e-abstract book

IRC 2025 BANGKOK

International Rubber Conference 2025

Rubber Revolution : Balancing Nature and Innovation for a Sustainable Future

1-3 December 2025

Bangkok International Trade & Exhibition Centre, Bangkok, Thailand



Organised by :

Co-organisers :

International Rubber Conference 2025 (IRC 2025)

Organised by :

- The Polymer Society of Thailand (PST)
- International Rubber Conference Organisation (IRCO)

Co-organisers :

- National Metal and Materials Technology Center (MTEC)
- Rubber Industry Club, Federation of Thai Rubber Industry
- Hub of Talents in Natural Rubber, NRCT
- TechnoBiz Communications Co., Ltd.

Sponsors :

Platinum

- National Metal and Materials Technology Center (MTEC)
- Rubber Authority of Thailand (RAOT)

Gold

- Sumitomo Rubber Industries, Ltd.

Silver

- Struktol Company of America, LLC

Bronze

- KOKOKU Innovative Technology Ltd.
- Otani Tire Co.,Ltd.
- Prince of Songkla University
- PT Cabot Indonesia
- Saengthai Rubber Co., Ltd.

Supporting

- Bangkok Synthetics Co., Ltd.
- Behn Meyer Chemicals (T) Co., Ltd.
- MRS-Thailand
- Singha Corporation
- Union Belt Industries Co., Ltd.
- Yokohama Tire Manufacturing (Thailand) Co., Ltd.

Message from Chairman of the Organising Committee

The International Rubber Conference 2025 (IRC 2025) is held for the first time in Thailand, the world's number one supplier of natural rubber, during 1-3 December 2025, although we had previously organised the RubberCon before in 2013. We are honoured to be given an opportunity to host this event on behalf of the rubber societies throughout the world which are members of the IRCO. We promise to do our best to make the IRC 2025 a successful and memorable event as well as being beneficial to all the participants.

As we are well aware, the IRC is one of the leading and most widely known international rubber conference which has been organised since 1966. The Conference provides a forum for sharing new developments in the science, technology and engineering of rubbers and rubber products, including the issues of health, safety and environment in connection with the modern rubber industry. The objectives are to encourage and promote international progress in rubber science, technology and engineering, co-operation as well as involvement of the younger generation for sustainability of the rubber industry.

The theme of IRC 2025 is "Rubber Revolution: Balancing Nature and Innovation for a Sustainable Future". A rather emphatic theme reflects our beliefs that there is an increasing urgency for all of us to work harder and more effectively to achieve sustainability of the rubber industry. Therefore, the IRC 2025 focuses on the innovation of increasing uses of natural raw materials (particularly natural rubber which has unique attributes to help accelerate achievement of net zero emissions goal for the rubber industry), technologies supporting the circular economy of the rubber industry, design and manufacturing technologies for sustainable rubber products with also longer life, raising safety and lowering of negative impact on the environment of the rubber products and unexplored applications of rubbers and rubber composites. As an emphasis on the importance of natural rubber in contributing to sustainability of the rubber industry, a one day Natural Rubber Symposium is also organised in the IRC 2025 under the theme "Sustainability of Natural Rubber : Latest Challenge and Solutions". The NR Symposium provides a platform for discussing and exchanging expert ideas and opinions in order to tackle the critical issues facing the sustainability of natural rubber industry today."

On behalf of the Organising Committee of the IRC 2025, I would like to extend our gratitude to all of you who are actively participating in the IRC 2025, to help make the IRC 2025 a successful event. I also sincerely hope that you will obtain the benefits of learning and exchanging new knowledge and technology relating to the development of sustainable rubber industry, as well as be provided with a rare opportunity to meet, discuss and possibly network with outstanding international researchers.

Welcome to the IRC 2025 and to Thailand.



Dr. Krisda Suchiva
Chairman of the Organising Committee,
International Rubber Conference 2025

Message from the President of the Polymer Society of Thailand

Dear Participants,

On behalf of the **Polymer Society of Thailand**, it is my great pleasure and honour to welcome you to the **International Rubber Conference 2025 (IRC2025)**, held this year under the theme **"Rubber Revolution: Balancing Nature and Innovation for a Sustainable Future."**

It has been nearly ten years since our society first expressed the intention to host this prestigious conference. Today, we are delighted to see IRC return to Thailand — a country recognized as the **world's leading producer of natural rubber** and a vital contributor to the global rubber supply chain. Although the IRC embraces all types of rubber, both natural and synthetic, it is fitting that this year's conference highlights the indispensable role of **natural rubber**, a renewable biomaterial supporting millions of smallholder farmers while meeting the diverse needs of global industries.

We are proud to collaborate closely with the **International Rubber Conference Organisation (IRCO)** in organizing this event, which serves as one of the world's most influential platforms for scientists, technologists, industrial leaders, and policymakers in the rubber field. At a time when the rubber sector faces challenges related to supply, sustainability, climate change, and performance demands from emerging technologies, innovation has never been more crucial. From advanced material design and green processing to circularity and responsible sourcing, our community plays a pivotal role in shaping the future of rubber.

The theme of IRC2025 — balancing nature with innovation — reflects a shared vision: that progress in polymer and rubber science must go hand in hand with environmental stewardship, economic resilience, and the well-being of communities. As a natural, versatile, and high-performance biomaterial, natural rubber remains central to this journey, offering unmatched properties while contributing to a more sustainable future.

I sincerely hope that this conference will inspire new ideas, spark meaningful discussions, and forge lasting collaborations. May IRC2025 serve as a bridge connecting fundamental research, industrial applications, and global strategies for sustainability.

Thank you for joining us in Bangkok. I wish you all a fruitful, engaging, and memorable conference experience.

Sincerely,



Associate Professor Dr. Taweechai Amornsakchai
President, Polymer Society of Thailand

II CONFERENCE COMMITTEE II

Organising Committee

Chairman

Dr. Krisda Suchiva	Mahidol University

Committee

Prof. Pranee Phinyocheep	Mahidol University (Vice-Chairman)
Dr. Ittipol Jangchud	King Mongkut's Institute of Technology Ladkrabang (Vice-Chairman)
Dr. Kannika Sahakaro	Prince of Songkla University (Vice-Chairman)
Dr. Taweechai Amornsakchai	Mahidol University (Secretariat)
Mr. Adisak Kongwaree	Thai Rubber Glove Manufacturers Association
Mr. Boonharn Ou-Udomying	Rubber Industry Group, Federation of Thai Industry
Dr. Charoen Nakason	Prince of Songkla University
Mr. Ekachai Limpichotipong	Rubber Industry Group, Federation of Thai Industry
Dr. Ekwipoo Kalkornsurapranee	Prince of Songkla University
Dr. Kanoktip Boonkerd	Chulalongkorn University
Ms. Pannee Jirabunpaisit	National Research Council of Thailand
Dr. Pasaree Laokijcharoen	National Metal and Materials Technology Center
Mr. Peram Prasada Rao	TechnoBiz
Dr. Sunanta Chuayprakong	King Mongkut's University of technology North Bangkok
Dr. Surapich Loykulnant	National Metal and Materials Technology Center
Dr. Wirasak Smitthipong	Kasetsart University

Scientific Committee

Chairman

Prof. Pranee Phinyocheep	Mahidol University (Chairman)

Committee

Dr. Panya Sunintaboon	Mahidol University (Secretariat)
Dr. Anoma Thitithammawong	Prince of Songkla University
Dr. Chaiwat Raksakulpiwat	Suranaree University of Technology
Prof. Chakrit Sirisinha	Mahidol University
Dr. Charoen Nakason	Prince of Songkla University
Dr. Chorwayakron Phetphaisit	Naresuan University
Dr. Ekwipoo Karnkornsurapranee	Prince of Songkla University
Dr. Ittipol Jangchud	King Mongkut's Institute of Technology Ladkrabang
Prof. Jitladda Sakdapipanich	Mahidol University
Dr. Kannika Sahakaro	Prince of Songkla University
Dr. Kanoktip Boonkerd	Chulalongkorn University
Dr. Pongdhorn Sae-oui	National Metal and Materials Technology Center
Prof. Pramuan Tangboriboonrat	Mahidol University
Prof. Rathanawan Magaraphan	Chulalongkorn University
Dr. Sombat Thanawan	Mahidol University
Dr. Supa Wiraset	Mahidol University
Dr. Supitta Suethao	Kasetsart University
Dr. Surapich Loykulnant	National Metal and Materials Technology Center
Dr. Taweechai Amornsakchai	Mahidol University
Dr. Wirasak Smitthipong	Kasetsart University

International Advisory Committee

Dr. Amir Hashim Yatim	Malaysian Rubber Glove Manufacturers Association, Malaysia
Dr. Amit Das	Leibniz-Institut Fur Polymerforschung Dresden, Germany
Prof. Anke Blume	University of Twente, Netherlands
Prof. Bagdagul Karaagac	Kocaeli University, Turkiye
Prof. Baochun Guo	South China University of Technology, China
Prof. Changwoon Nah	Jeonbuk National University, Korea
Dabo Philippe	AFICEP, France
Prof. Jacques W.M. Noordermeer	The Dutch Natural Rubber Foundation, Netherlands
Prof. James Busfield	Queen Mary University of London, UK
Prof. Jean Francois Pilard	Le Mans Université, France
Prof. Keon-Soo Jang	University of Suwon, Korea
Prof. Kinsuk Naskar	Indian Institute of Technology, Kharagpur, India
Prof. Liqun Zhang	Xi'an Jiaotong University, China
Prof. Markus Susoff	University of Applied Science of Osnabrück, Germany
Prof. Mikihito Takenaka	Kyoto University, Japan
Prof. Murat Sen	Hacettepe University, Turkiye
Dr. Nadras Othman	Universiti Sains Malaysia, Malaysia
Dr. Phan Trung Nghia	Hanoi University, Vietnam
Prof. Sabu Thomas	Mahatma Gandhi University, India
Prof. Seiichi Kawahara	Nagaoka University of Technology, Japan
Prof. Shinichi Sakurai	Kyoto Institute of Technology, Japan
Prof. Ulrich Giese	German Institute for Rubber Technology, Germany

Polymer Society of Thailand Committee

Advisory board

Prof. Supawan Tantayanon	Chulalongkorn University
Prof. Suda Kiatkamjornwong	Chulalongkorn University
Prof. Pattarapan Prasassarakich	Chulalongkorn University
Dr. Krisda Suchiva	Mahidol University
Prof. Suwabun Chirachanchai	Chulalongkorn University
Prof. Pranee Phinyocheep	Mahidol University
Dr. Chaya Chandavasu	PTT Global Chemical PCL

President

Dr. Taweechai Amornsakchai	Mahidol University

Committee

Dr. Amorn Chaiyasat	Rajamangala University of Technology Thanyaburi
Dr. Amornrat Lertworasirikul	Kasetsart University
Dr. Anucha Euapermkiati	PTT Global Chemical Public Co., Ltd.
Dr. Ittipol Jangchud	King Mongkut's Institute of Technology Ladkrabang
Dr. Kannika Sahakaro	Prince of Songkla University
Mr. Kongsak Dokbua	Plastics Institute of Thailand
Dr. Nattakarn Honsriphan	Silpakorn University
Dr. Pakorn Opaprakasit	Thammasat University
Dr. Panya Panya Sunintaboon	Mahidol University
Dr. Pasaree Laokijcharoen	National Metal and Materials Technology Center
Dr. Sararat Mahasaranon	Naresuan University
Dr. Sunanta Chuayprakong	King Mongkut's University of technology North Bangkok
Mr. Thongchai Oranrigsupak	The Federation of Thai Industries
Dr. Varawut Tangpasuthadol	Chulalongkorn University
Dr. Winita Punyodom	Chiang Mai University
Dr. Wonchalerm Rungswang	SCG Chemicals Company Limited

IRC 2025 Sponsors

Platinum

MTEC a member of NSTDA

การยางแห่งประเทศไทย
Rubber Authority of Thailand

Gold

SUMITOMO RUBBER INDUSTRIES

Silver

struktol®

Bronze

CABOT

KOKOKU INNOVATIVE TECHNOLOGY Ltd.

PSU PRINCE OF SONGKLA UNIVERSITY

OTANI DRIVING CONFIDENCE

SAENG THAI RUBBER

Supporting

bm BEHN MEYER Since 1840

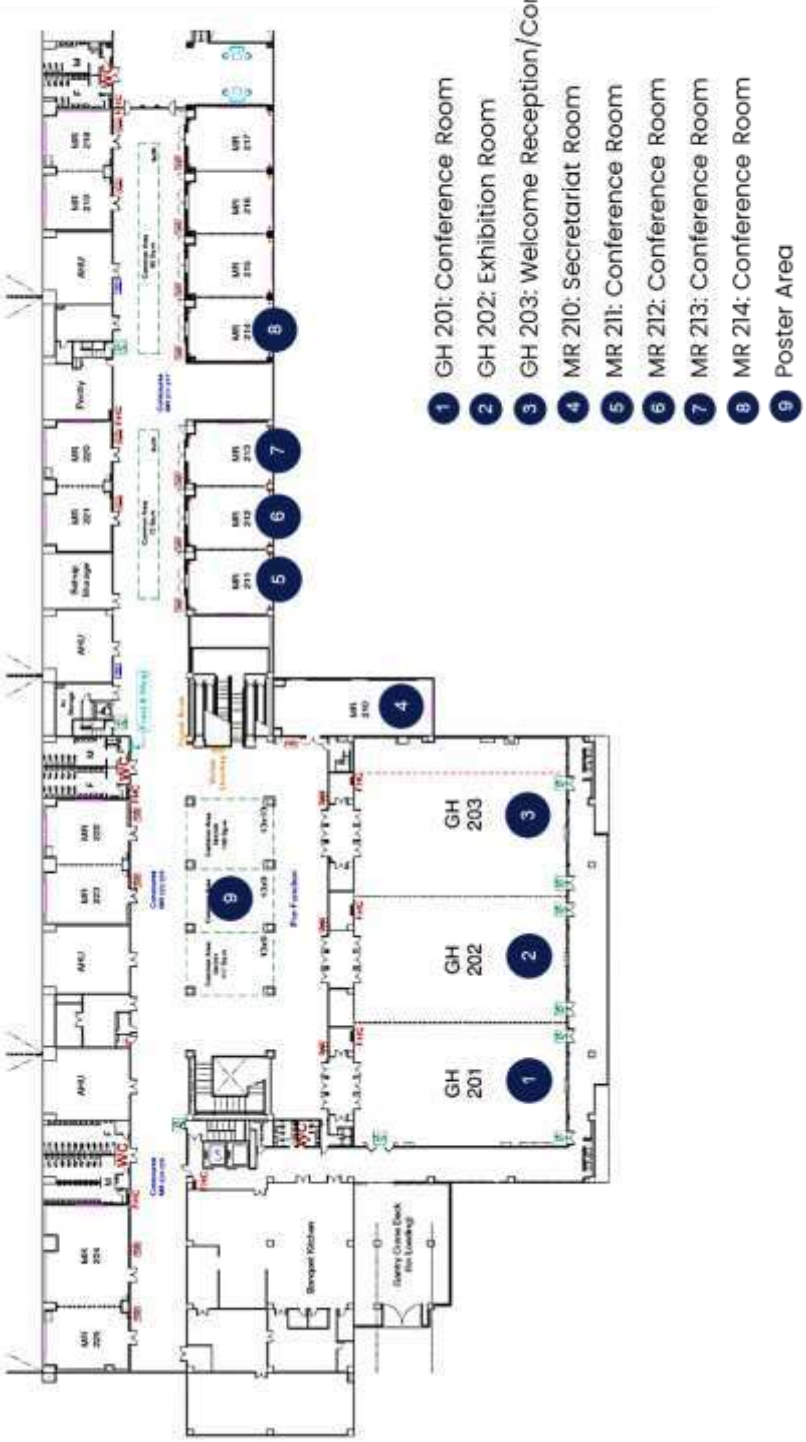
UBI CO.,LTD.

MRS-Thailand

BST

YOKOHAMA

Floor Plan


1 GH 201: Conference Room
2 GH 202: Exhibition Room
3 GH 203: Welcome Reception/Conference Room
4 MR 210: Secretariat Room
5 MR 211: Conference Room
6 MR 212: Conference Room
7 MR 213: Conference Room
8 MR 214: Conference Room
9 Poster Area
GH 201
GH 202
GH 203

Programme

December 1st, 2025

Time	Function
08:00-09:00	**Registration (Grand Hall)**
09:00-09:40	**Opening Ceremony (Grand Hall, GH 201)**
Plenary Lecture	
Session Chair	***Asst.Prof.Dr.Krisda Suchiva***
PL-01 **Plenary Lecture-1** 09:40-10:20	**Circular Economy -Limits and Chances in Rubber Recycling** ***Prof. Ulrich Giese*** German Institute for Rubber Technology, Germany
10:20-10:35	**Refreshment Break**
Session Chair	***Assoc.Prof.Dr.Taweechai Amornsakchai***
PL-02 **Plenary Lecture-2** 10:35-11:15	**Crack Resistance and Beyond: Fracture Mechanics in Strain Crystallizing and Liquid Crystal Elastomers** ***Prof. Kenji Urayama*** Kyoto University, Japan
Session Chair	***Prof. Pranee Phinyocheep***
PL-03 **Plenary Lecture-3** 11:15-11:55	**AI-driven Research and Multi-scale Simulation of Elastomer Materials** ***Prof. Liqun Zhang*** Xi'an Jiaotong University, China
11:55-13:00	**Lunch**
Keynote Lectures, Invited Lectures & Oral Presentations	
Session / Room	**Session I (MR 211)** **Natural Rubber, Bio-Based Rubbers and Rubber Chemicals**
Session Chairs	***Assoc.Prof.Dr.Charoen Nakason / Prof. Ulrich Giese***
KN-1 13:00-13:30	**Development of Fast Rubber Sheet Forming Method for Natural Rubber and Its Application** ***Seiichi Kawahara*** Nagaoka University of Technology, Japan

Dec. 1st, 2025 (MR 211)

IV-1 13.30-13:55	**Cellulose nanocrystal: Scalable production and Innovation Application** ***Jianming Zhang*** Qingdao University of Science and Technology, China
S1T6-O-01 13:55-14:15	**N-Vinylamides: Structural Isomers of Amino Acids Grafted onto Deproteinized Natural Rubber** ***Hiroharu Ajiro*** Nara Institute of Science and Technology, Japan
S3T3-O-22 14:15-14:35	**High-performance, Recyclable, and Multifunctional Nitrile Butadiene Rubber Based on Hydrogen and Urea Bonds** ***Dongmei Yue*** Beijing University of Chemical Technology, China
S1T6-O-03 14:35-14:55	**Chitosan-Reinforced Epoxidized Natural Rubber: Possible Design of Energy-Efficient Tire Tread Compounds** ***Nantinee Choosang*** Kasetsart University, Thailand
14:55-15:10	**Refreshment Break**
Session Chairs	***Assoc.Prof.Dr.Wirasak Smitthipong / Prof. Jitladda Sakdapipanich***
KN-6 15:10-15:40	**Engineering Allergy-Free Natural Rubber: Sustainable Deproteinization for Enhanced Industrial and Medical Performance** ***Jitladda Sakdapipanich*** Mahidol University, Thailand
S1T6-O-04 15:40-16:00	**Enhancing Ozone Resistance of TyreSidewall by Sustainable Replacement of Petroleum Wax with Bio-Based Additive** ***Tirthankar Bhandary*** HASETRI, India
S1T6-O-05 16:00-16:20	**Investigation of the Effect of the Amount of Zinc Borate on Cure Kinetics, Reversion, and Mechanical Properties of Natural Rubber in a Semi-Efficient Curing System** ***Davut Aksüt*** Hacettepe University, Turkey
S1T6-O-06 16:20-16:40	**Eco-Efficient Vulcanization: Analysis of a Sustainable Rubber Curing Package** ***Frances van Elburg*** University of Twente, the Netherlands
16:40-17:30	**Poster Session I**
18:00-20:00	**Welcome Cocktail Reception**

Dec. 1st, 2025

Session / Room	**Session II/1 (MR 212)** **Advancements in Sustainable Rubber Technology (1)**
Session Chairs	***Prof. Pattarapan Prasassarakich / Prof. Yuko Ikeda***
KN-2 13:00-13:30	**New Insights into Vulcanization Reactions for Green Rubber Technology** ***Yuko Ikeda*** Kyoto Institute of Technology, Japan
IV-2 13:30-13:55	**Self-Healing Rubber: An Advancing Technology for Smart Gloves** ***Patrick Tang Siah Ying*** Monash University Malaysia, Malaysia
S2T9-O-01 13:55-14:15	**Development of Carbon-Silica Dual Phase Filler for Application in Tyre Rubber Compounds –A Cost-Effective Material** ***Sampatrao Manjare*** Birla Institute of Technology and Science, India
S2T9-O-02 14:15-14:35	**Regeneration of Surface Sulfur Species on Pyrolysis Carbon Black** ***Ke Liu*** Qingdao University of Science & Technology, China
S2T9-O-03 14:35-14:55	**How Microcapsule-Enhanced Rubber Can Help Creating a Circular Economy** ***Katerina Filzer*** University of Twente, the Netherlands
14:55-15:10	**Refreshment Break**
Session Chairs	***Assoc.Prof.Dr.Ittipol Jangchud / Prof. Andreas Limper***
KN-7 15:10-15:40	**On the Path to Make a Black Magic Green –How to Minimize the CO_2 Footprint of Rubber Products** ***Andreas Limper*** Institut für Kunststoffverarbeitung RWTH Aachen, Germany
S2T9-O-04 15:40-16:00	**Chemical Degradation of End-of Life Tires** ***Heng Liu*** Qingdao University of Science and Technology, China
S2T9-O-05 16:00-16:20	**Thermo-Chemical Devulcanization of Sulfur-Cured Styrene–Butadiene Rubber (SBR) Using Diphenyldisulfide(DPDS)** ***Jonas Petzke*** Paderborn University, Germany
S2T2-O-11 16:20-16:50	**Reverse Molecular Reconstruction for Synthesizing High Performance Fluorinated Polyurea Elastomer** ***Donghan Li*** Shenyang University of Chemical Technology, China

Dec. 1st, 2025

16:40-17:30	**Poster Session I**
18:00-20:00	**Welcome Cocktail Reception**

Session / Room	**Session III/1 (MR 213)** **Advanced Rubber Materials and Novel Applications (1)**
Session Chairs	***Assoc.Prof.Dr.Kannika Sahakaro / Prof. Murat Sen***
KN-3 13:00-13:30	**Recent Trends in Adopting Sustainable Solution for Rubber Additives: How Chemistry Plays Significant Role?** ***Kinsuk Naskar*** Indian Institute of Technology Kharagpur, India
IV-3 13:30-13:55	**Effect of Molecular Architecture on the Thermal Stability of Poly(epichlorohydrin-co-ethylene oxide-co-allyl glycidyl ether) (GECO) Based Elastomers** ***Murat Sen*** Hacettepe University, Turkey
S3T5-O-01 13:55-14:15	**Boron-Containing Elastomer** ***Qi Wu*** Sichuan University, China
S3T5-O-02 14:15-14:35	**Effect of Non-Covalent Interactions on Epoxidized Natural Rubber: Structure-Properties Relationships** ***PhakamatLimarun*** Kasetsart University, Thailand
S3T5-O-03 14:35-14:55	**Sustainable Supramolecular Aqueous Adhesive with Moisture Resistance** ***Liying Zhang*** Qingdao University of Science & Technology, China
14:55-15:10	**Refreshment Break**
Session Chairs	***Assoc.Prof.Dr.Sitisaiyidah Saiwari / Prof. Sang Eun Shim***
KN-8 15:10-15:40	**Optimized Synthesis of Liquid Fluorosilicone Rubber with Improved Cold Resistance for Semiconductor Application** ***Sang Eun Shim*** Inha University, South Korea
S3T5-O-04 15:40-16:00	**Cellulose Nanocrystal-Based Aqueous Nanogel Photoinitiator for High-Performance Photocurable Hydrogel Elastomers** ***Quan Wang*** Qingdao University of Science & Technology, China

Dec. 1st, 2025 (MR 213)

S3T5-O-05 16:00-16:20	**Impact of Fused Filament Fabrication and Processing Parameters on the Performance of $BaTiO_3$-Piezoelectric Composites for Soft Robots** ***Sofiia Butenko*** EMPA, Switzerland
S3T5-O-06 16:20-16:40	**Enhancing the Piezoresistive Sensing Properties of TPE/CB Composites via Co-Continuous Structure Design through Natural Rubber Blending** ***Christopher Bascucci*** EMPA, Switzerland
16:40-17:30	**Poster Session I**
18:00-20:00	**Welcome Cocktail Reception**

Session / Room	**Session IV (MR 214)** **Progress in Rubber Characterisation**
Session Chairs	***Assoc.Prof.Dr.Ittipol Jangchud / Prof. Kenji Urayama***
KN-4 13:00-13:30	**Thermal History Effects on the Viscoelastic Response of Gum Natural Rubber: Temperature Induced Camel Structure and Influence on Extensional Rheology** ***Christopher G. Robertson*** Polymer Technology Services LLC, USA
IV-4 13:30-13:55	**Delayed Crystallization Response Inspired Waterborne Polyurethane with High Performance** ***Fei Chen*** Xi'an Jiaotong University, China
S4T7-O-01 13:55-14:15	**Formulations of Finite Hyperelasticity and Viscoelasticity Using Invariants of Stretch Tensors** ***Alexander Lion*** University of the Bundeswehr, Germany
S4T7-O-02 14:15-14:35	**Numerical Modeling of the Non-Isothermal Viscoelastic Flow Behavior of Rubber Compounds Based on the PHAN-THİEN TANNER (PTT) Model** ***HogenrichDamanik*** TU Dortmund, LsiiiAngewandte Mathematik, Germany
S4T7-O-03 14:35-14:55	**Method for Analyzing Mechanical Property Degradation of Polymer Materials Using Artificial Intelligence** ***Sangin Park*** Hyundai Motor Company, South Korea
14:55-15:10	**Refreshment Break**

Dec. 1st, 2025 (MR 214)

Session Chairs	***Dr.Pasaree Laokijcharoen / Prof. Changwoon Nah***
KN-9 15:10-15:40	**Some Considerable Factors in Laboratory Frictional Testing Rubbers** ***Changwoon Nah*** Jeonbuk National University, South Korea
S4T7-O-04 15:40-16:00	**Microstructural Modelling of Carbon Black Aggregates for Sustainable Next-Generation Tyre Design** ***Sarah Pedroni*** Queen Mary University of London, United Kingdom
S4T7-O-05 16:00-16:20	**Study on the Dispersion of Silica in SBR Using Time-Resolved Ultra Small Angle X-ray Scattering** ***Shotaro Nishitsuji*** Yamagata University, Japan
S4T7-O-06 16:20-17:30	**Correlative Analysis of Morphological and Functional Properties in High-Performance Elastomer Blends** ***Dean Vidakovic*** ZFE -Austrian Centre for Electron Microscopy & Nanoanalysis, Austria
16:40-17:30	**Poster Session I**
18:00-20:00	**Welcome Cocktail Reception**

Session / Room	**Session II/2 (GH 201)** **Advancements in Sustainable Rubber Technology (2)**
Session Chairs	***Assoc.Prof.Dr.Taweechai Amornsakchai / Dr. Amit Das***
KN-5 13:00-13:30	**The Crosslinking Dilemma in ENR: Evaluating Sulphur and Di-Acid Networks for Future-Ready Rubber Products** ***Amit Das*** Leibniz Institute of Polymer Research Dresden, Germany
IV-5 13:30-13:55	**Development of Helically-Wound Pineapple Leaf Fiber/NR Foam Composite for Near Zero-Volume Safety Devices** ***Taweechai Amornsakchai*** Mahidol University, Thailand
S2T1-O-01 13:55-14:15	**Application of Stearic Acid-Modified Silica in PCR Tread Compound** ***Farshid Zolala*** Barez Industrial Group, Iran

Dec. 1st, 2025 (GH 201)

S2T1-O-02 14:15-14:35	**Bio-Based Multifunctional Additive from Modified Illipe Butter for Silica Filled Tire Tread Compounds** ***Mohamad Irfan Fathurrohman*** PT. Riset Perkebunan Nusantara, Indonesia
S2T1-O-03 14:35-14:55	**The Utilization of Fly Ash from Different Resources as a Filler on the Properties of NR Compounds** ***Karnda Sengloyluan*** Prince of Songkla University, Thailand
14:55-15:10	**Refreshment Break**
Session Chairs	***Asst.Prof.Dr.Preeyanuch Junkong / Assoc.Prof.Dr.Kiadtisak Saenboonruang***
IV-6 15:10-15:40	**Natural Rubber Foam Containing Gamma-Synthesized Chitosan for the Utilization as Enhanced Heavy-Metal Sorbents** ***Kiadtisak Saenboonruang*** Kasetsart University, Thailand
S2T2-O-01 15:40-16:00	**Study on the Performance of Natural Rubber -Copper Coated Steel Wire with BCDB and BCoPD** ***Yuan Jin*** ReboNew Material Group, China
S2T2-O-02 16:00-16:20	**Carbon Black Coupling Agents for Improved Fuel Efficiency of Tyres** ***Max Dixey*** Queen Mary University of London, United Kingdom
S2T2-O-03 16:20-16:40	**Experimental Analysis of the Mixing Behavior of Ethylene-Propylene Diene Rubber (EPDM) in a Rubber Pin Extruder under Variation of Process Parameters and Mixing Elements** ***Leon Schmidt*** Paderborn University, Germany
16:40-17.30	**Poster Session I**
18:00-20:00	**Welcome Cocktail Reception**

December 2nd, 2025

Time	Function
8:00-9:00	**Registration**
Keynote Lectures, Invited Lectures & Oral Presentations	
Session / Room	**Session I (MR 211)** **Natural Rubber, Bio-Based Rubbers and Rubber Chemicals**
Session Chairs	***Dr.Philippe Dabo / Prof. Dariusz M. Bieliński***
KN-10 09:00-09:30	**Bio-Based Approach to Dispersion of Silica in NR** ***Dariusz M. Bieliński*** Institute of Polymer & Dye Technology, Poland
IV-7 09:30-09:55	**Synthesis of Polyester-Based Multiblock Copolymer Elastomers via A Cascade Polymerization Method** ***Yingfeng Tu*** Soochow University, China
S1T6-O-07 09:55-10:15	**Overview of SRI's Research Initiatives for Enhancing the Well-Being of Natural Rubber Stakeholders in Thailand** ***Lucksanaporn Tarachiwin*** Sumitomo Rubber (Thailand) Co., Ltd., Thailand
S1T6-O-08 10:15-10:35	**Research Progress on Modification and Functionalization of Natural Eucommia Ulmoides Gum** ***Hailan Kang*** Shenyang University of Chemical Technology, China
10:35-10:50	**Refreshment Break**
Session / Room	**Session I (MR 211)** **Natural Rubber, Bio-Based Rubbers and Rubber Chemicals**
Session Chair	***Prof. Pranee Phinyocheep***
KN-14 10:50-11:20	**Enhancing Coagulation Efficiency and Overcoming Uncoagulation Issues in Skim Latex Using Synthetic and Natural Creaming Agents** ***Charoen Nakason*** Prince of Songkla University, Thailand
S1T6-O-09 11:20-11:40	**Critical Concentration of Primary Amines for Preparation of Vulcanized Deproteinized Natural Rubber with Outstanding Mechanical Properties** ***Lam Ba Nguyen*** Nagaoka University of Technology, Japan

Dec. 2nd, 2025 (MR 211)

S1T6-O-10 11:40-12.00	**Removal of Proteins from Natural Rubber by Creaming Method** ***Anh Viet Ta*** Nagaoka University of Technology, Japan
12:00-13:00	**Lunch**
Session / Room	**Session II/1 (MR 211)** **Advancements in Sustainable Rubber Technology (1)**
Session Chairs	***Prof. Karine Mougin / Prof. Jinrong Wu***
KN-18 13:00-13:30	**Resolving the Microstructure of Natural Rubber and Its Influence on the Mechanical Properties** ***Jinrong Wu*** Sichuan University, China
IV-12 13:30-13:55	**Colour-Changing Smart Materials Inspired by Nature: Chameleon Effect** ***Karine Mougin*** Institutde Science des Matériaux de Mulhouse, France
S2T4-O-01 13:55-14:15	**Optimization of Calcium Nitrate to Compounded Latex Solid Content for Energy Saving in Latex Thin Film Forming** ***Wirach Taweepreda*** Prince of Songkla University, Thailand
S2T4-O-02 14:15-14:35	**Preparation and Characterization of Silica Filled Modified Natural Rubber: A Comparative Analysis of Pre-Dispersion and Conventional Techniques** ***Dalip Abdulraman*** Mahidol University, Thailand
S2T9-O-09 14:35-14:55	**The Reality of Sustainable Solution and the Economics of SME Rubber Industry: A Way Forward** ***Peram PrasadaRao*** Technobiz, Thailand
14:55-15:10	**Refreshment Break**
Session / Room	**Session I (MR 211)** **Natural Rubber, Bio-Based Rubbers and Rubber Chemicals**
Session Chairs	***Asst.Prof.Dr.Sunanta Chuayprakong / Assoc.Prof.Dr.Sitisaiyidah Saiwari***
IV-15 15:10-15:35	**Factors Affecting Biodegradability of Natural Rubber and Natural Rubber Products** ***Chomnutcha Boonmee*** National Metal and Materials Technology Center, Thailand

Dec. 2nd, 2025 (MR 211)

S1T6-O-11 15:35-15:55	**Synthetic Strategies and Mechanistic Studies of Liquid Rubber** ***Jing Hua*** Qingdao University of Science and Technology, China
S1T6-O-12 15:55-16:15	**Understanding and Controlling Storage Hardening in Natural Rubber via Phospholipid Network Disruption** ***Kittipong Insom*** Mahidol University, Thailand
S1T6-O-13 16:15-16:35	**New Non-Isocyanate Polyurethane Films Based on Natural Rubber** **Tharin Sensan** Prince of Songkla University, Thailand
16:35-17:30	**Poster Session II**
18:30-21:00	**Conference Dinner (Grand Hall: GH203)**

Session / Room	**Session II/1 (MR 212)** **Advancements in Sustainable Rubber Technology (1)**
Session Chairs	***Dr.Asira Fuongfuchat / Prof.Anke Blume***
KN-11 09:00-09:30	**Elucidating the Role of Nanoscale Interfaces and 3D Dispersion in Elastomer Nanocomposites: Connecting Microstructure to Viscoelastic Behavior** ***Ming Tian*** Beijing University of Chemical Technology, China
IV-08 09:30-09:55	**Greener Tire Tread Compounds by Reducing the Amount of Ingredients** ***Anke Blume*** University of Twente, the Netherlands
S2T9-O-07 09:55-10:15	**Upgrading Reclaimed Carbon from Tire Pyrolysis for Tire Rubber Applications** ***Purwonegoro Muljawan*** CABOT Corporation, Indonesia
S2T9-O-08 10:15-10:35	**Implementing Circular Economy Strategies in Power Transmission Belt Manufacturing** ***Aswathy T R*** JK FENNER India Limited, India
10:35-10:50	**Refreshment Break**

Dec. 2nd, 2025

Session / Room	**Session II/1 (MR 212)** **Advancements in Sustainable Rubber Technology (1)**
Session Chair	***Dr.Karnda Sengloyluan***
KN-15 10:50-11:20	**Driving Sustainability in Community Based Rubber Production: A Case of Energy and Waste Valorization in Thailand** ***Sumate Chaiprapat*** Prince of Songkla University, Thailand
S2T8-O-01 11:20-11:40	**Life Cycle Assessment of End-of-Life Tire Management Pathways: A Comparative Study** ***Yogesh Jadhav*** BITS Pilani K K Birla Goa Campus, India
S2T8-O-02 11:40-12:00	**Bridging Hydrophobic Silica Aerogels with Rubber Latexes via Hydrolysis Resistant Slurry Design** ***YanChun Han*** Qingdao University of Science & Technology, China
12:00-13:00	**Lunch**
Session / Room	**Session II/2 (MR 212)** **Advancements in Sustainable Rubber Technology (2)**
Session Chairs	***Prof. Pramuan Tangboriboonrat / Prof. Jeong Seok OH***
IV-11 13:00-13:30	**Greening the Elastomer Technology: Bio-Based Solid/Liquid Rubbers, Polyurethanes, and TPVs** ***Jeong Seok OH*** Gyeongsang National University, South Korea
IV-13 13:30-13:55	**Renewable Elastomeric Networks of Functionalized Ethylene-Propylene Copolymers** ***Yixian Wu*** Beijing University of Chemical Technology, China
S2T1-O-04 13:55-14:15	**Efficient and Gentle Processing of Rubber Compounds –How Continuous Milling Transforms Rubber Processing** ***Julia Uth*** UTH GmbH, Germany
S2T1-O-05 14:15-14:35	**Green Preparation and Performance Study of NRL/Biomass Composites via Non-Rubber Component Mediation and Spatial Confinement** ***Zhengtian Xie*** Sichuan University, China

Dec. 2nd, 2025 (MR 212)

S2T1-O-06 14:35-14:55	**Properties of Films from Deproteinized Natural Rubber Latex Produced via Membrane Separation Technology** ***Mohamad Akmal Absul Ramahm*** Malaysian Rubber Board, Malaysia
14:55-15:10	**Refreshment Break**
Session / Room	**Session II/2 (MR 212)** **Advancements in Sustainable Rubber Technology (2)**
Session Chairs	***Prof. Yixian WU / Prof. Sayant Saengsuwan***
IV-16 15:10-15:35	**Biocomposite Starch/NR-Grafted Hydrogels as Sustainable Coating Membranes for Slow-Release Fertilizers** ***Sayant Saengsuwan*** Ubon Ratchathani University, Thailand
S2T1-O-07 15:35-15:55	**Extrudable Vitrimeric Rubbers Enabled via Heterogeneous Crosslinking** ***Shuangjian Yu*** South China University of Technology, China
S2T1-O-08 15:55-16:15	**Lignin/Carboxylated Nitrile Rubber Composites: the Influence of Carboxyl Content on the Mechanical Properties of the Material** ***Hongbing Zheng*** PetroChina Shanghai Advanced Materials Research Institute Co., Ltd., China
S2T2-O-12 16:15-16:35	**Enhanced Gas Barrier Properties of Graphene Oxide/Rubber Elastomer Nanocomposites** ***Shipeng Wen*** Beijing University of Chemical Technology, China
16:35-17:30	**Poster Session II**
18:30-21:00	**Conference Dinner (Grand Hall: GH203)**

Session / Room	**Session III/1 (MR 213)** **Advanced Rubber Materials and Novel Applications (1)**
Session Chair	***Assoc.Prof.Dr.Pakorn Opaprakasit***
KN-12 09:00-09:30	**Wide-Angle X-Ray Diffraction Studies on Strain-induced Crystallization of Vulcanized Natural Rubber by Two-Step Biaxial Stretching** ***Shinichi Sakurai*** Kyoto Institute of Technology, Japan
IV-9 09:30-09:55	**Introduction of Reversible Bonds into Rubber Networks** ***Toshio Tada*** Sumitomo Rubber Industries, Ltd., Japan

Dec. 2nd, 2025 (MR 213)

S3T5-O-07 09:55-10:15	**α-Diimine Cobalt Complexes Bearing Axial Anagostic Interaction: A System for Accessing Ultra-High Molecular Weight Polybutadiene** ***Wang Xin*** Qingdao University of Science and Technology, China
S3T5-O-08 10:15-10:35	**Fe-Based Catalyst with Exogenous Electron Donor for Stereopolymerization of Butadiene and Isoprene** ***Xu Shiliang*** Qingdao University of Science and Technology, China
10:35-10:50	**Refreshment Break**
Session / Room	**Session III/2 (MR 213)** **Advanced Rubber Materials and Novel Applications (2)**
Session Chair	***Prof. Shinichi Sakurai***
KN-16 10:50-11:20	**Revisiting the Properties of Natural Rubber in Tire Industry and Development of NR-Based Sidewall Compounds for EV Passenger Cars** ***Kannika Sahakaro*** Prince of Songkla University, Thailand
S3T3-O-01 11:20-11:40	**Innovation Management for Commercial Success in the Rubber Industry Amid Shifting Global Market Forces** ***Matthew Thornton*** The Rubber Initiative, United Kingdom
S3T3-O-02 11:40-12:00	**Toward Sustainable Tire Development: Challenges and Emerging Solutions** ***Wisut Kaewsakul*** Walailak University, Thailand
12:00-13:00	**Lunch**
Session / Room	**Session III/2 (MR 213)** **Advanced Rubber Materials and Novel Applications (2)**
Session Chairs	***Assoc.Prof.Dr.Chaiwat Raksakulpiwat / Asst.Prof.Dr.Wisut Kaewsakul***
S3T3-O-03 13:00-13:20	**Surface-Functionalised Carbon Black as a High-Performance Filler in Elastomeric Compounds: Techniques and Potential** ***Rattapong Numard*** Queen Mary University of London, United Kingdom
S3T3-O-04 13:20-13:40	**Effect of Chemically Treated Pineapple Leaf and Hemp Fibers on the Interfacial Interaction and Mechanical Properties of Natural Rubber Composites** ***Siriwan Jansinak*** Kasetsart University, Thailand

Dec. 2nd, 2025 (MR 213)

S3T3-O-05 13:40-14:00	**Development of Thermoplastic Natural Rubber Composites for Wearable Shielding Materials** ***Akarapong Tuljittraporn*** Prince of Songkla University, Thailand
S3T3-O-06 13:55-14:15	**High-performance, Recyclable, and Multifunctional Nitrile Butadiene Rubber Based on Hydrogen and Urea Bonds** ***Dongmei Yue*** Beijing University of Chemical Technology, China
S3T3-O-07 14:15-14:55	**Development of Piezoresistive Sensor Prepared from PMMA-Grafted Natural Rubber Latex Filled Conductive Carbon Composites: Comparative of Conductive Carbon Fillers and Hybrid System** ***Arthittaya Chuaybamrung*** Prince of Songkla University, Thailand
S3T3-O-08 14:35-14:55	**Development of Hydroxyapatite from Eggshell Waste and Its application in SBR Composite** ***Chomsri Siriwong*** Khon Kaen University, Thailand
14:55-15:10	**Refreshment Break**
Session / Room	**Session III/2 (MR 213) Advanced Rubber Materials and Novel Applications (2)**
Session Chairs	***Dr.Toshio Tada / Assoc.Prof.Dr.Yeampon Nakaramontri***
IV-17 15:10-15.35	**Dual-Functional Natural Rubber Composites with Piezoresistive and Antibacterial Properties for Wearable Motion Detection** ***Yeampon Nakaramontri*** King Mongkut's University of Technology Thonburi, Thailand
S3T3-O-09 15:35-15:55	**Comparison of Growth and Transpiration in Micro-Cuttings and Budded Rubber Trees** ***Supat Isarangkool Na Ayutthaya*** Khon Kaen University, Thailand
S3T3-O-10 15:55-16:15	**Effectiveness of Participatory Ergonomic Training on Musculoskeletal Disorders Among Rubber Tappers: A Longitudinal Mixed-Effects Analysis** ***Warut Chanasit*** Prince of Songkla University, Thailand
S3T3-O-11 16:15-16:35	**Effects of Enhanced Ergonomic Training on Postural Risk Among Rubber Tappers: A Cluster Randomized Longitudinal Analysis** ***Chanon Kongkamol*** Prince of Songkla University, Thailand
16:35-17:30	**Poster Session II**
18:30-21:00	**Conference Dinner (Grand Hall: GH203)**

Dec. 2nd, 2025

Session / Room	**Session IV (MR 214)** **Progress in Rubber Characterisation**
Session Chairs	***Assoc.Prof.Dr.Ekwipoo Kalkornsurapranee / Prof. Ken Nakajima***
KN-13 09:00-09:30	**AFM Nanomechanics Connecting Macro-and Nanoscopic World** ***Ken Nakajima*** Institute of Science Tokyo, Japan
IV-10 09:30-09:55	**A Novel Value Approach of Natural Rubber for Emerging and Unexplored Applications** ***Ekwipoo Karnkornsurapranee*** Prince of Songkla University, Thailand
S4T7-O-07 09:55-10:15	**Chemical Fingerprinting for Environmental Detection of Tyre Rubber Emissions** ***Nick Molden*** Emissions Analytics Ltd., United Kingdom
S4T7-O-08 10:15-10:35	**Advancing Sustainability in Rubber Industries Involves Optimizing Testing Through the Utilization of Rubber Process Analyzer** ***Li Wan*** Alpha Technologies, China
10:35-10:50	**Refreshment Break**
Session / Room	**Session IV (MR 214)** **Progress in Rubber Characterisation**
Session Chair	***Prof. Jitladda Sakdapipanich***
KN-17 10:50-11:20	**Recent Advances in Reducing Hysteresis of Rubber Composites** ***Baochun Guo*** South China University of Technology, China
S4T7-O-09 11:20-11:40	**Rubber Blend Compatibility Analysis Using Large-Amplitude Oscillatory Shear (LAOS) on RPA** ***Zühra Çınar Esin*** Hacettepe University, Turkey
S4T7-O-10 11:40-12.00	**Performance Evaluation of Silicone Based Isolators under Varying Temperatures and Excitation Levels Using a Thermal Chamber Shaker** ***Erdem Rahmi SENOZ*** Aselsan, Turkey
12:00-13:00	**Lunch**

Dec. 2nd, 2025

Session / Room	**Session IV (MR 214)** **Progress in Rubber Characterisation**
Session Chairs	***Prof. Rathanawan Magaraphan / Prof. Baochun Guo***
KN-19 13:00-13:30	**Waste Tire Recycling: The Next Frontier Beyond Devulcanization for Low Carbon Living** ***Rathanawan Magaraphan*** Chulalongkorn University, Thailand
IV-14 13:30-13:55	**Facile Recycling Strategy for End-of Life Rubbers by Selective Cleavage of Cross-Linking Bonds** ***Ganggang Zhang*** South China University of Technology, China
S4T7-O-11 13:55-14:15	**Tribological Behavior of Soft Polymers Against Model Substrates** ***Sophie Bistac*** Université de Haute Alsace UHA LPIM, France
S4T7-O-12 14:15-14:35	**NR Film Visualization via AFM Imaging** ***Kim Song Tan*** Malaysian Rubber Board, Malaysia
S4T7-O-13 14:35-14:55	**AFM-Based Investigation of Polyisoprene-Inorganic Interface Adhesion at Multiple Scales** ***Hexuan Mao*** Institute of Science Tokyo, Japan
14:55-15:10	**Refreshment Break**
Session / Room	**Session IV (MR 214)** **Progress in Rubber Characterisation**
Session Chairs	***Dr.Panithi Wiroonpochit / Prof.Philippe Daniel***
IV-18 15.10-15.35	**Raman Spectroscopy Applied to Elastomers: From the History up to the New Smart Technological Developments** ***Philippe Daniel*** Le Mans University, France
S4T7-O-14 15.35-15:55	**Improving Seal Life Prediction: Faster Crack Growth Testing in HNBR** ***Orkid Ramekaj*** Queen Mary University, United Kingdom
S4T7-O-15 15.55-16:15	**Study on the Effect of Silane Coupling Agents on Mechanical Behavior of Silica-Filled Styrene-Butadiene Rubber under Elongation Using In Situ Nano-Palpation Atomic Force Microscopy** ***Maytawee Malineerat*** Institute of Science Tokyo, Japan

Dec. 2nd, 2025 (MR 214)

S4T7-O-16 16.15-16:35	**Friction Behaviour in Relation to Wear Morphology** ***Huong Thao Pham*** Queen Mary University of London, United Kingdom
16:35-17.30	**Poster Session II**
18:30-21:00	**Conference Dinner (Grand Hall: GH203)**

Session / Room	**Natural Rubber Symposium: GH 201**
Topic	**Sustainability of NR Supplies**
Session Chair	***Assoc.Prof.Dr.Charoen Nakason***
NRS-O-01 09:00-09:30	**Global Efforts to Ensure Sustainability of NR Supplies** ***Stefano Savi*** Global Platform for Sustainability of Natural Rubber
NRS-O-02 09:30-10:00	**The Role of Thailand Contributing to Sustainability of NR Supplies** ***Napawan Lekawipat*** Rubber Authority of Thailand, Thailand
Topic	**Quality of NR**
Session Chair	***Assoc.Prof.Dr.Ittipol Jangchud***
NRS-O-03 10:00-10:30	**Novel Green Technologies for Production of User-Friendly and Consistent Properties NR** ***Nantina Moonprasith*** National Metal and Materials Technology Center, Thailand
10:30-10:45	**Refreshment Break**
NRS-O-04 10:45-11:15	**From Tree to Technological Materials: Turning Natural Rubber into a Game Changer for More Sustainable and Performing Products** ***Poonyawat Prateeprat*** Michelin
Topic	**Biodegradation of NR and NR Products**
Session Chair	***Dr.Pairote Jittham***
NRS-O-05 11:15-11:45	**Perspective on Dipped Rubber Product Biodegradability: MRB Research Highlights and Future Pathways** ***Shabinah FilzaBinti Mohd Sharib*** Malaysian Rubber Board, Malaysia

Dec. 2nd, 2025 (GH 201)

NRS-O-06 11:45-12.15	**Study of Biodegradation Efficiency of Natural Rubber Products by Various Microorganism** ***Dr. Nattawut Boonyuen*** National Center for Genetic Engineering and Biotechnology, Thailand
12:15-13:00	**Lunch**
Topic	**Safety of NR Products**
Session Chair	***Prof. Jitladda Sakdapipanich***
NRS-O-07 13:00-13:30	**Reducing Extractable Protein in Latex Gloves to Lower Latex Allergy: Evidence from Thailand and International Studies** ***Naesinee Chaiear*** Khon Khan University, Thailand
NRS-O-08 13:30-14:00	**From Allergen to Assurance: A Comprehensive Review of Natural Rubber Product Safety and MRB's Strategic Role** ***Aziana Binti Abu Hassan*** Malaysian Rubber Board, Malaysia
Topic	**Challenge and Opportunity for Future Applications of NR**
Session Chair	***Assoc.Prof.Dr.Ekwipoo Karnkornsurapranee***
NRS-O-09 14:00-14:30	**Pioneering a Sustainable Biorefinery of Natural Rubber Serum for New Bioactives in Cosmetics, Food, Nutraceuticals, and Pharmaceuticals** ***Thanawat Pitakpornpreecha*** Prince of Songkla University, Thailand
NRS-O-10 14:30-15:00	**Utilizing Natural Rubber Seeds for Biorefinery** ***Koryu Kawatani*** Innovare, Japan
15:00-15:15	**Refreshment Break**
Topic	**Challenge and Opportunity for Future Applications of NR (Panel presentation and discussion)**
Session Chair	***Assoc.Prof.Dr.Kannika Sahakaro***
NRS-O-11 15:15-15:45	**Modified Natural Rubber: Current Progress, Opportunities, and Challenges.** ***Krishna Veni*** Malaysian Rubber Board, Malaysia
NRS-O-12 15:45-16:15	**Challenge for the Future of NR Latex and NRL Products** ***Amir Hashim Yatim*** Malaysian Rubber Glove Manufacturers Association, Malaysia

Dec. 2nd, 2025 (GH 201)

NRS-O-13 16:15-16:45	**Opportunity for Industrial Applications of NR** ***Banja Junhasavasdikul*** Innovation Group, Thailand
16:45-17:00	**Discussion**
16:35-17:30	**Poster Session II**
18:30-21:00	**Conference Dinner (Grand Hall: GH203)**

December 3rd, 2025

Time	Function
08:00-09:00	**Registration (Grand Hall)**
	Grand Hall: GH 201
Plenary Lecture	
Session Chair	***Assoc.Prof.Dr.Kannika Sahakaro***
PL-04 **Plenary Lecture-4** 09:00-09:40	**Sustainable Materials for Tyre Engineering** ***Sabu Thomas*** Mahatma Gandhi University, India
Session Chair	***Assoc.Prof.Dr.Ittipol Jangchud***
PL-05 **Plenary Lecture-5** 09:40-10:20	**Increasing the Circularity of Sulphur Crosslinked Natural Rubber** ***James Busfield*** Queen Mary University of London, United Kingdom
10:20-10:35	**Refreshment Break**
Session Chair	***Dr.Pasaree Laokijcharoen***
PL-06 **Plenary Lecture-6** 10.35-11:15	**Sustainable Mobility 2030 and Beyond –Role of Tyre and Rubber Industry** ***R. Mukhopadhyay*** JK Tyre& Industries Ltd., India
Keynote Lectures, Invited Lectures & Oral Presentations	
Session / Room	**Session I (MR 211)** **Natural Rubber, Bio-Based Rubbers and Rubber Chemicals**
Session Chair	***Dr.Karnda Sengloyluan***
S1T6-O-14 11:15-11:35	**Latex Serum Boosts Natural Rubber Strength** ***Katsuhiko Tsunoda*** Bridgestone Corporation, Japan
S1T6-O-15 11:35-11:55	**Green Synthesis of Zinc Oxide from Skim Latex Serum for Application in Rubber Vulcanization** ***Preeyanuch Junkong*** Mahidol University, Thailand
11:55-13:00	**Lunch**

Dec. 3rd, 2025 (MR 211)

Session Chairs	***Dr.Panithi Wiroonpochit / Prof.Seiichi Kawahara***
S1T6-O-16 13:00-13:25	**A New Antibacterial Hybrid Waterborne Polyurethane/Silica Coating Film Based on Natural Rubber** ***Nitinart Saetung*** Prince of Songkla University, Thailand
S1T6-O-17 13:25-13:45	**Degradation Trends in Plasticity and Viscosity of Selected Standard Philippine Rubber under Prolonged Storage** ***Shadam Suganob*** Department of Science and Technology Region IX - Philippines, the Philippines
S1T6-O-18 13:45-14:05	**Sustainable Yield Improvement and Quality Assessment of TSR10 Rubber from Two *Hevea Brasiliensis* Genotypes: Impact of Reduced Tapping Frequency Associated with Ethephon Stimulation** ***Hathainat Kum-ourm*** Sumitomo Rubber (Thailand) Co., Ltd., Thailand
S1T6-O-19 14:05-14:25	**Sustainable NZEROSILTM Silicas from Renewable Rice Husk** ***Danniel Liao*** Oriental Silicas Corporation Taiwan, Province of China
S1T6-O-20 14:25-14:45	**Mechanical Tailoring of Waterborne Epoxy Coatings on Metal Substrates Using Functionalized Natural Rubber Latex** ***Wasan Tessanan*** Pathumwan Institute of Technology, Thailand
14:45-15:00	**Refreshment Break**
Session Chair	***Dr.Wasan Tessanan***
S1T6-O-21 15:00-15:20	**Rubbery Soft Polymer Electrolyte Membrane with Nanomatrix Channel Prepared from Natural Rubber** ***Yoshimasa Yamamoto*** National Institute of Technology, Japan
S1T6-O-22 15:20-15:40	**The Development of Bio-Inspired Composites from Epoxidized Natural Rubber Using π–π Stacking and Cation–π Interactions** ***Kwanchai Buaksuntear*** Kasetsart University, Thailand
S1T6-O-23 15:40-16:00	**Effect of Crystal Orientation on Mechanical Strength of Polyisoprene Rubber under Bi-Axial Deformation** **Airi Sato** Bridgestone Corporation, Japan
16:00-16:30	**Best Student Presentation Award Ceremony**
16:30-17:00	**Closing Ceremony**

Dec. 3rd, 2025

Session / Room	**Session III/1 (MR 212)** **Advanced Rubber Materials and Novel Applications (1)**
Session Chair	***Prof. Maurice Brogly***
S3T5-O-09 11:15-11:35	**ECIU Rubber Chair -An Inter University Organisation Focused on Rubber Science and Intersectoral Impact** ***Rafal Anyszka*** Lodz University of Technology, Poland
S3T5-O-10 11:35-11:55	**Polyrotaxane-Based Hybrid Crosslinking for Tunable Elastic and Thermal Response in Epoxidized Natural Rubber** ***Anoma Thitithammawong*** Prince of SongklaUniversity, Thailand
11:55-13:00	**Lunch**
Session Chairs	***Assoc.Prof.Dr.Kannika Sahakaro / Assoc.Prof.Dr.Nadras Othman***
IV-19 13:00-13:25	**Optimizing Silica and Carbon Black Ratios for Enhanced Mechanical Performance of NR/BR/SSBR Blends** ***Nadras Othman*** Universiti Sains Malaysia, Malaysia
S3T5-O-11 13:25-13:45	**Actuation Programming of Liquid Crystal Elastomers** ***Binjie Jin*** South China University of Technology, China
S3T5-O-12 13:45-14:05	**Biomimetic Design and Development of Natural Rubber-Based Soft Robotics** ***Manus Sriring*** Mahidol University, Thailand
S2T2-O-10 14:05-14:25	**Inverse Vulcanization Forged Self - Motivated Polysulfide Silane: An Ultra-Efficient Architect in Engineering Silica-Rubber Interface** ***Dong Wang*** South China University of Technology, China
S3T5-O-14 14:25-14:45	**Elastomeric Ionomer Based on Maleated Bromobutyl Rubber** ***Subhan Salaeh*** Prince of Songkla University, Thailand
14:45-15:00	**Refreshment Break**
Session Chair	***Assoc.Prof.Dr.Polphat Ruamcharoen***
S3T5-O-15 15:00-15:20	**Properties and Crosslinking Mechanisms of 1,2-Polybutadiene Derivative-Based Rubber Formulations** ***Hiroki Hashimoto*** Nippon Soda Co., Ltd., Japan

Dec. 3rd, 2025 (MR 212)

S3T5-O-16 15:20-15:40	**Property and Application of Perfluoropolyether-Modified Functional Rubber** ***Zheming Tong*** PetroChina (Shanghai) New Materials Research Institute Co., Ltd., China
16:00-16:30	**Best Student Presentation Award Ceremony**
16:30-17:00	**Closing Ceremony**

Session / Room	**Session III/2 (MR 213)** **Advanced Rubber Materials and Novel Applications (2)**
Session Chair	***Assoc.Prof.Dr.Yeampon Nakaramontri***
S3T3-O-12 11:15-11:35	**Additive Manufacturing of Natural Rubber Latex for Sustainable Flexible Sensors** ***Panithi Wiroonpochit*** National Science and Technology Development Agency, Thailand
S3T3-O-13 11:35-11:55	**Construction of Recyclable Rubber Composites Based on Dynamic Bonding** ***Yuzhu Xiong*** Guizhou University, China
11:55-13:00	**Lunch**
Session Chair	***Assoc.Prof.Dr.Ittipol Jangchud***
S3T3-O-14 13:00-13:25	**Natural Rubber Latex-Based Tissue Engineering: The Pioneering Advances in Material for Sustainability** ***Masami Okamoto*** Toyota Technological Institute, Japan
S3T3-O-15 13:25-13:45	**Multidimensional Rubber Composite Utilizing Lignin as a Bio-Filler** ***Amit Kumar Sen*** Hari Shankar Singhania Elastomer and Tyre Research Institute, India
S3T3-O-16 13:45-14:05	**Sustainable Rubber Nanocomposites for Tyre Application by Silica Hairy Nanoparticles Fillers** ***Barbara Di Credico*** University of Milano-Bicocca, Italy
S3T3-O-17 14:05-14:25	**A Natural Rubber-Based Stretching Band and Its Machine Learning Validated Muscle Tension Mitigation** ***Nabil Hayeemasae*** Prince of Songkla University, Thailand

Dec. 3rd, 2025 (MR 213)

S3T3-O-18 14:25-14:45	**Thermoset–Rubber 2K Composite Systems: Material Combinations and Interfacial Reactions in a One-Step Injection Molding Process** ***Florian Löhr*** Paderborn University, Germany
14:45-15:00	**Refreshment Break**
Session Chair	***Assoc.Prof.Dr.Jareerat Ruamcharoen***
S3T3-O-19 15:00-15:20	**Advancing 3D Printing with Biobased Rubber: Photocurable and Extrudable Platforms for Functional Soft Materials** ***Nuttapol Risangud*** Chulalongkorn University, Thailand
S3T3-O-20 15:20-15:40	**Potential of Low-Temperature Vulcanized Natural Rubber Latex for Antimicrobial Applications** ***Rawiporn Promsung*** Prince of Songkla University, Thailand
S3T3-O-21 15:40-16:00	**Novel Triboelectric Nanogenerators for Self-Powered System by Using Fluorinated Wasted Rubber Powders** ***Huiqing Fan*** Northwestern Polytechnical University, China
16:00-16:30	**Best Student Presentation Award Ceremony**
16:30-17:00	**Closing Ceremony**

Session / Room	**Session IV (MR 214)** **Progress in Rubber Characterisation**
Session Chair	***Prof. Sophie Bistac***
S4T7-O-17 11:15-11:35	**In Situ Methods to Characterize Deformation-Induced Mechanisms in NR** ***Eric Euchler*** Leibniz Institute of Polymer Research Dresden, Germany
S4T7-O-18 11:35-11:55	**The Role of Deformation Mode on Rubber Hysteresis and Its Dependency on Viscoelasticity** ***Shouliang Nie*** Zhongce Rubber Group Co., Ltd., China
11:55-13:00	**Lunch**

Dec. 3rd, 2025 (MR 214)

Session Chairs	***Prof. Sabu Thomas / Assoc.Prof.Dr.Charoen Nakason***
IV-20 13:00-13:25	**Advancing Sustainable Rubber Recycling: Transforming NR and NBR Waste into Conductive Elastomers** ***Sitisaiyidah Saiwari*** Prince of Songkla University, Thailand
S4T7-O-19 13:25-13:45	**On the Decoupling of Chemical and Mechanical Surface Contributions in Soft Polymer Network Adhesion** ***Maurice Brogly*** UHA –LPIM, France
S4T7-O-20 13:45-14:05	**Wear Particle Formation Mechanism Investigated Using LAT100** ***Shinya Nakano*** Sumitomo Rubber Industries, Japan
S4T7-O-21 14:05-14:25	**Why Lab Studies Matter for Understanding Tyre Wear Emissions** ***Martin Stěnička*** Tomas Bata University in Zlin/ University Institute / Centre of Polymer Systems, Czech Republic
S4T7-O-22 14:25-14:45	**Study of Standard Laboratory for Testing Medical Rubber Gloves According to ISO/IEC 17025** ***Hassarutai Yangthong*** Kasetsart University, Thailand
14:45-15:00	**Refreshment Break**
Session Chair	***Asst.Prof.Dr.Sunanta Chuayprakong***
S4T7-O-23 15:00-15:20	***Visualizing Nanoscale Interface in Direct Adhesive Rubbers Containing Reversible Coordination Linkages*** ***Kim Hung NGUYEN*** Institute of Science Tokyo, Japan
S4T7-O-24 15:20-15:40	***Study on Delamination Mechanism of Rubber-Adhesive Interface in Sealing Materials*** ***Hiromu Kawasaki*** NOK Corporation, Japan
S4T7-O-25 15:40-16:00	***Analysis of Allergenic Proteins in Natural Rubber After Radiolysis by Mass Spectrometry Technique*** ***Adun Nimpaiboon*** Mahidol University, Thailand
16:00-16:30	**Best Student Presentation Award Ceremony**
16:30-17:00	**Closing Ceremony**

Dec. 3rd, 2025

Session / Room	**Session II/2 (GH 201)** **Advancements in Sustainable Rubber Technology (2)**
Session Chair	***Prof. Kinsuk Naskar***
S2T2-O-04 11:15-11:35	**Molecular Chain Structure Changes and Strain-Induced Crystallization Behaviors During Various Deformation of Segmented Polyurethane Elastomer** ***Kakeru Obayashi*** Kyoto University, Japan
S2T2-O-05 11:35-11:55	**Study of the Mullins Effect in Carbon Black-Filled Rubber by Atomic Force Microscopy** ***Takahiro Anzai*** NOK Corporation, Japan
11:55-13:00	**Lunch**
Session Chairs	***Assoc.Prof.Dr.Taweechai Amornsakchai / Prof. Bagdagul Karaagac***
IV-21 13:00-13:25	**Multifunctional Applications of Epoxidized Natural Rubber: From Gas Separation Membranes to Self-Healing and Adhesion Technologies** ***Bagdagul Karaagac*** Kocaeli University, Turkiye
S2T2-O-06 13:24-13:45	**Modelling of Elastomers under Dynamical Mechanical Loads** ***Michael Johlitz*** Institute of Mechanics, Germany
S2T2-O-07 13:45-14:05	**New Insights into Resins Behavior: Influence of Resin Softening Point on the In-Rubber Properties of Carbon Black-Filled SBR Compounds** ***Javier Alejandro and Araujo Morera*** University of Twente, the Netherlands
S2T2-O-08 14:05-14:25	**Influences of Sulfur Vulcanization System and Curative Content on Properties of Tire Tread Compounds Filled with Carbon Black/Silica Hybrid Filler** ***Puchong Thaptong*** National Science and Technology Development Agency, Thailand
S2T2-O-09 14:25-14:45	**Aluminum Soaps: A New Prospect for Rubber Application** ***Xiaorong Wang*** Hangzhou Zhongce Rubber Company, China
14:45-15:00	**Refreshment Break**
16:00-16:30	**Best Student Presentation Award Ceremony**
16:30-17:00	**Closing Ceremony**

Poster Presentation

December 1st, 2025 (16:40 - 17:30)

Poster Session I

Session I: Natural Rubber, Bio-based Rubbers and Rubber Chemicals

S1T6-P-01	**Design and Molecular Dynamics Simulation of Biomass Ion-Conductive Elastomer** ***Jiajun Qu*** Beijing University of Chemical Technology, China
S1T6-P-02	**Wide-Angle X-Ray Diffraction Studies on Thermal Melting Behavior of Crystallites Formed by Planar Elongation of Vulcanized Natural Rubber** ***Shoei Okamoto*** Kyoto Institute of Technology, Japan
S1T6-P-03	**Strain-Induced Crystallization of Carbon Black-Reinforced Vulcanized Natural Rubber by Biaxial Elongation** ***Hiroto Okumura*** Kyoto Institute of Technology, Japan
S1T6-P-04	**Study on Melting Behavior of Crystallites in Carbon Black-Filled Vulcanized Natural Rubber Upon High-Speed Shrinkage from Its Highly Elongated State** ***Maho Nakada*** Kyoto Institute of Technology, Japan
S1T6-P-05	**Natural-Rubber-Based Adhesives for Housefly (Musca domestica) Control** ***Kannika Hatthapanit*** National Metal and Materials Technology Center, Thailand
S1T6-P-06	**In Situ Silica Reinforced Natural Rubber: A Novel Approach for Enhanced Performance and Application** ***Suriyakamon Montha*** MTEC, National Science and Technology Development Agency, Thailand
S1T6-P-07	**Application of Ozone Treatment to Reduce Foul Odor in Cup Lump Rubber Production** ***Chaveewan Kongkaew*** National Metal and Materials Technology Center, Thailand
S1T6-P-08	**Changes in Nanostructural Changes During Tearing of Elastomeric Poly(butylene succinate)/poly(butylene succinate adipate) Blend Films** ***Kazuki Imai*** Kyoto Institute of Technology, Japan
S1T6-P-09	**Effect of Chitosan Bio-Based Filler on the Mechanical Reinforcement of ENR Composites** ***Ploypailin Juntosree*** Kasetsart University, Thailand
S1T6-P-10	**Identification and Reduction of Residual Allergenic Rubber Proteins in Natural Rubber Latex Gloves via Alkaline and Surfactant Treatments** ***Pimnaraporn Porncharukit*** Mahidol University, Thailand

S1T6-P-11	**Influence of Bio-Based Epoxidized Natural Rubber as a Compatibilizer on Thermoplastic Polyurethane/Natural Rubber Blends for 3D Printing Applications** ***Torfan Srisuwanno*** King Mongkut's University of Technology Thonburi, Thailand
S1T6-P-12	**Development of Natural Rubber Insulating Gloves: Influence of Latex Centrifugation and Leaching on Mechanical and Electrical Properties** ***Promsak Sa-nguanthammarong*** National Metal and Materials Technology Center (MTEC), Thailand
S1T6-P-13	**Evaluation of a Non-Traditional Preservative System for Enhancing Natural Rubber Latex Stability** ***Maneephan Sukkho*** Mahidol University, Thailand
S1T6-P-14	**Study on the Impact of Purified Natural Rubber Latex and Accelerators on Rubber Allergens in Natural Rubber Gloves** ***Pitchaya Theedee*** Mahidol University, Thailand
S1T6-P-15	**Optimized UVA-Irradiation Silane-Grafting onto Saponified Skim Rubber for Enhanced Silica-Natural Rubber Compatibility** ***Areeya Anuwatprakit*** Mahidol University, Thailand
S1T6-P-16	**Strain-Induced Crystallization Behaviors of Natural Rubber with Additional Lipids** ***Tomoaki Nakatsuka*** Kyoto University, Japan
S1T6-P-17	**Light-driven latex engineering: Scalable photopolymerization for semicrystalline polythioether nanoparticles** ***Cuong-Minh-Quoc Le*** Université de Haute-Alsace, France

Session III: Advanced Rubber Materials and Novel Applications

S3T3-P-01	**Preparation and Properties of In-situ Hydrogenated Nitrile Butadiene Rubber Latex** ***Zhiwei Yang*** Beijing University of Chemical Technology, China
S3T3-P-02	**Surface modification of UHMWPE fibers to enhance their interfacial adhesion with rubber** ***Wencai Wang*** Beijing University of Chemical Technology, China
S3T3-P-03	**Controllable Modification of Rubber Achieved Through Bio-based Inverse Vulcanized Compounds** ***Long Li*** Shenyang university, China

S3T3-P-04	**UiO-66-NH_2 for the Recovery of Catalyst in Hydrogenation Nitrile Butadiene Rubber and Its Repeated Hydrogenation** ***Hui Jiao*** Beijing University of Chemical Technology, China
S3T3-P-05	**Effects of Carbon Nanotube Size on Properties of Eucommia Ulmoides Gum Composite Materials: a Molecular Dynamics Study** ***Wenchi Han*** Shenyang University of Chemical Technology, China
S3T3-P-06	**Analysis of Internal Damage for CNT-Based Soft Nanocomposites** ***Keni Ma*** Kyoto University, Japan
S3T3-P-07	**Study on the Structural Control of Natural Rubber with Nanomatrix Structure and Its Vulcanization** ***Yuanbing Zhou*** Hainan University, China
S3T3-P-08	**Enhancing the Mechanical Properties of Uncrosslinked Epoxidized Natural Rubber through Non-Covalent Interactions** ***Muthita Phetpradab*** Kasetsart University, Thailand
S3T3-P-09	**A Mechanical Property and Thermal Stability of Natural Rubber Composite Reinforced with Multi-Walled Carbon Nanotubes/Carbon Black or Biochar** ***Punyarat Jantachum*** Udon Thani Rajabhat University, Thailand
S3T3-P-10	**Optimizing NR/EPDM/EVA Rubber Foam Formulations for Sustainable Ceiling Board Application** ***Natyada Jantawong*** Chulalongkorn University, Thailand
S3T3-P-11	**A Novel Approach to Using Waste Rubber as a Subsoil Amendment for Improving Soil Quality and Mitigating Hardpan Formation** ***Sirichai Pattanawanidchai*** National Metal and Materials Technology Center, Thailand
S3T3-P-12	**Development of Natural Rubber and Polycaprolactone Blends as Access Hole-Filling Materials for Dental Implant Applications** ***Panjaporn Wongwitthayakool*** Thammasat University, Thailand
S3T3-P-13	**Development of FIR-emitting Knee Supporter from Macca–Natural Rubber Composite for Osteoarthritis Relief** ***Varatnane Yaoprukse*** Mahidol University, Thailand

S3T5-P-01	**Manipulating the Properties of Polymer Vitrimer Nanocomposites by Designing Dual Dynamic Covalent Bonds** ***Zhenyuan Li*** Beijing University of Chemical Technology, China
S3T5-P-02	**Accelerated Prediction of Glass Transition Temperature in SSBR via Integrated Molecular Dynamics Simulation and Machine Learning Framework** ***Siqi Zhan*** Beijing University of Chemical Technology, China
S3T5-P-03	**Preparation of DES-containing Polyurethane Elastomer and Its Moisture-dependent Electrical Conductivity** ***Shogo Taketa*** Nagasaki University, Japan
S3T5-P-04	**A Facile Method in Fabricating Flexible Composite Elastomer with Large-Size Segregated Structures for Electromagnetic Interference Shielding** ***Liang He*** Beijing University of Chemical Technology, China
S3T5-P-05	**Highly Conductive Ag/pCF/MVQ Composite Rubber for Efficient Electromagnetic Interference Shielding** ***Yang Chen*** Beijing University of Chemical Technology, China
S3T5-P-06	**Texture Evolution and Mechanical Response of Cholesteric Liquid Crystal Elastomers with a Lying Helix Structure** ***Koudai Tanino*** Kyoto University, Japan
S3T5-P-07	**Simulation of Rubber Acoustic Coatings under Deep-Sea Pressure Based on Strain-Dependent Viscoelastic Properties** ***Liu Yue*** Beijing University of Chemical Technology, China
S3T5-P-08	**Influence of Vacancy Defect on Stretching Behavior of Liquid Crystal Elastomer Membrane** ***Takumi Kato*** Kyoto University, Japan
S3T5-P-09	**Bio-Based Polyurethane/Tannic Acid Composites with Adjustable Damping Property Enabled by Constructing Multiple Sacrificial Networks** ***Dexian Yin*** Beijing University of Chemical Technology, China
S3T5-P-10	**Changes in Nano Structure upon Uniaxial Stretching of Polyurethane Liquid-Crystalline Elastomers as Analyzed by Small-Angle X-ray Scattering** ***Yume Sugino*** Kyoto Institute of Technology, Japan

S3T5-P-11	**A Novel Properties of Rubber Formulated with 1,2-Polybutadiene Derivatives** ***Hokuto Ohura*** NIPPON SODA CO., LTD., Japan
S3T5-P-12	**Mechanically Robust and Moisture-Resistant Poly(thioether-thiourea) Elastomers with Glassy-State Self-Healing Capability** ***Haitao Wu*** Sichuan University, China
S3T5-P-13	**Self-Healing and Impact-Resistant Elastomer Based on a Novel Tetraoxadiborolane Dynamic Bonds** ***Shiyu Gu*** Sichuan University, China
S3T5-P-14	**UV-A Functionalization of Low Molecular-Weight Natural Rubber Latex Using TiO_2-Coated Hollow-Glass Beads as Photocatalyst** ***Kanokporn Wongnukoon*** Mahidol University, Thailand
S3T5-P-15	**Preparation and Characterization of Hydroxylated Natural Rubber via Epoxidation and Alkaline Ring-Opening** ***Thanita Suakamram*** Mahidol University, Thailand

December 2nd, 2025 (16:35 - 17:30)

Poster Session II

Session II: Advancements in Sustainable Rubber Technology

S2T1-P-01	**Preparation of High Performance Rubber Nanocomposites by Complex Coupling Agent System** ***Dengfeng Shi*** Beijing University of Chemical Technology, China
S2T1-P-02	**A Synergistic Enhancement of Bio-Based Eucommia Ulmoides Gum Nanocomposites through Epoxidized Natural Rubber and Silane Coupling Agent Integration: Advancements in High-Performance Engineering Tires** ***Zhi Chen*** Beijing University of Chemical Technology, China
S2T1-P-03	**Synthesis and Application of Novel Green Coupling Agents in Silica/Natural Rubber Composites** ***Shuaiqi Li*** Beijing University of Chemical Technology, China
S2T1-P-04	**Eco-Tread: The Compounds from Rice Husk Silica and Deproteinized Natural Rubber** ***Tran Dai Luat*** Hanoi University of Science and Technology, Viet Nam

S2T1-P-05	**Role of Lipase Enzyme in Controlling Storage Hardening and Mechanical Properties of Natural Rubber** ***Kattareen Boonchuay*** Mahidol University, Thailand
S2T1-P-06	**Sustainable Vulcanization of Natural Rubber Latex Using Electron Beam** ***Suthathip Sichumphuang*** National Metal and Materials Technology Center, Thailand
S2T1-P-07	**Comparative Evaluation of Natural Rubber Composites Reinforced with Macadamia Carbon and Carbon Black** ***Patcharapron Pimput*** Mahidol University, Thailand
S2T1-P-08	**Sustainable Rubber Compounding: Application of Silane-Grafted Palm Oil in Silica-Filled SBR/BR Blends** ***Chesidi Hayichelaeh*** Chulalongkorn University, Thailand
S2T1-P-09	**Cure Characteristics of NR Compounds with Sulfur Sludge from Biogas -Wastewater Treatment in Palm Oil Industry** ***Prachid Saramolee*** Walailak University, Thailand
S2T1-P-10	**Feasibility Study of Tamarind Shell Powder as a Bio-Based Secondary Accelerator for Rubber Flooring** ***Weenusarin Intiya*** National Science and Technology Development Agency (NSTDA), Thailand
S2T1-P-11	**Rubber Composites Reinforced with Carbon Black and Calcium Lignosulfonate** ***Ivan Hudec*** Slovak University of Technology in Bratislava, Slovakia
S2T1-P-12	**Rubber Composites Based on Devulcanized Tire Crumb and Lignin as A Stabilizer** **Ján Kruželák** Slovak University of Technology in Bratislava, Slovakia
S2T2-P-01	**Mediating Carbon Black-Natural Rubber Interface by Thioamide-Functionalized Polysulfide for Energy-Saving Composites** ***Ruoyan Huang*** South China University of Technology, China
S2T2-P-02	**Characterization of Polyisoprene Blended with Urethane Compounds** ***Takashi Kakubo*** The Yokohama Rubber Co., Ltd., Japan
S2T2-P-03	**Facile and Efficient Preparation of Functionalized Diene-Elastomers via Dynamic Covalent Polymerization** ***Xinglong An*** South China University of Technology, China

S2T2-P-04	**Development of Phosphorylated Cellulose Nanofibers/Natural Rubber Composites** ***Ryotaro Takayama*** Oji Holdings Corporation, Japan
S2T2-P-05	**Study on the Effect of Compatibilizer Content on the Mechanical Properties of NR/BR/NBR Blends** ***Kanokporn Sarikanon*** Kasetsart University, Thailand
S2T2-P-06	**Influence of Balanced Ratios between Mica and Carbon Black on Rheological and Mechanical Behaviors of Elastomeric Materials** ***Keon-Soo Jang*** University of Suwon, South Korea
S2T2-P-07	**Fatigue Properties of Rubber Composites with Different Glass Transition Temperatures** ***Jiaye Li*** Beijing University of Chemical Technology, China
S2T2-P-08	**Development of Tire Tread Formulations for Military Light-Truck Tires** ***Pairote Jittham*** National Metal and Materials Technology Center, Thailand
S2T2-P-09	**Enhancing Mechanical and Antibacterial Properties of Natural Rubber/Tire Waste Blends through Dual-Phase Processing Techniques** ***Napasorn Kingkohyao*** King Mongkut's University of Technology Thonburi, Thailand
S2T2-P-10	**Durazone D37 as a Potential Alternative to 6PPD: Balancing Ozone Resistance and Dynamic Performance** ***Chutima Saeheng*** National Metal and Materials Technology Center (MTEC), NSTDA, Thailand
S2T2-P-11	**Effect of Carbon Black and Barium Titanate Hybrid Filler on the Change of Electrical Signal in Epoxidized Natural Rubber Composites** ***Lyhav Boeurn*** King Mongkut's University of Technology Thonburi, Thailand
S2T2-P-12	**Predicting the Glass Transition Temperature of Polymer Based on Generative Adversarial Networks and Automated Machine Learning** ***Zhanjie Liu*** Beijing University of Chemical Technology, China
S2T4-P-01	**Deproteinization Process of Natural Rubber Latex by Membrane Filtration** ***Yoko Aoyama*** KOSEN-King Mongkut's Institute of Technology Ladkrabang, Thailand
S2T8-P-01	**Short-term Surface Nanostructure Change of Biodegradable Polyester Thin Films by Seawater Immersion Treatments** ***Nana Tsuji*** Kyoto Institute of Technology, Japan

S2T8-P-02	**Effect of Seawater Pressure on the Nanostructure Changes in Poly(l-lactic acid) Homopolymer and Poly(d, l-lactic acid) Blend Thin Films** ***Khanh-Van Thi Khuat*** Kyoto Institute of Technology, Japan
S2T8-P-03	**Effects of Proteins and Purification in Peroxide-Prevulcanized Natural Rubber Latex for Medical Devices** ***Thitipan Watcharakan*** Mahidol University, Thailand
S2T9-P-01	**A Sustainable Approach to Viscosity Control and Recycling of Over-matured Prevulcanized Latex in the Elastic Thread Industry** ***Nuorn Choothong*** Rajamangala University of Technology Rattanakosin, Thailand
S2T9-P-02	**Effective Degradation of Waste Tyre Rubber Using a Specific Treatment Process: A Chemi-Biological Method** ***Pritish Raj Shukla*** Birla Institute of Technology and Science- Pilani, K.K. Birla Goa Campus, India
S2T9-P-03	**Flame-Retardant Performance of Epichlorohydrin-Modified Reclaimed Tire Rubber** ***Selly Mitra Mailanda*** Chulalongkorn University, Thailand

Session IV: Progress in Rubber Characterisation

S4T7-P-01	**Development of an Integrated Design, Analysis and Evaluation System for Rubber Components** ***Changsu Woo*** Korea Institute of Machinery & Materials, Republic of Korea
S4T7-P-02	**Spatiotemporal Internal-Damage Distribution During Nonuniform Deformations in Filled Elastomers** ***Yuki Tokudome*** Kyoto University, Japan
S4T7-P-03	**AFM Nanomechanics of Vulcanized Rubber Containing Silica and Petroleum Resin** ***Makiko Ito*** Institute of Science Tokyo, Japan
S4T7-P-04	**Mixed-Mode Crack Propagation Criterion in Elastomers** ***Tomoki Mishima*** Kyoto University, Japan
S4T7-P-05	**Thermal Analysis of the Mullins Effect in Filler Reinforced Elastomers** ***Koshi Shimazaki*** Kyoto University, Japan

S4T7-P-06	**A Melt Crystallization and Dewetting Kinetics of Marine-Degradable Polyesters in Thin Films** ***Ryu Miyajima*** Kyoto Institute of Technology, Japan
S4T7-P-07	**A Resazurin Reduction Test for Rapid Evaluation of Natural Rubber Latex Putrefaction** ***Preeyawis Na Ubol*** The National Science and Technology Development Agency (NSTDA), Thailand
S4T7-P-08	**Establishment of a Library Database of Some Compounding Ingredients Using a Py-GC/MS Technique** ***Prin Tumwised*** Mahidol University, Thailand

Content

Plenary lecture

PL-01	Circular Economy - Limits and Chances in Rubber Recycling *Ulrich Giese and Jannik Laages*	1
PL-02	Crack Resistance and Beyond: Fracture Mechanics in Strain Crystallizing and Liquid Crystal Elastomers *Kenji Urayama*	3
PL-03	AI-driven Research and Multi-scale Simulation of Elastomer Materials *Liqun Zhang*	5
PL-04	Sustainable Materials for Tyre Engineering *Sabu Thomas and Milanta TOM*	7
PL-05	Increasing the Circularity of Sulphur Crosslinked Natural Rubber *James Busfield, Thomas Griggs, Anureet Kaur, Keizo Akutagawa and Biqiong Chen*	10
PL-06	Sustainable Mobility 2030 and Beyond – Role of Tyre and Rubber Industry *R. Mukhopadhyay*	13

Keynote Speaker

KN-01	Development of Fast Rubber Sheet-Forming Method for Natural Rubber and Its Application *Seiichi Kawahara and Yoshimasa Yamamoto*	14
KN-02	New Insights into Vulcanization Reactions for Green Rubber Technology *Yuko Ikeda and Hisayoshi Kobayashi*	16
KN-03	Recent Trends in Adopting Sustainable Solution for Rubber Additives: How Chemistry Plays Significant Role? *Kinsuk Naskar*	18
KN-04	Thermal History Effects on The Viscoelastic Response of Gum Natural Rubber: Temperature-Induced Camel Structure and Influence on Extensional Rheology *Christopher G. Robertson, Minglong Yao, Zhepeng Wang, Zhengying Li, Jiashun Yang, Chen Cheng and Xiaorong Wang*	19
KN-05	The Crosslinking Dilemma in ENR: Evaluating Sulphur and Di-acid Networks for Future-Ready Rubber Products *Amit Das*	20
KN-06	Engineering Allergy-Free Natural Rubber: Sustainable Deproteinization for Enhanced Industrial and Medical Performance *Jitladda Sakdapipanich*	21

KN-07	On the path to make a black magic green – how to minimize the CO_2 footprint of rubber products *Andreas Limper*	22
KN-08	Optimized Synthesis of Liquid Fluorosilicone Rubber with Improved Cold Resistance for Semiconductor Application *Sang Eun Shim, Jae Il So and Jin Sung Seo*	23
KN-09	Some Considerable Factors in Laboratory Frictional Testing Rubbers *C. Nah, G.-B. Lee, D. Abdulraman, P. Sunintaboon, P. Junkong, T. Amornsakchai and P. Phinyocheep*	25
KN-10	Bio-based Approach to Dispersion of Silica in NR *Dariusz M. Bielinski, Miroslawa Prochon, Agnieszka Kolodziejczak-Radzimska, Jakub Wreczycki, Mateusz Imiela and Teofil Jesionowski*	27
KN-11	Elucidating the Role of Nanoscale Interfaces and 3D Dispersion in Elastomer Nanocomposites: Connecting Microstructure to Viscoelastic Behavior *Ming Tian, Nanying Ning and Liqun Zhang*	29
KN-12	Wide-Angle X-Ray Diffraction Studies on Strain-Induced Crystallization of Vulcanized Natural Rubber by Two-Step Biaxial Stretching *Shinichi Sakurai, Yuki Jotatsu, Hiroto Okumura, Hiroyasu Masunaga, Yuji Kitamura, Katsuhiko Tsunoda and Kenji Urayama*	31
KN-13	AFM Nanomechanics Connecting Macro- and Nanoscopic World *Ken Nakajima*	33
KN-14	Enhancing Coagulation Efficiency and Overcoming Uncoagulation Issues in Skim Latex Using Synthetic and Natural Creaming Agents *Charoen Nakason, Sunida Kaewchuen and Azizon Kaesaman*	35
KN-15	Driving Sustainability in Community-Based Rubber Production: A Case of Energy and Waste Valorization in Thailand *Sumate Chaiprapat, Charongpun Musikavong, Juthamas Jaichuedee and Sayan Sdoodee*	37
KN-16	Revisiting the Properties of Natural Rubber in Tire Industry and Development of NR-based Sidewall Compounds for EV Passenger Cars *Kannika Sahakaro, Maimoon Himmawong, Warakorn Noisang and Pisit Pimrat*	39
KN-17	Recent Advances in Reducing Hysteresis of Rubber Composites *Baochun Guo, Dong Wang, Zhenghai Tang and Liqun Zhang*	41
KN-18	Resolving the Microstructure of Natural Rubber and Its Influence on the Mechanical Properties *Jinrong Wu, Junqi Zhang, Lingming Kong and Zhengtian Xie*	42
KN-19	Waste Tire Recycling: The Next Frontier beyond Devulcanization for Low Carbon Living *Rathanawan Magaraphan*	44

Invited Speaker

IV-01	Cellulose Nanocrystal: Scalable Production and Innovation Application *Jianming Zhang, Hongze Xu, Yunxiao Liu and Lu Zong*	45
IV-02	Self-Healing Rubber: An Advancing Technology for Smart Gloves *Siah Ying Tang, Darren Yi Sern Low and Janarthanan Supramaniam*	47
IV-03	Effect of Molecular Architecture on The Thermal Stability of Poly(Epichlorohydrin-Co-Ethylene Oxide-Co-Allyl Glycidyl Ether) (GECO) Based *Murat Şen, Anıl Tatlidilli and Davut Aksüt*	49
IV-04	Delayed Crystallization Response-Inspired Waterborne Polyurethane with High Performance *Fei Chen, Chenxi Huyan and Liqun Zhang*	51
IV-05	Development of Helically-Wound Pineapple Leaf Fiber/NR Foam Composite for Near Zero-Volume Safety Devices *Taweechai Amornsakchai, Wongsathorn Saitrong and Sorn Duangsuwan*	53
IV-06	Natural Rubber Foam Containing Gamma-Synthesized Chitosan for The Utilization as Enhanced Heavy-Metal Sorbents *Kiadtisak Saenboonruang, Thitiwan Intha, Ekachai Wimolmala and Pattra Lertsarawut*	55
IV-07	Synthesis of Polyester-based Multiblock Copolymer Elastomers via A Cascade Polymerization Method *Yingfeng Tu, Xueting Wan and Mujia Yang*	57
IV-08	Greener Tire Tread Compounds by Reducing the Amount of Ingredients *Anke Blume, Frances van Elburg, Fabian Grunert and Auke Talma*	59
IV-09	Introduction of Reversible Bonds into Rubber Networks *Toshio Tada*	60
IV-10	A Novel Value Approach of Natural Rubber for Emerging and Unexplored Applications *Ekwipoo Kalkornsurapranee*	62
IV-11	Greening the Elastomer Technology: Bio-Based Solid/Liquid Rubbers, Polyurethanes, and TPVs *Jeong Seok Oh*	65
IV-12	Colour-Changing Smart Materials Inspired by Nature: Chameleon Effect *Karine Mougin and Arnaud Spangenberg*	67
IV-13	Renewable Elastomeric Networks of Functionalized Ethylene-Propylene Copolymers *Y. X. Wu, Y. C. Wang, P. Y. Cheng, Z. Q. Zhang and S. Zhang*	68
IV-14	Facile Recycling Strategy for End-Of-Life Rubbers by Selective Cleavage of Cross Linking Bonds *Ganggang Zhang, Baochun Guo and Liqun Zhang*	70

IV-15	Factors Affecting Biodegradability of Natural Rubber and Natural Rubber Products *Chomnutcha Boonmee, Peeraphong Pokphat, Thanawadee Leejarkpai, Pongdhorn Saeoui, Surapich Loykulnant, Piyada Bussadee and Pattanop Kanokratana*	72
IV-16	Biocomposite Starch/NR-Grafted Hydrogels as Sustainable Coating Membranes for Slow-Release Fertilizers *Sayant Saengsuwan, Wilawan Lekkla, Pranee Nuinu, Siriwat Radabutra and Pitchayaporn Suwanakood*	74
IV-17	Dual-Functional Natural Rubber Composites with Piezoresistive and Antibacterial Properties for Wearable Motion Detection *Y. Nakaramontri, B. Sripornsawat and F. Clemen*	75
IV-18	Functionalized Polymer Surfaces Studied by Vibrational Spectroscopy and Applications *Philippe Daniel*	77
IV-19	Optimizing Silica and Carbon Black Ratios for Enhanced Mechanical Performance of NR/BR/SSBR blends *N. R. Mohamed and N. Othman*	78
IV-20	Advancing Sustainable Rubber Recycling: Transforming NR and NBR Waste into Conductive Elastomers *S. Saiwari, S. Salaeh, A. Thitithammawong and N. Hayeemasae*	80
IV-21	Multifunctional Applications of Epoxidized Natural Rubber: From Gas Separation Membranes to Self-Healing and Adhesion Technologies *Bagdagul Karaagac*	81

Oral Presentations

Session I: Natural Rubber, Bio-Based Rubbers and Rubber Chemicals

S1T6-O-01	N-Vinylamides: Structural Isomers of Amino Acids Grafted onto Deproteinized Natural Rubber *Hiroharu Ajiro, Sakiko Yashiro, Tran Thi Thuy, Nguyen Thu Ha, Nguyen Ngoc Mai, Seiichi Kawahara, Ryohei Ikura and Hiroaki Yoshida*	83
S1T6-O-02	Effects of Epoxidation Degree on Strain-Induced Crystallization and Mechanical Properties of Epoxidized Natural Rubber *Xiaohui Wu, Zixuan Wang, Han Song, Weixiao Song, Guo-Hua Hu and Liqun Zhang*	85
S1T6-O-03	Chitosan-Reinforced Epoxidized Natural Rubber: Possible Design of Energy-Efficient Tire Tread Compounds *Nantinee Choosang, Ploypailin Juntosree, Saree Phongphanphanee, Supitta Suethao and Wirasak Smitthipong*	87
S1T6-O-04	Enhancing Ozone Resistance of Tyre Sidewall by Sustainable Replacement of Petroleum Wax with Bio-based Additive *B. Tirthankar, C. Ajay, D. Sudeep, D. Saikat, C. Dipankar, D. Mahuya and M. Rabindra*	89
S1T6-O-05	Investigation of The Effect of The Amount of Zinc Borate on Cure Kinetics, Reversion, And Mechanical Properties of Natural Rubber In A Semi-Efficient Curing System *Davut Aksüt*	91
S1T6-O-06	Eco-Efficient Vulcanization: Analysis of a Sustainable Rubber Curing Package *F. Van Elburg, F. Grunert, M. Di Consiglio, A. Zych, Y. Shoda, A. Talma and A. Blume*	93
S1T6-O-07	Overview of SRI's Research Initiatives for Enhancing the Well-Being of Natural Rubber Stakeholders in Thailand *L Tarachiwin, K Kanyawararak, H Kum-ourm, K Charungchitaree, N Onozuka, A Matsuura, A Uesugii, Y Kitaura-Sakaguchi and T Tada*	95
S1T6-O-08	Research Progress on Modification and Functionalization of Natural Eucommia Ulmoides Gum *Hailan Kang, Feng Yang and Qinghogn Fang*	97
S1T6-O-09	Critical Concentration of Primary Amines for Preparation of Vulcanized Deproteinized Natural Rubber with Outstanding Mechanical Properties *Lam Ba Nguyen and Seiichi Kawahara*	99
S1T6-O-10	Removal of Proteins from Natural Rubber by Creaming Method *Viet Anh Ta, Seiichi Kawahara, Yoshimasa Yamamoto, Thuong Thi Nghiem and Nghia Trung Phan*	101
S1T6-O-11	Synthetic Strategies and Mechanistic Studies of Liquid Rubber *Jian Tang, Jinhui Liu, Yudong Liu, Kai Liu and Jing Hua*	103
S1T6-O-12	Understanding and Controlling Storage Hardening in Natural Rubber via Phospholipid Network Disruption *Kittipong Insom and Jitladda Sakdapipanich*	106

S1T6-O-13	New Non-Isocyanate Polyurethane Films Based on Natural Rubber *Tharin Sensan, Anuwat Saetung and Nitinart Saetung*	108
S1T6-O-14	Latex Serum Boosts Natural Rubber Strength *Katsuhiko Tsunoda, Yasuhiro Shoda, Yuji Kitamura and Kenji Urayama*	110
S1T6-O-15	Green Synthesis of Zinc Oxide from Skim Latex Serum for Application in Rubber Vulcanization *Preeyanuch Junkong and Sopinya Nithakor*	112
S1T6-O-16	A New Antibacterial Hybrid Waterborne Polyurethane/Silica Coating Film Based on Natural Rubber *Nitinart Saetung, Anutida Suwan, Nathapong Sukhawipat, Pamela Pasetto and Anuwat Saetung*	114
S1T6-O-17	Degradation Trends in Plasticity and Viscosity of Selected Standard Philippine Rubber Under Prolonged Storage *S. Suganob, R. Lim and R. Salazar*	116
S1T6-O-18	Sustainable Yield Improvement and Quality Assessment of TSR10 Rubber from Two Hevea brasiliensis Genotypes: Impact of Reduced Tapping Frequency Associated with Ethephon Stimulation *H. Kum-ourm, N. Onozuka, L. Tarachiwin, A. Matsuura, Y. Kitaura-Sakaguchi, L. Vaysse, R. Lacote, F. Gay, V. Ferrer, C. Bottier, S. Jantarasunthorn, J. Chaiyut, T. Lerksamran and S. Liengprayoon*	118
S1T6-O-19	Sustainable Nzerosiltm Silicas from Renewable Rice Husk *Danniel C. Liao, Tim Yu-Ting Lin, Spencer Lee, Chris Wu, Anthony Lin and W. Waddell*	120
S1T6-O-20	Mechanical Tailoring of Waterborne Epoxy Coating on Metal Substrate Using Functionalized Natural Rubber Latex *Wasan Tessanan, Sombat Thanawan, Taweechai Amornsakchai and Pranee Phinyocheep*	122
S1T6-O-21	Rubbery Soft Polymer Electrolyte Membrane with Nanomatrix Channel Prepared from Natural Rubber *Yoshimasa Yamamoto and Seiichi Kawahara*	124
S1T6-O-22	the Development of Bio-Inspired Composites from Epoxidized Natural Rubber Using Π–Π Stacking and Cation–Π Interactions *Kwanchai Buaksuntear, Phillip Kohl, Youli Li and Wirasak Smitthipong*	126
S1T6-O-23	Effect of Crystal Orientation on Mechanical Strength of Poly-Isoprene Rubber Under Bi-Axial Deformation *Airi Sato, Katsuhiko Tsunoda and Yuji Kitamura*	128

Session II: Advancements in Sustainable Rubber Technology

S2T1-O-01	Application of Stearic Acid-Modified Silica in PCR Tread Compound *Farshid Zolala*	130
S2T1-O-02	Bio-Based Multifunctional Additive from Modified Illipe Butter for Silica-Filled Tire Tread Compounds *M.I. Fathurrohman, S. Puspitasari, N.A. Kinasih and D.K. Arti*	133
S2T1-O-03	The Utilization of Fly Ash from Different Resources as a Filler on the Properties of NR Compounds *Karnda Sengloyluan, Apissara Komkay and Nattapon Uthaipan*	135
S2T1-O-04	Efficient and Gentle Processing of Rubber Compounds – How Continuous Milling Transforms Rubber Processing *Julia Uth, Annemarie Hillebrecht and Manuel Bessler*	137
S2T1-O-05	Green Preparation and Performance Study of NRL/Biomass Composites via Non-Rubber Component Mediation and Spatial Confinement *Zhengtian Xie, Shaoqi Huang, Junqi Zhang and Jinrong Wu*	139
S2T1-O-06	Properties of Films from Deproteinized Natural Rubber Latex Produced Via Membrane Separation Technology *Mohamad Akmal Abdul Rahim, Dazylah Darji and Nurul Hayati Yusof*	141
S2T1-O-07	Extrudable Vitrimeric Rubbers Enabled via Heterogeneous Crosslinking *Shuangjian Yu, Jialiang Chen, Baochun Guo, Siwu Wu and Liqun Zhang*	142
S2T1-O-08	Lignin/Carboxylated Nitrile Rubber Composites: the Influence of Carboxyl Content on the Mechanical Properties of the Material *Hongbing Zheng and Dongmei Yue*	144
S2T2-O-01	Study on the Performance of Natural Rubber - Copper Coated Steel Wire with BCDB and BCoPD *Jin Yuan, Yao Zhimin and Chen Zhaohui*	146
S2T2-O-02	Carbon Black Coupling Agents for Improved Fuel Efficiency of Tyres *M. J. J. Dixey and J. J. C. Busfield*	148
S2T2-O-03	Experimental Analysis of the Mixing Behavior of Ethylene-Propylene-Diene Rubber (EPDM) in a Rubber Pin Extruder under Variation of Process Parameters and Mixing Elements *L. Schmidt, J. Petzke, D. Kleinschmidt and F. Bruening*	150
S2T2-O-04	Molecular Chain Structure Changes and Strain-Induced Crystallization Behaviors During Various Deformation of Segmented Polyurethane Elastomer *Kakeru Obayashi, Ken Kojio and Kenji Urayama*	152
S2T2-O-05	Study of the Mullins Effect in Carbon Black-Filled Rubber by Atomic Force Microscopy *Takahiro Anzai, Yuichi Aoyagi, Xiaobin Liang and Ken Nakajima*	154
S2T2-O-06	Modelling of Elastomers under Dynamic Mechanical Loads *Michael Johlitz and Alexander Lion*	156

S2T2-O-07	New Insights into Resins Behavior: Influence of Resin Softening Point on the in Rubber Properties of Carbon Black-Filled SBR Compounds *Javier Araujo-Morera, Pilar Bernal-Ortega, Frances van Elburg, Elif Uzun, Hubert Gojzewski and Anke Blume*	157
S2T2-O-08	Influences of Sulfur Vulcanization System and Curative Content on Properties of Tire Tread Compounds Filled with Carbon Black/Silica Hybrid Filler *Puchong Thaptong, Pongdhorn Sae-Oui and Chakrit Sirisinha*	159
S2T2-O-09	Aluminum Soaps: New Prospect for Rubber Application *Xiaorong Wang*	161
S2T2-O-10	Inverse Vulcanization Forged Self-Motivated Polysulfide Silane: An Ultra-Efficient Architect in Engineering Silica-Rubber Interface *Dong Wang, Zhenghai Tang, Baochun Guo and Liqun Zhang*	163
S2T2-O-11	Reverse Molecular Reconstruction for Synthesizing High Performance Fluorinated Polyurea Elastomer *Donghan Li, Wangtong Li and Zhan Lu*	165
S2T2-O-12	Enhanced Gas Barrier Properties of Graphene Oxide/Rubber Elastomer Nanocomposites *Shipeng Wen, Long Zheng, Rui Zhang and Li Liu*	167
S2T2-O-13	Regulating Rubber-Filler Interface Using functionalized polysulfides *Zhenghai Tang, Dong Wang, Ruoyan Huang, Baochun Guo, Liqun Zhang*	169
S2T4-O-01	Optimization of Calcium Nitrate to Compounded Latex Solid Content for Energy Saving in Latex Thin Film Forming *Wirach Taweepreda and Sakorn Kaewthai*	170
S2T4-O-02	Preparation and Characterization of Silica-Filled Modified Natural Rubber: A Comparative Analysis of Pre-Dispersion and Conventional Techniques *D. Abdulraman, P. Sunintaboon, T. Amornsakchai, C. Nah and P. Phinyocheep*	172
S2T8-O-01	Life Cycle Assessment of End-of-Life Tire Management Pathways: A Comparative Study *Yogesh Jadhav and Sampatrao D Manjare*	174
S2T8-O-02	Bridging Hydrophobic Silica Aerogels with Rubber Latexes via Hydrolysis Resistant Slurry Design *Yanchun Han, Fangshuo Li, Feng Wang, Yongxin Duan, Boxiao Li and Jianming Zhang*	176
S2T9-O-01	Development of Carbon-Silica Dual Phase Filler for Application in Tyre Rubber Compounds – A Cost-Effective Material *Sampatrao D Manjare, Chandresh Dwivedi, Yogesh Jadhav, Ramakrishnan S and Tapas Ranjan Mohanty*	178
S2T9-O-02	Regeneration of Surface Sulfur Species on Pyrolysis Carbon Black *Ke Liu, Zejun Zhang, Jianming Zhang and Yongxin Duan*	179
S2T9-O-03	How Microcapsule-Enhanced Rubber Can Help Creating a Circular Economy *K. Filzer, K. Bandzierz, W. K. Dierkes, A. Blume and F. R. Wurm*	181

S2T9-O-04	Chemical Degradation of End-of-Life Tires *Heng Liu, Chunyu Zhang and Xuequan Zhang*	183
S2T9-O-05	Thermo-Chemical Devulcanization of Sulfur-Cured Styrene-Butadiene Rubber (SBR) Using Diphenyldisulfide (DPDS) *J. Petzke, D. Kleinschmidt and F. Bruening*	185
S2T9-O-06	Pyrolysis of Polychloroprene Rubber with Scavenger-Based HCl Neutralization *P. Srithavorn, J.J.C. Busfield and R. Volpe*	187
S2T9-O-07	Upgrading Reclaimed Carbon from Tire Pyrolysis for Tire Rubber Applications *Purwonegoro Muljawan*	189
S2T9-O-08	Implementing Circular Economy Strategies in Power Transmission Belt Manufacturing *T.R. Aswathy and T. Kalaivendhan*	190
S2T9-O-09	The Reality of Sustainable Solutions and the Economics of SME Rubber Industry: A Way Forward *Peram Prasada Rao*	192

Session III: Advanced Rubber Materials and Novel Applications

S3T3-O-01	Innovation Management for Commercial Success in the Rubber Industry Amid Shifting Global Market Forces *Matthew Thornton and Michael Clayton*	193
S3T3-O-02	Toward Sustainable Tire Development: Challenges and Emerging Solutions *Wisut Kaewsakul*	195
S3T3-O-03	Surface-Functionalised Carbon Black as A High-Performance Filler in Elastomeric Compounds: Techniques and Potential *Rattapong Numard, Keizo Akutagawa and James J.C. Busfield*	197
S3T3-O-04	Effect of Chemically Treated Pineapple Leaf and Hemp Fibers on the Interfacial Interaction and Mechanical Properties of Natural Rubber Composites *Siriwan Jansinak, Karine Mougin and Wirasak Smitthipong*	199
S3T3-O-05	Development of Thermoplastic Natural Rubber Composites for Wearable Shielding Materials *Akarapong Tuljittraporn, Nussana Lehman, Supakit Yonphan, Jakrapong Kaewkhao, Suchart Kothan, Siriprapa Kaewjaeng and Ekwipoo Kalkornsurapranee*	201
S3T3-O-06	High-Performance, Recyclable, and Multifunctional Nitrile Butadiene Rubber Based on Hydrogen and Urea Bonds *Dongmei Yue and Lin Wang*	203
S3T3-O-07	Development of Piezoresistive Sensor Prepared from PMMA-Grafted Natural Rubber Latex Filled Conductive Carbon Composites: Comparative of Conductive Carbon Fillers and Hybrid System *Arthittaya Chuaybamrung, Rawiporn Promsung, Ekwipoo Kalkornsurapranee, Yeampon Nakaramontri and Frank Clemans*	205

S3T3-O-08	Development of Hydroxyapatite from Eggshell Waste and Its Application in SBR Composite *Chomsri Siriwong, Jhiratchaya Buranawichit and A. Nintap*	207
S3T3-O-09	Comparison of Growth and Transpiration in Micro-Cuttings and Budded Rubber Trees *Supat Isarangkool Na Ayutthaya, Somyot Meetha, Adisak Khotchomphu, Supalerk Moonrungsee, Kamolchat Charungchitaree, Lucksanaporn Tarachiwin, Noriyuki Onozuka and Akari Uesugi*	209
S3T3-O-10	Effectiveness of Participatory Ergonomic Training on Musculoskeletal Disorders Among Rubber Tappers: A Longitudinal Mixed-Effects Analysis *Warut Chanasit, Apinya Chintrakul, Chutarat Sathirapanya and Chanon Kongkamol*	211
S3T3-O-11	Effects of Enhanced Ergonomic Training on Postural Risk Among Rubber Tappers: A Cluster-Randomized Longitudinal Analysis *Chanon Kongkamol, Apinya Chintrakul, Phachara Suklim and Atichart Kwanyuang*	213
S3T3-O-12	Additive Manufacturing of Natural Rubber Latex for Sustainable Flexible Sensors *Panithi Wiroonpochit, Sasitorn Srisawad, Siwaporn Srimongkol, Sutthinee Keawmaungkom, Ratanon Chotima and Nanthiya Hansupalak*	215
S3T3-O-13	Construction of Recyclable Rubber Composites Based on Dynamic Bonding *Yuzhu Xiong and Lingfeng Cui*	217
S3T3-O-14	Natural Rubber Latex-Based Tissue Engineering: the Pioneering Advances in Material for Sustainability *Masami Okamoto*	219
S3T3-O-15	Multidimensional Rubber Composite Utilizing Lignin as a Bio-Filler *S. Amit, G. Biswanath, C. Jagannath, M. Rabindra and G. Prasenjit*	221
S3T3-O-16	Sustainable Rubber Nanocomposites for Tyre Application by Silica Hairy Nanoparticles Fillers *B. Di Credico, L. Tripaldi, L. Tadiello, L. Conzatti, L. Giannini, M. D'arienzo, A. Causa, S. Mostoni, P. Stagnaro and R. Scotti*	223
S3T3-O-17	A Natural Rubber-Based Stretching Band and Its Machine Learning-Validated Muscle Tension Mitigation *N. Hayeemasae, N. Samerphob and N. Jehsoh*	225
S3T3-O-18	Thermoset–Rubber 2K Composite Systems: Material Combinations and Interfacial Reactions in A One-Step Injection Molding Process *Florian Löhr, Elmar Moritzer, Benjamin Klie and Ulrich Giese*	227
S3T3-O-19	Advancing 3D Printing with Biobased Rubber: Photocurable and Extrudable Platforms for Functional Soft Materials *N. Risangud, Z. A. Laksanaa, M. S. Arkana and S. Thongkham*	229
S3T3-O-20	Potential of Low-Temperature Vulcanized Natural Rubber Latex for Antimicrobial Applications *Rawiporn Promsung, Nussana Lehman, Ladawan Songtipya and Ekwipoo Kalkornsurapranee*	231

S3T3-O-21	Novel Triboelectric Nanogenerators for Self-Powered System by Using Fluorinated Wasted Rubber Powders *Huiqing Fan, Xiaohu Ren, Xiuze Che, Yuanbiao Gong and Weijia Wang*	233
S3T3-O-22	High-performance, Recyclable, and Multifunctional Nitrile Butadiene Rubber Based on Hydrogen and Urea Bonds *Dongmei Yue and Lin Wang*	235
S3T5-O-01	Boron-Containing Elastomer *Qi Wu and Jinrong Wu*	237
S3T5-O-02	Effect of Non-Covalent Interactions on Epoxidized Natural Rubber: Structure-Properties Relationships *Phakamat Limarun, Pairote Jittham and Wirasak Smitthipong*	238
S3T5-O-03	Sustainable Supramolecular Aqueous Adhesive with Moisture Resistance *Liying Zhang, Shuxue Wang and Jianming Zhang*	240
S3T5-O-04	Cellulose Nanocrystal-Based Aqueous Nanogel Photoinitiator for High Performance Photocurable Hydrogel Elastomers *Quan Wang, Yihan Sun, Xiaohui Hao and Jianming Zhang*	242
S3T5-O-05	Impact of Fused Filament Fabrication and Processing Parameters on the Performance of $BaTiO_3$-Piezoelectric Composites for Soft Robots *S, Butenko, F. Mongioi, T. Brugo, A. Ichangi and F. Clemens*	243
S3T5-O-06	Enhancing the Piezoresistive Sensing Properties of TPE/CB Composites via Co Continuous Structure Design through Natural Rubber Blending *Christopher Bascucci, Torfan Srisuwanno, Yeampon Nakaramontri, Josie Hughes and Frank Clemens*	245
S3T5-O-07	α-Diimine Cobalt Complexes Bearing Axial Anagostic Interaction: A System for Accessing Ultra-High Molecular Weight Polybutadiene *Xin Wang, Xuequan Zhang and Heng Liu*	247
S3T5-O-08	Fe-based Catalyst with Exogenous Electron Donor for Stereopolymerization of Butadiene and Isoprene *Shiliang Xu, Chunyu Zhang and Xuequan Zhang*	249
S3T5-O-09	ECIU Rubber Chair - An Inter-University Organisation Focused on Rubber Science and Intersectoral Impact *R. Anyszka*	250
S3T5-O-10	Polyrotaxane-Based Hybrid Crosslinking for Tunable Elastic and Thermal Response in Epoxidized Natural Rubber *A. Thitithammawong, K. Amin, S. Salaeh, S. Saiwari, B. Thongnuanchan and N. Hayeemasae*	252
S3T5-O-11	Actuation Programming of Liquid Crystal Elastomers *Binjie Jin, Baochun Guo and Liqun Zhang*	254
S3T5-O-12	Biomimetic Design and Development of Natural Rubber-Based Soft Robotics *M. Sriring, T. Watcharakan and C. Sirisinha*	256
S3T5-O-13	Epoxidized Natural Rubber and Its Composite-Based Sensors and Energy Harvesters *Titash Mondal*	257

S3T5-O-14	Elastomeric Ionomer Based on Maleated Bromobutyl Rubber *S. Salaeh, B. Marsri, S. Wiessner and A. Das*	259
S3T5-O-15	Properties and Crosslinking Mechanisms of 1,2-Polybutadiene Derivative-Based Rubber Formulations *Hiroki Hashimoto, Hokuto Ohura and Yasuhisa Shibata*	261
S3T5-O-16	Property and Application of Perfluoropolyether-Modified Functional Rubber *Zheming Tong, Yuzhi Feng, Zhiyang Tong, Shuai Xu, Yulin Yi and Guangbi Gong*	263

Session IV: Progress in Rubber Characterization

S4T7-O-01	Formulations of Finite Hyperelasticity and Viscoelasticity Using Invariants of Stretch Tensors *Alexander Lion and Michael Johlitz*	265
S4T7-O-02	Numerical Modeling of the Non-Isothermal Viscoelastic Flow Behavior of Rubber Compounds Based on the PHAN-THİEN-TANNER (PTT) Model *H. Damanik, A. Fatima, S. Turek, J. Petzke, D. Kleinschmidt and F. Bruening*	266
S4T7-O-03	Method for Analyzing Mechanical Property Degradation of Polymer Materials Using Artificial Intelligence *Sangin Park*	269
S4T7-O-04	Microstructural Modelling of Carbon Black Aggregates for Sustainable Next Generation Tyre Design *Sarah Pedroni, Lewis Tunnicliffe, Keizo Akutagawa and James J.C. Busfield*	271
S4T7-O-05	Study on the Dispersion of Silica in SBR Using Time-Resolved Ultra Small Angle X-ray Scattering *Shotaro Nishitsuji, Takayuki Yoshida, Daisuke Iwahara, Naoya Amino, Yuki Watanabe and Mikihito Takenaka*	274
S4T7-O-06	Correlative Analysis of Morphological and Functional Properties in High-Performance Elastomer Blends *Dean Vidakovic, Fatma Saraç, Nina Eggers, Bettina Taschner and Harald Plank*	276
S4T7-O-07	Chemical Fingerprinting for Environmental Detection of Tyre Rubber Emissions *Nick Molden, James Hobday and Ime Usen*	277
S4T7-O-08	Advancing Sustainability in Rubber Industries Involves Optimizing Testing Through the Utilization of Rubber Process Analyzer *Wan Li, Peih-Shyun Wu and Unal C. Yilmazoglu*	279
S4T7-O-09	Rubber Blend Compatibility Analysis Using Large-Amplitude Oscillatory Shear (LAOS) on RPA *Zühra Çinar Esin and Murat Şen*	281

S4T7-O-10	Performance Evaluation of Silicone-Based Isolators Under Varying Temperatures and Excitation Levels Using a Thermal Chamber Shaker *E.R. Senoz and U. Calik*	283
S4T7-O-11	Tribological Behavior of Soft Polymers Against Model Substrates *Sophie Bistac*	285
S4T7-O-12	NR Film Visualization via AFM Imaging *K S Tan, Evelyn Lim H M and Nurul Hayati Yusof*	286
S4T7-O-13	AFM-Based Investigation of Polyisoprene-Inorganic Interface Adhesion at Multiple Scales *Hexuan Mao, Xiaobin Liang and Ken Nakajima*	289
S4T7-O-14	Improving Seal Life Prediction: Faster Crack Growth Testing in HNBR *O. Ramekaj, J. Busfield and K. Akutagawa*	291
S4T7-O-15	Study on the Effect of Silane Coupling Agents on Mechanical Behavior of Silica-Filled Styrene-Butadiene Rubber Under Elongation Using in Situ Nano-Palpation Atomic Force Microscopy *M. Malineerat, M. Ito, X. Liang and K. Nakajima*	293
S4T7-O-16	Friction Behaviour in Relation to Wear Morphology *T.H. Pham, K. Akutagawa and J.J.C. Busfield*	295
S4T7-O-17	In Situ Methods to Characterize Deformation-Induced Mechanisms in NR *Eric Euchler, Lutz Zybell, Sven Wießner and Konrad Schneider*	297
S4T7-O-18	The Role of Deformation Mode on Rubber Hysteresis and Its Denpendency on Viscoelasticity *Shouliang Nie, Wei Huang and Xiaorong Wang*	299
S4T7-O-19	On the Decoupling of Chemical and Mechanical Surface Contributions in Soft Polymer Network Adhesion *M. Brogly*	301
S4T7-O-20	Wear Particle Formation Mechanism Investigated Using LAT100 *Shinya Nakano, Takanobu Kawamura and James J. C. Busfield*	303
S4T7-O-21	Why Lab Studies Matter for Understanding Tyre Wear Emissions *M. Stěnička, R. Stoček, M. Pöschl and S. Datta*	306
S4T7-O-22	Study of Standard Laboratory for Testing Medical Rubber Gloves According to ISO/IEC 17025 *Hassarutai Yangthong, Supitta Suethao and Wirasak Smitthipong*	308
S4T7-O-23	Visualizing Nanoscale Interface in Direct Adhesive Rubbers Containing Reversible Coordination Linkages *Hung K. Nguyen, Kyohei Kotani, Katsuhiko Tsunoda, Ken Nakajima*	310
S4T7-O-24	Study on Delamination Mechanism of Rubber-Adhesive Interface in Sealing Materials *Hiromu Kawasaki, Takahiro Anzai, Yuichi Aoyagi, Xiaobin Liang and Ken Nakajima*	312

S4T7-O-25 Analysis of Allergenic Proteins in Natural Rubber After Radiolysis by Mass Spectrometry Technique 314
A. Nimpaiboon

NR Symposium

NRS-O-01 Sustainability Risks are Business Continuity Risks: A Systemic Response through GPSNR's Assurance and Shared Investment Framework 316
S. SAVI

NRS-O-02 The Role of Thailand Contributing to Sustainability of Natural Rubber Supplies 317
N. Lekawipat

NRS-O-03 Novel Green Technologies for Production of User-friendly and Consistent Properties NR 318
N. Moonprasith, C. Kongkae, P. Suwandittaku, S. Montha, and S. Loykulnant

NRS-O-05 Perspective on Dipped Rubber Product Biodegradability: MRB Research Highlights and Future Pathways 319
Shabinah F. M. S., Aziana A. H. and Norhanifah M. Y

NRS-O-06 Study of Biodegradation Efficiency of Natural Rubber Products by Various Microorganism 320
N. Boonyuen, C. Suriyachadkun, P. Kwantong, S. Nuankaew, P. Kanokratana, C. Chuaseeharonnachai, S. Pattanawanidchai, P. Saeoui, T. Leejarkpai, V. Champreda, C. Boonmee and S. Loykulnant

NRS-O-07 Reducing Extractable Protein in Latex Gloves to Lower Latex Allergy: Evidence from Thailand and International Studies 323
N. Chaiear

NRS-O-08 From Allergen to Assurance: A Comprehensive Review of Natural Rubber Product Safety and MRB's Strategic Role 326
Aziana A. H.1 and Nurulhuda A. A.

NRS-O-09 Pioneering a Sustainable Biorefinery of Natural Rubber Serum for New Bioactives in Cosmetics, Food, Nutraceuticals, and Pharmaceuticals 327
T. Pitakpornpreecha

NRS-O-10 Utilizing Natural Rubber Seeds for Biorefinery 329
K. Kawatani1, J. Phojaroen2authorc

NRS-O-11 Modified Natural Rubber: Current Progress and Challenges in Malaysia 331
K. V. Baratha Nesan, N. H. Yusof and S. Ibrahim

NRS-O-12 Challenges for the Future of Natural Rubber Latex and NRL Products, and Its Oppourtunities 332
Amir Hashim M.Y., Tan C.Y., Nor Akilah Saidin and Felix Darrel

NRS-O-13 Challenges and Opportunities for Future Applications of Natural Rubber 333
B. Junhasavasdikul

Poster Presentations

Session I: Natural Rubber, Bio-Based Rubbers and Rubber Chemicals

S1T6-P-01	Design and Molecular Dynamics Simulation of Biomass Ion-Conductive Elastomer *Jiajun Qu, Liqun Zhang and Jun Liu*	336
S1T6-P-02	Wide-angle X-ray Diffraction Studies on Thermal Melting Behavior of Crystallites Formed by Planar Elongation of Vulcanized Natural Rubber *Shoei Okamoto, Hiroto Okumura, Maho Nakada, Shinichi Yagi, Huaizhong Xu, Hiroyasu Masunaga, Hideaki Takagi, Noriyuki Igarashi, Yuji Kitamura, Katsuhiko Tsunoda, Kenji Urayama and Shinichi Sakurai*	338
S1T6-P-03	Strain-Induced Crystallization of Carbon Black-Reinforced Vulcanized Natural Rubber by Biaxial Elongation *Hiroto Okumura, Shoei Okamoto, Maho Nakada, Yuki Jotatsu, Shinichi Yagi, Huaizhong Xu,Yuji Kitamura, Katsuhiko Tsunoda, Hiroyasu Masunaga, Kenji Urayama and Shinichi Sakurai*	340
S1T6-P-04	Study on Melting Behavior of Crystallites in Carbon Black-Filled Vulcanized Natural Rubber Upon High-Speed Shrinkage from Its Highly Elongated State *Maho Nakada, Shoei Okamoto, Hiroto Okumura, Taichi Uemura, Shinichi Yagi, Huaizhong Xu, Hiroyasu Masunaga, Yuji Kitamura, Katsuhiko Tsunoda, Kenji Urayama and Shinichi Sakurai*	342
S1T6-P-05	Natural-Rubber-Based Adhesives for Housefly (Musca domestica) Control *K. Hatthapanit, P. Wiroonpochit, B. Mulsena, T. Kaewprakob, Y. Chisti and N. Hansupalak*	344
S1T6-P-06	In Situ Silica Reinforced Natural Rubber: A Novel Approach for Enhanced Performance and Application *S. Montha, P. Suwandittakul, W. Intiya and C. Kongkaew*	349
S1T6-P-07	Application of Ozone Treatment to Reduce Foul Odor in Cup Lump Rubber Production *C. Kongkaew, P. Suwandittakul, S. Montha, P. Rakdee, N. Moonprasith and S. Loykulnant*	351
S1T6-P-08	Changes in Nanostructural Changes During Tearing of Elastomeric Poly (Butylene Succinate) / Poly (Butylene Succinate Adipate) Blend Films *Kazuki Imai, Keito Shimakawa, Ryu Miyajima, Nana Tsuji, Khuat Thi Khanh Van, Hiroyasu Masunaga, An Yingjun, Atsushi Takahara and Sono Sasaki*	353
S1T6-P-09	Effect of Chitosan Bio-Based Filler on The Mechanical Reinforcement of ENR Composites *Ploypailin Juntosree, Nantinee Choosang and Wirasak Smitthipong*	355
S1T6-P-10	Identification and Reduction of Residual Allergenic Rubber Proteins in Natural Rubber Latex Gloves via Alkaline and Surfactant Treatments *P. Porncharukit and J. Sakdapipanich*	357

S1T6-P-11	Influence of Bio-Based Epoxidized Natural Rubber as A Compatibilizer on Thermoplastic Polyurethane / Natural Rubber Blends for 3D Printing Applications *T. Srisuwanno, P. Luangchuang, C. Bascucci, F. Clemens and Y. Nakaramontri*	359
S1T6-P-12	Development of Natural Rubber Insulating Gloves: Influence of Latex Centrifugation and Leaching on Mechanical and Electrical Properties *Promsak Sa-nguanthammarong, Chayapha Nimsuwan, Chotiros Dokkhan and Bundit Putasaeng*	361
S1T6-P-13	Evaluation of A Non-Traditional Preservative System for Enhancing Natural Rubber Latex Stability *Maneephan Sukkho and Jitladda Sakdapipanich*	363
S1T6-P-14	Study on the Impact of Purified Natural Rubber Latex and Accelerators on Rubber Allergens in Natural Rubber Gloves *Pitchaya Theedee, Jinjutha Wiriyanantawong and Jitladda Sakdapipanich*	365
S1T6-P-15	Optimized UVA-Irradiation Silane-Grafting onto Saponified Skim Rubber for Enhanced Silica-Natural Rubber Compatibility *Areeya Anuwatprakit, Apisara Sillapasuwan and Jitladda Sakdapipanich*	367
S1T6-P-16	Strain-Induced Crystallization Behaviors of Natural Rubber with Additional Lipids *Tomoaki Nakatsuka, Yui Tsuji, Masunaga Hiroyasu and Keiji Numata*	369
S1T6-P-17	Light-driven latex engineering: Scalable photopolymerization for semicrystalline polythioether nanoparticles *Cuong-Minh-Quoc Le, Arnaud Spangenberg, Karine Mougin and Abraham Chemtob*	371

Session II: Advancements in Sustainable Rubber Technology

S2T1-P-01	Preparation of High Performance Rubber Nanocomposites by Complex Coupling Agent System *Dengfeng Shi, Hong Yao, Xuan Qin and Liqun Zhang*	372
S2T1-P-02	A Synergistic Enhancement of Bio-Based Eucommia Ulmoides Gum Nanocomposites Through Epoxidized Natural Rubber and Silane Coupling Agent Integration: Advancements in High-Performance Engineering Tires *Zhi Chen, Dexian Yin, Jichuan Zhang and Xiuying Zhao*	373
S2T1-P-03	Synthesis and Application of Novel Green Coupling Agents in Silica / Natural Rubber Composites *Shuaiqi Li and Xin Ye*	375
S2T1-P-04	Eco-Tread: The Compounds from Rice Husk Silica and Deproteinized Natural Rubber *Luat Dai Tran, Thang Manh Tran, Hang Thi Le, Hoang Van Nguyen, Thanh Binh Thi Bui, Hong Nhung Thi Le, Seiichi Kawahara and Nghia Trung Phan*	377
S2T1-P-05	Role of Lipase Enzyme in Controlling Storage Hardening and Mechanical Properties of Natural Rubber *K. Boonchuay, C. Sirisinha and A. Nimpaiboon*	379

S2T1-P-06	Sustainable Vulcanization of Natural Rubber Latex Using Electron Beam *S. Sichumphuang, C. Dokkhan, P. Kovitcharoenkul, C. Charaschimpleekul and P. Wiroonpochit*	381
S2T1-P-07	Comparative Evaluation of Natural Rubber Composites Reinforced with Macadamia Carbon and Carbon Black *Patcharapron Pimput and Jitladda Sakdapipanich*	382
S2T1-P-08	Sustainable Rubber Compounding: Application of Silane-Grafted Palm Oil in Silica-Filled SBR/BR Blends *C. Hayichelaeh, A. Mingsamoh and K. Boonkerd*	384
S2T1-P-09	Cure Characteristics of NR Compounds with Sulfur Sludge from Biogas Wastewater Treatment in Palm Oil Industry *P. Saramolee, P. Srithong, K. Sathaporn and K. Seneesrisakul*	386
S2T1-P-10	Feasibility Study of Tamarind Shell Powder as A Bio-Based Secondary Accelerator for Rubber Flooring *W. Intiya, P. Jittham, U. Tepsuwan, and P. Sae-oui*	388
S2T1-P-11	Rubber Composites Reinforced with Carbon Black and Calcium Lignosulfonate *I. Hudec, M. Džuganová, J and Kruželák*	390
S2T1-P-12	Rubber Composites Based on Devulcanized Tire Crumb and Lignin as A Stabilizer *J. Kruželák, M. Džuganová, I. Hudec, J. Hronkovič, J. Preťo*	392
S2T2-P-01	Mediating Carbon Black-Natural Rubber Interface by Thioamide Functionalized Polysulfide for Energy-Saving Composites *Ruoyan Huang, Dong Wang, Zhenghai Tang, Baochun Guo and Liqun Zhang*	394
S2T2-P-02	Characterization of Polyisoprene Blended with Urethane Compounds *Takashi Kakubo , Hirokazu Kageyama , Ryuga Honda, Sakito Sugii, Naoya Amino and Hiromu Saito*	395
S2T2-P-03	Facile and Efficient Preparation of Functionalized Diene-Elastomers via Dynamic Covalent Polymerization *Xinglong An, Siwu Wu, Baochun Guo and Liqun Zhang*	397
S2T2-P-04	Development of Phosphorylated Cellulose Nanofibers / Natural Rubber Composites *Ryotaro Takayama*	399
S2T2-P-05	Study on the Effect of Compatibilizer Content on the Mechanical Properties of NR/BR/NBR Blends *S. Kanokporn, C. Natchawut and K.Wirunya*	401
S2T2-P-06	Influence of Balanced Ratios between Mica and Carbon Black on Rheological and Mechanical Behaviors of Elastomeric Materials *Keon-Soo Jang, Won-young Jung, Seong-woo Cho and Tae-Hee Lee*	403
S2T2-P-07	Fatigue Properties of Rubber Composites with Different Glass Transition Temperatures *Shipeng Wen and Jiaye Li*	405

S2T2-P-08	Development of Tire Tread Formulations for Military Light-Truck Tires *Pairote Jittham, Puchong Thaptong and Pongdhorn Sae-Oui*	407
S2T2-P-09	Enhancing Mechanical and Antibacterial Properties of Natural Rubber/Tire Waste Blends through Dual-Phase Processing Techniques *N. Kingkohyao, T. Boonsiri and Y. Nakaramontri*	409
S2T2-P-10	Durazone D37 as A Potential Alternative to 6PPD: Balancing Ozone Resistance and Dynamic Performance *Chutima Saeheng and Puchong Thaptong*	411
S2T2-P-11	Effect of Carbon Black and Barium Titanate Hybrid Filler on the Change of Electrical Signal in Epoxidized Natural Rubber Composites *L. Boeurn, F. Clemens, Y. Nakaramontri, S. Srisawadi and T. Chanthasopeephan*	413
S2T2-P-12	Predicting the Glass Transition Temperature of Polymer Based on Generative Adversarial Networks and Automated Machine Learning *Zhanjie Liu and Jun Liu*	415
S2T4-P-01	Deproteinization Process of Natural Rubber Latex by Membrane Filtration *Yoko Aoyama, Yuzu Tomeba and Itsuha Kuga*	417
S2T8-P-01	Short-term Surface Nanostructure Change of Biodegradable Polyester Thin Films by Seawater Immersion Treatments *Nana Tsuji, Hiroto Osakaki, Keito Shimakawa, Ryu Miyajima, Kazuki Imai, Khanh-Van Thi Khuat, Hiroyasu, Masunaga, Yingjun An, Atsushi Takahara and Sono Sakaki*	419
S2T8-P-02	Effect of Seawater Pressure on the Nanostructure Changes in Poly(l-lactic cid) Homopolymer and Poly(d, l-lactic acid) Blend Thin Films *Khanh-Van Thi Khuat, Nana Tsuji, Ryu Miyajima, Kazuki Imai, Hiroyasu Masunaga, An Yingjun, Atsushi Takahara and Sono Sasaki*	421
S2T8-P-03	Effects of Proteins and Purification in Peroxide-Prevulcanized Natural Rubber Latex for Medical Devices *T. Watcharakan, M. Sriring, A. Nimpaiboon, P. Havanapan, N. Phungthanom, P. Tumwised, C. Sirisinha and K. Suchiva*	423
S2T9-P-01	A Sustainable Approach to Viscosity Control and Recycling of Over-Matured Prevulcanized Latex in the Elastic Thread Industry *Nuorn Choothong, Bawornkit Nekamanurak, Teerin Kongpun and Seiichi Kawahara*	426
S2T9-P-02	Effective Degradation of Waste Tyre Rubber Using A Specific Treatment Process: Chemi-Biological Method *Pritish R. Shukla, Utpal Roy and Sunil Bhand*	427
S2T9-P-03	Flame-Retardant Performance of Epichlorohydrin-Modified Reclaimed Tire Rubber *Selly M. Mailanda and Rathanawan Magaraphan*	429

Session III: Advanced Rubber Materials and Novel Applications

S3T3-P-01	Preparation and Properties of In-Situ Hydrogenated Nitrile Butadiene Rubber Latex *Yang Zhiwei and Yue Dongmei*	431
S3T3-P-02	Surface Modification of UHMWPE Fibers to Enhance Their Interfacial Adhesion with Rubber *Wencai Wang, Lijie Yin, Yichen Lu, Wei Li, Xiaotong Liu and Yanfeng Niu*	434
S3T3-P-03	Controllable Modification of Rubber Achieved Through Bio-based Inverse Vulcanized Compounds *Long Li, Jiayu Shi, Hailan Kang and Xiaodong Zhang*	435
S3T3-P-04	UiO-66-NH_2 for the Recovery of Catalyst in Hydrogenation Nitrile Butadiene Rubber and Its Repeated Hydrogenation *Hui Jiao and Dongmei Yue*	437
S3T3-P-05	Effects of Carbon Nanotube Size on Properties of Eucommia Ulmoides Gum Composite Materials: A Molecular Dynamics Study *Wenchi Han, Yue Pan and Qinghong Fang*	439
S3T3-P-06	Analysis of Internal Damage for CNT-Based Soft Nanocomposites *Keni Ma, Thanh-Tam Mai and Kenji Urayama*	441
S3T3-P-07	Study on the Structural Control of Natural Rubber with Nanomatrix Structure and Its Vulcanization *Yuanbing Zhou, Sujitra Onutai, Shuangquan Liao and Seiichi Kawahara*	443
S3T3-P-08	Enhancing the Mechanical Properties of Uncrosslinked Epoxidized Natural Rubber Through Non-Covalent Interactions *Muthita Phetpradab, Phakamat Limarun and Wirasak Smitthipong*	445
S3T3-P-09	A Mechanical Property and Thermal Stability of Natural Rubber Composite Filled with Multi-Walled Carbon Nanotubes / Carbon Black or Biochar *P. Jantachum, T. Khochai, A. Anlakhon and B. Khumpaitool*	447
S3T3-P-10	Optimizing NR/EPDM/EVA Rubber Foam Formulations for Sustainable Ceiling Board Application *N. Jantawong, K. Bunsreyneang, K. Boonkerd, K. Hancharoen and S. Poompradub*	449
S3T3-P-11	A Novel Approach to Using Waste Rubber as a Subsoil Amendment for Improving Soil Quality and Mitigating Hardpan Formation *S. Pattanawanidchai, P. Sae-Oui, S. Loykulnant and T. Kuankhamnuan*	451
S3T3-P-12	Development of Natural Rubber and Polycaprolactone Blends as Access Hole-Filling Materials for Dental Implant Applications *P. Wongwitthayakool, K. Hatthapanit, P. Wiroonpochit, C. Pongchumyen, S. Panyakrua and P. Gulgovit*	453
S3T3-P-13	Development of FIR-emitting Knee Supporter from Macca–Natural Rubber Composite for Osteoarthritis Relief *Varatnane Yaoprukse and Jitladda Sakdapipanich*	455

S3T5-P-01	Manipulating the Properties of Polymer Vitrimer Nanocomposites by Designing Dual Dynamic Covalent Bonds *Zhenyuan Li, Hengheng Zhao, Liqun Zhang and Jun Liu*	456
S3T5-P-02	Accelerated Prediction of Glass Transition Temperature in SSBR via Integrated Molecular Dynamics Simulation and Machine Learning Framework *Siqi Zhan, Jun Liu and Liqun Zhang*	458
S3T5-P-03	Preparation of DES-Containing Polyurethane Elastomer and Its Moisture-Dependent Electrical Conductivity *Shogo Taketa, Shintaro Yamaguchi, Hironobu Tahara and Hiroto Murakami*	460
S3T5-P-04	A Facile Method in Fabricating Flexible Composite Elastomers with Large-Size Segregated Structures for Electromagnetic Interference Shielding *Liang He, Yang Chen, Lijie Yin and Wencai Wang*	462
S3T5-P-05	Highly Conductive Ag/pCF/MVQ Composite Rubber for Efficient Electromagnetic Interference Shielding *Yang Chen, Liang He and Wencai Wang*	464
S3T5-P-06	Texture Evolution and Mechanical Response of Cholesteric Liquid Crystal Elastomers with a Lying Helix Structure *Koudai Tanino, Tsutomu Furuya, Tsuyoshi Koga and Kenji Urayama*	467
S3T5-P-07	Simulation of Rubber Acoustic Coatings under Deep-Sea Pressure Based on Strain-Dependent Viscoelastic Properties *Yue Liu and Xiuying Zhao*	468
S3T5-P-08	Influence of Vacancy Defect on Stretching Behavior of Liquid Crystal Elastomer Membrane *T. Kato, Y. Okumura, H. Kikuchi and K. Urayama*	470
S3T5-P-09	Bio-Based Polyurethane/Tannic Acid Composites with Adjustable Damping Property Enabled by Constructing Multiple Sacrificial Networks *Dexian Yin, Zhi Chen, Xin Wang, Xiuying Zhao and Liqun Zhang*	473
S3T5-P-10	Changes in Nano Structure upon Uniaxial Stretching of Polyurethane Liquid Crystalline Elastomers as Analyzed by Small-Angle X-ray Scattering *Yume Sugino, Tomoka Noda, Tatsuya Endo, Hideaki Takagi and Shinichi Sakurai*	474
S3T5-P-11	Novel Properties of Rubber Formulated with 1,2-Polybutadiene Derivatives *H. Ohura, H. Hashimoto and Y. Shibata*	476
S3T5-P-12	Mechanically Robust and Moisture-Resistant Poly(thioether-thiourea) Elastomers with Glassy-State Self-Healing Capability *Haitao Wu, Zhaoyang Yuan, Jing Zheng, Hao Wang, Mengjin Jiang and Jinrong Wu*	478
S3T5-P-13	Self-Healing and Impact-Resistant Elastomer Based on a Novel Tetraoxadiborolane Dynamic Bonds *Shiyu Gu, Nan Li, Qi Wu and Jinrong Wu*	480
S3T5-P-14	UV-A Functionalization of Low Molecular-Weight Natural Rubber Latex Using TiO2-Coated Hollow-Glass Beads as Photocatalyst *Kanokporn Wongnukoon and Jitladda Sakdapipanich*	482

S3T5-P-15 Preparation and Characterization of Hydroxylated Natural Rubber via Epoxidation and Alkaline Ring-Opening 484
Thanita Suakamram and Jitladda Sakdapipanich

Session IV: Progress in Rubber Characterization

S4T7-P-01 Development of an Integrated Design, Analysis and Evaluation System for Rubber Components 486
Changsu Woo, Sangee Choi and Sangkyun Kim

S4T7-P-02 Spatiotemporal Internal-Damage Distribution During Nonuniform Deformations in Filled Elastomers 488
Yuki Tokudome, Mai Thanh-Tam and Kenji Urayama

S4T7-P-03 AFM Nanomechanics of Vulcanized Rubber Containing Silica and Petroleum Resin 491
Makiko Ito, Kouki Azuma, Keisuke Chino, Xiaobin Liang and Ken Nakajima

S4T7-P-04 Mixed-Mode Crack Propagation Criterion in Elastomers 492
Tomoki Mishima, Thanh-Tam Mai, Katsuhiko Tsunoda and Kenji Urayama

S4T7-P-05 Thermal Analysis of the Mullins Effect in Filler Reinforced Elastomers 494
Koshi Shimazaki, Kakeru Obayashi, Katsuhiko Tsunoda and Kenji Urayama

S4T7-P-06 A Melt Crystallization and Dewetting Kinetics of Marine-Degradable Polyesters in Thin Films 496
Ryu Miyajima, Nana Tsuji, Kazuki Imai, Hiroto Osakaki, Keito Shimakawa, Khanh-Van Thi Khuat, Hiroyasu Masunaga and Sono Sasaki

S4T7-P-07 A Resazurin Reduction Test for Rapid Evaluation of Natural Rubber Latex Putrefaction 498
Preeyawis Na Ubol, Chayanoot Kositanont and Waluree Thongkam

S4T7-P-08 Establishment of A Library Database of Some Compounding Ingredients Using A Py-GC/MS Technique 501
P. Tumwised, S. Wirasate and C. Sirisinha

Plenary Lectures

IRC 2025
BANGKOK, THAILAND

International Rubber Conference 2025 (IRC 2025)

International Rubber Conference 2025 (IRC2025)
1-3 December 2025 @ BITEC, Bangkok, Thailand

Circular Economy - Limits and Chances in Rubber Recycling

ULRICH GIESE[1], JANNIK LAAGES[1]

[1] *Deutsches Institut fütr Kautschutechnologie e. V., Eupener Straße 33, 303519 Hannover, Germany*

e-mail address: ulrich.giese@dikautschuk.de

Keywords: Circular Economy, Rubber Recycling, Devulcanization, Network structures

1. Introduction and Objective of the research

Global rubber production reached 30.9 million tons in 2024, which corresponds to an increase of 1.9% compared to the previous year [1]. Over the world even over 13.5 million tons of used tires are generated (1 t NR equiv. to 0.6 t CO_2, 1 t synt. rubber equiv. 3 to 6 t CO_2). [2, 3] This constantly growing market, which is also associated with a corresponding increase in used rubber, therefore poses a significant environmental problem. According to EU Directive 2008/98/EC, the handling of waste is defined with a focus on the contribution to the protection of the environment and human health. [4]. It emphasizes the importance of proper waste management techniques, recovery and recycling to reduce pressure on resources and improve their use. This directive establishes a waste hierarchy, which requires genuine resource. The goal of the research was the development of an optimized extreme efficient devulcanization process for tire tread materials with environmental friendly or non toxic devulcanization agents. The systematic study considers especially different network structures and NR and s-SBR-compounds as praxis relevant and as model vulcanizates.

2. State of the art

The recycling of elastomers acc. to the idea of circular economy is difficult. The chemical cross-linking (vulcanization) of a rubber matrix to form an elastomer, in conjunction with the entropy elasticity of the polymer, is a basic prerequisite for high elasticity (recovery after mechanical stress). The wide-meshed cross-linking resulting from covalent bonds using sulfur or other cross-linking chemicals is generally not or only partially reversible, so that the material cannot be given a new shape without degradation of the polymer matrix. Mechanical, physical, energetic or pyrolysis recycling strategies therefore only allows limited reuse of the elastomer matrix, which is very valuable as a raw material. Mechanical recycling processes use rubber granulate (GTR) without breaking up the cross-linking, but only achieve limited application possibilities. Small amounts of GRT (appr. < 10 wt-%) in a fresh rubber matrix lead to an extreme decrease of physical properties. [5]. This effect can be partially avoided by functionalization of the GRT. [6] Further the use of rubber powder or GTR for products like flooring materials may be limited by REACH regulation because of potential content of cancerogenic PAHs. [7] Chemical devulcanization processes attempt to selectively split energetic weak S–S -bridges. But with increasing devulanization degree and use of higher temperatures this lead inevitably to unspecific polymer chain scission. The devulcanization of especially natural rubber elastomers using mainly environmental toxic diphenyl-disulfide is investigated for NR- or EPDM -materials, but a complete devulcanization cannot be achieved. [8, 9] As a further strategy, pyrolysis and component extraction (recycled carbon blacks [10], silica, S-recovery) aims to recover individual raw materials, but completely loses the basic polymer structure.

3. Used methods and approaches

First the efficiency and selectivity of several devulcanization agents were carried out in a study using sulfur crosslinked dimethyl-butene model vulcanizates. The vulcanizates (dimers) as well the reaction products from the devulcanization process were analyzed by means of LC-MS and SEC. [11] In a second research

devulcanization was carried out on NR- and s-SBR (silica) -based tread compounds using various chemical degradation aids, incl. components from bio- resources. The vulcanizates were prepared with a systematic variation of crosslink structures. Especially in the case of the SBR-sliica-compounds the effect of silanes were identified The devulcanization agents were optimally distributed in the rubber matrix by means of a diffusion process followed subsequently by thermo-chemical devulcanization. The devulcanization success was quantified and evaluated by means of sol/gel analyses. New compounds using reclaim were characterized for their physical properties.

4. Main Results

From the model studies on dimethylbutene as well from the sutdies on the tread components it is clear, that only the weak S-S-bonds in CV-crosslinked materials can be degraded specifically. In NR-tread componds a high devulcanization degree of higher than 90 % were acchieved using Di-octylpentasulfide (DOPS) in combination with the diffusion process for incorporation of the devulcanization agent into the vulcanizate. S-SBR-Silica systems show an contrary effect by oxidative aging. The crosslink density increased after the devulcanization process because of high stbitiy of the network.

5. Conclusion and main findings

The devulcanization process on NR-and SBR-tread materials with systemaused was found to be highly selective with respect to the degradation of crosslinking sites. The results of this work contribute to a fundamental understanding of the influencing factors for successful feedstock recycling of sulfur-crosslinked elastomers.

References

1. Malaysian Rubber Council (2025): Rubber Industry Overview. URL: https://www.myrubbercouncil.com/industry/world_production.php
2. Jawjit, Warit, Carolien Kroeze, and Suwat Rattanapan, Journal of cleaner production 18.5 (2010): 403-411.
3. Flannery, Brian P., and Jan W. Mares, Resources for the Future: Washington, DC, USA (2022): 1-16.
4. EU-Richtlinie 2008/98/EG („DIRECTIVE 2008/98/EC OF THE EUROPEAN PARLIAMENT AND OF THE COUNCIL of 19 November 2008, on waste and repealing certain Directives
5. A. Spittel, Diss., University Hannover/DIK 1996
6. A. Amash, U. Giese, R. H. Schuster, Kautsch. Gummi Kunstst. 55 (2002) 218
7. A. Diekmann, U. Giese*, I. Schaumann , Chemosphere 220 (2019) 1163-1178
8. Rajan, V., Dierkes, W. K., Noordermeer, J. W. & Joseph, R. *Rubber chemistry and technology* 78, 572–587 (2005).
9. Dijkhuis, K. A., Noordermeer, J. W. & Dierkes, W. K. , *European Polymer Journal* 45, 3302–3312 (2009)
10. „blackcycle-project.eu About the Project,“ 2021. [Online]. Available: https://blackcycle-project.eu/about-the-project/. [20 07 2021].
11. U. Giese, M. Hess, Paper 98, ISSN 1547-1977, Fall 184th Technical Meeting of the Rubber Division of the American Chemical Society, Inc., Cleveland, OH, October 8-10, 2013;
12. Y. Laages, Diss. DIK/University of Hanover, 2023

Crack Resistance and Beyond: Fracture Mechanics in Strain Crystallizing and Liquid Crystal Elastomers

Kenji Urayama

Department of Material Chemistry, Kyoto University, Kyoto 615-8510, Japan

urayama.kenji.2s@kyoto-u.ac.jp

Keywords: Fracture, Crack, Rubber Elasticity, Strain Induced Crystallization, Liquid Crystal Elastomer

This talk presents our recent advancements in understanding the fracture mechanics of rubber materials, from strain-crystallizing natural rubber (NR) to liquid crystal elastomers (LCEs). By integrating high-speed imaging, digital image correlation, high-speed thermography, custom-made biaxial tensile testing, and micro-beam scanning WAXS, we elucidate how nonlinear mechanical responses contribute crack resistance.

In NR, strain-induced crystallization (SIC) significantly enhances crack-growth resistance. However, the spatial confinement and heterogeneity of SIC near crack tips have made experimental characterization challenging. Our recent work [1] visualizes inhomogeneous distributions of strain and crystallinity in the crack-tip region (**Figure 1**). Local crystallinity correlates primarily with the principal major strain (ε_1), reflecting a narrow distribution of strain biaxiality. The stress field was computed using a hyperelastic model based on multiaxial stress-strain data.[2] Importantly, stress intensifies sharply within the SIC zone as the crack-tip is approached, providing quantitative evidence that strain hardening underlies NR's high fracture resistance. This methodology was extended to carbon-black-reinforced NR[3], demonstrating that filler-induced strain amplification enlarges the SIC zone. In a related study,[4] we elucidated the influence of strain biaxiality on SIC by stretching NR sheets with a central hole, which induced a gradient of local deformation from quasi-uniaxial to nearly equal-biaxial.

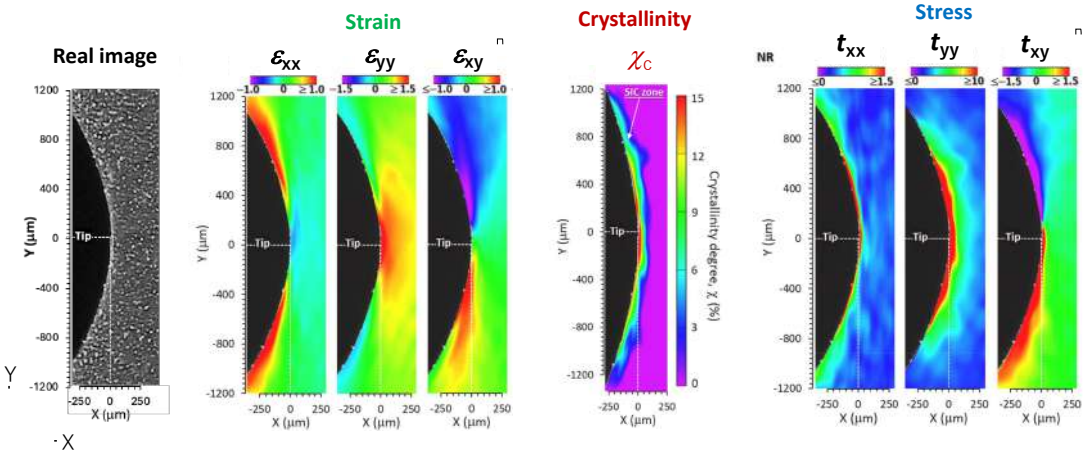


Figure 1. (Far left) Optical image of the region near the crack tip in unfilled natural rubber. (From left to right) Spatial distribution of principal strain, crystallinity, and stress fields, obtained through a combination of DIC, μ-beam scanning WAXS, and hyperelastic modeling.[1,2]

SIC exemplifies a "flaw-resistant" toughening mechanism that strengthens materials locally near flaws. In contrast, liquid crystal elastomers (LCEs) represent a fundamentally different "flaw-tolerant" strategy, enabled by their liquid-like elasticity. LCEs exhibit "soft elasticity", where deformation coupled with director rotation requires minimal mechanical energy[5]. Under unequal biaxial stretching, LCEs equalize stress in orthogonal directions,[6] revealing their in-plane liquid-like mechanics. This property leads to unconventional fracture behavior under tensile tearing [7]: In standard elastomers (e.g., SBR), strain progressively localizes at the crack tip, eventually causing fracture (**Figure 2**). In contrast, in isotropic-genesis polydomain nematic elastomers (I-PNEs), initial strain concentration near the crack tip saturates at a threshold, after which the far field deforms preferentially, leading to a nearly uniform strain distribution (**Figure 2**). Only after this homogenization, conventional strain concentration and fracture occur. This behavior, arising from the in-plane liquid-like elasticity in I-PNEs, suppresses mechanical contrast around flaws and thus mitigates stress localization. The resulting "flaw-tolerant" mechanism—based on strain delocalization rather than resistance—offers a novel design principle distinct from conventional toughening strategies in soft polymer materials.

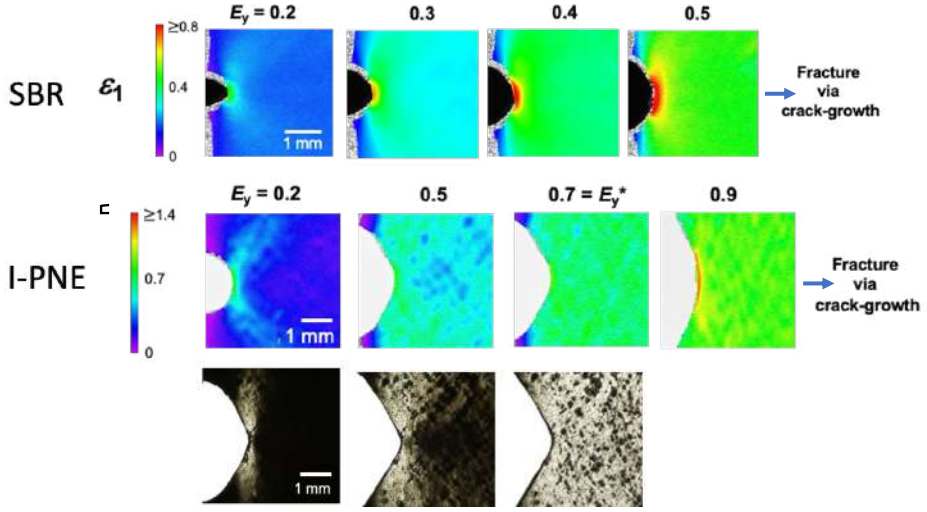


Figure 2. Evolutions of spatial distribution of principal maximum true strain (ε_1) during quasi-static tensile tearing tests for SBR and I-PNE at various applied macroscopic true strains (E_y). Corresponding optical transmission images are displayed alongside the strain maps. The turbid and transparent regions represent the polydomain and monodomain textures, respectively.[7]

References: [1] Mai TT, Yasui T, Tanaka R, Masunaga H, Kabe T, Tsunoda K, Sakurai S, Urayama K, *Adv. Sci.*, 2024; 2307741. [2] Mai, TT, Tsunoda K, Urayama K, *J. Mech. Phys. Solids*, 2024; 193: 105895. [3] Mai TT, Yasui T, Tanaka R, Jotatsu Y, Masunaga H, Kabe T, Tsunoda K, Sakurai S, Urayama K, *ACS Appl. Mater. Interf.* accepted for publication. [4] Nozaki D, Mai TT, Tsunoda K, Urayama K, *Macromolecules*, 2025; 58: 4059 (2025). [5] Terentjev EM, *Macromolecules*, 2025; 58: 2792. [6] Tokumoto H, Hao Z, Takebe A, Kamitani K, Kojio K., Takahara A, Bhattacharya K, Urayama, K, *Sci. Adv.*, 2021; 7: eabe9495. [7] Imai S, Tokudome Y, Mai TT, Urayama K, *ACS Mater. Lett.*, 2025; 2805.

AI-driven Research and Multi-scale Simulation of Elastomer Materials

Liqun Zhang[1,2]

[1] *College of Chemical Engineering, Xi'an Jiaotong University, Xi'an 710049, Shanxi*

[2]*State Key Laboratory of Organic-Inorganic Composites, College of Materials Science and Engineering, Beijing University of Chemical Technology, Beijing 100029, China.*

e-mail address of the presenting author (liqunzhang@xjtu.edu.cn)

Keywords: Natural Rubber, Solution-polymerized styrene-butadiene rubber, molecular dynamics simulation, Machine learning, Polymer property prediction

With the rapid advancement of AI and multi-scale modeling, the performance prediction and structural optimization of rubber materials have entered a new era. This study develops six cross-scale modeling frameworks integrating data augmentation and machine learning (ML) to address key performance aspects of natural rubber (NR) and solution-polymerized styrene-butadiene rubber (SSBR), including strain-induced crystallization (SIC), tensile stress, and glass transition temperature (T_g), providing a comprehensive framework for efficient design and optimization.

NR, known for its excellent mechanical properties attributed to SIC, has attracted significant scientific interest. While molecular dynamics (MD) simulations can investigate structural impacts on SIC at the molecular scale, their computational complexity limits widespread use. Integrating machine learning with MD offers a promising approach to speed up simulations while maintaining accuracy. In **Work 1**[1], a crystallinity prediction algorithm specifically aimed at the SIC properties of natural rubber materials was developed. With the data enhancement algorithm, the high evaluation value of the prediction model ensures the accuracy of the computational simulation results. The method includes (1) an XGBoost model to predict NR crystallinity; (2) a generative adversarial network (GAN) data augmentation algorithm to optimize the utilization of the limited training data; and (3) an analysis of the effects of phospholipid and protein percentage, hydrogen bond strength, and non-hydrogen bond strength on crystallinity, using feature importance analysis.

Work 2[2] addresses the challenge of predicting the tensile stress of NR with limited MD simulation data, which is a crucial mechanical property for this material. A machine learning framework involving three stages is proposed: (1) utilizing a Variational Autoencoder (VAE) to rapidly expand the data diversity; (2) employing Ordinary Kriging (OK) to label the VAE-generated virtual samples; and (3) training Gradient Boosting Regression (GBR) models by using relevant data on tensile stress in NR. The results demonstrate that the generated data exhibits enhanced rationality, significantly improving the accuracy and reliability of various regression models. This approach provides an effective solution to the problem of data scarcity in MD simulations.

SSBR, known for its low rolling and wet skid resistance, is ideal for eco-friendly tires. T_g is a key performance parameter, but testing it experimentally is time-consuming. In **Work 3**[3], all-atom MD simulations provided the foundational training data, and ML techniques were used to predict SSBR's T_g based on four key structural components. To address limited sample sizes, a novel approach combining OK and Nearest Neighbor Interpolation (NNI) was employed, improving upon methods relying solely on NNI. XGBoost showed superior performance with high R^2. The NNI-OK-XGBoost approach was validated with four new structural combinations, demonstrating its efficiency

and accuracy in predicting SSBR's T_g across varying compositions. This work offers a fast and accurate method for predicting the T_g of polymeric materials with limited samples.

Work 4[4] develops a quantitative structure-property relationship model linking SSBR's T_g to its structural properties. A dataset of 68 data sets from literature was used to create a predictive ML model for SSBR's structural design. To address small sample sizes, a framework combining GAN and the Tree-based Pipeline Optimization Tool (TPOT) is proposed. GAN generates additional samples to expand the dataset, and TPOT automatically identifies the best model and parameters. Experimental results show that this approach significantly improves model performance, increasing R^2 from 0.745 to 0.985. The GAN-TPOT framework highlights the potential of combining generative models with automated ML to enhance materials science research.

Work 5 investigates the influence of SSBR sequence structure on T_g using ML models. Natural language processing (NLP) techniques were introduced to represent polymer sequences, and data was augmented using the Wasserstein GAN with gradient penalty (WGAN-GP). T_g predictions were made using a CNN-LSTM model. The hybrid model, combining NLP, WGAN-GP, and CNN-LSTM, achieved an R^2 of 0.94 and MAE of 3.68, demonstrating strong performance and generalization across datasets. This study showcases the innovative use of WGAN-GP and NLP techniques in enhancing polymer sequence data and advancing polymer material design.

The stress-strain curve is crucial for SSBR performance optimization. MD simulations, though useful for exploring microscopic mechanisms, are often conducted at higher strain rates than experiments, leading to discrepancies in stress values. To address this, **Work 6** developed an ensemble learning framework combining transfer learning, hybrid LSTM-MLP, and XGBoost. A dataset of 100 simulated stress-strain curves from 20 SSBR molecular systems at 5 strain rates, along with five experimental curves, was used. The model was pre-trained on simulated data and fine-tuned with experimental data, overcoming MD simulation limitations and producing stress-strain predictions that matched experimental results. Comparative studies validated its effectiveness.

Acknowledgement

This work is supported by the National Science Fund for Excellent Young Scholars (52122311), the National Natural Science Foundation of China (52373222), and the Open Project of State Key Laboratory of Supramolecular Structure and Materials (Grant number sklssm202512).

References

1. Chen Q, Liu Z, Huang Y, Hu A, Huang W, Zhang L, Cui L, Liu J, *Langmuir*, 2023, 39 (48), 17088–17099.
2. Hu A, Liu Z, Chen Q, Zhan S, Li Q, Cui L, Liu J, *J. Mater. Inform.*, 2024, 4 (3).
3. Zhan S, Huang W, Dong C, Chen Q, Zhao H, Duan P, Hu A, Li Q, Li Y, Liu J, Zhang L, *Mater. Today Commun.*, 2024, 40, 110181.
4. Liu Z, Huo Y, Chen Q, Zhan S, Li Q, Zhao Q, Cui L, Liu J, *MGE Adv.*, 2024, 2 (4), e78.

Sustainable Materials for Tyre Engineering

Milanta TOM[1,2], Sabu THOMAS[3,4,5,6,7]

[1]*School of Energy Materials, Mahatma Gandhi University, Kottayam 686560, Kerala, India*

[2]*Univ. Bretagne Sud, UMR CNRS 6027, IRDL, F-56100 Lorient, France*

[3]*International and Inter University Centre for Nanoscience and Nanotechnology, School of Energy Materials, and School of Nanoscience and Nanotechnology, School of Chemical Science, Mahatma Gandhi University, Kottayam 686 560, Kerala, India,*

[4]*Department of Physics and Electronics, CHRIST (Deemed to Be University), Bengaluru, 560029, Karnataka, India*

[5]*Department of Chemical Sciences, University of Johannesburg, P.O. Box 17011, Doornfontein, 2028 Johannesburg, South Africa.*

[6]*TrEST Research Park, TC-4/2322, GEM Building , Opposite College of Engineering Trivandrum, Kulathoor Rd, Sreekariyam, Trivandrum, Kerala 695016, India*

[7]*Center of Excellence in Polymeric Materials for Medical Practice Devices, Department of Chemical Engineering, Faculty of Engineering, Chulalongkorn University, Bangkok 10330, Thailand.*

(sabuthomas@mgu.ac.in)

Keywords: Sustainability, renewable materials, bio-based additives, recycled materials, green tyres.

The tyre industry faces a critical challenge in balancing performance demands with environmental sustainability. Conventional tyre materials rely heavily on petroleum-derived polymers, fillers, and oils, leading to significant carbon footprints and waste generation. There is a need to explore the utilization of sustainable materials—renewable, bio-based, and recycled—for advanced tyre engineering applications [1,2].

Bio-based elastomers offer renewable, carbon-efficient alternatives to synthetic rubber derived from petrochemicals, addressing both environmental and supply chain challenges. Natural rubber (Hevea brasiliensis) remains a primary renewable elastomer with excellent resilience and tensile properties [3]. Guayule rubber (Parthenium argentatum) offers a hypoallergenic, non-tropical alternative with comparable elasticity and improved environmental adaptability [4]. Dandelion rubber is regarded as a promising rubber due to its high content of cis-1,4-polyisoprene, similar to traditional Hevea rubber [5]. Additionally, fully green rubbers derived from plant oils provide tremendous possibilities [6].

Reinforcement using biopolymer nanofillers such as nanocellulose, nanochitin, and nanostarch significantly enhances modulus, wear resistance, and gas barrier properties while reducing filler load and density [7]. Recent research shows that these bio-based fillers can partially replace traditional fillers like carbon black, providing improvements in mechanical properties, rolling resistance, and reducing the environmental impact of tyres [8]. To replace petroleum-based plasticizers, plant-derived oils such as soybean and sunflower oils are employed as sustainable processing aids, improving compound flexibility and oxidative stability [9]. The use of silica derived from rice husk ash provides a renewable reinforcing filler with high purity and improved wet grip and rolling resistance [10]. Moreover, recycled materials—including devulcanized rubber, recovered carbon black (rCB) from end-of-life tyres, and polyester fibers derived from recycled PET bottles—enhance circularity and resource efficiency in tyre production [11].

Collectively, these innovations contribute in developing of sustainable tyres that maintain high performance, durability, and cost competitiveness while significantly reducing environmental impact. The synergistic integration of renewable and recycled resources marks a pivotal step toward sustainable tyre manufacturing and a circular materials economy.

Acknowledgement

The authors would like to express their gratitude to Mahatma Gandhi University, Kottayam 686 560, Kerala, India, and Department of Physics and Electronics, CHRIST (Deemed to Be University), Bengaluru, 560029, Karnataka, India.

References

1. Sampath, M., Konikkara, N., David, S., Rath, J. P., & SKP, A. Advancements in sustainable materials for environmentally responsible tyre production: a comprehensive review. RSC Sustainability, 2025, 3, 4336-4363.
2. https://www.recovery-worldwide.com/en/artikel/sustainable-materials-in-tire-production-3932606.html
3. Hirata, Y., Kondo, H., & Ozawa, Y. Natural rubber (NR) for the tyre industry. In Chemistry, manufacture and applications of natural rubber. Woodhead Publishing. 2014, 325-352.
4. Rousset, A., Amor, A., Punvichai, T., Perino, S., Palu, S., Dorget, M., ... & Chemat, F. Guayule (Parthenium argentatum A. Gray), a renewable resource for natural polyisoprene and resin: composition, processes and applications. Molecules, 2021, 26(3), 664.
5. Das, S., Satpathi, H., Roopa, S., & Gupta, S. D. Sustainability of the tire industry: Through a material approach. In Applied biopolymer technology and bioplastics. Apple Academic Press. 2021, 53-98.
6. Tang, S., Li, J., Wang, R., Zhang, J., Lu, Y., Hu, G. H., ... & Zhang, L. Current trends in bio-based elastomer materials. SusMat, 2022, 2(1), 2-33.
7. Visakh, P. M. Rubber Based Bionanocomposites: Applications: State of Art and New Challenges. Rubber Based Bionanocomposites: Applications, 2025, 1-21.
8. Tom, M., Mohanty, T. R., Thomas, S., Seantier, B., Grohens, Y., Ramakrishnan, S., & Mohamed, P. K. Investigating the synergism and partial replacement of carbon black by cellulose nanofibers in natural rubber-based tyre tread composites. Polymer, 2025, 325, 128302.
9. Bernal-Ortega, P., van Elburg, F., Morera, J. A., & Blume, A. Bio-based resins: Exploring the use of bio-based resins as an alternative to TDAE oil in tire tread compounds-as part of the journey toward fully sustainable treads. 2024.
10. Chundawat, N. S., Parmar, B. S., Deuri, A. S., Vaidya, D., Jadoun, S., Zarrintaj, P., ... & Chauhan, N. P. S. Rice husk silica as a sustainable filler in the tire industry. Arabian Journal of Chemistry, 2022, 15(9), 104086.

11. Sienkiewicz, M., Janik, H., Borzędowska-Labuda, K., & Kucińska-Lipka, J. Environmentally friendly polymer-rubber composites obtained from waste tyres: A review. Journal of cleaner production, 2017, 147, 560-571.

International Rubber Conference 2025 (IRC2025)
1-3 December 2025 @ BITEC, Bangkok, Thailand

Increasing the circularity of sulphur crosslinked natural rubber

Thomas Griggs[1], Anureet Kaur[1], Keizo Akutagawa [1], Biqiong Chen[2], James J. C. Busfield[1],

[1] *School of Engineering and Materials Science, Queen Mary University of London, Mile End Road, London, E1 4NS, UK.*

[2] *Department of Chemistry, University of Liverpool, Crown Street, Liverpool, L69 7ZD, UK.*

j.busfield@qmul.ac.uk

Keywords: recycling, sustainability, disulphide bonds, chemical inhibitors, selective breakdown.

Natural rubber (NR) is a very widely used rubber, with the worldwide demand in 2025 exceeding 15 million tonnes globally (1). Its predominant usage is in the tyre industry, which uses about 70% of the global NR production. NR is a bio-sourced material, being produced using sap from Havea Brasiliensis trees. However, issues around biodiversity, deforestation and soil degradation are increasingly important issues associated with commercial rubber tree plantations (2). This establishes a vital need to recycle already existing NR materials. This is traditionally very difficult due to the presence of permanent crosslinks in rubber products that are essential to ensure the mechanical properties (such as modulus or strength) are appropriate for most industrial applications. One of the most common crosslinking mechanisms, utilises sulphur-based chemistry. In this case carbon molecules present on the NR backbone are targeted by sulphur radicals, creating permanent sulphur linkages between neighbouring NR chains. These permanent crosslinks inhibit flow, which limits the recycling potential.

A broad range of technologies have been investigated to breakdown the crosslinks. Examples of devulcanization approaches include chemical (3), microwave (4) or ultrasonic methodologies (5), or more recently specialized milling processes allowing for selective breakdown of bonds (6). Alternative recycling routes for existing NR products include pyrolysis/energy recovery (7,8), or simple grinding up of the rubber into crumb, for use in applications such as playground flooring, or tarmac (9).

Depending on the formulation of the compound, particularly the ratio between sulphur and accelerator, variable lengths of the sulphur linkages are formed. Of these linkages, the focus of our research lies in the disulphide bond, which shows a highly reversible nature (10). When cleaved, the disulphide bond will result in two sulphur radicals, which under certain conditions can undergo radical neutralisation and which may then reform (Figure 1).

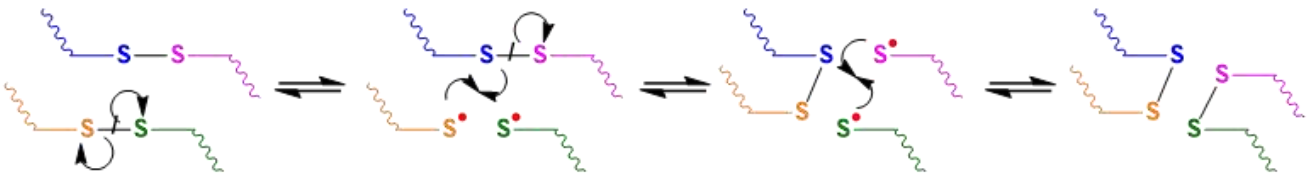


Figure 1. Reversible disulphide radical formation and neutralization reaction

While this reaction is largely spontaneous and uncontrolled, the addition of chemical inhibitors can nullify these reactions under standard conditions, only allowing for the restructuring of the disulphide bonds to occur under specific processing conditions. A range of inhibitors have been investigated, with the most promising being Copper (II) Methacrylate (CuMA). Over a range of curing systems, namely conventional (11) and semi-efficient (SEV) vulcanisations, both filled and unfilled, the addition of very small volume fractions of inhibitor has been shown to produce materials with high levels of recyclability, at recycled content levels greater than 50 wt%.

Through the addition of the inhibitor system, simple mechanical breakdown is sufficient to achieve the high levels of recyclability required, with no additional solvents or chemicals required. The method of breakdown does however show a distinct impact on the final properties of the recycled materials. Several different methodologies of breakdown have been investigated, including simple shearing on a two-roll mill, cryo-milling, and solid-state shear milling. This investigation of the recycling efficiency has allowed an understanding of both the detailed breakdown mechanism and temperature profile to be evaluated.

Utilising the optimised conditions for breakdown, as well as the optimal amount of the chemical inhibitor, a model NR compound equivalent to one that would be found in many industrial applications (an SEV crosslinked system with 50 phr carbon black), was seen to be almost completely recyclable even at a reincorporation rate of 50% recyclate (Figure 2).

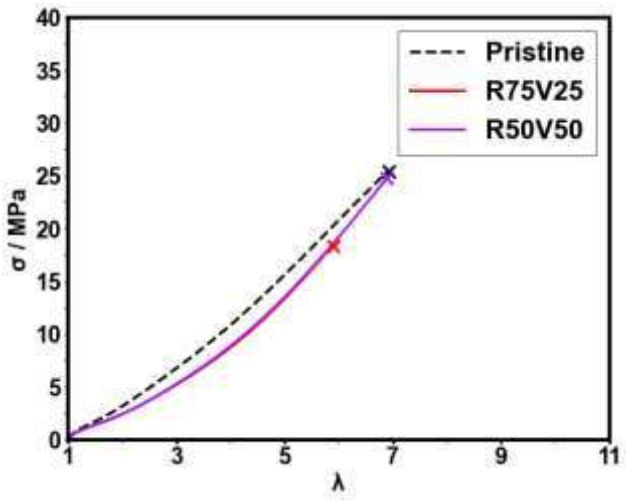


Figure 2. Stress-Extension Ratio curve for the pristine and recycled model filled SEV compounds.

Acknowledgement

This work was supported by the Engineering and Physical Sciences Research Council (EPSRC) grant EP/W018977/1.

References

1. ANRPC revises up natural rubber demand in 2024. Eur. Rubber J. 10. https://www.european-rubber-journal.com/article/2094013/anrpc-revises-up-natural-rubber-supply-demand (2023).
2. Environmental Impact of Rubber – Sustainability Matters. Ball Science, https://ballscience.net/environmental-impact-of-rubber-sustainability-matters/

3. Kojima, M., Ogawa, K., Mizoshima, H., Tosaka, M., Kohjiya, S. & Ikeda, Y. Devulcanization of sulfur-cured isoprene rubber in supercritical carbon dioxide. Rubber Chem. Technol. 76, 957–968 (2003). https://doi.org/10.5254/1.3547784
4. Scuracchio, C. H., Waki, D. A. & da Silva, M. L. C. P. Thermal analysis of ground tire rubber devulcanized by microwaves. J. Therm. Anal. Calorim. 87, 893–897 (2007). https://doi.org/10.1007/s10973-005-7419-8
5. Pelofsky, A. Process for dissolving solid rubber articles such as tires into a liquid vehicle using ultrasonic energy. US Patent 3,725,314 (filed 25 June 1971; granted 3 April 1973).
6. Innes, J. R., Siddique, N., Thompson, G., Wang, X., Coates, P., Whiteside, B., Benkreira, H., Caton-Rose, F., Lu, C., Wang, Q. & Kelly, A. The influence of devulcanization and revulcanization on sulfur cross-link type/rank: Recycling of ground tire rubber. ACS Omega 9, 29175–29188 (2024). https://doi.org/10.1021/acsomega.4c06159
7. Martínez, J. D., Puy, N., Murillo, R., García, T., Navarro, M. V. & Mastral, A. M. Waste tyre pyrolysis – A review. Renew. Sustain. Energy Rev. 23, 179–213 (2013). https://doi.org/10.1016/j.rser.2013.02.038
8. Amari, T., Themelis, N. J. & Wernick, I. K. Resource recovery from used rubber tires. Resour. Policy 25, 179–188 (1999). https://doi.org/10.1016/S0301-4207(99)00025-2
9. Flores Medina, N., Garcia, R., Hajirasouliha, I., Pilakoutas, K., Guadagnini, M. & Raffoul, S. Composites with recycled rubber aggregates: Properties and opportunities in construction. Constr. Build. Mater. 188, 884–897 (2018). https://doi.org/10.1016/j.conbuildmat.2018.08.069
10. Cremlyn, R. J. An Introduction to Organosulfur Chemistry. John Wiley & Sons (1996). https://www.wiley.com/en-us/An+Introduction+to+Organosulfur+Chemistry-p-9780471955122
11. Kaur, A., Fefar, M.M., Griggs, T., Akutagawa, K., Chen, B., Busfield, J.J.C. Recyclable Sulfur Cured Natural Rubber With Controlled Disulfide Metathesis. Communications Materials 5, 212, (2024) https://doi.org/10.1038/s43246-024-00651-9

Sustainable Mobility 2030 and beyond–Role of Tyre and Rubber Industry

Dr. R Mukhopadhyay

Director R&D-JK Tyre; Director & CE-Hari Shankar Singhania Elastomer & Tyre Research Institute

Chairman, Indian Rubber Institute, 437 Hebbal Industrial Area, Mysore

Email: rm@jkmail.com

Since beginning of the civilisation the concept of mobility was prevalent in the society to fulfil various requirements of the mankind. The modes of mobility evolved from the beginning itself, depending on the societal requirement. This evolution process also brought various technological development that enabled to transform pre-historic animal driven mobility to auto-mobility. The global automobile industry confronts a profound movement of transition. Today the automotive eco system is an engine for prosperity but it is also a major driver for environmental degradation. This sector will continue to grow with huge requirement for natural resources. However, natural resources are limited and hence alternate sources are the only option that can keep this sector afloat through sustainable mobility.

As the global community moves toward a low-carbon, resource-efficient, and equitable future, sustainable mobility is no longer a distant vision - it is a pressing mandate. The transportation sector contributes nearly 24% of direct CO_2 emissions from fuel combustion, and tyres - though often overlooked - play a pivotal role in both the environmental impact and technological advancement of vehicles.

The tyre and rubber industry stands at the intersection of innovation, sustainability, and mobility. By 2030 and beyond, its role in transforming how we move will be critical — not just in enabling energy efficiency, but in shaping a truly circular and resilient value chain. Key challenges driving the transformations are decarbonisation pressures, resource constraint, end-of life management and the mobility shift

The role of tyre and rubber industry in enabling sustainable mobility are material innovation and green chemistry, performance optimization for energy efficiency, smart & connected tyres, circular economy & life cycle management, collaborative eco-system and policy alignment.

The journey towards sustainable mobility is not linear, but 2030 and beyond the tyre and rubber industry to be a strategy enabler of sustainable transport system from being a component provider. In the presentation all the aspects mentioned above will be discussed.

Keynote Lectures

IRC 2025
BANGKOK, THAILAND

International Rubber Conference 2025 (IRC 2025)

International Rubber Conference 2025 (IRC2025)
1-3 December 2025 @ BITEC, Bangkok, Thailand

Development of Fast Rubber Sheet-Forming Method for Natural Rubber and Its Application

Seiichi KAWAHARA[1], Yoshimasa YAMAMOTO[2]

[1] *Nagaoka University of Technology, Department of Materials Science and Technology, Niigata, Japan.*

[2] *National Institute of Technology, Tokyo College, Department of Chemical Science and Engineering, Tokyo, Japan.*

(kawahara@mst.nagaokaut.ac.jp)

Keywords: Natural rubber, Island-nanomatrix structure, Latex, Spray drying, Vulcanization

1. Introduction

The method of preparing rubber sheets by spraying latex onto a heated metal surface—referred to as the Fast Rubber Sheet Forming (FRSF) method—has the potential to attract significant attention, as it may represent a paradigm shift in the processing of natural rubber obtained from the Para rubber tree (*Hevea brasiliensis*), transitioning from a conventional dry process to a water-based process. This approach aligns with the increasing demand for purification, compounding, modification, and nanostructure control to be conducted at the latex stage, given that natural rubber is originally harvested as latex, in which rubber particles with an average diameter of approximately 1 μm are dispersed in water. In water-based processing, various reagents and fillers are mixed into the latex; however, due to differences in specific gravity, heavier materials tend to sink while lighter ones float, making uniform dispersion within the latex extremely challenging. To overcome this issue, it is essential to develop a technique that can rapidly dry the rubber before such separation occurs. In this study, we investigated the conditions for forming rubber sheets and their effects on water content, gel content, structure, and mechanical properties of natural rubber (NR) prepared by the FRSF method. Rubber sheets were formed by spraying latex onto heated metallic surfaces at both laboratory and pilot scales. At the laboratory scale, NR latex was sprayed onto a hot plate preheated to 140, 150, 160, or 170 ºC and dried for 15, 30, 45, or 60 seconds to produce rubber sheets. At the pilot scale, latex was sprayed onto a rotating metal roll preheated to 150 ºC and dried for 45 seconds before the rubber sheet was scraped off the roll surface. The factors affecting drying efficiency during sheet formation were investigated by measuring the water content of the resulting sheets. The impact of sheet-forming conditions on rubber degradation was examined through gel content analysis, NMR, and FTIR spectroscopy. Mechanical properties were evaluated by measuring the tensile stress and strain at break of NR films. Furthermore, the FRSF method was applied to protein-free natural rubber latex.

2. Fast Rubber Sheet-Forming Method

NR sheets were prepared from latex by the FRSF method at 140, 150, 160, and 170 °C for 15, 30, 45, and 60 sec. Figure 1 shows enlarged FTIR spectra for NR dried at 50 oC (NR-50) and NR prepared by the FRSF method at 140, 150, 160, and 170 °C for a drying time of 60 sec. Absorbance peaks at 1630 cm^{-1}, 1660 cm^{-1}, and 1740 cm^{-1} appeared in all spectra, which were identified to the C=O

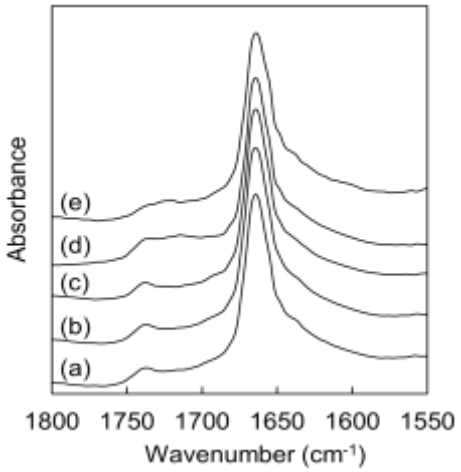


Figure 4. FTIR spectra of ^{1}H NMR spectra of (a) NR-50, (b)NR(140-60), (c) NR(150-60), (d) NR(160-60), (e) NR(170-60).

stretching vibration of amide I band of proteins, the C=C stretching vibration of isoprene units, and the C=O stretching vibration of fatty acid esters, respectively. The FTIR spectra for NR prepared by the FRSF method at 140 oC for 60 sec (NR(140-60)) and NR(150-60) were similar to that for NR-50, whereas they were distinguished from the spectra for NR(160-60) and NR(170-60). For instance, a new absorbance peak appeared at about 1720 cm^{-1} in the spectra for NR(160-60) and NR(170-60), which was attributed to the C=O stretching vibration of carbonyl groups of aldehydes and ketones, formed by the oxidative degradation. These results implies that the oxidative degradation of NR prepared by the FRSF method on small-scale was promoted at the elevated drying temperatures, i.e., 160 and 170 °C, but not at 140 and 150 °C.

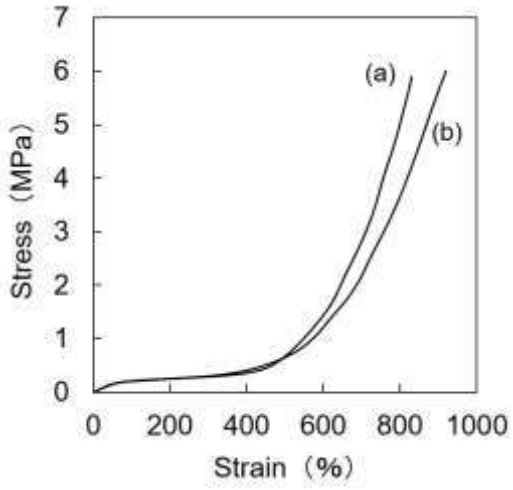


Figure 2 Stress-strain curve of (a) NR-50-control and (b) NR(150-45-LS).

Figure 2 shows stress-strain curves for NR-50-control and NR(150-45-LS). The tensile strength of NR prepared by the FRSF method on large-scale was improved, compared to that of NR-50-control. For instance, the stress at break of NR(150-45-LS) was 6 MPa, which was slightly higher than that of NR-50-control, i.e., 5.9 MPa. Meanwhile, the abrupt increase in stress occurred at the same strain of 500% for both NR-50-control and NR(150-45-LS). These results imply that the structural integrity was maintained for NR prepared by the FRSF method on large-scale as the abrupt increase in stress and stress at break of NR are attributed to the rapid strain-induced crystallization due to the long sequences of *cis*-1,4-polyisoprene units.

3. Application of FRSF method to vulcanization

Figure 3 shows stress-strain curves for natural rubber vulcanizate prepared from the rubber film formed by the FSRS method (latex-mixed natural rubber vulcanizate) and mechanically mixed natural rubber vulcanizate. The stress of the latex-mixed natural rubber vulcanizate drastically increased at a strain of 5, whereas that of the mechanically mixed natural rubber vulcanizate did at a strain of 6. The M_{100} of the latex-mixed natural rubber vulcanizate was almost the same as that of the mechanically mixed natural rubber vulcanizate, reflecting the same crosslink density of the vulcanizates. In contrast, the M_{300} of the latex-mixed natural rubber vulcanizate was higher than that of the mechanically mixed natural rubber vulcanizate. This may be attributed to the rapid strain induced crystallization of the latex-mixed natural rubber vulcanizate due to the improved vulcanization compared to the mechanically mixed natural rubber vulcanizate; that is, the improved vulcanization may result in the longer average sequence length of *cis*-1,4-isoprene units. In fact, the value of stress at break (T_b) of the latex-mixed natural rubber vulcanizate was larger than that of the mechanically mixed natural rubber vulcanizate.

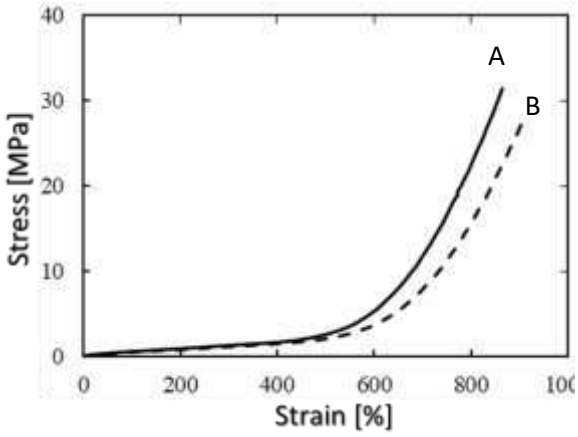


Figure 6 Stress-strain curves for latex-mixed natural rubber vulcanizate (A) and mechanically mixed natural rubber vulcanizate (B).

International Rubber Conference 2025 (IRC2025)
1-3 December 2025 @ BITEC, Bangkok, Thailand

New Insights into Vulcanization Reactions for Green Rubber Technology

Yuko Ikeda[1,2], Hisayoshi Kobayashi[2]

[1] *Research Institute for Production Development, Shimogamo, Sakyo, Kyoto 606-0805, Japan.*

[2] *Professor Emeritus, Kyoto Institute of Technology, Matsugasaki, Sakyo, Kyoto 606-8585, Japan.*

e-mail address of the presenting author (kyoto.rubber.science.lab@gmail.com)

Keywords: Vulcanization, Reaction mechanism, Zinc oxide, Stearic acid, *N*-Cyclohexyl-2-benzothiazole sulfenamide

Vulcanization is the most traditional and conventional chemical process in the rubber industry [1,2]. Almost all rubber products, including the pneumatic tires of automobiles and airplanes, are still manufactured using the vulcanization. In 1839, Goodyear discovered the vulcanization; since then, ongoing innovation has occurred, improving upon the processability and mechanical properties with accelerators, activators, retarders, etc. However, the vulcanization mechanism has not been fully clarified owing to the complicated chemical reactions that occur between rubber, elemental sulfur, and other cross-linking reagents at each step. In 2009, Ikeda *et al.* reported that combining zinc oxide (ZnO) with the other curing reagents was crucial for the chemical cross-linking of the rubber molecules and controlling the structural network inhomogeneity in the sulfur cross-linked isoprene rubber through small-angle neutron scattering [3]. The proposed two-phase inhomogeneous network structure consisted of network domains of high network-chain density embedded in the rubber network matrix (the mesh network). The results also indicated that the mesh size in the two-phase inhomogeneous structure was controlled by the amounts of ZnO and stearic acid (StH). In addition, the findings of the *in situ* time-resolved zinc *K*-edge X-ray absorption fine structure (XAFS) spectroscopy showed that two kinds of sulfur cross-linking reactions for the mesh and network domain formations occurred separately and almost simultaneously [4]. In this conference, reaction mechanisms of the two types of sulfur cross-linking reactions are presented.

Regarding the formation of the mesh network, the dinuclear bridging bidentate zinc/stearate complex (intermediate **I**) composed of $[Zn_2(\mu\text{-}O_2CC_{17}H_{35})_2]\cdot 4X$, where X was a OH group, H_2O, and/or rubber segment, was found to play a role of activator under heating to accelerate the sulfur cross-linking reaction by using a combination of *in situ* time-resolved zinc *K*-edge XAFS spectroscopy and *in situ* time-resolved FT-IR spectroscopy together with the density functional theory calculations [5-7]. The reaction mechanism is shown in **Figure 1** [7]. The intermediate **I** was generated at high temperature of curing by a reaction of ZnO and StH or from zinc stearate. Interestingly, an electron transfer from π-electron clouds of the isoprene rubber molecules to the generated intermediates was found to activate the sulfur cross-linking reaction. A dispersion effect of isoprene rubber for the dinuclear bridging bidentate zinc/stearate complexes to the rubber matrix was also observed to form a highly homogeneous mesh network structure [7,8]. On the formation of the network domain, a mechanism of sulfur cross-linking reaction on the ZnO surface will be explained in the conference. Depending on the amounts of vulcanization reagents, the network domains were found to form their continuous phases of network-domain clusters and network-domain networks, which show a reinforcement effect [9]. These results will be useful for materials design of green rubber products in a sustainable low-carbon society.

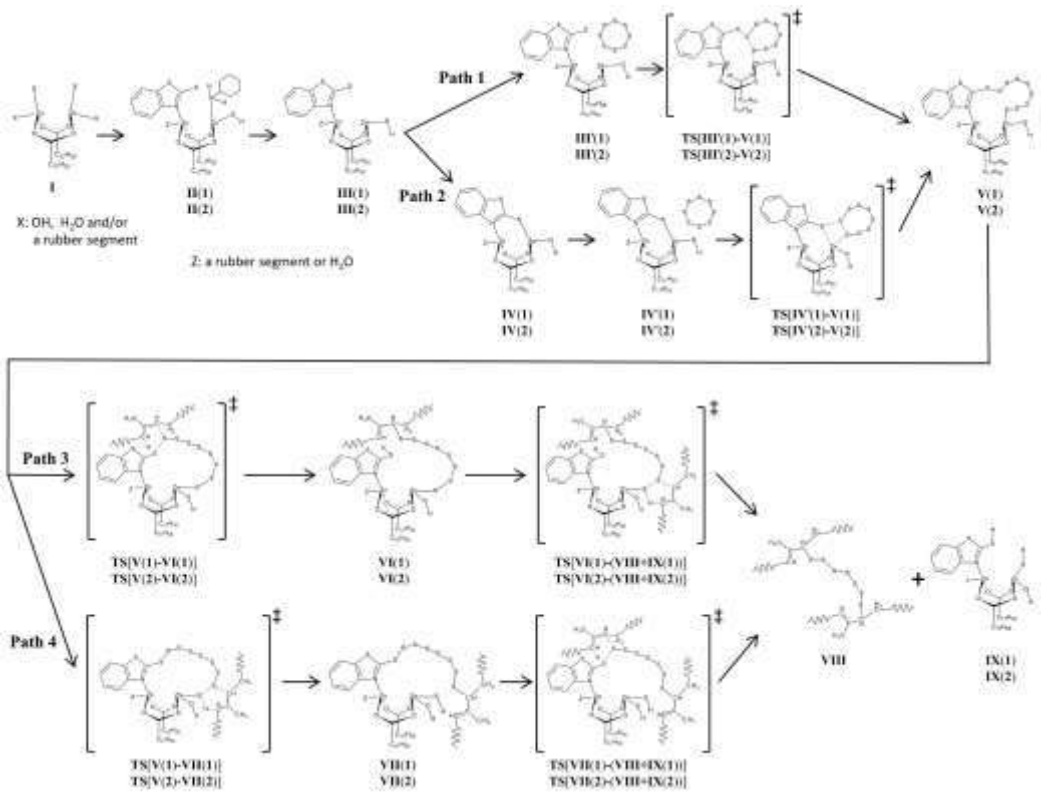


Figure 1. The highly possible reaction scheme of the *N*-cyclohexyl-2-benzothiazole sulfenamide-accelerated vulcanization to generate sulfur cross-linked isoprene rubber.

Acknowledgement

This work was supported by JSPS KAKENHI (B) (Grant Numbers: JP22H02144 & 23K23412) and the JST ALCA program (Grant Number: JPMJAL1501). The XAFS experiments were performed at the BL-14B2 in the SPring-8 with the approval of the Japan Synchrotron Radiation Research Institute (JASRI) (Proposal Nos. 2009A1929, 2009B2044, 2010A1778, 2010B1928, 2012A1419, 2012B1891, 2013A1828, 2013B1840, 2014A1574, 2017A1611). The authors also thank to Drs. Y. Yasuda, Y. Sakaki, K. Miyaji, A. Tohsan, P. Junkong, T. Phakkeeree, Mr. T. Ohashi, and other students for their supports.

References

1. Chapman, A. V., *et al*., *Natural Rubber Science and Technology*, Roberts, A. D., Ed., Oxford University Press, Oxford, 1988; p.511.
2. Ikeda, Y., *et al*., *Rubber Science: A Modern Approach, Second Ed.*, Springer, Singapore, 2024.
3. Ikeda, Y., *et al*., *Macromolecules*, 2009; 42: 2741.
4. Yasuda, Y., *et al*., *Macromol. Chem. Phys.*, 2014; 215: 971.
5. Ikeda, Y., *et al*., *Macromolecules*, 2015; 48: 462.
6. Ikeda, Y., *et al*., *Organometallics,* 2019; 38: 2363.
7. Ikeda, Y. *et al.*, *Organometallics*, 2022; 41, 1942.
8. Miyaji, K., *et al*., *Macromolecules*, 2020; 53: 8438.
9. Ikeda, Y., *et al*., *Rubber Chem. Technol.*, 2022; 95: 161.

Recent Trends in Adopting Sustainable Solution for Rubber Additives: How Chemistry Plays Significant Role?

Prof. Dr. Kinsuk Naskar [1]

[1] *Professor, Rubber Technology Centre, Indian Institute of Technology, Kharagpur, Kharagpur, India*

knaskar@rtc.iitkgp.ac.in

Keywords: Sustainability, Renewable Resources, Sustainable Additive, Vitrimer chemistry

Recent innovations in eco-friendly rubber additives stemmed from the growing global focus on sustainability, aiming to minimise environmental impacts while retaining or enhancing material efficiency. Current trends in adopting sustainable solutions for rubber additives emphasise progress in bio-based, renewable, and non-toxic chemical formulations, advancements in recycling technologies, and the adoption of green chemistry concepts.

Trending research highlights the potential benefits of innovations in renewable resources, which include bio-based activators, fillers, processing oils, and resins, as well as antioxidants and antiozonants sourced from agricultural waste and industrial by-products. Furthermore, it illustrates advancements in green chemistry methodologies for the synthesis of antioxidants, antiozonants, plasticisers, and vulcanising agents. Bio-based rubber processing aids, such as accelerators, antioxidants, and antiozonants, contribute to reducing the emission of toxic or hazardous compounds during end usage, hence ensuring environmental protection and preserving ecological balance.

Progress in green chemistry has enabled the modification of bio-derived materials to enhance their compatibility with rubber matrices and augment their reinforcing qualities. Lifecycle Assessment (LCA) is an essential tool to assess the environmental effects of several rubber processing additives in order to ensure compliance to international sustainability objectives. The integration of sustainable additives presents numerous technical and economic challenges, such as compatibility with current formulations, performance consistency, efficiency, and scalability of production. These difficulties can be addressed via case studies that illustrate successful industrial applications and cooperative initiatives throughout the supply chain.

References

1. Sarkar, P., & Bhowmick, A. K. (2017). Sustainable rubbers and rubber additives. Journal of Applied Polymer Science, 135(24).

Thermal history effects on the viscoelastic response of gum natural rubber: Temperature-induced camel structure and influence on extensional rheology

Minglong Yao,[1] Zhepeng Wang,[1] Zhengying Li,[1] Jiashun Yang,[1] Chen Cheng,[1] Xiaorong Wang,[1] and Christopher G. Robertson[2,3*]

[1]*Center for Frontier Research and Technology, Zhongce Rubber Group Co., Ltd., Hangzhou, Zhejiang 310008, China;*

[2]*Centre of Polymer Systems, University Institute, Tomas Bata University in Zlin, tr. Tomase Bati 5678, 76001, Zlin, Czech Republic;*

[3]*Polymer Technology Services LLC, Akron, Ohio 44333, USA;*

*Speaker; chris168robertson@gmail.com

After cooling natural rubber (NR) gum polymer (raw elastomer) from 80 °C to temperatures below 0 °C, we observe two viscoelastic relaxation responses near 16 °C and 51 °C in a subsequent heating scan using dynamic mechanical analysis (DMA) in an oscillatory shear rheometer. Prior isothermal crystallization at temperatures from -35 to -15 °C does not change the location or intensity of these dynamic mechanical events. This relaxation behavior, which we call *camel structure* due to the two characteristic humps in the DMA response, consistently shows up for gum NR but is not present for crosslinked NR or for synthetic polyisoprene (isoprene rubber; IR) with 98.7% cis-1,4 microstructure. Differential scanning calorimetry (DSC) reveals two weak endothermic local peaks for gum NR in the same general temperature regions as noted for the DMA humps, which suggests that two populations of residual crystalline nuclei may be responsible for the viscoelastic behavior. The camel structure in gum NR is unchanged across multiple repeated cooling and heating scans, and the structure has an influence on strain hardening in extensional rheology, which will be discussed.

The Crosslinking Dilemma in ENR: Evaluating Sulphur and Di-acid Networks for Future-Ready Rubber Products

Amit DAS
Leibniz Institute of Polymer Research Dresden, Germany
das@ipfdd.de

Keywords: Epoxidized Natural Rubber, Di-acid Crosslinking, Ionic Network, Self-Healing Rubber

This study presents an alternative crosslinking approach for epoxidized natural rubber. By introducing imidazolium ions, the rubber's backbone undergoes a transformation, resulting in the formation of ionic stickers as reversible cross-linking points. This process turns the rubber into an ionomer with unique characteristics, such as self-healing and re-processability. Furthermore, it is also observed that the thermal stability of such rubber composites is improved in a high extent. These reversible ionic bonds contribute to the network structure's thermal stability, flexibility and dynamics. Various analyses, including FTIR and impedance spectroscopy were conducted to characterize the chemical structure, demonstrating the promising mechanical properties of the transformed ENR. These unconventionally crosslinked rubbers, when combined with suitable fillers, can be potentially incorporated in specific quantities for practical applications, including tire applications and non-tire heat resistance product applications. By introducing these materials, the self-healing functionality and enhanced durability can be achieved in the specified application.

Acknowledgement

The author gratefully acknowledges the research grant provided by Sumitomo Rubber Industries, Japan.

References

1. Mandal, S, Verners, O, Euchler, E, Kundu, A, Zimmerer, C, Bernhardt, R, Tada, T., Heinrich, G, Wießner, S and Das, A, 2025, *Sustainable Materials and Technologies*, 2025, 43, p.e01243.

Engineering Allergy-Free Natural Rubber:

Sustainable Deproteinization for Enhanced Industrial and Medical Performance

Jitladda Sakdapipanich[1]*

Rubber Research Group, Department of Chemistry, Faculty of Science, Mahidol University, Nakhon Pathom 73170, Thailand.

*Corresponding author: jitladda.sak@mahidol.ac.th

Keywords: Sustainable Natural Rubber, Allergy-Free Gloves, Deproteinization, Saponification, Latex Allergy Prevention, Smart Biomaterials

Natural rubber latex remains a critical biomaterial owing to its exceptional mechanical strength and renewable origin. However, its intrinsic allergenic proteins have historically posed significant health risks, particularly in medical and occupational environments. This research presents a sustainable approach to produce highly purified natural rubber latex through deproteinization and saponification processes, yielding deproteinized natural rubber (DPNR) and saponified natural rubber (SPNR).

The developed latexes demonstrate markedly reduced extractable protein levels, effectively eliminating major allergens such as *Hev b*1, *b*3, *b*5, and *b*6.02, as confirmed by ELISA and SDS-PAGE analyses. Vulcanized gloves fabricated from DPNR and SPNR exhibit superior barrier properties, enhanced tensile strength exceeding ASTM standards, and improved elasticity, contributing to user comfort and extended product lifespan. Additionally, the gloves possess lighter coloration and lower water absorption, offering enhanced visual and tactile quality.

Compared to conventional latex gloves, these allergy-free products mitigate type I hypersensitivity reactions while preserving the advantageous properties of natural rubber. This integrated strategy addresses both health and sustainability imperatives by reducing reliance on synthetic alternatives and promoting safer use of natural rubber in healthcare and industrial applications. Overall, this work establishes a scalable model for producing eco-efficient, high-quality natural rubber gloves that align with circular economy practices and future global standards in personal protective equipment.



Fig. 1 Scenarios of natural rubber latex from *Hevea* rubber tree to sustainable products

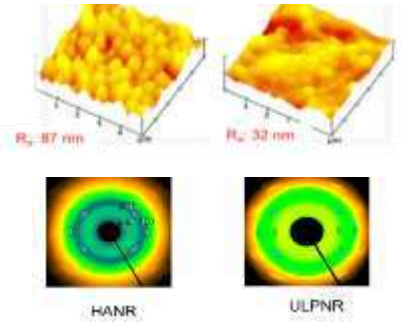


Fig. 2 Surface morphology from AFM analysis and WAXD patterns of HANR and ULPNR

On the path to make a black magic green – how to minimize the the CO_2 footprint of rubber products

Andreas Limper

Institut für Kunststoffverarbeitung RWTH Aachen, Germany

Climate change is a serious threat to humanity. Recent natural disasters show that swift action must be taken to reduce CO_2 emissions. Rubber products are indispensable to us today. We must therefore find ways to reduce their carbon footprint.

The presentation shows the CO_2 balance of two typical rubber products. It looks at the raw materials on the one hand and the processing on the other. In this way, conclusions can be drawn as to where improvements in the ecological balance can be achieved most effectively.

Trends for the use of more ecological raw materials will be shown.

Finally, examples of how resource consumption can be optimised are presented in both the materials and processing areas.As shown, modern process technologies can save a lot of energy by new machine concepts but also by a better process control. Besides this, efficient ways to save material consumption by new compounding concepts will be demonstrated.

International Rubber Conference Organisation

International Rubber Conference 2025 (IRC2025)
1-3 December 2025 @ BITEC, Bangkok, Thailand

Optimized Synthesis of Liquid Fluorosilicone Rubber with Improved Cold Resistance for Semiconductor Application

Sang Eun Shim, Jae Il So, Jin Sung Seo

Department of Chemistry & Chemical Engineering, Inha University, Incheon, S. Korea.

e-mail address of the presenting author (seshim@inha.ac.kr)

Keywords: Fluorosilicone rubber, Cold resistance, Synthesis, Thermal Properties

Fluorosilicone, which contains siloxane segments and fluorinated groups, has substantially different properties than polydimethylsiloxane (PDMS) owing to the presence of fluoroalkyl groups [1]. Fluorosilicone has various properties, such as waterproofing, resistance to oil, fuel, and solvents, low-temperature resistance, and excellent film-forming properties derived from the trifluoropropyl groups and siloxane backbone [2,3]. Currently, fluorosilicone elastomers are widely used as sealing materials for gasoline, fuel, and aircraft because of their ability to seal at low temperatures and reduce the possibility of fuel penetration. Owing to the growing demand for versatile hybrid materials that can withstand harsh conditions (below −40 °C), fluorosilicone copolymers are becoming promising materials that can overcome the limited operating temperature of conventional rubber.

In general, fluorosilicone is synthesized through the ring-opening polymerization (ROP) of 1,3,5-trimethyl-1,3,5-tris(3,3,3-trifluoropropyl)cyclotrisiloxane (F-D_3). Compared to the hydrolysis-condensation of fluorosilanes, synthesizing fluorosilicone through ROP has advantages, such as facile reactions, inexpensive raw materials, and a high molecular weight [4]. Herein, we synthesized fluoro-vinyl-methyl-silicone (FVMQ) as the main chain of fluorosilicone rubber and fluoro-hydride-methyl-silicone (FHMQ) as a crosslinker of fluorosilicone rubber, using TMAS as the initiator as shown in Figure 1. For the optmizing the thermal and mechanical properties of FVMQ, the combinations of the monomer mixture was varied by changing the amount of D_4, Vinyl-D_4, F-D_3, and initiator. In addition, vinyl group-containing polyhyderal oligomeric silsesquioxane (POSS) was prepared and used as a filler to improve the mechanical properties of FVMQ. liquid-fluorosilicone rubber (F-LSR) with various viscosities and fluorine content was prepared by hot press molding by adding silica as a filler. Finally, the thermal and mechanical properties of the synthesized F-LSRs with different molecular weights and fluorine content were investigated.

All FVMQs were synthesized as random copolymers, and the ratios of the functional groups were almost identical to their theoretical values, with errors of less than 2% determined by ^{1}H- and ^{29}Si-NMR. Furthermore, the molecular weight of the FVMQs could be controlled by changing the loading of the end-blockers. The synthesized FHMQ was also successfully optimized to achieve an MH block content of more than 10% and a viscosity of less than 1000 cP. The mechanical properties of all F-LSRs were confirmed: (1) the hardness of F-LSR increased as the proportion of fluorine in the chain increased; (2) at a constant fluorine ratio, elongation was proportional to the molecular length, and (3) the tensile strength was the greatest in F-LSR-400-f5. In TGA, it was confirmed that the thermal stability of the synthesized F-LSR at high temperatures decreased as the fluorine group increased. Conversely, elastic retention and brittleness at low temperatures improved with a high ratio of fluorine groups and long molecular chain lengths.

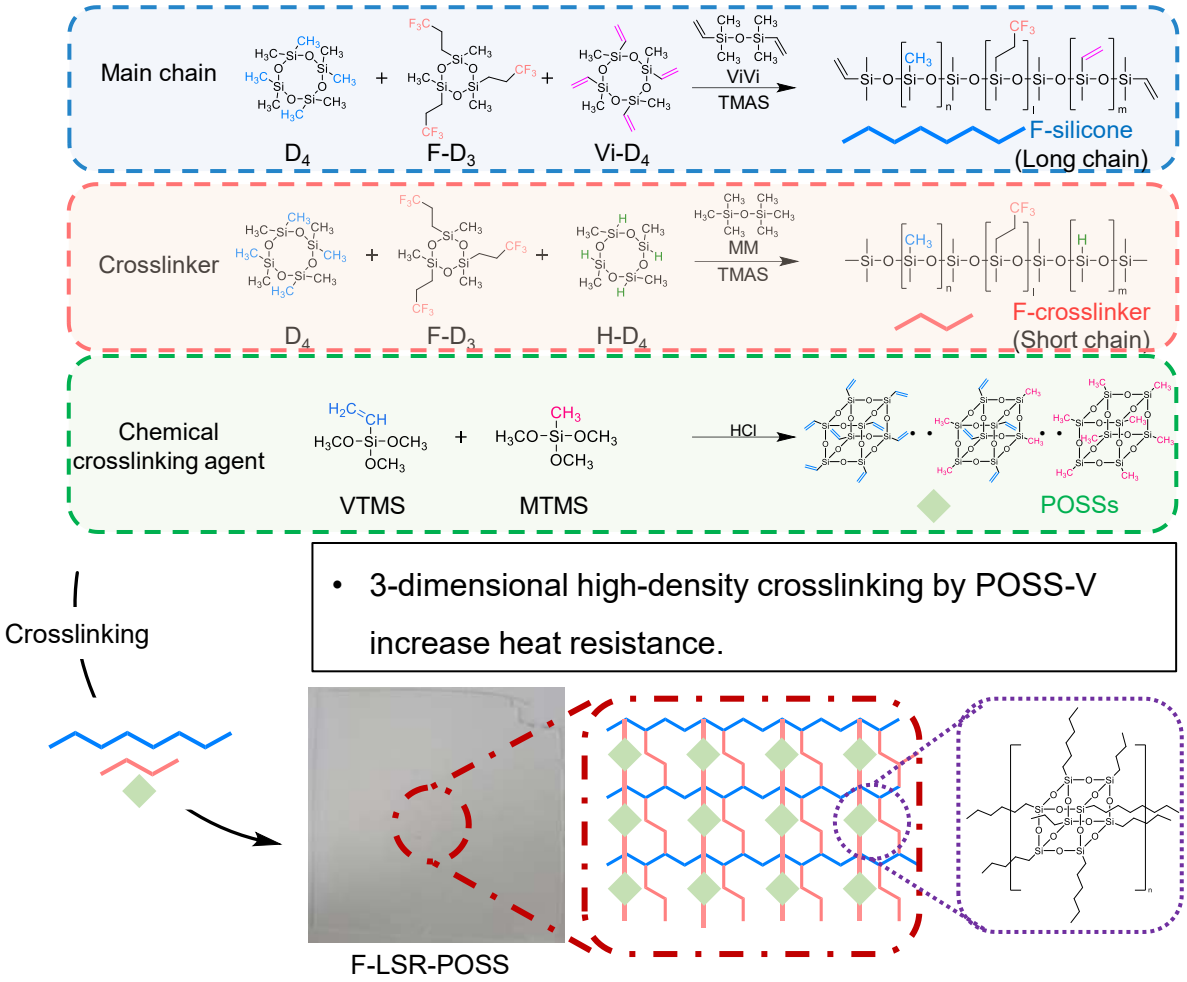


Figure 1. Schematic of all processes for synthesizing fluorosilicone and manufacturing liquid silicone rubber.

Acknowledgement

This work was supported by the Technology Innovation Program (20011100) funded by the Ministry of Trade, Industry & Energy (MOTIE, Republic of Korea).

References

1. Yang, Z.; Bai, Y.; Meng, L.; Wang, Y.; Pang, A.; Guo, X.; Xiao, J.; Li, W. *Eur. Polym. J.* 2022; 163: 110903.
2. Indulekha, K.; Behera, P.K.; Rajeev, R.; Gouri, C.; Ninan, K. *J. Fluor. Chem*. 2017; 200: 24.
3. Li, B.; Chen, S.; Zhang, J. *Polym. Chem*. 2012; 3,: 2366.
4. Cui, Y.; Jiang, W.; Li, D.; Niu, C.; Feng, S. *e-Polymers* 2011; 11: 77.

Some Considerable Factors in Laboratory Frictional Testing Rubbers

C. NAH[1,2], G.-B. LEE[1], D. ABDULRAMAN[2], P. SUNINTABOON[2], P. JUNKONG[2],
T. AMORNSAKCHAI[2], P. PHINYOCHEEP[2]

[1]*Department of Polymer-Nano Science and Technology, Jeonbuk National University*
567 Baekje-daero, Deokjin-gu, Jeonju 54896, Republic of Korea
[2]*Department of Chemistry, Faculty of Science, Mahidol University,*
999 Phutthamonthon Sai 4 Road, Salaya, Nakhon Pathom 73179, Thailand
(cnah@jbnu.ac.kr)

Keywords: Rubber, Wear, Cutting, Chipping, Frictional Energy

In tire industries, one of the challenging tasks is to predict properly the resistance of tires in service against abrasive wearing and cutting/chipping based on the data from the corresponding laboratory tests [1]. The poor correlation might come from the difference in various testing conditions such as temperature, applied loading, and texture of counter surfaces between the laboratory and field tests.

The resistance of tires in service against cutting and chipping by the sharp objects on the road is often evaluated by the B. F. Goodrich laboratory tester [2]. The field performance of two typical treads compounds for truck/bus tires based on natural rubber (NR) and butadiene rubber (BR) was compared with those from the laboratory test. A plausible reason was proposed in explaining the discrepancy between the laboratory and field tests by considering the frictional energy input into rubber specimen (**Figure 1**).

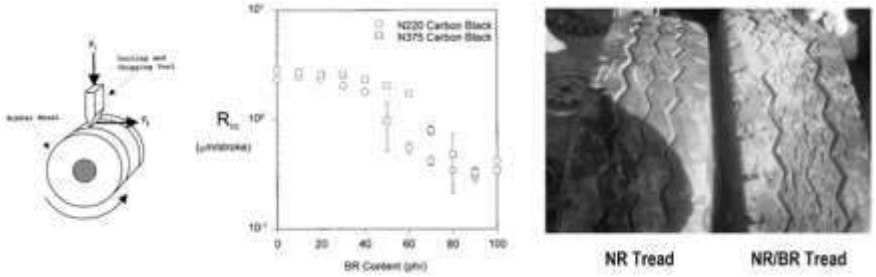


Figure 1. The laboratory cutting and chipping test (left) and truck/bus tire test on a harsh road condition (right) [reprinted from reference 3].

The rate of abrasion of various synthetic rubber compounds was estimated by a blade-type laboratory abrasion tester [4,5], and a fairly good correlation was found with the rate of crack growth as a function of the frictional energy input or tearing energy indicating the mechanical abrasive failure is governed by the progressive crack growth mechanism (**Figure 2**) [1].

The tire wear test was performed for the selected tread compounds, and it was compared with the results by the laboratory abrasion tests (blade abrader and DIN). For an improved correlation between the laboratory and field tests, the wear severity (frictional energy input) and the wear rate dependence with the frictional energy input should be carefully considered. It is noteworthy that when the smearing occurs, especially at lower frictional energy region during laboratory wear test, it should be eliminated by spreading dry powders like talc. A reasonably good correlation was found between blade and DIN abrader at relatively higher frictional energy regions (harsher wear condition). At

lower frictional energy region (milder wear condition), the rate of abrasion from the blade abrader was found to predict well the tire wear performance, which was provided by the Hankook Tire.

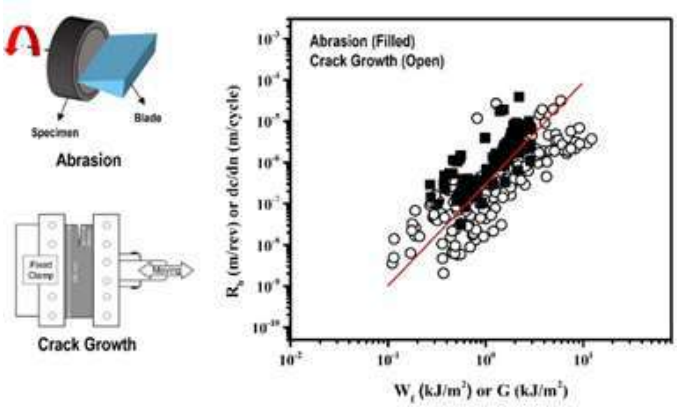


Figure 2. Correlation between abrasion and crack growth behavior [5].

Acknowledgement

This work was supported by the Technology Innovation Program (20010851, an advanced butadiene rubber and a functional complex development for super abrasion tire) funded By the Ministry of Trade, Industry & Energy (MOTIE, Korea). The authors would like to thank the Hankook Tire and the MIRAE Scientific Instruments Inc. for sharing the data.

References

1. Grosch KA, Schallamach A, *Rubber Chem. Technol*., 1966; 39: 287.
2. Beatty JR, Miksch BJ, *Rubber Chem. Tech*., 1982; 55: 1531.
3. Nah C, Jo BW, Kaang S, *J. Appl. Polym. Sci*., 1998; 68: 1537.
4. Gent A, Nah C, *Rubber Chem. Technol*., 1996; 69: 819.
5. Nah C, *Unpublished work*, 2025.

Bio-based Approach to Dispersion of Silica in NR

Dariusz M. BIELINSKI[1], Miroslawa PROCHON[1], Agnieszka KOLODZIEJCZAK-RADZIMSKA[2], Jakub WRECZYCKI[1], Mateusz IMIELA[1], Teofil JESIONOWSKI[2]

[1] *Lodz University of Technology, Faculty of Chemistry, Institute of Polymer & Dye Technology, Stefanowskiego 12/16, 90-924 Lodz, Poland.*

[2] *Poznan University of Technology, Faculty of Chemical Technology, Institute of Chemical Technology and Engineering, Berdychowo 4, 60-965 Poznan, Poland.*

e-mail address of the presenting author: dariusz.bielinski@p.lodz.pl

Keywords: Natural Rubber, Silica, Surface modification, Protein hydrolyzates, Mechanical properties

The filler-rubber interaction is a key parameter for the reinforcement of rubber. Silica is the most essential and cost-effective reinforcing filler in the rubber industry after carbon black. The silica reinforcement mechanism with a non-polar elastomer, like natural rubber (NR), is complicated by the presence of polar functional groups on the filler surface. Polar nature of silica causes filler-filler interactions by forming hydrogen bonds. Therefore, sizeable non-dispersed silica clusters remain in a non-polar rubber matrix [1]. To avoid these strong filler-filler interactions and to improve compatibility between rubber and silica, the filler surface needs to be modified. This can be done using a coupling agent that has functional groups capable of linking both rubber and silica. Silanization is the most popular and effective covalent coating method for modifying the surface of a material rich in hydroxyl groups, such as silica [1-3]. Proteins present in NR exhibit a similar, although not as strong, effect as silane in hydrophobizing silica surface [4]. The objective of studies was to check the possibility of replacing conventional silane compatibilizers with cheap protein derivatives, obtained from recycled natural products like sulfur containing amino acids or protein hydrolyzates, in rubber technology. It could open new direction of research towards bio-elastomeric composites.

Commercial precipitated silica was subjected to surface modification with amino acids (L-cysteine, cystine or methionine), keratin produced from the wastes of poultry (P) or tanning industry (K), as well as acidic (HKK) or enzymatic hydrolyzates of keratin made of bird feather (HP) or bovine hair (HK). In the case of LC and protein hydrolyzates, wet treatment was applied to modify silica surface, whereas for waste proteins, which are not soluble in water, silica was ground with keratin in a ball mill. The effects obtained were compared to silica surface treatment with commercial silanes: 3-Aminopropyltriethoxysilane or 3-Mercaptopropyltrimethoxysilane.

The above modifications were compared from the point of view of the degree of coverage and the elemental composition of the filler surface, determined from elemental analysis, and confirmed by thermogravimetric analysis (TGA), infrared spectroscopy (FT-IR) and nuclear magnetic resonance (^{29}Si NMR). FT-IR spectra and TGA confirm the modification of silica surface, with the highest effect observed, comparable to silane treatment, in the case of protein hydrolyzates, followed by the modification with L-cysteine. Most likely, the presence of thiol groups in the amino acid molecule, being absent in the case of the other amino acids studied, is responsible for the highest degree of its adsorption on filler surface. Protein molecules seem too big for effective chemical interactions with the filler surface, rather modifying rubber macromolecules, contrary to its hydrolyzates. Unlike silanization, the modification with the low molecular weight protein derivatives, does not seem to

interfere with the sulfur vulcanization process, achieving an increase in the vulcametric torque at the level of the rubber mixture filled with native silica. Despite good compatibility of amino acids with natural rubber [5], the most likely, increased mechanical properties of the NR vulcanizates can be subscribed to physical entanglements of the molecules grafted to the filler surface with macromolecules of the rubber matrix (resembling Velcro effect), without any increase of bound rubber (BdR), according to the scheme presented in Figure 1.

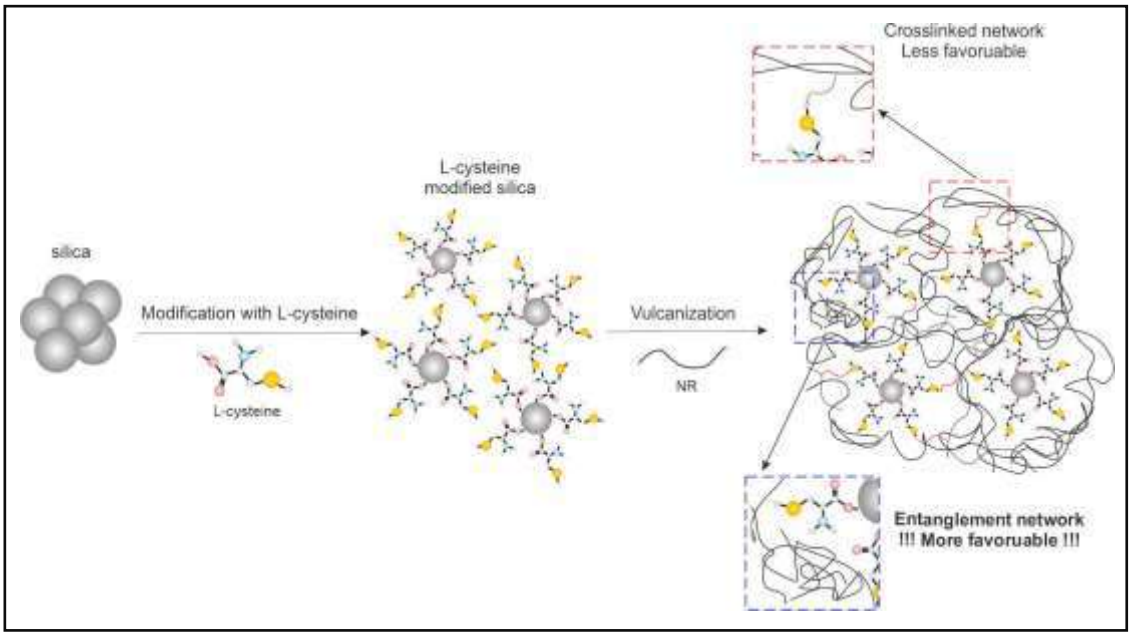


Figure 1. Proposed behaviour of L-cysteine grafted silica in rubber matrix

The proposed mechanism of modified silica - rubber interactions results in increase of the crosslink density of vulcanizates, due to significant contribution of physical crosslinks, as well as a change in the crosslink structure, dominated by longer ones, contrary to the vulcanizates filled with filler subjected to mercaptosilane treatment. The replacement of silica coupling agents with L-cysteine or the protein hydrolyzates results in improvement of the filler macro-dispersion, demonstrated by higher values of dispersion index (DI, ISO 11345) and SEM-EDS mapping, as well as indicated by lower Payne effect. It additionally makes possible to eliminate diphenyl guanidine, decomposing to toxic aniline, from sulfur curing system of rubber [6]. The changes to crosslink density and structure, together with improved filler dispersion and unchanged BdR content, result in increase of tensile strength (TS) due to significantly increased elongation at break (Eb) values (ISO 37), but contrary to silanization - decreasing stiffness of NR vulcanizates.

References

1. Neethirajan J, Parathodika AR, Hu G-H, Naskar K, *Funct. Comp. Mater.*, 2022; 3: 7.
2. Meon W, Blume A, Luginsland H-D, Uhrlandt S, in: Rodgers B ed., *Rubber Compounding: Chemistry and Applications*, Marcel Dekker Inc., New York, 2004; Ch. 7.
3. Ansarifara A, Azharb A, Ibrahima N, Shiaha SF, Lawton JMD., *Int. J. Adh. & Adhes.*, 2005; 25: 77.
4. Sarkawi SS, Dierkes WK, Noordermeer JWM, Proc. *11th Fall Rubber Colloquium*, Hannover, DIK 2014.
5. Kavichat K, Tulyapong T, Anuwat S, Siriwat S, Nattapong N, *Procedia Chemistry*, 2016; 19: 447.
6. Debnath SCh, Das A, Basu D, Heinrich G, *Kautsch. Gummi Kunstst.*, 2013; 1-2: 25.

Elucidating the Role of Nanoscale Interfaces and 3D Dispersion in Elastomer Nanocomposites: Connecting Microstructure to Viscoelastic Behavior

Ming Tian [1,2], Nanying Ning [1,2], Liqun Zhang [1,2]

[1] *State Key Lab of Organic-Inorganic Composites, Beijing University of Chemical Technology, Beijing 100029, China.*

[2] *Key Laboratory of Carbon Fiber and Functional Polymers, Ministry of Education, Beijing University of Chemical Technology, Beijing 10029, China.*

tianm@mail.buct.edu.cn

Keywords: interface, three-dimensional dispersion, quantitative characterization, elastomer nanocomposites, viscoelastic properties

Filler reinforced elastomer nanocomposites have significant applications in high-performance tires, aerospace, and other industries. The macroscopic performance of these nanocomposites is closely related to the interfacial interaction between filler and elastomer, as well as the dispersion structure of filler in the matrix. However, traditional characterization methods have limited resolution, making it challenging to elucidate the relationship between nanoscale microstructures (interfacial properties, dispersion structure) and the macroscopic performance of nanocomposites. Consequently, it is difficult to provide clear guidance for high-performance material design and preparation. In this study, by virtue of the high-resolution of Quantitative Nanomechanical Mapping Technique of Atomic Force Microscopy (AFM nanomechanics), a method for quantitatively characterizing the interfacial structure (interfacial thickness, nanomechanical properties) of elastomer nanocomposites is established. To ensure accurate measurements of nanomechanical properties by AFM nanomechanics, Johnson-Kendall-Robert (JKR) contact mechanics model that is more suitable for soft materials like rubber have been applied to analyze Young's modulus. The double layer structure of interface was directly identified based on AFM nanomechanics images and was further directly evidenced by the morphology of bound rubber observed through high resolution transmission electron microscopy. [1-4] Simultaneously, a method for quantitatively characterizing the three-dimensional dispersion structure of fillers in matrix is developed by combining Three-Dimensional Scanning Transmission Electron Microscopy (3D-STEM) with nanoscale resolution and Synchrotron X-ray Computed Tomography (X-ray CT) with a micrometer-level field of view. Using this method, the dispersion structure of fillers that ranges from several nanometers to dozens of microns, including the homogeneity and size of fillers, the compactness of agglomerates, and the branching degree and connectivity of agglomerates and filler networks, were quantified. The reliability of this method is demonstrated through the observation of the Payne effect in elastomer nanocomposites. [5-7] Based on the above quantitative characterization methods, the influence of the properties of rubber and fillers on the multi-scale microstructure (interface properties, dispersion structure) of nano-composites, as well as their relationship with macroscopic properties, especially their viscoelastic performance, has been further revealed. This study provides valuable guidance for the design and preparation of high-performance elastomer materials.

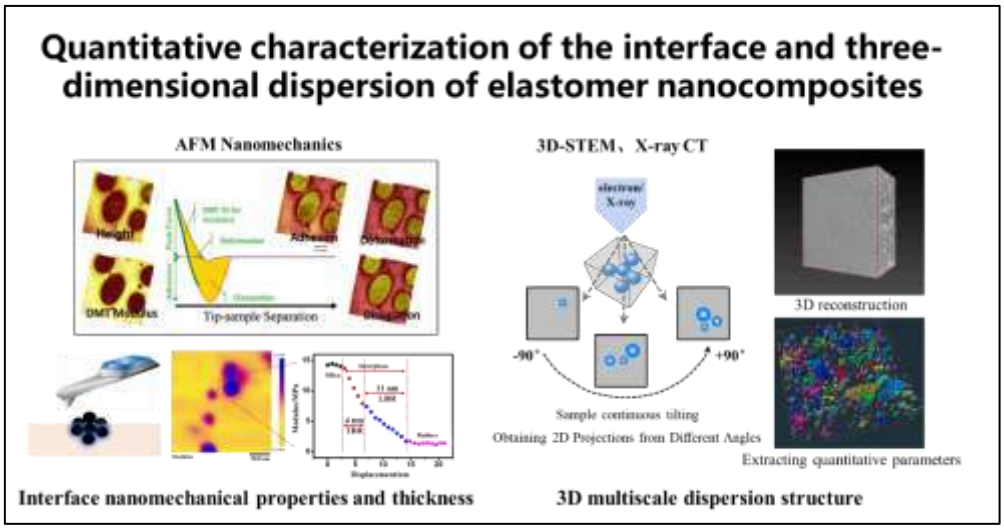


Figure 1. Quantitative characterization of the interface and three-dimensional dispersion of elastomer nanocomposites

Acknowledgement

The financial supports of the National Natural Science Foundation of China (Grant No.52127804 and 51373012) are gratefully acknowledged.

References

1. Chenchen Tian, Ming Tian*, et al. *Compos Sci Technol*., 2024, 258: 110847.
2. Chenchen Tian, Ming Tian*, et al. *Polymer*, 2023, 271: 125798.
3. Chenchen Tian, Ming Tian*, et al. *Compos Sci Technol*., 2022, 222: 109367.
4. Chenchen Tian, Ming Tian*, et al. *Compos Part B-Eng*., 2020, 193: 108048.
5. Xiangyan Li, Ming Tian*, et al. *Compos Part A-Appl S*., 2022, 152: 106722.
6. Xiangyan Li, Ming Tian*, et al. *Composites Part B: Engineering*., 2021, 212: 108687.
7. Xiangyan Li, Ming Tian*, et al. *Compos Part A-Appl S*., 2020, 131: 105778.

Wide-Angle X-Ray Diffraction Studies on Strain-Induced Crystallization of Vulcanized Natural Rubber by Two-Step Biaxial Stretching

Shinichi SAKURAI[1], Yuki JOTATSU[1], Hiroto OKUMURA[1], Hiroyasu MASUNAGA[2], Yuji KITAMURA[3], Katsuhiko TSUNODA[3], Kenji URAYAMA[4]

[1] *Department of Biobased Materials Science, Kyoto Institute of Technology, Matsugasaki, Sakyo-ku, Kyoto 606-8585, Japan.*

[2] *Japan Synchrotron Radiation Research Institute (JASRI), Sayo-gun, Hyogo 679-5198, Japan.*

[3] *Bridgestone, 3-1-1 Ogawa Higashicho, Kodaira, Tokyo 187-8531, Japan.*

[4] *Department of Material Chemistry, Kyoto University, Kyoto-Daigaku Katsura, Nishikyo-ku, Kyoto 615-8510, Japan.*

e-mail address of the presenting author (shin@kit.ac.jp)

Keywords: Vulcanized Natural Rubber, Strain-Induced Crystallization, Two-Step Biaxial Stretching, Wide-Angle X-Ray Diffraction, Synchrotron Radiation

Natural rubber (NR), in addition to its elastomeric properties, has the property of not breaking down even when momentary stress is applied during large deformation. The phenomenon of strain-induced crystallization (SIC), whereby polymer chains are oriented and crystallize when rubber is elongated, is known to play an important role in exhibiting these properties. It has been noted that crystallites formed by SIC in vulcanized NR cause a significant increase in tension during uniaxial elongation, but there are few reports on SIC of NR under multiaxial elongation. In the actual operating environment of NR, it is important to clarify the correlation between SIC and mechanical strength under complex deformation modes such as multiaxial elongation, since strain occurs under conditions similar to those of multiaxial elongation. Therefore, in this study, the behavior of SIC in two-step biaxial stretching of NR was investigated using wide-angle X-ray diffraction (WAXD) at the synchrotron radiation facility.

Although most of the published works are focused on SIC upon the uniaxial stretching, more complicated deformation mode should be examined in order to understand the characteristic features of SIC in the real circumstances of utilizing the elastomeric materials. Since the studies on SIC upon the simultaneous biaxial stretching has been examined, we decided to focus on the case of the two-step biaxial stretching for further understanding the SIC phenomena. For this purpose, we conducted 2-dimensional WAXD measurements along with the two-step biaxial stretching at the synchrotron radiation facilities. The precise measurements enabled us to accurately determine the onset of SIC. Additionally, melting behaviors of crystallites, which were already formed in the first-step stretching, during the second-step stretching process were examined.

Experiments were conducted under the condition that the specimen was extended only in the vertical direction (Y-direction) and subsequently elongated in the horizontal direction (X-direction) with the vertical direction fixed. To grip the specimen by jaws without slippage, the specially designed specimen as shown in Figure 1 was used. The specimen is cross-shaped with a cylindrical protrusion at each end to avoid slippage of the specimen sheet out from the jaw during elongation, bearing a round-shaped dimple with thinner thickness in its central portion. This was designed to be

more easily deformed under a given strain, as compared to the remained four arm portions (limbs) of the specimen. It was required to calibrate the real strain of the dimpled portion by video-recording the deformation process of the mesh lattice (with 1 mm spacing of the lattice pattern) during the deformation of the specimen. Note that the lattice pattern was stamped on the surface of the dimpled portion in prior to installing the specimen. Then, it was found that the dimpled portion can be elongated up to 4-flod of the elongation ratio for the condition of the apparatus operation with maximum stroke between the two crossheads. The incident X-ray beam was introduced at the center of the dimple of this sheet specimen for the WAXS measurements during the biaxial elongation.

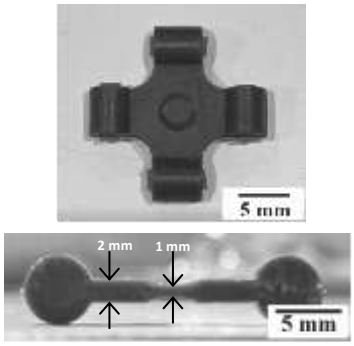


Figure 1. Cross-shaped specimen for the biaxial elongation.

The 2d-WAXD were performed at BL03XU of SPring-8, Japan Synchrotron Radiation Research Institute, Japan. The incident X-ray beam was introduced to the specimen from its normal direction. The exposure time of the X-ray beam was 20 s for each 2d-WAXD pattern measurement. PILATUS 1M (DECTRIS, Switzerland) was used as a two-dimensional detector. The distance from the specimen to the detector was set to 25 cm. The wavelength of X-ray (λ) was set at 0.08 nm.

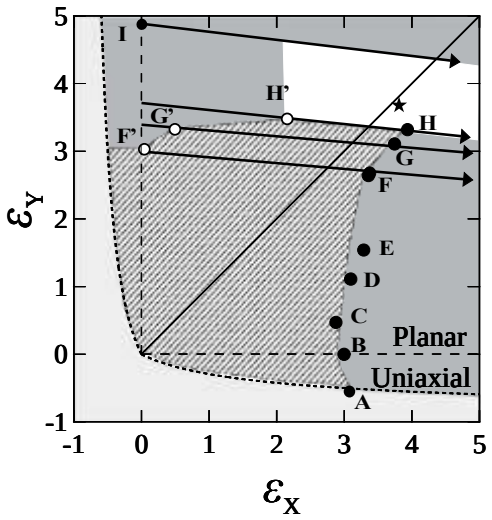


Figure 2. States of SIC shown in the plot of ε_Y vs ε_X for the case of the two-step biaxial elongation (elongation in the Y direction first and then elongation in the X direction). The gray zone indicates that the crystallites formed by the SIC stably exist while the black hatching zone indicates no occurring of the SIC. Experimental exploration has not yet been conducted in the white zone. Star symbol indicates the onset of SIC for the case of the equi-biaxial elongation.

The results are shown in Figure 2, where ε_X is the nominal strain in the X-direction and ε_Y is that in the Y-direction. Points A~ E (●) are the points where SIC formation was confirmed during elongation. When the first-step elongation was beyond the F' point, the SIC took place. In the existence of the SIC crystallites, the specimen was then subjected to the second-step elongation in the X-direction by keeping ε_Y constant. For this kind of experiment, it was found that the SIC crystallites were sometimes melted away. The points F'~G' (○) pinned down such points. In such stepwise stretching, we consider that the complexity of SIC behaviors is related to the orientational state of the polymer chains in the amorphous region. Based on the comprehensive and thorough examination, it was concluded that the SIC upon the two-step biaxial stretching was completely different from any other cases of SIC upon different stretching processes. Finally, we made the comprehensive conclusion that SIC is dependent on the strain histories or the strain routes in other words.

Acknowledgement

This work was financially supported by JST CREST grant number JPMJCR2091, Japan.

AFM Nanomechanics Connecting Macro- and Nanoscopic World

Ken NAKAJIMA[1]

[1] *Institute of Science Tokyo, Tokyo, Japan.*

e-mail knakaji@mct.isct.ac.jp

Keywords: AFM Nanomechanics, Heterogeneous Deformation, Strain-induced Crystallization, Reinforcement Mechanism

Atomic force microscope (AFM) nanomechanics is a useful tool for linking the nanoscale world inside rubber with the macroscopic properties of rubber [1]. Using AFM nanomechanics, which can visualize various nano-mechanical properties such as elastic modulus, our group have clarified various unsolved problems related to rubber. In this presentation, I will introduce the latest developments in this field.

An understanding of the microscopic deformation behavior of crosslinked rubber is key to gaining insight into the mechanisms of the mechanical properties of rubber materials. In this study, we measured isoprene rubber (IR) under uniaxial tensile strain using AFM nanomechanics to track the microscopic deformation of the IR rubber and to visualize the stress distribution at the nanoscale [2]. The results showed that affine deformation, a classical theory in rubber deformation, did not occur at the microscopic scale, and interesting nanoscale heterogeneous deformation behavior was observed as shown in Figure 1(a)-(d). Based on the AFM experimental results, we proposed a microscopic elongation behavior model that takes into account the heterogeneity of the crosslink density shown in Figure 1(e). In addition, we observed microcrystalline structures at the 10 nm scale at high strain, which is believed to be the first time that strain-induced crystallization (SIC) has been visualized in real space. The direct observation of SIC provides an important reference for the investigation of the self-reinforcing mechanisms of crystalline rubber.

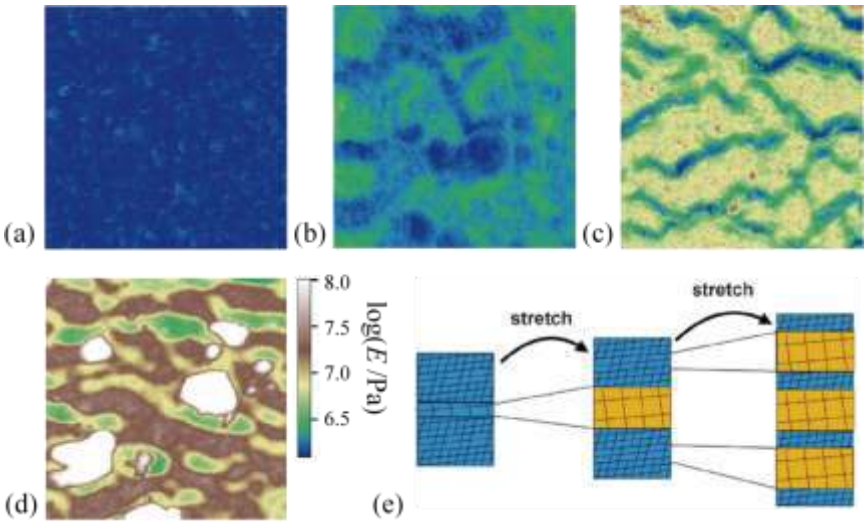


Figure 1. Elastic modulus mappings of IR vulcanizates (a) unstretched; (b) stretched to λ = 100%; (c) stretched to λ = 300% (d) stretched to λ = 500%. The scan sizes are 1.0 µm × 1.0 µm. (e) Schematic diagram of the microscopic deformation behavior based on this transformation process.

An *in-situ* AFM nanomechanical technique can be utilized to directly visualize the micromechanical behaviors of polymer nanocomposites during compressive [3] or tensile [4] strain. We obtained a stress distribution image of carbon black (CB)-filled IR at the nanoscale, with tracing the microscopic deformation behaviors of CB particles. CB filled rubbers exhibited heterogeneous local microscopic deformations, which were related to the dispersion of CB particles in rubber matrices. The local stress distributions of the rubber composites showed heterogeneity, and the stresses were concentrated in the regions near the CB particles during compression as shown in Figure 2(a)-(d). The area of stress concentration gradually expanded with increasing strain and eventually formed a stress network structure as schematically shown in Figure 2(e). This stress network bore most of the macroscopic stress and was considered the key reinforcement mechanism of CB-filled rubber. Based on the image data from the AFM experiments, we used finite-element method (FEM) simulations to reproduce the microscopic deformation process of CB-filled rubber. The stress distribution images simulated by FEM showed heterogeneity consistent with AFM.

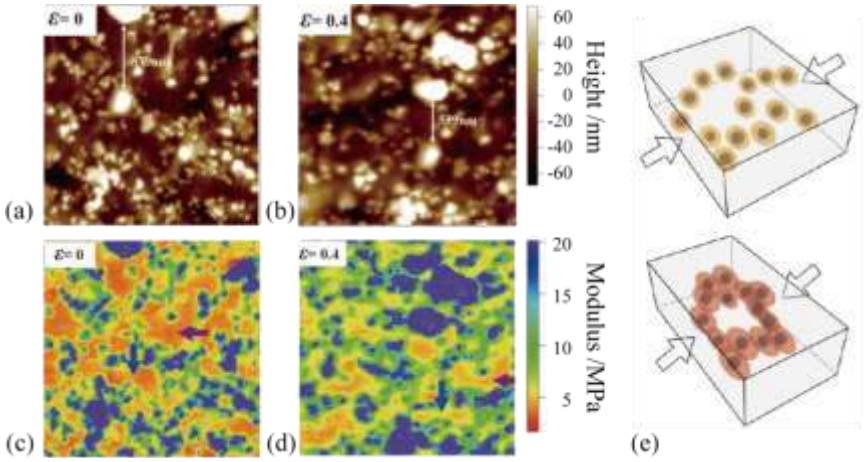


Figure 2. *In-situ* AFM height images of CB-filled IR at macroscopic compressive strains ε = (a) 0 and (b) 0.4. (c) (d) The corresponding modulus images. The scan size is 3.0 μm. (e) Schematic diagram of the formation of stress network.

Acknowledgement

This work was partly supported by JST-Mirai Program Grant Number JPMJMI18A2, Japan and partly supported by JSPS Grant-in-Aid for Scientific Research (B) 23K26714.

References

1. Nakajima K, Ito M, Nguyen HK, Liang X, *Rubber Chem. Technol.*, 2017; 90: 272.
2. Liang X, Nomura R, Iwabuki H, Ito M, Nakajima K, *Polymer*, 2025; 333: 128649.
3. Liang X, Kojima T, Ito M, Amino N, Liu H, Koishi M, Nakajima K, *ACS Appl. Mater. Interf.*, 2023; 15: 12414.
4. Liang X, Liu H, Maeda N, Suzuki M, Ito M, Amino N, Koishi M, Nakajima K, *Macromolecules*, 2025; (*https://doi.org/10.1021/acs.macromol.5c00844*)

Enhancing Coagulation Efficiency and Overcoming Uncoagulation Issues in Skim Latex Using Synthetic and Natural Creaming Agents

Charoen Nakason,[1] Sunida Kaewchuen, [2] Azizon Kaesaman[2]

[1]*Faculty of Science and Industrial Technology, Prince of Songkla University, Surat Thani, Thailand,* [2]*Faculty of Science and Technology, Prince of Songkla University, Pattani,*

The challenge of effectively coagulating skim latex and overcoming its resistance to coagulation after long-term storage was addressed through the use of creaming agents derived from both synthetic and natural sources. Specifically, poly(acrylic acid-co-acrylamide) (AA-co-AM), tamarind kernel powder (TKP), and hydroxyethyl cellulose (HEC) were applied to pre-condition the skim latex via creaming. These agents promote the aggregation of rubber particles by forming interfacial interactions, thereby enabling coagulation with dilute acid rather than the concentrated sulfuric acid typically used in industrial processes. This approach also resolves the issue of latex remaining uncoagulated after extended storage, which is commonly attributed to the presence of stabilizing anions. Stock solutions of the creaming agents were prepared at concentrations of 10 wt% for AA-co-AM, 3 wt% for TKP, and 2 wt% for HEC. Their molecular structures were confirmed through infrared spectroscopy. The creaming agents were then added to skim latex at varying dosages (1.0–14 wt%) and stored at room temperature for 1 to 4 days to allow phase separation. The upper cream layer, enriched in rubber content, was subsequently coagulated using only 10 wt% sulfuric acid after the serum layer was removed. The resulting dry skim rubber was evaluated through a series of tests, including Mooney viscosity, plasticity retention index (PRI), dirt content, ash content, nitrogen content, and standard curing and mechanical properties. Optimal creaming performance was achieved with 0.8 wt% AA-co-AM, 7.0 wt% TKP, and 12.0 wt% HEC. Importantly, the use of these agents significantly reduced the amount of acid required for coagulation—by approximately 50–67% compared to untreated skim latex. Furthermore, the recovered skim rubber exhibited key properties consistent with those of industrial-grade products available in the local market, including Mooney viscosity (61–82), as well as satisfactory values of Po, PRI, tensile strength, elongation at break, and hardness.

References:

1. Kaesaman, A., Kaewchuen, S., Nakason, C. (2024). Implementing eco-friendly creaming agents to address coagulation issues and minimize acid consumption in skim natural rubber latex processing, Industrial Crops and Products, 222, Part 1, 119499. https://doi.org/10.1016/j.indcrop.2024.119499.
2. Kongkaew, C., Loykulnant, S., Chaikumpollert, O. and Suchiva, K. (2010), Creaming of skim natural rubber latex with chitosan derivatives. J. Appl. Polym. Sci., 115: 1022-1031. https://doi.org/10.1002/app.31072

Driving Sustainability in Community-Based Rubber Production: A Case of Energy and Waste Valorization in Thailand

Sumate CHAIPRAPAT[1], Charongpun Musikavong[1], Juthamas Jaichuedee[1], Sayan Sdoodee[2]

[1] *Department of Civil and Environmental Engineering, Faculty of Engineering, Prince of Songkla University, Hat Yai, Songkhla 90110, Thailand.*

[2] *Department of Plant Science, Faculty of Natural Resources, Prince of Songkla University, Hat Yai, Songkhla, Thailand.*

e-mail address of the presenting author (sumate.ch@psu.ac.th)

Keywords: Smoked Sheet Rubber, Zero waste, Carbon neutrality, Local enterprise, Energy conservation

Facing the challenges of the new global environmental agenda, Thailand must mobilize both governmental units and private sectors to drive a collective transition towards sustainability. It is undeniable that past human activities have failed to maintain societal and environmental balance, as reflected in the underachievement of several Sustainable Development Goals (SDGs). To address this, Thailand has adopted the Bio-Circular-Green Economic Model (BCG), a framework emphasizing the nation's strengths in biodiversity and cultural wealth. Aligned with the Sufficiency Economy Philosophy (SEP), BCG promotes the use of appropriate technologies and local innovations to maximize resource efficiency and minimize waste. However, while larger corporations possess the capital and expertise to adapt, local and community enterprises often require additional support. Globally, the Paris Agreement from COP21 initiated a commitment to limit global warming to 1.5°C above pre-industrial levels. Thailand pledged at COP26 to achieve carbon neutrality by 2050 and net-zero greenhouse gas emissions by 2065. Achieving these targets demands technology transfer, capacity building, and systematic collaboration. A structured approach involving carbon footprint evaluation, emission reduction, and offsetting is being pursued to meet these goals.

Since 2015, the PSU Energy Systems Research Institute has supported local Smoked Sheet Rubber Cooperatives (SSRCs) through initiatives promoting sustainable energy and environmental practices. Historically, SSRCs, established under government policy in 1994-1995, served as processing hubs for smallholder rubber farmers. Today, around 300 SSRCs remain active, many struggling with high production costs and environmental challenges such as wastewater and odor emissions.

Research revealed that effluent from rubber factories, when properly treated and managed, could improve crop yields and reduce the use of chemical fertilizers, demonstrating a win-win solution for environmental and economic gains. Further advancements include the installation of biogas production systems and solar energy systems at pilot cooperatives like Ban Sai Kao and Yung Thong, leading to significant reductions in energy use, production costs, and CO_2 emissions—up to 425 tons of CO_2eq per year, equivalent to a 31% reduction. Treated wastewater is also reused for plantation irrigation, contributing to a circular economy model. Recently, efforts have extended towards achieving carbon neutrality certification for SSRCs. Yung Thong Cooperative has become a learning center promoting sustainable practices. Ongoing activities include the registration of organizational carbon footprints, expansion of wastewater reuse systems, and deployment of carbon offset strategies through rubber and palm tree plantations. Ultimately, the goal is to establish Thailand's first carbon-neutral rubber cooperative and to expand these sustainable models to broader sectors including schools, local government units, industries, and communities, amplifying national impact under the BCG framework.

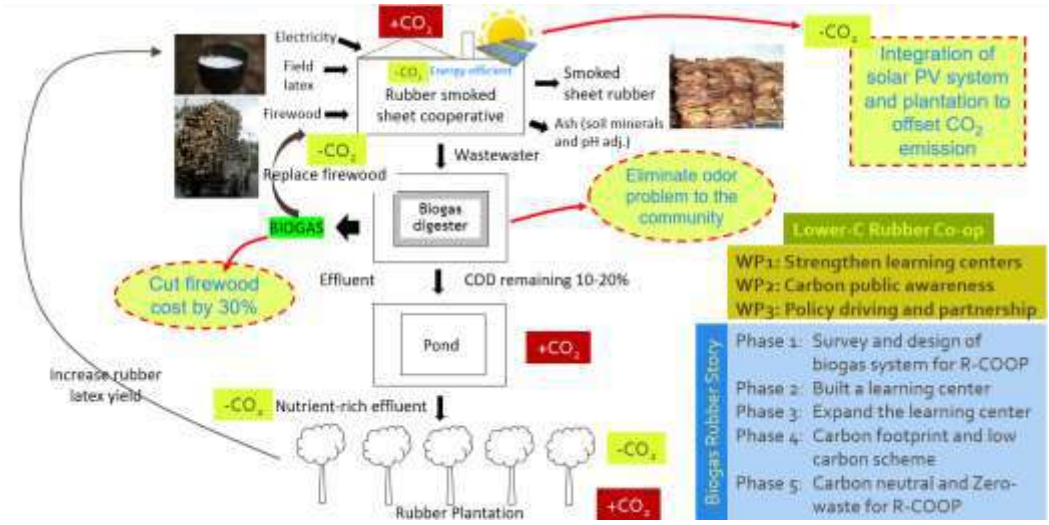


Figure 1. Carbon neutral model for rubber smoked sheet cooperatives



Figure 2. Installation of renewable energy and carbon offsetting scheme

Acknowledgment

The authors would like to acknowledge Thailand Research Fund, National Research Council of Thailand, the Ministry of Energy, Rubber Authority of Thailandฯ and Chevron Thailand Exploration and Production, Ltd. for supports in research, extension, and promotion of the work.

References

1. Chaiprapat, S., Sdoodee, S. “Effects of wastewater recycling from natural rubber smoked sheet production on economic crops in southern Thailand” (2007) Resources, Conservation and Recycling, 51 (3), pp. 577-590.

International Rubber Conference 2025 (IRC2025)
1-3 December 2025 @ BITEC, Bangkok, Thailand

Revisiting the Properties of Natural Rubber in Tire Industry and Development of NR-based Sidewall Compounds for EV Passenger Cars

Kannika SAHAKARO[1], Maimoon HIMMAWONG[1], Warakorn NOISANG[1], Pisit PIMRAT[2]

[1] *Faculty of Science and Technology, Prince of Songkla University, Pattani Campus, Muang, Pattani 94000 Thailand*

[2] *Rubber Industry Division, Rubber Authority of Thailand, Phaholyothin Road, Ladyao, Chatuchaak, Bankok 10900*

*e-mail address: kannika.sah@psu.ac.th

Keywords: natural rubber, STR20, RSS3, tire sidewall, EV tires

Natural rubber (NR) is an essential material for tire production, and it has been used for several parts that require its distinctive properties, like high strength, low heat build-up, good dynamic properties, and excellent adhesion. A sustainability move worldwide makes NR attracting more interest to be adopted as a raw sustainable material. It is known that NR production is subjected to region due to climate conditions, and it has variation in NR properties due to various factors such as clones, ages, rainfall and humidity, production process. In the tire industry, two main forms of NR are utilized, namely Technical Standard Rubber (TSR) and Ribbed Smoked Sheet (RSS). This work shows how the STR20 (Standard Thai Rubber 20) and RSS3 differ in terms of their processing, mechanical- and dynamic properties. The properties of the blends of these two NR forms with butadiene rubber (BR) are then demonstrated. Thereafter, a development of NR/BR tire sidewall compounds for electric vehicle (EV) passenger cars is revealed.

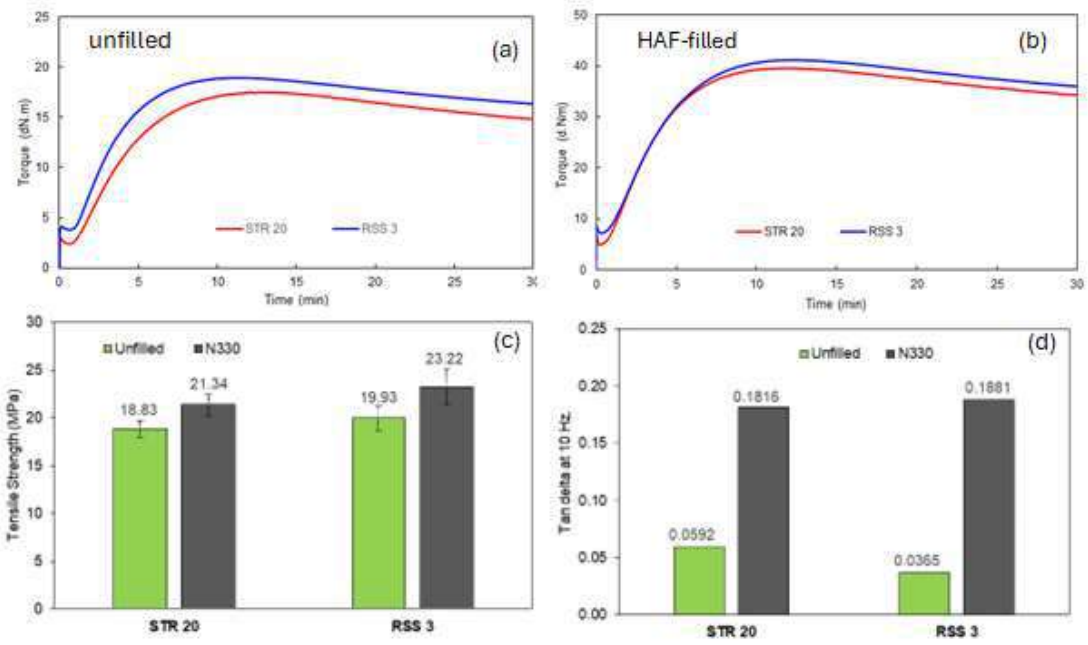


Figure 1. Properties of unfilled- and HAF-filled-compounds comparing the use of STR20 vs. RSS3

The two NR forms in the raw rubber state clearly show different Mooney viscosities and Mooney stress relaxation rates, reflecting their different macrostructures, like the overall network formed and gel originated from their non-rubber constituents. Once they are compounded either without or with filler, the uncured compounds with STR20 and RSS3 show different processing

properties stemming from their original viscosities. The cure, tensile and dynamic properties of the unfilled compounds consisting of STR20 and RSS3 also show different behaviors related to their original viscosity. However, the HAF-filled compounds show similar properties.

The use of STR20 or RSS3 in HAF-filled NR/BR blends for sidewall compounds results in very similar vulcanizate properties, especially the dynamic properties. The STR20 was then chosen for further study in the development of tire sidewall compounds. For EV tires, the sidewall shall have increased hardness and modulus while maintaining satisfactory flexibility and fatigue resistance. Three different grades of BR were compared. A special grade of BR with syndiotactic polybutadiene as dispersed resin in the high cis-BR was explored for its potential to be used to achieve the required hardness while maintaining its flexibility, in comparison with the conventional BR.

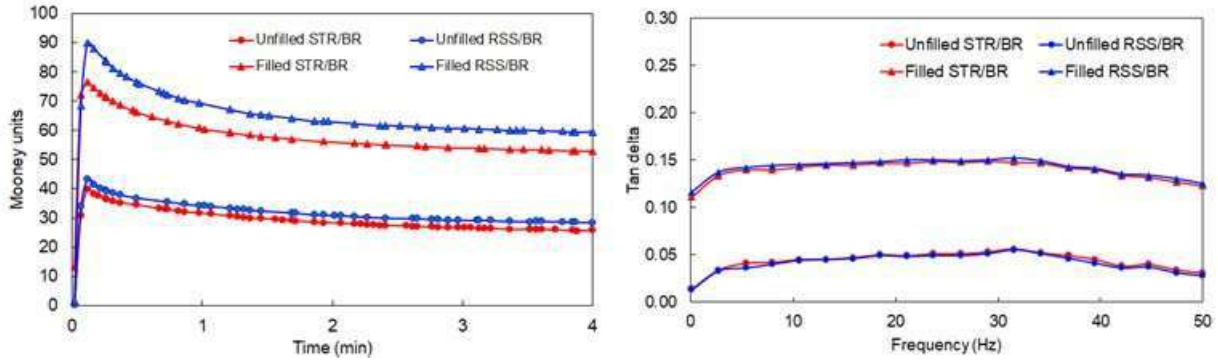


Figure 2. Mooney viscosities and tan delta at 60 °C of unfilled- and HAF-filled NR/BR blends

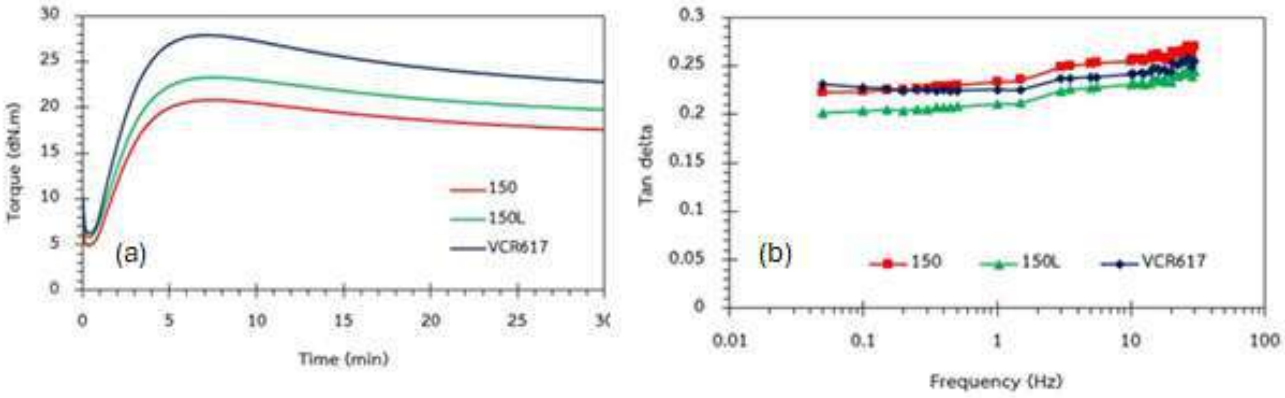


Figure 3. Cure curves and tan delta at 60 °C of filled-NR/BR blends with different BR grades

Acknowledgement

Part of this work was financially supported by the National Research Council of Thailand.

Recent Advances in Reducing Hysteresis of Rubber Composites

Baochun Guo*, Dong Wang, Zhenghai Tang, Liqun Zhang

Institute of Emergent Elastomers, School of Materials Science and Engineering, South China University of Technology, Guangzhou, China.

psbcguo@scut.edu.cn

Keywords: Rubber, Particle, Interface, Heterogeneous crosslinking, Hysteresis

Rubber composites for tires, due to their inherent viscoelasticity, convert substantial mechanical energy into heat during their service under dynamic loading, leading to an increased rolling resistance and fuel consumption for tire products. Heat generation also has a number of detrimental effects such as decreasing mechanical properties, accelerating material ageing and even failure of rubber composites. Reducing the hysteresis and heat generation of rubber composites is therefore of great importance for saving energy and extending service life of rubber products. Key scientific issues in developing the rubber materials with low heat generation include: (1) the interfacial manipulation of particle-reinforced rubber composites and (2) the elucidation of structure-property relationship in the intrinsically reinforced non-filing rubbers. In this talk, the authors summarize related advances in reducing the hysteresis of rubbers. (1) Efficient strategies for interfacial manipulation of particulate-reinforced rubber composites were proposed [1-5]. Various interfacial coupling agents have been designed and synthesized to achieve in-situ and efficient interfacial modification during the processing of rubber composites, resulting in improved particle dispersion, enhanced interfacial interactions and reduced heat generation in rubber composites. (2) A heterogeneous multiphase network of rubber was proposed and designed [6-7], enabling rubber composites with intrinsic reinforcement and extremely low heat generation. The reinforcing mechanism for the soft matrix-induced large extension of hard rubber (SMILE of HR) was revealed. This strategy breaks through the inherent contradiction between mechanical reinforcement and heat build-up in traditional reinforced rubbers.

Acknowledgement

These works were funded by the National Science Fund for Distinguished Young Scholars (51825303), the National Natural Science Foundation of China (52322303, 52073097 and 52130305), the Guangdong Basic and Applied Basic Research Foundation (2023B1515020085).

References

1. Wang J., Wu S., Fang S., et al. *Composites Communications*, 2024; 50: 102002.
2. Fang S., Yu S., Wu S., *Composites Science and Technology*, 2022; 225: 109482.
3. Wang D., Tang Z., Huang R, et al. *Chemistry of Materials*, 2023; 35: 764.
4. Wang D., Tang Z., Huang R., et al. *Macromolecules*, 2022; 55: 8485.
5. Wang D., Chen J., Tang Z., et al. *Macromolecules*, 2024; 57: 470.
6. Fang S., Li F., Liu J., et al. *Nano Energy*, 2021; 83: 1052822.
7. Zhang C., An X., Tang Z., *Macromolecules*, 2021; 54: 11522.

International Rubber Conference 2025 (IRC2025)
1-3 December 2025 @ BITEC, Bangkok, Thailand

Resolving the Microstructure of Natural Rubber and Its Influence on the Mechanical Properties

Junqi Zhang[1], Lingming Kong[1], Zhengtian Xie[1], JINRONG WU[1,*]

[1] *National Key Laboratory of Advanced Polymer Materials, College of Polymer Science and Engineering, Sichuan University, Chengdu, Sichuan, 610065.*

e-mail: wujinrong@scu.edu.cn

Keywords: Natural rubber, strain-induced crystallization, network structure

Natural rubber (NR) is widely utilized in critical fields such as healthcare, aviation, and national defense due to its exceptional comprehensive properties. Global research efforts have increasingly focused on elucidating the structure-property relationships of NR. Previous studies have explored the hierarchical microstructure of pristine NR, including its cis-1,4 structure, ultra-high molecular weight, non-rubber components, and terminal networks, as well as their impacts on mechanical performance. However, traditional processing methods inevitably alter these pristine structures, posing challenges for understanding their intrinsic roles and hindering the development of high-performance NR materials.

To address this issue, we prepared NR samples with distinct preservation levels of pristine structures: VNRL (prevulcanized latex film) and VNR (mechanically mixed vulcanizate), ensuring identical total cross-linking densities. Comparative studies on surface morphology, network homogeneity, entanglement behavior, and mechanical properties revealed that VNRL exhibits a more uniform cross-linked network, higher entanglement density, and a microscopic skeleton formed by non-rubber components. In situ synchrotron wide-angle X-ray diffraction (WAXD) analysis of strain-induced crystallization (SIC) demonstrated that although VNRL shows slightly delayed crystallization onset and lower crystallinity indices ($3.4 < \text{strain} < 6$), but it can form larger crystallite and higher crystallinity indices at high strains ($\geqslant 6$), achieving fracture strength compared to VNR. The homogeneous network also enables VNRL to withstand larger strains, while the non-rubber skeleton enhances tear resistance and energy dissipation.

Building on these insights, we developed a nondestructive latex-based mixing method. The resulting NR (LNR) retains pristine entanglements and forms a homogeneous, low-defect network. Compared to conventional mechanically mixed NR (MNR), LNR exhibits enhanced modulus (2.37 MPa), tensile strength (37.3 MPa), toughness (77.3 MJ/m^3), and fatigue threshold (258 J/m^2). The improved mechanical properties are highly related to the SIC behaviors, including earlier crystallization onset, larger crystallites, and higher ultimate crystallinity. This work establishes a microstructure-guided strategy for designing high-performance NR and demonstrates its potential for extreme-condition applications.

Acknowledgement

This work was supported by the National Natural Science Foundation of China (Grant No. 52173058; Grant No. 52403072), and the National Key R&D Program of China (2022YFD2301202).

.

References

1. Kong L, Zhang J, Huang S, Zhang R, Li J, Xie Z, Wu J. *Macromolecules*, 2025, 58, 6: 3109-3118.
2. Zhang J, Huang S, Kong L, Sakdapipanich J, Zhang R, Xie Z, Wu J. *Macromolecules*, 2024, 57: 11727-11737.

Waste Tire Recycling: The Next Frontier beyond Devulcanization for Low Carbon Living

Rathanawan MAGARAPHAN [1,2 *]

[1]*Polymer Processing and Polymer Nanomaterials Research Unit, Petroleum and Petrochemical College, Chulalongkorn University, Bangkok 10330, Thailand*

[2]*Center of Excellence in Green Materials for Industrial Application, Chulalongkorn University, Bangkok 10330, Thailand*

[*]Corresponding author / E-mail address: Rathanawan.K@chula.ac.th

Keywords: Waste tire, Recycle, Devulcanization, Low carbon, Ground tire rubber

In order to move forward, we need tires. Hence, the demand for tires continues to grow, and today, we face a large accumulation of used tires, which contribute significantly to environmental pollution. These waste tires are typically collected, recovered and used in different ways e.g. energy production, construction materials, landscaping mulch, floor mats, and crafts. For industrial reuse, they are ground into fine powder known as ground tire rubber (GTR). GTR can undergo devulcanization through thermal or chemical treatments, transforming it into reclaimed rubber that can be reprocessed and revulcanized, serving as an eco-friendly alternative in the production of new rubber products.

The thermomechanical with chemicals devulcanization are investigated; selected chemicals were used in comparison to the common devulcanizing agent, diphenyl disulfide. The devulcanization degree of the reclaimed rubbers (D-GTR) achieved more than 80%. When sulfur cross-links are broken, thiol end groups are reformed, enabling thiol-ene reactions [1-2]. By adding unsaturated natural-based compounds containing polar groups, surface adhesion is enhanced. The obtained products (FD-GTR) are green reclaimed-tire rubber with more value-added. They shows low contact angle and good adhesion to metal sheets as confirmed by 180 degree-peel test.

This modification to the reclaimed rubber brings higher glass transition temperature, broadened tan δ and higher storage modulus than those of the reclaimed rubber. It implies that the wasted tire can be processed and used as a sound absorber, electrical and thermal insulators for metal sheet or other polar materials. In other words, this innovation expands the industrial applications of reclaimed rubber, especially in building materials.

Acknowledgement

The author would like to express her gratitude to the National Research Council of Thailand (NRCT) for providing research funding.

.

References

1. Markl E, Lackner M, *Materials, 2*020; 13(5): 1246.

2. Joseph A M, George B, Madhusoodanan K N, Alex R, *Rubber Chem.&Technol.*, 2016; 89(4): 653.

Invited Lectures

IRC 2025
BANGKOK, THAILAND

International Rubber Conference 2025 (IRC 2025)

Cellulose nanocrystal: Scalable production and Innovation Application

Jianming Zhang[1], Hongze Xu[1], Yunxiao Liu[1], Lu Zong[1]

[1] *Key Laboratory of Rubber-Plastics, Ministry of Education/Shandong Provincial Key Laboratory of Rubber-Plastics, Qingdao University of Science & Technology, Qingdao 266042, China*.

zjm@qust.edu.cn

Keywords: Cellulose nanocrystals, Bio-based materials, Graft polymer

Cellulose nanocrystals (CNCs), derived from the world's most abundant natural polymer, are an emerging class of green nanomaterials. Their exceptional stiffness, high specific surface area, biodegradability, and rich surface chemistry make them ideal, sustainable reinforcements for the rubber industry. Beyond mechanical reinforcement alone, distinctive attributes—such as amphiphilicity and a propensity to form chiral nematic phases—unlock opportunities for high-performance, multifunctional rubber composites. Over the past decade, our team has emphasized green, efficient CNC production and high-value applications. We have developed a suite of surface-modification strategies, including polymer grafting [1-2] and small-molecule functionalization, to create polymer-grafted CNCs with tailored interfacial compatibility [3].

Recently, our focus has shifted from "reinforcement" toward "functionalization," leveraging CNCs' intrinsic properties to enable new functions: **(1) In Rubber Industry**: using CNC amphiphilicity as a "green dispersing aid" to homogenize traditional additives (e.g., sulfur, accelerators) within the rubber matrix, thereby improving vulcanization efficiency and the consistency of mechanical properties. **(2) In Photonic Materials**: by precisely controlling chiral-nematic self-assembly, we fabricate CNC/rubber photonic elastomer films with vivid structural colors that display stimulus-responsive color changes (e.g., strain, solvent vapor), offering pathways to smart sensors and anti-counterfeiting coatings. **(3) In Bio-based Materials**: by exploiting the supramolecular networks formed by polymer-grafted CNCs, we develop bio-based thermoplastic elastomers combining high strength, reprocessability, and self-healing; capitalizing on their optical properties and biocompatibility, we further explore their use as smart artificial-tendon systems. Collectively, our work establishes a robust scientific and technological foundation for the industrialization and high-value utilization of CNCs.

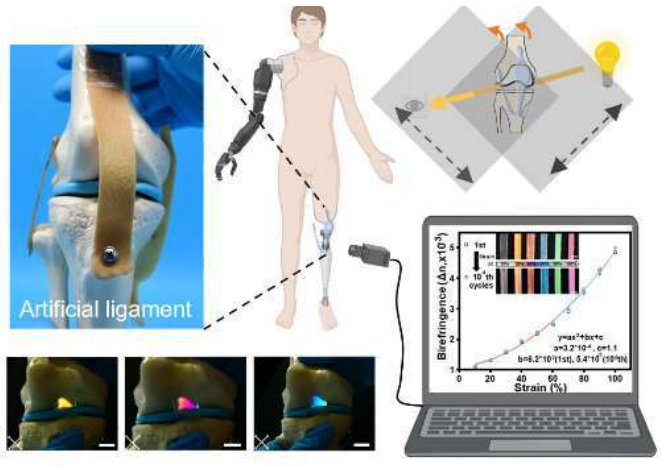


Figure 1. CNC-PVA hydrogel artificial ligament and intelligent sensing application display

Acknowledgement

Financial supports from the National Natural Science Foundation of China (No. 52473037)

References

1. Yunxiao L, Hongze X, Lijuan Z, Jianming Z, *Green Chem. J.*, 2023, 25: 3027-3033.
2. Yunxiao L, Yunjie L, Hui Z, Xinran L, Zhengqing K, Lijuan Z, Heng L, Jianming Z, *Green Chem.*, 2021, 23: 8581.
3. Xiangdong H, Hao W, Yunxiao L, Jian H, Yongxin D, Jianming Z, *Macromolecules*, 2025, 58: 2508–2520.

Self-Healing Rubber: An Advancing Technology for Smart Gloves

Siah Ying TANG[1*], Darren Yi Sern LOW[1], Janarthanan SUPRAMANIAM[2]

[1] *Department of Chemical Engineering, School of Engineering, Monash University Malaysia, 47500 Bandar Sunway, Selangor Darul Ehsan, Malaysia.*

[2] *School of Pharmacy, Monash University Malaysia, 47500 Bandar Sunway, Selangor Darul Ehsan, Malaysia*.

*E-mail: patrick.tang@monash.edu

Keywords: Self-healing rubber, gloves, autonomous, chemical resistance, supramolecular polymer.

Self-healing rubbers represent a transformative and revolutionary advancement in polymer science with significant potential across sectors such as tires, personal protective equipment, soft electronics and smart textiles. Through tailoring and customizing polymer chemistry and leveraging reversible intrinsic chemical interactions, self-healing properties can be effectively combined with rubber matrices.

In our Colloids and Polymers research group, we are developing next-generation rubber gloves that integrate intrinsic self-healing capabilities through engineered supramolecular rubber networks [1, 2]. These reversible non-covalent interactions enable autonomous repair of micro-damages through bond reformation, as shown in **Figure 1**. This provides rubber gloves with extended lifespan and maintaining material integrity and protection under stress. Our innovation addresses a critical need in high-risk environments, such as in chemical handling, agriculture, and heavy industrial manufacturing, where torn gloves are often reused or unchanged [3]. This increases the dermal exposure of users towards hazardous substances. By fine tuning the healing dynamics and chemical resistance during material formulation, we aim to create durable reusable gloves that offer both performance and environmental advantages. This approach not only enhances user safety, but also contributes towards reducing glove waste, presenting a sustainable alternative for industrial applications with advancing self-healing technology.

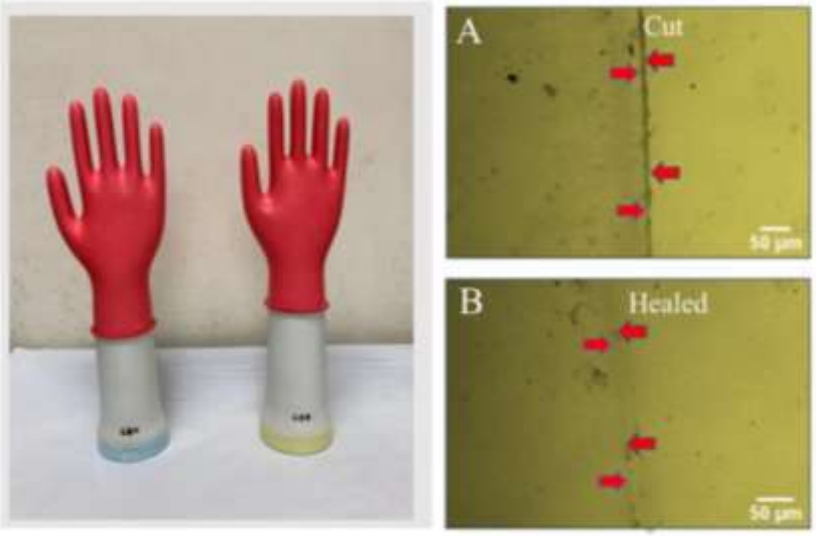


Figure 1. (Left) Self-healing rubber glove prototype; (Right) Optical microscopy image of (A) freshly cut and (B) self-healed rubber sample.

References

1. Low DYS, Supramaniam J, Goh BH, Manickam S, Tang SY, *Adv. Funct. Mater.*, 2024; 34:2401345.
2. Supramaniam J, Low DYS, Wong SK, Leo BF, Goh BH, Tang SY, *Chem. Eng. J.*, 2021; 437:135440.
3. Supramaniam J, Low DYS, Wong SK, Goh BH, Leo BF, Tang SY, *Sci. Rep.*, 2021; 12:4275.

International Rubber Conference 2025 (IRC2025)
1-3 December 2025 @ BITEC, Bangkok, Thailand

Effect of Molecular Architecture on the Thermal Stability of Poly(epichlorohydrin-co-ethylene oxide-co-allyl glycidyl ether) (GECO) Based Elastomers

Murat ŞEN[1,2], Anıl TATLIDİLLİ[1], Davut AKSÜT[2]

[1] *Polymer Science and Technology Division, Hacettepe University, Institute of Science, Ankara, Turkey*.

[2] *Hacettepe University, Department of Chemistry, Polymer Chemistry Division, 06800, Ankara, Turkey*.

e-mail address of the presenting author (senmura3@gmail.com)

Key Words: Hydrin polymers, molecular architecture, thermal stability, thermal degradation behavior.

The increasing demand for high-temperature-resistant and vibration-damping materials in advanced technological industries such as aerospace, defense, and automotive has highlighted the limitations of conventional rubbers [1]. Although materials such as natural rubber, nitrile rubber, butyl rubber, chloroprene, and silicone rubbers are widely used for vibration damping, their insufficient resistance to high temperatures, UV radiation, ozone, and oil swelling significantly limits their applications.

Epichlorohydrin-based elastomers have gained importance in recent years due to advancements in synthesis techniques [2]. Epichlorohydrin (ECH)-based polymers are categorized into three main groups based on their structural differences: epichlorohydrin homopolymer (PECH or CO), a random copolymer of epichlorohydrin and ethylene oxide (ECO), and a terpolymer consisting of epichlorohydrin, ethylene oxide, and allyl glycidyl ether (GECO). The molecular architecture of ECH-based elastomers plays a crucial role in determining their key properties, such as high thermal stability, resistance to heat and chemicals, and damping performance.

In this study, four commercial GECO terpolymers, T3102, T3108, T3000LL, and T3100, were selected for evaluation. The compounds were prepared using a Thermo-Haake Rheomix OS Lab mixer, following specified formulations. The curing behavior of the compounds was analyzed using an Alpha Technologies MDR 2000-B (USA) Moving Die Rheometer (MDR). The prepared samples underwent thermal aging at 120 °C for a total of 24 days, with different aging durations. Mechanical and chemical properties were evaluated before and after aging. The changes in mechanical properties caused by aging were assessed in accordance with the ASTM D412 standard.

The influence of terpolymer molecular architecture on thermal aging resistance was examined using spectroscopic and thermogravimetric analyses. FTIR spectroscopy was used to detect chemical changes induced by aging, while thermal lifetime was estimated from TGA data using the Flynn-Wall-Ozawa method.

The tensile strengths of elastomers with and without 6PPD were evaluated after various aging periods at 120 °C. The results for tensile strength and elongation at break indicate that molecular architecture is a key factor influencing the thermal stability of hydrin-based elastomers. Among the systems studied, T3102 which has the highest ECH and lowest AGE content exhibited the best thermal stability.

Furthermore, 6PPD was found to be a highly effective thermal stabilizer for hydrin-based elastomers. While the tensile strength of all 6PPD-free hydrin elastomers decreased from approximately 8 MPa

to below 1 MPa after three weeks of thermal aging, systems containing 1 phr 6PPD retained approximately 50% of their mechanical properties. These results demonstrate that 6PPD is a critical and beneficial additive not only due to its compatibility with the polymer matrix but also for further enhancing the already inherent thermal stability of hydrin polymers.

Acknowledgments

The authors gratefully acknowledge financial support from The Scientific and Technological Research Council of Türkiye, under the 2224-A Grant Program for Participation in Scientific Meetings Abroad.

References

[1] Thangapandian N, Satthiyaraju M, GaneshKumar P, Sivalingam V. Investigation of vibration, flexural, tribological and flame retardant properties on rubber crumb-reinforced polymer composites. Progress in Rubber, Plastics and Recycling Technology. 2024;40(3):305-319. doi:10.1177/14777606231220420

[2] Baggett JM, Pruitt ME. (Dow Chemical Co.) Patent US2871219.1959.

[3] Şen M, Soydas O, Aksüt A, "Preparation and characterization of high damping poly(epichlorohydrin) and poly(epichlorohydrin-co-ethylene oxide-co-allyl glycidyl ether) elastomers: I. Effect of curing system and blending on the damping properties Reactive and Functional Polymers, 2023; 184:105520. DOI:10.1016/j.reactfunctpolym.2023.105520

[4] Yalaki Y, Şen M." Effect of molecular and structural architecture of poly(epichlorohydrin-coethylene oxide-co-allyl glycidyl ether) on the properties of its elastomers", Polym Adv Technol. 2024;35:e6592. https://doi.org/10.1002/pat.6592

Delayed Crystallization Response-Inspired Waterborne Polyurethane with High Performance

Chenxi Huyan[1], Fei Chen[1], Liqun Zhang[1,2]

[1] *State Key Laboratory of Fluorine and Nitrogen Chemicals, School of Chemical Engineering and Technology, Xi'an Jiaotong University, Xi'an, Shaanxi, 710049, P.R. China*

[2] *Center of Advanced Elastomer Materials, State Key Laboratory of Organic-Inorganic Composites, Beijing University of Chemical Technology, Beijing, 100029, P.R. China*

feichen@xjtu.edu.cn

Keywords: Waterborne polyurethane, Toughness, Delayed crystallization, Hydrogen bonding, Sustainable elastomer

Waterborne polyurethane elastomers (WPUE), synthesized in aqueous solutions, represent a revolutionary sustainable alternative to thermoplastic polyurethane elastomers (TPUE), which are typically produced using organic solvent. This shift significantly reduces VOC emissions[1]. However, WPUE often lacks the mechanical strength of TPUE produced through traditional synthetic methods, limiting its potential as a sustainable option[2]. This work aims to overcome this performance gap by introducing a high-performance WPUE (HPWPUE) by leveraging a self-reinforcement mechanism known as the delayed crystallization response (DCR).

Our success lies in the use of symmetrical monomers that enhance the formation of a dynamic biphase structure, promoting the formation of hydrogen bonding during stretching and enabling crystallization at higher strains. When HPWPUE is stretched, steric hindrance from hydrophilic segments causes hard domains to break into isolated segments, increasing the stretch ratio and necessary for the co-crystallization of hard-soft segment at high strain, while this process is accompanied by the destruction of hydrogen bonds, providing additional energy dissipation for HPWPUE. Beyond a stretch ratio (λ) of about 20, the hard segments align with the soft segments, resulting in co-crystallization that significantly enhances strength and toughness [3,4]. Ultimately, the DCR process enables the HPWPUE to achieve an exceptional toughness of 0.959 GJ/m³ and a high strength of 81.8 MPa, surpassing to those of both commercial TPUE systems and TPUE materials reported in most academic studies (Figure 1).

The critical prerequisites for DCR-based reinforcement were identified as: First, interchain hydrogen bonding must provide sufficient energy dissipation to prevent premature chain breakage during stretching. Second, the elastomer should not have a highly cross-linking structure, as this can hinder molecular rearrangements and lead to stress concentration. Third, the hard-domain structures within the polyurethane network cannot pack tightly, as this would impede their dissociation and reorganization during stretching. Finally, the elastomer chain segments should exhibit a strong tendency to crystallize upon alignment. Moreover, the material can be scaled up into large-area transparent films (1.5 m × 1.5 m × 1 mm), demonstrating industrial relevance.

By leveraging our insights into mechanical enhancement through DCR, this work establishes a blueprint for designing next-generation sustainable elastomers with superior performance. Future research will further refine the applicability of the DCR strategy, expanding its impact across diverse

polymeric systems and accelerating the transition toward high-performance, environmentally responsible materials.

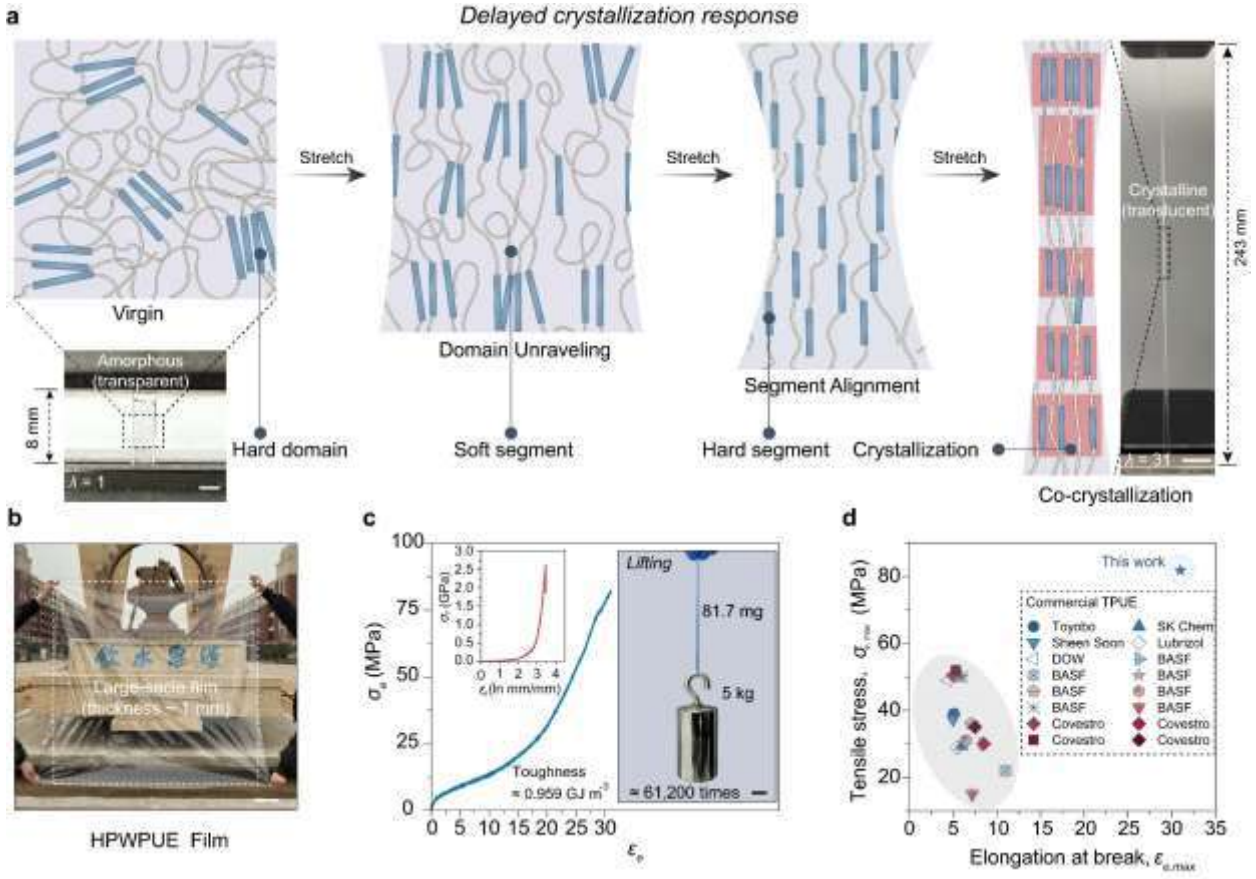


Figure 1. Microstructural changes in our HPWPUE during the DCR process and their mechanical properties

Acknowledgement

This work is supported by National Natural Science Foundation of China (No. 22205174, No. 22178278 and No. 22308271), National Key Research and Development Program of China (2022YFF0503503), the Research Fund for Shaanxi Province's "One School, One Policy" Project" and the Programme of Introducing Talents of Discipline to Universities (B23025).

References

1. Shi X, Wang Z, Liu S, Xia Q, Liu Y, Chen W, Yu H, Zhang K, *Nat. Sustain.*, 2024; 7: 315–325.
2. Chen SY, Kokalari I, Parnell SR, Smith GN, Zeng BH, Way TF, Chuang FS, Rwei SP, *Langmuir*, 2023; 39: 10033–10046.
3. Liu C, Morimoto N, Jiang L, Kawahara S, Noritomi T, Yokoyama H, Mayumi K, Ito K, *Science*, 2021; 372: 1078–1081.
4. Hartquist CM, Lin S, Zhang JH, Wang S, Rubinstein M, Zhao X, *Sci. Adv.*, 2023; 9: eadj0411.

Development of Helically-Wound Pineapple Leaf Fiber/NR Foam Composite for Near Zero-Volume Safety Devices

Taweechai AMORNSAKCHAI[1, 2], Wongsathorn SAITRONG[2], Sorn DUANGSUWAN[2]

[1] *Center of Sustainable Energy and Green Materials, Faculty of Science, Mahidol University, Nakhon Pathom, Thailand.*

[2] *Department of Chemistry, Faculty of Science, Mahidol University, Nakhon Pathom, Thailand.*

e-mail address of the presenting author (taweechai.amo@mahidol.ac.th)

Keywords: pineapple leaf fiber, NR foam tape, biochar, zero-waste, near-zero-volume

1. Introduction & Concept

A closed-loop, carbon-negative platform is introduced using natural rubber (NR) reinforced with pineapple leaf fiber [1] (PALF, 10 phr) and foamed in situ via unidirectional tape + helical mandrel winding. Unlike fabric laminates, tape off-cuts are fully recyclable by re-compounding. No extrusion, no injection, no solvent—only ambient winding + single-step cure in hot air oven (150 °C) with optional external coating for color and waste reduction. Fiber moisture + blowing agent (if needed, adjustable per desired expansion) generate internal pressure, creating cross-plied foam structures that:

- Collapse to ≥10 mm thickness (minimum 2 × wall; up to 87 % volume reduction)
- Recover in <10 s
- Replace rigid plastics (HDPE, LDPE, PVC, PU) and heavy solid NR in shape-retaining applications.



Figure 1. Helical winding process on a mandrel (left) and SEM of closed-cell foam microstructure (right)

2. Sustainability Framework

Table 1. Sustainability Pillars of the Proposed Pineapple Leaf Fiber/NR Foam Tape Platform

Pillar	Implementation	Benefit
Biogenic carbon	PALF 10 phr + pineapple-leaf biochar (5–30 phr) replaces carbon black	Carbon-negative lifecycle
Zero-waste	Tape trimmings re-melted; external color coating minimizes scrap	Closed material loop
Low-energy forming	Hot air oven cure vs. high-pressure molding	Reduced energy use
Compact logistics	Fold-flat design (tunable ≥10 mm thickness)	Up to 87 % volume reduction

3. Proof-of-Concept: Self-Inflating Rescue Float

A 0.9 m × ~500 g fold-flat rescue float fits in a compact cylindrical pack (Ø12 × 16 cm) and springs back instantly to full cylindrical shape upon unpacking due to the helically-wound foam tube structure—no CO_2 cylinder required. Modular 30 cm segments are connected with a one-way valve (air in only). A 30-s video demonstration will be shown during the presentation, demonstrating 80 kg buoyancy.

4. Proposed Applications (Compression-Driven)

- Self-erecting traffic delineator
  - Rebounds after 1.5 t rollover
  - Safer than HDPE/PVC/PU: no sharp fragments, absorbs 70 % impact energy
- Foldable pressure hose (3 bar target)
- Shatter-proof anti-glare panels

5. Challenges & Mitigation Roadmap

- Long-term compression set during fold-flat storage
  - Limit minimum flattened thickness to ≥10 mm (2×wall) → prevent permanent deformation
  - Tune compression level (10–20 mm) → balance 70–87 % volume saving vs. recovery time
  - Silica 5 phr → 58 % set reduction [2]
  - Optimize vulcanization system (CV, EV, or semi-EV) → tailored cross-link density for improved set resistance [3]
- Environmental durability (≥ 5-year service life)
  - External protective coating → UV & ozone barrier
  - Antioxidant system → weather resistance
  - Accelerated weathering (QUV-B) → verify long-term recovery
  - Field exposure trial (roadside, 12 months)

6. Conclusion

This zero-waste, near-zero-volume platform is expected to transform 1.2 Mt Thai pineapple waste into lightweight, shape-retaining, safer-than-plastic safety infrastructure—offering a promising alternative beyond tensile-focused rubber composites.

Acknowledgement

This research project is supported by Mahidol University (Fundamental Fund: fiscal year 2023 by the National Science Research and Innovation Fund (NSRF); Grant No. FF-069/2566) and Thailand Textile Institute.

References

1. Kengkhetkit N, Amornsakchai T, *Materials & Design*, 2014; 55: 292.
2. Vishvanathperumal S, Anand G, *Silicon*, 2022; 14: 3523.
3. Ehabe E E, Farid S A, *European Polym. J.* 2001; 37: 329.

Natural rubber foam containing gamma-synthesized chitosan for the utilization as enhanced heavy-metal sorbents

Thitiwan INTHA[1,2], Ekachai WIMOLMALA[3], Pattra LERTSARAWUT[4],
Kiadtisak SAENBOONRUANG[1,2]

[1] *Department of Applied Radiation and Isotopes, Faculty of Science, Kasetsart University, Bangkok 10900, Thailand*

[2] *Special Research Unit of Radiation Technology for Advanced Materials (RTAM), Faculty of Science, Kasetsart University, Bangkok 10900, Thailand*

[3] *Polymer PROcessing and Flow (P-PROF) Research Group, Division of Materials Technology, School of Energy, Environment and Materials, King Mongkut's University of Technology Thonburi, Bangkok 10140, Thailand*

[4] *Nuclear Technology Research and Development Center, Thailand Institute of Nuclear Technology (Public Organization), Nakhon Nayok 26120, Thailand*

e-mail address of the presenting author (kiadtisak.s@ku.th)

Keywords: Natural rubber foam, heavy metals, chitosan, gamma irradiation, wastewater

This study investigated the development of sustainable and eco-friendly heavy metal sorbents by incorporating gamma-synthesized chitosan (CS) into natural rubber foam (NRF) in order to meet the urgent need to manage industrial wastewater contamination, especially from toxic metals such as copper (Cu), lead (Pb), zinc (Zn), and cadmium (Cd), using environmentally friendly, biodegradable materials. Chitosan, derived from the deacetylation of chitin (CT), is a biopolymer known for its strong metal-binding affinity due to its abundant amino groups ($–NH_2$). However, conventional chitosan synthesis involves hazardous chemical conditions. As a result, the present work explored gamma irradiation as a green, pre-treatment step to enhance the efficiency of chitosan synthesis and its subsequent heavy-metal adsorption performance in NRF composites.

To prepare the samples for the study, chitin powder obtained from shrimp shells was irradiated at gamma doses ranging from 0 to 100 kGy and then deacetylated in 40% sodium hydroxide (NaOH) at 100 °C for 1 h to obtain CS powder. The irradiated CS exhibited increased degrees of deacetylation (%DD), with a maximum of 81.3% observed at 60 kGy (CS60). CS was then added to NRL at 0, 3, 6, and 9 phr, and the foams were prepared using the Dunlop method. The resulting NRF samples were characterized for their morphology, functional groups, thermal stability, mechanical properties, density, and pore structure.

The results demonstrated that the incorporation of CS increased surface area and density of NRF, particularly in samples with 9 phr CS60. The foams exhibited open-cell structures with evenly distributed CS particles. Mechanical testing revealed increased compression set and hardness with higher CS content, indicating enhanced rigidity due to the presence of CS. Thermal analysis showed no significant degradation up to 480 °C, confirming the material's thermal stability.

Additionally, the heavy metal adsorption performance of the developed foams was tested using standard solutions (25 mg/L) of Cu, Pb, Zn, and Cd. The NRF composite with 9 phr CS60

exhibited the highest removal efficiencies: 94.9% for Cu, 82.5% for Pb, 91.4% for Zn, and 97.0% for Cd. These improvements were attributed to increased amino group content and surface area, promoting electrostatic interaction with metal ions. Although the removal capacity per unit mass (mg/g) showed less variation due to increased sample density, the reusability tests revealed sustained adsorption over three cycles, with Cu adsorption remaining at 83% in the sample containing CS60.

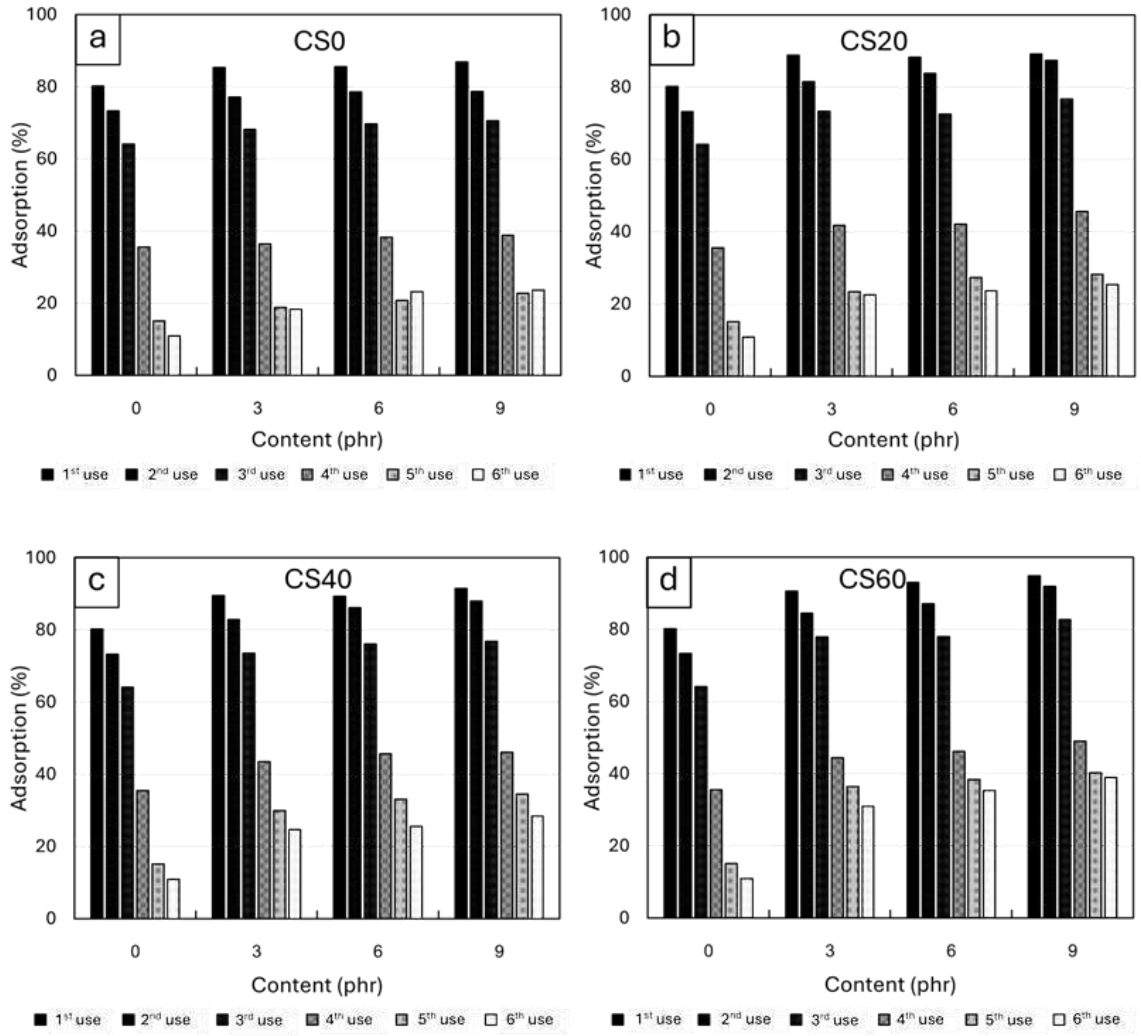


Figure 1. Copper (Cu) adsorption abilities for NRF containing varying contents of (a) CS0, (b) CS20, (c) CS40, and (d) CS60, determined for a total of six cycles of use.

Acknowledgement

This research was funded by Kasetsart University (Bangkok, Thailand) through the Graduate School Fellowship Program; and the Kasetsart University Research and Development Institute (KURDI) (Bangkok, Thailand) through grant number FF(KU) 51.67.

References

1. Intha T, Wimolmala E, Lertsarawut P, Saenboonruang K, *Sustainability*, 2024; 16: 6282.

Synthesis of Polyester-based Multiblock Copolymer Elastomers via A Cascade Polymerization Method

Yingfeng Tu[1], Xueting Wan[1], Mujia Yang[1]

[1] *College of Chemistry, Chemical Engineering and Materials Science, Soochow University, Suzhou, China.*

(tuyingfeng@suda.edu.cn)

Keywords: polyester, cascade polymerization, block copolymer, cyclic ester, elastomer

Polyesters are typically synthesized via condensation polymerization between diacids and diols, or by ring opening polymerization of lactones. However, these two techniques have complementary merits and drawbacks. Condensation polymerization can produce functional aliphatic polyesters directly by the introduction of the desired groups into monomers, yet the accompanying side reactions due to the high reaction temperature and long polymerization time make it unsuitable for the preparation of high molecular weights polyesters. ROP can produce polyesters with a high molecular weight and low polydispersity, yet the functional groups are hard to be introduced into polyester backbones due to the lack of suitable monomers.

Here we introduce a new cascade polymerization method, i.e., polycondensation-coupling ring-opening polymerization (PROP), for the synthesis of polyester copolymers using cyclic esters and diols as monomers (Figure 1). The cascade polymerization mechanism has been proved by the polymerization kinetics studies and the observation of polymerization intermediates. Thermodynamics studies indicate PROP is an entropy-driving polymerization process. By the combination of chain-growth and step-growth polymerization together in one system, PROP has the merits of fast polymerization speed, easy to handle with mild polymerization conditions, good tolerance of functional groups, and high molecular weights of polyesters are achievable. When use polyether diols as macromonomer, poly(ether esters) multiblock copolymers (mBCPs) can be obtained. These poly(ether ester) mBCPs have potential applications in thermoplastic elastomers and energy storage materials.

The cascade polymerization technique is capable to prepare thermoplastic elastomers with high strength and toughness. By introducing metal-ligand coordination bonds as sacrificial bonds into mBCP elastomers, ultra-strong and tough elastomers with a double crosslinked supramolecular network structure are prepared, using terpyridine diol, polyether diol and cyclic esters as monomers. By using diamine and cyclic esters as monomers, poly(ester amide) elastomers can be obtained.

It should be noted, the cyclic ester monomers can be prepared from the recycled polyesters, based on the ring-chain equilibrium in dilute solutions. Thus a value-added route for chemical recycling of polyesters is established, using recycled cyclic esters as monomers to prepare high performance poly(ether ester) elastomers. We believe this method is a promising chemical recycling route for polyesters.

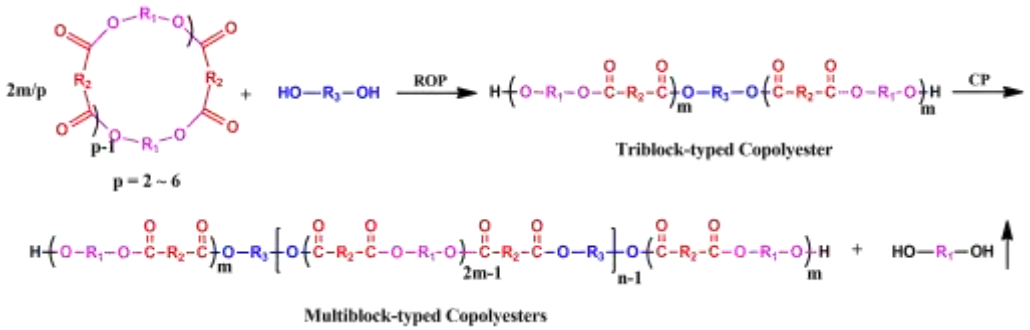


Figure 1. Schematic illustration of cascade polycondensation-coupling ring-opening polymerization method.

Acknowledgement

The financial support from the National Natural Science Foundation of China (Grants 22231008 and 22071167) is gratefully acknowledged.

References

1. Z. Li, J. Wang, X. Li, Y. Wang, L.-J. Fan, S. Yang, M. Guo, X. Li, and Y. Tu, *ACS Macro Lett.* 2020; 9: 1655.
2. X. Wan, J. Jiang, Y. Tu, S. Xu, J. Li, H. Lu, Z. Li, L. Xiong, X. Li, Y. Zhao and Y. Tu, *Polym. Chem.* 2021; 12: 6022.
3. J. Chen, S. Wang, J. Huan, Z. Li, X. Yang, X. Li, Y. Tu, *Macromolecules* 2024; 57: 4054.

Greener Tire Tread Compounds by Reducing the Amount of Ingredients

Anke Blume, Frances van Elburg, Fabian Grunert and Auke Talma

University of Twente, Faculty of Engineering Technology, Department of Mechanics of Solids, Surfaces & Systems (MS3), Chair of Elastomer Technology & Engineering, Enschede, The Netherlands

(a.blume@utwente.nl)

Keywords: sustainability, sulfur curing; SSBR; vinyl content; accelerator; Zinc oxide; stearic acid

Since Charles Goodyear discovered the method of sulfur curing Natural Rubber in 1839, many studies have been carried out to understand its mechanism. Currently, the broadly accepted mechanism includes an activated accelerator complex formed by Zinc oxide, stearic acid, accelerators and sulfur. Furthermore, it is also broadly accepted that the coupling of the sulfur to the polymer takes place in the allylic position to the double bond. Modern passenger car tire treads no longer contain Natural Rubber but instead a blend of Solution Styrene Butadiene Rubber and Butadiene Rubber, filled with a silica/silane system.

By using a tire tread compound based on a blend of high vinyl SSBR and high-cis BR, a different reaction mechanism for the sulfur curing takes place. The direct coupling via a sulfur radical is the dominant mechanism in such a rubber compound. The generally assumed coupling to the allylic position is only valid, e.g., in NR, when there are no vinyl groups. The direct sulfur coupling in a high-vinyl SSBR does not need any activators nor DPG; the presence of an activator for the sulfur ring opening like TBBS is sufficient. It can be considered that the coupling of the silane to the polymer, attached already to the silica surface, follows the same mechanism, a direct coupling via a sulfur radical. Therefore, a new tire tread compound should be based on high-vinyl SSBR/high-cis BR without ZnO, without stearic acid and without DPG. With this, the manifold inter-actions in the typical silica/silane filled green tire tread compound are significantly reduced, avoiding unwanted reactions like the interaction of stearic acid with silane which negatively influences the silica/silane coupling.

The abraded wear particles from such new tires will be less harmful for the environment. These tire wear particles do not contain any Zn species which are toxic to aquatic systems. The use of DPG can also be avoided, since this releases harmful aniline. This will have a very positive effect on the overall microplastic pollution caused by tire wear. Furthermore, the big particles of ZnO are not well dispersed in the rubber matrix. By leaving them out, the compounds do not contain these inhomogeneous spots which can be the origin of abrasion. For this reason, the wear resistance from such tire tread compounds is expected to be better.

This new tire tread compound contains less ingredients which also reduces the production costs. It leaves two environmentally critical substances out: Zinc species as well as DPG. This unique new approach of reducing the number of substances without compromising the in-rubber performance enables the design of a more sustainable, more eco-friendly tire tread compound and paves the way for further innovations.

Introduction of Reversible Bonds into Rubber Networks

Toshio Tada,

Sumitomo Rubber Industries, Ltd., 3-6-9, Wakinohama-cho, Chuo-ku, Kobe 651-0072, Japan.

t-tada.cx@srigroup.co.jp

Keywords: Reversible bond, Boroxine network, Recycle

Introduction

With growing interest in environmental issues, the tire industry is developing a framework for establishing a sustainable society. Recycling materials from end-of-life tires is one potential solution toward a sustainable society by reducing the usage of raw materials. However, material recycling from end-of-life tires through devulcanization is uncommon, likely due to technical limitations and environmental impact. To address this issue, the introduction of reversible bonds into the rubber network is a possible approach. In this study, the introduction of ionic bonds to commercial rubber is investigated through a relatively simple reaction pathway.

Firstly, recent advancements have focused on the molecular design and functionalization of styrene-butadiene rubber (SBR) to further enhance performance [1]. Ionic modification of SBR, especially through in-chain grafting, has shown remarkable effects on improving the dispersion of silica particles and enhancing the mechanical properties of tire compounds. This study explores the use of catalyst-free nitrile N-oxides for the ionic functionalization of solution-polymerized SBR, aiming to achieve high-performance tires with enhanced strength and reduced rolling resistance.

Experimental Section

The study synthesized nitrile N-oxides with carboxylic acid and pyridine groups and used them to modify SSBR both in solution and in the solid state. Characterization techniques included 1H NMR, FT-IR, gel permeation chromatography, DSC, and tensile tests. The modification process involved refluxing a THF solution of SSBR and nitrile N-oxides or mechanically kneading the mixture at elevated temperatures.

Materials and Methods

The study utilized various chemicals and materials, including 2-hydroxy-1-naphthaldehyde, ethyl 6-bromohexanoate, and SSBR, sourced from reputable suppliers. Characterization techniques included 1H NMR, FT-IR, gel permeation chromatography, DSC, and tensile tests.

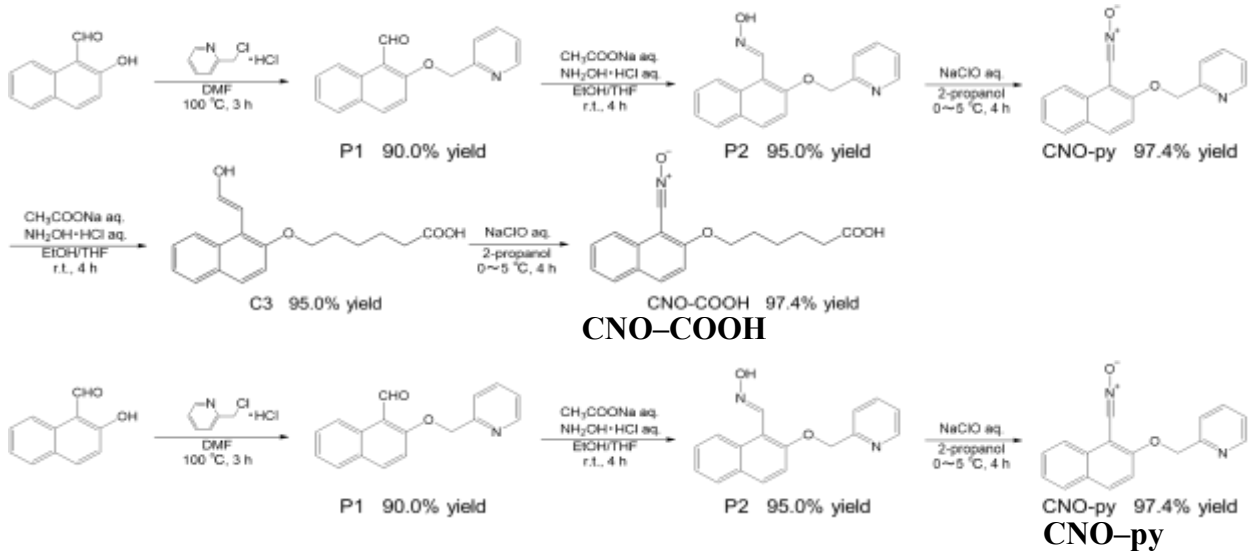
Synthesis of Nitrile N-Oxides

Nitrile N-oxides with carboxylic acid (CNO–COOH) and pyridine (CNO–py) groups were synthesized through a series of reactions starting from 2-hydroxy-1-naphthaldehyde. The synthesis involved steps such as esterification, hydrolysis, oximation, and oxidation, yielding high-purity products confirmed by NMR and FT-IR analyses.

Modification of SSBR

The SSBR was modified using the synthesized nitrile N-oxides both in solution and in the solid state. In the solution method, a THF solution of SSBR and nitrile N-oxides was refluxed, followed by precipitation with methanol. For solid-state modification, SSBR and nitrile N-oxides were mechanically kneaded at elevated temperatures. Both methods achieved high conversion rates of C=C bonds, with the solid-state method being more efficient.

The modified SSBRs were characterized using various techniques. 1H NMR confirmed the successful grafting of nitrile N-oxides onto SSBR.



Scheme 1. Synthetic pathways for CNO-COOH and CNO-py

Results and Discussion

Two N-oxides with carboxyl and pyridyl group (CNO-COOH and CNO-py) were synthesized as reactive modifiers for SSBR. The modification of SSBR with either N-oxide was performed by refluxing a THF solution containing a mixture of SSBR and N-oxide. In addition to the solution-based method, this study also employed the solid-state modification via kneading, achieving over 95% conversion in just 15 minutes. The glass transition temperature of pyridine and COOH-modified SSBRs increased, due to the introduction of bulky side groups onto the polymer backbone. The stress-strain relations of pyridine and COOH-modified SSBR are shown in Figure 1. A significant reinforcing effect was observed in the stress-strain relation for the blend of pyridine and COOH-modified SSBR, due to the hydrogen bond network between pyridine and carboxylic acid. The presence of hydrogen bonds between the introduced functional groups was confirmed through FT-IR spectroscopy, and these bonds contributed to enhanced mechanical properties.

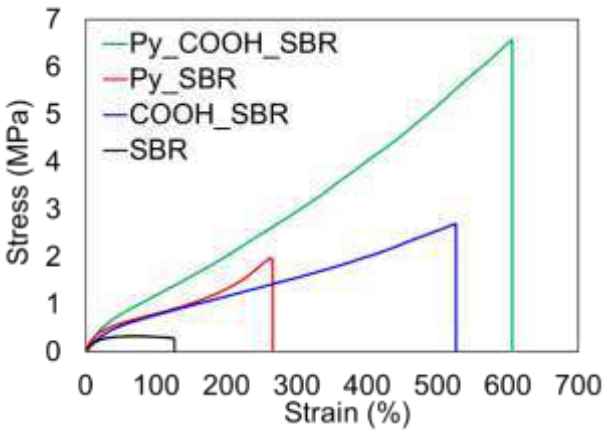


Figure 1. Stress-strain relation of pyridine and COOH modified SSBR and its mixture.

References

1. Jiang L, Manai D, Kawasaki S, Mabuchi T, Tada T, Takata T, *Eur. Polym. J.*, 2025; 223: 113653.

International Rubber Conference 2025 (IRC2025)
1-3 December 2025 @ BITEC, Bangkok, Thailand

A Novel Value Approach of Natural Rubber for Emerging and Unexplored Applications

Ekwipoo Kalkornsurapranee

Division of Physical Sciences, Faculty of Science, Prince of Songkla University, Songkhla, Thailand.

e-mail address of the presenting author (ekwipoo.k@psu.ac.th)

Keywords: natural rubber, patches, stain motion sensors, radiation shielding

Natural rubber (NR) is gaining importance due to its beneficial properties, including high strength, elasticity, rebound resilience, and low heat buildup. However, its application is limited by poor resistance to oil, heat, and oxidation, as well as the presence of non-rubber components that can cause allergic reactions in humans. Synthetic rubbers (SR) were developed to overcome these limitations for various applications, owing to their tailored structure and better purity control for achieving unique properties (Table 1) [1].

With increasing environmental awareness, the significantly lower Carbon Footprint (CFP) of natural rubber is highly advantageous (NR: approx. 0.28 g CO2e/kg, vs. SBR, EPDM, and NBR: 2.4, 2.83, and 3.07 kg CO2e/kg, respectively) [2]. Therefore, greater efforts are being made to utilize NR as a substitution for synthetic rubber in various products. To expand the application range of NR, it is essential to mitigate its existing limitations through dedicated research and development, such as chemical modifications, blending, and composite formation.

In-depth scientific investigations have provided new approaches for novel applications. Accordingly, natural rubber has been successfully developed for applications such as transdermal patches, flexible radiation shielding, and strain motion sensors, overcoming specific technical challenges and achieving new performance benchmarks (Table 2). Furthermore, lifestyle products with a better environmental impact, such as bio-leather, were also successfully developed. The findings of these studies and the science behind them will be presented.

Table 1 Common ranges of properties of different rubber types

Properties	Natural Rubber (NR)	Styrene Butadiene Rubber (SBR)	Ethylene Propylene Diene Monomer (EPDM)	Nitrile Butadiene Rubber (NBR)
Carbon footprint (CO_2e/kg)	0.28	2.47	2.83	3.07
Service Temperature (℃)	<100	<100	120-150	100-120
Rebound resilience (%)*	30-70	25-55	30-55	10-50
Tensile strength (MPa)*	15-30	7-30	7-18	7-25
Oil resistance	Poor	Poor	Poor	High
Ozone resistance	Poor	Poor	High	High

*Room temperature

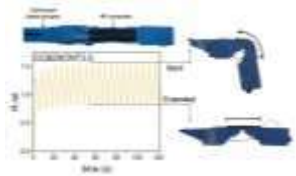
Table 2 Novel applications based-NR and its description

Transdermal Patches Made from Natural Rubber



A transdermal patch using natural rubber (NR) has been successfully developed. The primary challenge was creating an allergy-free patch [3] with excellent adhesion properties. The developed formulation has passed safety checks through medical regulations on animal and human volunteers, achieving FDA clearance. Adhesion performance was evaluated using standard lab shear and T-peel tests [4]. The developed patch demonstrated superior adhesion performance with significantly less residual adhesive left on the skin surface. This improved performance is attributed to a mechanism involving mechanical interlocking coupled with hydrogen bonding between the adhesive and the skin. This patch is now a core component of colostomy bags, providing a high-performance, skin-friendly alternative to conventional adhesives.

Strain Sensor Detection Made from Natural Rubber Composite



A natural rubber (NR) composite has been developed for strain sensing, exhibiting enhanced sensing performance. Although many NR-based strain sensors exist, they often display an undesirable "secondary peak" or non-smooth pattern peaks. These peaks generate noise signals, which are detrimental to sensor accuracy. The main objective of this work was to achieve a clear, low-noise signal. This was accomplished by meticulously controlling the distance between cross-linking points using a novel curing technique, along with precise filler distribution control. Experimental results confirm that this dual-control approach significantly improves sensor stability. The developed NR composite demonstrates a higher Gauge Factor (GF) [5] and greater elongation at break compared to previously developed flexible materials like TPU and silicone, indicating superior sensitivity and flexibility

Wearable Radiation Shielding Made from Natural Rubber Composite



A natural rubber composite for X-ray shielding has been developed. The main challenge of this work was achieving the uniform distribution of metallic filler into the NR matrix while maintaining good mechanical properties. Different high-atomic number metallic fillers were investigated to achieve effective X-ray shielding. The resulting rubber composite exhibits a lower Half Value Layer (HVL) [6] compared to traditional shielding materials such as glass, concrete, and lead [7]. This result demonstrates the superior radiation attenuation capability of the new composite, meaning it can achieve the same level of shielding with significantly reduced thickness, making it much better suited for wearable applications.

Leather-like Material Made from Natural Rubber/Agricultural Waste Composite



The processing conditions for a bio-leather composite made from natural rubber and agricultural waste have been optimized. The main challenge was finding a delicate temperature balance: the high temperature required for natural rubber vulcanization versus the thermal degradation sensitivity of the agricultural waste filler. Successful development involved identifying a precise processing window that enables adequate vulcanization while preserving the filler's structural integrity. Compared to commercial materials [8] like PVC and PU, the developed bio-leather exhibits superior mechanical properties and offers a variety of different texture experiences. Importantly, the product has a significantly lower Carbon Footprint (CFP), estimated to be 2-4 times less than synthetic alternatives

Acknowledgement

The authors gratefully acknowledge the support from Prince of Songkla University for the provision of facilities and resources for this research

References

1. Smith J R, Jones A B, *Handbook of Rubber Technology and Materials*, Global Tech Publishing, 2020.
2. Thailand Greenhouse Gas Management Organization (TGO), Carbon Label Project, Website, Accessed June 2, 2025.
3. Wanitsuwan W, Krainara P, Kalkornsurapranee E, et al., J. Innov. Res. Med. Sci., 2019; 4: 525.
4. Songtipya L, Songtipya P, Sengsuk T, et al., Compos. Commun., 2021; 27: 100880.
5. Promsung R, Georgopoulou A, Nakaramontri Y, Kalkornsurapranee E, Clemens F, Appl Mater Today, 2024; 39: 102302.
6. Intom S, Kalkornsurapranee E, Johns J, et al., J. Rad. Phys. Chem., 2020; 174: 108772.
7. Kalkornsurapranee E, Intom S, Lehman N, et al., Mater. Res. Innov., 2020; 26: 8.
8. Sourprae K, Kalkornsurapranee E, Lehman N, et al., J. Phys. Sci., 2022; 33: 65.

Greening the Elastomer Technology
: Bio-Based Solid/Liquid Rubbers, Polyurethanes, and TPVs

Jeong Seok OH[1]

[1] *Department of Materials Engineering and Convergence Technology, ReCAPT, Gyeongsang National University, 501, Jinju-daero, Jinju, Republic of Korea.*

(ohjs@gnu.ac.kr)

Keywords: Bio-based rubber, Liquid rubber, Eco-polyol, Spent coffee grounds, Bio-based TPV

The advancement of elastomer technology has marked a new era of sustainable materials, significantly impacting industries that rely on flexible, durable, and eco-friendly solutions. This presentation explores the recent green advancements in three key elastomeric categories: Bio-based rubber, Polyurethane foams, and Thermoplastic vulcanizates (TPVs).

Bio-based rubbers signify a significant shift toward using renewable resources. These materials are made from plants and biomass, allowing for the creation of elastomers with a lower environmental impact. This eco-friendly approach reduces dependence on finite petrochemical sources and helps to lower carbon emissions, contributing to a more sustainable and circular economy. The synthesis and characterization of solid and liquid polymers were studied, exploring the transformative potential of farnesene, dibutyl itaconate, and styrene through emulsion and Diels-Alder reactions [1-2].

Polyurethane foam, commonly used in applications like automotive sound absorption parts, has experienced a significant green transformation. The research focuses on advancing bio-based polyurethane foams by developing bio-polyols sourced from bio-waste. In particular, we emphasize the synthesis of bio-polyols from spent coffee grounds, which shows promise for delivering performance comparable to traditional counterparts while greatly reducing environmental impact. The properties of the foams were investigated [3-4].

Reprocessability is one of the significant advantages of thermoplastic vulcanizates (TPVs) because of environmental protection and resource-saving requirements. Owing to the sustainability and environmental friendliness of bio-based polymers, we adopted bio-based polypropylene (PP) and EPDM rubber as the two components to produce a new bio-based thermoplastic vulcanizates (TPV) by dynamic vulcanization. This study investigated physical properties and characterized bio-based TPVs to propel these materials to innovation.

Thus, these sustainable elastomers not only address the growing demand for greener alternatives but also force the elastomer industry towards a circular economy.

Acknowledgement

This work was supported by the project from the department of Ministry of Trade, Industry, and Energy, Republic of Korea and the Glocal University 30 Project Fund of Gyeongsang National University in 2025.

References

1. Sahu P, Oh J, *Ind. Eng. Chem. Res.*, 2022; 61: 11815.
2. Sahu P, Ko J, Ha J, Oh J, *Ind. Eng. Chem. Res.*,2023; 62: 8726.
3. Paria P, Lee J, Jeong S, Sahu P, Park S, Oh J, *J. Polym. Environ.*, 2024; 32: 1616.
4. Lee J, Kim G, Paria S, Jeong S, Sahu P, Park S, Oh J, *J. Elastomer Plast*., 2025, online

International Rubber Conference Organisation

International Rubber Conference 2025 (IRC2025)
1-3 December 2025 @ BITEC, Bangkok, Thailand

Colour-changing smart materials inspired by nature: Chameleon effect

Karine Mougin[1], Arnaud Spangenberg[1]

[1] *Institut de Science des Matériaux de Mulhouse, 15 rue Jean Starcky, 68057 Mulhouse, France*

Karine.mougin@uha.fr

Keywords: Color-changing materials, Hybrid nanomaterials, Colloidal Nanoparticles

Nature's inventiveness often inspires human innovation. Indeed, numerous living organisms rapidly alter their appearance in response to changes in their environment. For instance, the most famous one is chameleon that is able to change color for camouflage, by adjusting the spacing of tiny, crystal-like cells called iridophores, which reflect light at different wavelengths. Inspired by these impressive examples, researchers have developed different strategies to create surfaces or materials able to adapt and change of color in response to their surroundings too. Actually, today, there are various sensitive, reactive, these so-called **intelligent compounds transform and change color in response of an external disturbance** such as the effect of temperature, optical excitation or mechanical stimulation (stretching, shock).

Our approach was also inspired from nature and **t**he idea was to create a novel hybrid material able to color change of surfaces at will [l]. The key element of this novel technology is based on the combination of two phenomena observed in the nature and transferable to material science: plasmonic and structural colors. The developed functional nanomaterials are composed of colloidal metallic nanoparticles (NPs) that are properly synthesized and assembled into polymer to ensure a variety of plasmonic colors under mechanical stresses.

The characteristics of these new hybrid materials can be defined as an "***Intelligent***" material as it is able to achieve the required color on demand, "***Active***" as it responds quite instantaneously to a customer demand (Figure 1). Changing colors on demand is a new approach to modify consumer products. These impressive results in coloring have been motivated by combining plasmonic colors with different polymer and technologies to produce surface colors at will. These nature-inspired innovations are advancing applications in robotics, consumer products (inks, paints), wearable tech, sustainable packaging and medical products.



Figure 1. Color changing material: a. Polyvinylalcohol polymer filled with Au NPs under mechanical stress b. 3D printed polyurethane polymer nanocomposite under hydric stress c. Scheme of photothermal activation of a nanocomposite.

Acknowledgement

The authors thank CNRS financial support.

References

1. K.Mougin *et al, Advanced Functional and Structural Thin Films and Coatings*, 2022,; 74: 847.

Renewable Elastomeric Networks of Functionalized Ethylene-Propylene Copolymers

Y. C. WANG, P. Y. CHENG, Z. Q. ZHANG, S. ZHANG, Y. X. WU

State Key Laboratory of Chemical Resource Engineering, Beijing University of Chemical Technology, Beijing, China.

e-mail address of the presenting author (wuyx@buct.edu.cn)

Keywords: Elastomer, Ionic aggregation, Hydrogen bond, Coordination bond

Ethylene-propylene-diene rubber (EPDM), one of the most common commercial elastic materials due to its remarkable elasticity, heat resistance, and superior electrical insulation properties can be synthesized via coordination copolymerization of ethylene, propylene with nonconjugated diene. EPDM is typically vulcanized via a curing process with peroxide or sulfur to form the chemically cross-linked networks to improve its mechanical performance and chemical resistance. The resulting cross-linked EPDM contains irreversible covalent linkages, which make it difficult to be recycled at the end of its service life.

In order to obtain reversibly cross-linked polar EPDMs (*rc*EPDM) with high mechanical properties and reusability, the copolymerization of ethylene, propylene and 5-ethylidene-2-norbornene (ENB) was achieved to prepare EPDM with different contents of ENB. Then the C=C double bonds in the ENB units in the above EPDM could be converted into carboxylic functional groups *via* light-mediated thiol-ene reaction, leading to the production of the functionalized EPDM with various contents of carboxylic side groups. Subsequently, a six-coordination stable structure of Ni^{2+} with two carboxylate ligands and two sulfur atoms in side chains of ethylene-propylene copolymers can be constructed to form 3D physically cross-linked networks. The reversibly cross-linked polar ethylene-propylene copolymer elastomers (*rc*EPDMs) with triple noncovalent cross-linking sites of hydrogen bonds, ionic aggregation and 6-coordination Ni^{2+} bonds can be successfully *in-situ* prepared. The *rc*EPDM networks with Ni^{2+} having a coordination number of 6 (*rc*EPDM-Ni^{2+}) behave much higher cross-linking density than their analogues with Zn^{2+} having a coordination number of 4 (*rc*EPDM-Zn^{2+}). The *rc*EPDM-Ni^{2+} networks exhibit high tensile strength of 19.0 MPa at elongation of 587%. The mechanical properties of *rc*EPDM-Ni^{2+} networks containing triple cross-linking sites are superior to those of networks containing hydrogen and coordination bonds, as well as those containing ionic aggregation and coordination bonds. The hysteresis energy of *rc*EPDM-Ni^{2+} networks increases by 19 times and the strain recovery reaches 95% when the strain gradually increases from 50% to 400%, which is attributed to the synergy of noncovalent cross-linking sites. The renewable cross-linked EPDM elastomers would have potential applications in organic-inorganic composite materials, bonding agents, sealing parts, and reusable elastomers.

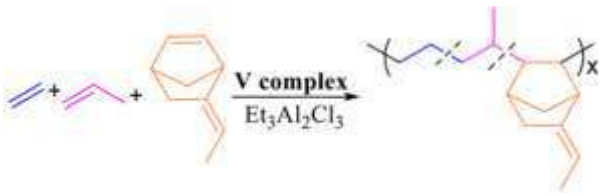


Figure 1. Terpolymerization of ethylene, propylene and ENB using V complex/$Et_3Al_2Cl_3$ catalytic system

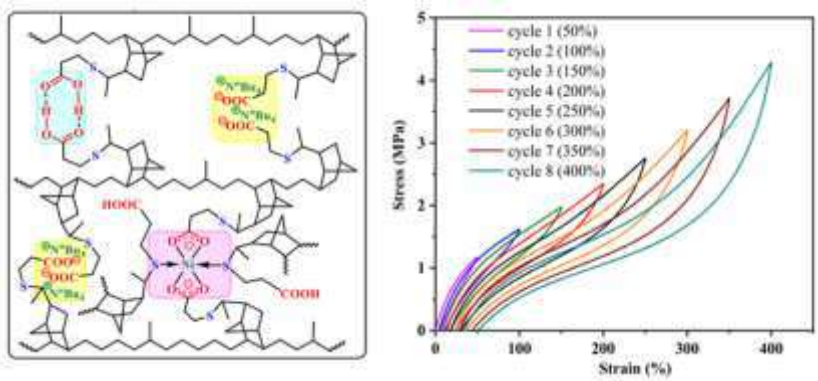


Figure 2. *rc*EPDM networks with noncovalent cross-linking sites and their cyclic tensile test curves

Acknowledgement

The financial supports from the National Nature Science Foundation of China (grant no. 21774006 and 21634002) are greatly appreciated.

References

1. Bravaya N, Faingol'd E, Badamshina E. Sanginov E, *Polym. Sci., Ser. C*, 2020; 62: 1.
2. Wang, Y, Zha, H, Cheng P, Zhang S, Liu X; Wu Y, *Chinese J. Polym. Sci.*, 2024; 42: 84.
3. Zhang X, Li H, Xiang B, Liu X, Zhang S, Wu Y, *Polymer Chemistry*, 2024, 15: 2148.
4. Lo'pez-Barro'n C, Lu J, Throckmorton J, Passino H, Gopinadhan M, *Macromolecules*, 2024, 57: 2729.
5. Wang Y, Cheng P, Zhang S, Wu Y, *Macromolecules*, 2025, 58: 7301.

Facile recycling strategy for end-of-life rubbers by selective cleavage of cross-linking bonds

Ganggang Zhang[1], Baochun Guo[1*], Liqun Zhang[1,2,3*]

[1] Institute of Emergent Elastomers, School of Materials Science and Engineering, South China University of Technology, Guangzhou 510640, China.

[2] State Key Laboratory of Organic/Inorganic Composites Beijing University of Chemical Technology, Beijing 100029, China.

[3] School of Chemical Engineering and Technology, Xi'an Jiaotong University, Xi'an 710049, China

e-mail address of the presenting author (scutgang2023@scut.edu.cn; psbcguo@scut.edu.cn; zhanglq@mail.buct.edu.cn)

Keywords: Recycle, devulcanization, cross-linking

Covalent cross-linking is necessary to achieve high elasticity and proper mechanical properties, but it also prevents reprocessing or recycling of the material, resulting in serious resource waste and environmental problems at their end of life. It is estimated that around 30 million tons of rubber waste are generated annually. Tires are highly engineered and complex assemblage of components, including rubber materials, reinforcing fillers, textiles, metal, etc.; hence, the management of waste tires is a serious technological, economic, and ecological challenge.

The reclamation of waste rubbers is preferred to other recycling methods, which is conducive to improving the mechanical properties of the reclaimed rubber. During the reclaiming process, the three-dimensional network of waste rubbers can be destroyed because physical and chemical treatments break their cross-linking bonds or main chain bonds. The current rubber reclaiming technologies make it difficult to selectively break the cross-linking bonds without destroying the rubber backbone, resulting in the macromolecular chains shortening and deterioration of the mechanical properties of the reclaimed rubber (Figure 1). Therefore, the obtained products from the current reclaiming methods are "down cycled", the mechanical properties and processability of which are greatly reduced compared to that of the original product. Although the recycling technology is used already in industrial settings, reclaimed rubber still can only replace partially virgin rubber in practical applications. To obtain high-performance reclaimed rubbers, it is highly desirable but challenging to explore an efficient and feasible rubber reclaiming method and theory, which could selectively break the S-S and C-S cross-linking bonds without destroying rubber main chains, thereby obtaining the high molecular weight, linear and soluble reclaimed rubber. Hence, the exploration of green and effective chemical reagents for the selective cleavage of cross-linking bonds is of great importance. Moreover, a facile, mild, and efficient chemical recycling strategy should emerge as a new and next-generation reclaiming technology and initiate a real recycling loop. Herein, we report a facile, mild and efficient chemical recycling strategy for end-of-life of NR. The sulfur-sulfur (S−S) bonds could be selectively cleaved by devulcanizing agent in sulfur-vulcanized rubbers. We demonstrate that has excellent devulcanization effect on cross-linked rubbers. The influence of DTT content, reaction temperature, and reaction time on devulcanization degree and sol faction was investigated. The devulcanization degree and quality of the treated rubbers were evaluated by equilibrium swelling experiments combined with the Horikx model.

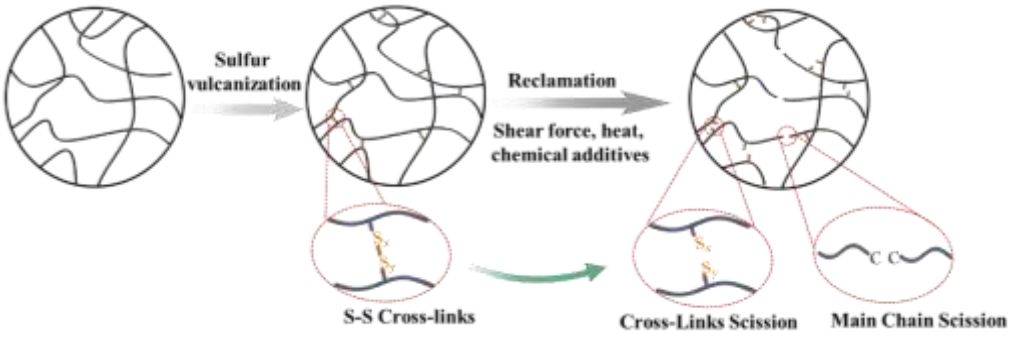


Figure 1. The bond-breaking mechanism within the crosslinked network during the reclaimed process

Our group has reported a facile, green, and promising strategy to introduce the cleavable bonds into the chemically cross-linked networks of diene-typed rubbers, thus achieving closed-loop recycling by a chemical process. The basic principle is that the cleavable bonds within the cross-linked networks could be cleaved selectively under mild conditions. Consequently, these cross-linked rubbers could be degraded into linear and soluble macromolecular chains. As a proof of concept, a commercial carboxylated nitrile rubber (XNBR) is efficiently cross-linked by a bio-based epoxidized soybean oil (ESO), without any toxic additives (Figure 2). ESO exhibits an excellent plasticization effect and excellent scorch safety for XNBR. The cross-linking density and mechanical properties of the ESO-cured XNBR can be manipulated in a wide range by changing simply varying the content of ESO. Furthermore, the end-of-life elastomer materials demonstrate a closed-loop recovery by selectively cleaving the ester bonds, resulting in very high recovery of the mechanical performance of the recycled composites. This strategy provides an unprecedented green avenue to cross-link diene elastomers and a cost-effective approach to further recycle the obtained cross-linked elastomers at high efficiency.

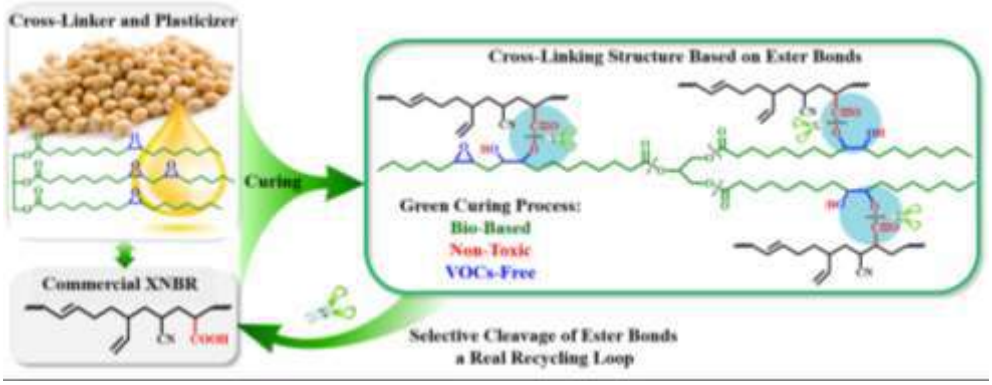


Figure 2. The cross-linking strategy based on ESO for XNBR via epoxy-acid reaction

Acknowledgement

The work was funded by the National Natural Science Foundation of China (52473094), and the GJYC program of Guangzhou (2024D01J0085).

References

1. Zhang GG, Guo BC, Zhang LQ, *Marcomolecules.*, 2025, DOI: 10.1021/acs.macromol.5c00494
2. Zhang GG, Feng HR, Liang K, Wang Z, Guo BC, Zhang LQ, *Science Bulletin* 65 (11), 889-898.

Factors Affecting Biodegradability of Natural Rubber and Natural Rubber Products

Chomnutcha Boonmee[1], Peeraphong Pokphat[1], Thanawadee Leejarkpai[1], Pongdhorn Saeoui[1], Surapich Loykulnant[1], Piyada Bussadee[2], Pattanop Kanokratana[2]

[1] *National Metal and Materials Technology Center (MTEC), National Science and Technology Development Agency (NSTDA), Khlong Nueng, Khlong Luang, Pathum Thani 12120, Thailand.*

[2] *National Center for Genetic Engineering and Biotechnology (BIOTEC), National Science and Technology Development Agency (NSTDA), Khlong Nueng, Khlong Luang, Pathum Thani 12120, Thailand*

(chomnutcha.boo@mtec.or.th)

Keywords: Natural rubber, Latex gloves, Air dried sheet, Biodegradation, Weight loss

Scope and objective

The biodegradability of natural rubber (NR) and NR products is influenced by environmental conditions, microbial activity, and material properties. This study aimed to investigate the key factors affecting the degradation of air-dried rubber sheet (ADS) and NR gloves under long-term aerobic and anaerobic burial at ambient and high temperatures.

Literature review

Natural rubber (NR) possesses high elasticity and excellent mechanical properties, which make it widely used in products such as gloves, tires, and rubber bands. Thailand is a leading producer and exporter of NR, resulting in significant rubber waste from both manufacturing and product use. The biodegradability of NR is influenced by multiple factors, including the type of microorganisms, their extracellular enzymes, rubber type, sample thickness, and environmental conditions such as temperature, oxygen availability, and humidity. Known rubber-degrading microorganisms, including *Streptomyces*, *Nocardia*, and *Gordonia*, exhibit different degradation strategies, either forming clearing zones on latex agar or adhering directly to rubber surfaces. Most studies have investigated isolated cultures in controlled media, providing limited insight into natural degradation processes. Due to the slow nature of NR biodegradation, long-term experiments under conditions that closely resemble real environments are necessary to evaluate the effects of these factors on degradation.

Methods

ADS and NR latex gloves were buried under aerobic and anaerobic conditions at ambient temperature and 52 °C for 360 days. Weight loss was measured to assess degradation. Surface morphology was examined via scanning electron microscopy (SEM), and microbial community composition on material surfaces was analyzed to identify dominant rubber-degrading bacteria.

Results

1) Appearance changes

The visual appearance of ADS and NR latex gloves during degradation under aerobic and anaerobic conditions was evaluated. Under aerobic conditions, ADS disintegrated into small pieces by 360 days at 52 °C, while specimens at ambient temperature largely retained their square shape. NR latex gloves at 52 °C fragmented by 270 days and were completely degraded by 360 days, whereas

at ambient temperature, some small fragments remained. Under anaerobic conditions, both materials maintained their shape and surface integrity, with no significant changes regardless of temperature.



Figure 1. Visual appearance of ADS and NR latex gloves after 360 days of degradation

2) Percentage of weight loss

Both ADS and NR latex gloves showed clear degradation only under aerobic burial conditions. ADS exhibited weight losses of 41.8% at ambient temperature and 56.6% at 52 °C. NR latex gloves degraded more rapidly, with 82.1% weight loss at ambient temperature and complete degradation at 52 °C. No significant degradation occurred under anaerobic conditions. The faster degradation of NR latex gloves was attributed to their lower thickness.

3) Change in surface morphology

SEM analysis showed clear surface deterioration of both ADS and NR latex gloves under aerobic conditions, whereas only minimal changes were observed under anaerobic conditions. ADS exhibited progressive roughness, erosion, and cavity formation at ambient temperature and 52 °C, while NR latex gloves developed cracks and holes, leading to complete structural breakdown at 52 °C after 360 days. In contrast, specimens under anaerobic conditions maintained mostly smooth surfaces with only slight roughening at certain time points, consistent with their insignificant weight loss.

4) Bacterial communities during rubber degradation

At ambient temperature, *Nocardia* was the major genus, accounting for >90% on NR latex gloves at 90 days, though its abundance decreased after 180 days with *Acinetobacter* increasing (~10%). For ADS at ambient temperature, *Nocardia* remained dominant (45–60%) followed by *Streptomyces* (20–30%). In contrast, *Mycobacterium* dominated samples incubated at 52 °C regardless of material type or incubation time. These results indicate that incubation temperature strongly shapes the community structure of rubber-degrading bacteria.

Conclusions

Natural rubber degradation depends on oxygen, temperature, and material properties. Aerobic conditions and high temperature accelerated degradation, particularly for NR latex gloves. SEM confirmed surface deterioration consistent with weight loss, and bacterial community analysis highlighted temperature as the key factor shaping dominant rubber-degrading genera.

Significance

These findings shed light on how environmental conditions influence NR biodegradation and microbial community dynamics, providing guidance for more effective and sustainable rubber waste management.

International Rubber Conference 2025 (IRC2025)
1-3 December 2025 @ BITEC, Bangkok, Thailand

Biocomposite Starch/NR-grafted Hydrogels as Sustainable Coating Membranes for Slow-Release Fertilizers

Sayant Saengsuwan[1,2], Wilawan Lekkla[1], Pranee Nuinu[1], Siriwat Radabutra[1,2], Pitchayaporn Suwanakood[3],

[1]*Innovation and Sustainability in Advanced Natural Rubber and Polymers (ISANRAP) Research Group, Ubon Ratchathani University, Ubon Ratchathani, 34190*

[2]*Department of Chemistry and Center of Excellence for Innovation in Chemistry (PERCH-CIC), Faculty of Science, Ubon Ratchathani University, Ubon Ratchathani, 34190*

[3]*Department of Bioscience, Faculty of Science, Ubon Ratchathani University, Ubon Ratchathani, Thailand*

e-mail: sayant.s@ubu.ac.th

Keywords: Sustainable agriculture, Biodegradable membrane, Slow-release fertilizer, Biochar, Natural rubber, Starch

To enhance soil fertility and promote sustainable agriculture, biodegradable and efficient slow-release fertilizers (SRFs) are essential. This study aimed to develope biocomposite hydrogels composed of modified natural rubber (NR), cassava starch (CSt), and rice straw biochar (RSBC) as eco-friendly, low-cost coating membranes for urea-based SRFs. NR was grafted with glycidyl methacrylate (GMA) to obtain NRG, improving compatibility with CSt and RSBC. The hydrogels were synthesized with a fixed NRG:CSt weight ratio of 1:1, while RSBC content varied from 0–10 wt%. Results revealed that water swelling increased with RSBC content up to 7.5 wt%, correlating with morphological changes observed via SEM, where pore size initially increased (up to 5 wt%) and then decreased due to micro-pore formation at higher RSBC levels. Thermal stability and biodegradation of the hydrogels were enhanced by RSBC incorporation, although agglomeration at higher RSBC contents reduced homogeneity. The hydrogels were coated onto urea pellets three times, followed by an outer wax coating to yield UHBxW formulations (x = wt% RSBC). The UHB7.5W formulation significantly prolonged urea release in aqueous media, extending nutrient availability for over a week, with only 23% of urea released within that period—compared to pure urea, which was fully released within 6 hours. Greenhouse trials using tomato plants demonstrated that UHB7.5W-treated plants showed superior height and fruit biomass relative to those treated with conventional urea and controls. Additionally, the UHBxW formulations exhibited higher biosafety compared to urea and biochar-free SRFs. These findings demonstrate that NRG/CSt/RSBC hydrogels offer a biodegradable, efficient, and biosafe solution for sustainable fertilizer delivery.

Acknowledgement

This work has received funding support from the NRSF, Thailand. The authors also acknowledge the center of excellent for innovation in chemistry (PERCH-CIC), Ministry of Higher Education, Science, Research and Innovation for some partial supports.

Dual-Functional Natural Rubber Composites with Piezoresistive and Antibacterial Properties for Wearable Motion Detection

B. SRIPORNSAWAT[1], F. CLEMEN[2], Y. NAKARAMONTRI[1]

[1]*Sustainable Polymer & Innovative Composite Materials Research Group, Department of Chemistry, Faculty of Science, King Mongkut's University of Technology Thonburi, Bangkok 10140, Thailand.*

[2]*Department of Advanced Materials and Surfaces, Empa-Swiss Federal Laboratories for Material Science and Technology, Ueberlandstrasse 129, 8600, Dübendorf, Switzerland.*

e-mail address of the presenting author (yeampon.nak@kmutt.ac.th)

Keywords: Natural rubber composites, Piezoresistive sensors, Deep eutectic solvent (mDES), Zinc oxide–silica ($ZnO–SiO_2$), Antibacterial activity

This study aims to develop multifunctional natural rubber (NR) composites with enhanced piezoresistive sensitivity and antibacterial properties for application in wearable motion detection and soft robotics. The overarching goal is to engineer dual-functional materials that combine mechanical robustness, electrical responsiveness, and hygienic performance for integration into dynamic environments, particularly in health-monitoring and human-machine interface systems. Although NR is widely recognized for its elasticity and mechanical resilience [1], its application in electronic sensing remains limited due to its non-polar nature, which inhibits the dispersion and interaction of conductive fillers [2]. To address this, conductive NR composites were formulated using a hybrid filler system consisting of carbon nanotubes (CNTs) and conductive carbon black (CCB), along with a modified deep eutectic solvent (mDES) synthesized in-house. Additionally, modified zinc oxide supported on silica ($ZnO–SiO_2$) was introduced to impart antibacterial functionality while further supporting crosslinking during vulcanization. Past research has demonstrated that hybrid CNT/CCB fillers improve the electrical conductivity of rubber matrices through the formation of percolated networks [3,4]. However, inconsistent sensing behavior under strain, particularly during cyclic deformation, remains a challenge. Meanwhile, modified ZnO has been extensively studied for its antibacterial performance and its catalytic role in crosslinking rubber chains, particularly when engineered as nanostructures dispersed within the matrix. Recent work also highlights the role of ionic conduction pathways and filler–matrix compatibility in tuning the piezoresistive response.

Building on these insights, this study introduces a dual approach that combines hybrid carbonaceous fillers with mDES and $ZnO–SiO_2$ to simultaneously achieve tunable electromechanical sensitivity and antibacterial protection. The NR composites were prepared *via* melt mixing, incorporating CNT and CCB at a fixed 20:30 phr ratio, while the solution of both mDES and $ZnO–SiO_2$ were dissolved and added together at varying concentrations. It was found that, when applied to a soft tendon-actuated structure, the sensor delivered noise-free, interpretable signal patterns aligned with actuator motion. To evaluate antibacterial properties, composites filled with $ZnO–SiO_2$ were tested against *Escherichia coli* and *Staphylococcus aureus*. The results demonstrated 90.0% bacterial reduction within 8 hours and 99.9% within 24 hours, attributed to sustained Zn^{2+} release and reactive oxygen species (ROS) generation from the well-dispersed $ZnO–SiO_2$ particles [5]. This antibacterial performance, combined with the high sensitivity and mechanical resilience of the composites, presents an ideal material candidate for wearable electronics requiring contact with human skin or environments prone to microbial contamination. In conclusion, this work introduces a dual-functional NR composite material that synergistically integrates piezoresistive sensing and antibacterial

properties via CNT/CCB-mDES networks and ZnO–SiO_2 additives. The successful elimination of inconsistent signal behavior and improved durability under cyclic loading highlight the material's readiness for integration into flexible sensors and soft robotic systems, as seen the summary in Figure 1.

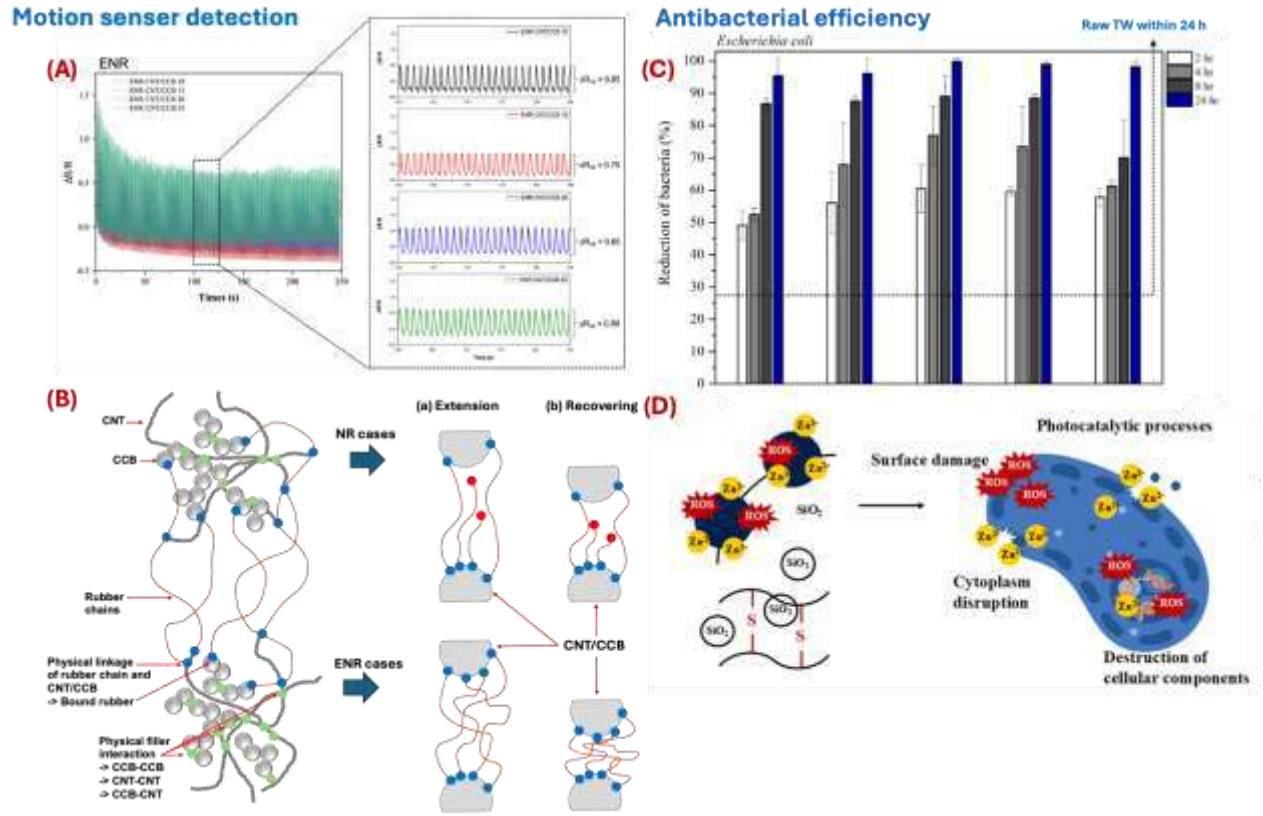


Figure 1. Indication of composite performance based on (A) the relative resistance response signal, (B) the proposed model illustrating the interaction between CNT/CCB and rubber molecules, (C) the antibacterial efficiency over a 0–24 h period, and (D) the antibacterial mechanism associated with the use of modified ZnO–SiO_2.

Acknowledgement

This work was supported by King Mongkut's University of Technology Thonburi (KMUTT), Thailand Science Research and Innovation (TSRI) , and National Science, Research and Innovation Fund (NSRF) Fiscal year 2026 Grant number FRB680074/0164.

References

1. Wattanasarn H, Ngennam T, Boonkirdram S, Thanachayanont C, *Appl. Mater. Today*, 2023; 35: 101955.
2. Georgopoulou A, Srisawadi S, Wiroonpochit P, Clemens F, *Polymers*, 2023; 15: 2410.
3. Banerjee SS, Arief I, Berthold R, Wiese M, Bartholdt M, Ganguli D, Mitra S, Mandal S, Wallaschek J, Raatz A, Heinrich G, Das A, *Appl. Mater. Today*, 2021; 25: 101219.
4. Nakaramontri Y, Pichaiyut S, Wisunthorn S, Nakason C, *Eur. Polym. J.*, 2017; 90: 467–484.
5. Yi W, Wang Y, Wang G, Tao XJ, *Polym. Test.*, 2012; 31: 677–684.

Functionalized Polymer Surfaces Studied by Vibrational Spectroscopy and Applications

Philippe DANIEL

Institut des Molécules et Matériaux du Mans - IMMM UMR CNRS 6283, Le Mans University, France

Email : philippe.daniel@univ-lemans.fr

Keywords: *Functionalized surfaces; Polymer; Raman; IR*

Abstract: This presentation focuses on the development of Polymer functionalized surfaces coupled to vibrational spectroscopy, either Raman scattering, either Infra-red (IR) spectroscopy and the applications o. If IR is a well-known tool in material chemistry, Raman spectroscopy appears as a less developed technique especially for applications in bioscience and biochemistry. However, IR and Raman are both very useful because they are generally non-destructive and non-invasive and with a fingerprint character. The recent technological improvements of IR and Raman spectroscopies will be exhibited. For instance the new rapid imaging techniques, enhanced techniques (SERS), Spatially Offset Raman Spectroscopy (SORS) which is a variant of Raman spectroscopy that enables highly accurate chemical analysis of objects beneath obscuring surfaces, and recent and promising applications will be given in different fields. In the frame of the state of art, we will present different recent and promising applications studied by Raman spectroscopy and Infrared spectroscopy and how these both techniques can bring very valuable information including food safety, health, industry…

Optimizing Silica and Carbon Black Ratios for Enhanced Mechanical Performance of NR/BR/SSBR blends

N. R. MOHAMED[1], N. OTHMAN[2]

[1] *Faculty of Applied Sciences, University Teknologi MARA Perlis Branch, 02600 Arau, Perlis, Malaysia.*

[2] *School of Materials and Mineral Resources Engineering,Engineering Campus, Universiti Sains Malaysia, 14300 Nibong Tebal, Penang, Malaysia.*

srnadras@usm.my

Keywords: Silica, carbon black, ternary rubber blends.

Carbon black (CB) and silica are widely used as reinforcing fillers to improve the performance of rubber materials. Previous studies have explored the combination of these two fillers to enhance both the mechanical and dynamic properties of natural rubber (NR) vulcanizates, due to the distinct advantages each offers [1]. However, the optimal CB/silica ratio for maximizing the performance of ternary rubber blends remains unclear. This study investigates the effect of hybrid CB/silica fillers in a ternary blend of natural rubber (NR), butadiene rubber (BR), and solution styrene-butadiene rubber (SSBR) in a 65/30/5 ratio, commonly used in pre-cured tyre tread liners. Filler compositions ranging from 4/64 to 36/32 (CB/Silica) were evaluated. Silane is incorporated with silica to enhance filler dispersion and improves rubber–filler interaction [2]. In this work, silane was added proportionally to silica loading based on its CTAB surface area, as defined in Equation 1 [3] :

$$\text{phr (silane)} = 0.00053 \times \text{phr filler} \times \text{CTAB}$$

Table 1. Formulation for various CB/Silica compositions

Ingredients	CB/silica compositions				
	4/64	**12/56**	**20/48**	**28/40**	**36/32**
SMR 10CV	65	65	65	65	65
BR	30	30	30	30	30
SSBR	5	5	5	5	5
Carbon Black	4	12	20	28	36
Silica	64	56	48	40	32
Process oil	13	13	13	13	13
Coupling agent	5.66	4.96	4.25	3.54	2.83
Processing aid I	1	1	1	1	1
Processing aid II	1	1	1	1	1
Zinc Oxide	4	4	4	4	4
Stearic Acid	2	2	2	2	2
Antioxidant	2	2	2	2	2
Antiozonant	1	1	1	1	1
Accelerator	1.5	1.5	1.5	1.5	1.5
Sulfur	1.5	1.5	1.5	1.5	1.5
Retarder	0.35	0.35	0.35	0.35	0.35

In cure characteristics, compositions such as 12/56 and 20/48 showed higher minimum (M_L) and maximum (M_H) torque values. The optimum cure time (t_{90}) remained fairly consistent for 4/64, 12/56, and 20/48, while it decreased slightly to 8.4 minutes at 36/32. An increasing trend in delta torque suggests a rise in crosslink density, although a performance drop was observed at 28/40 with

only 3.45 phr silane. Mooney viscosity increased with silica loading up to 56 phr, consistent with the rise in M_L, as seen in the 12/56 compound. However, a decline beyond 56 phr suggests reduced filler–rubber interaction, likely due to dispersion limits.

The highest crosslink density was observed at 64 phr silica and declined gradually as CB increased. A sharp 15–20% drop was noted at 28/40 with 3.45 phr silane, attributed to weaker filler–matrix bonding, which recovered when silane was increased to 4.2 phr. Silica-rich compounds (56–64 phr) demonstrated improved crosslinking and tensile strength, with the highest strength recorded for 4/64, and the lowest again at 28/40. The 300% modulus peaked at 20/48, and the highest reinforcement index was seen in 20/46, indicating a well-balanced formulation in terms of stiffness and flexibility.

Tear strength results showed that 20/48 and 36/32 compositions performed on par with the control. Generally, tear strength improved with increasing CB and decreasing silica, except at 28/40 with reduced silane. Wear resistance was highest in the control, followed closely by 12/56, which also exhibited a higher 300% modulus and better filler dispersion, as indicated by a lower Payne effect. The improved wear performance of 12/56 is further supported by its increased hardness and reinforcement index, consistent with earlier findings correlating high reinforcement with lower abrasion loss.

Finally, storage modulus measurements confirmed strong filler–filler interactions in high-silica compounds such as 4/64 and 12/56, with the highest G′ observed at 0.28% strain. In contrast, the 28/40 composition with 3.45 phr silane—approximately 16% less than the control—showed reduced storage modulus, reflecting better filler dispersion. These findings align with the Payne effect results, reinforcing the conclusion that silica enhances stiffness, while optimal silane loading ensures effective dispersion and mechanical performance.

Acknowledgement

This research was financially funded by the Malaysian Rubber Council (MRC) under MRC Industry Linkage Fund (Ref. no.; ILF/17/006). We would also like to acknowledge the Eversafe Rubber Works Sdn Bhd for the technical support and processing facilities, for fnancially funding this research, and fnally, Universiti Sains Malaysia (Grant No. 304/PBahan/6050400/E123) for the other facilities.

References

1. Rattanasom N, Saowapark T, Deeprasertkul C. Reinforcement of natural rubber with silica/carbon black hybrid filler. Polym Test. 2007;26:369–77.

2. Neethirajan J, Parathodika AR, Hu G-H, Naskar K. Functional rubber composites based on silica-silane reinforcement for green tire application: the state of the art. Functional Composite Materials. 2022;3:7.

3. Kaewsakul W, Sahakaro K, Dierkes WK, Noordermeer JWM. Flocculation Kinetics and Filler-Rubber Interaction in Silica-Reinforced NR Compounds. 186th Technical Meeting of Rubber Division. 2014. p. 1–20.

Advancing Sustainable Rubber Recycling: Transforming NR and NBR Waste into Conductive Elastomers

S. SAIWARI[1], S. SALAEH[1], A. THITITHAMMAWONG[1], N. HAYEEMASAE[1]

[1] *Department of Rubber Technology and Polymer Science, Faculty of Science and Technology, Prince of Songkla University, Pattani Campus, Pattani, 94000, Thailand.*

sitisaiyidah.s@psu.ac.th

Keywords: Rubber recycling, Devulcanization, Conductive elastomers, Carbon nanotubes

The increasing accumulation of waste rubber poses serious environmental challenges due to its non-degradable crosslinked structure. This work presents a sustainable strategy to upcycle natural rubber (NR) and nitrile rubber (NBR) waste into value-added elastomeric materials. Three recycling approaches: physical, thermomechanical, and thermochemical devulcanization processes were applied to waste NR, producing recycled rubbers with different crosslink densities. Physically devulcanized NR retained a more intact rubber network, enabling superior mechanical properties and promoting segregated networks of carbon nanotubes (CNTs) at low filler loading. A remarkably low electrical percolation threshold was obtained for highly crosslinked domains. To further broaden waste utilization, the recycled NBR was also studied. Recycled NBR was blended with NR at various ratios and reinforced with CNTs. NR-rich blends exhibited reversion behavior, while recycled NBR-rich blends demonstrated plateau curing with enhanced thermal stability. CNTs incorporation improved modulus, tensile strength, and curing kinetics, though elongation decreased due to reduced chain mobility. Electrical conductivity increased with CNTs loading, and lower percolation thresholds were observed in recycled NBR-rich blends due to residual crosslinked networks promoting CNTs connectivity. This study highlights the viability of converting rubber waste into high-performance recycled rubbers/CNTs composites, supporting circular economy and sustainable materials development.

Acknowledgement

This research was supported by National Science, Research and Innovation Fund (NSRF) and Prince of Songkla University (Grant No. SAT6601125d and SAT6505064S).

References

1. S. Saiwari, S. Nobnop, Y. Bueraheng, A. Thitithammawong, N. Hayeemasae and S. Salaeh, ACS Appl. Polym. Mater. 2022. 4(10), 7463.
2. S. Salaeh, S., and Kao-ian, P. Polym. Test. 2022, 108, 107493.

Multifunctional Applications of Epoxidized Natural Rubber: From Gas Separation Membranes to Self-Healing and Adhesion Technologies

Bagdagul KARAAGAC[1,2]

[1] *Kocaeli University Engineering Faculty, Chemical Engineering Dept., Kocaeli, Turkey.*

[2] *Sheffield Hallam University, Materials and Engineering Research Institute (MERI), Sheffield, UK.*

bkaraagac@kocaeli.edu.tr; B.Karaagac@shu.ac.uk

Keywords: Epoxidized natural rubber (ENR), Gas separation, Tyre inner liners, Anti-reversion

Epoxidized natural rubber (ENR), a chemically modified derivative of natural rubber obtained through controlled epoxidation of latex with organic acids, has emerged as a versatile elastomer with wide application potential owing to its reactive epoxy functionalities, tuneable polarity, and compatibility with diverse fillers [1,2]. The present work summarizes several recent investigations on the utilization of ENR in advanced rubber technologies, targeting sustainability, improved performance, and functional properties.

In the field of gas separation membranes, ENR-based composite matrices were designed for the first time for CO_2/CH_4 separation in biogas purification applications. By tailoring the epoxidation degree, crosslink density, and incorporating natural fillers such as clinoptilolite, bentonite, and halloysite nanotubes, promising improvements in permeability and CO_2 diffusion selectivity were demonstrated. For tyre inner liner compounds, ENR/NR blends reinforced with wollastonite were developed as an alternative to butyl rubber, showing superior gas barrier performance, improved mechanical strength, and enhanced interfacial adhesion between layers through curing system compatibility and filler–matrix interactions. Similarly, ENR incorporation in cushion gum compounds significantly increased adhesion strength to re-treaded tyre carcasses, where synergistic effects of ENR with phenolic resin, bismaleimide, and optimized sulphur curing systems were identified as key factors [3]. In the area of reinforcement and adhesion, ENR was further exploited in coating compounds for nylon and polyester cords to enhance adhesion durability under long curing cycles, and in NR/ENR–carbon fibre composites to achieve high tensile modulus and aging resistance for vibration and bearing applications. ENR's reactive backbone also enabled self-healing rubber technologies. The combination of lignin, a bio-based filler, with 1,3-bis(citraconimidomethyl)benzene (CIMB) induced reversible covalent interactions via Diels–Alder and Alder–ene mechanisms, providing up to 85% recovery of mechanical properties under optimized conditions. Lignin further contributed to improved thermal stability and curing efficiency in ENR and NBR compounds [4]. Finally, ENR proved effective in preventing marching cure behaviour in chloroprene rubber vulcanization when used alongside conventional anti-reversion agents (CIMB, HVA-2). By stabilizing crosslinks and enabling predictable cure kinetics, ENR contributed to enhanced processability and reliability. ENR was also applied in cable sheath formulations, where epoxy-silane modified wollastonite and ENR improved oil resistance, interphase compatibility, and thermal performance.

Overall, these studies highlight the multifunctionality of ENR as a reactive elastomeric platform for gas separation, adhesion technologies, self-healing systems, sustainable filler incorporation, and reinforcement strategies. The findings underline ENR's potential to serve as a sustainable, high-performance alternative to petroleum-based rubbers in next-generation industrial applications.

Acknowledgement

This study was funded by KOU-BAP (Grant no: FOA-2023-3167 and FBA-2021-2617), TUBITAK (Grand no: 5240042, 123M175, 221M572, 3170880, 2209-B). Authors gratefully thank KOU-BAP and TUBITAK for their valuable support.

References

1. Ismail, H., *J Elast. Polym.*, 2001; 33:34.
2. Rahman, M.A., Sartore, L., Bignotti, F., di Landro, L., *ACS Appl. Mater. Interfaces*, 2013; 5: 1494.
3. Öter, M., Karaağaç, B., *J. Rubber Res.*, 2020; 23: 333.
4. Yeşil, B., Ünügül, T., Karaağaç, B., *eXPRESS Polym. Lett.*, 2023; 17: 704.

Oral Presentations

IRC 2025
BANGKOK, THAILAND

International Rubber Conference 2025 (IRC 2025)

Session I : Natural Rubber, Bio-based Rubbers and Rubber Chemicals

Oral Presentations

International Rubber Conference 2025 (IRC2025)
1-3 December 2025 @ BITEC, Bangkok, Thailand

N-Vinylamides: Structural Isomers of Amino acids Grafted onto Deproteinized Natural Rubber

Hiroharu Ajiro[1,2,3], Sakiko Yashiro[1], Tran Thi Thuy[4], Nguyen Thu Ha[4], Nguyen Ngoc Mai[4], Seiichi Kawahara[5], Ryohei Ikura[1], , Hiroaki Yoshida[1]

[1] *Medilux Research Center, Nara Institute of Science and Technology, Takayama-cho 8916-5, Ikoma, Nara 630-0192, Japan*

[2] *Data Science Center, Nara Institute of Science and Technology, Takayama-cho 8916-5, Ikoma, Nara 630-0192, Japan*

[3] *Graduate School of Science and Technology, Nara Institute of Science and Technology, Takayama-cho 8916-5, Ikoma, Nara 630-0192, Japan*

[4] *School of Chemistry and Life Sciences, Hanoi University of Science and Technology, No.1 Dai Co Viet Street, Hai Ba Trung district, 10000 Hanoi, Vietnam*

[5] *Nagaoka University of Technology, 1603-1 Tomioka-cho, Nagaoka, Niigata 940-2137, Japan*

e-mail address of the presenting author (ajiro@ms.naist.jp)

Keywords: Natural rubber, Deproteinization, *N*-Vinylamide

Natural rubber (NR) is a vital material, prized for its exceptional elasticity and strength, with ongoing research focused on optimizing its performance and broadening applications. Key strategies involve blending NR with materials like carbon nanotubes for enhanced mechanical and electrical properties, and biomass-derived fillers for improved biodegradability. Additionally, chemical modifications,[1] such as grafting synthetic polymers or epoxidizing NR,[2] yield robust composites with diverse functionalities. Understanding NR's unique properties stems from detailed structural analyses (e.g., NMR, X-ray diffraction), which show it's primarily polyisoprene with crucial proteins and phospholipids.[3] These analyses highlight that NR's mechanical properties are significantly influenced by both its composition and intricate particle morphology. However, proteins in NR can cause instability and allergic reactions, prompting extensive protein removal efforts. While this may sometimes reduce mechanical strength, maintaining NR's superior properties after deproteinization (DPNR) necessitates replicating its unique nanomatrix structure.[4]

In this study, the authors propose using poly(*N*-vinylamide), a structural isomer of proteins, as a protein substitute. They hypothesize that its structural similarity will allow it to fulfill the role of proteins in NR. Their study explores grafting *N*-vinylamide monomers directly onto DPNR particles, aiming to overcome the challenge of grafting hydrophilic monomers onto hydrophobic rubber in aqueous environments and ultimately improve NR's mechanical strength.

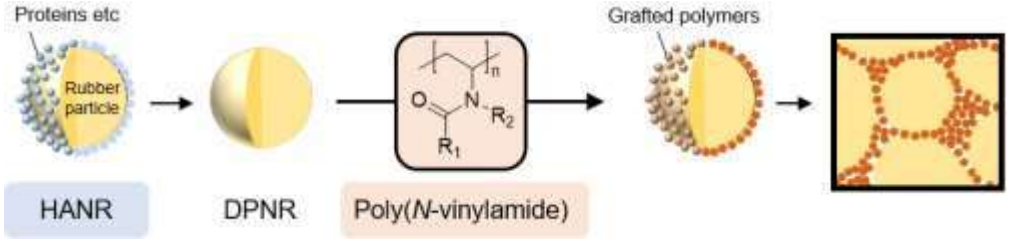


Figure 1. Chemical modification of poly(*N*-vinylamide) on DPNR.

We selected three monomers: *N*-vinylacetamide (NVA), *N*-vinylformamide (NVF), and *N*-methyl-*N*-vinylacetamide (NMVA), and the sample preparation conditions were listed in the Table 1, varying ratio ranged from 0.5 mol/kg to 2.0 mol/kg and initiators with 0.033 mol/kg and 0.066 mol/kg, resulting in total 8 samples for NVA, NVF, and NMVA, respectively.

Table. Sample preparation.

Samples	Monomer [mol/kg dry rubber]	TBHPO,TEPA [mol/kg dry rubber]
(1)	0.5	0.033
(2)	1.0	
(3)	1.5	
(4)	2.0	
(5)	0.5	0.066
(6)	1.0	
(7)	1.5	
(8)	2,0	

Our research successfully grafted N-vinylamide monomers (NVF, NVA, MNVA) onto deproteinized natural rubber (DPNR) using oxygen-radical-initiated surface modification. Despite low inherent reactivity, efficient and selective grafting was achieved, confirmed by FT-IR and elemental analysis.

Mechanical testing, as shown in the tensile data, revealed significant improvements: nearly 70% of grafted samples surpassed HANR in tensile strength. Notably, it achieved the highest performance (15.48 ± 0.64 MPa, 1361 ± 29% strain). TEM and AFM analyses confirmed the restoration of the nanophase-separated "island-nanomatrix" morphology, correlating with mechanical reinforcement. Optimal properties required only moderate nitrogen content, indicating extensive grafting isn't essential.

These findings suggest that protein-isomeric *N*-vinylamides can effectively replace proteins in natural rubber by structurally reproducing its original morphology. This offers a promising, sustainable approach to natural rubber design with potential for broader biomimetic applications.

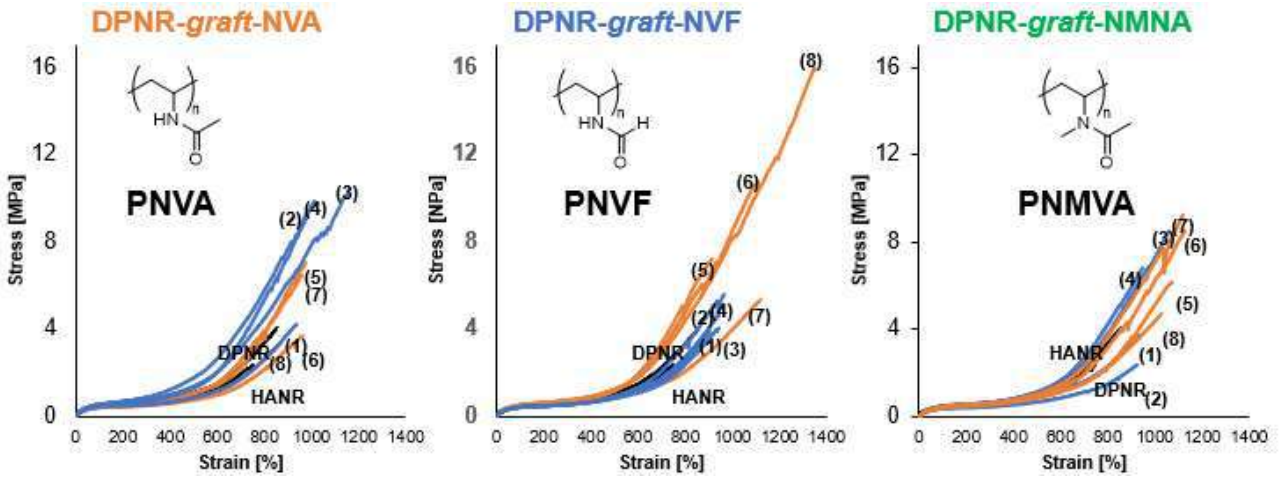


Figure 2. Tensile tests of DPNR-*graft*-poly(*N*-vinylamide)s.

References

1. Wichaita W, Promlok D, Sudjaipraparat N, Sripraphot S, Suteewong T, Tangboriboonrat P, *Eur. Polym. J.* 2021; 159: 110740.
2. Nuinu P, Sirisinha C, Suchiva K, Daniel P, Phinyocheep P, *J. Mater. Res. Technol*. 2023; 24: 2155.
3. Tarachiwin L, Sakdapipanich J, Ute K, Kitayama T, Tanaka Y. *Biomacromolecules* 2005; 6: 1858
4. Kawahara S, Chaikumpollert O, Akabori K, Yamamoto Y, *Polym. Adv. Technol.* 2011; 22, 2665.

International Rubber Conference 2025 (IRC2025)
1-3 December 2025 @ BITEC, Bangkok, Thailand

Effects of epoxidation degree on strain-induced crystallization and mechanical properties of epoxidized natural rubber

Xiaohui Wu [1], Zixuan Wang[1, 2], Han Song[1], Weixiao Song[1], Guo-Hua Hu[2], Liqun Zhang[1]

1 Beijing University of Chemical Technology, Beijing 100029, China

2 Université de Lorraine, CNRS, LRGP, F-54000 Nancy, France

wuxiaohui@mail.buct.edu.cn

Keywords: Epoxidized natural rubber, Strain-induced crystallization, Mechanical properties, Molecular chain orientation

Natural rubber (NR), as a biobased material, stands out for its unparalleled performance, including high tensile strength, tear strength, and excellent crack propagation resistance. The superior mechanical performance of natural rubber mainly stems from the self-reinforcement effect of its strain-induced crystallization (SIC). The epoxidation degree significantly influences the microstructure and macro-performance of epoxidized natural rubber (ENR).

In summary, the effect of epoxidation on SIC behavior, mechanical properties, and molecular chain orientation evolution in ENR has been studied. WAXD analysis indicates that the order of crystallinity at a fixed strain follows the sequence ENR10(Epoxy natural rubber with an epoxy degree of 10) > ENR5(Epoxy natural rubber with an epoxy degree of 5) > ENR20 (Epoxy natural rubber with an epoxy degree of 20)> NR > ENR33(Epoxy natural rubber with an epoxy degree of 33) > ENR50(Epoxy natural rubber with an epoxy degree of 50). This sequence is also reflected in the mechanical properties, highlighting the significant reinforcing role of SIC in enhancing mechanical performance. Notably, ENR10 exhibits the best tensile strength of 30.8 MPa and tear strength of 35.9 kN/m, representing increases of 27.8% and 40.2%, respectively, compared to NR. Further analysis using polarized FTIR confirms the preferential orientation capability of optimal epoxidation degrees and their promoting effect on molecular chain orientation. However, excessive epoxy groups can limit molecular chain orientation due to significant steric hindrance and interactions. By using AFM, fibril high-modulus regions were captured in stretched rubber, which can be attributed to the SIC-associative phase enduring high stress. Additionally, we propose a possible pathway for the influence of epoxidation degree on mechanical properties. The tensile process of ENR can be divided into three regions.

The first region occurs when the strain is below the crystalline strain, where the rubber matrix only undergoes elastic deformation. The second stage spans the transition from crystalline strain onset to the beginning of “stress-upturn” strain. SIC occurs first in NR and ENR (E≤20) and forms crystallites within the cross-linked network. However, the relaxation of amorphous chains leads to a plateau in stress increase. The third stage extends from the onset of stress-driven strain to the fracture strain. The crystallites formed from SIC act as stronger network points, creating an effective crystallite network that dissipates energy, as evidenced by higher tensile strength, tear strength, and modulus. NR and ENR (E≤20) possess more crystallites, resulting in superior mechanical properties. Conversely, for ENR (E>20), the excessive content of epoxy groups reduces the number of crystallites, consequently limiting the strength of the crystallites network. This ultimately results in a decrease in tear and tensile strength for ENR (E>20).

These new insights suggest that ENR with a low degree of epoxidation possesses higher mechanical performance due to the significant self-reinforcing effect of SIC, making it an attractive biobased rubber for advanced engineering rubber products.

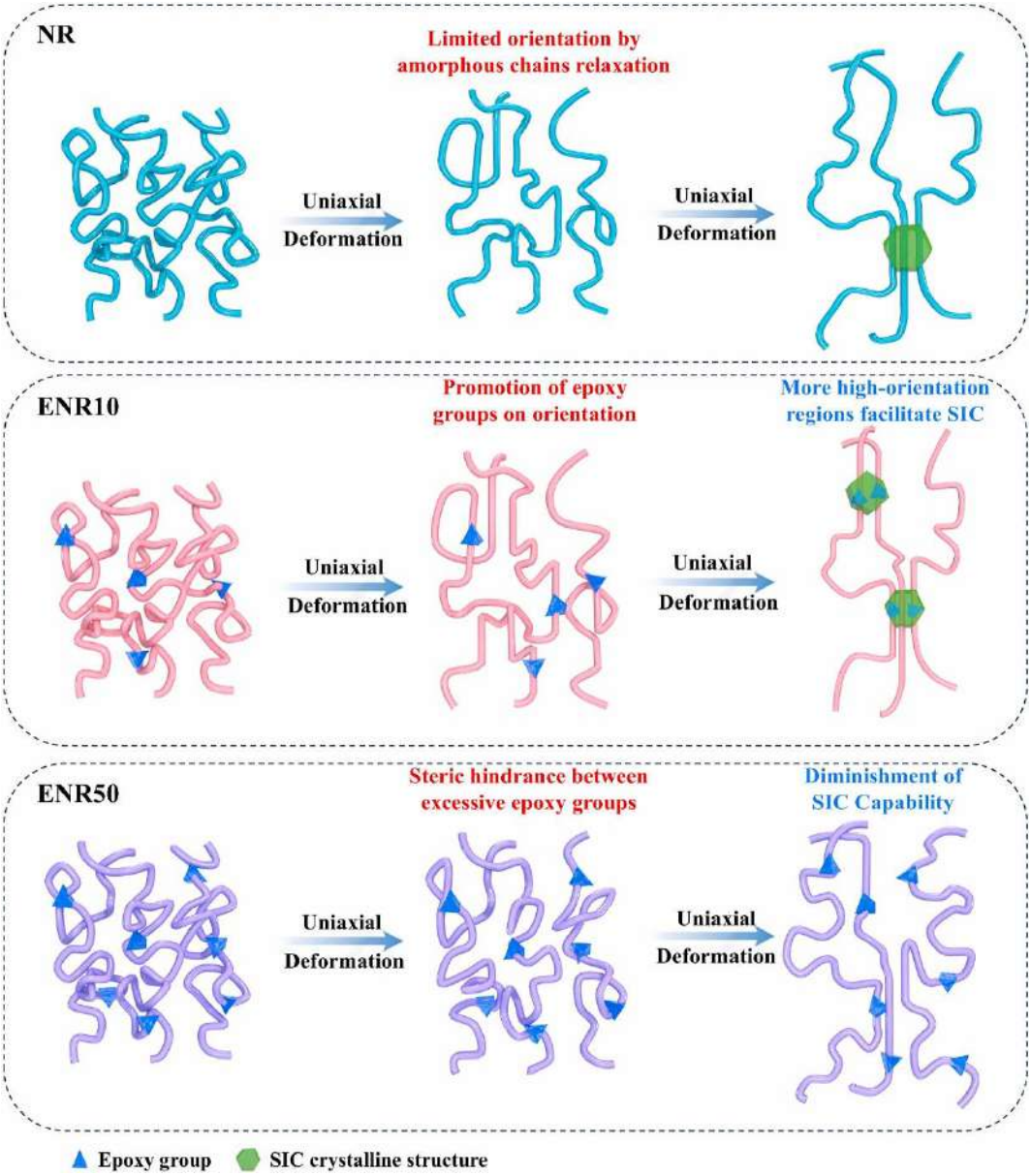


Figure 1. Proposed pathway of microstructure evolution during stretching of NR, ENR10, ENR50.

Acknowledgement

This work was supported by the National Key Research and Development Program of China (2022YFB3704800, 2022YFB3704802, 2022YFB3704801)

References

1. Li Y, Wang Z, Song H, et al. *Composites Communications*, 2025, 56: 102356.
2. Wang Z, Song H, Wang R, et al.. *Polymer*, 2025: 128541.
3. Wang Z, Li Y, Song W, et al. *Journal of Applied Polymer Science*, 2022, 139(30): e52682.

Chitosan-reinforced epoxidized natural rubber: possible design of energy-efficient tire tread compounds

Nantinee Choosang[1,2], Ploypailin Juntosree[1], Saree Phongphanphanee[1], Supitta Suethao[1,3], Wirasak Smitthipong[1,3]

[1] *Specialized Center of Rubber and Polymer Materials in Agriculture and Industry (RPM), Department of Materials Science, Faculty of Science, Kasetsart University, Bangkok, 10900, Thailand*.

[2] *Bangkok Metropolis Motor Co., Ltd., Samut Sakhon* 74110, *Thailand.*

[3] *Hub of Talents in Natural Rubber, National Research Council of Thailand (NRCT), Bangkok 10900, Thailand*.

E-mail address of the presenting author: nantinee.ch@ku.th

Keywords: Epoxidized natural rubber, chitosan, mechanical properties, tire, energy-saving property

The development of energy-efficient rubber tread compounds offers a promising route to reducing energy consumption and enhancing tire performance. In this study, natural rubber (NR) was epoxidized via performic acid epoxidation. This produced epoxidized natural rubber (ENR) as shown in Figure 1. It was then compounded with bio-derived chitosan (CTS) at loadings of 10, 20, 30, 40, and 50 phr (Table 1). The resulting materials were prepared and subsequently characterized under uncrosslinked condition. The aim of this work was to investigate the influence of chitosan content on physical and viscoelastic properties of tread formulation, with an ultimate goal of reducing rolling resistance and advancing sustainable tire technologies. Previous literature has demonstrated the potential of ENR as a reactive rubber matrix with enhanced polarity and compatibility toward bio-based fillers [1-2]. Chitosan, a biopolymer derived from chitin, has shown promising reinforcing and self-healing effects in rubber matrices [3]. ENR offers enhanced oil resistance and filler–matrix compatibility, making it a promising alternative to natural rubber [4]. Its polar epoxy groups enhance interactions with hydrophilic fillers, while chitosan further improves mechanical properties via biocompatibility and hydrogen bonding [5]. In addition, the incorporation of chitosan has been reported to enhance mechanical performance and thermal resistance in rubber composites [6].

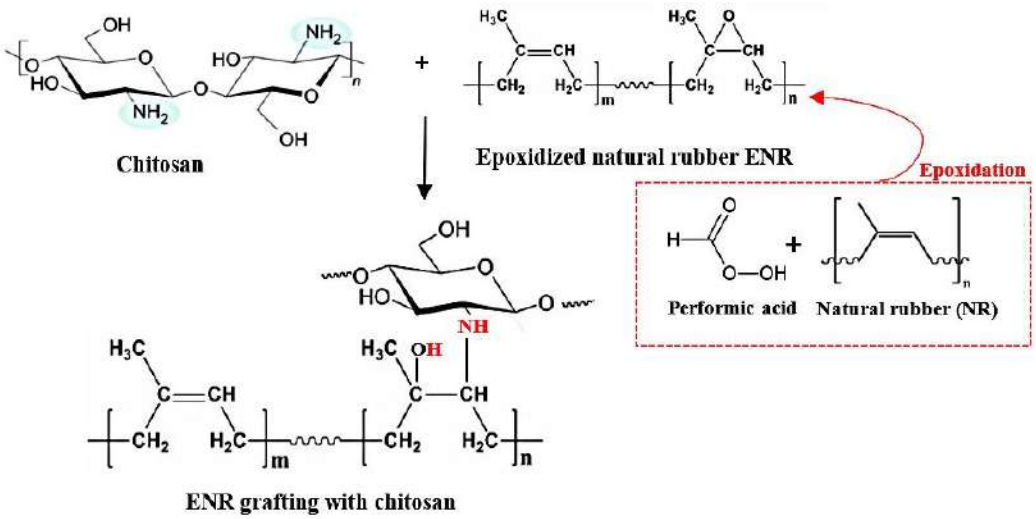


Figure 1. Proposed mechanism of grafting chitosan onto ENR

Table 1. Formulations of ENR and ENR composites*

Formulations [phr]	ENR	CTS10	CTS20	CTS30	CTS40	CTS50
ENR-25	100	100	100	100	100	100
Chitosan	-	10	20	30	40	50

* The unit "phr" denotes parts by weight per hundred parts of rubber. The compounds were prepared in uncrosslinked state.

In this study, ENR with about 25% epoxidation was prepared and confirmed using NMR. ENR–chitosan composites were characterized for processability, mechanical reinforcement, and energy efficiency by Mooney viscosity, tensile testing, and dynamic mechanical analysis (DMA). The tan δ at 60 °C from DMA was used to estimate the rolling resistance of tread tire. Chemical interactions between ENR and chitosan were investigated using Fourier-transform infrared spectroscopy (FTIR), while scanning electron microscopy (SEM) revealed the dispersion of fillers. These combined methods provided a thorough understanding of how filler–matrix interactions affect the performance of green tire materials. The results showed that tensile strength improved with chitosan concentration up to an optimal loading, Higher chitosan contents caused agglomeration and reduced efficiency. The optimal chitosan loading was around 30 phr, compromising improved tensile strength with manageable compound stiffness. DMA data revealed a higher storage modulus and decreased tan δ, indicating the potential for rolling resistance reduction and thus improved energy efficiency in tire performance. DSC measurements confirmed Tg shifts consistent with filler–matrix interactions, while morphological analysis confirmed good dispersion at optimal filler contents, contributing to the overall reinforcement effect. Incorporating chitosan into ENR-based tread compounds enhanced mechanical properties and energy-saving potential, supporting their suitability for green tire applications. However, processing challenges, such as filler dispersion and increased compound stiffness, must be addressed. This finding demonstrates that careful control of chitosan content is crucial for maximizing the benefits of bio-based fillers in sustainable tire tread formulations. Future work will focus on optimizing energy efficiency based on vulcanized condition.

Acknowledgement

This work was supported by Bangkok Metropolis Motor Company Limited through the provision of venues and research grants. The authors also acknowledge the Specialized Center of Rubber and Polymer Materials in Agriculture and Industry (RPM), Department of Materials Science, Faculty of Science, Kasetsart University, Bangkok, Thailand, for financial support of the experimental results.

References

1. Buaksuntear K, Panmanee K, Wongphul K, Lim-arun P, Jansinak S, Shah U.D, Smitthipong W, *Polymer.*, 2024; 291: 126626.
2. Buaksuntear K, Kohl P, Li Y, Smitthipong W, *ACS Appl. Polym. Mater.*, 2025; 7: 3576−3587.
3. Mathew M, Dominic C.D.M., Neenu K.V., Begum P.M.S, Dileep P., Kumar T.G.A., Sabu A.A., Nagane D, Parameswaranpillai J, Badawi M, *Carbohydr. Polym.*, 2023; 310: 120700.
4. Raju G, Haris M.R.H.M, Azura A.R., Eid A.M.A.M., *ACS Omega*., 2020; 5: 28760−28766.
5. Riyajan, S.A., Sukhlaaied W, *Mater. Sci. Eng., C.*, 2013; 33: 1041-1047.
6. Ali Q, Taweepreda W, Techato K, *Polym. Test.*, 2020; 82: 106294.

International Rubber Conference 2025 (IRC2025)
1-3 December 2025 @ BITEC, Bangkok, Thailand

Enhancing Ozone Resistance of Tyre Sidewall by Sustainable Replacement of Petroleum Wax with Bio-based Additive

B. Tirthankar[1], C. Ajay[1], D. Sudeep[1], D. Saikat[1], C. Dipankar[2], D. Mahuya[3] and M. Rabindra[1]

[1]*Hari Shankar Singhania Elastomer and Tyre Research Institute, India*

[2]*Department of Polymer Science and Technology, University of Calcutta, India*

[3]*Greater Kolkata College of Engineering and Management, India*

e-mail address of the presenting author (tirthankar@hasetri.com)

Keywords: Petroleum wax; Sustainable, Tyre, Ozone resistance, Bio, Ecofriendly, Natural, Sidewall

The growing demand for sustainable alternatives in the automotive industry has driven the exploration of renewable resources to replace petroleum-derived materials. Tyre wax, a critical component in tyre compounds, plays a key role in protecting rubber from ozone degradation by forming a surface layer of migrating hydrocarbons. However, these hydrocarbons can crystallize on the surface, giving the tyre a dull appearance. To enhance both appearance and durability, a biobased rubber chemical was investigated for use in the sidewalls of Passenger Car Radial (PCR) tyres. In this study, petroleum-based wax used in the tyre compound was partially and completely substituted by the bio-based additive.

The study found that identifed bio-based additive did not affect vulcanization, processability, or the stress-strain behavior of the compound. Performance evaluations, including dynamic mechanical analysis at 30 °C, 70 °C, and 100 °C, as well as fatigue-to-failure testing, showed comparable results to traditional petroleum-based waxes. Moreover, this bio-based additive demonstrated superior ozone damage resistance and improved the tyre surface's shininess, highlighting its potential as a sustainable and effective antiozonant in tyre formulations.

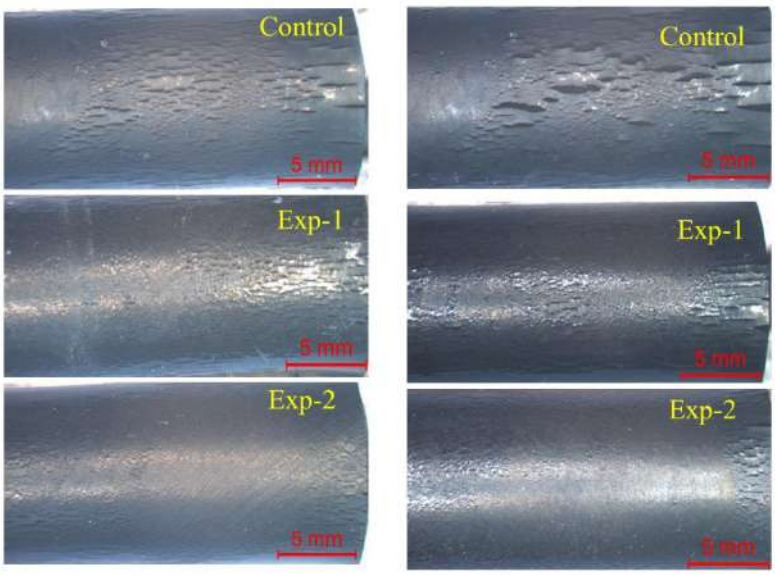


Figure 1. Optical Microscopy images of control with wax, Exp-1 for partial substitution and Exp-2 representing complete substitution of wax after 24hr (LHS) and 72hr (RHS) ozone exposure.

Acknowledgement

Authors sincerely thank Hari Shankar Singhania Elastomer and Tyre Research Institute (HASETRI), Mysore for their technical support, research facilities and financial support and to the conference organizing committee for this opportunity to contribute in balancing nature and innovation for a sustainable future.

References

1. Ossefort ZT (1958) ASTM Special Technical Publication 229: 38.
2. Lattimer RP, Layer RW (1990) Protection of rubber against ozone Rubber Chemistry and Technology 63(3): 426-450.
3. Tucker H (1985) ASTM Special Technical Publication 229: 269.
4. Huntink NM, Datta RN, Noordermeer JWM (2004) Addressing durability of rubber compounds. Rubber Chemistry and Technology 77(3): 476-511
5. Hu X, Zhao HN, Tian Z, Peter KT, Dodd MC, et al. (2022) Transformation product formation upon heterogeneous ozonation of the tire
6. rubber antioxidant 6PPD (N-(1,3-dimethylbutyl)-N′-phenyl-pphenylenediamine). Environ Sci Technol Lett 9(5): 413-419.
7. Sugandha S, Satish A, Somaiya NKJ (2020) Optimisation and evaluation of 2,2,4-trimethyl-1,2-dihydroquinoline (TMQ) and alkyl derivative of phenylene diamine (6PPD) and characterisation of rubber valcanisates. Research Journal of Chemistry and Environment 24(4): 107-117.
8. Budiarto (2017) The effect of antioxidant concentration of N-isopropyl-N-phenyl-p-phenylenediamine, and 2,2,4-trimethyl-1,2-dihydroquinoline and mixing time of physical properties, thermal properties, mechanical properties and microstructure on natural rubber compound. International Conference on Chemistry, Chemical Process and Engineering, Yogyakarta, Indonesia, 1823: 020068.
9. Xu J, Hao Y, Yang Z, Li W, Xie W, et al. (2022) Rubber antioxidants and their transformation products: environmental occurrence and potential impact. Int J Environ Res Public Health 19(21): 14595.
10. Ignatz-Hoover F, To BH, Datta RN, De Hoog AJ, Huntink NM, et al. (2003) Chemical additives migration in rubber. Rubber Chemistry and Technology 76(3): 747-768.

Investigation of the Effect of the amount of zinc borate on cure kinetics, reversion, and mechanical properties of natural rubber in a semi-efficient curing system

Davut AKSÜT[1]

[1] *Hacettepe University, Department of Chemistry, Polymer Chemistry Division, 06800, Ankara, Turkey.*

(davut.aksut@hacettepe.edu.tr)

Key Words: Natural rubber, zinc borate, cure kinetics, reversion, mechanical properties.

Reversion is the deterioration of the network structure in isoprene-based rubbers vulcanized with sulfur caused by high temperatures and extended curing times. This condition manifests as a decrease in torque values in the curing curves, resulting in a reduced cross-link density. Consequently, rubber properties like tensile strength, tear resistance, and solvent resistance are weakened **[1].** Natural rubber (NR) is commonly used in the aviation, aerospace, and tire industries because of its excellent elasticity and mechanical properties. Polysulfide bonds formed during the curing of NR rubber with sulfur systems above 140 °C are broken, leading to reversion. This decreases the crosslink density, which negatively impacts the physical properties and performance of the final product **[2].**

This study investigates the effect of zinc borate (ZnB) on the vulcanization kinetics, reversion behavior, and mechanical properties of natural rubber cured with the Semi-Efficient Vulcanization (SEV) system. The role of ZnB in improving crosslink density and reversion resistance was also systematically assessed. NR compounds with different amounts of ZnO and ZnB were prepared using a laboratory two-roll mixer at 40°C and 50 rpm for 20 minutes. Curing curves of four series of NR compounds were measured at 150, 160, 170, and 180 °C for 20 minutes using an Alpha Technologies MDR 2000-B (USA) Moving Die Rheometer (MDR). Based on these data at the specified temperatures, the effect of ZnB on curing kinetics was analyzed using the Isayev-Deng model. Values from R_{300} and R_{600} were calculated at each temperature and are given in Figures 1a and 1b.

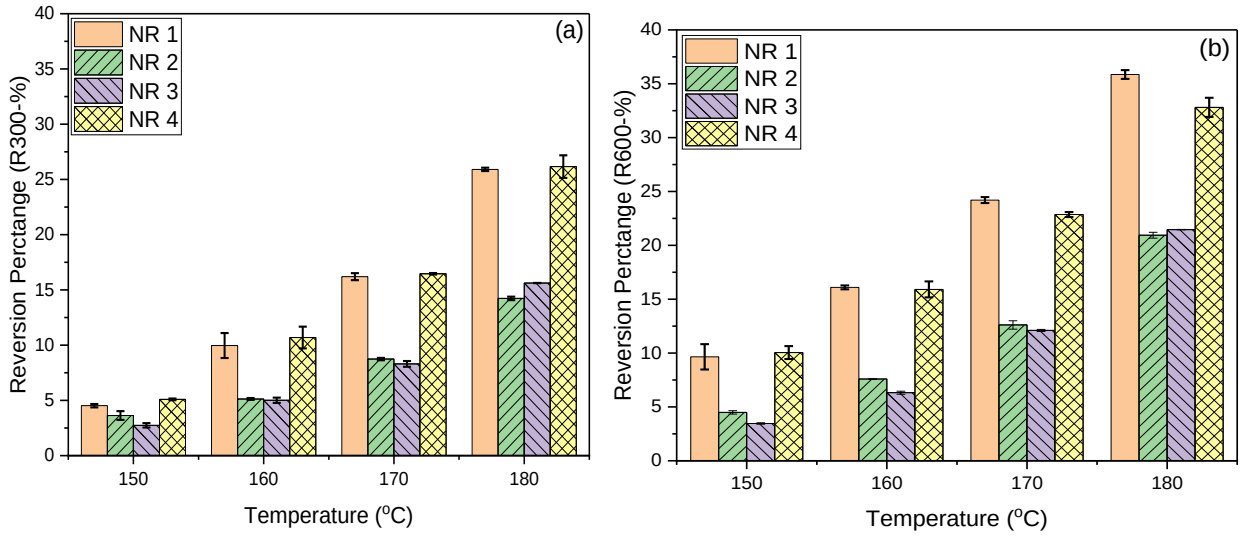


Figure 1. The reversion percentage of NR series blends at R_{300} (a) and R_{600} (b) times are at 150 °C, 160 °C, 170 °C, and 180 °C.

This research indicates that reversion rates for compounds containing both ZnO and ZnB (NR2, and NR3) are significantly lower than those for compounds containing either ZnO or ZnB alone(NR1 and NR4). Specifically, the onset of reversion is delayed, and the reversion percentage decreases to 65% in the compound with equal parts of ZnO and ZnB. Mechanical properties, such as stress-strain curves and Shore A hardness of vulcanizates molded from compounds containing ZnO and ZnB at 180°C, were investigated based on different curing times (optimum curing time (t_{90}), R_{300} (t_{90} + 5 min), and R_{600} (t_{90} + 10 min). The crosslink densities of the test samples cured at 180°C for t_{90} and R_{600} times of compounds with different proportions of ZnO and ZnB, calculated using the Lee-Pawlowski-Coran (LPC) method and the Flory-Rehner equation, support the mechanical test data.

The swelling ratios and crosslink density (XLD) values of the NR series samples, cured at 180 °C according to the curing times t_{90} and R_{600}, were determined using the Flory–Rehner equation and are presented in Figures 2a and 2b, respectively.

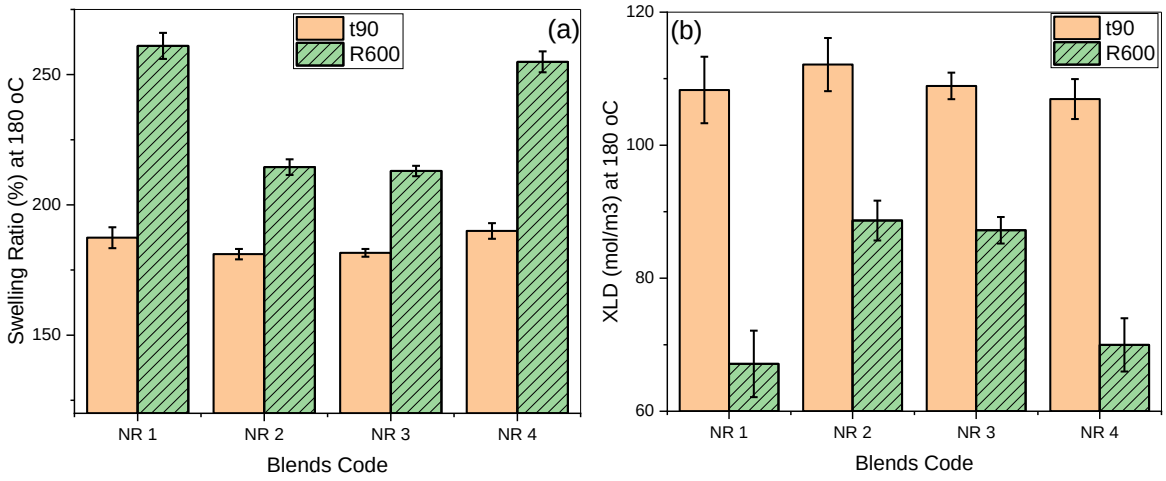


Figure 2. Swelling rates and XLD value of NR series blends at 180 °C with t_{90} and R_{600} times.

It was observed that ZnB, when used together with ZnO, provided industry-acceptable reversion resistance at high temperatures.

Acknowledgments

The author would like to acknowledge the BOREN Institute (Turkey) for kindly providing the non-hydrated zinc borate and its associated technical information.

The author gratefully acknowledge financial support from The Scientific and Technological Research Council of Türkiye, under the 2224-A Grant Program for Participation in Scientific Meetings Abroad.

References

[1] D. Bornstein, R.J. Pazur, Polymer Testing, Volume 88, 2020, 106524. https://doi.org/10.1016/j.polymertesting.2020.106524.
[2] Eric Leroy, Anouar Souid, Rémi Deterre, Polymer Testing, Volume 32, Issue 3, 2013, Pages 575-582. https://doi.org/10.1016/j.polymertesting.2013.01.003.

International Rubber Conference 2025 (IRC2025)
1-3 December 2025 @ BITEC, Bangkok, Thailand

Eco-Efficient Vulcanization: Analysis of a Sustainable Rubber Curing Package

F. VAN ELBURG[1], F. GRUNERT[1], M. DI CONSIGLIO[2],
A. ZYCH[2], Y. SHODA[2], A. TALMA[1], A. BLUME[1]

[1] *University of Twente, Elastomer Technology and Engineering, Drienerlolaan 5, Enschede, Netherlands.*

[2] *Bridgestone Europe NV/SA, Italian Branch, Technical Center, Via del Fosso del Salceto 13/15, Rome, Italy.*

e-mail address of the presenting author (f.a.vanelburg@utwente.nl)

Keywords: Vulcanization, Tires, Sustainability.

Zinc oxide and stearic acid are generally added to rubber compounds to activate the curing reaction with sulfur. Various studies have investigated the curing mechanism involving these activators [1-3]. Due to the possible environmental implications, an eco-friendlier curing system is desired. Despite extensive research, a suitable alternative resulting in comparable properties has not yet been found [4].

A recent publication reported that zinc oxide and stearic acid are unnecessary for curing high-vinyl S-SBR compounds [5]. Similar maximum torques and shorter scorch times were obtained for the compound without activators, suggesting that the activators function as retarders. Furthermore, the removal of N,N'-Diphenylguanidine (DPG) resulted in a slight increase in the scorch time. The study concluded that both zinc oxide and DPG can be omitted to create an eco-friendlier curing system. Nevertheless, optimization of the system is required to achieve appropriate scorch times and a less pronounced marching modulus.

This eco-friendlier curing package needs to be further researched to understand the curing mechanism better in order to efficiently optimize the system. Therefore, compounds with and without activators, as well as with and without DPG were analyzed (**Tab. 1**). To get insight into the influence of the silica/silane system on the curing reaction, filled and unfilled samples were evaluated.

Table 1. Rubber formulations

Components [phr]	**Sample notations**									
	1.TBBS	**2.TBBS**	**3.TBBS**	**4.TBBS**	**4.Sulfur**	**1.TBBS (UF)**	**2.TBBS (UF)**	**3.TBBS (UF)**	**4.TBBS (UF)**	**4.Sulfur (UF)**
S-SBR[a]	80	80	80	80	80	80	80	80	80	80
BR[b]	20	20	20	20	20	20	20	20	20	20
Silica	80	80	80	80	80	-	-	-	-	-
TESPD[c]	6.2	6.2	6.2	6.2	6.2	-	-	-	-	-
TDAE[d]	37.5	37.5	37.5	37.5	37.5	-	-	-	-	-
Zinc oxide	2.5	2.5	-	-	-	2.5	2.5	-	-	-
Stearic acid	2.5	2.5	-	-	-	2.5	2.5	-	-	-
Sulfur	1.4	1.4	1.4	1.4	1.4	1.4	1.4	1.4	1.4	1.4
TBBS[e]	2.0	2.0	2.0	2.0	-	2.0	2.0	2.0	2.0	-
DPG[f]	1.5	-	1.5	-	-	1.5	-	1.5	-	-

[a] Solution Styrene Butadiene Rubber, [b] Butadiene Rubber, [c] Bis(trietohxysilylpropyl)disulfide, [d] Treated Distillate Aromatic Extract, [e] N-tert-butyl-2-benzothiazole sulfenamide, [f] N,N'-Diphenylguanidine

The rheometer curves, cured Payne effect (filled compounds), stress-strain behavior, and dynamic mechanical analysis (DMA) of the samples were measured. Different trends, for example in the maximum torque values of the rheometer curves, for the filled and unfilled compounds were

obtained, suggesting strong differences in the crosslink network. The cured Payne effect, stress-strain behavior, and DMA results also suggested variations in crosslink densities. Therefore, the Thiol-Amine method was performed to get insight into the crosslink network structure. **Fig. 1** shows the calculated mono-, di- and polysulfidic content of the filled and unfilled compounds.

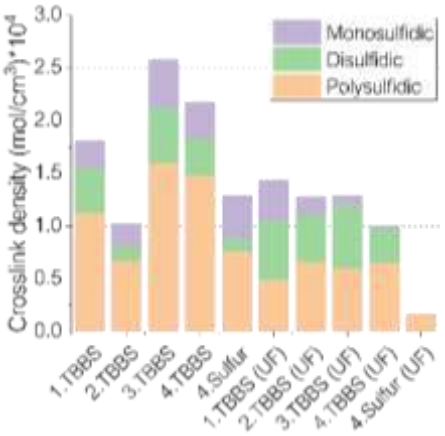


Figure 1. Crosslink structure of both filled and unfilled compounds.

The differences in the total crosslink density of the compounds are in line with the variations obtained in the other measurements. For example, the total crosslink densities showed a linear correlation with the obtained delta torque values of the rheometer curves. Although the silica likely influences the Thiol-Amine results, the differences in trends become clear. Based on the results, it can be concluded that the silica/silane system plays a large role in the curing reaction. The results especially show that the activators not only act as retarders as described by Blume et al. [5] but also interfere with the curing reaction. However, this only occurs in the filled system. In the unfilled compound, the crosslink density of the compound with activators (2.TBBS (UF)) is slightly higher than the compound without activators (4.TBBS(UF)). Possibly, the silane influences the formation of the zinc complex, which traps either the sulfur, the accelerator, or both. Besides, the results show that the crosslink formation happens in absence of any activators and accelerators, likely via a direct coupling between the sulfur and vinyl groups of S-SBR, as explained by Blume et al. [5]. Possibly, this reaction is enhanced by the presence of silane.

Based on this study, it becomes clear that the silica/silane system affects the curing behavior of the compound, which needs to be taken into consideration when optimizing the curing package. Further research is needed to understand which chemical reactions take place between the curing ingredients and the silica/silane system.

References

1. Ikeda Y, Yasuda Y, Ohashi T, Yokohama H, Minoda S, Kobayashi H, Honma T. *Macromolecules*, 2015; 48: 462.
2. Butuc S, Van Leerdam K, Rossenaar B, Swart J, Geurts F, Bossinga-Geurts B, Verwer P, Talma A, Blume A, *Polymer Testing*, 2023; 117: 107843.
3. Ignatz-Hoover F, To B. "Vulcanization," in *Rubber Compounding: Chemistry and Applications*, Boca Raton, Florida, USA: CRC Press, 2016; 472.
4. Moneypenny H, Menting K, Gragg F. "General Compounding," in *Rubber Compounding: Chemistry and Applications*, Boca Raton, Florida, USA: CRC Press, 2016; 366.
5. Blume A, Van Elburg F, Grunert F, Talma A. *Molecules*, 2024; 29: 5198.

International Rubber Conference 2025 (IRC2025)
1-3 December 2025 @ BITEC, Bangkok, Thailand

Overview of SRI's research initiatives for enhancing the well-being of natural rubber stakeholders in Thailand

L Tarachiwin[1], K Kanyawararak[1], H Kum-ourm[1], K Charungchitaree[1], N Onozuka[2], A Matsuura[2], A Uesugii[2], Y Kitaura-Sakaguchi[2], T Tada[2]

[1]*R&D Department, Sumitomo Rubber (Thailand) Co., Ltd., Rayong, Thailand.*

[2]*R&D HQ, Sumitomo Rubber Industries, Ltd., Kobe, Japan.*

(lucksanaporn-t@sumitomorubber.co.th)

Keywords: sustainable natural rubber, tissue culture NR tree, low tapping frequency, low odor NR

Sumitomo Rubber Industries, Ltd. (SRI) is one of the leading global tire manufacturers committed to promoting sustainability both across economic and social dimensions. Our mission is to harmonize human prosperity with environmental stewardship throughout all business activities. As natural rubber (NR) is a key raw material in the tire industry, we strive to securing its sustainable use. With rising concerns on low NR productivity, labor shortage and environmental issues of smallholders can result in unsustainable of NR production. Through our company's Sustainable Natural Rubber (SNR) Policy, we aim to ensure the long-term viability of NR by supporting human well-being throughout the entire supply chain.

As the world's leading NR producer and exporter, Thailand plays a critical role in the global supply chain. To support sustainable development in NR sector, SRI has launched three key research initiatives in Thailand in collaboration with Thai and internatioal partners targetting upstream and midstream production challenges;

1. Propagation of NR tree by tissue culture (TS) technology for enhancing NR latex yield has successfully produced the first prototype TS tree for future propagation technology development. The TS production process is shown in **Figure 1**.

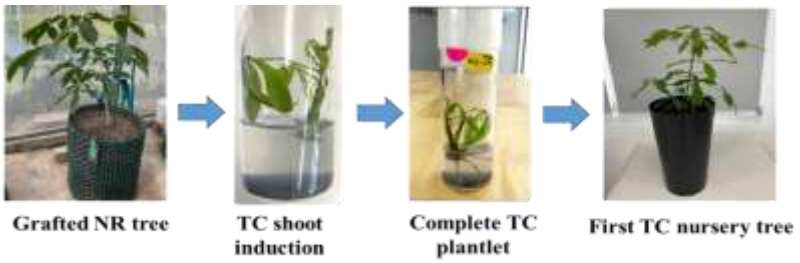


Figure 1. TC tree production from grafted tree by tissue culture technique

2. Low tapping frequency with ethephon stimulation practice shows the efficiency on securing NR latex yield of RRIM600 and RRIT251 clonal, without showing any significant negative impact on NR property as comparable as conventional method as illustrated in **Table 1**. This offers a viable solution to future labor scarcity, while maintaining rubber performance.

Table 1. Physical properties of TSR10-like rubber sample

Rubber properties	RRIM600	RRIT251

	Conventional	Low tapping frequency with ethephon	Conventional	Low tapping frequency with ethephon
Mooney Viscosity (a. u.)	85.2 ± 2.5 [b]	86.2 ± 1.7 [b]	96.4 ± 1.2 [a]	94.9 ± 1.4 [a]
P_0 (1/100 mm)	49.6 ± 1.5 [b]	49.0 ± 1.2 [b]	55.2 ± 0.6 [a]	54.1 ± 0.8 [a]
PRI (%)	84.5 ± 1.1 [a]	83.5 ± 1.2 [a]	81.5 ± 0.8 [a]	81.7 ± 0.6 [a]
M_w (kg mol^{-1})	1527 ± 45 [b,c]	1482 ± 36 [c]	1677 ± 30 [a]	1647 ± 37 [a,b]

Values not connected by same letter are significantly different according to Tukey-Kramer test (P = 5%).

3. Process improvement in TSR20 production reduces the index of causative bad odor substances by 90%, significantly minimizing putrefactive odor in NR factory.

These initiatives mark our company's attempt on developing new technologoies for future commerical scale application with socio-economic and environmental benefits. Future implementation efforts aim to equip smallholders with practical solution for sustainable NR utilization in the tire industry.

Acknowledgement

The authors would like to express their sincere gratitude to CIRAD, Kasetsart University, and Khon Kaen University for their valuable contributions to these researches. We also extend our thanks to Sumirubber Thai Eastern Plantation Co., Ltd. for providing the research sites and natural rubber samples.

References

1. Kum-ourm H , Liengprayoon S, Onozuka N, Vaysse L, Tarachiwin L, Lacote R, Chaiyut J, Jantarasunthorn S, Lerksamram T, Cakpo C B, Gay F, Ferrer V, Char C, Matsuura A, Sakaguchi-Kitaura Y, Miyagi-Inoue Y, Bottier C, Ind. Crops Prod., 2025; Manuscript submitted for publication.
2. Liengprayoon S, Kum-ourm H, Vaysse L, Lacote R, Chaiyut J, Jantarasunthorn S, Lerksamram T, Gay F, Ferrer V, Char C, Onozuka N, Tarachiwin L, Matsuura A, Sakaguchi-Kitaura Y, Miyagi-Inoue Y, Bottier C, Ind. Crops Prod., 2025; Manuscript submitted for publication.
3. Tarachiwin T, Kanyawarak K, Charungchitaree K, Matsuura A, Okada A, Miyagi-Inoue Y, Ichikawa N, 2022; Recent research activities for sustainable natural rubber development in Thailand. Oral presentation at the RubberCon2022, Kuala Lumpur, Malaysia.

Research Progress on Modification and Functionalization of Natural Eucommia Ulmoides Gum

Hailan Kang*, Feng Yang, Qinghogn Fang

Key Laboratory for Rubber Elastomer of Liaoning Province, College of Materials Science and Engineering, Shenyang University of Chemical Technology, Shenyang, 110142, China.

Correspondence to: Hailan Kang (E-mail: kanghailan@syuct.edu.cn)

Keywords: Eucommia ulmoides gum; Chemical modification; Shape memory; Electromagnetic shielding; Wave absorption

Eucommia ulmoides gum (EUG) is a unique crystalline natural polymer material, primarily extracted from the fruits, bark, and leaves of the Eucommia ulmoides tree. Its molecular backbone consists of trans-1,4-polyisoprene, rich in double bonds and possessing a symmetric, ordered structure, which endows it with unique rubber-plastic duality. Owing to the high reactivity of EUG's double bonds, functionalization has been achieved through chemical modifications such as epoxidation, sulfonation, and degradation. Epoxidation combined with chemical grafting has enabled the development of high-elasticity and self-healing EUG materials through the formation of multiple hydrogen bonds. Sulfonation enhances intermolecular polar interactions, leading to the creation of EUG-based high-damping materials and potent adhesives. Through controlled degradation, liquid EUG has been synthesized and subsequently incorporated into epoxy resin composites for application in anti-corrosion coatings. By leveraging the tunable crystalline domains and cross-linked networks of EUG, EUG-based thermoplastic vulcanizates (TPV) with shape memory properties have been prepared via dynamic vulcanization technology. Furthermore, crystalline-crosslinked network synergy enables heat-, electricity-, and magnetism-responsive EUG shape-memory materials. Further enhancing comprehensive functionality, a triple-network synergistic regulation strategy has been employed: chemical cross-linking networks strengthen mechanical properties; residual crystalline networks improve environmental resistance; and nanofillers (carbon materials/MXene) construct conductive pathways. This strategic design has significantly improved the performance of EUG-based composite materials, enabling the development of flexible EUG electromagnetic shielding and wave-absorbing materials, thereby expanding the functional and high-performance application scope of EUG.

Reference

1. Kang H, Cui Y, Li X, Hu J, Ni H, Li D, Li L, Fang Q, Zhang J. Biobased and Biodegradable Shape Memory Polymers of Eucommia Ulmoides Gum and Polycaprolactone via Dynamic Vulcanization. Industrial & Engineering Chemistry Research, 2024, 63, 11218–11229.
2. Han L, Kang H,* Luo T, Hu J, Cui Y, Li D, Li L, Zhang J, Fang Q. Enhanced EMI shielding effectiveness of green Eucommia ulmoides gum composites through heterogeneous and crystalline structures. Industrial Crops and Products, 2024, 219: 119033.

3. Li L, He Z, Wang Z, Kang H,* Li D, Fang Q. Sustainable eucommia ulmoides gum composites with outstanding electromagnetic wave absorption properties. Composites Communications, 2024 (48), 101945.
4. Kang H, Luo S, Du H, Han L, Li D, Li L, Fang Q. Bio-based Eucommia ulmoides gum composites with high electromagnetic interference shielding performance. Polymers, 2022, 14, 970.
5. Li L, Luo S, Li D, Wang Na, Kang H,* Fang Q. Thermal and electrical dual-triggered shape memory Eucommia ulmoides gum derived from renewable resources. Polymer Composites, 2022, 43, 378-388.
6. Kang H, Gong M, Xu M, Wang H, Li Y, Fang Q, Zhang L. Fabricated biobased Eucommia ulmoides gum/polyolefin elastomer thermoplastic vulcanizates into a shape memory material. Industrial & Engineering Chemistry Research, 2019, 58(16), 6375-6384.

Critical Concentration of Primary Amines for Preparation of Vulcanized Deproteinized Natural Rubber with Outstanding Mechanical Properties

LAM BA NGUYEN[1], SEIICHI KAWAHARA[1]

[1] *Nagaoka University of Technology, 1603-1, Kamitomioka-machi, Nagaoka, Niigata, 940-2188, Japan*

Presenting author: s235002@stn.nagaokaut.ac.jp

Keywords: Critical concentration, Deproteinized Natural Rubber, Accelerated sulfur vulcanization, Amine compound, Zinc complex.

Introduction:

Vulcanized deproteinized natural rubber (DPNR) with outstanding mechanical properties may be prepared by incorporating amine compounds into the standard vulcanization formula. This is because the amine compounds can act as ligands, which coordinate to zinc with 2-mercaptobenzothiazole (MBT) to form zinc complexes necessary for the accelerated sulfur vulcanization. However, the excess amount of amine compounds may result in unexpected phenomena, i.e., surface segregation, crystallization, side reactions, and so forth. Therefore, we must determine the prominent amount of amine compounds for the accelerated sulfur vulcanization of DPNR. In the previous work, Suchiva. *et al.* [1] found that proteins promote the vulcanization of NR, while Pamanuluk. *et al.* [2] reported that proteins contribute to the homogenous dispersion of zinc into NR. This implies the importance of nitrogen-containing compounds in the accelerated sulfur vulcanization. In fact, Wei. *et al.* [3] reported that the use of octylamine, up to 2 phr, in the vulcanization of washed NR improved the homogeneity of the crosslinking network. In the present study, octadecylamine (ODA) and octamethylenediamine (OMDA) were used as amine compounds to promote the accelerated sulfur vulcanization. The resultant vulcanized DPNR were evaluated by measuring curing characteristics, crosslink density, mechanical properties, and the structure of crosslinking junctions.

Table 1. Vulcanization formulas for vulcanized DPNR

Components [phr]	**Sample notations**		
	Control-vulcanized DP	**DP-ODA**	**DP-OMDA**
DPNR	100	100	100
Zinc oxide	5	5	5
Stearic acid	1	1	1
ODA	-	0.2, 0.4, 0.6, 1.0, 1.4, 1.8, 2.2, 2.6, 3.0, 3.6, 4.2, 4.8, 5.4, 6.0	-
OMDA	-	-	0.1, 0.2, 0.4, 0.6, 0.8, 1.0, 1.2, 1.4, 1.6, 1.8
TBBS accelerator	0.7	0.7	0.7
Sulfur	3	3	3

Experimentals:

Natural rubber latex used in the present study was a commercial high-ammonia natural rubber (HANR) latex with a total solids content (TSC) of 60 w/w% obtained from Thailand and supplied by Fukuwa Rubber Co., Ltd., Japan. Deproteinized natural rubber (DPNR) was prepared from HANR by ordinary procedure reported in elsewhere, followed by drying at 50 °C for a week under reduced pressure [4]. DPNR was vulcanized with various amounts of ODA and OMDA together with

compounding agents shown in Table 1, using an internal mixer. Vulcanized DPNR sheets were prepared by pressing the DPNR compounds at 150 °C under a pressure of 15 MPa for the optimal vulcanization time (t_{90}). Cure characteristics of the NR compounds were measured using a rotorless rheometer (RLR-4) at 150 °C. The vulcanized samples were swollen with toluene to determine crosslink density. Structure of crosslinking junctions were determined by Rubber-state NMR spectroscopy, using a Field-Gradient Magic Angle Spinning (FG-MAS) probe.

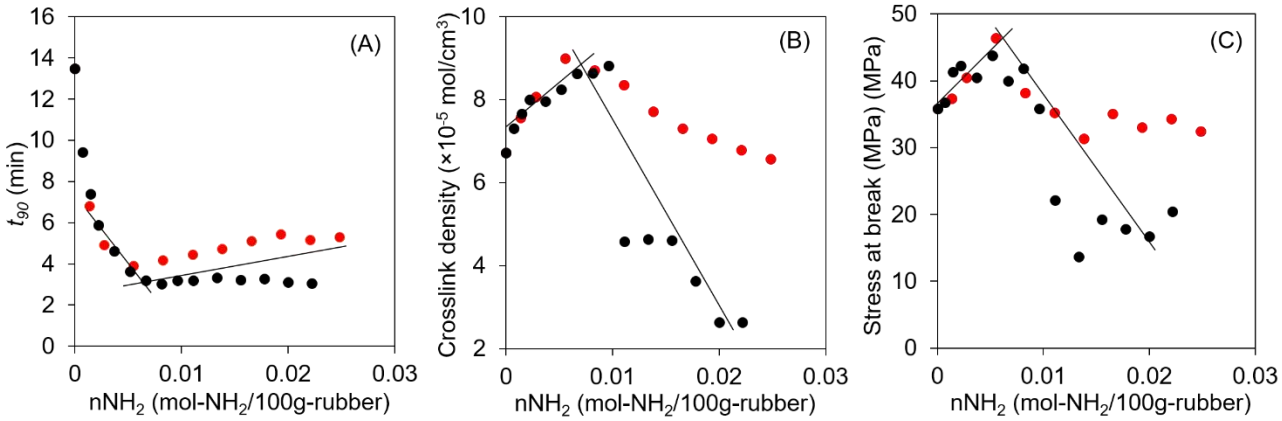


Figure 1. Plot of (A) optimal vulcanization time (t_{90}), (B) Crosslink density, and (C) Stress at break versus mole of NH_2 group in 100 g-rubber (Black: DP-ODA; Red: DP-OMDA)

Results and discussion:

Figure 1(A) shows a plot of optimal vulcanization time (t_{90}) for DPNR versus mole of NH_2 group in 100 g-rubber. The t_{90} shortened for DP-ODA and DP-OMDA as the mole of NH_2 group in 100 g-rubber increased until it reached to mimimum at approximately 0.007 mol-NH_2/100 g-rubber, and then it gradually increased. This implies that the prominent mole of NH_2 group in 100 g-rubber was approximately 0.007 mol-NH_2/100 g-rubber for not only DP-ODA but also DP-OMDA. Figure 1(B) shows a plot of crosslink density for vulcanized DPNR versus mole of NH_2 group in 100 g-rubber. The crosslink density of DP-ODA and DP-OMDA increased as the mole of NH_2 group in 100 g-rubber increased, until it reached the maximum at also approximately 0.007 mol-NH_2/100 g-rubber, and then it abruptly decreased. This implies that the prominent mole of NH_2 group in 100 g-rubber for the formation of crosslinking junctions was approximately 0.007 mol-NH_2/100 g-rubber for not only DP-ODA but also DP-OMDA. Figure 1(C) shows a plot of stress at break for vulcanized DPNR versus mole of NH_2 group in 100 g-rubber. The stress at break also increased for both DP-ODA and DP-OMDA as the mole of NH_2 group in 100 g-rubber increased, and it also reached the maximum at approximately 0.007 mol-NH_2/100 g-rubber, after that, it also abruptly decreased. Consequently , we found that the prominent mole of NH_2 group in 100 g-rubber were consistent, i. e., approximately 0.007 mol-NH_2/100 g-rubber for t_{90}, crosslink density, and stress at break for not only DP-ODA but also DP-OMDA.

References

1. Suchiva K, Kowitteerawut T, Srichantamit L, *J. Appl. Polym. Sci.*, 2000; 78: 1495–1504.
2. Pamanuluk K, Sato A, Thuong N, Nghia P, Kosugi K, Yamamoto Y, Kawahara S, *Polymer*, 2024; 307:127272.
3. Wei Y, Zhu D, Zhang J, Wang H, Zhou M, Liao S, *Int. J. Biol. Macromol.*, 2023; 250: 126202.
4. Chaikumpollert O, Yamamoto Y, Suchiva K, Kawahara S, *Colloid Polym. Sci.*, 2012; 290(4): 331-338.

Removal of proteins from natural rubber by creaming method

Viet Anh TA[1], Seiichi KAWAHARA[1], Yoshimasa YAMAMOTO[2], Thuong Thi NGHIEM[3], Nghia Trung PHAN[3]

[1]*Nagaoka University of Technology, Nagaoka, Japan*

[2]*National Institute of Techonology, Tokyo College, Tokyo, Japan*

[3]*Hanoi University of Science and Technology, Hanoi, Vietnam*

(s247013@stn.nagaokaut.ac.jp)

Keywords: protein-free natural rubber, precipitation, creaming method

Introduction

Proteins present in natural rubber (NR) must be efficiently removed, as they cause latex allergy, a Type I hypersensitively reaction that may lead to anaphylaxis. [1] One effective method for protein removals is the creaming process, which reduces protein solubility in water by increasing the ionic strength. This technique separates components based on density differences - rubber particles rise to the top, while proteins remain in the serum below. In recent years, alternative methods such as centrifugation and ultrasonication have also been developed for protein removal.[2] [3] However, even after purification, NR may still contain nitrogenous compounds that can trigger latex allergies. Therefore, more efficient protein removal techniques are essential to improve the quality and safety of NR. The creaming method is particularly well-suited for protein separation as it leverages high ionic strength to induce a salting-out effect [4]. The method is simple, cost-effective, and scalable. Overall, this approach shows strong potential for the producing low-protein NR suitable for medical and other high-purity applications. In the present study, the creaming process was further developed based on this principle.

Experimental section

Natural rubber latex used in the present study was a commercial high-ammonia natural rubber (HANR) latex (approximately 60 w/w% dried rubber content-TSC). The latex was first diluted with deionized water to 30 w/w% TSC, and then mixed with 2 w/w% NaOH (Kishida Chemical) and 1 w/w% sodium dodecyl sulfate (Kishida Chemical). The mixture was incubated at ambient or elevated tempeartues for 24 hours. After cooling, 0.1 w/w% urea (Nacalai Tesque Inc.) was added, followed by gradual addition of a 10 w/w% creaming agent. After the creaming process, the skim fraction was recovered and redispersed in deionized water. This washing step was repeated twice. The resulting latex was then concentrated and dried to prepare as-cast films for analysis. The samples were characterized using the Kjeldahl method and tensile testing.

Results and discussion

Table 1 shows the nitrogen content of HANR and purified rubber after creaming process. The nitrogen content of HANR was 0.194 w/w%. After the first creaming step, this value decreased to 0.034 w/w%. Subsequent separations further reduced the nitrogen content to 0.016 w/w% after the second creaming and 0.005 w/w% after the third. A single centrifugation of the third cream fraction further lowered the nitrogen content to 0.002 w/w%. These results demonstrate that the creaming method is highly effective for removing proteins from natural rubber at the latex stage.

Figure 1 presents the stress–strain curves for as-cast film prepared from HANR latex and the 3rd cream fraction after centrifugation. Both curves exhibited the characteristic stress upturn behavior of natural rubber. The stress at break of HANR was 2.66 MPa, whereas it decreased to 1.3 MPa after three times of creaming. This reduction may be explained to be due to the removal of proteins, which results in a decomposition of the physical crosslinking junctions of the gel fractions. In our previous studies, we found that the stress of natural rubber increased abruptly as the strain increased due to the strain-induced crystallization (SIC), whereas that of protein-free natural rubber didn't exibit the abrupt increase due to the decomposition of the physical crosslinking junctions of the gel fractions [4].

From the results, we proved that protein-free natural rubber was prepared by multi-step creaming andcentrifugation of HANR latex.

Table 1. The nitrogen content of creams obtained after the creaming process

Specimen	%N (w/w%)
HANR	0.194
1st separation	0.034
2nd separation	0.016
3rd separation	0.005
3rd separation (After centrifugation)	0.002

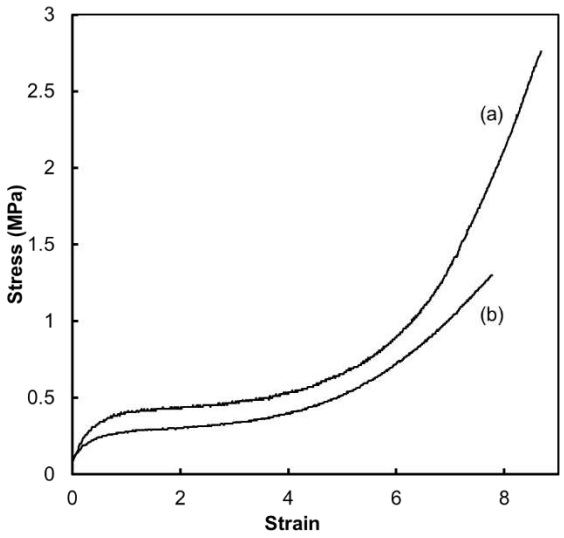


Figure 1. Stress-strain curves of (a) HANR, (b) the 3rd cream after centrifugation

Conclusion

The creaming process combined with centrifugation effectively removed proteins from natural rubber, reducing nitrogen content to 0.002 w/w%. The rubber retained its characteristic stress–strain behavior, confirming the method's potential for producing clean, low-protein NR.

References

1. Kawahara, S.; et al. *Polym. Adv. Technol.* 2004, 15, 181 – 184.
2. Kang, B.; Tang, H.; Zhao, Z.; Song, S. *ACS Omega* 2020, *5*, 6229.
3. Sengar, A. S.; Thirunavookarasu, N.; Choudhary, P.; Naik, M.; Surekha, A.; Sunil, C. K.; Rawson, A. *Appl. Food Res.* 2022, *2* (2).
4. Chaikumpollert, O.; Yamamoto, Y.; Suchiva, K.; Nghia, P. T.; Kawahara, S. *Polym. Adv. Technol.* 2012, 23, 825.

International Rubber Conference 2025 (IRC2025)
1-3 December 2025 @ BITEC, Bangkok, Thailand

Synthetic Strategies and Mechanistic Studies of Liquid Rubber

Jian Tang[1], Jinhui Liu[1], Yudong Liu[1], Kai Liu[1], Jing Hua[1],

[1] *Key Laboratory of Rubber-Plastics, Ministry of Education / Shandong Provincial Key Laboratory of Rubber-plastics, Qingdao University of Science and Technology, Qingdao 266042, P.R. China.*

(huajing72@qust.edu.cn)

Keywords: Anionic polymerization, Liquid rubber, Polybutadiene

Liquid rubber refers to low-molecular-weight rubbers (typically 1000–10000 g·mol^{-1}) with good fluidity at ambient temperature. High-vinyl polybutadiene liquid rubber, owing to its excellent heat resistance, low shrinkage, and favorable dielectric properties, has been widely used in high-frequency electronic applications such as 5G copper-clad laminates and semiconductor encapsulation [1]. Conventionally, it is synthesized via anionic polymerization, where producing low-molecular-weight products requires excessive organolithium initiators, leading to high costs and residual metal concerns [2]. With lithium resources increasingly constrained, this challenge is exacerbated. To address it, we propose a Pulsed Chain Transfer Polymerization (PCTP) strategy [3], which enables initiator regeneration through cyclic chain transfer, thereby affording high-vinyl content products with controlled/living characteristics while reducing initiator consumption by over an order of magnitude.

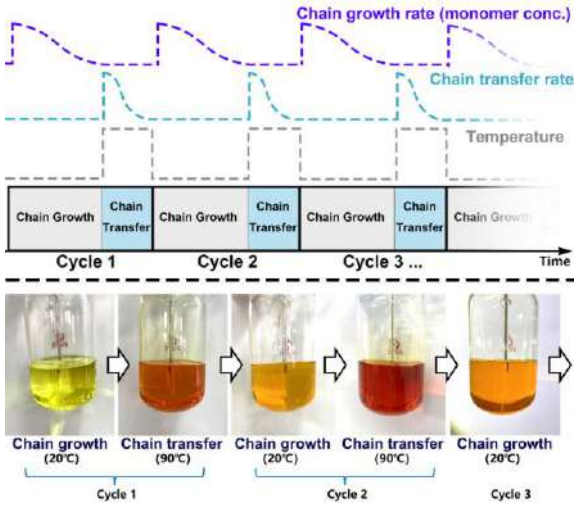


Figure 1. Schematic illustration of the pulsed chain transfer polymerization process

It is well known that diene anionic polymerization in toluene is usually accompanied by random chain transfer, leading to broadened molecular weight distributions. In contrast, PCTAP is fundamentally different from conventional chain-transfer polymerization. As illustrated in Figure 1, PCTAP strictly separates polymerization and chain-transfer steps, essentially operating as a sequence of "active" polymerization cycles, followed by controlled chain transfer after each cycle. Polymerization first proceeds at low temperature, where active chain growth occurs. At the end of each chain-growth stage, chain transfer is triggered by heating. Because all polymer chains are nearly equal in length and no monomer remains in the system, the molecular weight distribution of the resulting "dead" polymers is extremely narrow. This chain transfer proceeds through the formation of benzyl lithium (BnLi), thereby regenerating the initiator. Upon further monomer addition, BnLi

acts as the initiator for the next cycle. Thus, by alternating temperature control and intermittent monomer feeding, initiator recycling is achieved, enabling the synthesis of large amounts of polymer with only a small quantity of initiator.

The 1,2-selectivity of the polymerization can also be tuned by varying the ligand structure. We further propose a new model of regioselectivity in anionic polymerization based on "conformational constraint" and steric effects [4]. Guided by this model, highly efficient catalytic systems can be designed, affording products with 1,2-structural unit contents approaching 100%.

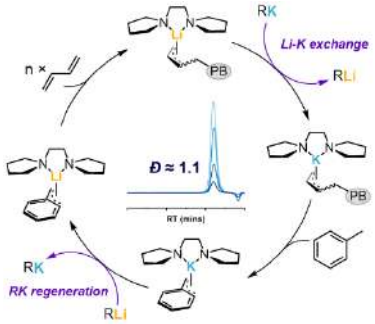


Figure 1. Mechanism of pulsed chain transfer polymerization

Compared with the conventional n-BuLi/Lewis base systems, PCTAP introduces catalytic amounts of n-BuK and a 1,2-dipyrrolidinylethane ligand, which enables temperature-responsive control over chain transfer. This strategy effectively addresses the long-standing issues in the preparation of low-molecular-weight polymers, including excessive initiator consumption, high residual metal content, and broad molecular weight distribution, provides a new pathway for the cost-effective and controlled synthesis of high-vinyl liquid polybutadiene rubbers.

Acknowledgement

Financial support for this work was provided by the National Natural Science Foundation of China (contract grant number 52373010).

References

1. Zhang, Y., Liu, Z., Zhang, X., & Guo, S. (2021). Sandwich-layered dielectric film with intrinsically excellent adhesion, low dielectric constant, and ultralow dielectric loss for a high-frequency flexible printed circuit. *Industrial & Engineering Chemistry Research*, *60*(31), 11749-11759.
2. Forens, A., Roos, K., Dire, C., Gadenne, B., & Carlotti, S. (2018). *Accessible microstructures of polybutadiene by anionic polymerization*. Polymer, 153, 103-122.
3. Tang, J., Liu, Y., Liu, J., Zhang, J., Xie, Z., Hua, J., & Li, Z. (2025). "Pulsed" Chain Transfer Anionic Polymerization: A Green and Cost-Effective Approach for Controlled Polymer Synthesis. *Angewandte Chemie, 137*(19), e202500761.

4. Tang, J., Fu, Y., Hua, J., Zhang, J., Peng, S., & Li, Z. (2024). Unlocking regioselectivity: steric effects and conformational constraints of Lewis bases in alkyllithium-initiated butadiene polymerization. *Chemical Science*, *15*(48), 20493-20502.

Understanding and Controlling Storage Hardening in Natural Rubber via Phospholipid Network Disruption

Kittipong Insom[1] and Jitladda Sakdapipanich[1,2]*

[1] *Rubber Research Group, Department of Chemistry, Faculty of Science, Mahidol University, Nakhon Pathom 73170, Thailand*

[2] *The Rubber and Rubber Glove Academician Association, Bangkok, 10900, Thailand*

Presenting author: kittiponginsom@yahoo.com

*Corresponding author: jitladda.sak@mahidol.ac.th

Keywords: Natural Rubber, Storage Hardening, Phospholipids, Hydroxylamine

Abstract

Storage hardening in natural rubber (NR) is a time-dependent phenomenon that significantly impairs its processability, as prolonged storage leads to increased gel content, higher Mooney viscosity, and elevated hardness. This study provides an updated perspective on the molecular mechanisms underlying storage hardening, highlighting the role of phospholipid-derived long-chain fatty acid esters located at the ω-terminal ends of rubber molecules. Evidence from both long-term and accelerated storage experiments indicates that proteins are not the primarily contributors to gel formation, whereas the ester groups in phospholipids play a central role in network structure development as shown in **Figure 1**. The influence of environmental humidity is also underscored, with high-moisture conditions shown to suppress hardening by inhibiting intermolecular crosslinking reactions.

Additionally, the efficacy of polar chemical additives, particularly hydroxylamine, in mitigating storage hardening was critically assessed. Hydroxylamine was demonstrated to disrupt hydrogen bonding and cleave phospholipid-based branch points, thereby effectively stabilizing NR during storage. Collectively, these insights establish a mechanistic framework for understanding and controlling storage hardening in NR and propose practical strategies for its mitigation in industrial applications.

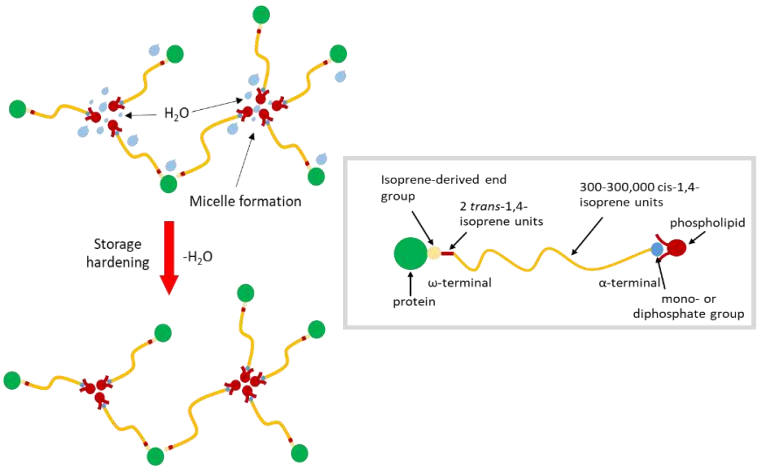


Figure 1 Proposed gel-like structure of NR after storage hardening

References

1. Sriring M, Nimpaiboon A, Kumarn S, Sirisinha C, Sakdapipanich J, Toki S, *Polym. Test*., 2018;70:127.
2. Kumarn S, Churinthorn N, Nimpaiboon A, Sriring M, Ho C-C, Takahara A, *et al*., *Langmuir*. 2018;34(43):12730.

New non-isocyanate polyurethane films based on natural rubber

Tharin SENSAN[1], Anuwat SAETUNG[2], Nitinart SAETUNG[1]

[1]*Division of Physical Science, Faculty of Science, Prince of Songkla University, Hatyai campus, Songkhla, Thailand.*

[2]*Department of Rubber Technology and Polymer Science, Faculty of Science and Technology, Prince of Songkla University, Pattani campus, Pattani, Thailand*

6810230001@psu.ac.th

Keywords: Non-isocyanate polyurethane (NIPU), Natural rubber (NR), Polyurethane films, Bio-based polymers

Green polyurethane is a trending research topic, aiming for safe and eco-friendly materials from bio-polyols derived from natural oils like palm, soybean, and sunflower. However, these bio-polyols often have low molecular weights, which negatively impact the polyurethane's mechanical properties, such as tensile strength and elasticity. To overcome this, natural rubber is being explored as a better bio-polyol source, potentially yielding higher molecular weights and improved polyurethane mechanical properties [1]. Along with these efforts, non-isocyanate polyurethanes (NIPUs) are gaining interest due to their greener synthesis, avoiding toxic isocyanates by using polyaddition of cyclic carbonates with amines and transurethanization of dicarbamates with polyols reactions [2]. This offers a safer and more sustainable approach to polyurethane production.

In this work, we focus on the synthesis of non-isocyanate polyurethane films using a bio-polyol based on natural rubber and dicarbamate. In the first approach, we synthesized bio-based polyols from *cis*-1,4-polyisoprene (natural rubber, NR) using epoxidation into epoxidized natural rubber (ENR). Then we used selective cleavage of double bonds via oxidation and transformed it into carbonyl telechelic natural rubber (CTNR), and then hydroxyl telechelic natural rubber (HTNR) via a reduction reaction [3] (**Figure 1**). The HTNR was successfully obtained from epoxidation of NR latex with epoxide unit content in ENR of 2.91%, resulting in an average molar mass of 3000 g/mol as confirmed by GPC, and the molecular structures of HTNR were confirmed by ^{1}H-NMR and FTIR.



Figure 1. Synthesis of hydroxyl telechelic natural rubber (HTNR) from natural rubber

The synthesis of dicarbamate was achieved using 1,6-diaminohexane and dimethyl carbonate as reactive substances, and 1,5,7-triazabicyclo[4.4.0]dec-5-ene (TBD) as a catalyst [4], The study on the influence of temperature (80, 100, 120, 150°C) revealed that the dicarbamate yields were 65%, 74%, 76%, and 70%, respectively. This trend demonstrates an initial increase in yield with temperature, peaking at 120°C, followed by a decrease at 150°C. This suggests a temperature-dependent yield limit. Structural analysis of the dicarbamate obtained at 80, 100, and 120°C using FTIR and ^{1}H-NMR confirmed their expected structures, as shown in **Figure 2**. However, the sample from 150°C showed a deformation of the –NH peak at 3300 cm^{-1} in its FTIR spectrum, while its ^{1}H-NMR spectrum showed an affected peak at 4.7 ppm. These spectral changes indicate the degradation of the dicarbamate structure due to side reactions at high temperatures.

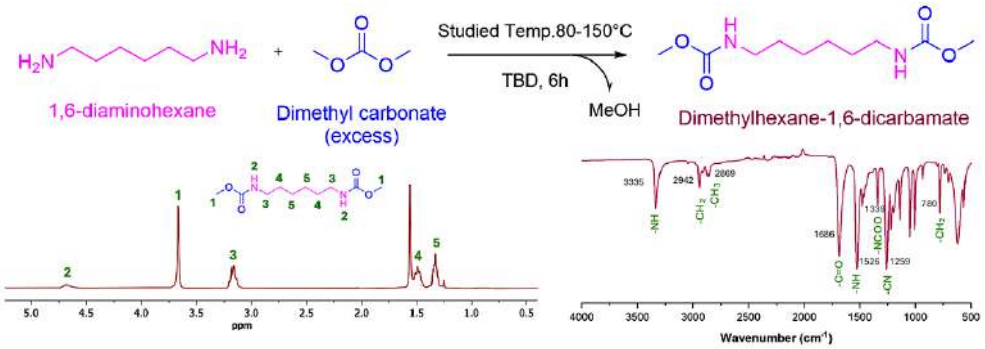


Figure 2. Synthesis and characterization of Dimethylhexane-1,6-dicarbamate

Hydroxy-terminated non-isocyanate polyurethane (NIPU) was synthesized from polyol and dicarbamate, utilizing a KOMe catalyst with the addition of 1,4-butanediol as a chain extender to increase the NIPU's hard segment structure, as illustrated in **Figure 3**. Experimental conditions revealed that temperature significantly affected NIPU's yield and properties, with higher temperatures optimizing reaction rates. Increased chain extender content enhanced both the hard segment structure and the resulting better mechanical properties of the NIPU.

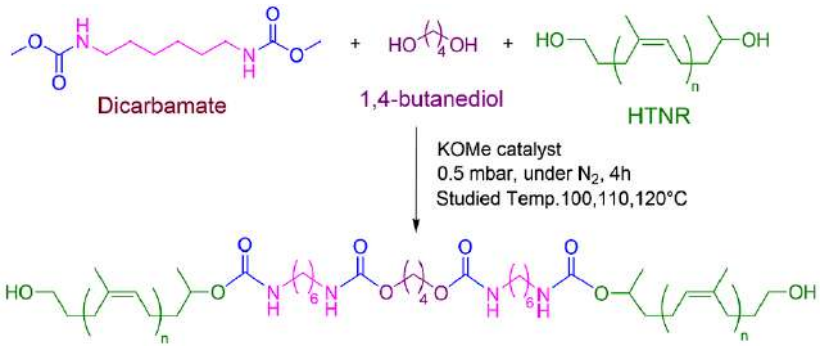


Figure 3. Synthesis of hydroxy-terminated non-isocyanate polyurethane (NIPU)

This work shows the success of preparing non-isocyanate polyurethane films from a natural rubber-based polyol, a highly renewable resource. This greener process avoids toxic isocyanates, offering a significant advancement in green polyurethane development for films in biomedical applications.

Acknowledgement

This research was supported by Prince of Songkla University, Thailand Science Research and Innovation (TSRI), and National Science, Research and Innovation Fund (NSRF); Grant No. FF68/SCI6801143S

References

1. Sukhawipat N, Saetung N, Pilard J-F, Bistac S, Saetung A, *J. Appl. Polym. Sci*, 2017; 135: 45715.
2. Stachak P, Łukaszewska I, Hebda E, Pielichowski K, *Materials*, 2021; 14 (13): 3497.
3. Saetung A, Rungvichaniwat A, Campistron I, Klinpituksa P, Laguerre A, Phinyocheep P, Pilard J, *J. Appl. Polym. Sci.*, 2010; 117 (3): 1279–1289.
4. Boisaubert P, Kébir N, Schuller A-S, Burel F, *European Polymer Journal*, 2020; 138: 109961.

International Rubber Conference 2025 (IRC2025)
1-3 December 2025 @ BITEC, Bangkok, Thailand

Latex Serum Boosts Natural Rubber Strength

Katsuhiko TSUNODA[1], Yasuhiro Shoda[2], Yuji KITAMURA[1], Kenji URAYAMA[3]

[1] *Sustainable and Advanced Materials, Bridgestone Corporation, 3-1-1 Ogawahigashi-Cho, Kodaira, Tokyo, Japan*

[2] *Material Innovation & Development, Bridgestone Europe, Via del Fosso del Salceto, 13/15, Rome, Italy*

[3] *Department of Material Chemistry, Kyoto University, Nishikyo-ku, Kyoto, Japan*

e-mail address of the presenting author (katsuhiko.tsunoda@bridgestone.com)

Keywords: Natural Rubber, cis 1,4-polyisoprene, SIC, Strength, Serum

According to forecasts, the number of automobiles worldwide in 2050 is expected to increase by approximately 1.6 times compared to 2015. With this rapid growth in vehicle numbers, the demand for tires is also expected to expand proportionally. Tires are not merely consumable items; they are highly complex products that significantly contribute to fuel efficiency, driving safety, and comfort. Not only improving fuel efficiency by reducing rolling resistance for lowering CO_2 emissions, but also improving resource productivity become significant for addressing the rapid increase in demand and contributing for realizing sustainable society.

Natural rubber (NR), cis 1,4-polyisoprene, is bio-sourced material, produced from the latex of Hevea Brasiliense, covers more than 50% of the rubber used in tire industry. NR exhibits strain induced crystallization (SIC), which enables it to perform excellent mechanical strength and crack growth resistance. We have reported that NR shows 20°C high threshold temperature and 2 folds faster threshold strain rate for producing SIC generated strength than that of synthetic isoprene rubber, IR[1]. These differences cannot be fully explained by stereoregularity alone. The SIC behavior of NR has long been a subject of extensive investigation in polymer science. Studies have focused on the role of non-rubber components such as proteins and lipids for terminally modified isoprene chains in SIC enhancement. Resent structural analyses have revealed that the ω-terminals of cis-1,4-polyisoprene end chains contain dimethylallyl group, and the α-terminals contain hydroxy or ester functionalities[2]. These terminal modifications are hypothesized to establish stable physical network structures, which would facilitate SIC. Despite the wide variety of research on NR's chemical architecture has been carried out, direct strategies for optimizing and maximizing its SIC performance is not fully clarified.

When NR latex is subjected to centrifugation, it separates into three layers: the rubber particle layer, the serum layer, and the bottom fraction layer. The main component in serum layer is L-Quebrachitol (QA), and normally discarded as waste during rubber production in coagulation process[3]. QA is a naturally occurring cyclic compound with multiple hydroxyl functional groups. We tried to re-introduce dried serum (DS) to NR as it would interact with the end terminal functional groups and promotes the development of higher-order structures resulting in enhancing SIC performance. Compound formulation is shown in Table-1. DS is prepared from NR Latex (PB260, DRC30%) in laboratory. Figure-1 shows tearing energy (G) as a function of initial notch length (c_o) for NR, IR, DS incorporated NR (NR-DS) and DS incorporated IR (IR-DS) vulcanizates in edge crack test method at 20°C and strain rate of $0.5s^{-1}$. In this relationship, G increases with increasing c_o and drop to constant value at c_o^*. Maximum G in $c_o<c_o^*$ region correspond with SIC enhancement strength, G_{-SIC}, and constant G in $c_o^*<c_o$ region is strength merely associated with viscoelastic energy

dissipation, G_{-c}[1]. DS incorporation to NR drastically enhances G_{-SIC}, whereas no enhancement in IR. This enhancement effect can more clearly be observed in temperature effect measurement. G_{-SIC} as a function of temperature is summarized in figure-2. G_{-SIC} decreases with increasing temperature and disappear at threshold temperature, T^*. NR-DS shows higher G_{-SIC} over the measured temperature range, and worth to note that 20°C higher T^* than NR. Again, this DS incorporation effect is not observed at all in IR. Viscoelastic measurement with un-vulcanized samples show clear differences in relaxation slope between NR and NR-DS, whereas no difference between IR and IR-DS. Relaxation slope reduces with DS incorporation to NR indicating development of higher order structure. Wide angle X-ray scattering is also conducted, and SIC kinetic enhancement is confirmed in NR-DS. These data suggests that with incorporating DS to NR, SIC kinetic is surprisingly enhanced by higher order structure development via polymer chain end linkage resulting higher G_{-SIC}.

Table 1. Sample compositions

Components [phr]	**Sample notations**			
	NR	**NR-DS**	**IR**	**IR-DS**
NR[a]	100	100		
IR[b]			100	100
DS[c]		4		4
ZnO	5	5	5	5
Stearic acid	2	2	2	2
Anti-degradant 6PPD	1	1	1	1
Sulfur	1.5	1.5	1.5	1.5
Accelerator CBS	1.5	1.5	1.5	1.5

[a] Natural rubber (RSS#3), [b] IR2200 (ENEOS Materials, Co.,), [c] Dried Serum from Latex PB260, DRC30%

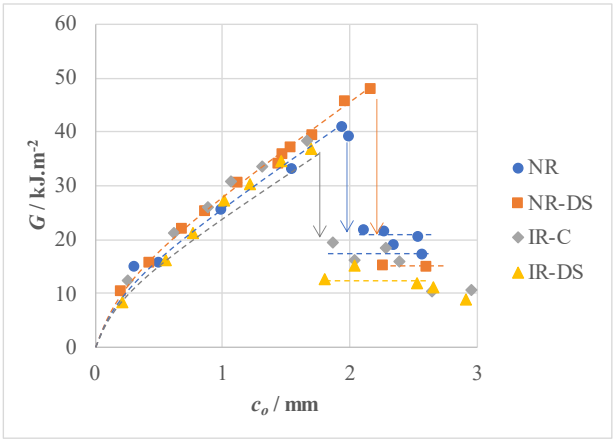


Figure 1. G as a function of co at 20°C, 0.5s^{-1}

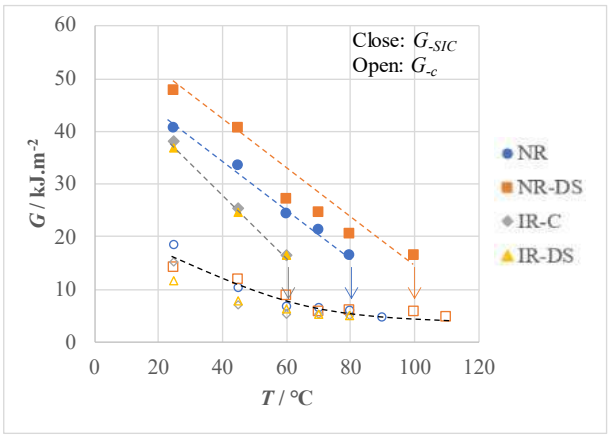


Figure 2. G_{-SIC} and G_{-c} as a function of T at 0.5s^{-1}

Acknowledgement

Authors acknowledge funding from JST CREST through grant number JPMJCR2091.

References

1. Tsunoda K, Kitamura Y, Urayama K, *Soft Matter*, 2023; 10: 1966.
2. Oouchi M, Ukawa J, Ishii Y, Maeda H, *Biomacromolecules*, 2019; 20: 1394
3. Herculano, R. D. et al., Biomaterials Advances, 2024; 157: 213739

Green Synthesis of Zinc Oxide from Skim Latex Serum for Application in Rubber Vulcanization

Sopinya NITHAKORN[1] and Preeyanuch JUNKONG[1]

[1] *Department of Chemistry, Faculty of Science, Mahidol University, Ratchathewi, Bangkok, Thailand.*

preeyanuch.jun@mahidol.ac.th

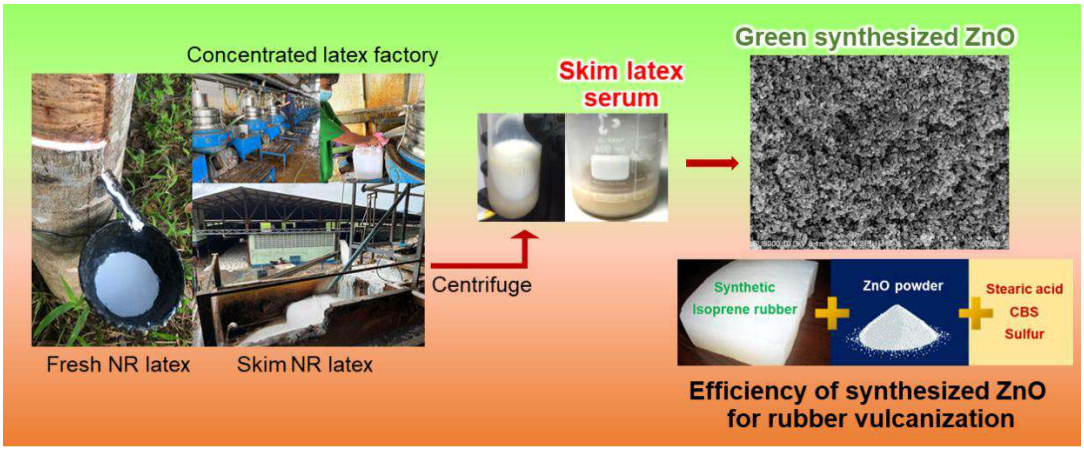
Keywords: Skim latex serum, ZnO, Green synthesis, Activator, Rubber vulcanization

This research introduced a sustainable approach for the synthesis of zinc oxide (ZnO) using skim latex serum wastewater as a natural reducing and capping agent. ZnO was synthesized through a green method by varying the skim latex serum volumes and zinc precursor concentrations. The ZnO yield was maximized at a serum volume of 5 ml, with a decline observed at higher volumes. Field emission scanning electron microscope revealed that the morphologies of ZnO varied depending on the volume of serum added. In contrast, the zinc precursor concentration had less impact on morphology but affected the yield and size of ZnO. Powder X-ray diffraction confirmed the formation of ZnO with a hexagonal wurtzite structure [1] for all samples. Fourier-transform infrared (FT-IR) spectra of all synthesized ZnO revealed the presence of characteristic ZnO absorption bands and functional groups in the skim latex serum, thereby verifying its function as a capping agent in ZnO synthesis. Optimal synthesis conditions (5 ml of serum and 0.01 M zinc precursor) produced ZnO with a high yield, uniform morphology, and fine particle size.

To evaluate the synthesized ZnO in rubber application, synthesized ZnO with optimal conditions was selected, referred to as sZnO. The FT-IR spectra of IR compounds that were heated at various time intervals showed that sZnO formed strong interactions with stearic acid to create Zn(II) carboxylate coordination in both monodentate and syn-syn bridging bidentate forms [2,3], similar to commercial ZnO (cZnO). This suggested that sZnO acted as an effective vulcanization activator, comparable to cZnO.

IR vulcanizates with sZnO exhibited fast curing behavior (short scorch time, low cure time, high cure rate index). Nevertheless, it showed a lower crosslink density compared to IR vulcanizates with cZnO, which is was likely due to more extensive crosslinking formation around sZnO clusters, leading to reduced crosslinking throughout the IR matrix. Compared to cZnO, sZnO-based vulcanizates exhibited lower tensile strength, modulus, hardness, and abrasion resistance, but higher elongation at break attributed to the lower crosslink density of sZnO-based vulcanizates.

Overall, the green synthesis of ZnO from skim latex serum wastewater offers a promising alternative to conventional methods, transforming industrial waste into value-added materials. This aligns with Sustainable Development Goal 6 (SDG 6) [4] by promoting the reuse of industrial wastewater. The successful application of sZnO in rubber compounding highlights its potential for producing stretchable and soft rubber products, contributing to environmentally conscious and resource-efficient material development.



Acknowledgement

This work was financially supported by a Young Researcher Grant from Mahidol University, Thailand, in 2020 (Grant Number: IO 863090090000). Additionally, this project received partial funding from the National Research Council of Thailand (NRCT) and Mahidol University (Grant Number: N42A660548). The authors are thankful for instrumentation support for the X-ray diffractometer (XRD, Bruker, D2 Phaser) from the Mahidol University-Frontier Research Facility (MU-FRF) and scientists of MU-FRF, Nawapol Udpuay, Dr. Suwilai Chaveanghong, and Bancha Panyacharoen for their kind assistance. The authors would like to thank Assoc. Prof. Pranee Phinyocheep for her advice. Also, the authors extend our thanks to Dr. Adul Nimpaiboon, Ms. Kattareen Boonchuay, and Mr. Prin Tumwised, the staff of the Rubber Technology Research Centre, Mahidol University, Thailand for their experimental support.

References

1. Jung M-H and Chu M-J. *J. Mater. Chem. C*. 2014; 2(32): 6675.
2. Junkong P., Morimoto R., Miyaji K., Tohsan A., Sakaki Y. and Ikeda Y. *RSC. Adv*., 2020; 10, 4772.
3. Ikeda Y., Sakaki Y., Yasuda Y., Junkong P., Ohashi T., Miyaji K. and Kobayashi H. *Organometallics*. 2019; 38, 2363.
4. United Nations. (2025, June 27). Sustainable Development Goal. https://sdgs.un.org/goals.

A New Antibacterial Hybrid Waterborne Polyurethane/Silica Coating Film Based on Natural rubber

Nitinart SAETUNG[1], Anutida SUWAN[1], Nathapong Sukhawipat[2], Pamela Pasetto[3], Anuwat Saetung[4]

[1] *Division of Physical Science, Faculty of Science, Prince of Songkla University, Hatyai campus, Songkhla, Thailand.*

[2] *Division of Polymer Engineering Technology, Department of Mechanical Engineering Technology, College of Industrial Technology, King Mongkut's University of Technology North Bangkok, Bangkok, Thailand.*

[3]*Institut des Molécules et Matériaux du Mans, UMR CNRS 6283, Le Mans Université, 72085 Le Mans Cedex 9, France*

[4]*Department of Rubber Technology and Polymer Science, Faculty of Science and Technology, Prince of Songkla University, Pattani campus, Pattani, Thailand*

e-mail address of the presenting author (nitinart.s@psu.ac.th)

Keywords: natural rubber, hybrid waterborne polyurethane, coating, biopolyol, antibacterial film

Bio-based waterborne polyurethane (WPU) coatings have attracted research interest for use in coatings due to the demand for environmentally friendly and renewable materials. Our research focused on natural rubber (NR), which is a renewable and environmentally friendly material with excellent physical properties. NR was synthesised into hydroxyl-telechelic natural rubber (HTNR) as a bio-polyol, which was used as a starting material to synthesise WPUs. However, the WPU exhibited strong hydrophilic characteristics, resulting in low water and corrosion resistance of the coatings, which limits the applications of WPU. One effective method to enhance the water resistance, hydrophobicity, and mechanical properties of WPU film is adding nanofillers into the WPU matrix. However, successful incorporation of silica into polyurethane systems requires compatibility between silica particles and the WPU matrix through surface modification of silica or by grafting silane coupling agents onto the polyurethane backbone. The modified WPU and functional nano-silica using click reaction can enhance the water resistance, hardness, thermal stability, and weather resistance of WPU. The click reaction is a novel technique for integrating nano-silica into the WPU matrix [1], offering advantages such as solvent-free processing and light exposure. However, the antibacterial activity of WPU is another limitation of WPU films. Improving antibacterial activity by introducing antibacterial agents into the WPU system is widely used to inhibit the growth of bacteria. Chitosan is one such green antibacterial agent and is widely used for this purpose. The ion charge of chitosan inhibits the growth of bacteria with opposite charges [2].

Therefore, the aim of this study is to explore the potential of silane-functionalised HTNR (SiHTNR) based polyols for synthesising waterborne polyurethanes. The influence of nano silica content on the properties of hybrid PU films was examined. Additionally, chitosan was used to assess antibacterial activity against bacteria such as ***E. coli, V. parahaemolyticus***, and ***S. aureus***.

The bio-polyol was synthesized from NR latex via epoxidation reaction to obtain epoxidized NR, followed by selective carbon-carbon double bond oxidation to obtain carbonyl telechelic oligomers, and was transformed to hydroxyl groups by reduction reaction to give HTNR as bio-polyol, with a molecular weight of 3,500 $g.mol^{-1}$. The modified silane-functionalized HTNR (SilaneHTNR) via thiol-ene click reaction using (3-mercaptopropyl) trimethoxysilane (MPTMS) and Darocur1173 as photoinitiator, as shown in **Fig. 1**. The chemical structure of SilaneHTNR was confirmed by ^{1}HNMR and ^{29}SiNMR spectroscopy. Hybrid WPU was synthesized from SilaneHTNR, dimethylolpropionic

acid (DMPA), and hexamethylene diisocyanate (HDI) by emulsion polymerization. The 20% nanosilica at 1, 3, and 5 %wt was added into hybrid WPU with stirring rate of 50 rpm for 1 h before casting into Teflon molds. The preparation of antibacterial hybrid WPU film was prepared by adding 10% of CS solution at 200 ppm into hybrid WPU and then cast on the Teflon molds, for 48 h and dried in the hot air oven at 60 ^{o}C, for 24 h.

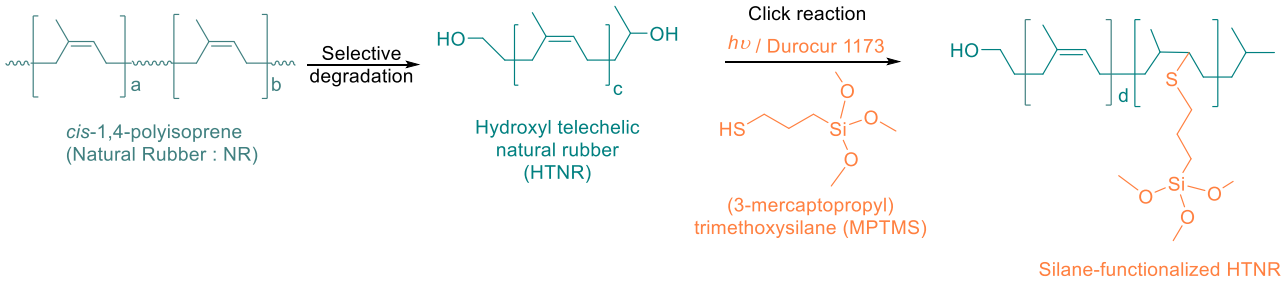


Fig. 1 Synthesis of SilaneHTNR

The TEM image showed interactions in silica-silica particles and the silica-hybrid WPU matrix, leading to a larger particle size with increasing nanosilica content. The water contact angle of silica-hybrid WPU showed higher hydrophobic characteristics of films with increasing nanosilica content. In addition, the tensile strength and thermal stability of films were improved by increasing nanosilica content. Moreover, the silica-hybrid WPU films showed significantly enhanced inhibition of *V. Parahaemolyticus*, *S. aureus* and *E. coli* of 100%, 85%, and 38% respectively.

These results demonstrated that the new antibacterial hybrid WPU from silane-modified polyols based on HTNR has significantly enhanced its water resistance, mechanical stability, and antibacterial performance, and is an alternative for eco-friendly materials coating.

Acknowledgement

This research project is supported by **The Royal Golden Jubilee Ph.D. ProGramme (RGJ)**, National Research Council of Thailand (NRCT, N41A640237), Fundamental fund (Grant No. SCI6505099S), Hub of Talents in Natural Rubber, National Research Council of Thailand (NRCT), Bangkok, Thailand.

References

1. Suwan, A.; Sukhawipat, N.; Saetung, A.; Saetung, N.; Pasetto, P. *Prog. Org. Coat.* **2025**, *201*, 109109. DOI: https://doi.org/10.1016/j.porgcoat.2025.109109
2. Qin, Y.; Li, P.; Guo, Z. *Carbohydr. Polym.* **2020**, *236*, 116002. DOI: https://doi.org/10.1016/j.carbpol.2020.116002.

Degradation Trends in Plasticity and Viscosity of Selected Standard Philippine Rubber Under Prolonged Storage

S. Suganob, R. Lim, R. Salazar
Department of Science and Technology – Region IX, Zamboanga City, Philippines
rosemarie.salazar@ro9.dost.gov.ph

Keywords: Philippine rubber, Plasticity, Viscosity, Long-term storage, Mechanical properties

The mechanical stability of Standard Philippine Rubber (SPR) during storage is essential for ensuring consistent quality in processing and end-use applications. This study aimed to evaluate the degradation trends in plasticity and viscosity of selected SPR grades—SPR 20, SPR 5, and SPR L—during prolonged storage, and to assess whether the rates of degradation differ among these grades. Rubber samples were stored under ambient conditions away from direct sunlight for a period of 40 weeks. Weekly measurements were taken for Mooney Viscosity (ISO 289-1), Initial Plasticity (ISO 2007), and Plasticity Retention Index (ISO 2930). Literature has shown that natural rubber undergoes spontaneous crosslinking during storage, unlike synthetic polyisoprene which tends to soften. According to Gan [1], this phenomenon—known as storage hardening—alters processing properties due to slow crosslinking reactions involving abnormal groups in the rubber matrix. Analysis of Covariance (ANCOVA) was applied in this study to determine whether degradation rates (slopes), shown in Figures 1 and 2, significantly differed among the three SPR grades. Results showed no statistically significant differences at the 0.05 significance level for Mooney Viscosity ($p = 0.2844$), Initial Plasticity ($p = 0.0888$), and PRI ($p = 0.0850$). Based on regression models and minimum property thresholds for PRI, shown in Figure 3, estimated shelf-life was approximately 113 weeks for SPR 5, 120 weeks for SPR L, and 135 weeks for SPR 20. These findings suggest that the three SPR grades exhibit similar mechanical resilience under long-term storage. Future studies may explore the influence of different environmental conditions or packaging systems on rubber shelf-life behavior.

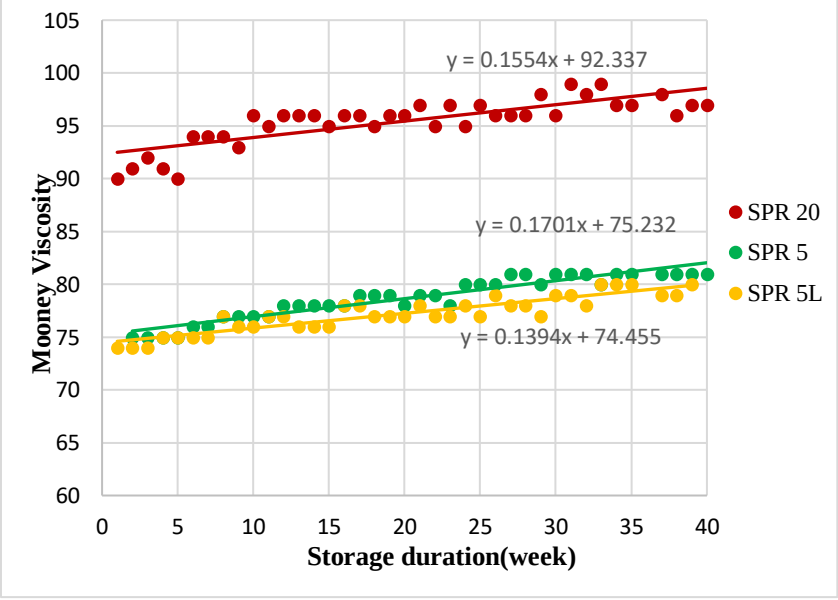


Figure 1. Mooney Viscosity vs. Storage Duration for Standard Philippine Rubber Grades

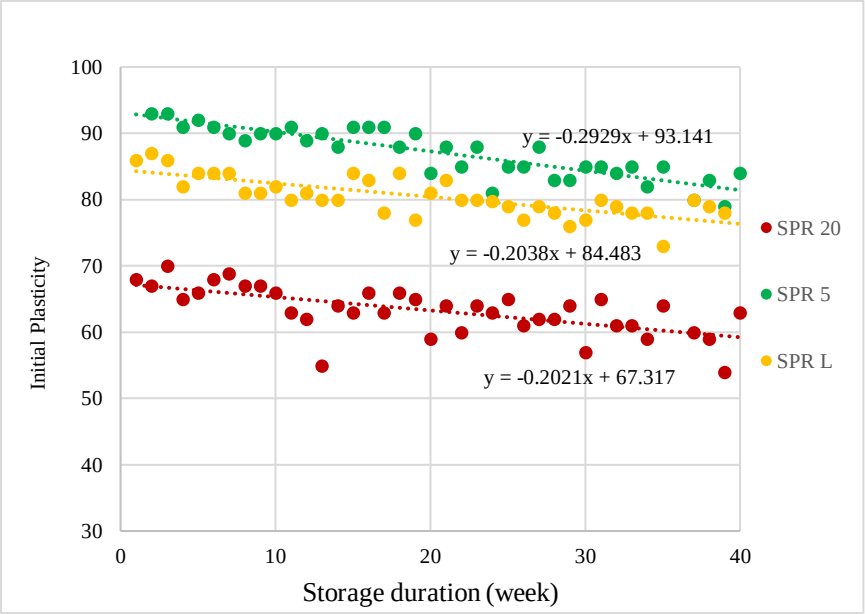


Figure 2. Initial Plasticity vs. Storage Duration for Standard Philippine Rubber Grades

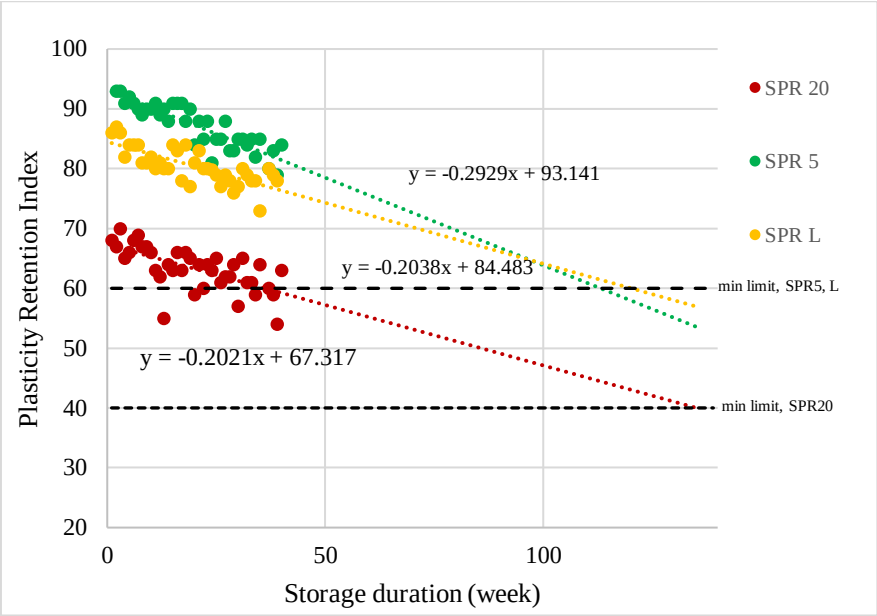


Figure 3. Shelf-Life Projection of Standard Philippine Rubber Grades Based on PRI Limit

Acknowledgement

The authors would like to express their deepest gratitude to the management of the Department of Science and Technology – Region IX for their support and funding of this research. Special thanks to Ms. Calamohoy and Mr. Ang for their generosity in providing the samples.

References

1. Gan, S.-N. (2006). Storage Hardening of Natural Rubber. Journal of Rubber Research, University of Malaya, pp. 1939–1948. Published online: 22 Sep 2006.

International Rubber Conference 2025 (IRC2025)
1-3 December 2025 @ BITEC, Bangkok, Thailand

Sustainable Yield Improvement and Quality Assessment of TSR10 Rubber from Two *Hevea brasiliensis* Genotypes: Impact of Reduced Tapping Frequency Associated with Ethephon Stimulation

H. Kum-ourm[1], N. Onozuka[2], L. Tarachiwin[1], A. Matsuura[2], Y. Kitaura-Sakaguchi[2], L. Vaysse[3,4], R. Lacote[5,6], F. Gay[5,6], V. Ferrer[4,7], C. Bottier[3,4], S. Jantarasunthorn[8], J. Chaiyut[8], T. Lerksamran[8], S. Liengprayoon[8]

[1]*R&D Department, Sumitomo Rubber (Thailand) Co., Ltd., Rayong, Thailand 21140*

[2]*R&D HQ, Sumitomo Rubber Industries Co., Ltd., Kobe, Japan*

[3]*CIRAD, UPR BioWooEB, F-34398 Montpellier, France.*

[4]*BioWooEB, Univ Montpellier, CIRAD, Montpellier, France.*

[5]*CIRAD, UMR ABSys, F-34398 Montpellier, France.*

[6]*ABSys, Univ Montpellier, CIHEAM-IAMM, CIRAD, INRAE, Institut Agro, Montpellier, France.*

[7]*CIRAD, UPR BioWooEB, 10900 Bangkok, Thailand.*

[8]*KAPI, Kasetsart University, Chatuchak, Bangkok 10900, Thailand*

(hathainat-k@sumitomorubber.co.th)

Keywords: *Hevea brasiliensis*, sustainability, ethephon, latex yield, rubber quality, molecular structure

Natural rubber (NR) is a crucial raw material in tire production. Ensuring its sustainability involves optimizing yield, maintaining product quality, and addressing challenges like low productivity and labor shortages. Ethephon stimulation is commonly employed to enhance latex yield, particularly under low tapping frequencies; however, its systematic effects on the rubber's biochemical composition, molecular structure, and physical properties remain underexplored. This study aims to assess the impact of ethephon stimulation on the latex yield, biochemical properties, molecular structure and physical properties of TSR10-like samples prepared from two *Hevea brasiliensis* clones (RRIM600 and RRIT251).

Field trials were conducted from 2020 to 2023 in the area of the Sumirubber Thai Eastern Plantation Company Limited (STEP) in Northeast Thailand, a non-traditional area for rubber cultivation. Two tapping systems were compared: conventional tapping (S/2 d2) and low tapping frequency with ethephon application (S/2 d3 ET 2.5% Pa 1(1)).

Reduction of tapping frequency with the use of ethephon stimulation significantly increased latex yield per tapping, sustaining the total production per tree and promoting resource-efficient harvesting. Yield (kg/tree) increased by 24% in RRIM600 and by 12% in RRIT251. Importantly, the ethephon-treated system had minimal impact on key biochemical components, such as protein content that ranged from 2.45–2.56% in RRIM600 and 2.40–2.55% in RRIT251, while lipid content varied between 2.46–2.57% in RRIM600 and 2.52–2.64% in RRIT251. No significant differences ($p > 0.05$) were observed in the properties and molecular structure indicators of dry rubber, including Mooney viscosity, gel content, and initial and post-aging plasticity (P_0, P_{30}, ASHT), as well as average molecular weight. The clone of *Hevea brasiliensis* (RRIT251 and RRIM600) had a more significant effect

on the biochemical composition, molecular structure, and physical properties of TSR10-like rubber compared to the tapping system.

Table 1. Physical properties and molecular structure of TSR10-like rubber sample

Rubber properties	RRIM600		RRIT251	
	Conventional	Low tapping frequency with ethephon	Conventional	Low tapping frequency with ethephon
Mooney Viscosity (a. u.)	85.2 ± 2.5 [b]	86.2 ± 1.7 [b]	96.4 ± 1.2 [a]	94.9 ± 1.4 [a]
Gel (% w/w dry matter)	7.4 ± 1.0 [a]	9.3 ± 1.0 [a]	9.6 ± 0.8 [a]	10.6 ± 1.0 [a]
M_w (kg mol^{-1})	1527 ± 45 [b,c]	1482 ± 36 [c]	1677 ± 30 [a]	1647 ± 37 [a,b]

Values not connected by same letter are significantly different according to Tukey-Kramer test (P = 5%).

These findings highlight a breakthrough in sustainable rubber production by being one of the first to systematically evaluate ethephon stimulation under reduced tapping frequency in a non-traditional rubber cultivation area and ensuring that reduced-frequency tapping, combined with ethephon application, can enhance latex productivity with minimal impact on rubber quality. This practice contributes to the long-term sustainability of natural rubber production, as evidenced by secure latex production with a lower workforce. Besides environmental impacts and genotype responses across diverse agroclimatic zones on rubber production and NR quality, the adoption of farmers and socio-economic aspects should also be explored.

Acknowledgement

The authors gratefully acknowledge the support of Sumi Rubber Thai Eastern Plantation Co., Ltd. for providing the field site and natural rubber samples essential to this study.

References

1. Kum-ourm H, Liengprayoon S, Onozuka N, Vaysse L, Tarachiwin L, Lacote R, Chaiyut J, Jantarasunthorn S, Lerksamram T, Cakpo C B, Gay F, Ferrer V, Char C, Matsuura A, Sakaguchi-Kitaura Y, Miyagi-Inoue Y, Bottier C, *Ind. Crops Prod., 2025; Manuscript submitted for publication.*
2. Liengprayoon S, Kum-ourm H, Vaysse L, Lacote R, Chaiyut J, Jantarasunthorn S, Lerksamram T, Gay F, Ferrer V, Char C, Onozuka N, Tarachiwin L, Matsuura A, Sakaguchi-Kitaura Y, Miyagi-Inoue Y, Bottier C, *Ind. Crops Prod., 2025; Manuscript submitted for publication.*
3. Lacote R, Gabla O, Obouayeba S, Eschbach J-M, Rivano F, Dian K, Gohet E, *Field Crops Res.*, 2010; 115: 94–98.
4. Liengprayoon S, Chaiyut J, Sriroth K, Bonfils F, Sainte-Beuve J, Dubreucq E, Vaysse L, *Eur. J. Lipid Sci. Technol.*, 2013; 115: 1021–1031.

International Rubber Conference 2025 (IRC2025)
1-3 December 2025 @ BITEC, Bangkok, Thailand

Sustainable NZEROSIL™ Silicas from Renewable Rice Husk

DANNIEL C. LIAO, TIM YU-TING LIN, SPENCER LEE, CHRIS WU, ANTHONY LIN, W. WADDELL

ORIENTAL SILICAS CORPORATION, #99, Li-Yu Kou, Li-Yu Village, Sanyi Miaoli Taiwan

Email: dliao@oscsilica.com

Keywords: Precipitated Silica, BET Surface Area, Microgranule, Silica Dispersion, Passenger Car Tire Tread

Precipitated silica in passenger car (PCR) tire treads desirably increases wet traction, decreases rolling resistance, and maintains wear. Oriental Silicas Corporation makes easily dispersible Tokusil® 255EG granules and highly dispersible Eecosil® 350MG microgranules (BET surface area ~170 m^2/g), and high surface area Eecosil® 230G granules and Eecosil® 230MG microgranules (BET ~210 m^2/g). Two chemical reaction steps are needed, see Equations 1 & 2. Sodium silicate is made from crystalline quartz sand (Figure 1) or recycled cullet (broken glass), see Figure 2. Our sustainable NZEROSIL™ net zero emission silicas are made from bio-renewable rice husk, see Figure 3. Amorphous reinforcing silicas are continuous batch manufactured (Figure 4) by reaction of sulfuric acid with sodium silicate.

Equation 1. $SiO_2 + Na_2CO_3 \rightarrow n\,(SiO_2)Na_2O + CO_2$

Equation 2. $n\,(SiO_2)Na_2O + H_2SO_4 \rightarrow n\,SiO_2 + Na_2SO_4 + H_2O$



Figure 1. Dry (Furnace) Process to make Sodium Silicate from Minerals (Crystalline Quartz).



Figure 2. Wet (Autoclave) Process to make Sodium Silicate from Recycled Cullet (Broken Glass).



Figure 3. Furnace Process Ashes Renewable Rice Husk as Starting Material for Sodium Silicate.

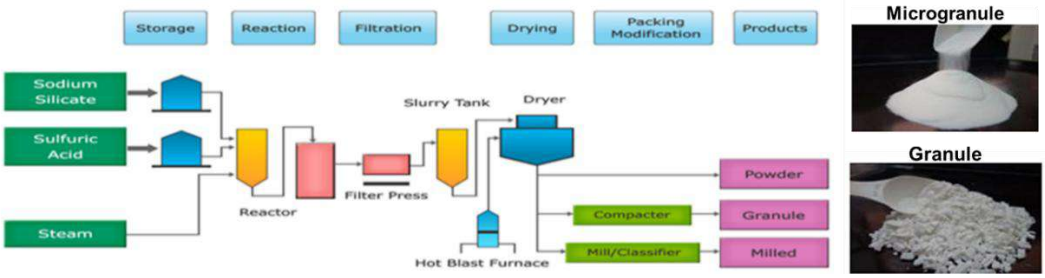


Figure 4. Manufacturing Process of Amorphous Silica by Sodium Silicate reaction with Acid.

Compounds are formed inside a Kobelco BB-2 1.5L mixer. 100-phr Eecosil® 230MG in a 75/25 SSBR/cis BR PCR tread was studied at zero, 2- and 6-phr of a zinc processing additive. 6-phr was selected to optimize the 300% elongation and silica dispersion. Four mix sequences were then studied: 4-pass, two 5-pass with a different remill stage, and a 6-pass mix with two remill stages. SEM @100X / ImageJ analysis gave %-white areas and average particle sizes (Figure 5), and lower is better.

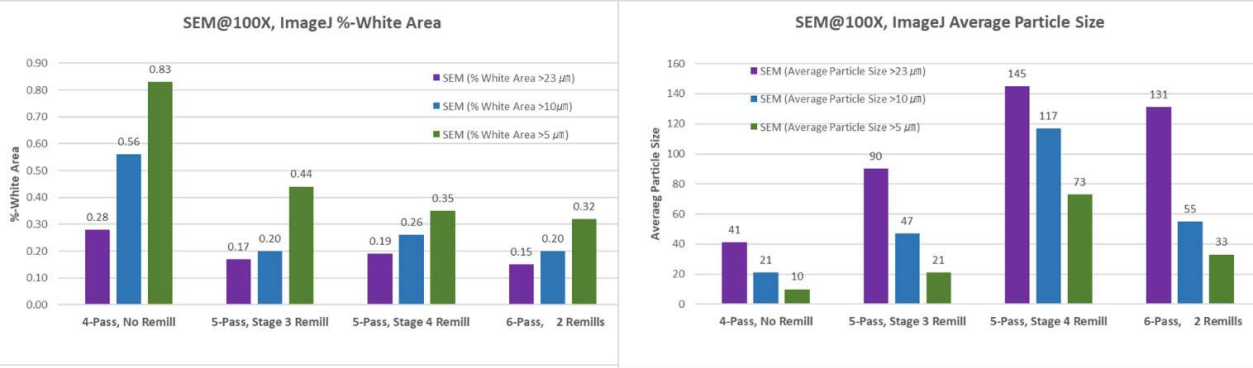


Figure 5. %-White areas (left) and Average particle sizes (right) of four difference mix sequences.

The 5-Pass, Stage 3 Remill mix was selected to evaluate sustainable NZEROSIL™ RH-230G granules from renewable rice husk versus other silicas, and showed NZEROSIL™ RH-230G gave equivalent properties to Eecosil® 230MG microgranules and a competitor Silica 1 within about 10% (Figure 6). Elongation to break is higher, and rolling resistance from tangent delta at 60°C is lower. %-White areas and average particle sizes are similar, see Figure 7.

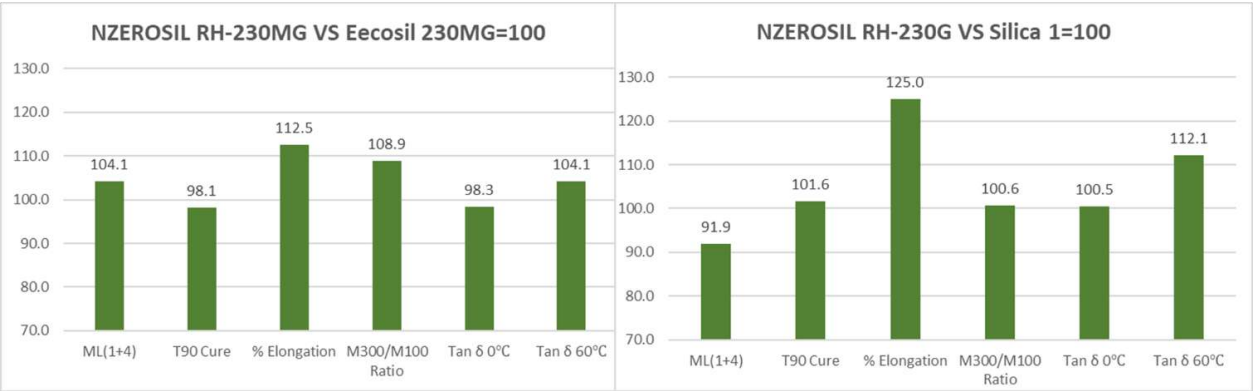


Figure 6. NZEROSIL™ 230G properties relative to Eecosil® 230MG (left) and Silica 1 (right).

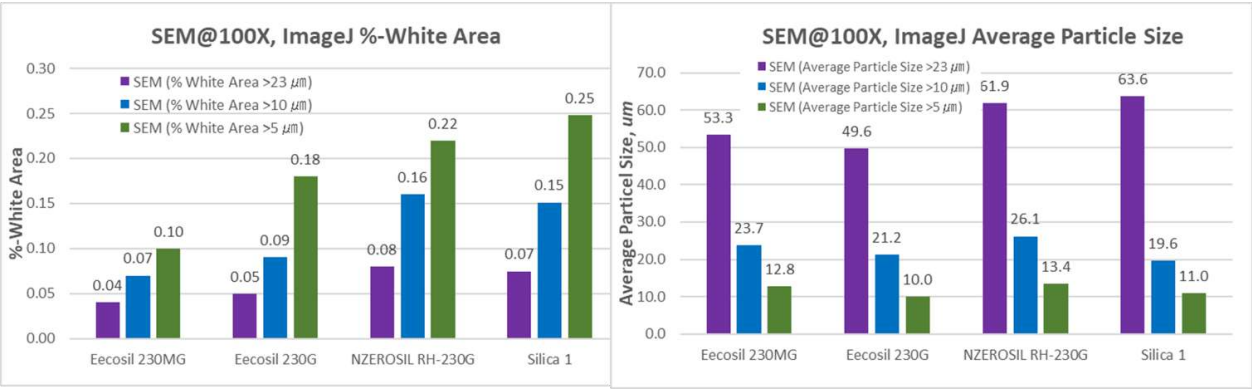


Figure 7. %-White areas (left) and Average particle sizes (right) of four difference silica treads.

Sustainable NZEROSIL™ RH-350MG (BET ~170 m^2/g) and NZEROSIL™ RH-230G (BET ~210 m^2/g) reinforcing precipitated silicas are commercial starting from the bio-renewable rice husk.

Mechanical Tailoring of Waterborne Epoxy Coating on Metal Substrate Using Functionalized Natural Rubber Latex

Wasan Tessanan[1,2], Sombat Thanawan[3], Taweechai Amornsakchai[1], Pranee Phinyocheep[1]

[1]*Department of Chemistry, Faculty of Science, Mahidol University, Bangkok 10400, Thailand*

[2]*Department of Industrial Technology and Innovation Management, Faculty of Science and Technology, Pathumwan Institute of Technology, Bangkok 10330, Thailand.*

[3]*Rubber Technology Research Center, Faculty of Science, Mahidol University, Phutthamonthon Sai 4, Nakhon Pathom 73170, Thailand*

e-mail address of the presenting author (wasan.t@pit.ac.th)

Keywords: Waterborne epoxy, Functionalized natural rubber, Coating application, Mechanical properties, Sustainability

Volatile organic compounds (VOCs), commonly found in the petrochemical, paint, and coating industries, are recognized as significant environmental pollutants and potential health hazards. As a result, there is growing global concern among stakeholders, leading to the implementation of stricter regulations aimed at reducing VOC emissions in polymer coating technologies. To address the concerns surrounding VOC emissions, waterborne coating systems, where water replaces volatile organic solvents, have gained substantial traction, making them an environmentally friendlier option. These coatings are favored for their notable attributes, including non-toxicity, non-flammability, widespread availability, and significantly lower VOC emissions.

Among various types of water-dispersible coatings, epoxy-based waterborne resin has gained substantial attention due to the superior characteristics of its cured films, such as excellent adhesion, strong interfacial bonding, effective corrosion resistance, high thermal stability, and robust chemical durability. Despite its excellent performance, highly crosslinked epoxy materials often suffer from inherent brittleness, which limits their applicability in certain domains. To overcome this drawback, synthetic and natural elastomers [1,2] have been incorporated to enhance the toughness of epoxy-based thermosetting materials. However, identifying a sustainable and environmentally friendly alternative, such as natural rubber and its derivatives in the latex form, remains a significant challenge.

In this study, two types of functionalized natural rubber with a molecular weight of 70,000 g/mol, including hydroxyl-functionalized natural rubber (NR-OH) and low molecular weight epoxidized natural rubber (LENR), were synthesized in latex form using an eco-friendly method. The NR-OH latex was prepared via the oxidative degradation reaction using hydrogen peroxide as an oxidizing agent, while the LENR latex was prepared through sequential epoxidation with in situ performic acid, generated from hydrogen peroxide and formic acid [3,4], followed by oxidative degradation using hydrogen peroxide. The rubbers' chemical structures and molecular weights were characterized before blending (10 - 30 wt.%) with an epoxy/amine hardener emulsion and applied onto metal substrates. After curing at room temperature for 1, 3, and 7 days, mechanical tests revealed that LENR improved film adhesion without compromising scratch resistance, achieving up to 4B adhesion rating after 3 days, compared to 3B for the neat epoxy. In contrast, NR-OH resulted in reduced adhesion and scratch resistance. The examples of cross-hatch adhesion test of waterborne

epoxy resin without and with functionalized natural rubber for 1 day of curing time at room temperature are shown in Figure 1. The enhanced performance of LENR is likely due to chemical interactions between epoxide groups and the curing system, while NR-OH may rely on weaker hydrogen bonding. These findings demonstrate the potential of NR-based additives, particularly LENR, as sustainable reinforcements for waterborne epoxy coatings, supporting the development of environmentally friendly coating technologies.

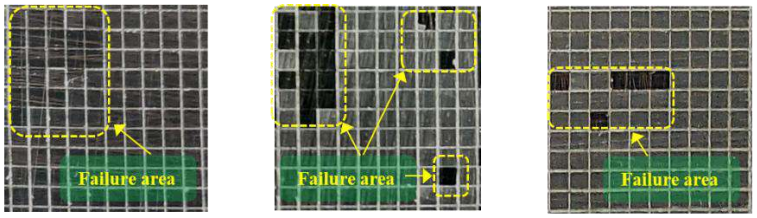


Figure 1. Examples of cross-hatch adhesion test of waterborne epoxy resin without and with functionalized natural rubber; Epoxy/20NR-OH and Epoxy/20LENR for 1 day of curing time at room temperature

Acknowledgement

The authors thank the National Research Council of Thailand for financial support (Grant no. NRCT-165/2564). The instrument facilities provided by the Department of Chemistry and Rubber Technology Research Center, Faculty of Science, Mahidol University, are appreciated.

References

1. Ruamcharoen P, Umaree S, Ruamcharoen J, *J. Mater. Sci. Eng.*, 2011; 5, 504.
2. Niu C, Du K, Xu Z, Li Z, Li T, Wang R, *J. Appl. Polym. Sci.*, 2023; 140: e54002.
3. Tessanan W, Phinyocheep P, *Iran. Polym. J.*, 2022; 31: 455.
4. Koeipudsa N, Phinyocheep P, *Polym. Compos.*, 2024; 45, 4524.

International Rubber Conference 2025 (IRC2025)
1-3 December 2025 @ BITEC, Bangkok, Thailand

Rubbery Soft Polymer Electrolyte Membrane with Nanomatrix Channel Prepared from Natural Rubber

Yoshimasa YAMAMOTO[1], Seiichi KAWAHARA[2]

[1] *National Institute of Technology, Tokyo College, Department of Chemical Science and Engineering, Tokyo, Japan.*

[2] *Nagaoka University of Technology, Department of Materials Science and Technology, Niigata, Japan.*

(yamamoto@tokyo-ct.ac.jp)

Keywords: Polymer electrolyte membrane, Nanomatrix channel, Natural rubber, Graft-copolymerization

1. Introduction

Rubbery soft polymer electrolyte membranes (PEMs) with a nanomatrix channel [1] prepared from natural rubber are sustainable functional materials that can potentially achieve an efficient proton transportation, which is required for flexible polymer electrolyte fuel cells to generate green electrical energy. This may be achieved by forming the nanomatrix channel consisting of hydrophobic polymer particles with a diameter of approximately 1 μm and nanochannel of a hydrophilic functional polymer that possesses a proton conductivity. In our previous studies [2], the PEM with the nanomatrix channel was prepared by graft-copolymerization of styrene on the surface of natural rubber particles followed by sulfonation with chlorosulfonic acid. The resulting PEM accomplished a high proton conductivity of 0.095 S/cm, outperforming Nafion117®. However, the PEM was too brittle for application in polymer electrolyte fuel cells because chlorosulfonic acid resulted in not only the sulfonation of grafted polystyrene but also the cyclization of natural rubber. To avoid this cyclization, styrene substituted with a sulfonic acid precursor such as a sulfonic acid ester could be used for the graft copolymerization. In this study, a rubbery soft PEM with a nanomatrix channel was prepared by graft-copolymerizing ethyl *p*-styrenesulfonate (SSEt) onto the surface of natural rubber particles in the latex stage, followed by hydrolysis with NaOH and cast film formation. The resulting PEM was characterized via ^{1}H-NMR spectroscopy, transmission electron microscopy (TEM), impedance analysis, and tensile testing.

2. Experiment

Natural rubber latex used in this study was deproteinized natural rubber (DPNR) latex. The graft copolymerization of SSEt was performed using *t*-butylhydroperoxide–tetraethylenepentamine as an initiator. The DPNR latex was charged with N_2 gas for 3 h at 30 °C, followed by the successive addition of the initiator (2.0×10^{-2} mol/kg-rubber) and SSEt (1.0 mol/kg-rubber). The reaction was conducted by stirring the latex at approximately 300 rpm for 3 h at 30 °C. A film of the graft copolymer of DPNR and poly(ethyl *p*-styrenesulfonate) (DPNR-*graft*-PSSEt) was prepared by casting the gross polymer latex into a Petri dish and drying under reduced pressure at 50 °C. The PSSEt homopolymer was removed from the gross polymer by extracting with a 3:1 acetone–2-butanone mixture in a Soxhlet apparatus under a N_2 atmosphere in the dark. The hydrolysis of DPNR-*graft*-PSSEt latex (ca. 2 w/w% DRC) was carried out with 0.1 mol/L NaOH solution at 85 °C for 3 h. The homo-polymer, poly(*p*-styrenesulfonic acid) (PSS), was removed from the gross polymer by immersing the as-cast film into 1 mol/L HCl solution for 24 h.

3. Results and Discussion

Figure 1 shows TEM images of DPNR-*graft*-PSS(1.0), DPNR-*graft*-PSS(0.75), and DPNR-*graft*-PSS(0.50), which were prepared via graft copolymerization of SSEt at concentrations of 1.0, 0.75, and 0.50 mol/kg-rubber, respectively, onto natural rubber. In these copolymers, the PSS contents were calculated to be 6.5%, 5.3%, and 4.4%, respectively, from the conversion and the

grafting efficiency of SSEt. The bright domains represent DPNR and the gloomy domains represent PSS owing to the staining of the ultrathin sections of DPNR-*graft*-PSS with RuO_4. As shown in Figure 1(a), the nanomatrix channel of DPNR-*graft*-PSS(1.0) was formed, in which the natural rubber particles with a diameter of approximately 1 μm were covered with a continuous nanochannel of PSS with a thickness of approximately 10 nm. In contrast, the nanochannel of DPNR-*graft*-PSS(0.75) was partially disconnected (Figure 1(b)). As shown in Figure 1(c), for DPNR-*graft*-PSS(0.50), some lumps of PSS with a diameter of about 50–100 nm existed on the surface of the natural rubber particles, forming a discontinuous nanochannel. These differences in the morphology may be attributed to the difference in the PSS content, with the PPS contents of 5.3% and 4.4% in DPNR-*graft*-PSS(0.75) and DPNR-*graft*-PSS(0.50), respectively, being insufficient to form a continuous nanochannel.

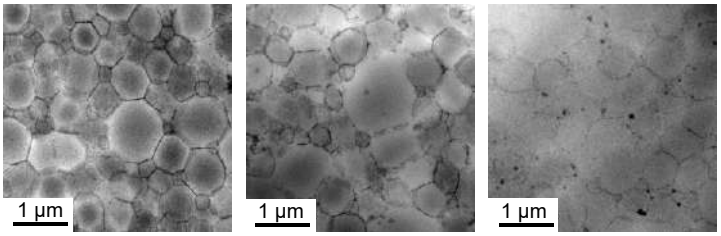


Figure 1. TEM images of (a) DPNR-*graft*-PSS(1.0), (b) DPNR-*graft*-PSS(0.75), (c) DPNR-*graft*-PSS(0.50).

Table 1. IEC and conductivity of DPNR, DPNR-*graft*-PSSEt, DPNR-*graft*-PSS, and Nafion117.

Specimen	Feed of SSEt (mol/kg-rubber)	IEC (meq/g)	Conductivity, σ (S/cm)[a]	σ* ((S/cm)/meq)[b]
DPNR	-	0.00	0.0	0.0
DPNR-*graft*-PSSEt	1.0	0.02	1.9×10^{-7}	2.8×10^{-4}
DPNR-*graft*-PSS(0.50)	0.50	0.11	3.2×10^{-5}	0.015
DPNR-*graft*-PSS(0.75)	0.75	0.15	1.4×10^{-3}	0.50
DPNR-*graft*-PSS(1.0)	1.0	0.22	8.1×10^{-3}	2.6
Nafion117®	-	0.87	4.6×10^{-2}	1.9

[a] Measured at 50℃,

[b] σ^* ((S/cm)/meq) = $\frac{\sigma}{\mathrm{IEC} \cdot t \cdot A \cdot d}$ *t*: thickness, *A*: surface area, *d*: density

Table 1 shows the ion exchange capacity (IEC) and proton conductivity (σ) measured at 50°C for DPNR, DPNR-*graft*-PSSEt prepared with SSEt of 1.0 mol/kg-rubber, DPNR-*graft*-PSS(1.0), DPNR-*graft*-PSS(0.75), DPNR-*graft*-PSS(0.50), and Nafion117®. The IEC and σ of DPNR were 0.00 meq/g and 0.0 S/cm, respectively, owing to the lack of a sulfonic acid group. Meanwhile, the corresponding values for DPNR-*graft*-PSSEt were 0.02 meq/g and 1.9×10^{-7} S/cm, suggesting that the hydrolysis of ethyl sulfonate in DPNR-*graft*-PSSEt slightly proceeded by immersing it into 1 mol/L HCl solution followed by drying before the measurement. In contrast, the IEC and σ of DPNR-*graft*-PSS depended significantly on the PSS content. Specifically, the IEC increased from 0.11 to 0.15 and then to 0.22 meq/g with increasing PSS content in DPNR-*graft*-PSS(0.50), DPNR-*graft*-PSS(0.75), and DPNR-*graft*-PSS(1.0), respectively. The IEC of DPNR-*graft*-PSS(1.0) was about one-fourth that of Nafion117® (0.87 meq/g). Similarly, the σ of DPNR-*graft*-PSS increased with increasing PSS content, reaching the highest value of 8.1×10^{-3} S/cm for DPNR-*graft*-PSS(1.0), but it was still lower than that of Nafion117® (4.6×10^{-2} S/cm). The efficiency of the proton transportation was investigated by estimating the proton conductivity per unit equivalent of sulfonic acid (σ*) from the values of IEC and σ. The estimated σ* values are shown in Table 1. The σ* of DPNR-*graft*-PSS(1.0) was approximately 1.4 times higher than that of Nafion117®, (1.9 (S/cm)/meq), which can be attributed to the formation of a continuous nanochannel of PSS, as shown in Figure 1(a). These results demonstrate that the PEM with a nanomatrix channel consisting of natural rubber and PSS achieved an efficient proton transportation.

References

1. Y. Yamamoto et al., *ACS Omega*, **2025**, *10*, 17576–17583.
2. S. Kawahara et al., *Macromolecules*, **2009**, *42*, 8557–8560.

The development of bio-inspired composites from epoxidized natural rubber using π–π stacking and cation–π interactions

Kwanchai Buaksuntear[1], Phillip Kohl[2], Youli Li[2], Wirasak Smitthipong[1,3]

[1] *Specialized Center of Rubber and Polymer Materials in Agriculture and Industry (RPM), Department of Materials Science, Faculty of Science, Kasetsart University, Bangkok 10900, Thailand.*

[2] *Materials Research Laboratory and BioPACIFIC MIP, University of California, Santa Barbara, California, 93106, United States.*

[3] *Hub of Talents in Natural Rubber, National Research Council of Thailand (NRCT), Bangkok 10900, Thailand.*

E-mail address of the presenting author: buaksuntear.k@gmail.com

Keywords: Functionalized NR, epoxidation, π-π stacking interactions, cation-π interactions, CB dispersion

Natural rubber (NR), also known as *cis*-1,4-polyisoprene, is derived from *Hevea brasiliensis* plants. NR exhibits good elasticity and mechanical properties. However, the oxidation is occurred due to the double bonds in molecules [1]. The chemical modifications are widely used to improve the properties of NR such as epoxidation process, which is the substitution of the double bond with the epoxide group, producing epoxidized natural rubber (ENR) [1]. In terms of rubber processing, carbon black (CB) is commonly used as a reinforcing filler. However, filler aggregation of CB in rubber products is one of the important problems, which is related to the complicated mixing in rubber manufacturing and high energy loss [2]. Therefore, the bio-inspired mechanism (i.e. mussel-inspired polymers) has been used to improve the mechanical properties of elastomer using non-covalent interactions [3]. The present research aims to improve carbon black dispersion in ENR composites through aromatic non-covalent interactions such as π-π stacking and cation-π interactions. Initially, the epoxidation process was used for the modification of NR to produce ENR. Then, the 20 phr of dopamine (D) was grafted onto the ENR chain as shown in Figure 1. The CB content in the ENR composite was various at 30, 40, and 50 phr, respectively.

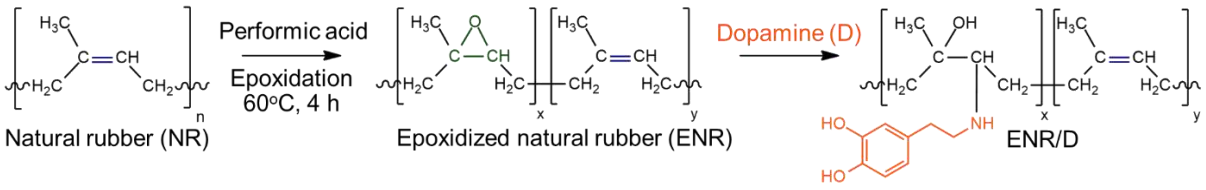


Figure 1. Epoxidation of NR and the D-functionalized molecules on the ENR chains (ENR/D) [4].

In this study, a variety of aromatic interactions (i.e. π-π stacking and cation-π interactions), which were observable by FTIR (1572 and 668 cm^{-1}) and Raman spectroscopy (1350 cm^{-1}), were obtained between the benzene ring in D-functionalized molecules on ENR chains and the surfaces of CB [4]. Interestingly, the small- and wide-angle X-ray scattering (SAXS/WAXS) revealed the slopes of ENR/CB with dopamine were lower than those of ENR/CB samples at a given concentration of CB. This indicated that the CB aggregates were broken and well dispersed in the D-functionalized ENR matrix by the π–π stacking and cation–π interactions between the benzene rings on the surfaces of CB and the dopamine. These results were in good agreement with the findings from the transmission electron microscope (TEM) and rubber process analyzer (RPA), which indicated that the π-π stacking and cation-π interactions enhanced the CB dispersion in the ENR composites [4].

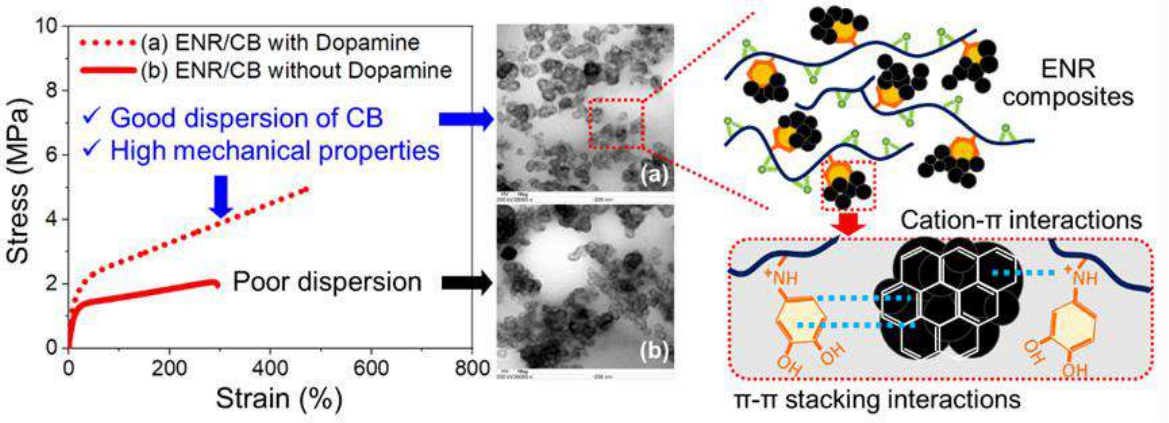


Figure 2. Stress-strain curves, TEM images, and model of the ENR composites with/without D [4].

Furthermore, the ENR/CB with dopamine exhibited the highest of the tensile properties (i.e. Young's modulus, tensile strength, and elongation at break) due to the effect of filler reinforcement and the non-covalent interactions as shown in Figure 2. Moreover, the decrease in tan δ from the dynamic mechanical analyzer (DMA) revealed a good energy-saving property (low energy loss) because of the well dispersion of the CB particles in the D-functionalized ENR matrix [4]. Finally, this research provides a novel approach based on a bio-inspired material to solve the CB aggregation problem in rubber products, resulting in the ENR composites with superior performance properties.

Acknowledgement

This research is funded by the Graduate School Fellowship Program in Agriculture and Agro-industry from the Agricultural Research Development Agency (Public Organization) as of fiscal year 2022. This research is also supported by the Capacity Building of KU Students on Internationalization Program (KUCSI), Kasetsart University as of fiscal year 2023, which is funded for K.B. to research studies at the University of California, Santa Barbara (USA). The use of BioPACIFIC SAXS instrument is supported by the BioPACIFIC Materials Innovation Platform of the National Science Foundation (NSF) under Award No. DMR-1933487 and Material Research Laboratory, UC Santa Barbara (USA). The research reported here made use of shared facilities of the UCSB MRSEC (NSF DMR 1720256), a member of the Materials Research Facilities Network (www.mrfn.org).

References

1. Buaksuntear K., Panmanee K., Wongphul K., Lim-arun P., Jansinak S., Shah D. U., Smitthipong, W., *Polymer*, 2024; 291: 126626.
2. Fauche R, Windey R, Pfeiffer H, Seveno D, Wevers M, *ACS Appl. Nano Mater*. 2024; 7: 3610.
3. Kim H., Lee J., Hong Y., Lim C., Lee D. W., Oh D. X., Waite J. H., Hwang D. S., *Chem. Mater.*, 2022; 34: 5074.
4. Buaksuntear K., Kohl P., Li Y., Smitthipong W., *ACS Appl. Polym. Mater.*, 2025; 7: 3576.

International Rubber Conference 2025 (IRC2025)
1-3 December 2025 @ BITEC, Bangkok, Thailand

Effect of crystal orientation on mechanical strength of poly-isoprene rubber under bi-axial deformation

Airi SATO[1], Katsuhiko TSUNODA[1], Yuji KITAMURA[1]

[1] *Sustainable and Advanced Materials, Bridgestone Corporation, 3-1-1 Ogawahigashi-Cho, Kodaira, Tokyo, Japan*

e-mail address of the presenting author (airi.sato@bridgestone.com)

Keywords: Natural Rubber, cis 1,4-polyisoprene, SIC, Strength, Wide-Angle X-Ray Diffraction,

Natural rubber (NR) is derived from the naturally occurring latex of Hevea Brasiliensis. NR exhibits exceptional mechanical strength due to strain-induced crystallization (SIC), a phenomenon in which polymer chains align and crystallize under deformation. This unique property not only contributes to product durability but also enhances resource efficiency. Owing to its distinctive SIC kinetics, NR accounts for over 50% of the rubber used in the tire industry. Moreover, natural rubber is a renewable resource that absorbs CO_2 during its growth. Enhancing the functionality of NR and expanding its applications are therefore considered beneficial from a nature-positive perspective.

NR and synthetic polyisoprene rubber (IR), which has the same cis-1,4-polyisoprene backbone, are known to exhibit different mechanical strengths. It has been reported that NR shows a threshold temperature for generating SIC driven strength that is more than 20 °C higher, and a threshold strain rate that is twice as fast as that of IR[1]. Furthermore, studies have shown a significant difference in the upper temperature limit for SIC-induced high mechanical strength between uniaxial and planar deformations in IR, whereas NR exhibits only a small difference between these deformation modes[2]. Additionally, the development of SIC has been found to be strongly influenced by local strain biaxiality, highlighting the importance of anisotropy in the SIC process[3].These findings imply that the orientation of SIC crystals is one of the key factor in determining SIC kinetics. However, there are very few reports addressing the differences in SIC orientation between NR and IR, and strategies for maximizing SIC performance remain unclear. Therefore, it is essential to investigate the detailed differences in SIC behavior between NR and IR. In this study, we investigated the SIC characteristics of NR and IR by conducting detailed analyses of lattice parameters, crystal size, and orientation using diffraction pattern analysis obtained from two-dimensional wide-angle X-ray scattering (WAXS).

Rubber samples, referred to as NR and IR , were formulated using the following process. NR gum (ribbed smoked sheet, RSS#3) or IR gum (IR2200, ENEOS Material Co.) was mixed with stearic acid (2 phr, i.e., 2 g per 100 g of rubber), ZnO (5.0 phr), N-1,3-dimethylbutyl-N'-phenyl-p-phenylenediamine (6PPD, 1 phr), N-cyclohexyl-2-benzothiazole sulfenamide (CBS, 1.5 phr), and sulfur (1.5 phr) using an internal mixer (Labo Plastomill, Tokoseiki Co.). The rubber specimen sheets were then vulcanized adopting hot press at 145 ℃ for a curing time of 21 minutes for NR and 37 minutes for IR. The WAXS experiments were conducted by uniaxially stretching ring-shaped specimens in the horizontal (X) direction at a strain rate of 0.05 mm/s. The use of ring-shaped specimens allows measurements to be performed without slippage during extension. X-ray beams were directed at the central part of the ring specimens to perform WAXS measurements during uniaxial stretching. 2D-WAXS measurements were carried out using a NANOPIX-WE (Rigaku) system. The incident X-rays were directed at the sample in the normal direction. The exposure time for each 2D-WAXS measurement was set to 6 seconds. A HyPix-6000 (Rigaku) detector was used

as the two-dimensional detector. The sample-to-detector distance was set to 70 mm, and the X-ray wavelength (λ) was 0.154 nm.

Figure-1 shows the strain applied to the ring specimen on the horizontal axis and the crystallinity calculated from the WAXS measurements on the vertical axis. In the comparison between NR and IR, it is worth to note that though NR shows smaller onset strain for crystallization, the slope is smaller, indicating a slower rate of crystallization. From the peaks of the (200), (120), and (002) planes, lattice parameters a, b, and c were calculated, and no differences were observed between NR and IR. Additionally, the crystal sizes along the a, b, and c axes at each strain were analyzed, and the crystal number density for each strain was also calculated. The results indicated that the rate of increase in number density from the SIC onset was comparable between NR and IR. Figure-2 shows a plot with the strain from the SIC onset in the horizontal axis and the degree of SIC orientation in the vertical axis. The degree of orientation was calculated using the peak from the (120). The degree of orientation of both NR and IR depends on strain. Since the degree of orientation at the onset remains nearly constant, but the slopes obtained from the linear approximation is different. These data would suggest that IR is more prone for highly oriented SIC after onset strain compared to NR. This difference in SIC orientation may be the origin of the difference in strength dependency for deformation mode between NR and IR.

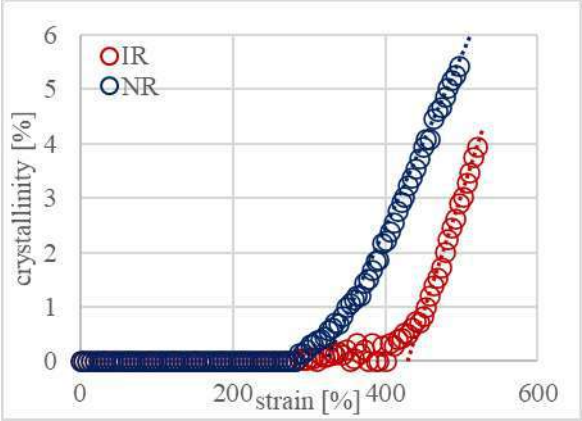


Figure 1. Crystallinity as a function of strain

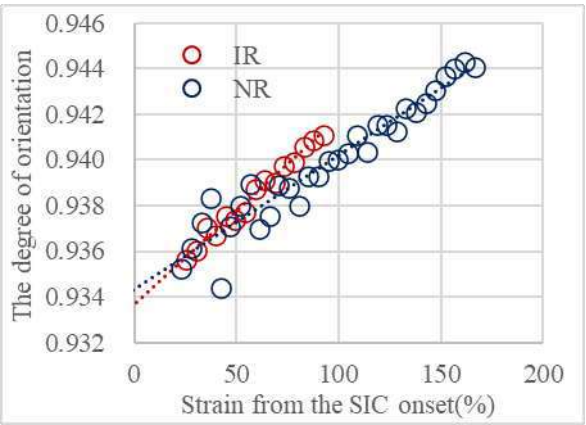


Figure 2. The degree of orientation as a function of strain from the SIC onset

Acknowledgement

Authors acknowledge funding from JST CREST through grant number JPMJCR2091.

References

1. Tsunoda K, Kitamura Y, Urayama K, *Soft Matter*, 2023; 19: 1966
2. Osumi R, Mai T-T, Tsunoda K, Urayama K, *Soft Matter*, DOI: 10.1039/D5SM00341E
3. Nozaki D, Mai T-T, Tsunoda K, Urayama K, *Maclomolecules*, 2025; 58(8): 4059

Session II : Advancements in Sustainable Rubber Technology

Oral Presentations

International Rubber Conference 2025 (IRC2025)
1-3 December 2025 @ BITEC, Bangkok, Thailand

Application of stearic acid-modified silica in PCR tread compound

FARSHID ZOLALA[1]

[1]*Process Engineering Specialist (compounding),Barez Industrial Group, Kerman, Ian.*

[1]Farshid2244@gmail.com

Keywords: Silica, Stearic acid, Rolling resistance, Tread compound

Abstract:

Silica is a key reinforcing filler in the rubber industry, particularly for high-performance tire tread applications. However, it has poor compatibility with nonpolar elastomers limit its dispersion and reinforcing efficiency. Surface modification of silica with stearic acid has been explored as an effective method to enhance its performance in tire tread compounds. This study investigates the effects of stearic acid-modified silica on the physical and mechanical properties of PCR tread compound. The modification process involves the esterification reaction between the hydroxyl groups (–SiOH) on the silica surface and the carboxylic acid group (–COOH) of stearic acid, resulting in a hydrophobic surface, containing 5% stearic acid modification, that improves better filler dispersion and polymer-filler interaction. This leads to reduce silica agglomeration due to decreased surface polarity, and better filler-matrix compatibility. Increase tensile strength, abrasion resistance, lower rolling resistance and wet skid properties.

Scope of the Research

The scope of this study is the exploration of surface functionalization of silica with stearic acid and its influence on silica dispersion, filler–polymer interactions, and tread compound properties.

Chemical Structure of Stearic Acid-Modified Silica

Stearic acid ($C_{18}H_{36}O_2$) contains a polar carboxyl group (-COOH) and a long hydrophobic alkyl chain. Its interaction with silica occurs via:

Hydrogen bonding between the -COOH and surface Si–OH groups. Covalent ester-like linkages (Si–O–C=O–R) formed through condensation under heat. Surface hydrophobization by alkyl chains extending outward, lowering surface energy and enhancing compatibility with elastomers [1, 2].

Characterization Techniques

To confirm surface modification, several analytical tools are used:

FTIR spectroscopy: detects C=O stretching (~1700 cm^{-1}) and C–H bands (~2850–2920 cm^{-1}), indicating stearic acid attachment [3]. TGA: quantifies organic content and grafting density by measuring weight loss of stearic acid upon heating [4]. SEM/TEM: observes morphological differences and improved dispersion.

Table 1. Sample compositions

Components [Phr]	Sample notations	
	N1	N2
SSBR 27.5 %Oil	110	110
BR	20	20
Silica	75	-
Modified Silica(5% stearic acid modification)	-	75
X50S (TESPT 50%)	12	12
Stearic Acid	1	1
Wax	1.5	1.5
ZnO	2.5	2.5
6PPD	2	2
DPG	1.2	1.2
CBS	1.7	1.7
Sulfur	1.6	1.6

Table 2. Test results

properties	Sample notations	
	N1	N2
T10 @160°C (min)	1.37	1.28
T50 @160°C (min)	4.45	4.14
T90 @160°C (min)	9.32	9.24
MH @160°C (lb.in)	12.2	12.8
Hardness (Shore A)	64	65
Modulus 300% (MPa)	8.4	8.5
Tensile Strength (MPa)	14.3	15.1
Elongation at Break (%)	347	332
Resilience @ 0 °C (%)	13	11.5
Resilience @ room temp. (%)	26	29
Resilience @ 70 °C (%)	60	63

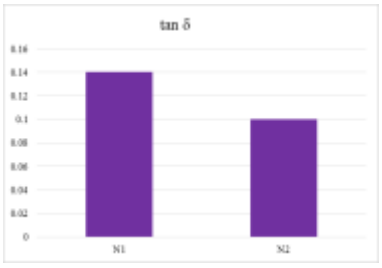


Figure 1. tan δ at 70°C , 10 Hz

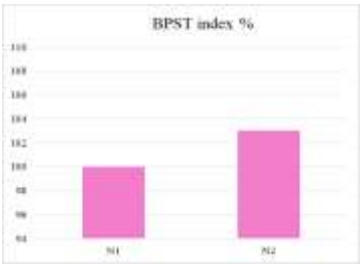


Figure 2. Wet skid resistance

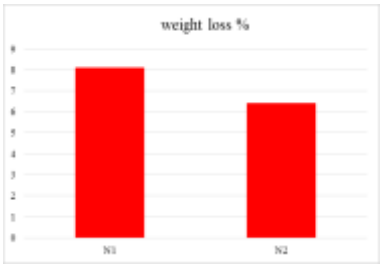


Figure 3. Abrasion resistance

Conclusion

Comparison was made between silica and modified silica in terms of properties and characteristics in the PCR tread compound. Characterization confirms the successful chemical interaction between stearic acid and silica. Based on the performance in the laboratory, the global compromise between rolling resistance, abrasion resistance and wet skid resistance for the tread compounds can be improved by replacing the silica with the modified silica. This is due to the improvement of polymer-filler interaction.

References

1. Li, Y., et al. Surface modification of silica with fatty acids and its effect on dispersion in rubber matrix. Journal of Applied Polymer Science, 2017.

2. Luo, Y., et al. Hydrophobization of silica with stearic acid for rubber reinforcement. Materials Chemistry and Physics, 2015.
3. Zhang, M., et al. Characterization of silica modified by fatty acids for rubber applications. Applied Surface Science, 2018.
4. Zhou, Y., et al. Thermal and structural analysis of fatty acid-modified silica particles. Thermochimica Acta, 2016.

International Rubber Conference 2025 (IRC2025)
1-3 December 2025 @ BITEC, Bangkok, Thailand

Bio-Based Multifunctional Additive from Modified Illipe Butter for Silica-Filled Tire Tread Compounds

M.I. FATHURROHMAN[1], S. PUSPITASARI[1], N.A. KINASIH[1] , D.K. ARTI[2]

[1] *PT. Riset Perkebunan Nusantara – Bogor Getas Research Unit, 1 Salak Rd, Bogor, West Java, Indonesia.*

[2] *Research Center for Advanced Material, National Research and Innovation Agency (BRIN), South Tangerang, Indonesia.*

irfanirri@gmail.com

Keywords: Biomaterial, multifunctional additive, silica-filled compound, tire tread

Diphenyl Guanidine (DPG) is one of the guanidine class rubber accelerators that could be used as a catalyst for silanization reactions in rubber filled with silica (Kaewsakul et al. 2013). The use of DPG results in improved filler dispersion within rubber matrix. However, during high temperatures of rubber compounding, DPG releases toxic and carcinogenic substances such as aniline; therefore, safe alternative DPG substitutions are required (Hayichelaeh et al., 2017). Illipe butter, a class of vegetable butter, is the alternate source of fatty acid. Modification of illipe butter into fatty amine was defined as attaching an amine of an alkanolamine compound in the fatty acid molecular chain of illipe butter to form amines complexed with fatty acid. Additionally, the presence of fatty acids in illipe butter promoted the processing capability of the uncured rubber compound. As the consequences, fatty amine is predicted to have a function as a rubber plasticizer and curing accelerator simultaneously.

In this present study, the role of bio MFA based on fatty amine synthesized from esterification of illipe butter and alkanolamine was investigated by arranging the concentration of fatty amine into SSBR/BR rubber blend filled with high disperse (HD) silica. Fatty amine was introduced as a potential alternative bio-based MFA in the rubber/silica/silane system to substitute DPG. We arranged fatty amine concentrations at 1.25 and 2.5 part(s) per hundred parts of rubber (phr) and combined them with DPG at equal ratio of DPG/fatty amine as 1.25/1.25 phr denoted MFA*, MFA, DPG/MFA, respectively. A rubber compound composed only of DPG was determined as a comparison. Filler-filler interaction, bound rubber, and curing characteristics of silica-filled rubber caompound were investigated. Furthermore, the magic traingle properties of tire tread compound such as abrasion resistance, wet grip and rolling resistance were were also studied.

The esterification of illipe butter into fatty amine was demonstrated by a notable distinction between the FTIR spectrums of fatty amine and illipe butter, as shown in Figure 1. The fatty amine spectrum displays a large absorption peak at 3360 cm^{-1}, attributed to the stretching of O-H groups generated by water production during the esterification step and/or the interaction of triethanoamine (TEA) with illipe butter. Furthermore, absorption peaks associated with the amide carbonyl (-CON-) functional group at 1652 cm^{-1}, C-O stretching at 1035 cm^{-1}, and C=C bending at 877 cm^{-1} were identified in the fatty amine spectrum. Moreover, the absorption peak at 1744 cm^{-1}, attributed to fatty acids in illipe butter, exhibits a minor shift to 1739 cm^{-1}, signifying the presence of C=O (ester) in the fatty amine spectrum as a result of the esterification of illipe butter.

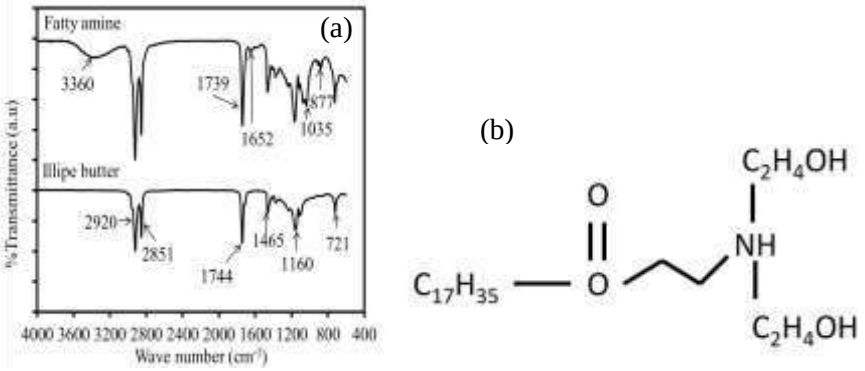


Figure 1. FTIR fatty amine compared to illipe butter (a), possible structure of fatty amine (b)

The result found that with the appropriate amount of MFA* reduced a filler-filler interaction and increased chemical bound rubber therefore fatty amine can function as activators for silanization and bio-plasticizer which play a similar role as filler dispersants. Furthermore, the presence of fatty amine at an appropriate amount of 1.25 phr provided the most favorable magic triangle of tire parameters since it reached maximum tan δ at 0°C, along with tan δ at 60°C and DIN volume loss at the minimum level as shown in Figure 2.

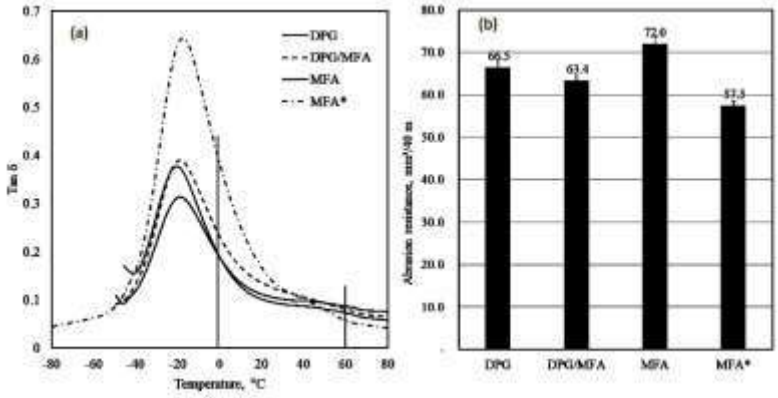


Figure 2. Tan δ vs temperature (a) DIN volume loss (b) of silica-filled tire tread vulcanizate

Acknowledgement

Authors highly acknowledge to Indonesia Endowment Fund for Education Agency (LPDP) and National Research and Innovation Agency (BRIN), Republic of Indonesia [RIIM Batch 2, Contract Number 86/IV/KS/11/2022, 2022] for supported research grant.

References

1. Hayichelaeh C, Reuvekamp LAEM, Dierkes WK, Blume A, Noordermeer JWM, Sahakaro K, *Rubber Chem. Technol.*, 2017; 90(4):651-666.
2. Heideman B, Noordermeer JWM, Datta RN, van Baarle B, *Rubber Chem Technol.*, 2006; 79(4):561-588.
3. Kaewsakul W, Sahakaro K, Dierkes WK, Noordermeer JWM, *Rubber Chem. Technol.*,2013; 86(2):313-329.
4. Park SS, Kil SG, Jang BM, Song KC, Kim, SK, *Polym Korea.*, 2021; 25(4):503-511.

The Utilization of Fly Ash From Different Resources as a Filler on the Properties of NR Compounds

Karnda Sengloyluan[1], Apissara Komkay[1], Nattapon Uthaipan[1]

[1] *Rubber Engineering Program, Interdisciplinary Department, Prince of Songkla University, Songkhla, Thailand.*

Karnda.s@psu.ac.th

Keywords: Fly ash, biomass filler, alternative filler, sustainability

Filler is widely used in rubber industry in order to improve the properties of rubber products, for example, carbon black and silica are generally used as reinforcing fillers in many high performance rubber products such as tire, bearing, engine mount, etc., calcium carbonate and clay are used to reduce the rubber product cost because of its low surface area and cheap. Those commercial fillers are produced by chemical synthesis or non-renewable resources. Due to the sustainability concern, the renewable filler resources are more investigated to replace the commercial fillers.

There are at least 80 biomass power plants located throughout Thailand. The biomasses used as a raw material to generate the electric power are quite varieties based on the agricultures in those areas such as paddy farm, rubber plantation, palm plantation, sugarcane field, and eucalyptus plantation. By-products from the incomplete combustion of the biomass power plants are fly ash and bottom ash. Fly ash consists of different proportions of metal oxide like SiO_2, Al_2O_3, CaO, Fe_2O_3, MgO and etc [1-3]. Fly ash was added into rubber compounds to study the properties of fly ash as an alternative filler. The study reported that mechanical properties of rubber could be influenced by particle size and filler content [1]. Comparison with clay and calcium carbonate, the use of fly ash in emulsion grade styrene butadiene rubber (ESBR) showed the similarity of the cure characteristics and mechanical properties [3]. However, the properties of fly ash silica filled natural rubber (NR) were lower than those of precipitated silica without any treatment because of different composition and surface characteristics. But the use of fly ash was not recommended to use in SBR compounds [4]. The interfacial interaction between fly ash and rubber could be improved by adding silane coupling agent, but the properties of filled rubber compounds and vulcanizates were somehow lower than the use of precipitated silica [5].

This project was studied the properties of different types of fly ash obtained from the biomass power plants in Thailand. The biomasses used as raw materials to produce the electric power were rice husk, bagasse, parawood, palm bunch and household waste. The fly ashes obtained from the power plants were milled and filtered to control the particle size not larger than 50 µm via a 300 mesh metal sieve. The properties of fly ashes were analyzed such as particle size, pH value and chemical compositions. The fly ashes were added into NR compounds for 30 phr, then testing the cure characteristics, mechanical properties and filler dispersion.

The fly ashes showed different chemical compositions, strong base characters and low surface areas. The fly ash-filled NR compounds were prepared on a two roll mill as the following formulations in Table 1. Then, cure characteristics of the compounds were tested at 150°C for 30 min as presented in Figure 1. It was found that scorch times and cure times of the compounds were clearly different according to the different types of biomasses to produce the fly ashes. The use of fly ashes at 30 phr led to increase tensile strength, elongation at break and tear strength, unless the use of fly ash from household waste ash. These results were obviously affected by different crosslink densities

and interfacial adhesion of fly ashes and NR phases according to a different metal oxide composition obtained in the fly ashes. These fly ashes showed a potential to use or replace non-reinforcing or semi-reinforcing fillers in some commercial applications such as rubber roofing, foam, rubber parts.

Table 1. Fly ash-filled NR compounds formulations with different types of fly ashes.

Components [phr]	**Sample notations**					
	NF1	**F1**	**F2**	**F3**	**F4**	**F5**
STR 5L[a]	100	100	100	100	100	100
Rice husk ash	-	30	-	-	-	-
Bagasse ash	-	-	30	-	-	-
Parawood ash	-	-	-	30	-	-
Palm bunch ash	-	-	-	-	30	-
Household ash	-	-	-	-	-	30
Processing oil	5	5	5	5	5	5
ZnO	5	5	5	5	5	5
Stearic acid	1	1	1	1	1	1
TMQ	1	1	1	1	1	1
CBS	1.5	1.5	1.5	1.5	1.5	1.5
Sulfur	1.5	1.5	1.5	1.5	1.5	1.5

[a] Standard Thai Rubber 5L

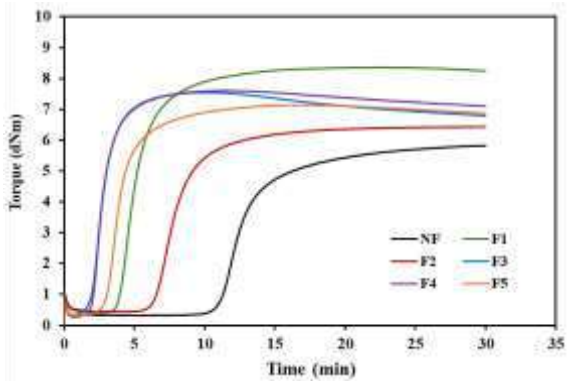


Figure 1. Cure characteristics of different types of fly ashes filled NR at 150°C

Acknowledgement

This project was granted by the Fundamental Fund 2023, No. RDO6601360d, the Research and Development Office, Prince of Songkla University. The research facilities were supported by the Faculty of Engineering, Prince of Songkla University.

References

1. Maan A, Kumar Niyogi U, Kumar Singh A, SinghMehra D, Rattan S, J. Polym. Mater., 2014; 31(4): 397.
2. Saowapark T, Sombatsompoop N, Sirisinha C, J. Appl. Polym. Sci., 2009; 112: 2552.
3. Dasgupta M, Kar S, Das Gupta S, Mukhopadhyay R, Bandyopadhyay A, Prog. Rubber Plast. Recycl. Technol., 2013; 29(3): 151.
4. Sombatsompop N, Thongsang S, Markpin T, Wimolmala E, J. Appl. Polym. Sci., 2004; 93: 2119.
5. Thongsang S, Sombatsompop N, Ansarifar A, Polym. Adv. Technol., 2008; 19: 1296.

International Rubber Conference 2025 (IRC2025)
1-3 December 2025 @ BITEC, Bangkok, Thailand

Efficient and Gentle Processing of Rubber Compounds – How Continuous Milling Transforms Rubber Processing

Julia Uth, Annemarie Hillebrecht, Manuel Bessler

UTH GmbH, Eisenhowerstrasse 7-9, 36041 Fulda/Germany

Presenting author: Julia Uth (juth@uth-gmbh.com)

Keywords: Continuous Milling, Rubber Processing, Rubber Compounds, Fine Mesh Straining, Homogenisation

Continuous Milling with Two-Roll Plasticiser (TRP) technology is a resource-efficient method for the economical and gentle processing of technical rubber compounds based on an open two-roll system. In conventional rubber production, final compound finishing either takes place in the mixing room through a highly automated and safe process – resulting in high costs due to blocked mixing capacity and strict temperature control – or on open mills, which enable gentle processing but present challenges related to manual labor and safety risks. Consequently, the rubber processing industry demands alternative solutions. Continuous Milling can fully replace automated downstream mixing stages in technical rubber production and offers an alternative processing route for remilling, blending, rework, or compounding applications.

Basic principles of Continuous Milling

The compact Continuous Milling process combines established rubber processing operations such as cracking, homogenizing, and discharging. Processing takes place across three zones along the continuous roll **(Figure 1)**. The length of the processing zones on the rolls are in general adapted to application and throughput and therefore vary between 1000 and 2500 mm of roll length. In the feeding zone materials of various shapes can be fed by a conveyor. During the process, a mechanically induced transformation occurs in the nip of the homogenization zone in which the material is plasticized and homogenized. The basis for a gentle process is a controlled temperature development (**Figure 2**). Adjustable roll speeds and gap settings optimize friction and improve compound homogeneity. A roll design tailored to technical rubber compounds also enables axial material transport from the feeding to the discharging zone, where the compound is directly extruded into defined strip dimensions. The process eliminates the need for operator intervention in the processing area, which is fully enclosed to ensure operator safety. At the same time, the specialized open two-roll system provides excellent accessibility for cleaning, making the equipment particularly suitable for frequent material or color changes. With its modular machine concept, UTH GmbH also offers the integration of a gear pump for gentle Fine Mesh Straining when impurities are present.

Development and Trials

Experimental trials were conducted using three representative compounds **(Table 1)** in order to evaluate the performance of the TRP-based Continuous Milling process. The results demonstrated a significant reduction in compound viscosity, while cure characteristics remained largely unaffected. For NR-based compounds, both storage and loss moduli exhibited a measurable decrease. In combination with the observed reduction in Mooney viscosity, these findings suggest that a controlled mechanical breakdown of molecular chains occurs during TRP processing. Importantly, the maintenance - or even improvement - of vulcanized properties indicates that this viscosity reduction is achieved without detrimental effects on the final compound performance. These results provide strong evidence that Continuous Milling constitutes a gentle yet effective

processing method for achieving high-quality rubber compounds. A comprehensive discussion of the experimental data and material-specific effects will be presented in detail during the lecture.

Current State of Development and Future Prospects

The Continuous Milling technology has been established in the tire industry for processing rework materials with throughputs up to 2,500 kg/h. Special process designs can provide options for tasks in rubber processing, such as preheating, mixing, and discharging. Additionally sustainable materials moving this state-of-the-art process into focus of application.

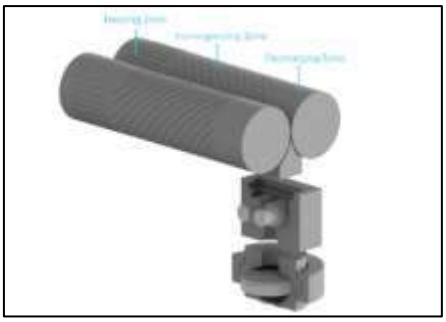


Figure 1. Processing takes place in different zones along the rolls, starting from the feeding zone.

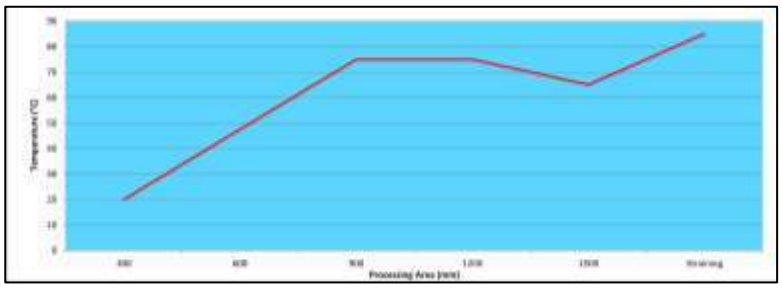


Figure 2. The graph shows the controlled temperature development along the rolls' length (processing area). Due to temperature circuits it's possible to take off temperature in discharging zone.

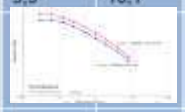
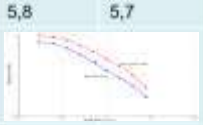
	NR/BR		BR		NR	
	BEFORE	AFTER ContMill	BEFORE	AFTER ContMill	BEFORE	AFTER ContMill
Mooney ML (1+4) 100°C	**102**	**82**	**49**	**47**	**44**	**35**
CureT95 [min]	9,9	10,1	42	41	5,8	5,7
Ampl-Sweep (1,67Hz, 50°C)						
Shore A - Hardness	66	64	43	43	76	75
Modul 300 [N/mm²]	12,5	10,8	4,0	4,1	8,6	8,7
Tensile strength [N/mm²]	24,1	23,8	11,3	11,8	14,5	16,7
Elongation at break [%]	499	519	654	683	454	503

Table 1. Compound Properties before and after Continuous Milling

References

All information is based on the results of studies conducted by UTH GmbH in collaboration with various research institutions and customer-specific tests.

Green Preparation and Performance Study of NRL/Biomass Composites via Non-Rubber Component Mediation and Spatial Confinement

Zhengtian Xie[1*], Shaoqi Huang[1], Junqi Zhang[1], Jinrong Wu[1*]

[1] *State Key Laboratory of Polymer Materials Engineering, College of Polymer Science and Engineering, Sichuan University, Chengdu 610065, China.*

zt-xie@scu.edu.cn

Keywords: Natural Rubber/Biomass Composites, Non-Rubber Component, Spatial Confinement, Green Preparation

The green and high-performance development of rubber materials represents a significant trend and urgent demand for the rubber industry. Natural rubber latex (NRL) biomass composites offer significant application potential in areas like weather balloons, medical devices, and eco-friendly packaging due to their renewability, low cost, and biodegradability. However, the inherent polarity of biomass materials impedes uniform blending with non-polar rubber matrices, resulting their reinforcement efficacy generally falls short of traditional fillers, severely limiting the development and practical application of these composites. Consequently, developing green, efficient composite technologies for NRL/biomass composites and enhancing their performance is a research imperative for the sustainable advancement of the rubber industry.

The mechanical properties of NRL/biomass composites are fundamentally linked to the dispersion state and network structure of the biomass within the rubber. To achieve efficient composite construction and performance optimization, extensive research has focused on novel coupling agents, chemical modification of rubber or biomass, and process condition regulation. For example, silane modification of chitosan improved its dispersion in NR, enhancing composite strength and toughness [1]. Similarly, epoxidation or carboxylation of NR increases its polarity, improving interactions with biomass molecules [2]. Fundamentally, these approaches enhance biomass compatibility in the rubber matrix through interfacial modification. However, they often compromise the properties of composites and require substantial chemical reagents and solvents, introducing pollution and process complexity. This significantly constrains NRL/biomass composites research and application. Therefore, exploring greener, more efficient preparation methods that circumvent interfacial chemical modification is crucial for high-performance NRL/biomass composites and sustainable industry growth.

Although the polyisoprene chains in NRL are non-polar, the latex particles possess a polar membrane layer comprising non-rubber components (proteins, phospholipids) rich in hydroxyl, amino, and carboxyl groups. This work exploits the interaction between these non-rubber components and biomass to improve dispersion and overcome interfacial incompatibility [3]. Kappa-carrageenan (k-type) and NRL were uniformly mixed under heating, then dried and coagulated to form composite films. Transmission electron microscopy (TEM) revealed that carrageenan remained uniformly dispersed post-drying, forming a continuous three-dimensional biomass network around the latex particles. Two-dimensional infrared spectroscopy further confirmed strong hydrogen bonding between polar groups (e.g., hydroxyl) of carrageenan and non-rubber components. Additionally, intrinsic gelation capability of carrageenan led to the formation of a spatially nested skeleton with rubber matrix during preparation. This spatial confinement effect further stabilized carrageenan

dispersion within the NRL. Utilizing this inherent interaction and nanoconfinement, we produced well-dispersed biomass composites exhibiting excellent tensile properties (14 MPa unvulcanized, exceeding 35 MPa vulcanization, as shown in **Figure 1**), outstanding tear resistance, and thermal responsiveness.

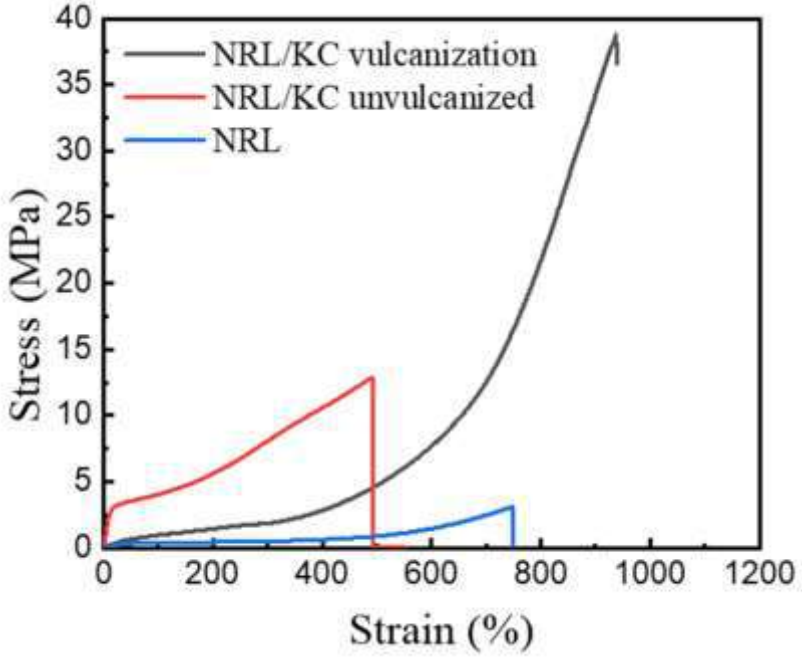


Figure 1. Mechanical performance of NRL and NRL/k-carrageenan composites (NRL/KC).

Acknowledgement

This work was supported by the National Natural Science Foundation of China (grant No. 52173058 and No. 52403072), and the National Key R&D Program of China (2022YFD2301202). The authors are indebted to the Shanghai Synchrotron Radiation Facility (SSRF) for providing the necessary beamline time and technical assistance in the experiments on the BL16B1 line.

References

1. Yin J, Hou J, Huang S, et al. Effect of Surface Chemistry on the Dispersion and pH-Responsiveness of Chitin Nanofibers/ Natural Rubber Latex Nanocomposites. Carbohydr. Polym. 2019, 207, 555–562.
2. Han H, Zhang X, Kuang W, et al. Self-Healing and Recyclable Elastomer Based on Epoxidized Natural Rubber and Carboxylated-Chitosan. Compos. Commun. 2023, 40, 101594.
3. Huang S, Xie Z, and Wu J, et al. Fully Biosourced, Vulcanization-Free, and Thermal-Responsive Natural Rubber Material. Macromolecules. 2024, 57, 1642–52.

International Rubber Conference 2025 (IRC2025)
1-3 December 2025 @ BITEC, Bangkok, Thailand

Properties of Films from Deproteinized Natural Rubber Latex Produced *Via* Membrane Separation Technology

Mohamad Akmal ABDUL RAHIM, Dazylah DARJI, Nurul Hayati YUSOF

Technology & Engineering Division, Rubber Research Institute Malaysia,

Malaysian Rubber Board, 47000, Sg. Buloh, Malaysia

*Corresponding author: akmal@lgm.gov.my

Keywords: Deproteinized natural rubber latex, membrane separation, latex processing and film properties

Deproteinized natural rubber (DPNR) latex has gained attention as a valuable material due to its reduced protein content, making it suitable for applications requiring hypoallergenic potential. DPNR can be produced *via* three primary methods: mechanical, chemical, and enzymatic reactions. Among these, the enzymatic route offers a sustainable, eco-friendly alternative, using biocatalysis to remove proteins while preserving natural rubber properties. In this study, DPNR latex was produced enzymatically and further processed using advanced membrane technology to increase its total solid content (TSC). The membrane technology played a crucial role in concentrating the latex, ensuring high purity, and achieving the desired TSC levels for downstream applications. The resulting concentrated DPNR latex was fabricated into cast and dipped films, and their properties were systematically compared with those of high-ammonia (HA) natural rubber latex. Key parameters such as latex properties, tensile properties, and residual protein content were assessed.

Acknowledgement

The authors are grateful for the financial support and facilities provided by the Malaysian Rubber Board. The authors also thank Hishamudin Samat, Noorafiza Fauzi and Mohd Faizal Abd Aziz for their technical assistance during the duration of the study.

Extrudable Vitrimeric Rubbers Enabled via Heterogeneous Crosslinking

Shuangjian Yu, Jialiang Chen, Baochun Guo, Siwu Wu, Liqun Zhang

[1] *Institute of Emergent Elastomers, School of Materials Science and Engineering, South China University of Technology, Guangzhou 510640, China.*

3053453086@qq.com

Keywords: Rubber, Dynamic covalent bond, Heterogeneous crosslinking, Recycling, Simulation

Cross-linked rubbers, as a typical thermosetting polymer, is difficult to reshape and reprocess once molded. In 2020, the global output of waste rubber exceeded 70 million tons. The current recycling methods of waste rubber such as incineration, production of rubber powder and reclaimed rubber is “downcycle”. A large amount of waste rubbers has led to serious “black pollution” and resource waste. Dynamic covalent chemistry provides a bran-new method for closed-loop recycle of crosslinked rubber. However, it is difficult to implant dynamic covalent bonds (DCBs) into rubber and regulate the network aggregation structure due to that there are the few reaction-active sites in the general rubber chains, and it is difficult to functionalize, and rubber processing must go through “black box” processes during mixing and crosslinking. Besides, the service temperature of the rubber is much higher than the glass transition temperature and the processing viscosity is high, which leads to a series of dilemmas of the DCB cross-linked rubber, such as the processing temperature difficult to relax, the service temperature easy to creep, the low mechanical properties, etc. More importantly, it cannot meet the requirements of continuous processing/molding process and performance in practical application. Around the above-mentioned issues, our team has carried out the systematic studies.

The key for the practical application of DCBs cross-linked rubber is to realize the continuous reprocessing. Recently, we pioneered a multiphase structural design strategy to obtain the first DCBs crosslinked rubber material with a recycle capability by extrusion [1,2]. Specifically, by introducing cross-linked granules with high-density DCBs into the cross-linked matrix with low-density DCBs, a multi-phase network with the strong interfacial bonding was adopted in DCBs cross-linked rubber. Based on the amplification of interfacial stress and the mechanochemical activation effect, the matrix strengthening and the accelerated network relaxation were simultaneously realized. For example, by crosslinking the raw rubber matrix with rubber particles rich in dynamic polysulfide bonds, an elastic skeletal network (ICE) dominated by rubber granules was created, which contained a slightly crosslinked plastic interfacial layer as binder (**Figure 1a**). Based on the thermomechanical actions, the plastic interface layer was able to flow, and the solid-state rubber granules can be repeatedly “ruptured and repaired” through the rapid exchange of dynamic polysulfide bonds at the interface, ultimately giving the overall material a stable repeated extrudability (**Figure 1b**). The recycled extrudate with excellent mechanical properties exhibited the high retention rate of mechanical properties (**Figure 1c**). Moreover, the material exhibited high strength, high elasticity and high creep resistance, which is significantly better than the commercially available TPVs. This not only provides a new idea for the development of a new generation of TPV, but also provides a potential solution for promoting the industrial application of DCBs crosslinked rubber [2].

To reveal the interface stress amplification effect in the multiphase network during the processing, we have recently constructed a multiphase model via coarse-grained molecular dynamics simulation [3,4]. Subsequently, tensile and shear force fields were respectively applied to the

multiphase model, and the stress distribution and evolution during the stress loading process of the multiphase network were systematically studied. During the stretching process, due to the significant differences in the deformation capabilities of the two phases and the interfacial stress concentration, the interfacial cross-links perpendicular to the stretching direction are mainly broken. During the shearing process, the lowly cross-linked phase exhibits viscous flow, while the highly cross-linked phase is forced to move synchronously. The velocity gradient between the two phases triggers rotational motion, significantly increasing the interfacial stress and eventually leading to the complete fracture of the interfacial crosslinked bonds. In short, even at small strains, the interfacial stress generated during the shearing process is significantly higher than that during the tensile process. Therefore, during the extrusion process, the shear flow dominates the rapid activation of the interface DCBs, thereby achieving efficient extrudable reprocessing of the heterogeneous network.

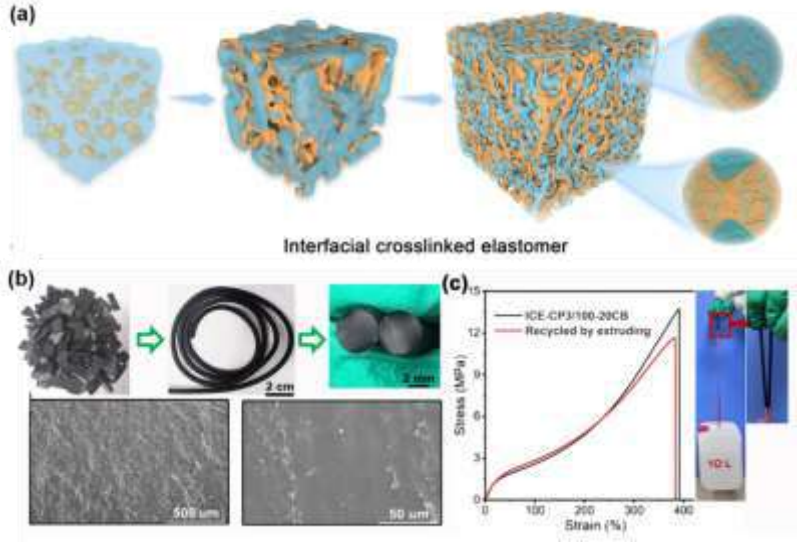


Figure 1. (a) Scheme for the formation process of the skeletal network via granule percolation and interfacial crosslinks. (b) Extrudable reprocessing of multiphase rubbers and their microscopic morphology on the surface/cross-section. (c) Tensile properties of the extruded sample and its load-bearing demonstration.

Acknowledgement

These works were funded by the National Science Fund for Distinguished Young Scholars (51825303), the National Natural Science Foundation of China (52130305), the Guangdong Basic and Applied Basic Research Foundation (2023B1515020085).

References

1. Yu S, Li F, Fang S, Yin X, Wu S, Tang Z, Zhang L, Guo B, *Macromolecules*, 2022; 55: 3236.
2. Yu S, Wu S, Fang S, Tang Z, Zhang L, Guo B, *Adv. Mater.*, 2023; 35: 2300856.
3. Chen J, Yu S, Wu S, Tang Z, Guo B, Zhang L, *Langmuir*, 2025; 41: 6353.
4. Chen J, Yu S, Wu S, Tang Z, Guo B, Zhang L, *Sci. China Mater.*, 2025; 68: 2032.

International Rubber Conference 2025 (IRC2025)
1-3 December 2025 @ BITEC, Bangkok, Thailand

Lignin/carboxylated nitrile rubber composites: the influence of carboxyl content on the mechanical properties of the material

Hongbing Zheng1,2, Dongmei Yue[2]

1PetroChina Shanghai Advanced Materials Research Institute Co.Ltd, Shanghai, PR China;

2Key Laboratory of Beijing City on Preparation and Processing of Novel Polymer Materials, Beijing , PR China.

e-mail address of the presenting author (zhenghongbing@petrochina.com.cn)

Keywords: Lignin, Carboxylation, NBR, Biomaterials, Composites

Nitrile rubber (NBR) exhibits excellent oil resistance, wear resistance, airtightness, and good physical and mechanical properties. On the other hand, lignin, a by-product of the pulp and paper industry, can serve as an ideal substitute for carbon black as a reinforcing agent for rubber. However, when NBR is directly compounded with lignin, achieving the desired reinforcing effect is challenging due to factors such as poor dispersion of lignin in the NBR matrix and poor compatibility with the NBR phase.

In this paper, we converted cyano groups into carboxyl groups through the hydrolysis reaction of NBR. By controlling the hydrolysis time, we successfully prepared two types of carboxylated NBR with different carboxyl contents (2.6 wt% and 6.0 wt%), named as IX-NBR and HX-NBR. Subsequently, the base NBR and the carboxylated NBR was processed into lignin/NBR composites via dry blending. Using the same basic formula and processed procedure, three types of nitrile butadiene rubber (NBR, IX-NBR, HX-NBR) with different carboxyl contents were compounded with lignin at different loadings (0, 10, 20, 30, and 40 parts). Basic formula (parts by mass/phr) as follows: NBR 100.0, ZnO 5.0, S 1.5, SA 1.0, DM 1.0, TMTD 0.2, sodium lignosulfonate (10.0, 20.0, 30.0, 40.0).

The results indicated that the introduction of carboxyl groups endowed NBR with higher polarity and reactivity, significantly enhancing the interfacial compatibility between lignin and the rubber matrix. The mechanical properties of the composite were greatly improved, with the mechanical strength increasing from 4.5 MPa without carboxyl groups to 13.8 MPa with high carboxyl content. The good dispersion of lignin also significantly improved the thermal stability of the composite. The carboxylation modification strategy of NBR provides a new approach for preparing high-performance NBR/biomass composites.

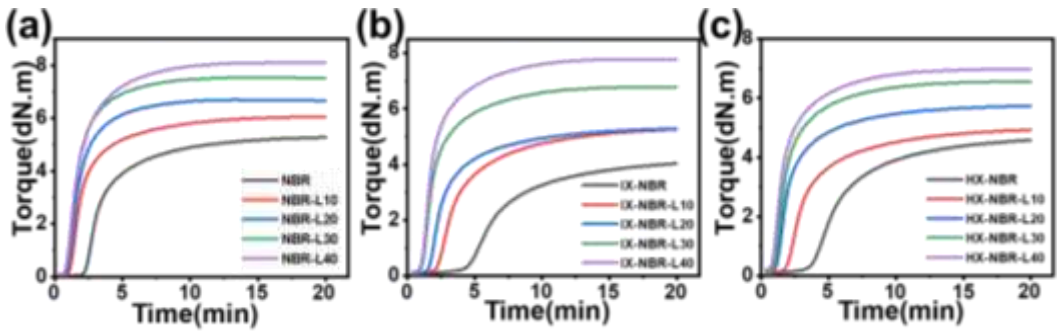


Figure 1. Vulcanization curve diagram of (**a**) NBR-L, (**b**) IX-NBR-L, and (**c**) HX-NBR-L.

From the torque curve in Figure 1, it can be seen that after completely replacing carbon black with lignin for reinforcement, the minimum torques of the composites during the vulcanization process becomes extremely low.

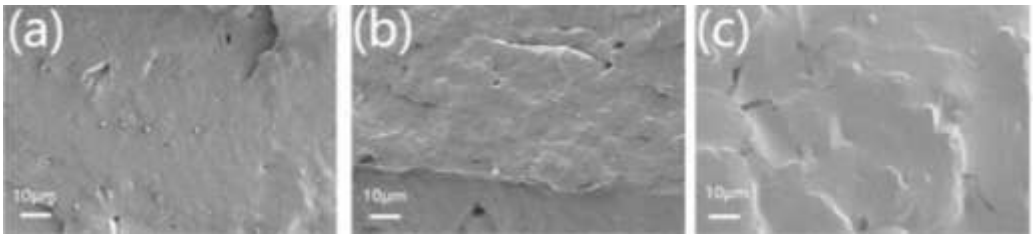


Figure 2. SEM images of (**a**) NBR-L20, (**b**) IX-NBR-L20, and (**c**) HX-NBR-L20.

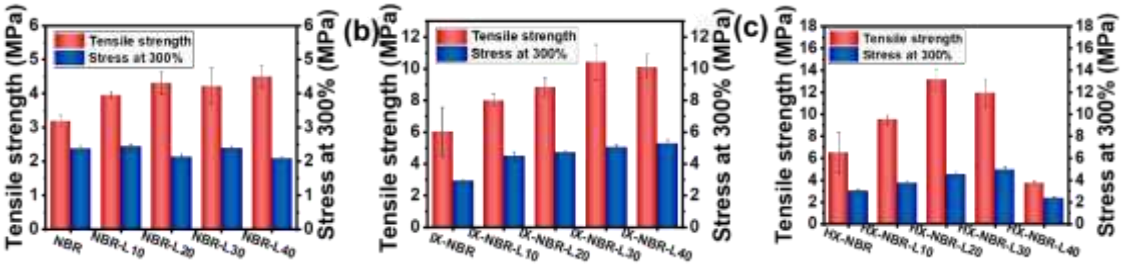


Figure 3. Maximum stress and 300% modulus at a fixed extension of (**a**) NBR-L, (**b**) IX-NBR-L, and (**c**) HX-NBR-L.

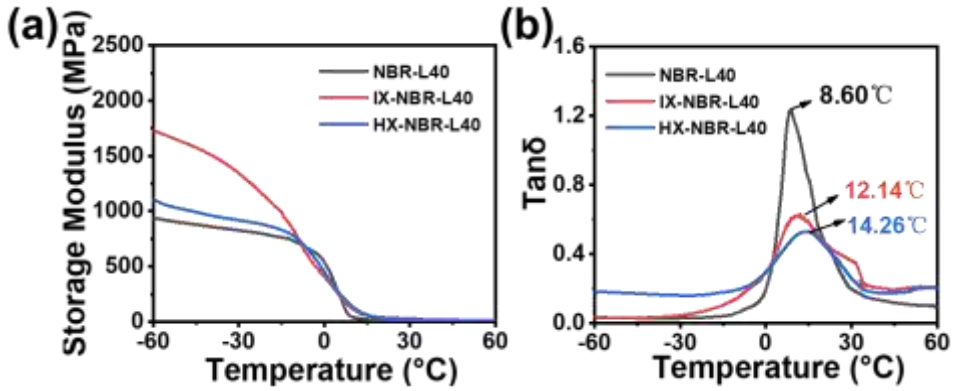


Figure 4. (**a**) Storage modulus and (**b**) Tan δ curves of XNBR/lignin compounds with three different carboxyl contents.

International Rubber Conference 2025 (IRC2025)
1-3 December 2025 @ BITEC, Bangkok, Thailand

Study on the Performance of Natural Rubber - Copper Coated Steel Wire with BCDB and BCoPD

Jin Yuan[1], Yao Zhimin[2], Chen Zhaohui[3]

[1] *Building 101, No.45 Caifuxingyuan, Lane 188, Maoting Road, Songjiang District, Shanghai, China.*

[2] *No. 8 Weisan Road, Lingang Industrial Park, Guanyun County, Lianyungang, China.*

[3] *School of Materials Science and Engineering, South China University of Technology, Guangzhou, China.*

jinyuan@rebochem.com

Keywords: Natural rubber, 2,2-dithiobis(phenylcitraconimido), Anti-reversion agent, Crosslink, Adhesion

The belt compounds of radial tires typically contain natural rubber (NR) and a conventional curing system with a relatively high proportion of polysulfide bonds. Consequently, these compounds are prone to reversion during the curing process and tire operation, resulting in a decline in mechanical properties and durability of tires. One of the most effective strategies to mitigate reversion is to incorporate anti-reversion agents into the rubber matrix. In this study, 1,3-bis(citraconimidomethyl)benzene (BCDB) and 2,2-dithiobis(phenylcitraconimido) (BCoPD) were employed as vulcanization functional additives to investigate their effects on reversion and other properties of the belt compound. The molecular structures of these compounds are depicted in Figure 1.

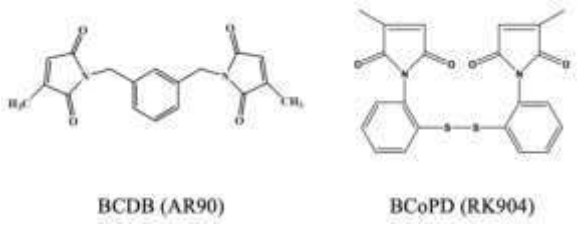


Figure 1. Chemical structures of anti-reversion agents AR90 and RK904

Extensive research has elucidated the mechanism of action of these additives. Figure 2 depicts the reaction mechanism of BCoPD with NR. During the normal curing phase, BCoPD engages in a Michael addition reaction with the polymer chain by bonding with sulfur. In the post-curing phase, BCoPD undergoes a Diels-Alder reaction with the conjugated diene generated by NR during reversion.

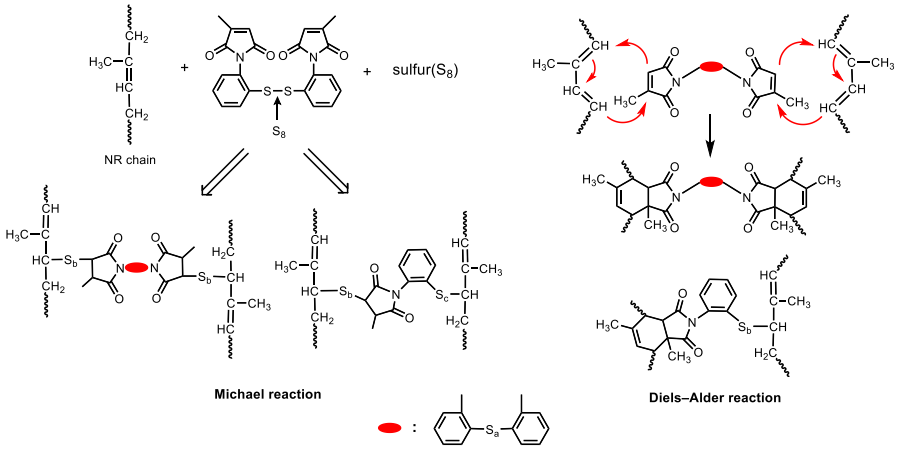


Figure 2. Reaction mechanism of BCoPD with NR

BCDB and BCoPD were incorporated into the belt compound to evaluate their impacts on curing characteristics, crosslink structure, physical-mechanical properties, heat build up performance, steel cord adhesion performance and dynamic mechanical properties. Additionally, density functional theory (DFT) calculations were utilized to analyze the frontier orbital energy levels of these additives, quantify their reactivity within rubber, and assess their anti-reversion performance.

The HOMO and LUMO orbital energy levels as well as the HOMO-LUMO Gap of NR (isoprene), BCDB and BCoPD were calculated using DFT. The results indicated that BCoPD exhibits higher reactivity with NR as shown in Figure 3. The compound test results indicated that both BCDB and BCoPD enhanced the maximum torque (M_H) of the natural rubber compound and extended the cure times (tc10 and tc90). Specifically, an equimolar amount of BCoPD exhibited higher M_H and longer tc10 and tc90 compared to BCDB. Equimolar BCDB resulted in lower R_{45} and R_{60} values. On the other hand, equimolar BCoPD led to a higher crosslink density (Xc), a greater proportion of polysulfide bonds, higher tensile strength, and lower heat build-up values and tan δ (at 60℃) for the vulcanized NR.

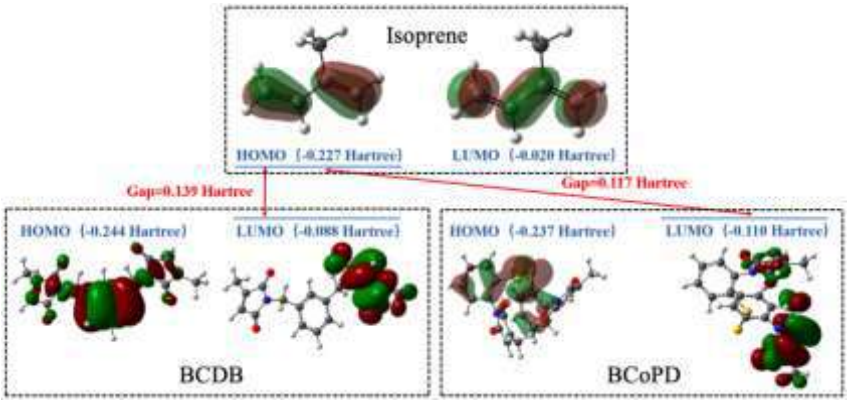


Figure 3. Frontier orbital energy levels of NR (isoprene), BCDB and BCoPD

Regarding the T-pull adhesion force of the belt compound (under conditions of unaged, heat aging, and moisture-heat aging), it initially increased and then decreased with increasing dosage of BCDB and BCoPD. Overall, BCoPD demonstrated higher T-pull adhesion strength than BCDB. Further investigation is needed to understand the decline in aged adhesion properties with increasing amounts of BCDB and BCoPD.

Acknowledgement

This research was successfully completed with the strong support of Professor Chen Zhaohui and his team from South China University of Technology. We are grateful for their contributions and assistance.

References

1. Bertelsen C. M., *Rubber-to-metal bonding: An investigation of chemical reactions and adhesion at the interface*, 2001.
2. Ignatz-Hoover F., To B., Terrill E., *Rubber World,* 2009; 32: 37.
3. Poh B. T., Kwok C. P., Lim G. H., *European Polymer Journal*, 1995, 223: 226.

Carbon Black Coupling Agents for Improved Fuel Efficiency of Tyres

M. J. J. Dixey[1], J. J. C. BUSFIELD[1]

[1] *School of Engineering and Materials Science, Queen Mary University of London, London, United Kingdom.*

e-mail address of the presenting author (m.dixey@qmul.ac.uk)

Keywords: Carbon Black, Reinforcement, Coupling Agent, Tyres, Fuel Efficiency

Carbon black coupling agents are molecules designed to increase the rubber-filler interaction. This is an especially important mechanism in the context of car tyres. Car tyre compounds containing carbon black suffer from hysteresis loss at low strains which presents itself as the Payne effect. This softening mechanism is responsible for increased rolling resistance and therefore increased fuel burn [1, 2]. To counteract this, formulators can take steps to stiffen compounds and reduce hysteretic loss. However, and according to the tyre 'magic triangle', an accompanying reduction in wet grip can be expected [3]. According to Dannenberg's molecular slippage model, rubber molecules are thought to undergo cyclic slippage across the carbon black filler under strain to yield the Payne effect [4]. This is a hysteretic mechanism and is therefore deleterious to fuel efficiency. The aforementioned carbon black coupling agents are designed to reduce this slippage and, like their silica-compatible silane analogs, are thought to reduce the Payne Effect by providing chemical linkages between the filler and the rubber molecules [1, 2, 3]. Figure 1 shows the structures of the coupling agents assessed. Both coupling agents bond to carbon black acid groups via an amine. One coupling agent (left) cross-links with the rubber during vulcanization via a sulfur moiety. The unsaturation in the other coupling agent (right) reacts with rubber chain free radicals which are formed as a result of chain scission during mixing [1].

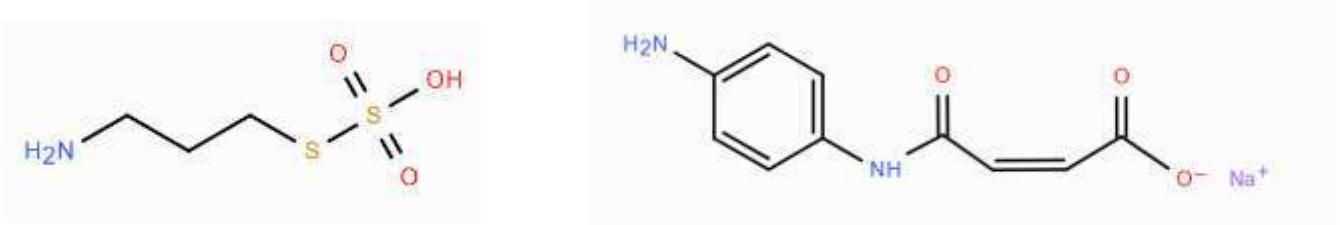


Figure 1. Molecular structures of assessed coupling agents

In the course of this work, various mechanical and mechanical-thermal testing methodologies have been and are being undertaken. In an initial stage, quasi-static cyclic stress-strain testing in tension was performed. The purpose of this testing was to calculate the hysteresis loss at specific strain levels. Figure 2 shows an example cyclic stress-strain curve produced with a control compound at a strain rate of $1s^{-1}$. The area encompassed by the hysteresis loop of the third cycle at each strain level is taken as the hysteresis area, which can be expressed in $J.m^{-3}$, and is an indicator of rolling resistance and wet grip. Dynamic Mechanical Analysis (DMA) in a shear sandwich configuration has also been undertaken to assess the effectiveness of the coupling agents in unvulcanized filled rubbers. A dynamic strain sweep from 0.01-10% at 1Hz and 34°C was utilized to assess the Payne effect (ΔG'). Figure 3 shows the characteristic Payne effect. The coupling agents in Compounds 2 and 3 show a reduction in the Payne effect relative to the control Compound 4. The reduction in $G'_{\gamma=0.01\%}$ for Compound 3 is thought to be as a result of improved dispersion reducing the filler-filler networking. The reason this does not occur with Compound 2, despite it also utilizing a coupling agent, is that some premature vulcanization may have occurred during mixing due to the presence of the sulfur. Future work will include DMA of vulcanized material to assess rolling

resistance and wet grip by reporting peak tan δ amplitude at 0°C and 70°C [5]. Chemical analysis methods such as bound rubber measurement and NMR will also be performed to characterise changes in the rubber-filler interaction.

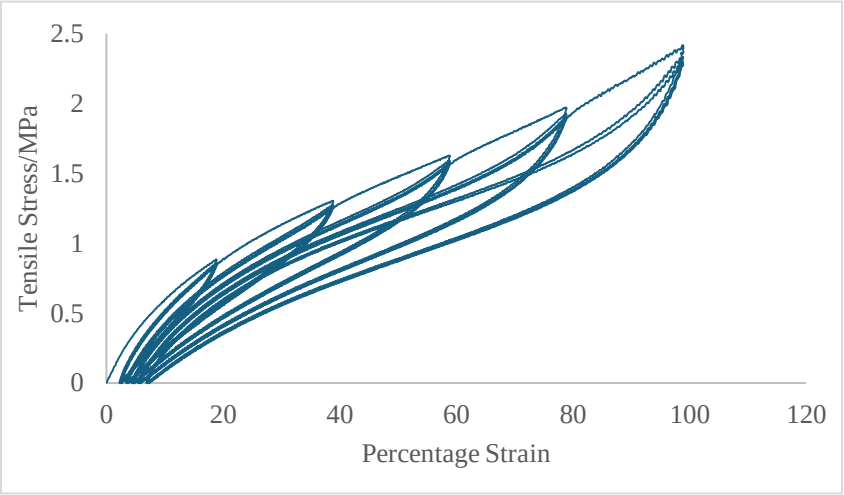


Figure 2. Quasi-static cyclic stress-strain testing of a model carbon black-filled car tyre rubber compound under tension

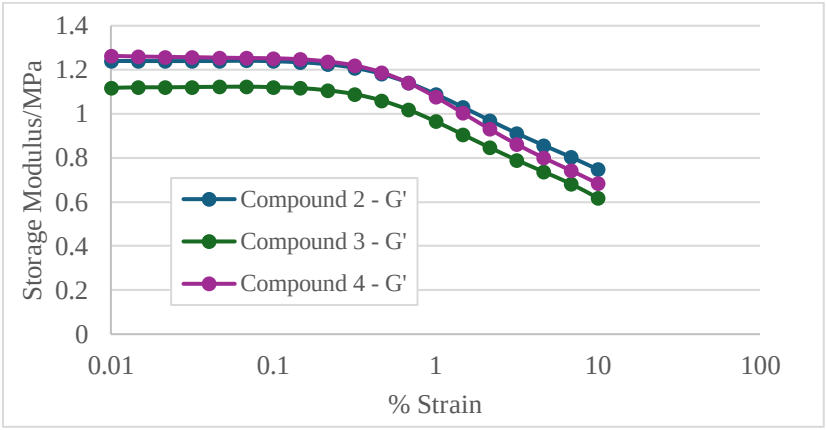


Figure 3. Effect of coupling agents on Payne effect as measured by Shear Sandwich DMA

Acknowledgement

The authors would like to express their gratitude to Continental AG who have kindly sponsored this project.

References

1. Uekita Y, Iyama H, Watanabe Y, Ozturk O. *Sumitomo Kagaki*, 2016
2. Chowdury S G, Pal K, Satpathi H, Bandyopadhyay A, Mukhopadhyay R, Bhattacharyya A, *Progress in Rubber, Plastics and Recycling Tech.*, 2019 1:17
3. Weng P, Tang Z, Guo B. *Polymer.*, 2020 190
4. Dannenberg E M, *Rubber Chemistry and Tech.*, 1975 48:3
5. Harris M, *https://www.tainstruments.com/applications-notes/sustainable-tire-rubber-a-comparison-of-silica-and-carbon-black-filled-tread-compounds-using-dma/*

International Rubber Conference 2025 (IRC2025)
1-3 December 2025 @ BITEC, Bangkok, Thailand

Experimental Analysis of the Mixing Behavior of Ethylene-Propylene-Diene Rubber (EPDM) in a Rubber Pin Extruder under Variation of Process Parameters and Mixing Elements

L. Schmidt[1], J. Petzke[1], D. Kleinschmidt[1], F. Bruening[1]

[1] *Kunststofftechnik Paderborn, Paderborn University, Warburger Straße 100, 33098 Paderborn, Germany*

jonas.petzke@ktp.uni-paderborn.de

Keywords: rubber extrusion, mixing, pin extruder, mixing section, ethylene-propylene-diene rubber (EPDM)

The rubber processing industry is increasingly confronted with challenges related to resource and energy efficiency in production. A major factor contributing to this issue is the inadequate mixing and poor homogeneity of rubber compounds during the extrusion process, which negatively affects the quality of the final products. In particular, both the thermal and material homogeneity of the compound at the die exit significantly influence the dimensional stability and uniform property distribution of the extrudate. Due to the highly viscous and multi-component nature of rubber compounds, achieving effective dispersive and distributive mixing in rubber extrusion is a non-trivial task. The current state of the art includes cold-fed pin extruders equipped with cylindrical pins that extend radially into the screw channel, continuously deforming and reorienting the rubber melt.

Given the high relevance of mixing quality in rubber extrusion, the topic has already been addressed in the literature. RÖTHERMEYER ET AL. [1] and KÖSTER ET AL. [2] described the fundamental mixing mechanisms in rubber extruders in their technical publications. Building on this, SUN ET AL. [3] conducted studies comparing the mixing behavior of extruders with and without pins. SCHÖPPNER ET AL. [4] and YAO ET AL. [5] further investigated mixing mechanisms in more detail, analyzing different rubber compounds under varying pin geometries.

This study focuses on the further analysis of the mixing behavior of a rubber compound based on ethylene–propylene–diene rubber (EPDM). The mixing quality is investigated under variation of key process parameters such as barrel and screw temperature, screw speed, and the screw design including the pin geometry. The latter is enabled by a modular screw equipped with an exchangeable screw tip.

Two identical EPDM compounds, pigmented in yellow and blue respectively, are used to assess mixing performance. The coloration allows for visual detection of the degree of mixing based on the formation of a green color upon blending. The compounds are simultaneously fed as strips into a cold-fed pin extruder from TROESTER GmbH & Co. KG (Hannover, Germany) with a 60 mm screw diameter. During the experiments, screw speeds of 10, 20, and 30 rpm as well as barrel and screw temperatures of 60 °C and 90 °C are tested. The screw consists of a base body with two flights and a pitch of 80 mm, configured with a conveying thread, and an exchangeable screw tip. Two tip designs are used: one with a pineapple mixing section and one with interrupted flights. Additionally, the diameter of the pins in the barrel (10 mm and 12 mm) is varied.

To analyze the mixing behavior, a steady-state extrusion process is first established. A “dead-stop” method is then applied, in which the extrusion is abruptly halted, and the compound is vulcanized in-situ along the entire screw length. The screw is then pushed out of the barrel, and the vulcanized rubber is unwound. Cross-sectional cuts and subsequent color analysis allow for evaluation of the material homogeneity along the screw. Furthermore, a temperature probe is installed downstream of the screw to assess the thermal homogeneity across the extrudate cross-section. In

addition to mixing quality, throughput is monitored over time to evaluate the economic efficiency of each process setting.

The results show that both process parameters – temperature and screw speed – as well as screw design and pin geometry have a significant influence on the material and thermal mixing quality of rubber extrudates. It was found that lower barrel and screw temperatures, due to the resulting higher viscosity and increased shear forces, lead to improved material mixing. A reduction in screw speed also has a positive effect on mixing quality, attributed to the formation of a low-viscosity boundary layer at high speeds, which promotes plug flow in the center of the channel and thus impairs mixing. Moreover, pin screw configurations were shown to provide superior mixing performance compared to the pineapple mixing section.

These findings offer new insights into the process design and control of cold-fed rubber extrusion. The knowledge generated in this study contributes to improving the efficiency and economic viability of the rubber processing industry by enhancing extrudate quality and minimizing waste.

Acknowledgement

The authors gratefully acknowledge the financial support provided by the German Aerospace Center (DLR) (IGF No. 01IF22861N). This research was funded by the Federal Ministry for Economic Affairs and Climate Action (BMWK). Furthermore, we would like to thank the companies represented in the project advisory committee for their valuable support and constructive collaboration.

References

1. Röthemeyer F, Sommer F, *Kautschuktechnologie*, 2013
2. Köster L, Perz H, Tsiwikis G, *Praxis der Kautschukextrusion*, 2007
3. Sun Y, Wang S, Huang S, Pan W, He Y, Jian R, *Polymers*, 2024; 16(13)
4. Schöppner V, Schadomsky M, Hopman C, Lemke F, *PROCEEDINGS OF PPS-31: The 31st International Conference of the Polymer Processing Society – Conference Papers*, 2015
5. Yao W, Takahashi K, Koyama K, Dai G, *Chemical Engineering Science*, 1997; 13: 21

Molecular chain structure changes and strain-induced crystallization behaviors during various deformation of segmented polyurethane elastomer

Kakeru Obayashi[1], Ken Kojio[2], Kenji Urayama[1]

[1] *Kyoto University, Nishikyo-ku, Kyoto 615-8510, Japan.*

[2] *Kyushu University, 744 Motooka, Nishi-ku, Fukuoka 819-0395, Japan.*

Obayashi.kakeru.8j@kyoto-u.ac.jp

Keywords: Polyurethane, Biaxial deformation, Microphase-separated structure, Strain-induced crystallization

Introduction

Uniaxial stretching deformation test is often used to evaluate the mechanical properties of polymer materials. However, not only uniaxial deformation but also multiaxial one takes place in practical use. So that the evaluation of molecular chain structure during biaxial deformation is important. It has been reported that strain-induced crystallization of natural rubber is hard to occur under biaxial deformation and, natural rubber does not crystallize under equi-biaxial deformation even at strain 3 [1]. Segmented polyurethane (SPU) has a multi-block structure and forms a microphase-separated structure. The hard segment (HS) domains work as physical cross-linking points. Since the cross-linking points are as large as several ten nm, the molecular chains between the cross-linking points easily might occur strain-induced crystallization even under multiaxial elongation. The purpose of this study is to clarify the changes in molecular chain structure and strain-induced crystallization behaviors of SPU using in situ small-angle X-ray scattering (SAXS) and wide-angle X-ray diffraction (WAXD) measurements during equi-biaxial deformation process.

Experimental

SPU with 25 wt% of HS contents was synthesized by a bulk one-shot method. Poly(oxytetramethylene) glycol (PTMG) was used as the soft segment (SS) component, and 4,4'-diphenylmethane diisocyanate and 1,4-butanediol were used for the HS one. The molecular chain structures of SPU film during equi-biaxial deformation process were analysed using in situ SAXS/WAXD measurements.

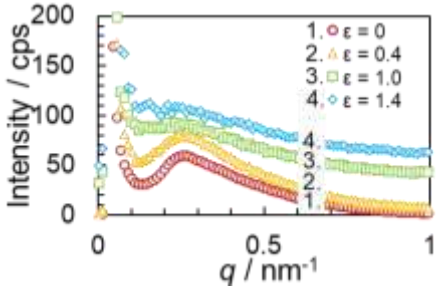


Figure 1. SAXS profiles of SPU during equi-biaxial deformation.

Results and discussion

Figure 1 shows SAXS profiles of SPU during equi-biaxial deformation. In the initial state, a broad peak was observed. This peak can be assigned to the spacing of isolated HS domains surrounded by a SS matrix. As the strain increased, the peak position slightly shifted to the high *q* region. This suggests the HS domain spacing, which corresponds to the distance between physical cross-linking points, decreased with strain increasing. Figure 2 shows (a) HS domain size and (b) HS domain spacing of SPU during equi-biaxial deformation. The HS domain size that was the size of physical cross-linking points, was calculated using a three-dimensional autocorrelation function. The HS domain

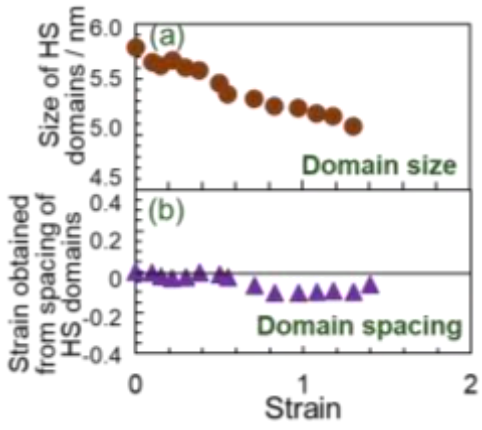


Figure 2. (a) HS domain size and (b) HS domain spacing of SPU during equi-biaxial deformation.

spacing were obtained from the Kratky plots of one-dimensional SAXS profiles. The HS domain size of SPU continued to decrease until broken. The HS domain spacing of SPU also decreased from strain 0.4. These results indicate that crush and break of the HS domains occurred with increasing strain.

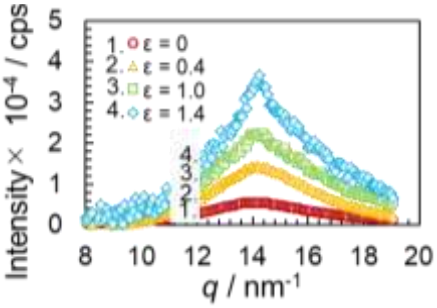


Figure 3. WAXD profiles of SPU during equi-biaxial deformation.

Figure 3 shows WAXD profiles of SPU during equi-biaxial deformation. A broad peak was observed at q = 14.0 nm^{-1} in the initial state. This peak is derived from the intermolecular chain distance. Although the crystallization peak was not clearly observed under biaxial deformation, the shape of the peak became slightly sharper at a strain (ε) ≥ 1. Moreover, the peak position was 14.3 nm^{-1}, which is consistent with the 020 peak position of the strain-induced crystallization of SS chains. These indicate that the diffraction peaks of strain-induced crystallization were overlapped the amorphous peak, and the strain-induced crystallization may occur even under biaxial deformation.

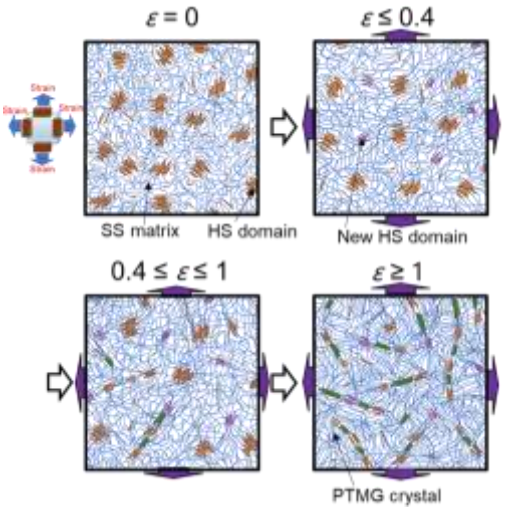


Figure 4. Schematic illustration of the molecular chain structure of SPU during equi-biaxial deformation.

Figure 4 shows schematic illustration of the molecular chain structure of SPU during equi-biaxial deformation. In the low strain region (ε < 0.4), the size and spacing of the HS domains decreased and remained constant. The microphase separation was induced and the formation of the HS domains progressed. In the region of 0.4 < ε < 1, the size and spacing of the HS domains decreased abruptly. Additionally, the crystallinity of the SS chains started to increase with strain. These results indicate that breakage of the HS domains occurred, microphase separation progressed, and the applied stress propagated well to the SS chains, which crystallized. Furthermore, it appeared that the orientation of the crystallized SS chains was random in the film plane. Since the size of the HS domains is within the 10 nm, the SS chains crystallized between the HS domains with the formation of bundles of extended PTMG chains. At the strain of ε > 1, both the size and spacing of the HS domains decreased with increasing strain. Moreover, the crystallinity of the SS chains increased, and the HS domain began to break above a strain 1. Unlike uniaxial deformation mode, in the case of equi-biaxial deformation mode of SPU, (1) "crush" of the HS domains occurred at strain around 0.4 and (2) strain induced crystallization occurred even for biaxial deformation mode.

Acknowledgement

This work was supported by JSPS KAKENHI (Grant Numbers 20H04640 and 24K01557), and JST PRESTO (JPMJPR2194), Japan. K.O. acknowledges the Kyushu University Support for Pioneering Research initiated by the Next Generation (SPRING; grant no. JPMJSP2136).

References

1. Chen X, Meng L, Zhang W, Ye K, Xie C, Wang D, Chen W, Nan M, Wang S, Li L, *ACS Appl. Mater. Interfaces*, 2019; *11* (50), 47535-47544.

International Rubber Conference 2025 (IRC2025)
1-3 December 2025 @ BITEC, Bangkok, Thailand

Study of the Mullins Effect in Carbon Black-Filled Rubber by Atomic Force Microscopy

Takahiro Anzai[1], Yuichi Aoyagi[1], Xiaobin Liang[2], Ken Nakajima[2]

[1]*NOK CORPORATION, 4-3-1 Tsujido-Shinmachi, Fujisawa-shi, Kanagawa-ken 251-0042 Japan*

[2]*Institute of Science Tokyo, 2-12-1 Ookayama, Meguro-ku, Tokyo 152-8550 Japan*

Anzai.13.Takahiro@jp.nokgrp.com

Keywords: Mullins effect, Cushion rubber, EPDM, Carbon black, In-situ AFM, Microstructure

INTRODUCTION

The spread of next-generation vehicles is progressing towards the realization of a low-carbon society. Cushion rubber is in high demand because it can fill gaps in electric vehicle batteries or other electric units, and it can control load during deformation. Therefore, it is necessary to understand the deformation characteristics of rubber. In a repeated tensile rubber test, a phenomenon occurs in which the second cycle shows a lower modulus of elasticity than the first cycle at the same strain. This phenomenon was investigated by Mullins et al.[1)] and is known as the "Mullins effect." Cushion rubber is used in an environment where repeated deformation occurs. Therefore, it is necessary to develop a rubber material which reduces the Mullins effect. On the other hand, the mechanism of the Mullins effect is not clear. Nakajima et al. are studying the microstructure of rubber by Atomic Force Microscopy (AFM)[2)]. However, it was very difficult to observe microstructural changes at the same position while stretching the rubber. Therefore, it was not possible to confirm which part and how the microstructure changed. In this study, in-situ AFM measurements were made of the same position while stretching the rubber by a specially designed compact tensile tester. Furthermore, the purpose of this study is to clarify the mechanism of the Mullins effect and to gain insights into the stress relaxation behavior and durability of rubber under repeated deformation. The findings obtained will directly contribute to improving the performance of not only cushion rubber but also a wide range of rubber products, such as automotive sealing materials, vibration-damping components, and insulating materials. In particular, if design guidelines for materials that reduce the Mullins effect can be established, it will be possible to enhance reliability and extend service life under cyclic loading conditions. This is expected to significantly contribute to the safety, comfort, and environmental compatibility of next-generation vehicles.

EXPERIMENTAL SECTION

Ethylene-Propylene-Diene terpolymer (EPDM) was used for the sample and carbon black was filled with 75phr. The rubber surfaces were cut on the side of the dumbbell test specimen using an ultramicrotome made by Leica Co., Ltd. It was set in a compact tensile tester, and microstructure were measured at each extension rate by AFM using a Bruker's Icon. Young's modulus was calculated by two-point JKR method.

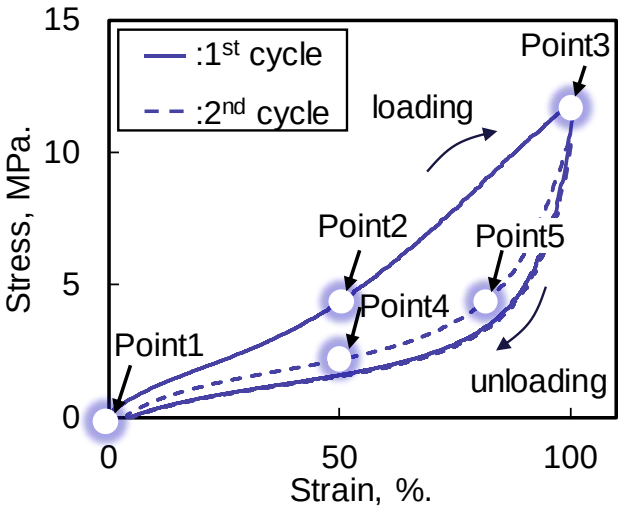


Figure 1. Stress-strain curves.

RESULTS AND DISCUSSION

AFM measurements were performed at each point in Fig. 1, and the results are shown in Fig. 2. Upon

stretching, regions with locally high Young's modulus were formed due to stress concentration. This is known as a "stress chain"[3]. Point 4 corresponds to a 50% stretch ratio in the second cycle, and the stress chain that had formed at Point 2 was found to have decreased. Point 5 was stretched to a stress level equivalent to that of Point 2, and a stress chain was observed at the same location as at Point 2. If the decrease in the stress chain at Point 4 were due to the breakage of molecular chains or the detachment of polymer chains from the filler surface, a stress chain should not reappear at the same location at Point 5 in Fig. 2. In other words, under the present experimental conditions, the results suggest that the decrease in stress is caused by local disentanglement of molecular chains, leading to a reduction in the stress chain. This is considered to be one of the primary factors contributing to the Mullins effect.

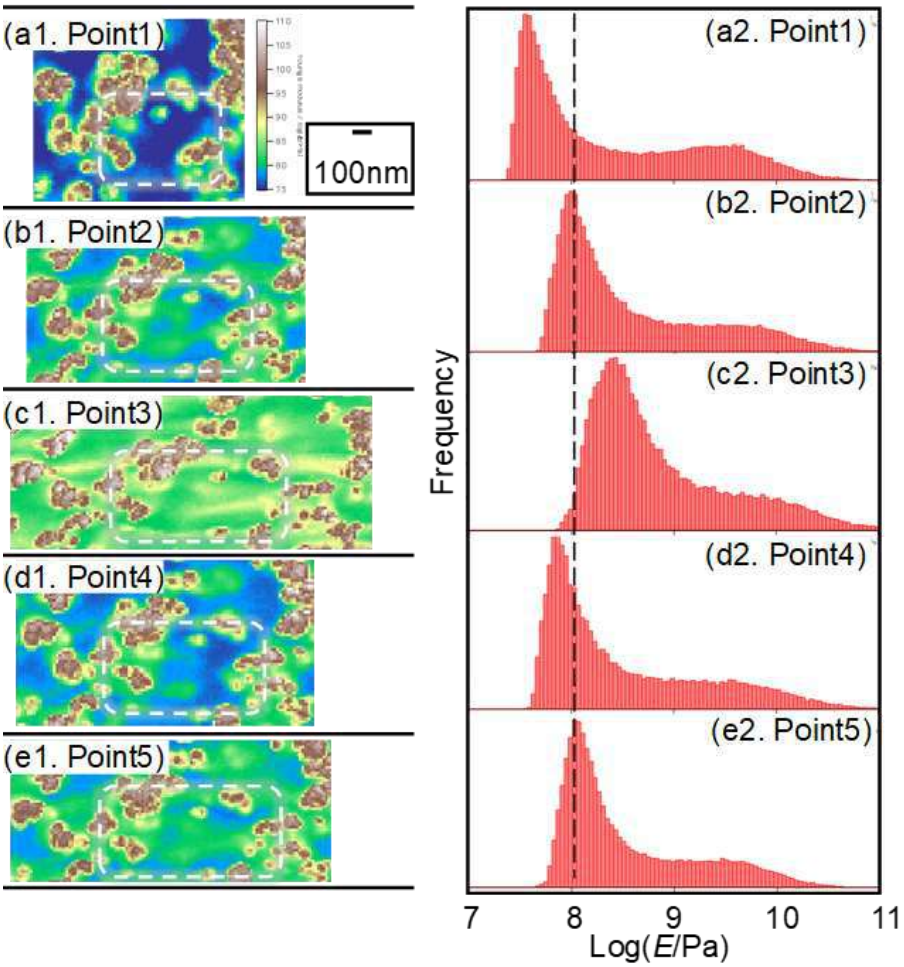


Figure 2. Young's modulus mapping and the corresponding histograms for 26.6 vol% CB/EPDM of (a1, a2) Point1, (b1, b2) Point2, (c1, c2) Point3, and (d1, d2) Point4. The stretching direction was crosswise in the Young's modulus mapping.

References

1) Mullins, L. *Rubber Chemistry and Technology*, **1969**, *42*, 339−362.

2) Xiaobin, Liang. Ken, Nakajima. *Macromolecules*, **2022**, *55*, 6023−6030.

3) Xiaobin, Liang. Makiko, Ito. Ken, Nakajima. *Polymers*, **2021**, *13*, 3922.

International Rubber Conference 2025 (IRC2025)
1-3 December 2025 @ BITEC, Bangkok, Thailand

Modelling of Elastomers under Dynamic Mechanical Loads

Michael Johlitz[1], Alexander Lion[1]

[1] *University of the Bundeswehr Munich, Werner-Heisenberg-Weg 39, 85579 Neubiberg, Germany.*

michael.johlitz@unibw.de

Keywords: Ageing, Modelling, Dynamic Material Properties

If elastomer components are exposed to heat and oxygen, as in internal combustion or electric engines, they age thermooxidatively and change their mechanical material properties over the course of their lifetime. This causes, for example, suspension and engine mounts to change both their static or elastic and their frequency-dependent dynamic transfer properties.

Based on original works of Arthur V. Tobolsky, the idea has been developed and manifested that during ageing at constant deformation the primary elastomer network degenerates and a secondary stress-free network evolves. Depending on how pronounced these two effects are, the elastomer can stiffen or soften during ageing.

In the past, the influence of thermooxidative ageing on the static or elastic material properties of elastomers has been very widely investigated experimentally and represented using material theory and continuum mechanics. There are considerably fewer studies on the influence of ageing on the frequency-dependent dynamic properties of elastomers. To the knowledge of the author, there are practically no studies in which this behaviour is modelled and simulated within the framework of continuum mechanics.

After a presentation of recent literature results related to the influence of ageing to the dynamic material properties of elastomers, a thermodynamical consistent continuum mechanical model is presented. It is able to depict the impact of chemical ageing on static and dynamic material properties of polymers. Both the parameters of the equilibrium stress as well as the elasticity parameters of the overstress and the relaxation times or viscosities can be formulated in dependence of ageing parameters. This model was motivated by a number of preliminary tests and showed qualitatively that it can describe the experimentally observed relationships.

This makes it now possible to describe the changes in the dynamic behaviour of elastomers caused by ageing. These changes usually cause the elastomer to stiffen and influence the frequency-dependent dynamic storage and loss modulus.

International Rubber Conference 2025 (IRC2025)
1-3 December 2025 @ BITEC, Bangkok, Thailand

New insights into Resins behavior: Influence of Resin Softening Point on the In-Rubber Properties of Carbon Black-Filled SBR Compounds

Pilar Bernal-Ortega[1], Frances van Elburg[1], Javier Araujo-Morera[1], Elif Uzun[1], Hubert Gojzewski[2], Anke Blume[1]

[1] *University of Twente, Faculty of Engineering Technology, Department of Mechanics of Solids, Surfaces & Systems (MS3), Chair of Elastomer Technology & Engineering, Enschede, The Netherlands*

[2] *2University of Twente, Faculty of Science and Technology, Department of Molecules & Materials, Sustainable Polymer Chemistry, Enschede, The Netherlands*

(j.a.araujomorera@utwente.nl)

Keywords: Resins, Softening Point, Rubber Compounding, Carbon Black, In-Rubber Properties

The growing demand for high-performance and environmentally sustainable products, combined with new restrictions on the use of aromatic oils, has driven the search of new ingredients as an alternative to traditional materials in the rubber industry. In this context, resins have raised significant attention, especially in the tire industry, as potential substitute for aromatic oils due to their plasticizing effect. In addition, resins are also frequently incorporated into tire formulation to improve wet traction performance. [1] However, despite their widespread application in the rubber industry, the behavior of resins in rubber compounds remains not fully understood. In particular, how their role changes with properties such as softening point (SP).

Resins are amorphous oligomers (200-4000 g/mol) derived from natural or petroleum-based monomers. They are characterized by their ability to modify the physical and mechanical properties of rubber compounds, acting as tackifiers, plasticizers, or reinforcing agents. Since resins are amorphous materials, they do not have a sharp melting point but a softening range. However, for practical purposes, the softening point (SP) is defined as a characteristic temperature withing this range at which the resin noticeably begins to soften and transition into a more flexible or tacky state. It significantly influences the processing and end-use performance of the rubber compound. [2-3]

This study explores the effect of the SP of resins on the in-rubber properties of Styrene Butadiene Rubber (SBR) compounds filled with N330 grade carbon black. Understanding the impact of the SP of resins on in-rubber properties is essential for selecting the most suitable resin for specific applications and optimizing its performance. Five Indene-Coumarone hydrocarbon resins (C9 type) with identical chemical bases but varying softening points (from 10 °C to 160 °C), were evaluated as a full replacement for Treated Distillate Aromatic Extracted (TDAE) oil. In-rubber properties analyzed included Mooney viscosity, cure behavior, Payne effect, Shore A hardness, stress-strain and dynamic properties. All results were compared to a TDAE oil-containing reference sample.

A comprehensive analysis shows that the SP of the hydrocarbon resins significantly influences the overall performance of the carbon black-filled SBR compounds. Low-SP resins exhibit Mooney viscosity values close to the reference, and show faster vulcanization kinetics compared to TDAE. In contrast, high-SP resins increase the Mooney viscosity values and delay the crosslinking reaction compared to TDAE reference. Mechanically, an increase in tensile strength and hardness is observed with increasing resin SP, behaving more and more like a secondary reinforcing filler within the rubber

matrix. All resin-containing samples show a significantly higher Payne effect compared to the TDAE reference, intensifying as the resin SP increases. This might be explained by poorer filler dispersion or the introduction of new interactions in the system due to the presence of the resin. [4] Dynamic Mechanical Analysis (DMA) reveals that increasing the resin SP leads to an increase in the glass transition temperature (T_g) of the rubber compound while the maximum peak of the loss factor (tan δ) decreases, indicating segmental mobility and damping behavior are reduced. Additionally, tan δ at both 0 °C and 60 °C, key indicators of wet traction and rolling resistance in tire performance, increases as the resin SP increases. Figure 1 summarizes the overall performance of the rubber compounds.

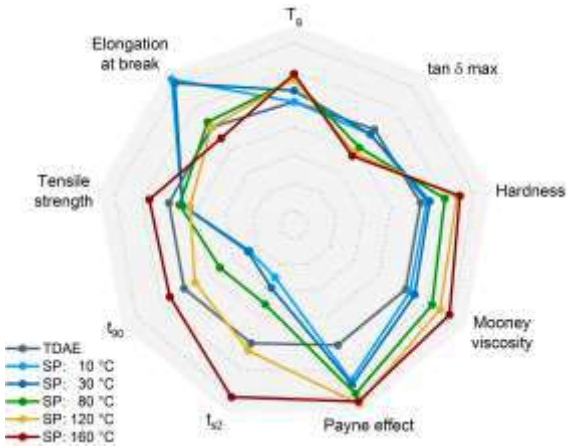


Figure 1. Overall performance of the studied rubber compounds

In conclusion, this study provides clear evidence that the softening point (SP) of resins critically determines their specific function within rubber compounds. Resins with lower SP act as a plasticizer enhancing the processability and molecular mobility, while resins with higher SP act as a reinforcing filler that enhance stiffness of the rubber compound. These findings provide a practical framework for tailoring the performance of rubber compounds through strategic resin selection. While this study was focused on one resin type and filler system, future studies should explore key characteristics such as the polarity, functional groups, and the overall behavior of different resins in silica-filled systems to broaden industrial applicability.

Acknowledgement

The authors thank Rain Carbon for kindly supplying the resins samples used in this study.

References

1. Shee B, Chanda J, Dasgupta M., Sen A. K, Bhattacharyya S. K, Das Gupta S, Mukhopadhyay, R, *J. Appl. Polym. Sci.*, 139.15 (2022): 51950.
2. Barlow F W, *Rubber compounding: principles, materials, and techniques.* CRC Press, 2018, 167-180.
3. Mildenberg R., Zander M., Collin G. *Hydrocarbon resins*. John Wiley & Sons, 2008, 41-73.
4. Bernal-Ortega P, van Elburg F, Araujo-Morera J, Gojzewski H, Blume A, *Polym. Testing*, 133 (2024): 108406.

Influences of Sulfur Vulcanization System and Curative Content on Properties of Tire Tread Compounds Filled with Carbon Black/Silica Hybrid Filler

Puchong THAPTONG[1], Pongdhorn SAE-OUI[1], Chakrit SIRISINHA[2]

[1] *MTEC, National Science and Technology Development Agency (NSTDA), 111 Thailand Science Park, Phahonyothin Road, Khlong Nueng, Khlong Luang, Pathum Thani, Thailand.*

[2] *Rubber Technology Research Centre, Faculty of Science, Mahidol University, Salaya Campus, Phutthamonthon 4 Road, Salaya, Nakhon Pathom, Thailand.*

(puchongt@mtec.or.th)

Keywords: Sulfur vulcanization system, Curative content, Tread, Properties

Tire tread plays a crucial role in overall tire performance. It not only functions to evacuate water to prevent hydroplaning, but also influences key performance aspects such as traction, fuel saving (FS), road noise, and service life. [1] Apart from tread pattern, tread compound has a significant impact on tire performance. Continuous efforts have been made to develop tread compounds providing excellent wet grip (WG), low rolling resistance, and high abrasion resistance, that aim to meet the performance requirements of modern vehicles, particularly electric vehicles. Among the various factors affecting tread compound performance, the vulcanization system plays an important role in determining the final performance of tire. Conventional vulcanization (CV), semi-efficient vulcanization (semi-EV), and efficient vulcanization (EV) systems differ primarily in the sulfur-to-accelerator ratio, which directly affects crosslink structure, [2] crosslink density, and consequently, tire performance. Therefore, the selection and optimization of the curing system and curative content to meet specific performance targets is a subject of considerable interest.

In this work, tire tread compounds filled with carbon black/silica (40/60) hybrid filler were studied. Two sulfur vulcanization systems, i.e., CV and semi-EV, were selected. For each system, the relative curative content (TBBS, TBzTD and sulfur) was varied from 100% to 140%. Comparison of mechanical properties, tire performance, and thermal ageing properties between the CV and semi-EV systems, at any given relative curative content, was discussed. The proper sulfur vulcanization system and relative curative content for balancing the tire performance and thermal ageing properties were also proposed.

The results showed that both scorch time (t_s1) and optimum cure time (t_c90) decreased with increasing relative curative content, while the cure rate index (CRI) tended to increase. Additionally, the CV system provided shorter t_s1 and t_c90, and a higher CRI, than the semi-EV system. As expected, the increase in relative curative content led to the enhanced crosslink density. At any given curative content, the CV system gave higher crosslink than the semi-EV system, attributed mainly to its greater sulfur content. Although hardness increased with increasing relative curative content, both tensile strength (TS) and elongation at break (EB) decreased. This reduction in TS is likely because the crosslink density exceeded the optimum level, leading to brittle behavior of the vulcanizates. [3] Surprisingly, the CV system demonstrated slightly lower TS than the semi-EV system despite the fact that CV system generally provides greater amount of polysulfidic linkages which enables crosslink exchange under stress. In this case, the brittle behavior from excessively high crosslink density might have overridden the crosslink structure effect. Furthermore, abrasion resistance improved with increasing relative curative content, with the semi-EV system showing slightly better resistance than

the CV system, possibly due to its greater strength mentioned earlier. Results also revealed that increasing relative curative content led to an improvement in WG and FS as indicated from tan δ at 0° and 60°, respectively. At any given relative curative content, the CV system showed better WG and FS than the semi-EV system. Both relative TS and relative EB after ageing at 100°C for 120 hours tended to decrease with increasing relative curative content, revealing the adverse effect on thermal ageing resistance. As expected, the semi-EV system provided better thermal ageing resistance than the CV system. No curative bloom was observed on the specimen surfaces of all compounds and vulcanizates.

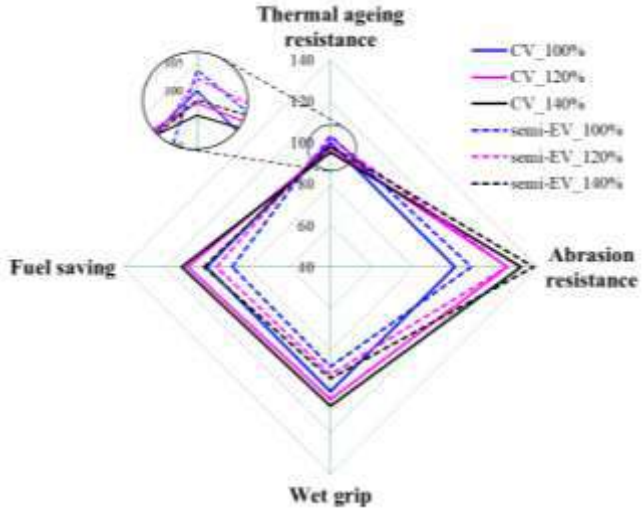


Figure 1. Normalized graph of tire performance and thermal ageing resistance at various relative curative contents and sulfur vulcanization systems

Based on the tread formulations in this study, the increased curative content resulted in the improvements of both CRI and crosslink density without causing curative bloom. While higher curative content caused negative effects on TS, EB, and thermal ageing resistance, it positively affected key tire performance aspects, i.e., WG, FS, and abrasion resistance. Compared to the semi-EV system, the CV system showed negative effects on TS, EB, abrasion resistance as well as thermal ageing resistance. However, it offered positive effects on WG and FS. Taken as a whole, the CV system with a relative curative content of 120% appears to offer a good balance between tire performance and thermal ageing resistance within the scope of this study.

Acknowledgement

Sincere appreciation is expressed to Thailand Research Fund (TRF) via Research and Researcher for Industries (RRi) and Siam Rubber Ltd., Part. for the financial support to this research (Grant No. PHD56I0074).

References

1. Giechaskiel B, Ferrarese C, Grigoratos T, *Vehicles*, 2025; 7(2): 29.
2. Kratina O, Pöschl M, Stoček R, *Polym. Degrad. Stab.*, 2024; 227: 110871.
3. Tavakoli M, Peyzari P, Tamaddon F, Zare-Banadkouki B, *Polym. Eng. Sci.*, 2025; 65(5): 2699-2713.

Aluminum Soaps: A New Prospect for Rubber Application

Xiaorong WANG[1,2]

[1] *School of Chemical Science and Engineering, Tongji University, Shanghai 200092, China.*

[2] *Center for Frontier Research & Technology, Hangzhou Zhongce Rubber Company, Zhejiang 310018, China.*

Email: xrwang@tongji.edu.cn

Keywords: Aluminum Soap, Additives, Filled Rubber, Rheological Behavior

The soaps commonly used in daily life are typically derived from metal carboxylates composed of elements from Groups 1 and 2 of the periodic table. These soaps are water-soluble due to their ionic nature, featuring a hydrophilic salt group at one end of the molecular structure and hydrophobic fatty hydrocarbon chains at the other—an arrangement that underpins their cleaning effect. However, elements from Groups 3 through 8 can also form metal soap compounds. Unlike sodium or potassium soaps, which rely on dissociable ionic bonds, these variants frequently involve covalent bonding and are generally insoluble in water but can dissolve in organic solvents. Notably, aluminum soaps demonstrate exceptional thickening capabilities: even a small quantity can elevate the viscosity of hydrocarbon solvents by several orders of magnitude and impart unique rheological properties.

In the rubber industry, wet traction and rolling resistance serve as critical metrics for tire manufacturing. When the car is driving on a road, the grip of the tire rubber will be greatly reduced due to the presence of water, which will affect the safety of driving. From a microscopic perspective, the key determinant of wet traction lies in the dynamic viscoelasticity of rubber materials. At this scale, anti-skid behavior arises from the frictional force resulting from energy losses during adhesion and deformation between rubber molecules and the road surface. This phenomenon, characterized by material hysteresis, occurs at vibration frequencies within the range of approximately 10^3-10^6 Hz. Rolling resistance, on the other hand, represents the energy required to maintain an entire tire rotation consistently over a road surface. The primary contributor to rolling resistance is also the hysteresis, occurring as the tire rolls through its footprint. Depending on rolling speed and temperature, the rolling resistance force also reflects the fraction of energy dissipated due to material hysteresis, however, at much lower frequencies, typically within the range of 10^{-1}-10^1 Hz. Optimizing the dynamic viscoelasticity of rubber is therefore a key strategy for simultaneously improving wet traction and minimizing rolling resistance in tire tread formulations.

Among the diverse metal soap compounds, aluminum soaps are poised to play an important role in the design and development of these rubber systems. Their appeal lies in their simplistic structure coupled with their great thickening ability. This combination allows them to modify and enhance the rheological properties of the rubber materials they are added to. Moreover, the synthesis methods for aluminum soaps of different structures are straightforward, typically involving reactions in aqueous solutions. These methods are not only easy to implement but also environmentally friendly, making aluminum soaps an attractive choice from a sustainability perspective. In addition, the use of multi-carboxylic acid compounds can synthesize aluminum-containing macromolecular polymers with linear and branched structures. Given these advantages, we anticipate that aluminum soaps will hold immense potential in future applications, particularly in tire rubbers.

In this presentation, I will outline the core findings from our decade-long research at Tongji University on aluminum soaps: a new frontier in rubber materials engineering. Our work has demonstrated that aluminum soaps with specifically tailored molecular architectures (as shown in several examples in Figure 1) can remarkably enhance tensile strength and mechanical resilience, while simultaneously reducing rolling resistance. These dual benefits not only support superior tire performance but also contribute to energy efficiency. We discovered that the thickening power of aluminum soap originates from the formation of spherical nanoparticles by soap molecules, which then aggregate into highly fractal networks in the dispersion medium. Remarkably, this nanoparticle formation occurs not only in small molecular organic media but also in long-chain macromolecular rubber matrices, such as styrene-butadiene rubber. Using aluminum soaps as an additive in rubber may reinforce the polymer matrix and offer rheological benefits in resulting rubber compounds. Furthermore, our team has explored the interplay between structural variations of aluminum soaps and their dispersion behavior in rubber matrices, revealing further opportunities for property tuning. These promising outcomes highlight the practical application potential of aluminum soaps of specially designed molecular structures in tread formulations.

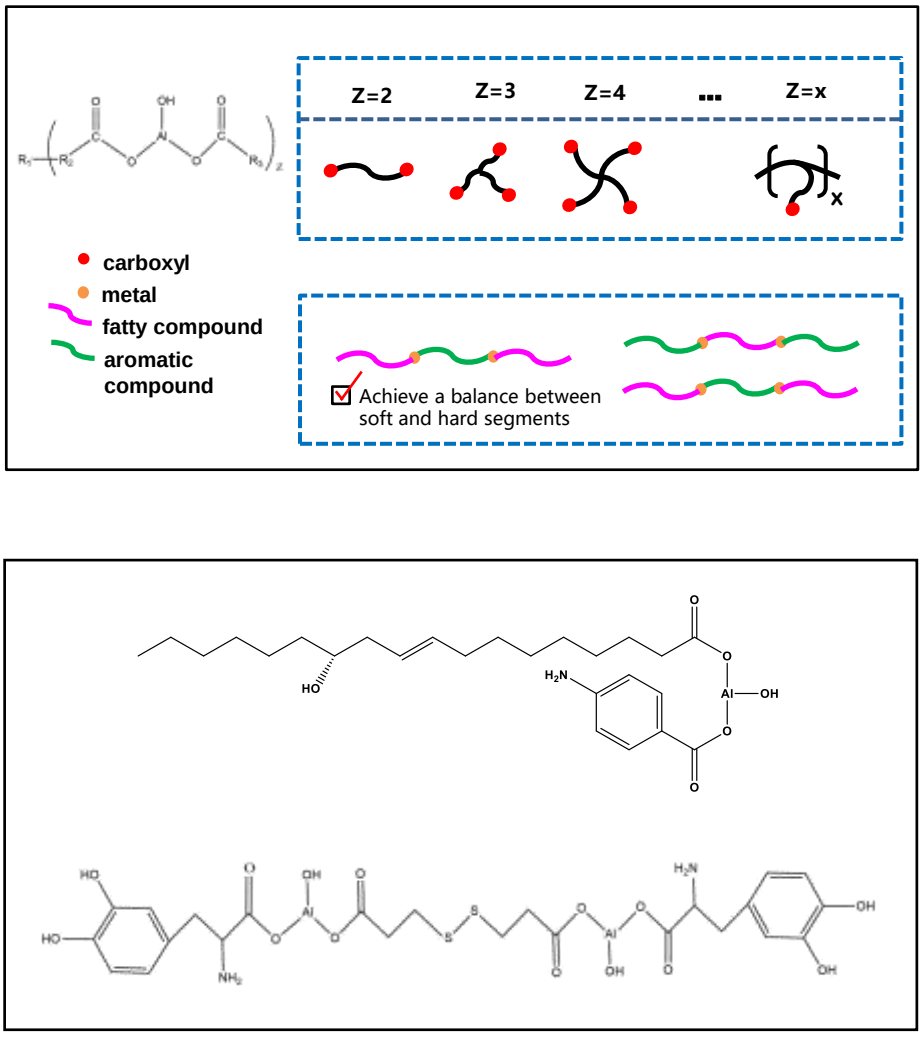


Figure 1. Structural Design of Aluminum Soap

International Rubber Conference 2025 (IRC2025)
1-3 December 2025 @ BITEC, Bangkok, Thailand

Inverse vulcanization forged self-motivated polysulfide silane: An ultra-efficient architect in engineering silica-rubber interface

Dong Wang, Zhenghai Tang*, Baochun Guo* and Liqun Zhang

Institute of Emergent Elastomers, School of Materials Science and Engineering, South China University of Technology, Guangzhou, China.

mszhtang@scut.edu.cn; psbcguo@scut.edu.cn

Keywords: inverse vulcanization • polysulfide silane • low hysteresis • interface engineering • composites

Incorporating sulfur-containing silane coupling agents (SSCAs) into silica-filled rubber composites is essential to improve the compatibility between silica and rubber matrix. However, the synthesis of conventional SSCA requires multi-step processes and organic solvent usage, and the silanization efficiency is rather low.[1-2]

In this talk, we presented the facile synthesis of a self-motivated polysulfide silane (PSTG, **Figure 1a**) via one-pot sequential inverse vulcanization of sulfur, methoxy polyethylene glycol acrylate (mPEG) and triethoxyvinylsilane (TEVS), and utilized it as a new-brand interfacial modifier for rubber composite. The successful synthesis of PSTG was confirmed by ^{1}H NMR and FTIR spectra (**Figure 1b and 1c**).

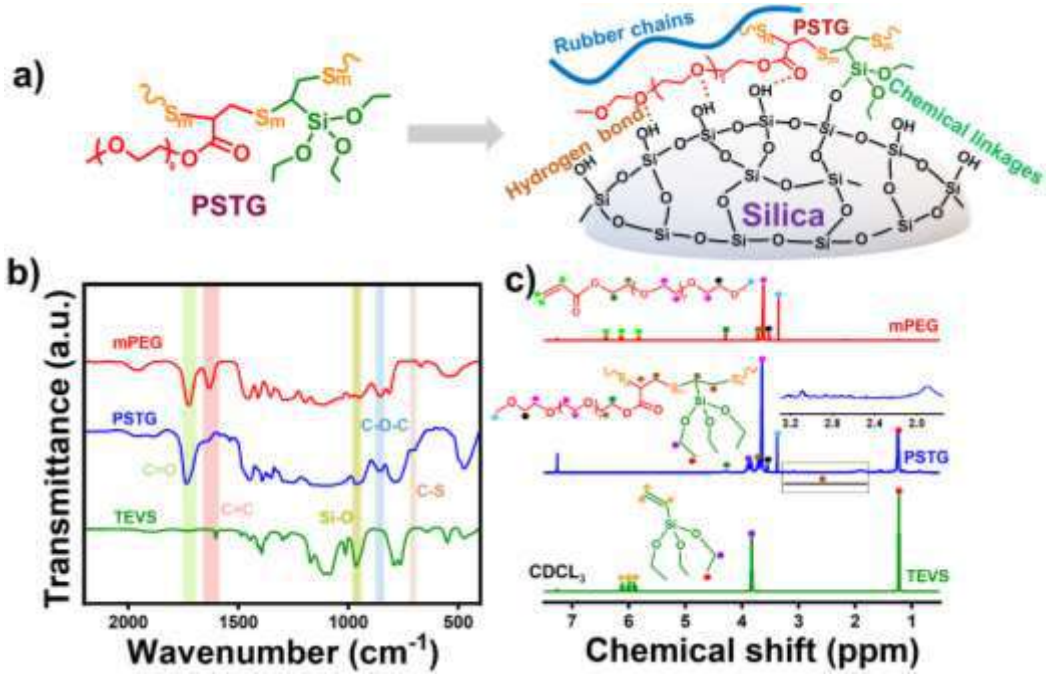


Figure 1. (a) Scheme illustration for the structure of PSTG and the proposed coupling mechanism. (b) FTIR spectra and (c) ^{1}H NMR spectra of mPEG, TEVS and PSTG.

In the tailored PSTG, the polyethylene glycol chains direct ethoxysilyl groups onto silica surface via hydrogen bond and subsequently promote the silanization reaction, and the polysulfide fragments couple with rubber chains during vulcanization (**Figure 1a**). As a result, the incorporation of PSTG greatly strengthens interfacial interactions and improves silica dispersion in rubber composites, resulting in remarkably higher static-mechanical properties and lower hysteresis loss when compared to the most widely used SSCA bis[γ-(triethoxysilyl) propyl] tetrasulfide at the same ethoxysilyl group content.

Acknowledgement

This work was funded by the National Natural Science Foundation of China (52322303 and 52130305), the Guangdong Basic and Applied Basic Research Foundation (2023B1515020085). We thank USAXS Beamline BL10U1 at SSRF (Shanghai Synchrotron Radiation Facility, China) for providing the beamtime.

References

1. Wang D., Tang Z., Huang R., et al. *Macromolecules*, 2022; 55: 8485.
2. Wang D., Chen J., Tang Z., et al. *Macromolecules*, 2024; 57: 470.

Reverse molecular reconstruction for synthesizing high performance fluorinated polyurea elastomer

DONGHAN LI[1], WANGTONG LI[1], ZHAN LU[1]

[1] *Shenyang University of Chemical Technology and Liaoning Key Laboratory of Polymer Materials Application Technology, Shenyang, China.*

Presenting author : lidonghan@syuct.edu.cn

Keywords: Reverse molecular reconstruction, Synthesis, fluorinated polyurea elastomer

Polyurea (PUA) is a high-performance material featuring a urea-linked structure (–NH–CO–NH–) and microphase-separated morphology, which provide exceptional mechanical strength, chemical resistance, and thermal stability, rendering it highly versatile for various applications. Introducing 'fluorine' into the PUA backbone effectively reduces its surface free energy. Furthermore, neighboring fluorine atoms align along the carbon chain in a helical pattern, providing strong shielding and protection for the molecular chain. This integration preserves the original mechanical properties of PUA while imparting exceptional hydrophobic and oleophobic characteristics, corrosion resistance, weathering resilience, as well as flame retardancy [1]. Consequently, fluorinated polyurea (FPUA) as the advanced fluoropolymer is attracting more attention. However, how to synthesize a high performance fluorinated soft segment (amino-terminated low-molecular-weight fluoropolymer, ATLF) is a key problem. Compared to complex forward synthesis methods, such as the functional initiator method, iodine transfer polymerization (ITP) [2-3] etc., this study propose a reverse molecular reconstruction strategy to transform fluororubber into ATLF via controlled oxidative degradation and decarboxylation amination. The resulting ATLF exhibits a high fluorine content (＞ 65 mol%), and excellent thermal stability with a decomposition temperature (T_d) exceeding 250°C.

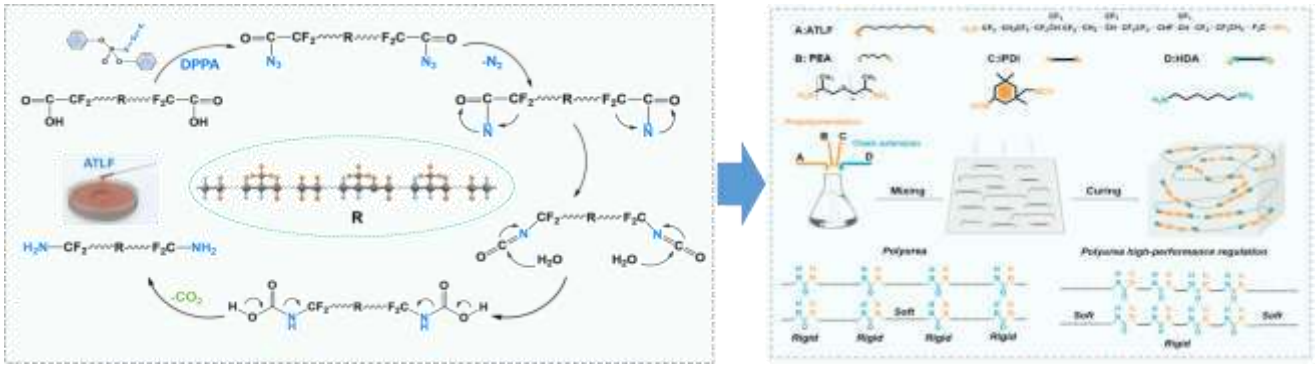
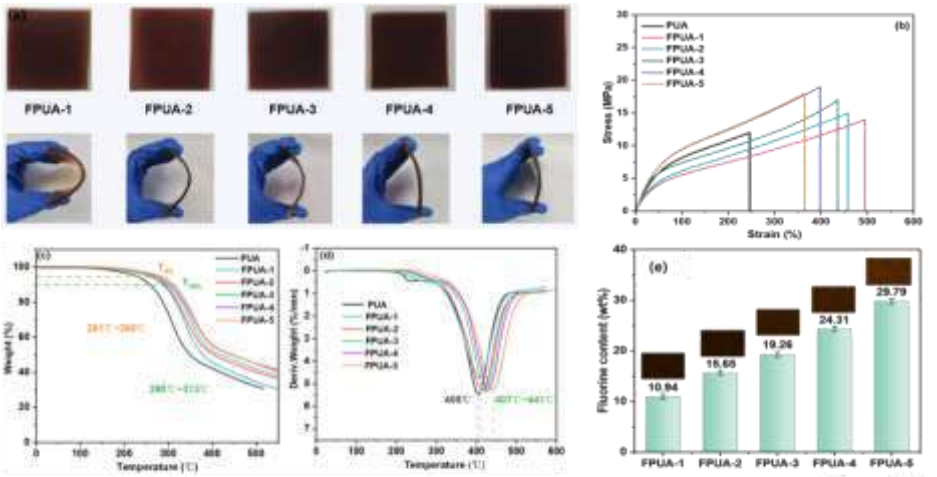


Figure 1. Synthesis mechanisms of ATLF and high-performance FPUA

Further, the synthesis of FPUA was carried out using the prepolymerization method, in which ATLF was employed as the first soft segment, poly(ether amine) D2000 (PEA) as the second soft segment, and isophorone diisocyanate (IPDI) coordinated with 1,6-hexanediamine (HDA) as the hard segment. The results show that compared to PUA, FPUA has superior thermal stability, mechanical properties, hydrophobicity, and chemical resistance, due to the introduction of high-energy C-F bonds and the inherently low surface energy of fluorocarbon compounds. The T_d of FPUA was higher than 260°C, with a tensile strength of up to 19MPa. Its hardness could be adjusted as required, and the water contact angle (WCA) reached up to 120°. In addition, the fluorine content of FPUA could be regulated within the range of 10~30 wt%, resulting in excellent hydrophobicity.



Sample	ATLF/mol	PEA/mol	HDA/mol	IPDI/mol
PUA	——	1.00	1.40	3.00
FPUA-1	1.00	1.00	1.16	3.95
FPUA-2	2.00	1.00	1.80	6.00
FPUA-3	3.00	1.00	2.80	8.50
FPUA-4	4.00	1.00	3.40	10.50
FPUA-5	5.00	1.00	4.00	12.50

Figure 2. (a) Effect of ATLF content on hardness of FPUA. (b) Effect of ATLF content on the mechanical properties of FPUA. (c) TGA thermograms of PUA and FPUAs. (d) DTG thermograms of PUA and FPUAs. (e) Effect of ATLF content on the fluorine content of FPUA. (f) AFM images of PUA and FPUA.

In summary, based on the 'reverse molecular reconstruction' strategy, this study demonstrates for the first time the mechanism by which the molecular chain structure of ATLF contributes to the improved overall performance of FPUA, thereby offering a theoretical foundation for designing high-performance FPUA materials.

Acknowledgement

This work was funded by the Youth talent support program of Liaoning Province (XLYC2203101); Natural Science Foundation of Liaoning Province (2023-MSLH-272); National Science Foundation Training Project for Excellent Young Scholars of SYUCT (2022YQ001).

References

1. Donghan L, Shurui N, Lu Y, Qinghong F, Hailan K, Long L, *Mater. Today Chem*, 2024; 42: 102382.
2. Donghan L, Shurui N, Lu Y, Fan J, Dawei Z, Qinghong F, Hailan K, Long L, *Adv.Mater*, 2025; 2501622.
3. Donghan L, Shurui N, Lu Y, Ping L, Qinghong F, Hailan K, Long L, Jia Y, *Adv.Sci*, 2025; 2501460.

Enhanced gas barrier properties of graphene oxide/rubber elastomer nanocomposites

Shipeng Wen[1], Long Zheng[1], Rui Zhang[1], Li Liu[1]

[1] *Beijing University of Chemical Technology, Beijing, China*

e-mail address of the presenting author (wensp@mail.buct.edu.cn)

Keywords: Graphene oxide, Rubber, Gas barrier

The high gas barrier property of an elastomer composite is of great significance for the application of tires and seals [1]. The complex filler network, crosslinking network, and strong covalent interfaces are the key factors in the formation of tortuous penetration paths for gas. Graphene oxide (GO) has been widely used in the elastomer composites due to its high reinforcing effect [2-4]. Notably, the large dimension of GO sheets leads to difficulties in gas/liquid penetration, making GO a suitable candidate for sealing composites.

In this research, different chemical modifications of GO and oriented GO structures were constructed to enhance the interfacial interactions and complex crosslinking networks. First, γ-mercaptopropyltriethoxysilane modified GO (MGO)/styrene-butadiene rubber (SBR) composites were prepared by the combination of the latex compounding method and thiol-ene click reaction [5]. Results showed the mercapto groups in MGO reacted with the vinyl groups in SBR molecules through thiol-ene click reaction during the crosslinking process at high temperature, thus forming strong chemical interactions at the interface in the form of GO-MPS-rubber and enhanced crosslinked networks. Meanwhile, the strong interface promoted the dispersion of MGO in SBR. The tensile strength and gas barrier properties of MGO/SBR composite improved by 19.0% and 37.5%, respectively, relative to the GO/SBR composite at 5 phr GO or RGO.

Second, sulfur-graphene oxide (S-GO) hybrids were prepared by in situ growth of sulfur on the surfaces of GO sheets [6]. The S-GO hybrids were also introduced into SBR using a green method of latex compounding. Results showed that sulfur melted and spread on the surface of the GO during the crosslinking process at high temperature. This process prevented the aggregation of GO and resulted in a fine dispersion of GO and complex filler networks in S-GO/SBR composites. More importantly, the sulfur particles on the GO surface not only aided the crosslinking of rubber molecules but also chemically reacted with the GO radicals generated at high temperature. This occurred by the homolytic cleavage of oxygen-containing groups, thereby constructing covalent interfaces between the GO and SBR molecules. Due to these strong interfaces and complex filler networks, the gas permeability coefficient of S-GO/SBR composites was decreased dramatically by 50.7% and 23.3% by comparison with that of pure SBR and GO/SBR composites, respectively.

Third, oriented layered filler networks in methyl vinyl silicone rubber (PDMS) composites were constructed to enhance their gas barrier properties [7]. GO was first functionalized by sodium dodecyl benzene sulfonate and cetyltrimethylammonium bromide to form amphiphilic GO (SCGO). Furthermore, SCGO and PDMS were mixed to form the water-in-oil type SCGO/PDMS Pickering emulsions. A porous PDMS masterbatch containing hollow SCGO shells was further obtained through freeze-drying the SCGO/PDMS Pickering emulsions. Following hot pressing, the hollow shells composed of SCGO sheets collapsed to form oriented filler networks within the PDMS

composites. When the content of SCGO was 3 phr, the gas barrier properties of SCGO/PDMS composites increased 85.7% relative to the pure PDMS. Meanwhile, the gas barrier properties of the SCGO/PDMS composites with oriented filler networks were 20–30% higher than those of the SCGO/PDMS composites with random filler networks at the same filler content.

The above researches provide a facile and effective method to design elastomer composites with high gas barrier used for tires, seals, packaging, and medical stoppers. Considering the processing complexity, scalability, and long-term stability, mercapto-functionalized GO/SBR composites are more easily fabricated at a large scale among the three composites. SCGO/PDMS composites are suitable for seals used in extreme low temperatures.

References

1. Guo B, Tang Z, Zhang L, *Prog Polym Sci*., 2016; 61: 29.
2. Yan N, Buonocore G, Lavorgna M, Kaciulis S, Balijepalli S K, Zhan Y Xia H, Ambrosio L, *Compos Sci Technol.*, 2014; 102: 74.
3. Song S H, Kim J M, Park K H, Lee D J, Kwon O S, Kim J, Yoon H, Chen X, RSC *Adv.*, 2015; 5: 81707.
4. Scherillo G, Lavorgna M, Buonocore G G, Zhan Y H, Xia H S, Mensitieri G, Ambrosio L, *ACS Appl Mater Interfaces*., 2014; 6: 2230.
5. Zheng L, Jerrams S, Su T, Xu Z, Zhang L, Liu L, Wen S, *Compos Part B-Eng.*, 2020; 197: 108186.
6. Zheng L, Jerrams S, Xu, Zhang L, Liu L, Wen S, *Chem Eng J*., 2020; 383: 123100.
7. Zhang R, Xu Z, Zheng L, Liu L, Wen S, Zhang L, *Polymer*., 2021; 235: 124273.

Regulating rubber-filler interface using functionalized polysulfides

Zhenghai Tang, Dong Wang, Ruoyan Huang, Baochun Guo, Liqun Zhang*

Institute of Emergent Elastomers, School of Materials Science and Engineering, South China University of Technology, Guangzhou 510640, China

*Email: mszhtang@scut.edu.cn

Abstract: The authors reported the synthesis of a series of functionalized polysulfides via inverse vulcanization strategy and used them as interfacial modifiers for rubber composites. Specially, amino, epoxy, and alkoxysilyl-functionalized polysulfides were synthesized by copolymerizing sulfur with functionalized comonomers. The coupling efficiency of the as-prepared polysulfides is prominent, remarkably improving filler dispersion and enhancing interfacial adhesion, which lead to significant decrease in the hysteresis loss of the rubber composites. By resolving the hierarchical structure across multiple length scales in the composites, the function mechanism of the functionalized polysulfides is disclosed, and the effects of molecular structure of polysulfides on the structures as well as quasi-static and dynamic mechanical properties of the composites are systematically investigated.

Reference

1. Ruoyan Huang, Dong Wang, Zhenghai Tang*, Baochun Guo*, Liqun Zhang*, Mediating Carbon Black-Natural Rubber Interface by Thioamide-Functionalized Polysulfide for Energy-Saving Composites, *J Mater Chem A*, 2025 DOI https://doi.org/10.1039/D5TA04129E
2. Senmao Yu, Zhenghai Tang, Dong Wang, Siwu Wu, Fei Chen, Baochun Guo* and Liqun Zhang, Reviving recovered carbon black as reinforcement for natural rubber by utilizing acylhydrazine-functionalized polysulfide as an intelligent interfacial modifier, *Polym Chem*, 2025, 16, 1949-1960
3. Senmao Yu, Zhenghai Tang*, Dong Wang, Baochun Guo*, Liqun Zhang, Toughening Rubber by in-situ Construction of Hierarchical Coordination Complexes with a Sulfur-Based Ionomer, *Macromolecules*, 2024, 57, 10120-10129
4. Dong Wang, Jialiang Chen, Zhenghai Tang*, Ruoyan Huang, Yilin Xiao, Jiadong Chen, Panchao Yin, Baochun Guo*, Liqun Zhang*, Exploring epoxy-functionalized polysulfide as a VOC-free and highly effective interfacial modifier for silica-filled rubber composites, Macromolecules, *Macromolecules* 2024, 57, 470-480
5. Dong Wang, Zhenghai Tang*, Ruoyan Huang, Yun Duan, Siwu Wu, Baochun Guo*, Liqun Zhang*, Interface Coupling in Rubber/Carbon Black Composites toward Superior Energy-Saving Capability Enabled by Amino-Functionalized Polysulfide, *Chem Mater*, 2023, 35, 764-772.
6. Dong Wang, Zhenghai Tang*, Ruoyan Huang, Haoming Li, Chengfeng Zhang, Baochun Guo*, Inverse Vulcanization of Vinytriethoxysilane: A Novel Interfacial Coupling Agent for Silica-filled Rubber Composites, *Macromolecules*, 2022, *55*, 8485

Optimization of Calcium Nitrate to Compounded Latex Solid Content for Energy Saving in Latex Thin Film Forming

Wirach Taweepreda[1], Sakorn Kaewthai[1,2]

[1] *Polymer Science Program, Division of Physical Science, Faculty of Science, Prince of Songkla University, Hat-Yai, Songkhla 90110, THAILAND.*

[2] *General Starch Limited, 3539 Rama 9 Soi 53, Phatthanakan Suan Luang, Bangkok 10250, THAILAND. .*

e-mail address of the presenting author (wirach.t@psu.ac.th)

Keywords: Latex Glove, Energy, Calcium Nitrate

The current practice of latex thin film forming is reducing compounded latex solid content by dilution with water as a cause of high energy consumption in drying process. Calcium nitrate is widely used in the dipping industry to produce gels of compounded latex on the 'formers' and was found that reduction of calcium nitrate content decrease the thickness of latex film without dilution of compound latex. In this study, the concentration of calcium nitrate and compounded latex solid content was optimized. The latex thin films forming on the ceramic former were characterization for film morphology using scanning electron microscopy (SEM). The physical properties of latex thin film are found to meet the requirements of ASTM D-3578-05 for natural rubber examination gloves.

Table 1. Thickness of vulcanized natural latex film on various of calcium nitrate concentration.

% Calcium Nitrate	Solid Contents 25 %	Solid Contents 35 %	Solid Contents 45 %
2	0.092±0.007	0.111±0.011	0.135±0.007
4	0.112±0.005	0.136±0.005	0.185±0.009
8	0.130±0.005	0.175±0.007	0.241±0.008
16	0.152±0.007	0.208±0.008	0.283±0.011

The vulcanized film thickness was incresed with increasing calcium nitrate concentration as shown in table 1 and figure 1. Calcium nitrate as coagulant coated porcelain former is then dipped into the compound latex. The coagulant strength and the "soak" time in the latex will determine the thickness of the glove. When the correct thickness has been reached the former is withdrawn from the latex and is the newly formed glove is ready for leaching.

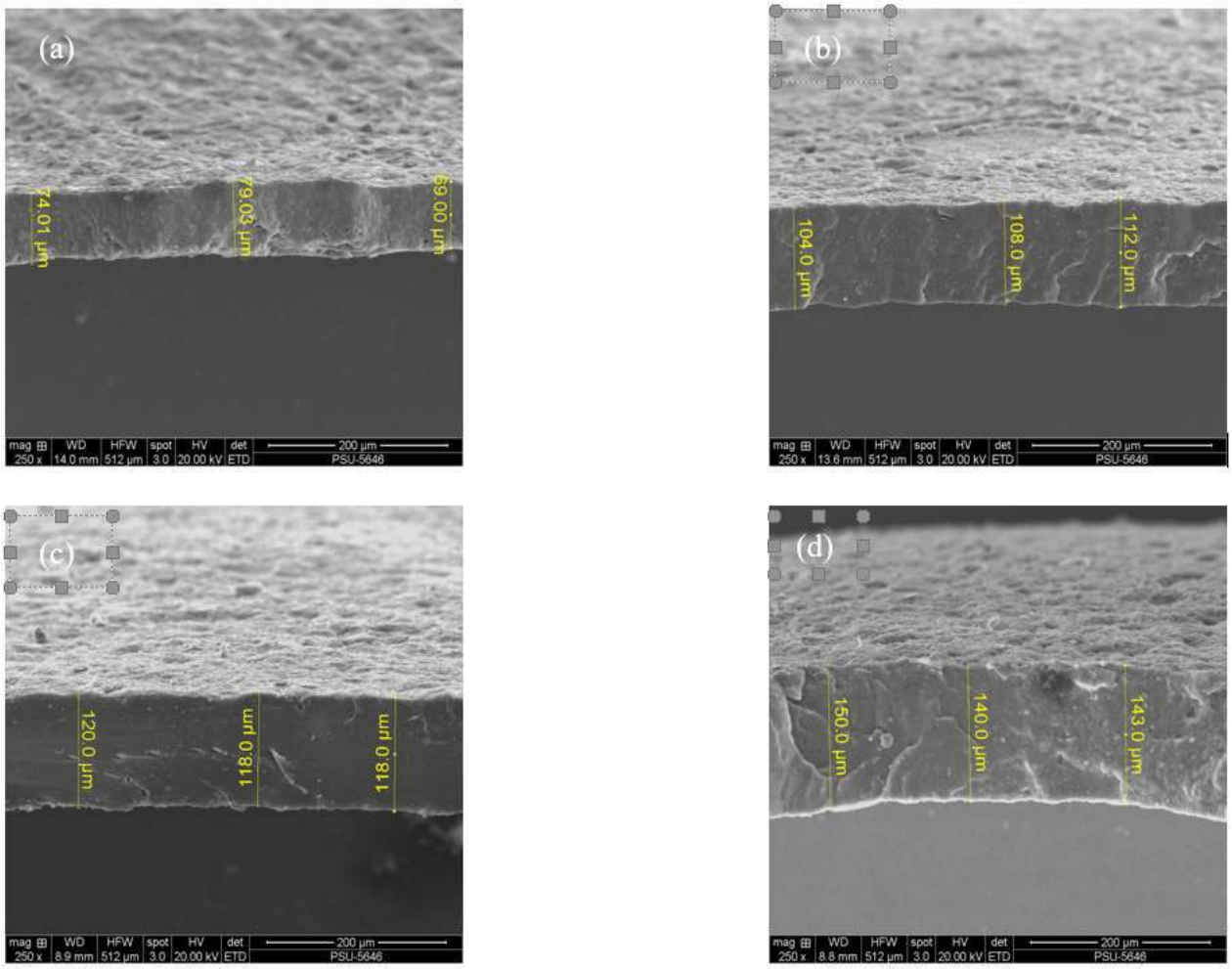


Figure 1. SEM images of vulcanized latex film cross-section by varying the calcium nitrated (N) concentration with solid content (SC) of compound latex (a) N2-SC25, (b) N4-SC25, (c) N8SC35, and (d) N16SC25.

References

1. S. Schlögl, M.-L. Trutschel, W. Chassé, I. Letofsky-Papst, R. Schaller, A. Holzner, G. Riess, W. Kern, K. Saalwächter, Photo-vulcanization using thiol-ene chemistry: Film formation, morphology and network characteristics of UV crosslinked rubber latices, Polymer, 55 (2014) 5584-5595.
2. M. Singh, J. Esquena, C. Solans, K. Booten, T.F. Tadros, Influence of hydrophobically modified inulin (INUTEC NRA) on the stability of vulcanized natural rubber latex, Colloids and Surfaces A: Physicochemical and Engineering Aspects, 451 (2014) 90-100.
3. P.R. Newswire, Medical Gloves Market: GCC Industry Analysis & Opportunity Assessment, 2016-2026, in: RPT-Medical-Gloves, Y, 2016.

Preparation and Characterization of Silica-Filled Modified Natural Rubber: A Comparative Analysis of Pre-dispersion and Conventional Techniques

D. ABDULRAMAN[1], P. SUNINTABOON[1], T. AMORNSAKCHAI[1], C. NAH[1,2], P. PHINYOCHEEP[1]

[1]Department of Chemistry, Faculty of Science, Mahidol University, Rama VI Rd., Payathai, Bangkok 10400, Thailand

[2]Department of Polymer-Nano Science and Technology, Jeonbuk National University, Jeonju 54896, Republic of Korea

(dalipraman.ab@gmail.com)

Keywords: Epoxide modified natural rubber, Silica-Rubber nanocomposite, Pre-dispersion method

Generally, incorporating high silica content into natural rubber (NR) leads to poor silica dispersion due to the polarity difference between the hydrophilic silica and the non-polar NR matrix. To overcome this incompatibility, modifying NR to have a higher polarity or adding a compatibilizer or a silane coupling agent can be implemented. Functionalization of NR into epoxidized NR was shown to enable the successful incorporation of high silica content (50 parts per hundred rubber, phr) using conventional mixing techniques [1]. A relatively low epoxide content (approximately 14 mol%) in the epoxidized NR without a silane coupling agent improved dispersion and interfacial interaction between the rubber matrix and silica filler, leading to superior mechanical properties compared to unmodified NR.

This study aims to develop mild and green conditions for incorporating high silica content in the modified natural rubber in latex stage without the use of a silane coupling agent. A small amount of polar group was introduced into the NR molecular structure via epoxidation reaction to enhance interactions with silica, thereby improving silica dispersion within the rubber matrix. A low degree of epoxide modified NR (5% epoxide content) (EMNR) latex was prepared by using a small amount of hydrogen peroxide and formic acid [2]. The EMNR latex was mixed with 40 phr silica prepared by pre-dispersion in water (EMNR/40SiP), compared with silica without pre-dispersion (EMNR/40Si) (see Figure 1), NR filled with untreated silica (NR/40Si) and NR with silica treated with bis-(3-triethoxysilylpropyl) tetrasulfide, TESPT (NR/40SiT).

The EMNR/40SiP latex was poured on a tray, followed by drying at 50 ^{o}C for 48 h, then compounded with curing agents by a two-roll mill. For conventional process, the EMNR latex was coagulated with methanol, washed with water, and dried, followed by mixing with silica and curing agents by a two-roll mill, designated as EMNR/40Si. The mechanical properties and tan δ at 60 °C of EMNR/40SiP were then compared with those of EMNR/40Si, NR/40Si, and NR/40SiT.

As shown in Table 1, EMNR/40SiP exhibited higher mechanical properties compared with EMNR/40Si, NR/40Si, and NR/40SiT. This properties' enhancement is attributed to strong interactions between silanol groups of silica and epoxide groups of EMNR, as well as an effective silica pre-dispersion method. Moreover, EMNR/40SiP showed a significantly low tan δ at 60 °C, indicating improved rolling resistance.

This study demonstrates that incorporating silica into modified natural rubber under mild and environmentally friendly conditions is feasible without the use of a silane coupling agent. By introducing a small amount of epoxide groups into the NR molecular structure and employing a pre-dispersion technique. These findings highlight the potential of the pre-dispersion approach,

combined with modified natural rubber at the latex stage, as a promising and environmentally friendly alternative for producing high-silica rubber composites — contributing to global warming mitigation efforts.

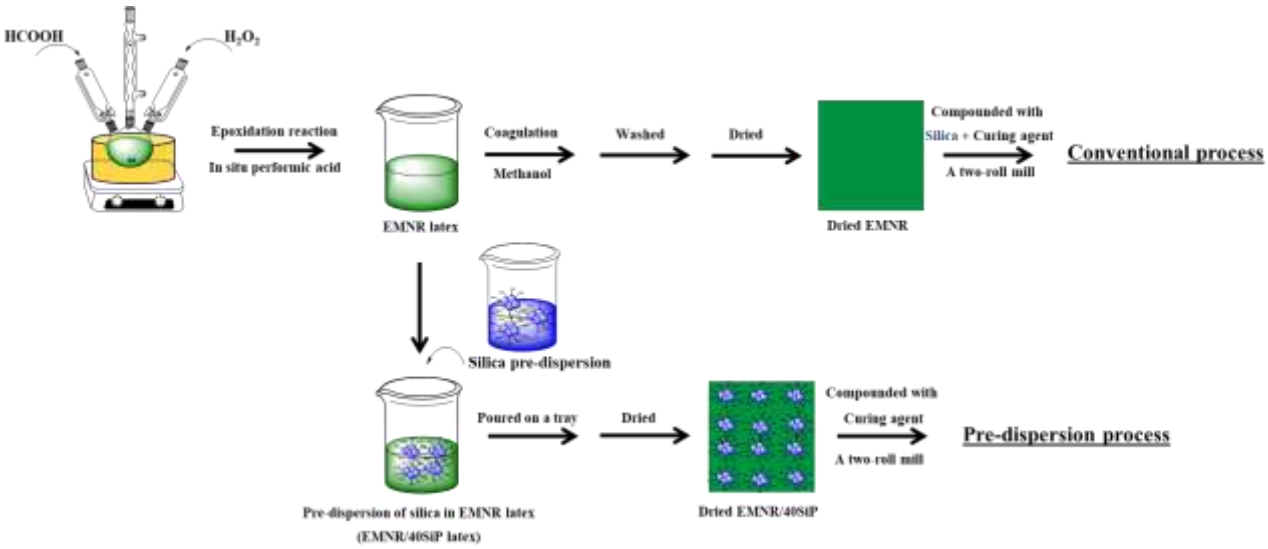


Figure 1. Diagram for preparation of EMNR filled with silica by pre-dispersion process compared with conventional process

Table 1. Mechanical properties and tan delta at 60 °C

Composites	Properties				
	100% Modulus (MPa)	Tensile strength (MPa)	Elongation at break (%)	Tear strength (MPa)	Tan delta at 60 °C
NR/40Si	1.09±0.07	10.19±0.95	557.72±17.85	35.75±0.01	0.0952
NR/40SiT	1.29±0.03	25.96±0.86	711.13±27.81	143.00±0.27	0.0458
EMNR/40Si	1.27±0.04	26.23±0.84	747.91±18.86	130.40±3.80	0.0801
EMNR/40SiP	1.37±0.04	31.26±0.50	771.41±15.50	151.78±0.90	0.0662

Acknowledgement

The authors thank the Department of Chemistry, and Rubber Technology Research Centre, Faculty of Science, Mahidol University for facilities and instruments in conducting this research.

References

1. Nuinu P, Sirisinha C, Suchiva K, Daniel P, Phinyocheep P, *J Mater Res Technol.*, 2023; 24: 2155-2168.
2. Tessanan W, Phinyocheep P, *Iranian Polymer Journal*, 2022; 31(4): 455-469

Life Cycle Assessment of End-of-Life Tire Management Pathways: A Comparative Study

Yogesh JADHAV[1], Sampatrao D MANJARE[2],

[1,2] *Advanced Sustainable Materials Lab, Department of Chemical Engineering, BITS Pilani, K. K. Birla Goa Campus, Zuarinagar, Goa, 403726, India.*

E-mail address of the presenting author (p20210100@goa.bits-pilani.ac.in)

Keywords: End-of-Life Tire, Life Cycle Assessment, Environmental Impact, Pyrolysis, Global warming

The End-of-Life Tire (ELT) management is major challenge in globe both environmentally and technically because of its complex composition and non-biodegradability. It is estimated that the annual generation of waste tire is approximately 1.5 billion worldwide contributing to the huge number of tires already placed in landfill and stockpiles [1]. Approximately, 4 billion ELTs are currently in stockpiles and landfills worldwide and it is expected to rise to 5 billion by 2030. When ELTs are disposed improperly in landfills, because of rainwater and runoff, it leaches the harmful chemicals such as heavy metals, organic compounds, and microplastics and creates better environments for harmful insects leading to soil and water pollution [2]. Proper ELT management, such as recycling and reuse, can reduce the reliance on incineration for disposal or landfilling [3].

This study presents a comprehensive Life Cycle Assessment (LCA) of various ELT management strategies, including incineration, pyrolysis (conventional and microwave), devulcanization, reclaim rubber production and ELT decontamination from 6PPD [4] to evaluate their environmental sustainability with selected impact categories. Using LCA Methodology, the evaluation was by midpoint impact categories like global warming potential, ozone layer depletion, acidification, photochemical ozone formation, terrestrial eutrophication and toxicity and endpoint categories human health, ecosystems and resources normalized to a functional unit of 1 kg of ELT processed.

Normalized to functional unit, in total 1.68 kg CO_2-eq. and 0.64 kg CO_2-eq. are emmitted from incinceration and conventional pyrolysis. The comparative results reveal that devulcanization and decontamination from 6PPD demonstrates consistently lower environmental impacts positioning those as a more sustainable alternative routes among others with reduction in 20%, 15% of kg CO_2-eq. respectively compared to incineration and conventional pyrolysis. Reclaim rubber production shows the reduction in global warming potential of 4.6% compared to conventional pyrolysis.

Findings from this study provide valuable insights for considering the sustainable process for ELT Management for particular application. The microwave assisted ELT decontamination from 6PPD is best sustainable alternative to other ELT Management pathways reducing approx. 20% of environmental burden whereas devulcanization stands the second considerable pathway with approx. 15% of environmental burden.

References

[1] I. Bianco, D. Panepinto, M. Zanetti, End-of-Life Tyres: Comparative Life Cycle Assessment of Treatment Scenarios, Applied Sciences 11 (2021) 3599. https://doi.org/10.3390/app11083599.

[2] A. Mohajerani, H. Kurmus, D. Conti, L. Cash, A. Semcesen, M. Abdurahman, M.T. Rahman, Environmental impacts and leachate analysis of waste rubber incorporated in construction and road materials: A review, Science of The Total Environment 835 (2022) 155269. https://doi.org/10.1016/j.scitotenv.2022.155269.

[3] D. Maga, V. Aryan, J. Blömer, A comparative life cycle assessment of tyre recycling using pyrolysis compared to conventional end-of-life pathways, Resour Conserv Recycl 199 (2023) 107255. https://doi.org/10.1016/j.resconrec.2023.107255.

[4] S. Najmi, P. Bhalode, M. Baker-Fales, B.C. Vance, E. Selvam, K. Yu, W. Zheng, D.G. Vlachos, End-of-life tire decontamination from 6PPD and upcycling, Nature Chemical Engineering 1 (2024) 597–607. https://doi.org/10.1038/s44286-024-00110-9.

Bridging Hydrophobic Silica Aerogels with Rubber Latexes via Hydrolysis-Resistant Slurry Design

Yanchun Han, Fangshuo Li, Feng Wang, Yongxin Duan, Boxiao Li, Jianming Zhang*

Key Laboratory of Rubber-Plastics, Ministry of Education/Shandong Provincial Key Laboratory of Rubber-plastics,

State Key Laboratory of Advanced Optical Polymer and Manufacturing Technology,

Qingdao University of Science and Technology, Qingdao, China.

hanyanchun02@163.com

Keywords: Silica aerogel, Rubber latex, Hydrophobic modification, Slurry, Aqueous stability

Silica aerogels (SAs) impart low density and excellent thermal insulation to polymer systems, yet incorporating hydrophobic SAs into aqueous rubber latex systems remains challenging due to their poor dispersibility and potential to destabilize the latex. Although previous studies have dispersed SAs in aqueous poly(vinyl alcohol) (PVA), the stability of such dispersions and their effectiveness as a bridging medium for latex integration have not been thoroughly evaluated, which limits practical application in latex compounding. This study systematically examines how surface chemistry governs hydrolytic stability, interfacial behavior, and latex compatibility in PVA-assisted aqueous processing. Two hydrophobic SAs were prepared, ethoxy-modified (E-SA) and methyl-modified (M-SA). Both initially form homogeneous PVA slurry, but E-SA rapidly hydrolyzes its surface $–OCH_2CH_3$ groups, releasing ethanol, becoming hydrophilic, and undergoing irreversible nanopore collapse. In contrast, M-SA maintains structural integrity and hydrophobicity because its $–Si(CH_3)_3$ groups are highly resistant to hydrolysis. This divergence dictates behavior during latex blending. Ethanol released from E-SA disrupts electrostatic and steric stabilization, inducing latex coagulation, whereas M-SA/PVA dispersions preserve colloidal stability across diverse latex systems. As a practical demonstration, M-SA-reinforced chlorosulfonated polyethylene (CSM) rubber latex composites show more than 50% reduction in thermal conductivity while maintaining chemical resistance, enabling high-performance insulating protective gloves and coatings. This work establishes a critical link between aerogel surface chemistry and aqueous processing stability, providing a mechanistic foundation for the rational design of water based rubber–silica aerogel composites and next-generation thermal insulation materials.

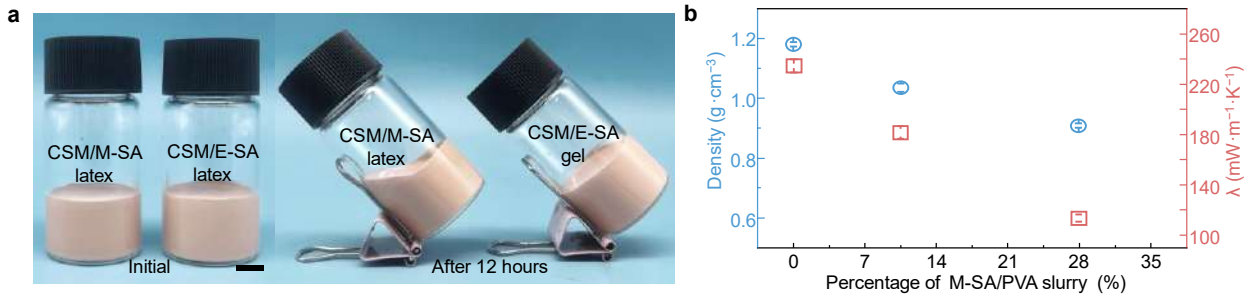


Figure 1. Compounding performance of CSM latex with E-SA/PVA and M-SA/PVA slurries, scale bar is 1cm

Acknowledgement

This work was supported by National Key Research and Development Program of China (2022YFC2603500, 2022YFC2603502), and Guangzhou Science and Technology Project (2024A04J4280). All the authors acknowledge this financial support.

References

1. Zhang J, Han Y, Zhang L, *Composites Science and Technology. J.*, 2024; 251: 110553.
2. Chen L, Li L, Zhang X, *Nature Communications. J.*, 2025; 16 (1): 2228.

Development of Carbon-Silica dual phase filler for Application in Tyre Rubber Compounds – A Cost-effective Material

Sampatrao D MANJARE[1], Chandresh DWIVEDI[1], Yogesh JADHAV[1], Ramakrishnan S[2], Tapas Ranjan MOHANTY[2]

[1]*Advanced Sustainable Materials Lab, Department of Chemical Engineering, BITS Pilani, K. K. Birla Goa Campus, Zuarinagar, Goa, 403726, India.*

[2]*Apollo Tyres Ltd., Global R&D Centre, Chennai, Tamil Nadu, 602118, India.*

E-mail address of the presenting author (manjare@goa.bits-pilani.ac.in)

Keywords: Carbon Black, Silica, Reinforcing filler, rubber, CSDPF, Pyrolysis

Reinforcing fillers, such as carbon black (CB) and silica, are indispensable for high-performance tyre compounds. CB enhances tensile strength, modulus, and abrasion resistance, whereas silica improves rolling resistance, wet grip, and ageing resistance. Combining them into a dual-phase filler (CSDPF) offers synergistic reinforcement by merging the conductive, high-structure characteristics of CB with the polar, energy-efficient features of silica. Conventional CSDPF production, however, remains complex, costly, and environmentally taxing. This study develops a cost-effective and sustainable CSDPF from end-of-life tyres (ELTs) via microwave pyrolysis and a novel flame-spray pyrolysis reactor, aiming to integrate circular resource recovery with simplified filler technology. Typically, carbon black–silica systems employ ratios between 40:60 and 60:40 to balance reinforcement and rolling resistance; this framework guided the design of the present formulation.

The produced CSDPFs, synthesised with 1–7 wt% silica incorporation, were used as partial replacements (57%) of conventional fillers, maintaining a constant total filler loading of 70 phr across all compounds. The control (R1) contained 40 phr N330 CB and 30 phr silica, while experimental formulations (E1–E3) replaced 40 phr CB with 40 phr CSDPF of varying compositions (1%, 3%, 5%, and 7% Si-CB). This approach isolated the effect of CSDPF composition without altering overall filler content. Incorporation of CSDPF improved rheological and mechanical behaviour: maximum torque rose from 13.82 dN·m (control) to 14.72 dN·m (5% CSDPF); tensile strength from 21.5 MPa to 23.1 MPa (7% CSDPF); modulus at 300% strain from 8.1 MPa to 11.5 MPa (5% CSDPF); and abrasion resistance by 30–40%, while rolling resistance index decreased to 91 at 3% CSDPF, indicating improved energy efficiency.

To substantiate its reinforcing capability, physicochemical characterisation was conducted. FTIR spectra confirmed dual-phase structure through C–H, C=O, and Si–OH/Si–O–Si bands, with silanol intensity rising alongside silica content. BET surface area (85–110 m^2/g) and DBP oil absorption (98-120 ml/100 g) demonstrated a well-developed aggregate network. Surface-free-energy analysis revealed balanced dispersive and polar components compared with pure CB and silica, ensuring improved compatibility with non-polar rubbers. Collectively, these features validate that CSDPF derived from ELTs can partially replace conventional fillers, deliver comparable or superior reinforcement while advance sustainability, cost reduction, and circular-economy integration for next-generation green tyre compounds.

Regeneration of Surface Sulfur Species on Pyrolysis Carbon Black

Ke Liu, Zejun Zhang, Jianming Zhang, Yongxin Duan*

Key Laboratory of Rubber-Plastics, Ministry of Education/Shandong Provincial Key Laboratory of Rubber-plastics, Qingdao University of Science and Technology, Qingdao, 266042

e-mail address of the presenting author (670192320@qq.com)

Keywords: Pyrolysis Carbon Black, Waste Tires, Rubber composites, Sulfur

Recovering pyrolysis carbon black (CBp) from waste tires provides a promising approach to conserving secondary resources and mitigating environmental hazards. However, the large particle size and high ash content of CBp, with the ash mainly consisting of ZnS and SiO_2, severely restrict its reinforcing capability [1-2]. In this work, we propose a low-cost and efficient strategy to completely convert surface ZnS into elemental sulfur, achieving the transformation of a harmful substance into a beneficial one. By exploiting the mild oxidizing property of H_2O_2 under weakly acidic conditions, ZnS was converted to elemental sulfur, while the average particle size of CBp was reduced from ~1900 nm to ~400 nm, accompanied by the removal of organosilicon impurities. Elemental sulfur increases the crosslink density in the rubber matrix, while the reduced particle size enhances the reinforcing ability of CBp, which contributes to improved mechanical properties such as tensile strength and wear resistance in the rubber. The formation of elemental sulfur was confirmed by X-ray photoelectron spectroscopy (XPS) and Raman spectroscopy. The upgraded CBp (CBp-H) exhibited significantly enhanced reinforcing performance in natural rubber (NR), with the mechanical properties of CBp-H/NR composites markedly surpassing those of commercial N660/NR composites. This study pioneers a novel, distinctive, and sustainable approach that facilitates the closed-loop recycling of waste tires and contributes to environmental sustainability.

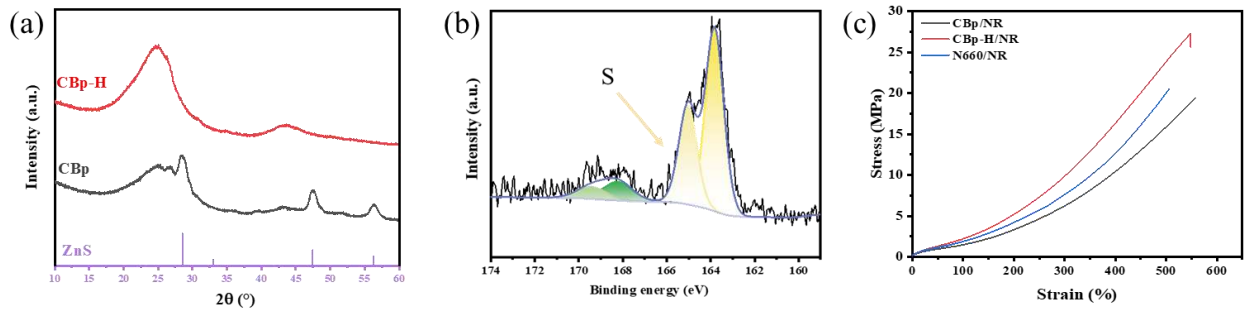


Figure 1. (a) The XRD patterns of CBp and CBp-H; (b) the high-resolution S 2p XPS spectrum of CBp-H; (c) representative stress–strain curves of natural rubber composites reinforced with CBp, N660 and CBp-H.

Acknowledgement

This work is supported by the National Key Research and Develop-ment Program of China (No. 2018YFC1902604) and Natural ScienceFoundation of Shan Dong province (2009ZRB019A4).

References

1. Jiang GS, Pan JQ, Deng WZ, Sun YZ, Guo J, *J. Clean. Prod.*, 2022; 374.
2. Liu K, Kong ZQ, Han YC, Zong L, Zhang JM, Duan YX, *J. Clean. Prod.*, 2024:482.

International Rubber Conference 2025 (IRC2025)
1-3 December 2025 @ BITEC, Bangkok, Thailand

How Microcapsule-enhanced Rubber Can Help Creating a Circular Economy

K. Filzer[1], K. Bandzierz[1,2], W. K. Dierkes[1], A. Blume[1], F. R. Wurm[1]

[1]*University of Twente, Drienerlolaan 5, 7522 NB Enschede, The Netherlands*

[3]*Apollo Tyres Global R&D B.V., Enschede, The Netherlands*

k.filzer@utwente.nl

Keywords: Devulcanization, Recycling, Microcapsules, Tires

A crucial part of rubber research is focused on recycling. This stems from the fact that only in the European Union alone, more than 300 million end-of-life tires are discarded each year.[1] However, those tire materials hold substantial value and should therefore be recycled and reused. Several devulcanization technologies have been developed, all based on a process in which a devulcanization agent (DA) is brought into the vulcanized material after its service life.[2] However, this poses a big challenge: How can the devulcanization agent be equally distributed within the rubber? A possible solution would be to bring in the DA already during the rubber mixing step, as at this stage, ingredients can be efficiently distributed within the elastomer matrix. However, the DA needs to be shielded during processing and service life, to avoid untimely degradation of the rubber product. Microcapsules could be a suitable tool to encapsulate the DA and protect it, as shown in thermoplastic materials, in order to distribute additives within the polymer matrix.[3] After its service life, the cargo of the microcapsules has to be released into the matrix. In the case of devulcanization of rubber, the DA will be released by breaking the microcapsules during the devulcanization step and thus will be able to devulcanize the rubber.

In this study, silica microcapsules were prepared by inverse miniemulsion according to an adjusted protocol of Jo et al., to obtain capsules of ~300 nm.[4] These microcapsules were loaded with DA (Figure 1) where the DA covers 13.5 wt% of the whole microcapsule. 20 phr microcapsules were then incorporated into 100 phr styrene-butadiene rubber (SBR). As a reference, empty microcapsules (without DA) were prepared in a similar manner and the same amount was incorporated into an SBR matrix. The incorporation of the capsules occurred during the standard rubber mixing process. It was shown in a previous study that the shear forces during mixing are not high enough to mechanically break the capsules.[5] Afterwards, the compounds were cured, granulated and devulcanized. Devulcanization was carried out in an internal mixer at 160 °C mixing temperature for 6 minutes in 66 g batches. The compound with loaded microcapsules was devulcanized without adding any further DA. The reference compound containing empty microcapsules was devulcanized with and without additional DA, both serving as references.

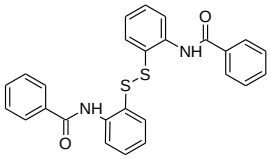


Figure 1. Chemical Structure of the used DA: 2,2′-Dibenzamido diphphenyl disulfide

A technique to determine the effectiveness of the devulcanization is the White Rubber Analysis:[2] The devulcanizate is blended with a white rubber compound in a 1:9 ratio (5g:45g). The part of the material which is fully devulcanized was blended homogenously with the white rubber,

while the insufficiently devulcanized part will be visible as black particles within the grey matrix. The results in Figure 2 indicate that the compound with microcapsules loaded with DA shows better devulcanization efficiency compared to the empty microcapsules with no DA present. This can be determined by more insufficiently devulcanized particles being visible for the compound with empty microcapsules compared to the others. When adding a DA before devulcanization to the compound with empty microcapsules, the properties of the devulcanizate are similar to the ones of the material with loaded microcapsules. This proves that the microcapsules can be mechanically broken through the shear forces during the devulcanization step, and that the DA is effectively set free.

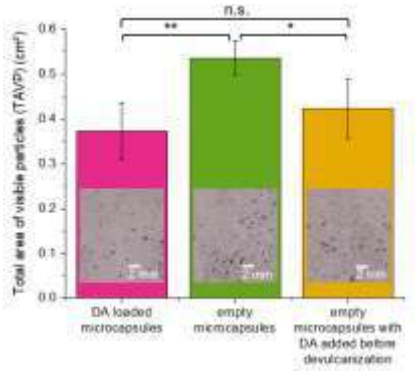


Figure 2. White rubber analysis results for compounds containing (left) DA loaded microcapsules, (middle) empty microcapsules, (right) empty microcapsules with DA added before devulcanization (a statistical analysis of the p-value is shown in the graph: *p < 0.05, **p < 0.01, n.s. = not significant).

This research provides valuable insights for the improvement of the devulcanization process using a DA shielded in a microcapsule. These microcapsules can effectively be dispersed during the rubber mixing step. This ensures that the DA can be homogenously distributed in the rubber before curing and is effectively shielded during processing of the rubber and service life of the tire. It was shown that the DA is released from the microcapsules during devulcanization and the effectiveness of this process is similar to the conventional process as shown by the white rubber analysis. This technology solves the problem of an inhomogeneous dispersion of the DA in vulcanized rubber.

Acknowledgement

The authors would like to express their gratitude to Apollo Tyres Global R&D B.V., Teijin Aramid and Evonik Operations GmbH for their support within this project.

References

1. Dabic-Miletic S, Simic V, Karagoz S, *Environ Sci Pollut Res*, 2021; 28: 68053.
2. Ghosh R, Mani C, Krafczyk R, Schnell R, Paasche A, Talma A, Blume A, Dierkes WK, *Polymers*. 2023; 15(13):2848.
3. Zhu X, Gojzewski H, Koshkina O, Wurm FR, *J. Chem. Eng.*, 2024; 491: 151903.
4. Jo SM, Jiang S, Graf R, Wurm FR, Landfester K, *Nanoscale*, 2020;12:24266-24272.
5. Filzer K, Bandzierz K, Blume A, Dierkes WK, Wurm FR, *Tire Technology Expo 2025* [conference presentation], 2025, March 3-5; Hannover, Germany.

International Rubber Conference 2025 (IRC2025)
1-3 December 2025 @ BITEC, Bangkok, Thailand

Chemical Degradation of End-of-life Tires

Heng Liu[1*], Chunyu Zhang, Xuequan Zhang,

[1] *School of Polymer Science and Engineering, Qingdao University of Science and Technology, Qingdao, China.*

hengliu@qust.edu.cn

Keywords: Degradation, waste tires, liquid rubber

Green recycling of end-of-life tires is of great significance for achieving the goal of carbon peaking and carbon neutrality.[1-2] In this study, a synergistic catalyst system of bis (cyclopentadienyl)zirconium dichloride/lithium aluminum hydride (Cp_2ZrCl_2/$LiAlH_4$) was designed to cleave the mainchain of polydiene rubber and de-crosslink of polysulfide bond, thereby achieving the chemical degradation of waste tires. It was found that such a system revealed extremely high efficiency in the degradation reaction, affording liquid polydiene rubber as final product in very short time. By adjusting the reaction temperature, catalyst equivalents, catalyst ratio, and other conditions, a series of liquid rubbers with different parameters (microstructure, chemical composition, molecular weight, and dispersity) can be obtained. Matrix-Assisted Laser Desorption/Ionization Time-of-Flight Mass Spectrometry (MALDI-TOF) analysis indicated that the recycled liquid rubber is mainly structured with *mono*-thiol functional group. Different types of polydiene based sulfur vulcanizates (polybutadiene rubber (PBR), styrene-butadiene rubber (SBR), polyisoprene rubber (IR), natural rubber (NR)) can be efficiently degraded to give liquid rubber products (LPBR, LSBR, LPIR, LNR). Additionally, all the recycled liquid rubbers, including LPBR, LPIP, LSBR, and LNR, can be further used as plasticizers to fill back into butadiene rubber and improve the processing performance of the rubber compound, affording vulcanizate with parallel mechanical properties to the commercial TDAE (treated distillate aromatic extract) involved counterpart. Furthermore, after degradation of waste tires, carbon black can also be recovered with a high efficiency (up to 83%), which is very similar to pristine carbon black in terms of morphology, size, and specific surface area. In general, the present system provides a *quasi*-closed-loop in upcycling end-of-life tires.

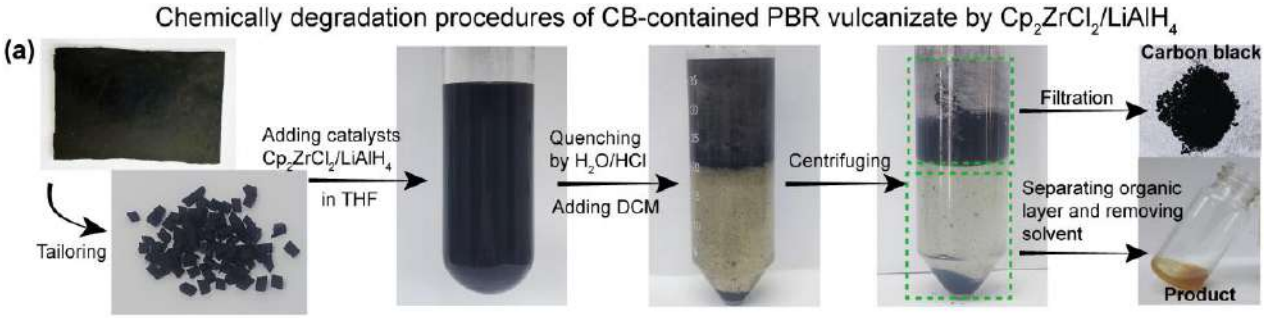


Figure 1. General procedures for chemical degradation of CB-contained polydiene vulcanizate by Cp_2ZrCl_2/LAH (reaction conditions: 0.535g PBR vulcanizate (0.0092 mol C=C bond), [Cp_2ZrCl_2]/[LAH]/[C=C] = 0.025/0.0/1, 60 °C, 20ml THF, 20 min).

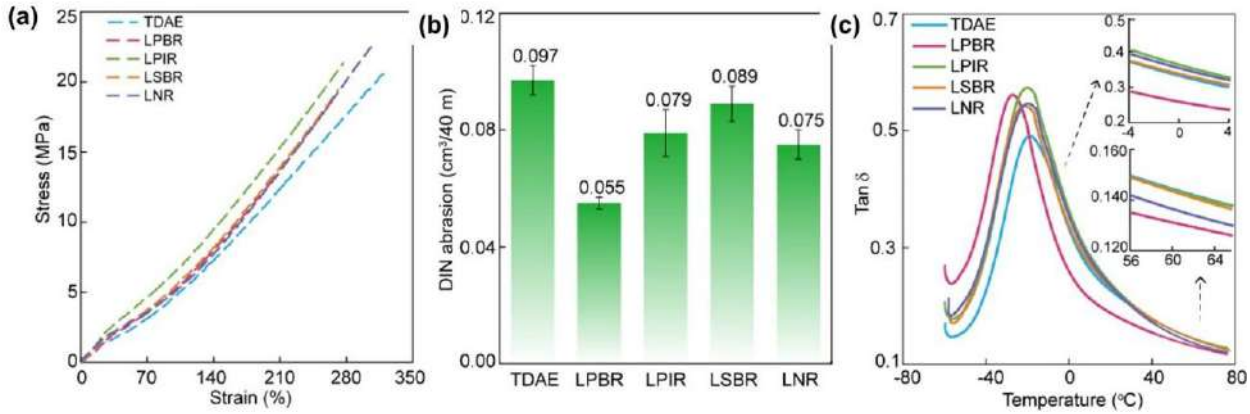


Figure 2. (a) Stress-strain curves of compounds containing TDAE oil and degraded LPRs. (b) DIN abrasion (volume loss) of compounds containing TDAE oil and degraded LPRs. (c) Tan δ−temperature curves of composites at 0.5% tensile strain.

Acknowledgement

This work was supported by National Natural Science Foundation of China (52573115), the project ZR2024ME117 supported by the Shandong Provincial Natural Science Foundation, and H.L. thanks to the Taishan Scholars Program (No. tsqn202211165) for the financial support.

References

1. S. Deng, R. Chen, S. Duan, Q. Jia, X. Hao, L. Zhang, *SusMat.* 2023, (3), 581–608.
2. G. Zhang, B. Guo, L. Zhang, *Macromolecules*, 2025, 58(12), 5883-5903.

International Rubber Conference 2025 (IRC2025)
1-3 December 2025 @ BITEC, Bangkok, Thailand

Thermo-Chemical Devulcanization of Sulfur-cured Styrene-Butadiene Rubber (SBR) Using Diphenyldisulfide (DPDS)

J. Petzke[1], D. Kleinschmidt[1], F. Bruening[1]

[1] *Kunststofftechnik Paderborn, Paderborn University, Warburger Straße 100, 33098 Paderborn, Germany*

jonas.petzke@ktp.uni-paderborn.de

Keywords: recycling, waste rubber, devulcanization, thermo-chemical, diphenyldisulphide

Recycling has gained significant importance in recent years due to the implementation of the European Union's Waste Framework Directive [1]. Global interest in the sustainable development of a resource-efficient circular economy, focused on reusing products that have reached the end of their life cycle, is continuously increasing. This trend is reflected in initiatives such as the policy recommendations of KreislaufwirtschaftPLUS [2]. To meet these demands, it is essential to develop new approaches that enable the recovery and reprocessing of raw materials from end-of-life products, facilitating their reintegration into the value chain. This is particularly relevant for the recycling of polymeric materials, especially elastomer waste. Due to their crosslinked structure and complex multi-component composition, elastomers pose a significant challenge for material recovery and remain insufficiently researched in this context.

In response to these challenges, numerous studies have investigated devulcanization, i.e., the cleavage of crosslinks between the polymer main chains, enabling subsequent reshaping. For instance, AOUDIA ET AL. [3] examined the devulcanization behavior of ground tire rubber (GTR) using microwave irradiation. SABZEKAR ET AL. [4] explored the use of chemical agents for selectively cleaving crosslinks in sulfur-cured natural rubber (NR), while GHOSH ET AL. [5] considered silane-based devulcanization strategies.

This study investigates the thermo-chemical devulcanization of a sulfur-cured styrene–butadiene rubber (SBR) compound, commonly used in passenger car tire formulations (GTR). Diphenyldisulfide (DPDS) is employed as the devulcanizing agent. The influence of DPDS concentration and process duration on the efficiency of the devulcanization process is systematically analyzed. The starting material is a granulated, crosslinked SBR-based GTR with particle sizes between 2.0 and 2.5 mm. The granules are dry-blended with 0, 5, and 10 wt% DPDS. Due to the melting point of DPDS (61 °C), the mixtures are preheated at 70 °C for 24 h in a circulating air oven to ensure adequate wetting of the rubber surface, which is expected to promote a more uniform reaction. The samples are then heated to a reaction temperature of 190 °C. At this temperature, thermal energy initiates the cleavage of sulfur bonds in both the GTR and the DPDS. The resulting DPDS radicals bind to the newly formed reactive sites in the rubber matrix, thereby preventing re-crosslinking. The mixtures are treated for varying durations of 5, 10, 15, 20, 25, 30, 35, 40 and 60 min.

Two methods are used to evaluate the degree of devulcanization. First, qualitative assessment is performed on a two-roll mill, where 10 g of each sample is passed 20 times through a 0.1 mm gap to form a thin sheet, allowing evaluation of plastic deformability. Second, a quantitative analysis is conducted based on ASTM D6814. After acetone extraction (24 h) and drying (70 °C, 24 h), the samples are swollen in 200 cm³ of toluene for 72 h. The swollen samples are weighed, dried again, and reweighed. The crosslink density v_e is calculated using the FLORY–REHNER equation (1):

$$v_e = \frac{-[\ln(1-V_r)+V_r+\chi_1 V_r^2]}{V_1\left(V_r^{\frac{1}{3}}-V_r\right)/2} \quad (1)$$

where V_r is the polymer volume fraction in the swollen state, χ_1 is the polymer–solvent interaction parameter, and V_1 is the molar volume of the solvent. The percentage degree of devulcanization is then determined by comparing the crosslink density of the devulcanized samples with that of the original, fully crosslinked GTR.

The results show that both DPDS concentration and treatment duration significantly influence the devulcanization efficiency. While extended treatment times enhance the devulcanization effect, increasing the DPDS content beyond a certain threshold does not yield further improvement, indicating an optimal concentration range. For example, starting from an initial crosslink density of 7.42×10^{-4} mol/cm^3, a treatment time of 5 min with 5 wt % DPDS led to a 33.6 % reduction, whereas 10 wt% resulted in only 17.4 %. The observed decrease in crosslink density may not be solely due to cleavage of crosslinking points but also to degradation of the polymer backbone. Although the bond dissociation energy of carbon–carbon bonds (348 kJ/mol) is significantly higher than that of carbon–sulfur (273 kJ/mol), disulfide (227 kJ/mol), or polysulfidic (251 kJ/mol) linkages, excessive energy input during thermo-chemical devulcanization can still cause C–C bond scission [6]. Further analysis of the sol–gel content is planned to evaluate backbone degradation.

These findings provide valuable insights into the recycling of sulfur-cured elastomers and contribute to the advancement of circular economy practices. The work supports the future reintegration of rubber waste, particularly from end-of-life tires, into the material cycle.

Acknowledgement

The authors gratefully acknowledge the financial support provided by the Federal Ministry for Research, Technology and Space (BMFTR). We also thank our project partners Gerlach Maschinenbau GmbH (Nettetal, Germany), Fricke und Mallah GmbH (Peine, Germany), and Zeppelin Systems GmbH (Friedrichshafen, Germany) for their excellent collaboration.

References

1. Bundesministerium für Umwelt; Naturschutz; Bau und Reaktorsicherheit (BMUB); Klimaschutzplan 2050 - Klimaschutzpolitische Grundsätze und Ziele der Bundesregierung, 2016
2. Bardow A, Bonten C, Carus M, Hopmann C, Lang R, Schopf M, Stapf D, Wilts H, Handlungsempfehlungen-Nationale-Kreislaufwirtschaftsstrategie, 2022,
3. Aoudia K, Azem S, Hocine N, Gratton M, Pettarin V, Seghar S, Recycling of waste tire rubber: Microwave devulcanization and incorporation in a thermoset resin, *Waste Management*, 2017; 471 – 481
4. Sabzekar M, Chenar M, Mortazavi Seyed, Kariminejad M, Asadi S, Zohuri G, Influence of process variables on chemical devulcanization of sulfur-cured natural rubber, *Polymer Degradation and Stability*, 2015; 88 – 95
5. Ghosh R, Mani C, Krafczyk R, Schnell R, Paasche A, Talma A, Blume A, Dierkes W, New Route of Tire Rubber Devulcanization Using Silanes, *Polymers*, 2023, 15, 2848. https://doi.org/10.3390/polym15132848
6. Ramarad S, Khalid M, Ratnam C, Luqman Chuah A, Rashmi W, Waste tire rubber in polymer blends: A review on the evolution, properties and future, *Progress in Material Science*, 2015, 72, 100 – 140. https://doi.org/10.1016/j.pmatsci.2015.02.004

Pyrolysis of Polychloroprene Rubber with Scavenger-Based HCl Neutralization

P. SRITHAVORN[1], J.J.C. BUSFIELD[1], R. VOLPE[1]

[1] *Intelligent Transport, School of Engineering and Materials Science, Queen Mary University of London, London, United Kingdom.*

j.busfield@qmul.ac.uk

Keywords: Pyrolysis, Polychloroprene rubber, HCl capture, Chlorine scavenger

Polychloroprene rubber (PCR) is widely used in industrial applications due to its excellent chemical resistance, mechanical strength, and long-term durability. However, its disposal presents environmental challenges, especially during pyrolysis, which releases hydrogen chloride (HCl) gas and produces harmful chlorinated compounds. Removing or capturing HCl is important to make PCR waste treatment more environmentally friendly. One promising solution is the use of solid scavengers. This study is designed to evaluate the performance of magnesium oxide (MgO), calcium oxide (CaO), and sodium hydroxide (NaOH) as reactive agents for HCl capture, and to estimate the optimal amount of each scavenger required.

Chlorine may be released as HCl gas, remain in the solid char, or form chlorinated compounds in the liquid phase (pyrolysis oil), so using only one detection method may give incomplete results [1]. Therefore, this study combines two techniques: (1) X-ray fluorescence (XRF) to measure residual chlorine in solid char, and (2) HCl sensors to detect real-time HCl gas release during pyrolysis. These two methods will help estimate the total HCl released and evaluate the scavenger's performance [2].

The experimental design involves preparing PCR particles (0.1–0.5 mm) blended with different sizes of MgO (20, 50 nm), CaO (150, 200 µm), and NaOH (150, 300 µm) at 50:50 and 60:40 ratios. Each setup will be pyrolyzed in a furnace: dried at 105 °C, heated to 300 °C and held for 1 hour, then ramped up to 600 °C and held for 2 hours. Chlorine capture is calculated using XRF data with the formula: Cl captured (%) = 100 – (Cl_{sample} × 100 / Cl_o) where Cl_o is the XRF peak height of Cl from the char of pure neoprene, and Cl_{sample} is the XRF peak height of Cl from the char of neoprene blended with scavenger.

For example, if the Cl peak drops from 1000 to 400 counts, this indicates that 60% of Cl was removed from the char, likely captured by scavengers such as MgO. Based on the equation: Cl captured = 100 - (40 × 100 / 1000) = 60%, this corresponds to a 60% Cl capture efficiency. It is estimated that 10 g of PCR would release approximately 0.105 mol of HCl, based on the chemical structure of polychloroprene. This estimate derives from the chlorine content in the monomer unit (C_4H_5Cl), which contains 38.4% Cl by weight, giving 3.84 g of Cl in 10 g of PCR (10 g × 38.4%). With 60% capture efficiency, the actual amount of HCl captured is 0.063 mol (0.105 mol × 60%). According to the stoichiometric reaction ($MgO + 2HCl \rightarrow MgCl_2 + H_2O$), 1 mol of MgO neutralizes 2 mol of HCl. Therefore, 0.0315 mol (1.27 g) of MgO would be required to fully react with the captured HCl.

This study investigates the influence of surface area and agglomeration on the HCl capture performance of nanosized MgO, in comparison with CaO and NaOH. Nanosized MgO (20–50 nm) offers a high surface area, providing more active sites for HCl to react, potentially enhancing capture efficiency. However, its high surface energy can lead to particle agglomeration, reducing the effective surface area and limiting contact with HCl gas, especially if dispersion in the rubber matrix is poor. In contrast, micron-sized CaO (150–200 μm) has a lower surface area but remains highly reactive and is less prone to agglomeration. NaOH is highly reactive with HCl, but its nanosized form is hygroscopic, sticky, and corrosive, making it difficult to handle in pyrolysis systems. Micron-sized NaOH is easier to manage but may react less uniformly if not well dispersed. By comparing these scavengers, this study aims to identify the most suitable option for PCR pyrolysis and contribute to the development of safer, more efficient waste treatment strategies for chlorinated rubber materials.

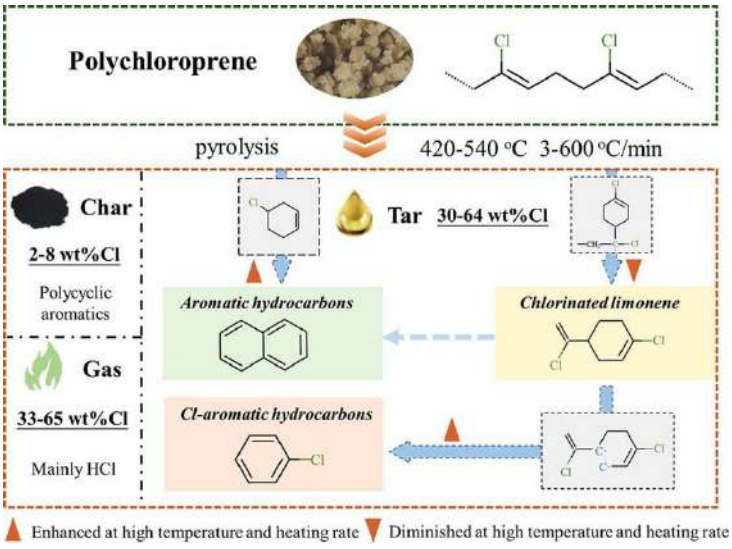


Figure 1. Pyrolysis of untreated polychloroprene (original PCR): Chlorine distribution in solid, liquid, and gas phases

Acknowledgement

This project was sponsored by ContiTech Company. The author would like to express sincere gratitude to the Royal Thai Government for the generous sponsorship and support throughout the course of this research.

References

1. Ren Y., Cao C., Hu H., Lei S, Yuan X., Li X., Yao H., Fuel, 2022; 317:123573.
2. Giri A., Yan H., Emamjomeh O., Cuoq F., Kwakkenbos G., Zijl A., Wong K., Energy&Fuels, 2024; 38:8649–8660.

Upgrading Reclaimed Carbon from Tire Pyrolysis for Tire Rubber Applications

Purwonegoro Muljawan

PT Cabot Indonesia Talavera Suite, 21st Fl., Unit 1-3 Jl. Letjen TB Simatupang, Kav. 22-26,

Jakarta, Cilandak 12430 Indonesia

e-mail address of the presenting author (Purwonegoro.Muljawan@cabotcorp.com)

Keywords: Reclaimed, Carbon, tire, pyrolysis, Carcass

Cabot has developed a product based on direct incorporation of 30% reclaimed carbon that enables reclaimed carbon use in more demanding tire carcass applications that traditionally require N300 series carbon blacks. In this presentation, Cabot will provide detailed application data in multiple tire carcass applications as compared to the typical N300 carbon blacks used. The use of reclaimed carbon from tire pyrolysis has been limited to modest loadings in the replacement of mostly low structure, semi-reinforcing carbon blacks in tire applications. Without upgrading the material, further use is extremely challenging.

Implementing Circular Economy Strategies in Power Transmission Belt Manufacturing

T.R. ASWATHY and T. Kalaivendhan

JK FENNER INDIA LIMITED, Madurai, Tamil Nadu, India 625016

e-mail address of the presenting author (aswathy.tr@jkfenner.com)

Keywords: Circular economy, Power transmission belts, Recovered carbon black, Hybrid filler system

Recovered carbon black (rCB) produced from waste tires through pyrolysis is getting attention from rubber good manufactures as it has emerged as a more environmentally friendly filler than regular carbon black (CB). The high percentage of carbon black in rCB can provide some properties equivalent to CB. However, the presence of inorganic materials may retard some essential properties like tensile strength and abrasion resistance. Although the rCB does have some inferiorities to it; to reduce the consumption of CB and increase the percentage of environmentally friendly fillers it is necessary to find a way to incorporate these fillers into rubber formulations without affecting the final properties. So, in this study various combinations of CB and rCB are used in ethylene propylene diamine (EPDM) -based rubber compounds to identify the exact ratio at which the best properties for dynamic applications are obtained. The properties of the CB and rCB used for the study are given in Table 1.

Table 1. The properties of regular as well as recovered carbon black used for the study.

Properties	CB,FEF (N-550)	rCB
Silica content	-	12%
Ash content	0.5%	10%
pH	7	7.5
Heating loss	<1%	1.5%

Starting from raw material level evaluation, the compound properties such as mechanical, rheological, and morphological were studied and reported in this paper. The CB and rCB have average particle sizes of 2080 nm and 562 nm, with corresponding specific surface areas of 13,770 m²/kg and 41,000 m²/kg, respectively. A 33% replacement of CB with rCB shows improvement in crucial properties like tensile strength and compression set. The tensile strength increases by 3% with the replacement of 20 Phr of CB with rCB. The compression set decreases by 18% for 20 Phr replacement of CB, which indicates even dispersion of fillers in the matrix. However, upon increasing the percentage of rCB in the formulations, a deterioration in mechanical properties was observed. The morphology of the composites was analyzed using AFM and TEM. From both results, it was clear that the replacement of 20 Phr of CB with rCB provides fine dispersion of fillers in the matrix. TGA was carried out to understand the degradation behavior upon the addition of rCB and confirms that the addition of rCB does not have any noticeable influence on the degradation pattern of the compounds. Hybrid filler-modified EPDM compounds based on power transmission belts were developed, and their physical and dynamic properties were studied. Positive results were obtained during these tests, confirming that a hybrid filler system containing CB and rCB, where rCB does not

exceed 33%, can be used as an environmentally friendly filler for applications like power transmission belts.

References

1. Dwivedi C, Manjare S, Rajan S K, *Compos B Eng.*, 2020; 200: 108346.
2. Anuar A U, Bonnia N N, Affandi N D N, Jamil N M, Hanapi N S M, Zawawi E Z E, *Malays. J. Microsc.*, 2024; 20: 259.

International Rubber Conference 2025 (IRC2025)
1-3 December 2025 @ BITEC, Bangkok, Thailand

The Reality of Sustainable Solutions and the Economics of SME Rubber Industry: A Way Forward

Peram Prasada Rao

TechnoBiz, Thailand

Email: peram.technobiz@gmail.com

Keywords: Sustainability, Rubber Industry Economics, SME Rubber Industry

The pursuit of sustainability has become a defining focus of the global rubber industry. Governments, investors, and end users increasingly expect manufacturers to adopt greener materials, energy-efficient processes, and transparent supply chains. However, for small and medium-sized enterprises (SMEs) that dominate the rubber sector in many developing economies, the transition toward sustainable practices remains a formidable challenge.

While large corporations can invest in advanced technologies, waste-reduction systems, and environmental certifications, SMEs often face financial limitations, market volatility, and a shortage of technical expertise. The high cost of implementing green technologies and compliance systems frequently outweighs immediate business returns. In addition, fragmented supply chains and inconsistent policy support make it difficult for smaller enterprises to translate sustainability goals into practical action.

This presentation examines the reality of sustainable transformation in the SME rubber sector, analyzing the economic and operational barriers that hinder progress. Drawing on industry observations and case examples from Asia, it highlights the gap between ambitious sustainability policies and the day-to-day realities of production-driven enterprises. It also explores emerging success stories where SMEs have achieved measurable improvements through innovation, resource efficiency, and collaboration within industrial clusters.

The discussion concludes with pragmatic recommendations for bridging the divide between environmental responsibility and business viability. It calls for a more inclusive framework involving governments, large corporations, and knowledge organizations to provide shared infrastructure, simplified compliance systems, and targeted financial incentives.

Ultimately, the presentation argues that sustainable progress in the rubber industry will depend not on idealistic models but on realistic, economically viable pathways that empower SMEs to participate meaningfully in the sustainability movement—ensuring that growth and responsibility advance together.

Session III : Advanced Rubber Materials and Novel Applications

Oral Presentations

International Rubber Conference 2025 (IRC2025)
1-3 December 2025 @ BITEC, Bangkok, Thailand

Innovation Management for Commercial Success in the Rubber Industry Amid Shifting Global Market Forces

Matthew Thornton[1], Michael Clayton[2]
[1]*The Rubber Initiative, Everton, Nottinghamshire, UK*
[2]*The Rubber Initiative, Adelaide, Australia*
Email address of presenting author: matthew@therubberinitiative.com

Keywords: Sustainability, Technological Integration, Market Dynamics, Innovation Management.

The rubber industry, integral to global manufacturing and economic development, is currently experiencing substantial transformations driven by multifaceted global market forces. These forces encompass environmental pressures, evolving trade policies, technological advancements, and shifting consumer expectations, collectively necessitating a refined approach to operational and strategic frameworks. This abstract examines the pivotal role of innovation management as a mechanism to address these dynamic challenges, emphasising sustainability, technological integration, and market responsiveness as critical areas of focus.

The Imperative of Innovation in the Rubber Industry

The rubber industry is encountering an era of unprecedented complexity and opportunity, demanding a departure from conventional practices. Regulatory environments have become more stringent, particularly concerning ecological sustainability, while the advent of novel materials and geopolitical disruptions have redefined supply chains and production paradigms. Concurrently, the demand for environmentally responsible products has intensified, compelling firms to innovate across material science, manufacturing processes, and product applications.

In this context, innovation management emerges as an essential construct. It entails systematically cultivating inventive capacities and translating these into strategic initiatives, encompassing product development, operational efficiency, and competitive positioning. For the rubber sector, this paradigm involves not only advancing technical methodologies but also re-evaluating organisational models to align with global sustainability imperatives.

Sustainability: A Catalyst for Transformation

Foremost among the influences reshaping the rubber industry is the global prioritisation of sustainability. Both natural and synthetic rubber production have faced criticism for their environmental ramifications. Natural rubber cultivation is challenged by issues such as deforestation and biodiversity degradation, while synthetic rubber, derived from petrochemical processes, contributes significantly to greenhouse gas emissions.

Innovation management offers a strategic pathway to mitigate these environmental concerns. Enterprises are increasingly allocating resources to the development of bio-based rubber alternatives, advanced recycling technologies, and circular economy frameworks. For instance, the engineering of high-performance, sustainable rubber compounds represents a progressive step toward reducing reliance on conventional raw materials while adhering to international ecological benchmarks.

Technological Integration and Operational Enhancement

The integration of emergent technologies is revolutionising the rubber industry's operational landscape. Innovations such as Artificial Intelligence (AI), machine learning (ML), and the Internet of Things (IoT) are redefining supply chain management, enhancing quality assurance, and optimising production workflows. Innovation management facilitates the seamless incorporation of these technologies into foundational industry practices.

Examples include IoT-enabled sensors that provide real-time monitoring of production machinery, thereby minimising downtime and maximising efficiency. AI-powered analytics further enable organisations to forecast market trends with precision, tailoring their product strategies to maintain competitiveness in volatile markets.

Adapting to Evolving Market Dynamics

The rubber industry must contend with rapidly shifting market dynamics, including the ascendancy of emerging economies and fluctuating international trade policies. Innovation management equips organisations to identify and adapt to these changes through the cultivation of adaptive capabilities and strategic foresight. By fostering a culture of continuous improvement and agility, firms can anticipate market perturbations and recalibrate their approaches accordingly.

For instance, the automotive sector's expansion within developing regions presents substantial growth opportunities for rubber products such as tyres and seals. Firms that prioritise innovation in the development of lightweight, durable, and fuel-efficient rubber components are strategically positioned to capture market share in these regions.

Conclusions

The pursuit of commercial success within the rubber industry, amidst the turbulence of shifting global market forces, necessitates a robust commitment to innovation management. This framework enables firms to effectively address sustainability, leverage technological advancements, and navigate intricate market dynamics. By institutionalising innovation as a core organisational principle, businesses not only secure resilience against contemporary challenges but also establish a trajectory for sustained growth and leadership in the global manufacturing sector.

The presentation will provide a comprehensive exploration of the transformative impacts of sustainability, technological integration, and adaptive strategies within the rubber industry. By showcasing how innovation management serves as a critical enabler of these advancements, the session will delve into the practical applications and theoretical implications of emerging trends.

This research bridges interdisciplinary domains, combining insights from environmental science, technological innovation, and market analysis to propose actionable frameworks for industry transformation. Furthermore, the emphasis on bio-based alternatives, AI-driven efficiencies, and circular economies underscores the pioneering nature of the study, aligning it with global priorities in sustainability and strategic business practices. This presentation aims to stimulate dialogue, foster collaboration, and inspire future research directions in the realm of industrial innovation management for the global rubber sector.

International Rubber Conference 2025 (IRC2025)
1-3 December 2025 @ BITEC, Bangkok, Thailand

Toward sustainable tire development: Challenges and emerging solutions

Wisut KAEWSAKUL

Greener Elastomer Technology, Futuristic Science Research Center, School of Science,

Walailak University, Nakhon Si Thammarat, Thailand.

wisut.ka@wu.ac.th / wisutkaewsakul@gmail.com

Keywords: Rubber compound, tire performance, bio-based materials, rubber processing

Based on recent publications from industry and academia, this work highlights new sustainability trends in tire development, discusses the practical challenges, and outlines opportunities for further research.

Sustainability in tires – Sustainable aspect has become one of the key competitive factors in the tire industry today. Current efforts in this area focus on improving tire performance, reducing environmental impact, minimizing rubber particle pollution, and addressing a range of sustainability challenges.

Sustainable tire strategies primarily target three areas: performance, manufacturing, and recyclability. Figure 1 summarizes possible strategies towards improving tire sustainability. Greener production processes aim to lower energy consumption, utilize recovered energy, and improve the processability of rubber compounds. Additionally, incorporating renewable or bio-based materials, as well as safer chemical ingredients, further contributes to sustainability. One of the major concerns is the origin of natural rubber, which must be sustainably sourced. Ideally, natural rubber should be traceable and must not originate from deforested or monoculture plantations.

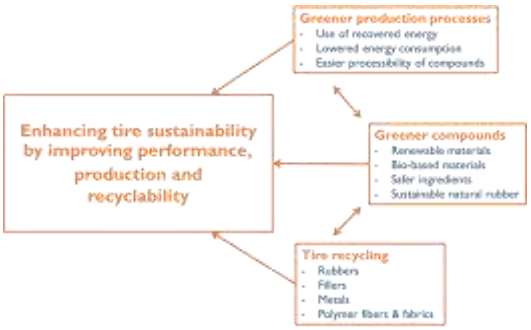


***Fig. 1**: Stretagies towards improved tire sustainability.*

To close the loop on tire life cycles, tires must be recyclable. However, their multi-material structure poses a challenge. Effective recycling requires that components such as rubber, fillers, metals, polymer cords, and fabrics can be separated. Progress is underway, and some recycled tire-derived products are already commercially available.

One of the biggest technical challenges is the recycling of vulcanized rubber. Vulcanization creates a chemically crosslinked macromolecular network via sulfide bonds, making the rubber durable but difficult to break down. Devulcanization involves cleaving these sulfide bonds without damaging the rubber backbone. Current research indicates that thermo-mechanical-chemical approaches are among the most effective, as they allow more controlled breakdown of the crosslinked network and better properties in the resulting material. Practical use of devulcanized rubber is usually 5–15 phr in tread compounds, sometimes up to 20–30 phr in inner liners or sidewalls, depending on devulcanization quality [1].

Continued improvements in tire performance – Tire performance enhancement remains a critical area of development. Two key factors influence tire performance: materials and processing. Intense competition drives ongoing innovation in rubber formulations, especially for tread and sidewall components. New generations of rubbers, fillers, processing oils, and curatives are regularly introduced. These materials require optimized mixing processes. For example, conventional silanized silica-filled compounds require higher mixing temperatures (around 150°C) to activate silane coupling reaction towards silica, whereas carbon black-based compounds are mixed at temperatures

around 110°C. These parameters are critical as they influence the degree of filler dispersion and chemical bonding within the compound as well as the energy consumption during processing [2].

Rolling resistance—a key performance metric—can be significantly reduced by replacing carbon black with silica as a reinforcing filler, indicated by the reduced tan δ at 60°C of the silica/TESPT silane compound as shown in Fig. 2. Silica, when combined with a silane coupling agent, forms strong chemical bonds with rubber, reducing energy loss and fuel consumption. In contrast, carbon black interacts primarily through physical interlocking, which leads to higher energy dissipation and thus higher rolling resistance [2]. The rolling resistance indicator (tan δ at 60°C) can typically be lowered by roughly 10-30%, and since every 10% reduction in the rolling resistance indicator leads to about a 1-2% improvement in fuel economy, this translates to approximately a 3-6% fuel saving for vehicles [3]. Ongoing advancements in both silica and silane technologies aim to further improve tire efficiency.

Resins also play a role in enhancing wet grip without compromising rolling resistance. Additionally, newer rubber materials and additives are being developed to enhance functionality, improve filler compatibility, simplify processing, or even eliminate certain mixing stages altogether [4]. Silane coupling agents remain a cornerstone of performance tuning, with continuous innovation to improve bonding strength, reduce Volatile Organic Compounds (VOCs), and enhance hysteresis properties [2,5].

A deep understanding of material behavior is essential for future advancements in sustainable tire design. Innovations in renewable rubbers, bio-based fillers, safer chemicals (e.g., zinc oxide alternatives, antidegradants, curatives, and processing oils), and novel filler-rubber interactions are currently all areas of active research and development.

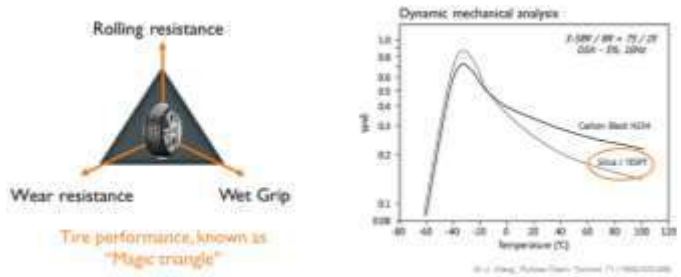


Fig. 2: *Magic triangle and rolling resistance indicator of silica- and carbon black based tire treads.*

The third corner of the tire performance "magic triangle"—abrasion resistance—is particularly complex. It is influenced by numerous factors, including road conditions, weather, driving style, and tire design. Laboratory Abrasion Tester (LAT100) is currently regarded as the best method for evaluating abrasion resistance. However, some studies show weak correlation between lab results and real-world tire wear, indicating a need for better predictive abrasion testing techniques [6].

Acknowledgement

The author gratefully acknowledges the grant sponsoring this participation in the IRC2025 conference, from Walailak University, Nakhon Si Thammarat, Thailand.

References

1. Markl E, Lackner M, *Materials*. 2020;13: 1246.
2. Kaewsakul W, Noordermeer J, Sahakaro K, Sengloyluan K, Saramolee P, Dierkes W, Blume A, in: Chemistry, Manufacture and Applications of Natural Rubber, Elsevier, UK, 2021.
3. The National Academy of Sciences, Tires and Passenger Vehicle Fuel Economy, Transportation Research Board Special Report 286, US, 2006.
4. Vleugels N, Pille-Wolf W, Dierkes W, Noordermeer J, *Rubber Chem. Technol.*, 2015; 88: 65.
5. Luginsland H-D, Röben C, *Int. Polym. Sci. Technol*., 2016; 43: 1.
6. Hoeksma M, Kaewsakul W, van der Heide E, Matthews D, Blume A, Conference Proceeding, The 15th Fall Rubber Colloquium (KHK), Hannover, Germany, 10-12 Sep. 2024.

International Rubber Conference 2025 (IRC2025)
1-3 December 2025 @ BITEC, Bangkok, Thailand

Surface-Functionalised Carbon Black as a High-Performance Filler in Elastomeric Compounds: Techniques and Potential

Rattapong NUMARD, Keizo AKUTAGAWA, James J.C. BUSFIELD
School of Engineering and Materials Science, Queen Mary University of London, UK
(r.numard@qmul.ac.uk)

Keyword: Carbon black surface activity; filler reinforcement; tyre tread application

The optimisation of polymer–filler interactions plays a critical role in the development of tyre tread compounds, particularly in addressing the trade-offs between rolling resistance, wet grip, and wear resistance. Modern tread formulations focus on enhancing the interfacial bonding between reinforcing fillers and elastomeric matrices. Carbon black and silica are the most commonly used fillers in passenger car tyre treads due to their reinforcing capabilities. In silica-based systems, the use of silane coupling agents significantly increases the polymer–filler interactions, leading to better overall tread performance, especially by reducing rolling resistance and improving wet grip. Surface modification of carbon black (CB) is an effective strategy to enhance rubber reinforcement by tuning polymer–filler interactions. Conventional CBs like N234 have low surface activity, limiting interfacial bonding with non-polar elastomers such as natural rubber (NR). Oxidative treatments increase the number of oxygen-containing groups (–OH, –COOH), improving filler dispersion and interfacial adhesion. In contrast, graphitisation at >2500 °C reduces surface functionality and promotes sp^2 ordering. [1]

In this study, surface modification techniques for carbon black were employed to alter its surface activity. Surface deactivation was achieved through high-temperature treatment conducted at 800°C and 1100 °C for 1 hour under an inert nitrogen atmosphere. The experimental setup for thermal treatment is illustrated in Figure 1(a). Conversely, surface activation was carried out via a wet chemical method using hydrogen peroxide (H_2O_2, 30 wt%). The oxidation reaction was performed at 80 °C for 1 hour, followed by thorough washing with deionised water. The treated carbon black was then dried in an oven at 120 °C for 24 hours. The experimental setting is shown in Figure 1(b)



(a) High-heat treatment



(b) Oxidation treatment

Figure 1. The carbon black surface modification technique.

Table 1. The XPS survey the elemental composition of high-heat treatment CB

Sample	**Element at. %**		
	Carbon	Oxygen	Sulphur
CB_pristine	95.23	4.31	0.46
CB_800°C	96.52	3.00	0.47
CB_1100°C	97.79	1.73	0.48

From the high-heat treatment process, the XPS results show that the oxygen content decreases as the temperature increases, which allows the carbon black surface to develop more graphitic domains and become more ordered in structure.

In this study, an Xplore micro-compounder was used to prepare the rubber compounds. Natural rubber was employed as the polymer matrix, and each surface-modified carbon black was incorporated at a loading of 50 phr. Additionally, standard compounding ingredients -including activators, antioxidants, and curing agents- were incorporated to complete the formulation. In Figure 2 the preliminary results, strain sweep DMA at 60°C, showed the Payne effect was most pronounced in Deactivated Carbon Black (DCB) filled compounds, indicating weaker filler–rubber interactions. In contrast, Control Carbon Black (CCB) demonstrated a lower Payne effect, suggesting stronger interfacial bonding interactions. The energy dissipation indicated by the loss modulus with the highest energy dissipation was DCB, and the Oxidised Carbon Black (OCB) showed the lowest. tan δ which is also related to tyre tread energy consumption or the tyre tread rolling resistance showed similar trends. Further work has characterised the nature of all of the carbon blacks, both oxidised and deactivated CB, using XPS, BET and Raman spectroscopy. The viscoelasticity of the rubber compound will be investigated. The morphological techniques, such as AFM, are used to map out the polymer matrix phase.

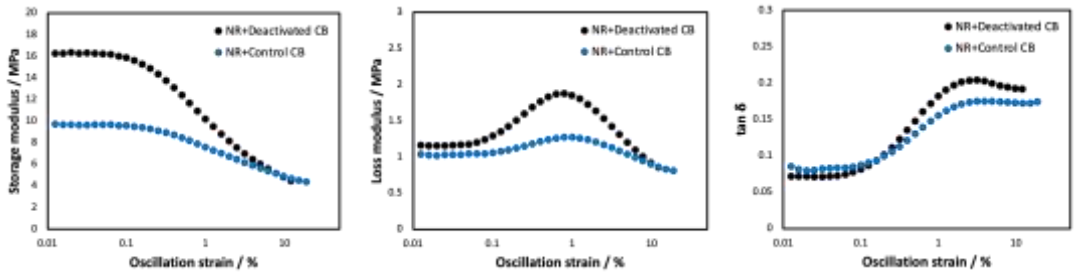


Figure 2. The storage modulus(E'), loss modulus(E") and tan δ at 60°C of rubber with different surface activity of carbon black, respectively.

Acknowledgement

The authors would like to thank the Royal Thai Government for supporting student scholarships and Soft Matter Group, Queen Mary University of London.

References

1. Donnet JB, editor. CRC Press; 1993 May 13.
2. Park SJ, Seo MK, Nah C. J of colloid and interface science., 2005; 291(1):229-35.

Effect of chemically treated pineapple leaf and hemp fibers on the interfacial interaction and mechanical properties of natural rubber composites

Siriwan Jansinak[1], Karine Mougin[2], Wirasak Smitthipong[1,3,*]

[1] *Specialized Center of Rubber and Polymer Materials in Agriculture and Industry (RPM), Department of Materials Science, Faculty of Science, Kasetsart University, Bangkok 10900, Thailand.*

[2] *Institute of Materials Science of Mulhouse, CNRS – UMR 7361, University of Haute-Alsace, France.*

[3] *Hub of Talents in Natural Rubber under National Research Council of Thailand (NRCT), Bangkok 10900, Thailand.*

E-mail address of the presenting author: siriwan.jan@ku.th

Keywords: Natural rubber, Pineapple leaf fiber, Hemp fiber, Chemical treatment, Rubber composites

Development of sustainable and environmentally friendly materials have been increasingly promoted. Biomaterials including natural fibers (NFs) derived from renewable plants and animals have been widely used due to their biodegradability, availability and low environmental impact. Natural rubber (NR), an important agricultural product of Thailand, can be reinforced with fibers to enhance its mechanical properties in composite applications. However, the interface compatibility between hydrophilic fibers and hydrophobic NR matrix is limited due to the difference in polarity, resulting in insufficient adhesion. To overcome this limitation, surface modification techniques have been employed to improve the adhesion of the interface and improve the overall properties of the composite [1-2]. In this research, surface-modified pineapple leaf fibers (PALF) and hemp fibers (HF) were co-molded with NR to form rubber composites, with the fibers content varying at 25, 50 and 75 phr as shown in Figure 1.

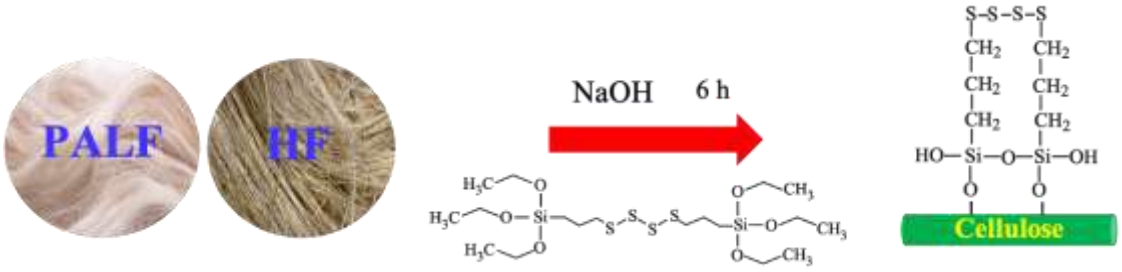


Figure 1. Natural fiber treatment process: PALF or HF was treated by NaOH and then silane 69 for 6 h to link the silane 69 on the surface of natural fibers

The NR composite was fabricated in a sandwich-like configuration, with the outer layers composed of NR and the core layer consisting of natural fibers, as illustrated in Figure 2. Surface characterization was characterized by Fourier Transform Infrared Spectroscopy (FTIR), X-ray Photoelectron Spectroscopy (XPS), and X-ray Diffraction (XRD). The surface of PALF and HF was modified through sequential treatment with a sodium hydroxide solution followed by a silane coupling agent. This chemical treatment resulted in the reduction of hemicellulose content. Composites reinforced with both untreated and surface-treated PALF and HF exhibited improved modulus and tensile strength in proportion to fiber loading [3].

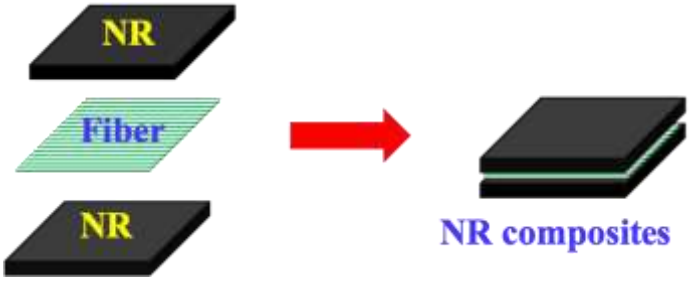


Figure 2. Preparation of sandwich-structured rubber composites

Nevertheless, when the fiber contents exceeded 50 phr, a significant decrease in stress was observed, likely due to the excessive fiber content impairing the structural integrity of the rubber matrix. Additionally, Single fiber pull-out tests indicated that superior interfacial adhesion to the rubber matrix was exhibited by the chemically modified fibers, compared to the untreated ones [4]. Moreover, Young's modulus of composite samples was observed to increase with increasing fiber content, and increased by 1,500 % treated PALF at 50 phr Furthermore, NR-PALF sample represented the highest Young's modulus compared with NR-HF sample, owing to PALF's higher cellulose content. This enhancement was attributed to the removal of surface impurities and lignin, which facilitated better interaction between the silane agents and the fiber surfaces. As a result, the incorporation of surface-modified fibers was found to enhance the mechanical performance of the rubber composite. Therefore, the developed NR-natural fiber composite could be applied for potential applications in vabration damping engineering.

Acknowledgement

This research was supported by the Capacity Building of KU Students on Internationalization Program (KUCSI) as of fiscal year 2024, which is funded by the International Affairs Division (IAD) and Faculty of Science, Kasetsart University (Thailand). Finally, the Specialized center of rubber and polymer materials in agriculture and industry (RPM), Department of Materials Science, Faculty of Science, Kasetsart University, is gratefully acknowledged for providing the facilities used in this research.

References

1. Wong D, Fabito G, Debnath S, Anwar M, Davies I. J, *C. Materials.*, 2024; 13: 100261.
2. Chollakup R, Suethao S, Suwanruji P, Boonyarit J, Smitthipong W, *Ref. Compos. & Adv. Mater.*, 2021; 30.
3. Smitthipong W, Suethao S, Shah D, Vollrath F, *Polym. Test.*, 2016; 55.
4. Thaiwattananon S, Thanawan S, Amornsakchai T, *IOP Conf. Ser.: Mater. Sci. Eng; 2023;* 012017.

International Rubber Conference 2025 (IRC2025)
1-3 December 2025 @ BITEC, Bangkok, Thailand

Development of Thermoplastic Natural Rubber Composites for Wearable Shielding Materials

Akarapong TULJITTRAPORN[1], Nussana LEHMAN[1], Supakit YONPHAN[2,3], Jakrapong KAEWKHAO[2,3], Suchart KOTHAN[4], Siriprapa KAEWJAENG[4], Ekwipoo KALKORNSURAPRANEE[1]

[1] *Division of Physical Sciences, Faculty of Science, Prince of Songkla University, Hat-Yai, Thailand.*

[2] *Physics program, Faculty of Science and Technology, Nakhon Pathom Rajabhat University, Nakhon Pathom, Thailand.*

[3] *Center of Excellence in Glass Technology and Materials Science (CEGM), Nakhon Pathom Rajabhat University, Nakhon Pathom, Thailand.*

[4] *Center of Radiation Research and Medical Imaging, Department of Radiologic Technology, Faculty of Associated Medical Sciences, Chiang Mai University, Chiang Mai, Thailand.*

(akarapong04@gmail.com)

Keywords: Thermoplastic natural rubber, Radiation shielding, Composites, Flexible shielding

Radiation such as gamma rays or X-rays has been widely applied in various fields, including medicine, hospitals, agriculture and laboratories. Different types and doses of radiation have their own benefits. On the other hand, radiation can cause damage to life and the environment. Therefore, recommendations for safety to prevent radiation exposure should consider 3 factors: time, distance and shielding [1]. Lead has been the preferred material for radiation shielding due to its high density and atomic number. However, lead's toxicity, high.[2] Recent research has focused on materials with high atomic numbers, such as bismuth (Bi) and barium (Ba), that can be incorporated into flexible polymer composites [3].

This study aims to develop flexible radiation shielding materials based on thermoplastic natural rubber composites. TPNR were prepared by natural rubber (NR) / Polybutylene adipate terephthalate (PBAT) and using bismuth oxide (Bi_2O_3) and barium sulfate ($BaSO_4$) as radiation shielding fillers or composites. TPNR composites were prepared with a composition of NR 40 and PBAT 60 wt.%, various contain of Bi_2O_3 and $BaSO_4$ at 0, 20, 60, 100 and 150 php. by internal mixer. The properties such as tensile strength, elongation at break, hardness and specific gravity of TPNR composites were investigated. The morphology was investigated composites dispersion by using Scanning Electron Microscopy (SEM-EDX). Gamma-ray shielding properties were measured under the exposure of gamma rays in the energy range of 0.223-0.662 MeV by Compton scattering technique. X-ray shielding properties were measured with a high-frequency digital radiography X-ray machine at 70-120 kVp and 40 mAs.

The results shown in Figure 1 indicate that the gamma-ray shielding properties such as the values of mass attenuation coefficient (μ_m), effective atomic number (Z_{eff}), and effective electron density (N_{eff}) of materials, increased with increasing amounts of composites. Similar trends were observed for X-ray shielding properties. SEM analysis confirmed a composites distribution within

polymer matrix. The Bi_2O_3 shown radiation shielding properties better than barium sulfate due to the higher atomic number. TPNR composites exhibited good flexible that conformed due to mechanical properties as shown in table 1. The obtained results confirm that TPNR composites can be effectively used as an alternative flexible radiation shielding material.

Table 1. Mechanical properties of TPNR composites

Properties	Concentration (php)								
	0	20		60		100		150	
		$BaSO_4$	Bi_2O_3	$BaSO_4$	Bi_2O_3	$BaSO_4$	Bi_2O_3	$BaSO_4$	Bi_2O_3
Tensile strength (MPa)	6.73 ±0.12	5.01 ±0.02	6.27 ±0.12	4.80 ±0.13	5.51 ±0.62	4.74 ±0.13	3.41 ±0.29	4.21 ±0.14	3.07 ±0.35
Elongation at break (%)	560 ±17	554 ±11	353± 21	555 ±3	236 ±20	404 ±2	224 ±1	155 ±3	152 ±1
Hardness (shore A)	65 ±0.81	72.8 ±0.84	67.8 ±1.09	74.4 ±1.34	73.6 ±0.55	76.2 ±0.84	74.5 ±0.58	78.2 ±0.84	75.2 ±1.26
Specific gravity	1.084	1.212	1.262	1.487	1.632	1.693	1.888	1.923	2.247

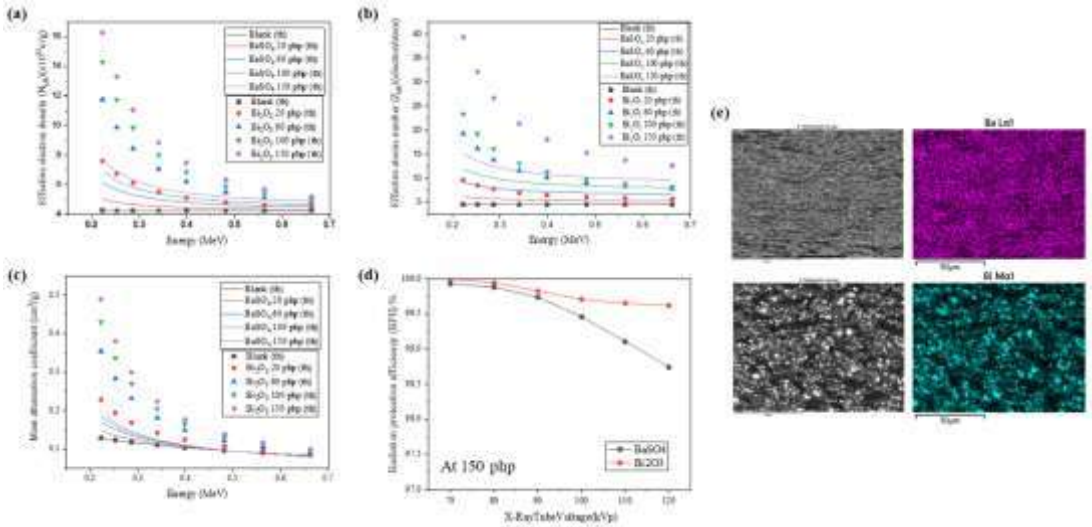


Figure 1. (a) The theoretical values of $N_{eff.}$ (b) The theoretical values of $Z_{eff.}$ (c) The theoretical values of μ_m. (d) The X-rays radiation protection efficiency (RPE%) of TPNR composites with 150 php (e) Morphology and composites distribution by using SEM/EDX testing method.

Acknowledgement

The authors also would like to thank Faculty of Science, Prince of Songkla University for sample preparation and facilities support.

References

1. Rudychev VG, Azarenkov NA, Girka IO, Rudychev YV, Nuclear Engineering and Technology. 2023;55(2):690–5.
2. Verdipoor K, Alemi A, Mesbahi A, Radiation Physics and Chemistry. 2018;147:85–90.
3. Intom S, Kalkornsurapranee E, Johns J, Kaewjaeng S, Kothan S, Hongtong W, et al, Radiation Physics and Chemistry. 2020;172:108772.

High-performance, Recyclable, and Multifunctional Nitrile Butadiene Rubber Based on Hydrogen and Urea Bonds

Dongmei Yue[1], Lin Wang[1]

Beijing University of Chemical Technology, Beijing, China.

e-mail address of the presenting author (yuedm@mail.buct.edu.cn)

Keywords: Nitrile butadiene rubber, High-performance, Recyclability, Multifuncation

Nitrile Butadiene Rubber (NBR) is widely used in auto parts, petroleum exploration, sealing parts, and other fields because of its outstanding performance.[1] However, raw NBR usually needs to be crosslinked with sulfur or peroxide[2,3] before it can be utilized, which impeding the reprocessing and recycling of NBR, leading to resource wastage and environmental pollution. Thus, it is urgent to search for a new crosslinked network to realize NBR with reprocessability and recyclability.

In recent years, to enable the recyclability and reusability of NBR, researchers have integrated dynamic bonds into NBR *via* a range of modification strategies. For example, Chen *et al*. designed a network composed of Fe^{3+}-catechol group coordination bonds.[4] Wang *et al*. introduced reversible alkoxyamine (C-ON) bonds into the dynamic cross-linked network of NBR.[5] It's evident that while dynamic characteristics are attainable by introducing metal coordination bonds and reversible alkoxyamine (C-ON) bonds, there are several challenges including intricate fabrication processes, inferior mechanical properties, and low efficiency in reprocessing. Consequently, the development of a straightforward, effective, and innovative dual dynamic crosslinking network for NBR elastomers is of great significance.

In this work, a series of novel polyurea NBR elastomer materials (IPDI-ATBN-PPD) were designed and synthesized by a one-pot ternary polymerization reaction of amino-terminated liquid nitrile rubber (ATBN), isophorone diisocyanate (IPDI) and p-phenylenediamine (PPD) without any catalyst. The presence of urea bonds not only provides a large number of hydrogen bonding sites between the molecular chains, but also exhibits the remarkable microphase separation properties of thermoplastic elastomers. This approach endows NBR with enhanced dynamic characteristics and significant recyclability. As a result, the as-synthesized multifunctional NBR elastomer (I-$A_{0.5}$-$P_{0.5}$) exhibits excellent tensile strength (19.9 Mpa, Figure 1c), toughness (93.7 MJ m^{-3}, Figure 1c), low glass transition temperature (-52 ℃, Figure 1a), and low compression cold resistance coefficient (0.15 at -55 ℃, Figure 1f), which are comparable to those of conventionally covalently crosslinked NBR. The elastomer retains mechanical integrity after multiple rounds of recycling (retaining 81% of its original tensile strength after five reprocessing cycles, Figure 1e). To broaden the application of NBR products, I-$A_{0.5}$-$P_{0.5}$ was crosslinked with sulfur and its performance was compared with NBR vulcanizates of different acrylonitrile contents. It shows excellent oil resistance and low temperature resistance (Figure 1g and 1h). Surprisingly, it can also possess the ability to be reprocessed multiple times. (Figure 1i) This new multifunctional thermoplastic NBR elastomer is of great significance in solving the problem of difficult recycling of traditional NBR and is expected to replace traditional covalently cross-linked NBR. This synthesis strategy is readily adaptable to industrial processes and offers a scalable route to produce recyclable NBR for demanding applications.

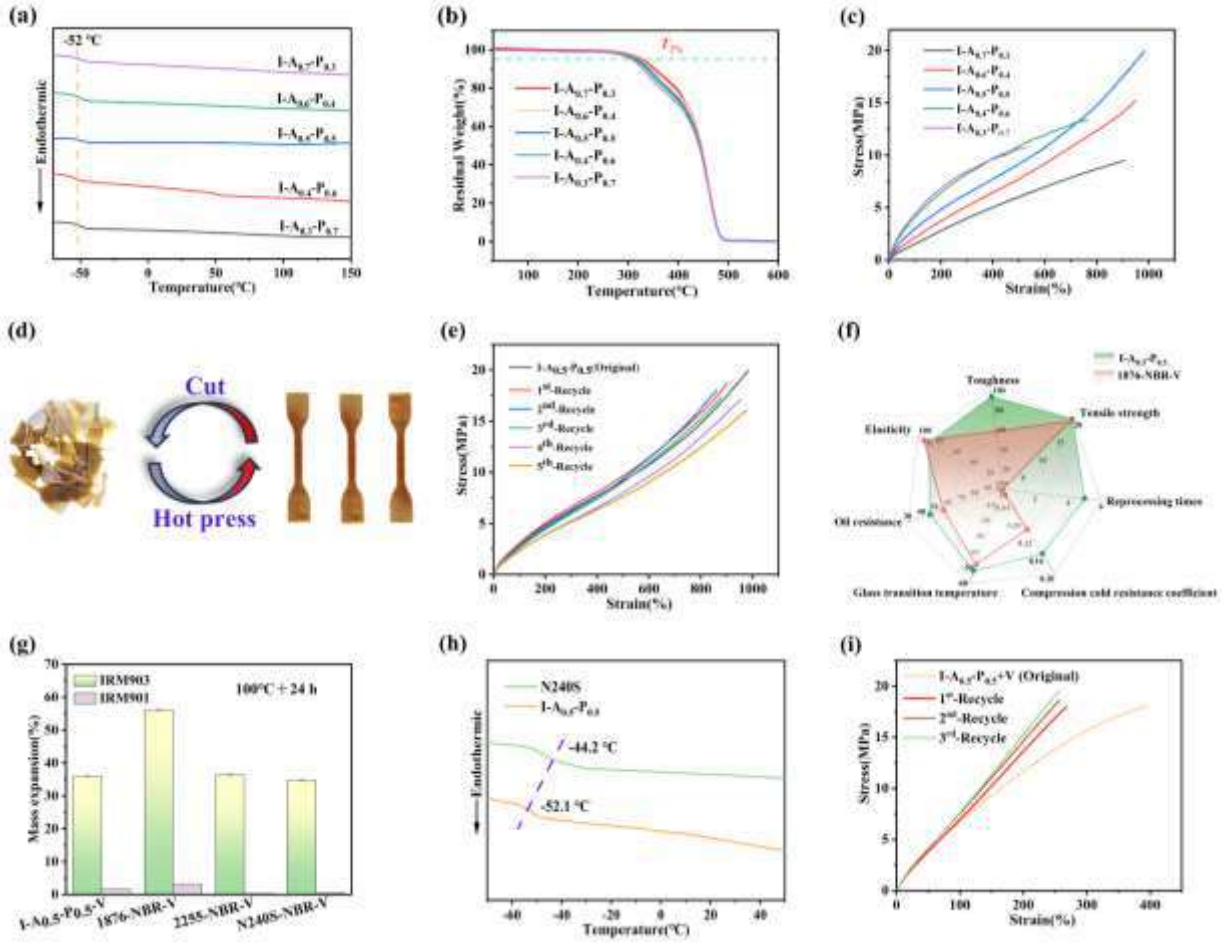


Figure 1. (a) DSC curves, (b) TGA curves, (c) Stress–strain curves of IPDI-ATBN-PPD. (d) Photograph of I-$A_{0.5}$-$P_{0.5}$ recycled dumbbell strip. (e) Stress–strain curves of original and recycled samples. (f) Comparison of I-$A_{0.5}$-$P_{0.5}$ and 1876-NBR-V. (g) Oil resistance of I-$A_{0.5}$-$P_{0.5}$-V, 1876-NBR-V, 2255-NBR-V, and N240S-NBR-V. (h) DSC curves of N240S and I-$A_{0.5}$-$P_{0.5}$. (i) Stress–strain curves of original and recycled samples.

Acknowledgement

This work was supported by the Taishan Industrial Experts Program, the National Key R&D Program of China (2022YFB3704700), and the National Science and Technology Major Special Projects (2024ZD0603000).

References

1. Wan S H, Du P, Guo Z Y, You L X, Mao Y W, He X R, *Polym. Compos.*, 2024, 45, 2462-2473.
2. Zhang R, Yuan X, Sun R, Zhang B, Geng Z, Li Z, Liu G, *Polym. Compos.*, 2023, 44, 1929-1939.
3. Forghani N, Maghsoud Z, Ramezanian N, Appl. Surf. Sci., 2023, 639, 158114.
4. Chen Z, Yan M, Cao L, Huang J, Cao X, Yuan D, Chen Y, *Ind. Eng. Chem. Res.*, 2019, 58, 3912-3920.
5. Wang X P, Xue K X, Wu H J, *Ind. Eng. Chem. Res.*, 2024, 63, 9779-9789.

International Rubber Conference 2025 (IRC2025)
1-3 December 2025 @ BITEC, Bangkok, Thailand

Development of Piezoresistive Sensor Prepared from PMMA-Grafted Natural Rubber Latex Filled Conductive Carbon Composites: Comparative of Conductive Carbon Fillers and Hybrid System

Arthittaya CHUAYBAMRUNG[1], Rawiporn PROMSUNG[1], Ekwipoo KALKORNSURAPRANEE[1], Yeampon NAKARAMONTRI[2], Frank CLEMANS[3]

[1] *Division of Physical Sciences, Faculty of Science, Prince of Songkla University, Songkhla, Thailand.*

[2] *Sustainable Polymer & Innovative Composites Material Research Group, Faculty of Science, King Mongkut's University of Technology Thonburi, Bangkok, Thailand.*

[3] *Laboratory for High Performance Ceramics, Empa, Swiss Federal Laboratories for Materials Science and Technology, Dübendorf, Switzerland*

e-mail address of the presenting author (arthittaya2875@gmail.com)

Keywords: Grafted natural rubber, Conductive carbon fillers, Piezoresistive sensor

Current flexible sensor technologies frequently encounter challenges such as complex fabrication processes, high manufacturing costs, and sensitivity degradation over time. Furthermore, many existing polymer-based conductive composites suffer from issues like poor filler dispersion, weak interfacial adhesion between the conductive elements and the polymer matrix, and a compromised balance between electrical conductivity and mechanical flexibility [1]. These issues often lead to suboptimal piezoresistive performance, characterized by low sensitivity, significant hysteresis, and limited long-term stability.

This study aims to develop novel piezoresistive sensors based on polymethyl methacrylate (PMMA)-grafted natural rubber (NR) composites with enhanced mechanical strength, electrical property, and sensing stability. NR latex was grafted with 10 wt% PMMA and crosslinked using glutaraldehyde. Conductive fillers were incorporated, including CNT (1 phr) and hybrid fillers (CNT: CCB 1:20 phr). The composites were characterized by electrical properties, mechanical performance (modulus, tensile strength, elongation at break), and piezoresistive response under dynamic cyclic strain (0-100% strain for 10 cycles reported through relative resistance (R_{rel}) change).

Grafted-PMMA improved polymer polarity and stiffness, leading to stronger filler–matrix interactions [2]. CNT provided excellent reinforcement, resulting in high modulus, tensile strength, and elongation at break in grafted NR/CNT composites, as shown in Figure 1. However, the incorporation of hybrid fillers reduced the mechanical performance due to poorer dispersion and unfavorable inter-filler interactions [3, 4], which consistent with the specific gravity results that revealed significantly higher filler distribution compared to the composites containing only CNT [5, 6] Piezoresistive testing revealed that grafted NR/CNT composites demonstrated superior sensitivity, drift magnitude, and stable cyclic performance compared with NR-based and hybrid-filler composites.

Piezoresistive sensor application, for applications requiring stable and reliable strain sensing the grafted NR/CNT composite appears to be the most promising candidate due to its high sensitivity, low hysteresis, and excellent long-term stability under cyclic loading. The other composites, particularly those with the NR matrix or the mix filler in grafted NR, show limitations in terms of stability, noise signal, or significant drift, which would hinder their performance as reliable strain sensors.

Grafted-PMMA NR/CNT composites show outstanding mechanical and piezoresistive properties, making them strong candidates for flexible and wearable strain sensor applications. Their high sensitivity and stability position them as promising materials for next-generation durable sensing technologies.

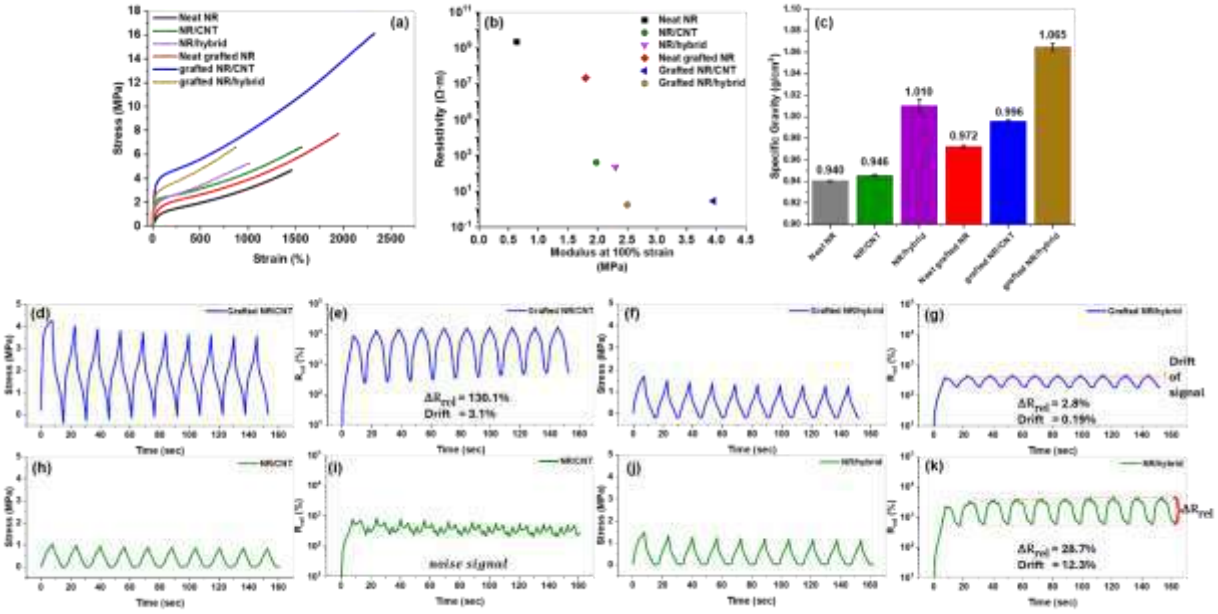


Figure 1. The stress-strain curves (a), resistivity (b), specific gravity (c) and relation of stress and time (d-k) of the composites with the R_{rel} as a function of time during the dynamic tests in 10 cycles at 0-100 % strain.

Acknowledgement

This research project is also supported by National Research Council of Thailand (NRCT): (N41A640236). The authors also would like to thank KMUTT and Empa-Swiss Federal Laboratories for Materials Science and Technology for their invaluable technical support.

References

1. Liu, J.; Tian, G.; Yang, W.; Deng, W. *Soft Science*. OAE Publishing Inc., 2022.
2. Chuaybamrung, A.; Promsung, R.; Clemens, F.; Nakaramontri, Y.; Johns, J.; Kalkornsurapranee, E. *Iran Polym J.,* 2025.
3. Nakaramontri, Y.; Nakason, C.; Kummerlöwe, C.; Vennemann, N. *Rubber Chem. Technol.,* 2016, *89* (2), 272–291.
4. Wang, X. D.; Wang, J. C.; Biswas, S.; Kim, H.; Nam, I. W. *Sensors* 2020, *20* (7).
5. Nasruddin; Setianto, W.B.; Yohanes, H.; Atmaji, G.; Lanjar; Yanto, D.H.Y.; Wulandari, E.P.; Wiranata, A.; Ibrahim, B. *Appl. Sci.* **2023**, *13*, 1277.
6. Hutagaol, P.; Suryanto, E.; Suryani, E. *AIP Conf. Proc.* 2020

Development of hydroxyapatite from eggshell waste and its application in SBR composite

Chomsri Siriwong[1], Jhiratchaya Buranawichit, A. Nintap[1]

[1] *Department of Chemistry, Faculty of Science, Khon Kaen University, Khon Kaen, 40002 Thailand.*

schoms@kku.ac.th

Keywords: Eggshell, Hydroxyapatite, Styrene butadiene rubber

This research focuses on the preparation of hydroxyapatite (HAP) from eggshells for use as a filler in styrene butadiene rubber (SBR). Initially, HAP was synthesized using calcium source derived from eggshells as raw material. The prepared HAP was subsequently surface-modified with two types of coupling agents: polyethylene glycol (PEG) and *bis*-(3-triethoxysilylpropyl) tetrasulfide (TESPT) through ball milling process. The unmodified and surface-modified HAP were characterized using various analytical techniques including FTIR, XRD, TGA, and SEM. The HAP fillers were then incorporated into SBR using a two-roll mill, and rubber compounds were prepared according to the formulation presented in Table 1. The influence of HAP loading (10-40 phr) on vulcanization behavior, mechanical properties, and dispersion characteristics in rubber matrix was investigated for both unmodified and surface-modified HAP.

Table 1 Rubber formulation used in this study.

Ingredient	Amount (phr)
SBR	100
Filler[a]	0, 10, 20, 30, 40
ZnO	5
Stearic acid	1
CBS	0.5
TMTD	1.5
S8	2

[a] = HAP, TESPT-modified HAP (T-HAP), and PEG-modified HAP (P-HAP)

The cure characteristics of the compounds, including minimum torque (M_L), maximum torque (M_H), scorch time (t_s1), optimum cure time (t_c90), and torque difference, are presented in Table 2. The results revealed that the synthesized HAP exhibited relatively large particle size, porous structure, and high specific surface area. Upon incorporation into SBR, both scorch time and optimum cure time decreased with increasing HAP content. At equivalent loading levels, HAP modified with TESPT and PEG demonstrated shorter scorch time and optimum cure time compared to unmodified HAP. Furthermore, the incorporation of TESPT-modified HAP provided the most significant improvement in overall mechanical properties of SBR, followed by PEG-modified HAP and unmodified HAP, respectively.

Table 2 Cure characteristic of the SBR filled with various filler types and loadings.

Sample Name	Filler Loading (phr)	M_L (dN.m)	M_H (dN.m)	ΔM (dN.m)	t_S1 (min)	t_C90 (min)
SBR	0	0.66 ± 0.00	12.71±0.07	12.05±0.07	1.73±0.01	5.64±0.09
SBR/HAP	10	0.88 ± 0.01	13.47±0.13	12.59±0.12	1.58±0.02	5.55±0.46
	20	0.81±0.02	13.62±0.05	12.81±0.03	1.64±0.01	5.29±0.43
	30	1.00±0.09	14.46±0.09	13.46±0.09	1.11±0.00	4.81±0.00
	40	1.45±0.00	15.38±0.04	13.94±0.04	1.31±0.00	4.05±0.10
SBR/P-HAP	10	0.83±0.00	13.32±0.00	12.49±0.00	1.39±0.00	3.42±0.05
	20	1.00±0.00	14.33±0.11	13.33±0.11	1.07±0.00	2.60±0.02
	30	1.15±0.00	15.52±0.00	14.37±0.00	0.93±0.00	1.95±0.00
	40	1.27±0.00	16.53±0.14	15.26±0.14	0.80±0.00	1.43±0.04
SBR/T-HAP	10	0.82±0.00	13.87±0.09	13.04±0.09	1.60±0.00	4.36±0.04
	20	0.99±0.00	15.26±0.01	14.27±0.01	1.53±0.00	4.08±0.00
	30	1.09±0.00	16.55±0.00	15.46±0.00	1.42±0.00	3.60±0.00
	40	1.31±0.00	17.92±0.00	16.61±0.00	1.38±0.00	3.52±0.01

Acknowledgement

The authors would like to express their gratitude to the Department of Chemistry, Faculty of Science, Khon Kaen University, for financial support

References

1. Rivera EM, Araiza M, Brostow W, Castaño VM, Díaz-Estrada JR, Hernández R, Rodríguez JR, *Mater. Let.*,1999; 41: 128.
2. Salman AD, Tatjána J, Al-Mayyahi MA, Ibrahim RI, Abdullah TA, Khader EH, IOP Conf. Ser.: Mater. Sci. Eng., 2020; 765: 012006.

International Rubber Conference 2025 (IRC2025)
1-3 December 2025 @ BITEC, Bangkok, Thailand

Comparison of Growth and Transpiration in Micro-Cuttings and Budded Rubber Trees

Supat ISARANGKOOL NA AYUTTHAYA[1], Somyot MEETHA[1], Adisak KHOTCHOMPHU[2]
Supalerk MOONRUNGSEE[3], Kamolchat CHARUNGCHITAREE[3], Lucksanaporn TARACHIWIN[3],
Noriyuki ONOZUKA[4], Akari UESUGI[4]

[1] *Department of Horticulture, Faculty of Agriculture, Khon Kaen University, Khon Kaen, Thailand.*

[2] *Sumirubber Thai Eastern Corporation Co., Ltd, Udon Thani, Thailand.*

[3] *Sumitomo Rubber (Thailand) Co., Ltd, Rayong, Thailand.*

[4] *Sumitomo Rubber Industries, Ltd, Kobe, Japan.*

e-mail address of the presenting author (isupat@kku.ac.th)

Keywords: Tissue culture, Trunk girth, Sap flow, Transpiration, Water use, Micro-cutting

Green budding is a commonly used technique for rubber tree propagation; however, it often results in variability in tree growth. A newer method, such as micro-cutting or tissue culture, has been introduced to improve the uniformity of rubber tree saplings. This study aimed to evaluate the growth and its relationship with sap flow in micro-cutting and budded rubber trees. The experiment was conducted in the experimental field of Sumirubber Thai Eastern Plantation Co., Ltd., located in Udon Thani, Thailand. The sampled rubber trees (clone RRIM600) were two years old. The trunk girth of both micro-cutting (MC) and budded trees (BD) was measured from April 2024 to April 2025. Additionally, sap flow was measured in four trees per propagation technique using the transient thermal dissipation method with a dual-probe sensor based on Granier's design.

The third-year growth results showed that MC had a larger trunk girth than BD (Figure 1). For both propagation methods, trunk girth increased during the wet season and decreased during the dry season. Variation in trunk girth, as indicated by the standard deviation, was lower in MC trees compared to BD trees. The maximum and daily sap flux densities (Figure 2A and 2B) were higher in BD trees than in MC trees during May to June 2024; however, no significant differences were observed between the two propagation methods during the main rainy season (July to October 2024). In contrast, tree transpiration (Figure 2C) in MC trees was higher than in BD trees from July 2024 to February 2025, suggesting that the greater transpiration in MC trees may have contributed to their enhanced growth. These findings indicate that, in the RRIM600 clone, the MC propagation technique not only reduced growth variation but also promoted greater tree growth, potentially associated with higher transpiration rates.

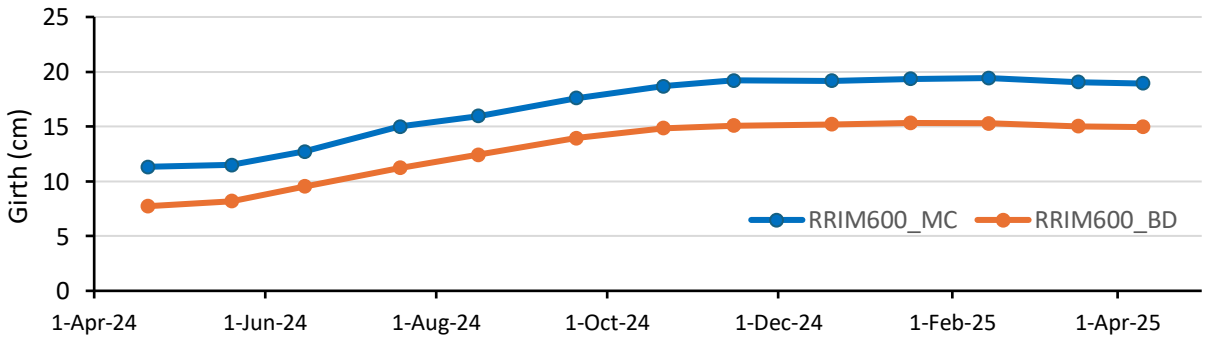


Figure 1. Change of girth of the rubber tree clone RRIM600 was propagated by micro-cutting (MC) and budded trees (BD) from April 2024 to April 2025

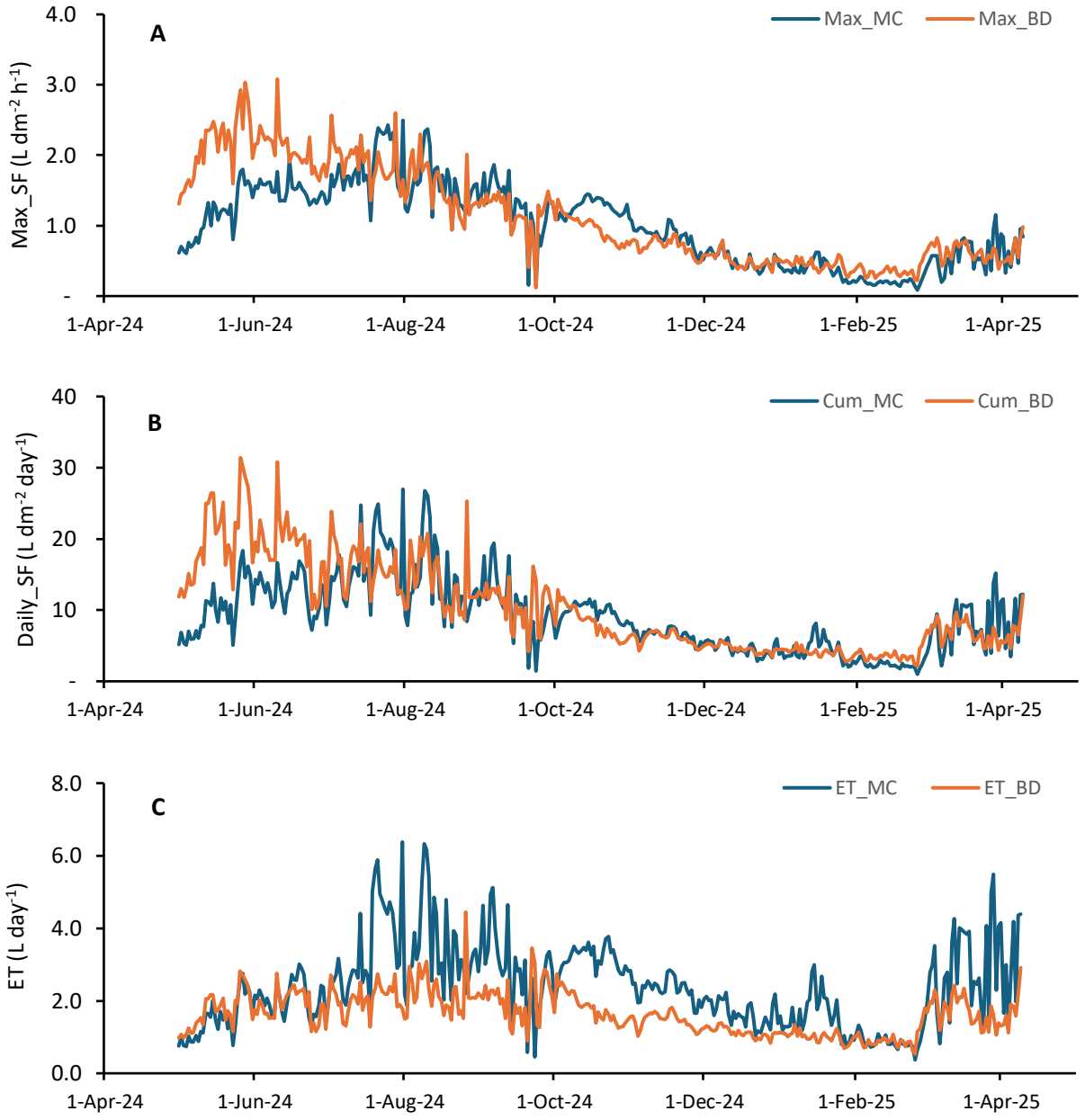


Figure 2. Maximum sap flux density (A), daily sap flux density (B), and tree transpiration (C) of rubber tree clone RRIM600 propagated by micro-cutting (MC) and budding (BD) from May 2024 to April 2025.

Acknowledgement

We gratefully acknowledge the support of Sumitomo Rubber Industries, Ltd., for this research.

References

1. Isarangkool Na Ayutthaya S, Do FC, Pannengpetch K, Junjittakarn J, Maeght JL, Rocheteau A, Cochard H. *Tree Physiol. 2010;* 30:139-148.
2. Isarangkool Na Ayutthaya S, Do FC, Pannangpetch K, Junjittakarn J, Maeght JL, Rocheteau A, Cochard H. *Tree Physiol. 2011;* 31: 751-762.

International Rubber Conference 2025 (IRC2025)
1-3 December 2025 @ BITEC, Bangkok, Thailand

Effectiveness of Participatory Ergonomic Training on Musculoskeletal Disorders Among Rubber Tappers: A Longitudinal Mixed-Effects Analysis

Warut CHANASIT[1], Apinya CHINTRAKUL[2], Chutarat SATHIRAPANYA[1], Chanon KONGKAMOL[1]

[1] *Department of Family and Preventive Medicine, Faculty of Medicine, Prince of Songkla University, 90110, Songkhla, Thailand.*

[2] *Division of Safety, Occupational Health and Environment, Songklanagarind Hospital, Faculty of Medicine, Prince of Songkla University, 90110, Songkhla, Thailand.*

(warutchanasit@gmail.com)

Keywords: Occupational ergonomics, Musculoskeletal disorders, Rubber tappers, Participatory intervention, Rubber Authority of Thailand

Work-related musculoskeletal disorders (WMSDs) are prevalent among rubber tappers due to repetitive motions and awkward postures [1]. The Rubber Authority of Thailand (RAOT) has been conducting 5-day rubber tapping training courses for over 10 years; however, the long-term effectiveness on post-training musculoskeletal health outcomes remains unclear. Despite this occupational group representing over 10 million workers globally with high MSD prevalence (52.9-66%), no systematic reviews have identified participatory ergonomic interventions specifically designed for rubber tappers. This study addresses this critical research gap by evaluating the effectiveness of the first longitudinal participatory ergonomic intervention specifically tailored for rubber tapping operations, integrating worker-driven problem-solving with comprehensive occupational health strategies to reduce work-related body pain and discomfort.

A cluster-randomized longitudinal study conducted in 2025, followed 120 rubber tappers enrolled in 5-day rubber tapping training courses conducted by RAOT across 4 areas in Songkhla Province, Thailand, for 90 days post-training (time 0,30,60, and 90 days). Training clusters were randomly allocated to receive either enhanced occupational ergonomic training (OER, n=66) or standard training (STG, n=54). Both groups received standard training on knife maintenance and tapping techniques, while OER participants additionally received a 1-hour participatory ergonomic intervention including: (1) interactive sessions where rubber tappers identified their own postural risk factors, awkward working positions, and work-related pain points, (2) collaborative development of posture correction techniques for tapping and latex collection, (3) self-care management training for musculoskeletal health, and (4) medical consultation guidance [2]. Data collection included demographic characteristics, health behaviors (sleep, exercise, alcohol consumption and smoking habits), rubber tapping data, and psychological wellbeing (the Depression, Anxiety and Stress Scale-21: DASS-21 and WHO Quality of Life-BREF: WHOQOL-BREF)

Work-related musculoskeletal disorders were assessed using Cornell Musculoskeletal Discomfort Questionnaires (CMDQ) [3]. CMDQ composite scores were calculated by multiplying frequency, discomfort intensity, and work interference ratings for each body region. The questionnaire assessed 14 anatomical regions bilaterally. Composite scores for each segment were classified into five severity levels: none (0), mild (1.5-4.5), moderate (5-14.5), severe (15-45), and very severe (60-90). Each body segment was dichotomized as "pain" (moderate/severe symptoms) or "no pain" (none/mild symptoms). Participants were classified as having musculoskeletal disorders if they reported pain in any body segment.

Statistical Analysis: The primary analysis employed generalized linear mixed-effects models (GLMM) with binomial distribution and logit link function to account for the longitudinal nature of the data and clustering within work areas.

Results: OER participants significantly reduced musculoskeletal disorders compared to standard training (OR=0.17, 95% CI: 0.04-0.66). Disorder prevalence decreased by 2% per follow-up time point (OR=0.98, 95% CI: 0.97-0.99). Risk factors included inappropriate sleep latency (OR=3.4, 95% CI: 1.42-8.16) and mild-moderate anxiety (OR=3.6, 95% CI: 1.32-9.82), while higher health beliefs and self-efficacy were protective (as table 1).

Table 1. Mixed-Effects Logistic Regression Models of Factors Associated with Work-Related Musculoskeletal Disorders in Rubber Tappers (n=120)

	Model 1			**Model 2**		
Parameters	Odds Ratios	CI	p	Odds Ratios	CI	p
(Intercept)	2.54	0.35 – 18.35	0.356	3.99	0.51 – 31.42	0.189
Time	0.98	0.97 – 0.99	**<0.001**	0.98	0.97 – 0.99	**<0.001**
Group (ref: STG)						
OER	0.16	0.04 – 0.63	**0.009**	0.17	0.04 – 0.66	**0.011**
Sleep latency (ref: appropriate)						
Inappropriate	3.36	1.30 – 8.06	**0.007**	3.40	1.42 – 8.16	**0.006**
DASS21: anxiety						
Normal	ref	-	-	ref	-	-
Mild/moderate	3.94	1.44 – 10.77	**0.008**	3.6	1.32 – 9.82	**0.012**
Severe	3.95	0.95 – 16.41	0.059	3.91	0.95 – 16.08	0.059
Susceptibility[a]	0.58	0.34 – 0.99	**0.046**			
Selfcare[b]				0.54	0.32 – 0.90	**0.018**
Marginal R^2 / Conditional R^2	0.178 / 0.768			0.184 / 0.768		

Susceptibility[a]: from health belief model; excellent/good, ref:moderate/poor
Selfcare[b] : from selfefficacy; excellent/good, ref:moderate/poor

Conclusions: Participatory ergonomic training significantly reduces musculoskeletal disorders among rubber tappers. Combined with sleep hygiene and anxiety management, the intervention shows amplified benefits. These findings provide strong evidence for policy recommendations to the Rubber Authority of Thailand (RAOT) to integrate participatory ergonomic modules into its existing national training curricula for rubber tappers and to establish robust occupational health monitoring systems specifically for rubber tappers, ideally facilitated by local Health Promoting Hospitals.

Acknowledgement

We acknowledge the Rubber Authority of Thailand (RAOT) for study collaboration and the National Science, Research and Innovation Fund (NSRF) for funding support.

References

1. Varghese A, Panicker VV, *Med Lav.*, 2022; 1:13.
2. Tangadulrat N, Wattanapisitkul P, Kaewmanee T, et al., *Ind Eng Manag Syst.*, 2019; 710–718.
3. Hedge A, Morimoto S, McCrobie D, *Ergonomics*, 1999; 1333-1349.

Effects of Enhanced Ergonomic Training on Postural Risk Among Rubber Tappers: A Cluster-Randomized Longitudinal Analysis

Chanon KONGKAMOL[1], Apinya CHINTRAKUL[2], Phachara SUKLIM[3], Atichart KWANYUANG[3]

[1] *Department of Family and Preventive Medicine, Faculty of Medicine, Prince of Songkla University, 90110, Songkhla, Thailand.*

[2] *Division of Safety, Occupational Health and Environment, Songklanagarind Hospital, Faculty of Medicine, Prince of Songkla University, 90110, Songkhla, Thailand.*

[3] *Department of Biomedical Sciences and Biomedical Engineering, Faculty of Medicine, Prince of Songkla University, 90110, Songkhla, Thailand.*

(chanon.kon@psu.ac.th)

Keywords: Occupational ergonomics, REBA, Rubber tappers, Participatory intervention, Rubber Authority of Thailand

Work-related musculoskeletal disorders (WMSDs) are prevalent among rubber tappers due to repetitive motions and awkward postures [1]. While the Rubber Authority of Thailand (RAOT) has conducted traditional 5-day training courses for over 10 years, systematic research utilizing evidence-based ergonomic assessment tools remains limited in the rubber tapping sector. This study evaluated the effectiveness of enhanced occupational ergonomic training in reducing Rapid Entire Body Assessment (REBA) assessed postural risk among rubber tappers, representing one of the first comprehensive longitudinal evaluations of training interventions for rubber tapping activities.

As part of a larger cluster-randomized trial conducted in 2025, this sub-study followed 30 rubber tappers who received enhanced occupational ergonomic training from RAOT courses in Hat Yai area, Songkhla Province, Thailand, for 90 days post-training (time 0, 30, 60, and 90 days). Participants received standard training on knife maintenance and tapping techniques, plus an additional 1-hour participatory occupational health education, self-care management, and medical consultation guidance [2]. The enhanced training component included participatory risk identification sessions where participants demonstrated their current tapping techniques, received individualized corrective feedback on posture optimization, and practiced proper body mechanics during simulated tapping scenarios. The program emphasized practical application of ergonomic principles specific to rubber tapping activities. Data collection included demographic characteristics, rubber tapping data, and postural risk assessment using REBA at each time point. Participants were asked to perform their usual rubber tapping techniques at two different heights: low-level tapping (knee-to-waist level) and normal-level tapping (waist-to-shoulder level). Video recordings were captured using two cameras positioned at 45° and 135° angles to ensure comprehensive postural analysis.

REBA assessments were conducted independently by three trained evaluators: two physiotherapists and one occupational medicine physician with ergonomics expertise. Inter-rater reliability was ensured through consensus discussions when initial assessments differed. All evaluators were blinded to group allocation and time point sequence.

Statistical Analysis: REBA scores were dichotomized into "very high risk" (≥8) and "lower risk" (<8). Generalized linear mixed-effects models (GLMM) examined factors associated with very high postural risk, with random intercepts at participant level.

Results: Enhanced ergonomic training demonstrated significant improvements in postural risk over time. Very high risk prevalence (REBA ≥8) decreased significantly from 96.7% at baseline to 78.3% at 90 days (18.4% absolute reduction, 19.0% relative improvement). The improvement was more pronounced for waist-to-shoulder level tapping (93.3% to 65.0%, 30.3% relative reduction) than for knee-to-waist level tapping (100% to 91.7%, 8.4% relative reduction). Waist-to-shoulder level tapping demonstrated significantly lower odds of very high postural risk compared to knee-to-waist level tapping as demonstrated in Table 1.

Table 1. Mixed-Effects Logistic Regression Model of Factors Associated with Very High Postural Risk (REBA ≥8) in Rubber Tappers (n=30, observations=240)

	Right side			**Left side**		
Parameters	Odds Ratios	CI	p	Odds Ratios	CI	p
(Intercept)	1899.195	112.116 – 32171.501	**<0.001**	832.432	74.883 – 9253.686	**<0.001**
Time	0.97	0.953 – 0.988	**0.001**	0.973	0.957 – 0.990	**0.002**
Tapping level[a]	0.016	0.002 – 0.107	**<0.001**	0.028	0.006 – 0.135	**<0.001**
Marginal R^2 / Conditional R^2	0.422 / 0.739			0.365 / 0.702		

Tapping level[a]: Waist to shoulder (ref: knee to waist)

Conclusions: Enhanced occupational ergonomic training significantly reduces postural risk among rubber tappers. The intervention demonstrated sustained effectiveness over 90 days follow-up period, with pronounced improvements observed in waist-to-shoulder level tapping positions. However, knee-to-waist level tapping remains inherently high risk, requiring additional ergonomic interventions such as adjustable tools or alternative techniques. These findings support implementing evidence-based ergonomic training programs in agricultural occupational health initiatives and advocate for policy-level integration of postural risk assessment in national training curricula for high-risk agricultural occupations.

Study limitations include the single-site design in southern Thailand and relatively small sample size (n=30), which may limit generalizability to other rubber plantation regions. Additionally, the 90-day follow-up period, while sufficient to demonstrate sustained effects, may not capture longer-term behavioral maintenance.

Acknowledgement

We acknowledge the Rubber Authority of Thailand (RAOT) for study collaboration and the National Science, Research and Innovation Fund (NSRF) for funding support.

References

1. Varghese A, Panicker VV, *Med Lav.*, 2022; 1:13.
2. Tangadulrat N, Wattanapisitkul P, Kaewmanee T, et al., *Ind Eng Manag Syst.*, 2019; 710–718.

Additive Manufacturing of Natural Rubber Latex for Sustainable Flexible Sensors

Panithi Wiroonpochit[1*], Sasitorn Srisawad[1], Siwaporn Srimongkol[1], Sutthinee Keawmaungkom[1], Ratanon Chotima[2], Nanthiya Hansupalak[3,4]

[1] *National Metal and Materials Technology Center, National Science and Technology Development Agency, Phahonyothin Road, Pathum thani, 12120 Thailand*

[2] *Department of Chemistry, Faculty of Science, Naresuan University, Pitsanulok 65000, Thailand*

[3] *Department of Chemical Engineering, Faculty of Engineering, Kasetsart University, Bangkok 10900, Thailand*

[4] *Specialized Center of Rubber and Polymer Materials for Agriculture and Industry, Faculty of Science, Kasetsart University, Bangkok 10900, Thailand*

E-mail : panithiw@mtec.or.th

Keywords: natural rubber latex, additive manufacturing, 3D printing technology, flexible sensor, piezoresistive materials

Natural rubber (NR) latex, a renewable and highly elastic biopolymer, holds tremendous potential for the development of eco-friendly flexible and wearable sensors. However, integrating NR latex into advanced additive manufacturing has been challenging due to its colloidal nature and processing limitations. In this work, we present a novel green additive manufacturing approach — a customized vat-based 3D printing technology — specifically designed for NR latex. This innovative process enables precise, customizable fabrication while ensuring homogeneous dispersion of conductive fillers.

By incorporating conductive carbon black (CCB) up to 12 phr or acetylene black (AB) 3-12 phr as fillers into pre-vulcanized NR latex, we developed highly stretchable and sensitive piezoresistive composites. The 3D-printed NR composites demonstrated excellent mechanical properties, with elongations at break exceeding 700%, and high electromechanical sensitivity, achieving gauge factors up to 361.4 and reliable detection of small strains (<10%).

Furthermore, the sensor performance of conductive NR composites with varying AB contents was systematically investigated. The results showed that AB content significantly influenced both sensitivity and stretchability. Optimized sensors exhibited outstanding electromechanical performance, with gauge factors up to 361.4 in the strain range of 210–300%. Pre-stretching further enhanced performance by improving signal stability, reducing hysteresis, and increasing linearity (R^2 = 0.99), though with a slight reduction in gauge factor. Dynamic durability tests confirmed stable and repeatable responses over 5,000 stretching cycles, with rapid response times of 0.06–0.10 s and reliable small-strain detection, demonstrating their suitability for real-time human motion monitoring applications.

Collectively, these advancements in green additive manufacturing and conductive NR composite design establish a new pathway toward sustainable, high-performance flexible electronics and wearable devices.

Acknowledgement

This work was funded by This research has received funding support from the National Science Research and Innovation Fund (NSRF) and the National Science and Technology Development Agency (NSTDA) through the Fundamental Fund with grant no. 4707963 and IRPC Public Co., Ltd., Thailand for gifting conductive filler.

References

1. S. Srimongkol, P. Wiroonpochit, K. Utra, R. Sethayospongsa, P. Muthitamongkol, B. Methachan, N. Butsri, S. Srisawad, Polymers for advanced technology, 2022, 1-12.
2. A. Georgopoulou, S. Srisawadi, P. Wiroonpochit, F. Clemens, Polymers. 2023, 15, 2410.

Construction of recyclable rubber composites based on dynamic bonding

Yuzhu Xiong*[1]; Lingfeng Cui[1]

[1]*College of Materials and Metallurgical Engineering, Guizhou University, Guiyang, China*

*E-mail: xyzhu789@126.com

Keywords: polyurethane rubber, multiple hydrogen bonding, disulfide bonding, post-recycling reinforcement

Due to the irreversibility of the three-dimensional network structure formed through covalent cross-linking, it is difficult to recycle the cross-linked polyurethane rubber, leading to environmental pollution and unsustainable industrial development. The construction of covalent adaptive networks (CANs) in polyurethane rubber systems has proven to be a straightforward and effective strategy for enabling self-healing and recyclability in thermoset polyurethane rubber materials [1]. However, it is worth noting that during the heat recycling process of CAN polyurethane rubber, almost unavoidable side reactions such as oxidation and permanent cross-linking occur, which lead to the degradation of mechanical properties post-reprocessing [2], and the mechanical properties deteriorate as the number of operations increases. In fact, most of the previous research has reported recycling efficiencies <80% for CAN elastomers [3-5], resulting in unsatisfactory performance after recycling for sustainable use. In addition, at this stage, more attention is paid to how to improve the mechanical properties of polyurethane rubber, and there are few reports on how to improve the recycling performance of CAN polyurethane rubber materials. Therefore, it is a challenge to develop a polyurethane rubber material with recycling and re-enforcement functions in the field of polymer materials, which has generally enhanced mechanical properties (tensile strength, elongation at break, modulus, toughness) after recycling process.

The tensile strength of APSilica/IPU without any addition (0wt%-APSilica/IPU) was recorded at 0.37 MPa with an elongation at break of 221%. Upon increasing the APSilica content, significant enhancements in tensile strength, modulus, and toughness were observed. Specifically, the addition of 14.5wt% (2 g) of APSilica resulted in tensile strength, modulus, and toughness of 2.8 MPa, 3.1 MPa, and 4.5 MJ/m³, respectively, representing increases of 654%, 667%, and 864% compared to 0-APSilica/IPU. These improvements are attributed to the reinforcing effects of APSilica, which not only enhances the material's mechanical properties but also increases the cross-linking density and the content of multiple hydrogen bonds within the system, contributing significantly to mechanical performance enhancement.

The changes in surface scratches were monitored using an optical microscope. Significant contraction of the scratches on sample 14.5wt%-APSilica/IPU was observed after 8 hours of healing at 80 °C, demonstrating the composite's robust healing capability. Furthermore, intact thin sections can be prepared by cutting the sample and subjecting it to a 45-minute reshaping treatment at 100 °C and 10 MPa, demonstrating the sample's reprocessability. The mechanical properties of the samples exhibited an upward trend with each cycle of processing. Compared to the initial sample, after two

cycles of processing, the mechanical properties of the samples were generally enhanced (tensile strength increased by 16.2% to 3.0 MPa, elongation at break increased by 9.7% to 342%, modulus increased by 33.6% to 3.3 MPa and toughness increased by 34.1% to 5.9 MJ/m^3). This enhancement in mechanical properties is attributed to the breakage of disulfide bonds which generate sulfur radicals, reacting with the side vinyl groups on the IPU molecular chain to form a denser cross-linking network at elevated temperatures.

x-APSilica/IPU polyurethane rubber composite system can undergo recycling through an enhanced mechanism, as depicted in Figure 1 During the recycling process, disulfide bonds break at elevated temperatures to form sulfur radicals. These radicals predominantly engage in two reaction processes: (i) they reconnect to form new disulfide bonds, thereby preserving the recyclability of the original samples; and (ii) they establish new cross-linking points with the side chains of the polymer, thus increasing the cross-linking density of the system. This increase in cross-linking density is primarily responsible for the enhanced mechanical properties of the recycled polymer materials, which is crucial for cyclic processing.

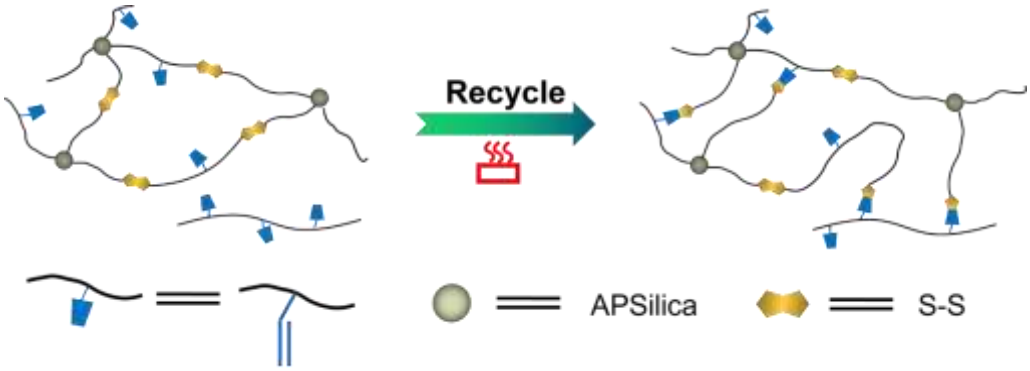


Figure 1. x-APSilica/IPU polyurethane rubber composite system recyclable enhancement mechanism

References

1. Ou, Z.; Peng, W.; Rong, M.; Zhang, M. *Macromolecules.* **2022**, 55: 262-269.
2. Trinh, B.; Owen, P.; Vanderheide, A.; Gupta, A. Mekonnen TH. *ACS Appl. Mater. Interfaces.* **2023**, 5: 8890-8906.
3. Billa, S.; Vislavath, P.; Bahadur, J.; Rath, S.; Ratna, D.; Manoj, N.; Chakraborty, B. *ACS Appl. Polym. Mater.* **2023**, 5: 3079-3095.
4. Liu, W.; Huang, J.; Gong,Z.; Fan, J.; Chen, Y. Healable. *Polymer.* **2022**, 252, 124900.
5. Wang, F.; Zhang, C.; Han,Y.; Yi, G.; Mao, Z.; Li, J.; Li, Z.; Wang, W. J. *Polym. Sci.* **2024**, 62: 2147-2156.

International Rubber Conference 2025 (IRC2025)
1-3 December 2025 @ BITEC, Bangkok, Thailand

Natural rubber latex-based tissue engineering: The pioneering advances in material for sustainability

Masami Okamoto [1]

[1] *Toyota Technological Institute, 2-12-1 Hisakata, Tempaku, Nagoya 468 8511, Japan*

okamoto@toyota-ti.ac.jp

Keywords: Natural rubber latex, Biocomposite, Cartilage, Mechanical properties, Normoxia

Our research has explored the sustainability of tissue engineering and regenerative medicine (TERM). The TERM has been studied for many years by biomedical engineers and scientists with the primary aim of improving patients' quality of life (QOL) and finding a permanent cure for their disease.

Unfortunately, the focus during this period was on the application of the materials developed, rather than their source. Researchers now recognize that it is possible to explore sources of sustainable and environmentally friendly natural-based materials with similar/better performance than those being sought. It is time to reflect on previous study and make research on TERM more circular, despite the regulatory challenges of FDA approval. Our research aims to shift the TERM paradigm toward sustainable and circular biomaterial sourcing.

Biomaterials with various functions are important not only for applications in the fields of TERM, but also for the elucidation of pharmacology. The development and discovery of new biomaterials is constantly being driven by researchers around the world. Natural rubber latex (NRL) is derived from the lactiferous sap of the *Hevea brasiliensis* (para rubber tree) and has been used in traditional medicine as vegetal-origin functional biomaterials [1].

To further the knowledge of NRL nanoparticles in TERM, we investigated the chondrogenic ability of NRL nanoparticles in vitro on human mesenchymal stem cells (hMSCs) under hypoxia. NRL (solid content of 35.3 wt%) nanoparticles enhanced the cell proliferation of hMSCs. The results demonstrate a higher biocompatibility of NRL nanoparticles without a significant reduction in the viability of hMSCs [2].

We have successfully fabricated the cartilage/NRL biocomposites via hMSC spheroids under hypoxic conditions, where the administration of NRL nanoparticles shows the suppression of spheroid contraction due to cellular proliferation of hMSCs. The NRL nanoparticles were found to act as a major component providing surface heterogeneity of the spheroid, resulting in a mechanically stable structure with an 8-fold higher modulus compared to the control (without NRL), as revealed by atomic force microscopy microindentation (refer to the reference [3]).

In addition, genetic analysis revealed that NRL particles also induce cartilage differentiation of hMSCs. In hypoxia the expression of SRY-box 9 (SOX9) gradually increases throughout 21 days of culture (Fig. 1a). However, no statistical difference between spheroids with and without NRL is observed. The expression of Aggrecan is over 6-fold at 14 days in comparison to control (Fig. 1b). This suggests that the cartilage cultured with NRL nanoparticle produce a large amount of aggrecans. The collagen type-II (Col-II) is up-regulated at day 14. The expression level in NRL-loaded spheroids

is more than 4-fold in comparison with the control (Fig. 1c). The expression level of SOX9, aggrecan and Col-II are higher in the spheroid, indicating that chondrogenic differentiation is successfully induced with the administration of NRL nanoparticles under hypoxic condition. The expression level in hypoxic microenvironment is significantly greater than that observed under normoxis (Fig. 1d-f), indicating that the chondrogenesis of hMSCs is promoted in the hypoxic microenvironment.

Our group concluded that NRL particles are biomaterials that can be applied to bio-engineering. We succeeded in fabricating cartilage/NRL biocomposite materials by forming hMSC spheroids for the first time. Major breakthroughs in latex technology are yet to come. Further efforts are needed to investigate the viscoelastic and long-term properties of the biocomposites for cartilage tissue.

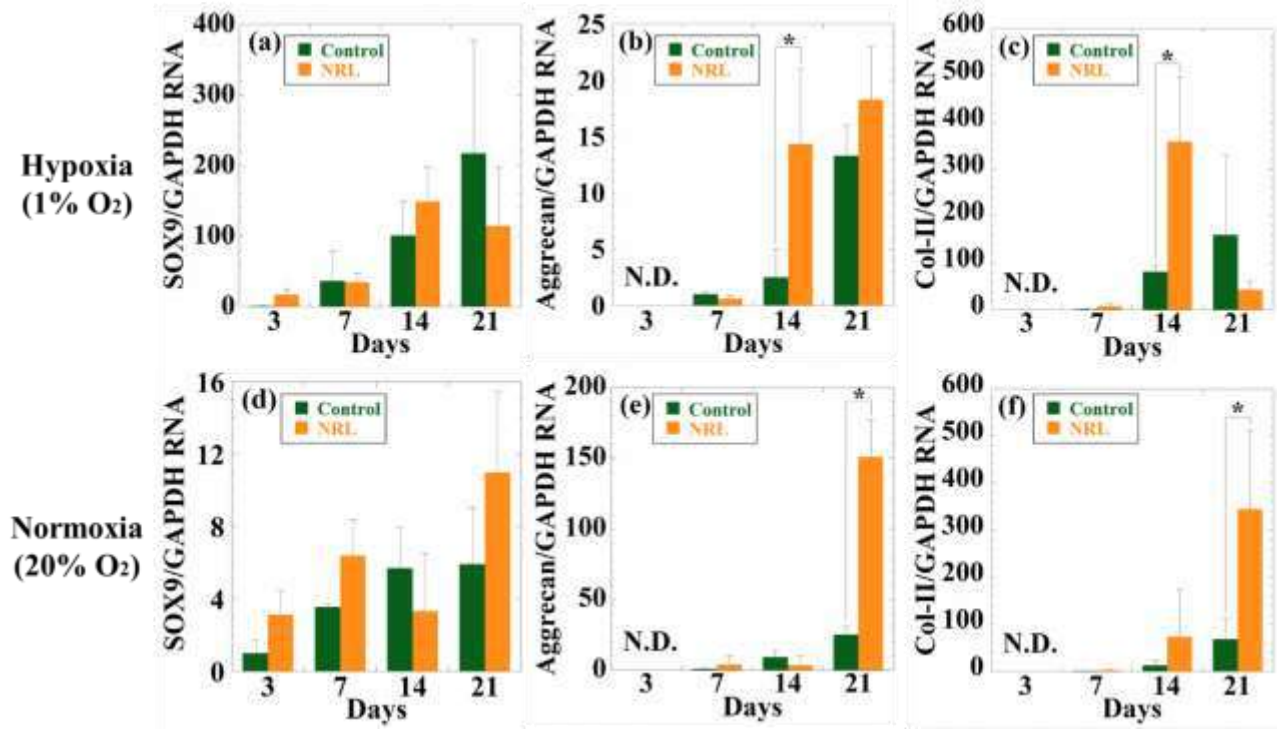


Figure 1. RT-PCR analysis of the chondrogenic gene expression of (a) and (d) Sox9, (b) and (e) aggrecan, (c) and (f) Col-II, for hMSCs cultured with NRL nanoparticles of 0.32 mg/mL at different time interval (3, 7, 14, and 21 days) under both normoxic (a–c) and hypoxic (d–f) conditions. Data were normalized to those of control at day 3 for (a and d) or at day 7 for (b, c, e, and f) and were expressed as mean ±S.D. (n=3).
* Indicates $p < 0.05$. N.D. indicates data were not detected.

Acknowledgement

This work was supported by the KAKENHI of the Ministry of Education, Sports, Science and Technology, Japan.

References

1. Gurib-Fakim A, *Mol Aspects Med.* **2006**; 27(1): 1.
2. Kinoshita M, Okamoto Y, Furuya M, Okamoto M, *Mater. Today Chem.*, **2019**; 2: 315.
3. Okamoto Y, Kinoshita M, Okamoto M, *Nanocomposites*, **2020**; 6: 137.

International Rubber Conference 2025 (IRC2025)
1-3 December 2025 @ BITEC, Bangkok, Thailand

Multidimensional rubber composite utilizing lignin as a bio-filler

S. Amit[1], G. Biswanath[1], C. Jagannath[1], M. Rabindra[1], G. Prasenjit

[1]*Hari Shankar Singhania Elastomer and Tyre Research Institute, India*

e-mail address of the presenting author (amit.sen@jkmail.com)

Keywords: Sustainability and Circular economy, scalable lignin-rubber production, eco-friendly material

The rubber industry's reliance on petroleum-based filler materials significantly contributes to CO_2 emissions and resource depletion, posing a substantial hindrance to sustainability and the circular economy. Consequently, the industry is exploring bio-based alternatives that maintain performance while reducing environmental impact. Lignin, a renewable, aromatic polymer derived from lignocellulosic biomass, is a promising candidate. Its abundance, high carbon content, renewability, and antioxidant and mechanical properties make lignin an attractive resource for rubber reinforcement. However, current lignin incorporation methods are often energy-intensive and rely on unsustainable chemicals and processes, limiting industrial adoption. Also, the incorporation of lignin into rubber poses processing challenges, primarily due to its limited compatibility with the rubber matrix. Its inherent polarity and strong self-interactions result in poor dispersion and weak interfacial adhesion, adversely affecting the performance properties of the compound. This research aims to overcome these barriers by developing a novel approach to integrate lignin nanoparticles into rubber composites. A controlled liquid phase mixing technology enables us to seamlessly incorporate 20-30 phr of lignin without sacrificing major mechanical properties. With an 11% higher bio-material content, a 17% higher elongation at break, and a 12% benefit at tanδ@70 °C, a significant improvement in lignin dispersion was achieved. The effective interaction of lignin-rubber alleviates the potential issues related to lignin utilization in terms of volume and application areas, thereby promoting lignin on a multidimensional scale and guiding the industry toward sustainability and an environmentally conscious model.



Figure 1: FESEM image showed that Trial 2 has comparable filler dispersion to the reference.

Acknowledgement

The authors sincerely thank Hari Shankar Singhania Elastomer and Tyre Research Institute (HASETRI), Mysore, for their technical support, research facilities, and financial support, and to the conference organizing committee for this opportunity to contribute to balancing nature and innovation for a sustainable future.

International Rubber Conference 2025 (IRC2025)
1-3 December 2025 @ BITEC, Bangkok, Thailand

Sustainable Rubber Nanocomposites for Tyre Application by Silica Hairy Nanoparticles Fillers

B. DI CREDICO[1], L. TRIPALDI[1], L. TADIELLO[2], L. CONZATTI[3], L. GIANNINI[2], M. D'ARIENZO[1], A. CAUSA[2], S. MOSTONI[1], P. STAGNARO[3], R. SCOTTI[1]

[1] *Dept. of Materials Science, INSTM, University of Milano-Bicocca, Via R. Cozzi, 55, 20125 Milano, Italy.*

[2] *Pirelli Tyre SpA, Viale Sarca, 222, 20126 Milano, Italy.*

[3] *Istituto di Scienze e Tecnologie Chimiche (SCITEC) "G. Natta", Consiglio Nazionale delle Ricerche (CNR), Via De Marini 6, 16149 Genova, Italy*

barbara.dicredico@unimib.it

Keywords: Silica, Hairy Nanoparticles, Rubber Nanocomposites, Rolling Resistance, Green Tyre.

The current open challenge of the tyre industry is to identify possible design strategies to reduce the environmental impact throughout the life cycle of tyre using environmentally friendly materials, also able to reduce energy consumption and CO_2 emissions. To design sustainable rubber nanocomposites (NCs), the reinforcement effect should go hand in hand with the formation of an extended percolative filler network, a good filler dispersion and distribution, and an effective interaction of fillers with rubber, producing filler network structures. This has important technical implications on the dynamic loading of tyre materials, especially for the reduction of rolling resistance, directly linked to fuel efficiency and emission reduction. Consequently, despite the performing and established use of silica as a reinforcing filler in rubber NCs, alternative fillers are considered to develop a more sustainable tyre [1].

To achieve this objective, our strategy has been to exploit the effect of silica fillers self-assembly in anisotropic structures with the purpose of obtaining rubber materials having lower Payne effect and consequently low hysteresis. To induce the formation of the self-assembled anisotropic fillers superstructure, we embedded in a rubber matrix the silica hairy nanoparticles (HNPs) [2], which consist of a core of silica surrounded by end-grafted polymer chains, ranging from low to high molecular weight. This design imparts tailored surface reactivity to the silica NPs for improved compatibility with rubber, eliminating the need of traditional coupling agents.

SiO_2 HNPs, having polybutadiene (PB) chains as polymeric brushes, were prepared with different degrees of PB grafting density (Figure 1). The structure, morphology and surface chemistry of so-called SiO_2-HNP_X (X = 3, 4, 6 wt% of PB) were extensively investigated by multi-technique analysis. In particular, small-angle X-ray scattering (SAXS) analysis demonstrated that NP size increases from 27 to 29 till 31 nm after the SiO_2 functionalization with PB. Thus, rubber NCs were prepared by melt mixing the styrene-butadiene rubber (SBR) and SiO_2-HNP_X fillers, without using silane coupling agents, exploiting the compatibilizing effect of macromolecular PB shell. The specific organization of SiO_2-HNPs within the polymer matrix was inspected by transmission electron microscopy (TEM) and related to the mechanical properties of rubber NCs investigated through dynamic-mechanical tests. These reveal that moderately strong rubber−filler interactions exist in SBR NCs, which result in a high degree of structural order and a significant percolative HNPs network.

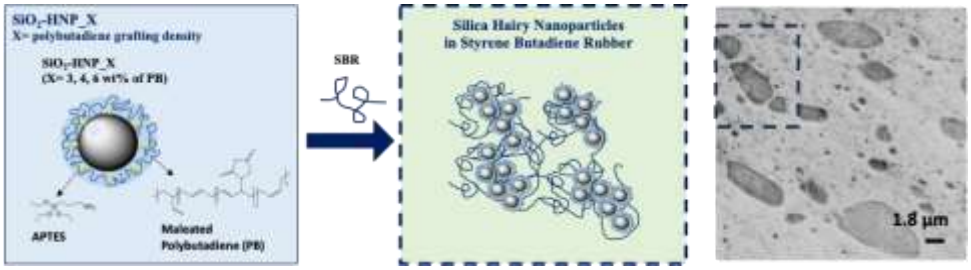


Figure 1. Schematic representation of the HNPs synthesis and their self-assembly in SBR NCs

It has been demonstrated that interfacial polymer coating of HNPs can tune the matrix chain confinement and thus, they appear to be a relevant way to reduce the energy dissipation of a compound for tyre use, either decreasing delta G' or decreasing tanδ value (Table 1), both strong predictors of the rolling resistance coefficient which determines vehicle energy consumption and CO_2 emissions. In particular, the V-SiO_2-HNP_6/SBR NC exhibited the highest reinforcement strength, largest stress at break and lowest elongation at break, while the V-SiO2-HNP_4/SBR NC exhibited the optimum balance between hysteresis and reinforcement.

Table 1. Values of G'(6%), Δ(G′(0.4%)-G′(10%)) and tanδ(6%) for V-SiO_2-HNP_X/SBR.

Sample	G′(6%) (MPa)	Δ(G′(0.4%)-G′(10%)) (MPa)	tanδ (6%)
V-SiO_2-ST/SBR	1.168 (± 0.05)	0.102 (± 0.02)	0.169 (± 0.01)
V-SiO_2-HNP_3/SBR	1.163 (± 0.05)	0.238 (± 0.02)	0.170 (± 0.01)
V-SiO_2-HNP_4/SBR	1.189 (± 0.05)	0.222 (± 0.02)	0.139 (± 0.01)
V-SiO_2-HNP_6/SBR	1.300 (± 0.05)	0.173 (± 0.02)	0.165 (± 0.01)

Thus, silica HNPs can build energy-dissipative anisotropic structures which act as additional cross-linking junctions reducing the chain relaxation and consequently enhancing the chain deformation. The tuning of NPs surface chemistry allows in principle to design an hoc modification system for any possible dienic rubber formulation, just by optimizing the choice of oligomer and degree of modification [3].

Acknowledgement

Laura Tripaldi thanks CORIMAV ("Consortium for the Research of Advanced Materials between Pirelli and Milano Bicocca University) for its support within the Doctoral Program

References

1. Di Credico B, Cobani E, Callone E, Conzatti L, Cristofori D, D'Arienzo M, Dirè S, Giannini L, Hanel T, Scotti R, Stagnaro P, Tadiello L, Morazzoni F, *Appl. Clay Sci.*, 2018, 152: 51.
2. Tripaldi L, Callone E, D'Arienzo M, Dirè S, Giannini L, Mascotto S, Meyer A, Scotti. R, Tadiello L, Di Credico B, *Soft Matter*, 2021, 17: 9434.
3. Di Credico B, Tripaldi L, Tadiello L, Conzatti L, Giannini L, D'Arienzo M, Causa A, Mostoni S, Stagnaro P, Scotti. R, *Mater. Today Chem.*, 2025, 45: 102678.

International Rubber Conference 2025 (IRC2025)
1-3 December 2025 @ BITEC, Bangkok, Thailand

A Natural Rubber-Based Stretching Band and Its Machine Learning-Validated Muscle Tension Mitigation

N. SAMERPHOB[1], N. JEHSOH[2], and N. HAYEEMASAE[2]

[1]*Division of Health and Applied Sciences, Faculty of Science,*

Prince of Songkla University, Hat Yai, Songkhla, 90112 Thailand

[2] *Department of Rubber Technology and Polymer Science, Faculty of Science and Technology, Prince of Songkla University, Pattani Campus, Pattani, 94000, Thailand*

e-mail: nabil.h@psu.ac.th

Keywords: natural rubber, stretching band, office syndrome, electromyography, heart rate variability

Natural rubber (NR) is an invaluable material and is known to have great properties such as high tensile strength, elasticity, abrasion resistance, and to name a few. This has brought NR into many applications. One of them is the exercise devices such as exercise bands, grips, mats, and others where the non-slip, and cushioned surfaces are concerned. It is well-known that these materials nourish a healthy body for the users. However, the physical responses while using these products are still largely unexplored. This study produced a few examples of exercise devices made from natural rubber. The efficiency was monitored through the mechanical properties of materials and the physical responses of volunteered subjects before, during, and after using the materials. The physical tracking covered the heart rate, Electromyography (EMG), Electroencephalography (EEG), Electrocardiography (ECG), hand strength, cognitive test, and satisfaction questionnaires [1]. The representatives of the NR products are the rubber stretching bands. The rubber stretching band was developed to prevent injury due to office syndrome

Here, the development initiated with formulating latex-based rubber using different rubber formulations having various crosslink densities and moduli. Each formulation was evaluated for mechanical properties including the crosslinking density, tensile strength, modulus, tear strength and set property. Subsequently, the optimized formulation was used to fabricate elastic bands, which were then evaluated for their effect on Sternocleidomastoid (STN), Trapezius (TRP), and Deltoid (DEL) muscle tension in healthy subjects during office-based task simulation. Control participants continued to sit for a period, while movement participants broke into the same posture for natural rubber bands, and commercial bands that were broken and used for exercise. Muscle activation was assessed using surface electromyography (sEMG) and analyzed with a Random Forest machine learning model [2].

Figure 1 shows the raw EMG signals of subjects at STN, TRP, and DEL over various sample types. A high signal response indicates the muscle contraction during applied activities. Using the NR stretching band showed a high degree of contraction while using NR stretching band, indicating the quick response when having simulated tasks. A nested analysis of ANOVA was conducted to examine how break types and task conditions affect muscle activity. The results showed a statistically significant effect of task type on DEL muscle activity ($F(4,159)=18.175$, $p < 0.001$). The Tukey post hoc test showed that all simulated office tasks caused a significant increase in DEL muscle activation when compared to the resting state ($p < 0.001$). In the control group, proofreading ($p=0.001$), typing ($p=0.002$), and creative tasks ($p=0.012$) led to significantly higher deltoid muscle activation than at the start of the period. The arithmetic task did not show a significant change in deltoid muscle activity. Text typing ($p=0.005$) caused a significant increase in deltoid muscle activity compared to the starting period for the participants in the movement group. When compared to resting, both proofreading and

typing ($p < 0.001$) significantly increased deltoid muscle activity among participants in the commercial rubber group. In the NR group, significant increases in deltoid muscle activity were observed for typing ($p=0.012$) and proofreading ($p=0.013$) significantly higher muscle activity than rest. Other tasks within this group were not significantly different. The study confirmed through sEMG analysis that NR bands provides resistance comparable to a standard spring stretcher, ensuring the modified band offers both therapeutic muscle activation and physiological benefits. This study provides strong evidence that using NR bands is an effective way to combat the physiological stresses of a sedentary office job.

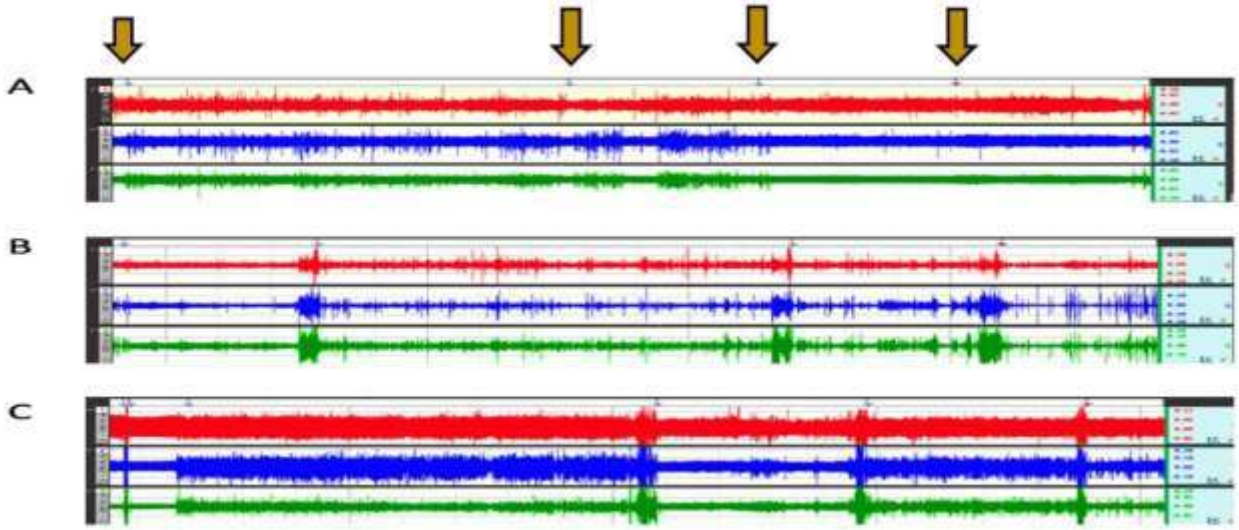


Figure 1. Raw EMG signals of subjects at STN, TRP and DEL over various sample types; Control (A), Normal movement (B), and NR stretching band (C).

Acknowledgement

The authors would like to express their gratitude to the grant sponsors through the grant number SCI6701108S.

References

1. Kwak C-J, Kim YL, Lee SM. (2016). Journal of Physical Therapy Science, 2016; 28(11): 3189–3196.
2. Jaroenngarmsamer P, Keawtongpan B, Rojanabenjakun P, Ounprasertsuk J, Benjanirat T, Krutchangthong S, Choawai S. Systematic Reviews in Pharmacy, 2020; 11: 10.

International Rubber Conference 2025 (IRC2025)
1-3 December 2025 @ BITEC, Bangkok, Thailand

Thermoset–Rubber 2K Composite Systems: Material Combinations and Interfacial Reactions in a One-Step Injection Molding Process

Florian Löhr[1], Elmar Moritzer[1], Benjamin Klie[2], Ulrich Giese[2]

[1]*Paderborn University, Warburger Straße 100, 33100 Paderborn, Germany*

[2]*Deutsches Institut für Kautschuktechnologie e. V., 30519 Hannover, Germany*

Corresponding author: florian.loehr@ktp.uni-paderborn.de

Keywords: thermoset–elastomer, 2K injection molding, interfacial adhesion, BMC, peel strength

Multicomponent composites consisting of hard and soft components are an essential part of modern product development. The production of hard–soft components by two-component (2K) injection molding is an established method for integrating functions into polymer components [1]. While thermoplastic–elastomer systems are widely established, thermoset–elastomer composites provide additional potential where particularly high resistance to temperature, media and creep is required [2,3]. Examples include components with integrated sealing or bearing functions in media-carrying systems or vibration-loaded applications. Two-component injection molding with direct interfacial adhesion increases process reliability and reduces the need for additional processing steps or external additives such as applied adhesion promoters [6]. Therefore, the aim of this work is the development of thermoset–elastomer composites produced in the 2K injection molding process without additional adhesion-promoting layers. The investigated material pairings have so far been insufficiently studied, particularly in the context of a one-step process with chemically active interfacial reactions [4,5]. An additional advantage of this approach lies in sustainability: direct adhesion in a one-step injection molding process replaces adhesives, mechanical joining methods and additional processing steps. This shortens the process chain and reduces the consumption of material and energy [6].

The experiments were carried out on the basis of a design of experiments (DoE). On the thermoset side, various reinforced phenolic molding compounds (PF), an epoxy molding compound (EP) and several bulk molding compounds (BMC) with different glass fiber contents were processed. In the BMC systems, two approaches were pursued: the variation of the release agent content and the control of the reaction kinetics through additives to improve interfacial compatibility. The rubber formulations investigated were natural rubber (NR, vulcanization time tc90: 11.5/6 min at 150/160 °C) with a shorter incubation time and hydrogenated nitrile butadiene rubber (HNBR, tc90: 17/9/3 min at 150/160/180 °C) with higher viscosity. The NR formulation also contained adhesion additives (Cohedur RS and A200), which form an in-situ resin during vulcanization and thus improve interfacial bonding. The process parameters included mold temperatures of 150–180 °C, elastomer injection speeds of 4–8 cm³/s, holding pressures of 150–450 bar and elastomer heating times of tc90 + 3 to 6 min.

The adhesion of the composites was characterized using peel tests. Depending on specimen geometry, both a 90° peel test according to VDI 2019 (Zwick Z010, v = 100 mm/min, width 19.75 mm, length 135 mm) and an alternative setup with an initial angle of approx. 110° (Zwick Z010, v = 100 mm/min, width 24.3 mm, length 44.5 mm) were used. In addition, fracture surfaces were analyzed to differentiate between adhesive and cohesive failure (Figure 1).

The results show that interfacial adhesion is strongly influenced by material selection and process parameters. With NR in combination with four PF grades, peel strengths between 1.1 ± 0.1 N/mm (n=5) and 10.3 ± 0.5 N/mm (n=5) were achieved – a relative increase of more than

800 %. Both adhesive and cohesive failure modes were observed. With HNBR, peel strengths of up to 13.4 ± 1.9 N/mm (n=4) were obtained at 160 °C. However, raising the mold temperature to 180 °C reduced adhesion to a maximum of 7.3 ± 1.5 N/mm (n=4; minimum 1.0 ± 0.1 N/mm, n=5), while epoxy molding compounds showed no adhesion under the same conditions. Initial experiments with BMC showed basic adhesion to both elastomers. With HNBR (maximum 3.1 ± 0.3 N/mm, n=5), more than twice the peel strength was achieved compared to NR (maximum 1.3 ± 0.1 N/mm, n=5). Adhesion was found to be strongly dependent on the adjusted curing kinetics.



Figure 1. Failure types in peel tests: (a) adhesive, (b) transition with rubber film, (c) cohesive with rubber residue

This study provides initial design guidelines for thermoset–elastomer composites without external adhesion promoters, with further improvements expected from tailored formulations and kinetic analyses.

Acknowledgement

The authors would like to thank the German Aerospace Center (DLR) for the financial support of the project (01L22604N), which is funded by the Federal Ministry of Economics and Climate Protection (BMWK). In addition, we would like to thank our cooperation partner, the German Institute of Rubber Technology, for the good collaboration.

References

1. Lange C, Hungerkamp T, Thermoplaste und Elastomere gemeinsam spritzgießen; Kunststoffe 12/2001; S. 36-42
2. Hopmann C, Menges G, Michaeli W, Mohren, P.: Spritzgießwerkzeuge – Auslegung, Bau, Anwendung. Carl Hanser Verlag, 7., neu bearbeitete Auflage, München, 2018
3. Palik M, Vernetzte Präzision – Duroplaste im Automobilbau. Carl Hanser Verlag, München, 2008
4. Thust T, Rezeptur- und Prozesseinflüsse auf das Haftverhalten beim Mehrkomponentenspritzgießen von Thermoplast-Elastomer-Verbundbauteilen am Beispiel PA6.6 – HNBR; Dissertation, Martin-Luther-Universität Halle-Wittenberg; 2014
5. DKG21. Entwicklung hochtemperatur- und medienbeständiger 2-Komponenten-Verbundwerkstoffe aus Duroplasten und Elastomeren zum Einsatz im Motorraum IGF-Vorhaben Nr. 20553N. Techn. Ber. Deutsche Kautschuk-Gesellschaft e. V. (DKG), 2021
6. Diedrich K M, Der Haftvermittlerfreie Kunststoff-Kautschuk-Verbund – Vorteile für Hersteller und Verbraucher; ACS Rubber Division Meeting; Savannah; 29. April - 01. Mai 2002

Advancing 3D Printing with Biobased Rubber: Photocurable and Extrudable Platforms for Functional Soft Materials

N. RISANGUD[1], Z. A. LAKSANAA[1], M. S. ARKANA[1], S. THONGKHAM[2]

[1]*Petroleum and Petrochemical College, Chulalongkorn University, Bangkok, Thailand*

[2]*National Nanotechnology Center, National Science and Technology Development Agency, Pathumthani, Thailand*

e-mail address of the presenting author (nuttapol.r@chula.ac.th)

Keywords: Rubber Composites, Biopolymer, Additive Manufacturing, Vat Photopolymerization, Fused Deposition Modelling

The integration of biobased elastomers into additive manufacturing (AM) presents an attractive route for the sustainable production of soft, functional components. However, their implementation across light-assisted and extrusion-based platforms remains constrained by material incompatibilities, limited mechanical performance, and insufficient scalability. This study presents a material strategy designed to enable biobased rubber composites for vat photopolymerization and fused deposition modelling (FDM), with an emphasis on mechanical integrity, printability, and cytocompatibility.

In this work, two distinct classes of rubber-based materials were formulated. The first system comprises a photocurable resin from unmodified natural rubber latex (NRL) reinforced with titanium dioxide nanoparticles, utilizing TPO photoinitiator to trigger photopolymerization, followed by post-curing at 60 °C for 24 hours. The second involves a thermoplastic composite based on poly(butylene succinate) (PBS) and epoxidized natural rubber (ENR) with talc filler, designed for low-temperature FDM. Both were systematically characterized in terms of rheology, thermal and mechanical behavior, morphology, and *in vitro* cytocompatibility using L929 fibroblasts (MTT assay).

Both systems demonstrated strong printability, mechanical performance, and cytocompatibility. The latex resin produced high-resolution, stretchable DLP constructs with close CAD fidelity (Figure 1A), while PBS/ENR filaments yielded ductile, low-warping lattices with high geometric accuracy (Figure 1B). The photocurable latex resin enabled DLP fabrication of elastomeric constructs with a tensile strength of ~1450 kPa, a modulus of ~700 kPa, and an elongation of more than 1200%. Notably, TiO_2 enhanced curing depth and mechanical reinforcement, with printed specimens showing dimensional errors of ±5–13% relative to the CAD design. Besides, the PBS/ENR composites exhibited balanced performance, with a tensile strength of ~14 MPa, a modulus of ~120 MPa, and an elongation of ~216%. Indeed, cytocompatibility was excellent, with cell viability exceeding 96% across all formulations.

Taken together, these findings demonstrate the versatility of rubber-based composites as multifunctional materials for both vat photopolymerization and extrusion-based AM platforms. By enabling compatibility across diverse printing modalities, the proposed systems establish a foundation for next-generation biomedical devices, orthotic insoles, and soft robotics, while addressing sustainability and performance requirements for scalable manufacturing.

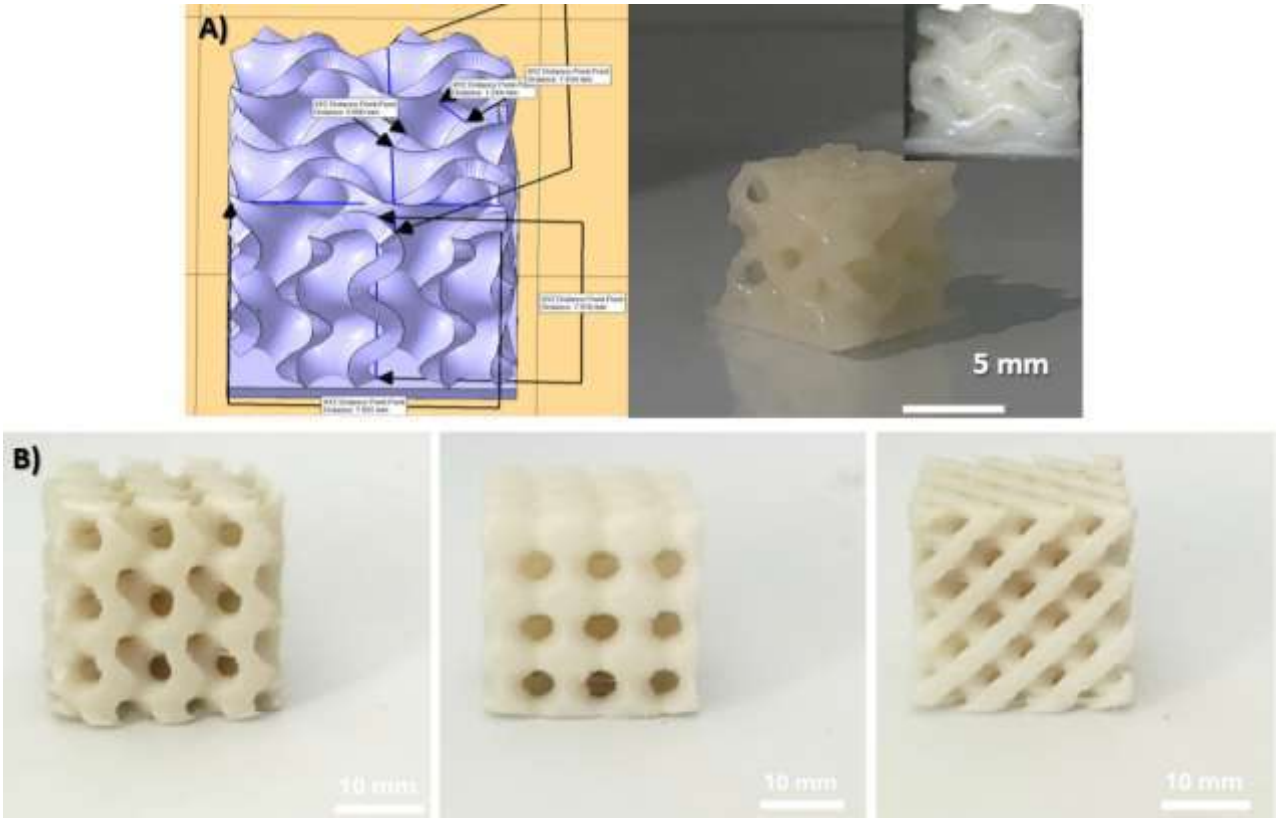


Figure 1. (A) Computer-aided design (CAD) model of a gyroid structure (left), and the corresponding 3D-printed construct using the photocurable natural rubber latex (PNLR) formulation (right) and (B) Photographs of 3D-printed lattice structures based on TPMS geometries, fabricated using PBS/ENR composite filaments *via* FDM. From left to right: Gyroid, Primitive, and Diamond structures.

Acknowledgement

This work was financially supported by the Rubber Authority of Thailand (RAOT).

International Rubber Conference 2025 (IRC2025)
1-3 December 2025 @ BITEC, Bangkok, Thailand

Potential of low-temperature vulcanized natural rubber latex for antimicrobial applications

Rawiporn PROMSUNG[1], Nussana LEHMAN[1], Ladawan SONGTIPYA[2], Ekwipoo KALKORNSURAPRANEE[1]

[1] *Division of Physical Sciences, Faculty of Science, Prince of Songkla University, Hat-Yai, Songkhla 90110, Thailand.*

[2] *Center of Excellence in Bio-based Materials and Packaging Innovation, Faculty of Agro-Industry, Prince of Songkla University, Hat-Yai, Songkhla, 90110, Thailand*

e-mail address of the presenting author (rawiporn.p@psu.ac.th)

Keywords: Natural rubber latex, Antimicrobial, Cinnamon oil, Glutaraldehyde, Low-temperature curing

Recently, with growing concerns over health, infection control, and the spread of antimicrobial-resistant pathogens, antimicrobial materials have gained significant attention not only in hospitals and healthcare environments but also in laboratories, home uses, and various non-medical sectors including, public transportation, food packaging and smart textiles. Their functionality is achieved through the incorporation of antimicrobial agent into surfaces or base materials like polymers, textiles and ceramics [1]. The most commonly used antimicrobial agents are silver nanoparticles, copper, zinc oxide, or organic essential oils. Cinnamon oil is one of the antimicrobial essential oils and is used in culinary and traditional medicine practices. It is obtained from the inner bark of cinnamon trees and contains cinnamaldehyde, cinnamic acid, and cinnamate, which are responsible for its antimicrobial activities [2]. Natural rubber (NR) becomes an attractive elastomeric polymer for flexible antimicrobial materials due to its standing properties such as high elasticity, elongation at break, resilience and strength. However, to achieve a NR product with high performance, NR typically requires high-temperature vulcanization (>100 °C) to achieve effective crosslinking by using the conventional sulfur curing agent. Nevertheless, with this high temperature, the essential oil might evaporate and cannot be used as an antimicrobial material [3].

In this present work, low-temperature vulcanization of NR latex has been performed at 50ºC by using glutaraldehyde (GA) as a curing agent. The antimicrobial material base-NR latex was prepared by incorporating cinnamon oil (CO) as an antimicrobial agent. The properties of cured antimicrobial NR-CO were compared with those of the uncured at 15 %wt of CO content. The antimicrobial NR-CO was verified its antimicrobial activity against *Escherichia coli (E. coli)*, *Staphylococcus aureus (S. aureus)* and *Aspergillus niger (A. niger)*. Mechanical properties in terms of modulus, tensile strength and elongation at break were also investigated using tensile testing.

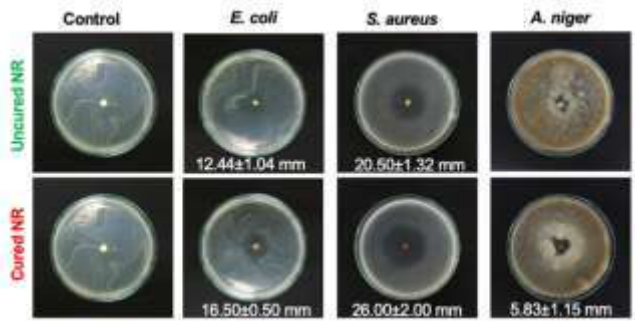


Figure 1. The qualitative antimicrobial activities against *E. coli*, *S. aureus* and *A. niger* of uncured and cured NR films filled with 15 %wt cinnamon oil and controlled samples.

As a result, the qualitative clearing zone or inhibition zone after the microbial infection is examined, as seen in Figure 1. It is observed that the controlled NR sample, which is an NR film without CO showed no clear zone for both uncured and cured NR samples. In contrast, the clearing zone can be clearly observed after the incorporation of 15 %wt CO into the NR especially the antimicrobial activity against *E. coli* and *S. aureus*. This indicates the antibacterial performance of the films by disrupting bacterial cell membranes, altering lipid profiles, inhibiting enzymes, and interfering with cell division. Moreover, it was clearly seen that the cured NR films exhibited better antimicrobial performance than the uncured NR films by increasing the clearing zone of 32 % for *E. coli*, 26 % for *S. aureus* and 100 % for *A. niger*. This might be due to the crosslinking of the NR molecular chain by GA curing agent. The crosslinking of the NR entrapped cinnamaldehyde which is the main component of CO and prevented the evaporation of CO during the preparation process [4, 5], leading to better antimicrobial performance of the cured NR films.

In addition, the overall mechanical properties of the uncured and cured NR films were summarized in Table 1. It was found that crosslinking NR by the GA curing has strongly affected the mechanical properties of NR films in terms of their modulus and tensile strength. The cured NR-CO15 film showed a tensile strength of 0.87 MPa and an elongation at break of 446%. Nevertheless, incorporation of 15 %wt CO into NR matrix showed a decreasing in 100% modulus and tensile strength but increased elongation at break compared to unfilled CO.

Therefore, this work is found to be beneficial in case of NR latex film that requires antibacterial performance. The additional advantage of this system is that the curing process occurs at low-temperature using GA and it can prevent the evaporation of essential oils that possess antibacterial properties. This indicates a great opportunity to develop and manufacture the NR latex film for antimicrobial materials such as industrial coating applications, active food packaging and so on.

Table 1. Overall mechanical properties of the uncured and cured NR films.

Sample	Properties		
	100% Modulus [MPa]	**Tensile strength [MPa]**	**Elongation at break [%]**
Uncured-CO0	0.32±0.03	0.78±0.05	414±31
Uncured-CO15	0.12±0.04	0.28±0.03	434±43
Cured-CO0	1.39±0.06	3.71±0.41	316±35
Cured-CO15	0.20±0.07	0.87±0.34	446±39

Acknowledgement

This research was supported by National Science, Research and Innovation Fund (NSRF) and Prince of Songkla University (Grant no. SCI6801314S and SCI6802083S). The authors would like to express their gratitude to the Faculty of Science, Prince of Songkla University, Hat Yai Campus.

References

1. Zhang Y.B., Liu X.Y., Jiang P.P., Li W.D., Wang Y.F., *Mod. Food Sci. Technol.*, 2015; 31: 31–35.
2. Sengsuk T., Songtipya P., Kalkornsurapranee E., Johns J., Songtipya L., *Polymers*, 2021; 13: 199.
3. Promsung R., Nakaramontri Y., Uthaipan N., Kummerlöwe C., Johns J., Vennemann N., Kalkornsurapranee E., *Express Polym. Lett.*, 2021; 15: 308–318.
4. Lucas-González R., Yilmaz B., Khaneghah A.M., Hano C, Shariati M.A., Bangar S.P., Goksen G., Dhama K., Lorenzo J.M., *Food Packag.*, 2023; 35: 101026.
5. Gong C., Lee M.C., Godec M., Zhang Z., Abbaspourrad A., *Food Hydrocoll*., 2020; 99: 105316.

International Rubber Conference 2025 (IRC2025)
1-3 December 2025 @ BITEC, Bangkok, Thailand

Novel Triboelectric Nanogenerators for Self-Powered System by using Fluorinated Wasted Rubber Powders

Huiqing FAN[1], Xiaohu REN[1], Xiuze CHE[1], Yuanbiao GONG[1], Weijia WANG[1]

[1] *State Key Laboratory of Solidification Processing, School of Materials Science and Engineering, Northwestern Polytechnical University, Xi'an 710072, China*

e-mail address of the presenting author (hqfan@nwpu.edu.cn)

Keywords: Triboelectric nanogenerator, Energy harvesting, Self-powered system, Wasted rubber

Energy plays a crucial role in human life. Currently, our energy consumption primarily depends on traditional fossil fuels, which are finite and non-renewable. As we continue to exploit and deplete these fossil resources, it becomes increasingly urgent to discover new forms of energy. Mechanical energy, which is omnipresent in our daily environment, exists in a variety of forms and is less susceptible to environmental influences. It stands out as a potential energy source that could be harnessed on a large scale. However, the methods for collecting mechanical energy are largely based on conventional electromagnetic generators. These devices struggle to effectively capture low-frequency and random energy from the environment due to their inherent operational principles. Enter the triboelectric nanogenerator, a novel energy collection device that has emerged as a promising avenue for micro-nano mechanical energy harvesting. It boasts several advantages, including high energy density, efficient conversion rates, lightweight design, affordability, a broad range of suitable materials, and ease of scaling up. Since its inception, there have been numerous reports on the friction-based nanogenerator, indicating a promising future. It has the potential to extract energy from biological motion, mechanical vibrations, airflow, and other forms of mechanical energy. This technology could power and drive portable electronic devices, environmental monitoring systems, medical equipments, and energy conversion applications.

To further develop the triboelectric nanogenerator, we must delve deeply into its working principle, expand its application scope, and facilitate its commercialization to alter the way people obtain energy and enhance the human living environment. To achieve numerous functional applications with the triboelectric nanogenerator, its output performance must be enhanced through the optimization of device structure and material properties, ensuring a more sensitive and stable output signal. Simultaneously, the flexibility, stability, environmental friendliness, and cost of the designed triboelectric nanogenerator must be considered to meet various application requirements. This paper takes the optimization of material properties and structural design as its starting point, aiming to address some challenges in constructing a self-powered system based on the friction nanogenerator. It encompasses exploring methods to improve the output performance of the triboelectric nanogenerator. Through correlation analysis, the working principle of the friction nanogenerator has been thoroughly investigated. A simple self-supplying energy system has been designed by integrating traditional energy collection methods. The self-charging energy supply unit has been optimized, and human kinetic energy has been harnessed, leading to the exploration of novel functional applications within the field of self-powered systems.

A contact-separation triboelectric nanogenerator utilizing solid waste has been designed and constructed. Waste rubber powder (WRP), with methodological modification as depicted in Figure 1, acts as the negative triboelectric electrode material. By employing waste rubber powder as the

negative friction electrode material and water-assisted oxidation porous aluminum as the positive friction electrode material, a contact-separation friction nanogenerator based on solid waste was developed. The open circuit voltage and short circuit current density increase as the particle size of the rubber powder decreases. Fluorosilane grafted onto the surface of WRP particles significantly enhances the electronegativity of the WRP surface, resulting in more friction charges when used as a friction electrode material. This, in turn, improves the output characteristics of the friction nanogenerator. The nanogenerator based on fluorinated rubber powder achieves an open circuit voltage of 265 V and a short circuit current density of 75 $mA \cdot m^{-2}$. When the external load resistance is 200 MΩ, the maximum power density reaches 4.6 $W \cdot m^{-2}$, which is 67 times greater than that of the nanogenerator based on unmodified rubber powder. Additionally, several novel nanogenerators utilizing various nanocomposites have been demonstrated for broader applications, such as energy harvesting from human motion.

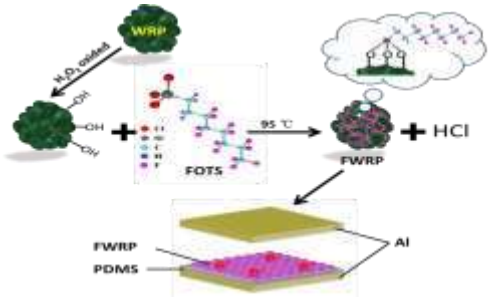


Figure 1. Schematic diagram of surface fluorinated modification for the wasted rubber powder (WRP) by using trichloro (1H,1H,2H,2H-perfluorooctyl) silane (FOTS) as negative electrodes of triboelectric nanogenerators

Acknowledgment

This work was supported by the National Nature Science Foundation (52372125, 52333009), the Shaanxi Provincial Science Foundation (2021GXLH-01-11), the Yulin Project (YLKG-2022-11), the 111 Program (B08040) of MOE of China. We would thank the Analytical & Testing Center of NPU (2024T008).

References

1. Ren X, Fan H, Ma J, Wang C, Zhao Y, Lei S, *ACS Sustainable Chem. Eng.*, 2017; 5: 1957.
2. Ren X, Fan H, Zhao Y, Liu Z, *ACS Appl. Mater. & Inter.*, 2016; 8: 26190.
3. Ren X, Fan H,Wang C, Ma J, Li H, Zhang M, Lei S, Wang W, *Nano Energy*, 2018; 50: 562.
4. Gong Y, Wang W, Che X, Su Y, Jia Y, Ren X, Fan H, *J. Mater. Chem. A*, 2024; 12: 24565.
5. Gong Y, Wang W, Cao J, Ren X, Jia Y, Duan Y, Wang B, Guo Q, Feng Y, Fan H, *J. Mater. Chem. A*, 2025; 13: 23756.
6. Che X, Fan Y, Su Y, Gong Y, Guo Q, Feng Y, Du D, Wang W, Fan H, *ACS Appl. Mater. & Inter.*, 2024; 16: 33517.
7. Che X, Fan H, Cao J, Fan Y, Jia Y, Duan Y, Guo Q, Feng Y, Wang W, *Nano Energy*, 2025; 143: 11275.

International Rubber Conference 2025 (IRC2025)
1-3 December 2025 @ BITEC, Bangkok, Thailand

High-performance, Recyclable, and Multifunctional Nitrile Butadiene Rubber Based on Hydrogen and Urea Bonds

Dongmei Yue[1], Lin Wang[1]

Beijing University of Chemical Technology, Beijing, China.

e-mail address of the presenting author (yuedm@mail.buct.edu.cn)

Keywords: Nitrile butadiene rubber, High-performance, Recyclability, Multifuncation

Nitrile Butadiene Rubber (NBR) is widely used in auto parts, petroleum exploration, sealing parts, and other fields because of its outstanding performance.[1] However, raw NBR usually needs to be crosslinked with sulfur or peroxide[2,3] before it can be utilized, which impeding the reprocessing and recycling of NBR, leading to resource wastage and environmental pollution. Thus, it is urgent to search for a new crosslinked network to realize NBR with reprocessability and recyclability.

In recent years, to enable the recyclability and reusability of NBR, researchers have integrated dynamic bonds into NBR *via* a range of modification strategies. For example, Chen *et al*. designed a network composed of Fe^{3+}-catechol group coordination bonds.[4] Wang *et al*. introduced reversible alkoxyamine (C-ON) bonds into the dynamic cross-linked network of NBR.[5] It's evident that while dynamic characteristics are attainable by introducing metal coordination bonds and reversible alkoxyamine (C-ON) bonds, there are several challenges including intricate fabrication processes, inferior mechanical properties, and low efficiency in reprocessing. Consequently, the development of a straightforward, effective, and innovative dual dynamic crosslinking network for NBR elastomers is of great significance.

In this work, a series of novel polyurea NBR elastomer materials (IPDI-ATBN-PPD) were designed and synthesized by a one-pot ternary polymerization reaction of amino-terminated liquid nitrile rubber (ATBN), isophorone diisocyanate (IPDI) and p-phenylenediamine (PPD) without any catalyst. The presence of urea bonds not only provides a large number of hydrogen bonding sites between the molecular chains, but also exhibits the remarkable microphase separation properties of thermoplastic elastomers. This approach endows NBR with enhanced dynamic characteristics and significant recyclability. As a result, the as-synthesized multifunctional NBR elastomer (I-$A_{0.5}$-$P_{0.5}$) exhibits excellent tensile strength (19.9 Mpa, Figure 1c), toughness (93.7 MJ m^{-3}, Figure 1c), low glass transition temperature (-52 ℃, Figure 1a), and low compression cold resistance coefficient (0.15 at -55 ℃, Figure 1f), which are comparable to those of conventionally covalently crosslinked NBR. The elastomer retains mechanical integrity after multiple rounds of recycling (retaining 81% of its original tensile strength after five reprocessing cycles, Figure 1e). To broaden the application of NBR products, I-$A_{0.5}$-$P_{0.5}$ was crosslinked with sulfur and its performance was compared with NBR vulcanizates of different acrylonitrile contents. It shows excellent oil resistance and low temperature resistance (Figure 1g and 1h). Surprisingly, it can also possess the ability to be reprocessed multiple times. (Figure 1i) This new multifunctional thermoplastic NBR elastomer is of great significance in solving the problem of difficult recycling of traditional NBR and is expected to replace traditional covalently cross-linked NBR. This synthesis strategy is readily adaptable to industrial processes and offers a scalable route to produce recyclable NBR for demanding applications.

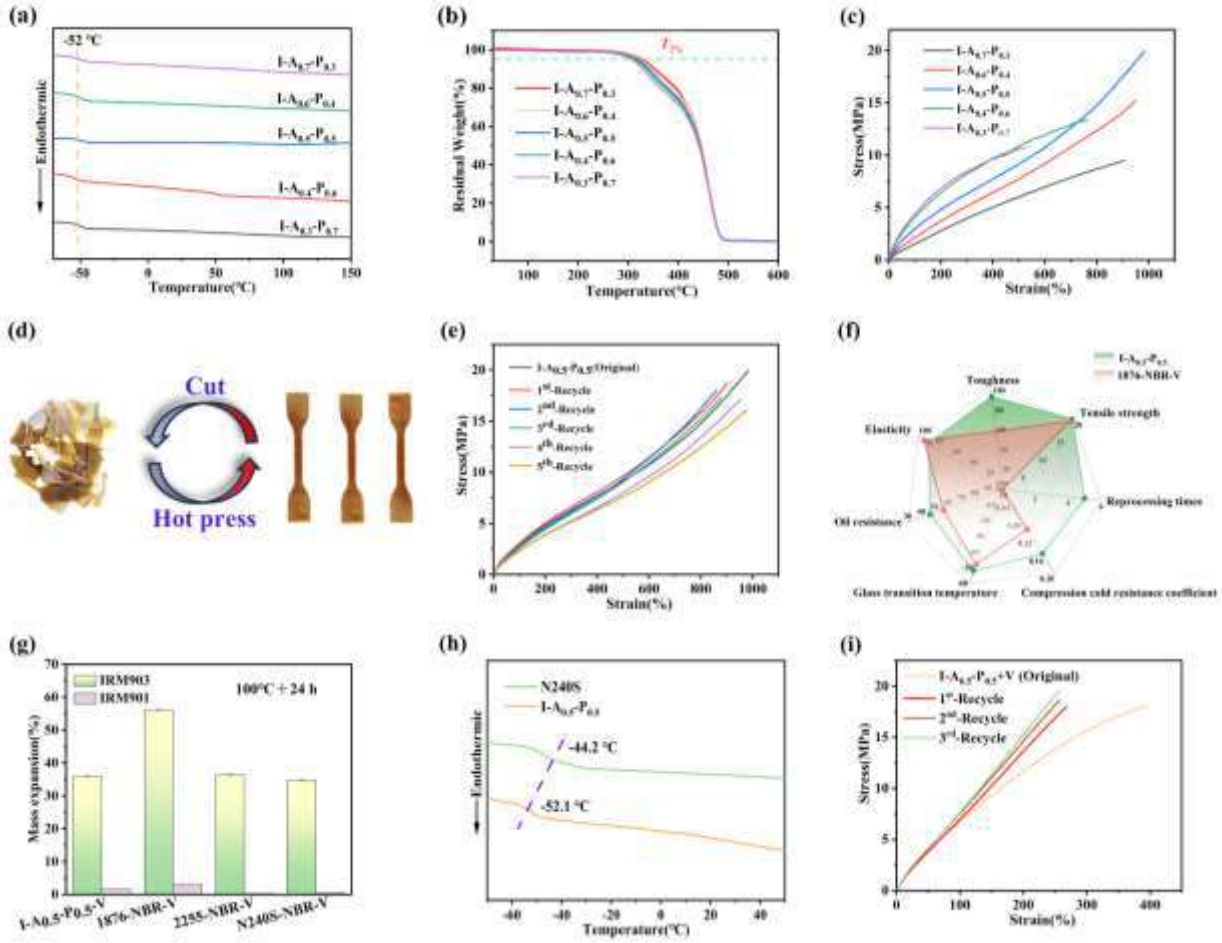


Figure 1. (a) DSC curves, (b) TGA curves, (c) Stress–strain curves of IPDI-ATBN-PPD. (d) Photograph of I-$A_{0.5}$-$P_{0.5}$ recycled dumbbell strip. (e) Stress–strain curves of original and recycled samples. (f) Comparison of I-$A_{0.5}$-$P_{0.5}$ and 1876-NBR-V. (g) Oil resistance of I-$A_{0.5}$-$P_{0.5}$-V, 1876-NBR-V, 2255-NBR-V, and N240S-NBR-V. (h) DSC curves of N240S and I-$A_{0.5}$-$P_{0.5}$. (i) Stress–strain curves of original and recycled samples.

Acknowledgement

This work was supported by the Taishan Industrial Experts Program, the National Key R&D Program of China (2022YFB3704700), and the National Science and Technology Major Special Projects (2024ZD0603000).

References

1. Wan S H, Du P, Guo Z Y, You L X, Mao Y W, He X R, *Polym. Compos.*, 2024, 45, 2462-2473.
2. Zhang R, Yuan X, Sun R, Zhang B, Geng Z, Li Z, Liu G, *Polym. Compos.*, 2023, 44, 1929-1939.
3. Forghani N, Maghsoud Z, Ramezanian N, Appl. Surf. Sci., 2023, 639, 158114.
4. Chen Z, Yan M, Cao L, Huang J, Cao X, Yuan D, Chen Y, *Ind. Eng. Chem. Res.*, 2019, 58, 3912-3920.
5. Wang X P, Xue K X, Wu H J, *Ind. Eng. Chem. Res.*, 2024, 63, 9779-9789.

Boron-Containing Elastomer

Qi WU[1], Jinrong WU[1]

[1] *College of Polymer Science and Engineering, National Key Laboratory of Advanced Polymer Materials, Sichuan University, Chengdu, China.*

e-mail address of the presenting author (wuqi57@scu.edu.cn)

Keywords: Elastomer, Boron, Dynamic nature.

The inherent uniqueness of the boron element and the dynamic nature of the covalent boron-oxygen bond are crucial components of boron dynamic chemistry. On the one hand, the boron atom possesses an empty p-orbital, which can interact reversibly with the electron donor to form a boron coordination bond. This reversibility leads to changes in the hybridization mode, configuration, and charge state of the boron center, resulting in the multifaceted variability of boron coordination bonds. On the other hand, dehydration/hydrolysis or transesterification processes between boron-oxygen bonds such as boric hydroxyl groups, boronic esters and boroxine cause the transformation of bonding methods, molecular configurations and network structures, resulting in the dynamic responsiveness of boron-oxygen covalent bonds. Consequently, based on boron dynamic interactions, boron-containing polymers exhibit excellent performance and great potential in fields such as intelligent response.

Leveraging these dynamic boron interactions, we have developed functional elastomers with various environmental response mechanisms, including photo response, thermal response and mechanical force response. This work broadening the types and potential application possibilities of boron-containing elastomers.

Acknowledgement

This work was supported by National Natural Science Foundation of China (Grant No. 52473061 and 52203064), China Postdoctoral Science Foundation (2023M732415).

References

1. Xiong, H., Zhang, L., Wu, Q., & Wu, J. *Sci. China Mater.*, 2024, 67(10): 3339-3346.
2. Cai, M., Hou, Y., Huang, Y., Gu, S., Xiong, H., Wu, Q., & Wu, J. *ACS Appl. Mater. Interfaces*, 2024, 16(42): 57760-57768.
3. Gu, S., Wu, Q., & Wu, J. *Mater. Horiz.*, 2024, 11(22): 5692-5700.

Effect of Non-covalent interactions on Epoxidized Natural Rubber: Structure-Properties Relationships

Phakamat Limarun[1], Pairote Jittham[2], Wirasak Smitthipong[1,3,*]

[1] *Specialized Center of Rubber and Polymer Materials in Agriculture and Industry (RPM), Department of Materials Science, Faculty of Science, Kasetsart University,Bangkok 10900, Thailand.*

[2] *National Metal and Materials Technology Center (MTEC), Khlong Luang, Pathum Thani 12120, Thailand.*

[3] *Hub of Talents in Natural Rubber under National Research Council of Thailand (NRCT), Bangkok 10900, Thailand.*

E-mail address of the presenting author (phakamat.li@ku.th)

Keywords: Natural Rubber, Epoxidized Natural Rubber, Self-healing Properties

Natural rubber (NR) is the primary raw material derived from the rubber tree (*Hevea brasiliensis*) [1]. This material exhibits a chemical structure of *cis*-1,4-polyisoprene and possesses several advantageous properties, including excellent flexibility, good tensile and tear resistance, low heat buildup, and high strength. However, NR is a non-polar and contains double bonds within its main chain structure. This molecular configuration results in poor resistance to ozone, oil, and various chemicals [2]. So, researchers commonly employ modification techniques to enhance properties of NR. The most widely used modification method involves epoxidation reactions, which convert NR into epoxidized natural rubber (ENR) [3].

This research focuses on enhancing mechanical and self-healing properties of NR through epoxidation modification combined with 2,4,5-Trihydroxy-DL-phenylalanine (DOPA) and ferric chloride ($FeCl_3$) solution. The present study examines the ENR systems incorporating to the DOPA, along with iron solution (Fe). ENR latex was prepared at 60 °C for 4 h to obtain 25% epoxide content. 20 phr of DOPA powder and 10 phr Fe^{3+} ions from $FeCl_3$ was mixed at room temperature for 24 h (Figure 1). The objective of this work is to understand how these combined modifications influence intermolecular interactions and resulting mechanical and thermal properties of the DOPA-functionalized ENR.

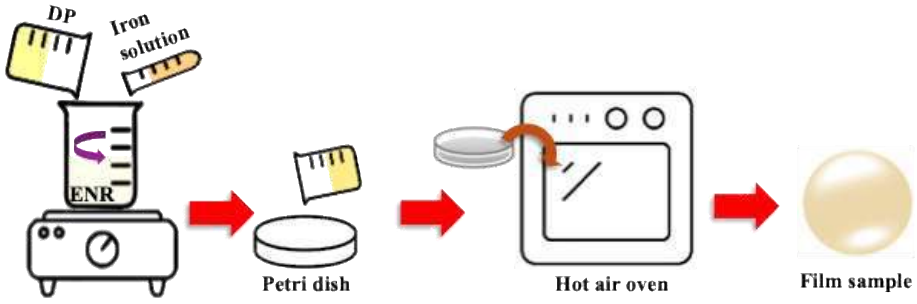


Figure 1. Preparation of modified ENR film samples

The modification of NR to form epoxide groups was confirmed by Nuclear Magnetic Resonance (NMR) and Fourier-Transform Infrared Spectroscopy (FTIR) analysis. The DOPA was covalently bonded to ENR through ring-opening of epoxide groups, then Fe^{3+} ions formed

coordination bonds with both nitrogen and oxygen atoms of DOPA. From the mechanical properties point of view, it was found that ENR undergoes strain-induced crystallization due to the close alignment of rubber molecular chains when stretched. The addition of DOPA (ENR/DOPA) resulted in hydrogen bond formation but no crystallization occurred due to the steric effect of DOPA molecules disrupting chain alignment. However, when iron was added (ENR/DOPA/Fe), the Young's modulus was significantly increased. Fe^{3+} ions and the amine/hydroxyl groups of DOPA generated coordination interactions, causing a clear increase in Young's modulus value [4]. Moreover, the ENR/DOPA/Fe film enhanced self-healing efficiency around 60% compared to ENR/DOPA (30%) and control ENR (15%) films.

The results of this research can be used for developing new rubber products with tunable mechanical and thermal properties, especially the self-healing capabilities. By controlling intermolecular interactions, enhanced mechanical properties and self-healing capabilities of rubber materials can be achieved [5].

Acknowledgement

This research was supported by The High-Quality Research Graduate Development Cooperation Project between Kasetsart University and the National Science and Technology Development Agency (NSTDA). The research facilities were also provided by the Specialized Center of Rubber and Polymer Materials in Agriculture and Industry (RPM), Department of Materials Science, Faculty of Science, Kasetsart University.

References

1. Payungwong, N., Wu, J., Sakdapipanich, J., *Polymer*, 2024; 308, 127419.
2. Buaksuntear, K., Panmanee, K., Wongphul, K., Lim-arun, P., Jansinak, S., Shah, D.U., Smitthipong, W., *Polymer*, 2024; 291, 126626.
3. Tessanan, W., Ratvijitvech, T., Thanawan, S., Amornsakchai, T., Phinyocheep, P., *Sci. Rep.*, 2024; 14, 26603.
4. Filippidi, E., Cristiani, T. R., Eisenbach, C. D., Waite, J. H., Israelachvili, J. N., Ahn, B. K., Valentine, M. T., *Science*, 2017; 358(6362), 502-505.
5. Li, L., Smitthipong, W., Zeng, H., *Polym. Chem.*, 2015; 6(3), 353-358.

International Rubber Conference 2025 (IRC2025)
1-3 December 2025 @ BITEC, Bangkok, Thailand

Sustainable Supramolecular Aqueous Adhesive with Moisture Resistance

Liying Zhang[1], Shuxue Wang[1], Jianming Zhang[1,2]

[1] *Qingdao University of Science & Technology, Qingdao, China.*

[2] *Key Laboratory of Rubber-Plastics, Ministry of Education/Shandong Provincial Key Laboratory of Rubber-plastics, Qingdao, China.*

b022020007@mails.qust.edu.cn

Keywords: Bio-adhesive, Cellulose nanocrystals, Non-covalent crosslinking, Humidity-resistance, On-demand debonding

Bio-based adhesives have attracted considerable attention as sustainable alternatives to petroleum-based counterparts, which raise environmental and ecological concerns. Despite this promise, their broader application remains limited by insufficient adhesion strength and poor humidity tolerance. [1] To address these challenges, we developed a bio-based aqueous adhesive comprising poly (acrylic acid)-grafted cellulose nanocrystals (CNC-PAA) [2] and poly (vinyl alcohol) (PVA). The adhesive constructs a dense supramolecular network through abundant non-covalent interactions, which enhances the flexibility of the adhesive film and thereby improves both cohesive strength and interfacial adhesion. It exhibits outstanding adhesive performance on various substrates, achieving a maximum lap-shear strength of 7.52 MPa on ceramic. The rigid CNC-PAA framework and its intrinsic hydrophilicity significantly improve stability under humid conditions as seen in Figure 1, allowing the adhesive to retain 75% of its maximum strength even at 100% relative humidity. Furthermore, the high density of hydrogen bonds and structured water confer robust adhesion at cryogenic temperatures (−196 °C). The reversible nature of hydrogen bonding also enables pH-responsive adhesion–dispersal cycles, affording recyclability and on-demand debonding. Importantly, the biomass-derived composition imparts inherent biodegradability. This work introduces a facile and scalable strategy to design high-performance, humidity-resistant, and recyclable bio-based adhesives, with potential applications in packaging, labeling, cryogenic storage, and beyond. While further optimization may be required for large-scale industrial adoption, this study highlights a promising pathway toward sustainable adhesive technologies.

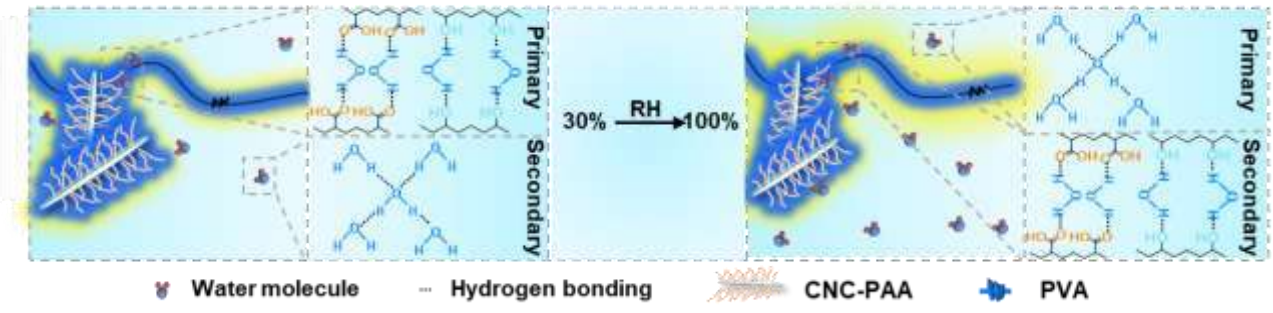


Figure 1. Schematic of the water in the hydratable polymer network of PVA/CNC-PAA adhesives, showing water/polymer bonding, weakened water/water bonding, and normal water/water bonding.

Acknowledgement

We acknowledge the financial support from the Youth Innovation Team Project of Shandong Province, China (No. 2023KJ311) and the China Postdoctoral Science Foundation (Certificate Number: 2023M732976).

References

1. Zeng G, Zhou Y, Liang Y, Zhang F, Luo J, Li J, Fang Z, *Chem Eng J*., 2022; 434: 134632.
2. Lu Y J, Li Z H, Xie Y Q, Liu Y X, Zhang J M, Zong L, *ACS Mater. Lett.*, 2024; 6: 976.

International Rubber Conference 2025 (IRC2025)
1-3 December 2025 @ BITEC, Bangkok, Thailand

Cellulose Nanocrystal-Based Aqueous Nanogel Photoinitiator for High-Performance Photocurable Hydrogel Elastomers

Quan Wang, Yihan Sun, Xiaohui Hao, Jianming Zhang*

Key Laboratory of Rubber-Plastics, Ministry of Education/Shandong Provincial Key Laboratory of Rubber-plastics, Qingdao University of Science and Technology, Qingdao, China.

1084032541@qq.com

Keywords: Photocurable hydrogels, Nanogel photoinitiators, Cellulose nanocrystals

Photocurable hydrogel elastomers (PHEs) offer rapid gelation, high spatial fidelity, and tunable mechanics for tissue engineering, drug delivery, flexible electronics, and soft robotics [1]. Yet commonly used photoinitiators suffer from cytotoxicity, poor water solubility, and oxygen inhibition, which lower conversion and compromise biocompatibility [2]. Here we report an aqueous nanogel photoinitiator constructed from cellulose nanocrystals (CNCs) coordinated with Fe^{3+}, which generates hydroxyl radicals through the conversion of Fe^{3+} to Fe^{2+}, initiating rapid and efficient polymerization of acrylate hydrogels (Figure 1a). The nanogel shows (i) colloidal stability in water without visible sedimentation for at least 30 days (at a content of 1.0 wt%); (ii) accelerated initiation kinetics compared with α-ketoglutaric acid, with a monomer conversion rate after 4 minutes of UV (365 nm, 70mW/cm^2) that is twice that of α-ketoglutaric acid, yielding rapid crosslinking even in high-water-content formulations (Figure 1b); (iii) reduced oxygen inhibition that supports open-air curing; (iv) broad optical responsiveness, allowing curing under ultraviolet and blue light; and (v) mechanical reinforcement of the network due to CNCs acting as nanoscale fillers, improving elasticity and toughness. These features position the nanogel as a biocompatible and sustainable photoinitiator for the rapid, precise fabrication of high-performance hydrogel elastomers.

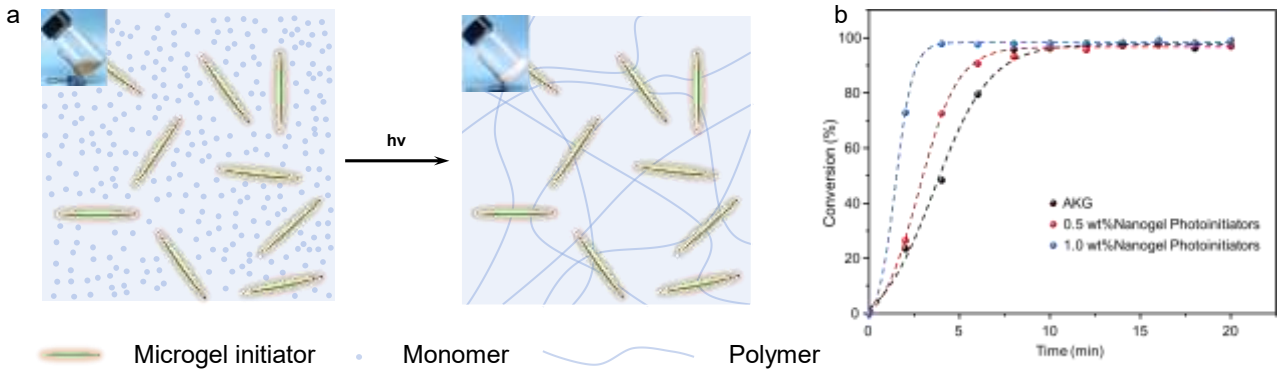


Figure 1. (a) Nanogel photoinitiator initiates polymerization under visible light, (b) Photopolymerization kinetics of acrylate monomers.

References

1. Lv Y, Xu Y, Zhang S, Xie S, Wang B, *Advanced Functional Materials. J.*, 2025: 2501904.
2. Zhang H, Sun Y, Chen G, Zeng D, Cheng Z, *Journal of Hazardous Materials. J.*, 2025; 139370.

International Rubber Conference 2025 (IRC2025)
1-3 December 2025 @ BITEC, Bangkok, Thailand

Impact of Fused Filament Fabrication and Processing Parameters on the Performance of $BaTiO_3$-Piezoelectric Composites for Soft Robots

S, BUTENKO[1,2], F. MONGIOI[3], T. BRUGO[3], A. ICHANGI[1], F. CLEMENS[1]

[1] *Swiss Federal Laboratories for Materials Science and Technology, Ueberlandstrasse 129, 8600 Dübendorf, Switzerland.*

[2]*Swiss Federal Technology Institute of Lausanne, Rte Cantonale, 1015 Lausanne, Switzerland.*

[3]*University Of Bologna, Via Zamboni, 33, 40126 Bologna BO, Italy*

sofiia.butenko@empa.ch

Keywords: Thermoplastic**,** Fused-filament fabrication (FFF), fused deposition modeling (FDM), Barium titanate composite, Piezoelectric sensors.

The advancement in soft robotics continues to drive interest in self-powered flexible integrable sensing materials that can withstand mechanical deformation while delivering a reliable electrical signal in response to tactile pressures. [1-2] Piezoelectric composites based on rubber matrix and ceramic fillers present a promising solution due to their inherent softness and electrical sensing capability. However, extrusion-based fabrication of such materials remains challenging due to incompatibilities between rubber and conventional 3D printing processes like fused filament fabrication/fused deposition modeling (FFF/FDM). To enable FFF/FDM processing, rubber must be blended with a thermoplastic binder. In this project, we investigate a composite based on thermoplastic styrene-based elastomer (TPS) matrix filled with barium titanate ($BaTiO_3$, BTO) particles as an intermediate step toward printable rubber-based piezoelectric materials. The present study focuses on understanding the electromechanical behavior of TPS–BTO composites fabricated via extrusion-based additive manufacturing.

A comprehensive study was conducted to evaluate the effect of different mixing and processing strategies on material performance. Two mixing approaches were examined: (i) blending a 50 vol% BTO masterbatch with pure TPS to achieve final BTO contents of 25 and 45 vol% (3D-MB), and (ii) direct mixing of BTO at 25 and 45 vol% with TPS (3D-DM). All mixtures were 3D printed under controlled conditions, and the influence of processing parameters - including print speed, nozzle temperature, and layer height - on piezoelectric coefficient was systematically analyzed (Table 1). To assess the functional behavior, electromechanical characterization was carried out on printed samples without and with electrical poling at different temperatures (Table 1).

Table 1. Determined parameters and their ranges of processing and post-processing

Process Parameter	Symbol	Unit	Range			Number of values
			Min.	Max.	Step	
Layer height	H	mm	0.2	0.4	0.1	3
Printing speed	v	ml/s	10	40	10	4
Nozzle temperature	T_{nozzle}	°C	180	220	20	3
Extrusion pattern	p	°	0°	90°	45°	3
Poling Field	P	kV/cm	10	50	40	2
Poling Temperature	T_{pol}	°C	25	100	75	2

Figure 1a–d presents the electrical characterization of samples 3D printed from composite feedstock prepared by direct mixing (3D-DM) and masterbatch (3D-MB). The output voltage of the 3D-MB sample was 65% higher than that of 3D-DM (Figure 1a), while the saturation of 3D-DM was

higher by 30, respectively. Figure 1b shows that the output voltage of the 3D-DM sample increased by 40% after poling, with a similar trend observed in polarization values before and after poling (Figure 1d). The microstructure of the 3D-printed samples, shown in the cross-sectional SEM images (Figure 1f), confirms that the ceramic filler particles were successfully embedded within the TPS matrix across both mixing strategies.

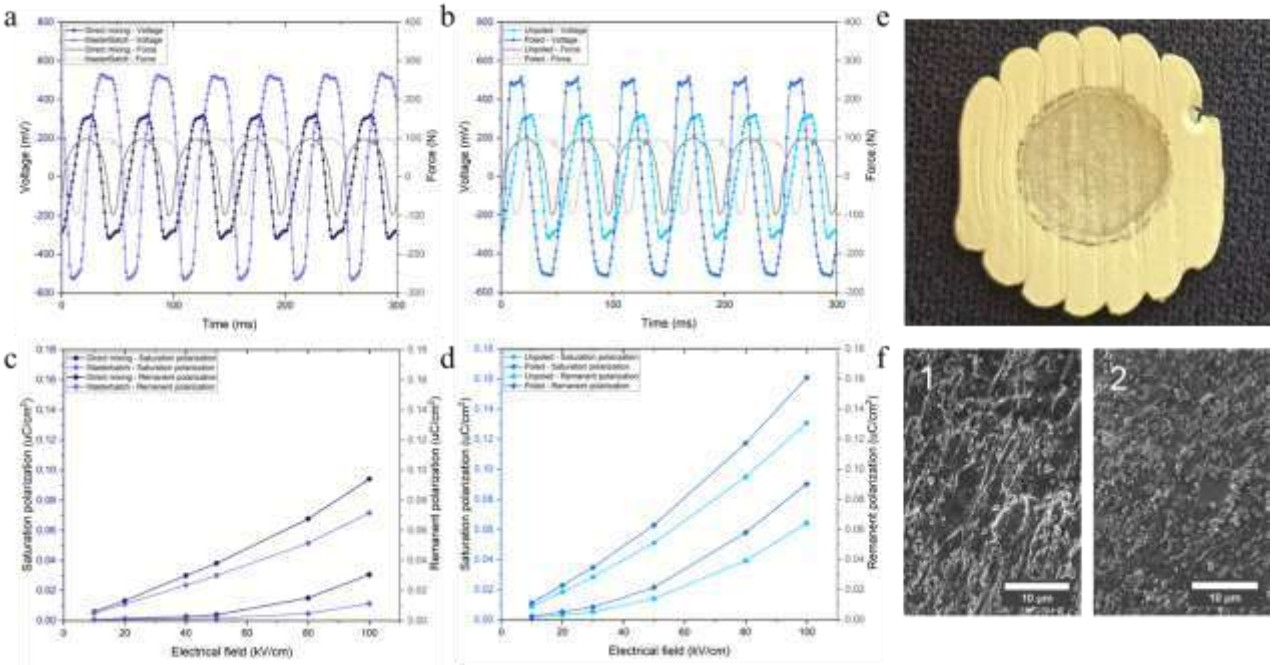


Figure 1. (a-d) shows the electrical characterization of 3D printed samples. (a–b) Voltage under periodic loading with a 110 N preload (baseline) and 100 N amplitude at 20 Hz, and (c–d) saturation and remanent polarization measured at 0.1 Hz frequency. Poling was performed at 100 °C for 10 minutes under an 80 kV/cm poling field. (e) photograph of a 3D-printed composite sample with silver electrodes. (f) cross-section SEM images of 3D printed composites prepared by (1) direct mixing and (2) masterbatch.

These results, supported by optimized electrical and structural characterization methods—including direct piezoelectric coefficient (d_{33}) quantification and microstructural evaluation—demonstrate a scalable approach for fabricating thermoplastic elastomer-based piezoelectric composites. The observed processing–structure–property relationships are critical for advancing fully 3D-printed piezoelectric sensors and enabling the integration of rubber-based composites into soft robotic systems with embedded sensing capabilities.

Acknowledgement

This project has received funding from the Swiss National Science Foundation (SNSF) research and innovation programme SPIRT under grant agreement No 223840 (SPRINT Project).

References

1. Habib M, Lantgios, I, Hornbostel, K, J. *Phys. D: Appl. Phys.*, 2022; 55: 423002
2. Qu J, Cui G, Li Z, Fang S, Zhang X, Liu A, Han M, Liu H, Wang X, Wang X, *Adv. Funct. Mater.*, 2024; 34: 2401311.

Enhancing the Piezoresistive Sensing Properties of TPE/CB Composites via Co-Continuous Structure Design through Natural Rubber Blending

Christopher Bascucci[1,3], Torfan Srisuwanno[2], Yeampon Nakaramontri[2], Josie Hughes[3], Frank Clemens[1]

[1]Laboratory of High Performance Ceramics, Empa, Swiss Federal Laboratories for Materials Science and Technology, Dübendorf, Switzerland

[2]Sustainable Polymer and Innovative Composites Material Research Group, Department of Chemistry, Faculty of Science, King Mongkut's University of Technology Thonburi, Bangkok, 10140, Thailand

[3]Computational Robot Design and Fabrication Lab, EPFL, Swiss Federal Institute of Technology Lausanne, Lausanne, Switzerland

Email: christopher.bascucci@empa.ch

Keywords: Soft robotics, Thermoplastic elastomers (TPE), Natural rubber (NR), Carbon nanomaterials (CNMs), Resistive sensors

Flexible and stretchable piezoresistive materials are attracting growing interest for use in wearable sensors and soft robotics, where large mechanical deformation must be accurately translated into stable and repeatable electrical signals [1]. Among the various materials being explored, thermoplastic styrene-based block copolymers (TPS), are emerging as promising candidates due to their unique combination of softness, elasticity, processability, and recyclability [2]. When filled with conductive particles such as carbon black (CB), TPS-based composites exhibit piezoresistive behavior, as their electrical conductivity responds to mechanical strain or pressure [3].

However, achieving reliable electromechanical performance at low percolation thresholds remains a challenge. In conventional TPS/CB systems, a CB content above 30 wt.% is needed to achieve reliable sensor signals. Consistent piezoresistive response, effective sensing performance (Figure 1a-d) and negligible polarization effect (Figure 1e-f) are typically observed only at high CB concentrations. These elevated filler contents lower the mechanical flexibility and increase stiffness and plastic deformation, which limit their practical utility in soft sensor applications.

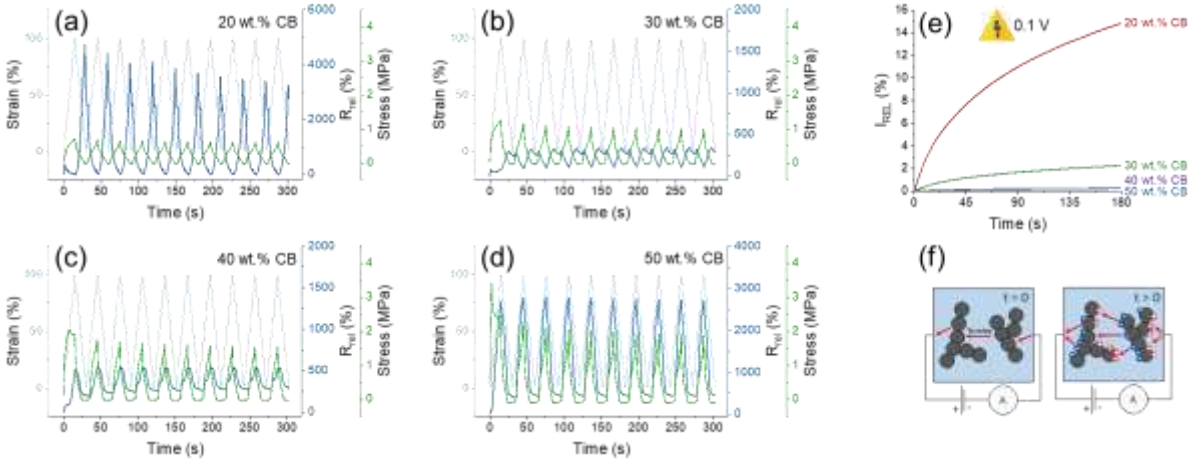


Figure 1. Dynamic mechano-electrical behavior of a TPS Shore 22A elastomer mixed with (a) 20 wt.% CB, (b) 30 wt.% CB, (c) 40 wt.% CB, and (d) 50 wt.% CB. (e) Polarization experiments under a constant applied voltage of 0.1 V. (f) Schematic illustration of the proposed polarization mechanism.

To address these limitations, this study introduces a novel materials strategy based on the creation of a co-continuous structure design via polymer blending [4]. Specifically, natural rubber (NR) is incorporated as a phase-separating component within the thermoplastic styrene (TPS) matrix

to form a thermoplastic vulcanizate (TPV) (Figure 2a). NR is selected not only for its excellent mechanical elasticity but also for its sustainable origin, contributing to reduced carbon emissions compared to synthetic elastomers [5].

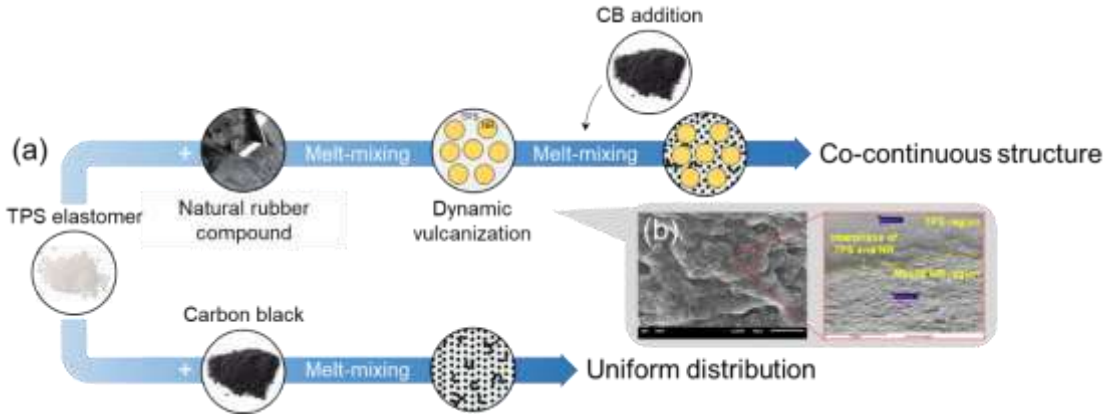


Figure 2. (a) Schematic of the fabrication process for uniformly dispersed TPS/CB and co-continuous TPS/NR/CB compounds. (b) SEM image showing the morphology of the TPS/NR/CB compound.

Four TPS materials with varying hardness levels (from Shore 71A to 25 00) were blended with 50 wt.% NR. This ratio was selected to promote the formation of a co-continuous structure while avoiding phase inversion. During melt mixing, the NR undergoes dynamic vulcanization, becoming a non-processable, crosslinked phase dispersed within the continuous TPS matrix, leading to a TPV microstructure. SEM micrographs illustrating the presence of discrete NR domains confirm the morphology (Figure 2b).

These TPS/NR systems will be further compounded with CB to evaluate their effect on functional properties. Both unfilled and filled samples will be thoroughly characterized in terms of:

- Electrical conductivity and percolation threshold
- Mechanical plasticity and stretchability
- Piezoresistive sensitivity and stability under static and dynamic loadings.

Electro-mechanical performance will be benchmarked against traditional TPS/CB composites lacking a co-continuous structure.

This work explores a novel approach to high-performance, flexible piezoresistive sensors by tailoring the microstructure through natural rubber (NR) blending. The co-continuous structure strategy is expected to reduce the required amount of conductive filler, thereby lowering material costs and enhancing overall mechanical and electrical performance. This supports the development of soft sensor platforms that are both more sustainable and higher-performing.

Acknowledgement

This research is part of the SAMS project (grant number IZCOZ0_213312) funded by the Swiss National Science Foundation (SNSF). The project is part of the COST Action EsSENce (grant number CA19118).

References

[1] S. S. Banerjee, I. Arief, R. Berthold, M. Wiese, M. Bartholdt, D. Ganguli, S. Mitra, S. Mandal, J. Wallaschek, A. Raatz, G. Heinrich, and A. Das, Appl. Mater. Today **25**, 101219 (2021).
[2] G. Holden, in *Applied Plastics Engineering Handbook (Third Edition)*, edited by M. Kutz (William Andrew Publishing, 2024), pp. 97–113.
[3] A. Georgopoulou and F. Clemens, ACS Appl. Electron. Mater. **2**, 1826 (2020).
[4] P. Pötschke and D. R. Paul, J. Macromol. Sci. Part C **43**, 87 (2003).
[5] A. Boonmahitthisud and K. Boonkerd, Curr. Opin. Green Sustain. Chem. **28**, 100446 (2021).

International Rubber Conference 2025 (IRC2025)
1-3 December 2025 @ BITEC, Bangkok, Thailand

α-Diimine Cobalt Complexes Bearing Axial Anagostic Interaction: A System for Accessing Ultra-High Molecular Weight Polybutadiene

Xin Wang,[1] Xuequan Zhang, [1] Heng Liu*,

School of Polymer Science and Engineering, Qingdao University of Science and Technology, Qingdao, China.

Corresponding author: hengliu@qust.edu.cn

Keywords: Polybutadiene, Ultra-high molecular weight, Anagostic interaction

Rubber materials require a combination of excellent elasticity, abrasion resistance, and mechanical strength to meet the stringent demands of high-performance applications such as tires, shock absorbers, etc. [1-2] By increasing molecular weight to a ultrahigh molecular weight (UHMW) level, although sometimes being accompanied by the reduced processability, synthetic rubbers can not only achieve enhanced tear resistance and durability, but also exhibit unique strain-induced crystallization behavior, further improving its overall performance.[3]

Cis-1,4-enriched polybutadiene (PBd) is a synthetic rubber valued for its high elastic recovery, superior abrasion resistance, etc., and currently finds wide application in the tire industry, conveyor belts, etc.[4] Nevertheless, accessing *cis*-1,4-enriched UHMW polybutadiene remains a significant challenge due to inevitable chain transfer reactions in most coordination polymerization systems, despite the material's promising superior mechanical properties. In this study, we satisfactorily find that, by introducing axial anagostic interaction into *α*-diimine $CoCl_2$ complexes (see Figure 1)—a typical system produces PBds with moderate molecular weights—the obtained catalysts could enable the synthesis of UHMWPBds with high catalytic activities.

When activated by ethylaluminum sesquichloride (EASC), the obtained complexes **Co1-Co2** not only exhibit high *cis*-1,4-selectivity (up to 97.7%), but also effectively suppress chain transfer reactions, as supported by density functional theory (DFT) calculations, enabling the synthesis of PBds with UHMW. The nature of the axial anagostic Co···H–C interaction was systematically elucidated using multiple complementary techniques. Mechanical testing revealed that the resulting UHMWPBds possess significantly enhanced tensile strength and elongation at break compared to commercial PBd materials.

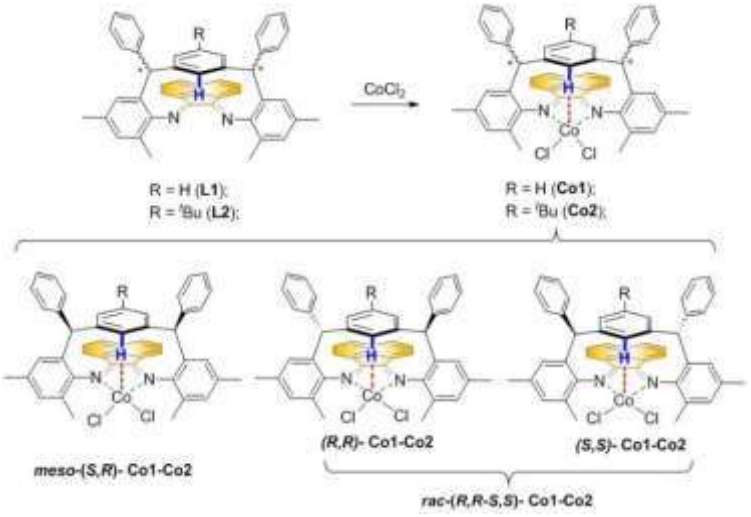


Figure 1. Synthetic procedure for the α-diimine cobalt complexes **Co1-Co2** bearing axial anagostic interaction Co…H-C.

Altough with UHMW, kinetic studies revealed that molecualr weight (M_w)witnessed an approximately linear increment over the first 80 minutes of polymerization to achieve a M_w of 72.0×10^4 g/mol, accompanied by relatively narrow molecular weight distributions (1.25~1.52) (Figure 2(1)). Due to the significantly increased molecular weight, the UHMWPBd obtained exhibited markedly enhanced mechanical properties, with a tensile strength of 3.36 MPa and elongation at break of 385.4% (Figure 2(2)) compared to 1.63 MPa and 253.6% for BR9000—a widely used PBd in tire production in China, which has a M_w of 42.5×10^4 g/mol and a PDI of 3.15. This substantial improvement suggests a higher degree of polymer chain entanglement in the UHMWPBd.

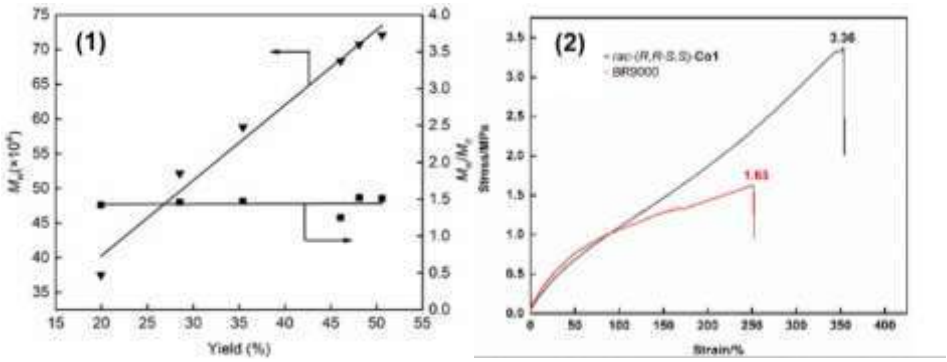


Figure 2. (1) The dependence of molecular weights and polydispersities on the monomer conversions; (2) stress-strain curves of UHMWPBd and BR9000.

Acknowledgement

This work was supported by National Natural Science Foundation of China (22071236), the Taishan Scholars Program (No. tsqn202211165).

References

1. Mahmood Q, Zeng Y, Yue E, Solan G A, Liang T, Sun W H, *Polym. Chem.*, 2017; 8: 6416.
2. Tugui C, Tiron V, Dascalu M, Sacarescu L, Cazacu M, *Eur. Polym. J.*, 2019; 120: 109243.
3. Wang L, Wang X, Hou H, Zhu G, Yang W, *Chem. Commun*., 2020, 56, 8846-8849.
4. Fu Y, Tang J, Hua J, *Dalton Trans.*, 2023; *52*: 13146.

International Rubber Conference 2025 (IRC2025)
1-3 December 2025 @ BITEC, Bangkok, Thailand

Fe-based Catalyst with Exogenous Electron Donor for Stereopolymerization of Butadiene and Isoprene

Shiliang Xu, *Chunyu Zhang, Xuequan Zhang

School of Polymer Science and Engineering, Qingdao University of Science and Technology, Qingdao, China.

Corresponding author: cyzhang@qust.edu.cn

Keywords: Coordination polymerization, Conjugated diene, Fe-based catalysts, Electron donor

Rubber materials remain an indispensable commodity material central to many diversified products essential in our modern lifestyle. The wide range of industrial applications for conjugated-diene rubbers can display different thermal, mechanical and physical properties depending on the possible chain microstructures [1-3]. Since the advent of Ziegler-Natta catalysts, the fine control of the regio/stereo-regularity of the chain microstructure can be reached, to some extent, only through coordination-insert polymerization. Therefore, the development of coordination polymerization catalyst systems with high temperature and high activity is significant.

Among the late transition metal-based catalysts, iron-based catalysts have shown broad application prospects in the preparation of functionalized polymers and other fields owing to their exceptional biocompatibility and abundance on earth and certain tolerance to polar functional groups. Early binary iron-based catalyst systems had poor activity and selectivity, and required low temperature polymerization. Later, adding electron donors was adopted to enhance catalytic performance by electronically and sterically modulating the active center [4-6]. Thus, identifying effective electron donors remains a key strategy for advancing iron-based catalyst development.

In this study, a novel iron-based catalyst system, $Fe(acac)_3$/IITP/AlR_3, was employed for the synthesis of syndiotactic 1,2-polybutadiene and 3,4-polyisoprene with high activity in hexane as reaction pathway shown in Figure 1 and their chemical structure characteristics presented in Figure 2.

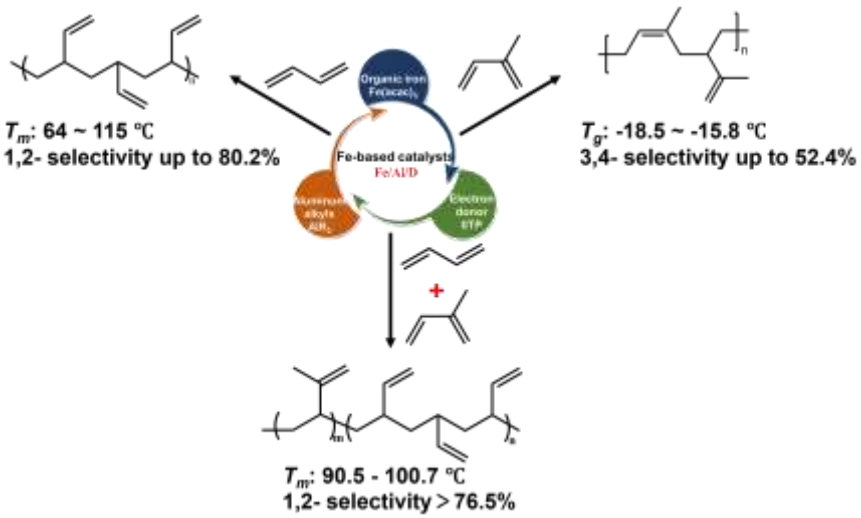


Figure 1. Homo-polymerization and copolymerization of butadiene and isoprene

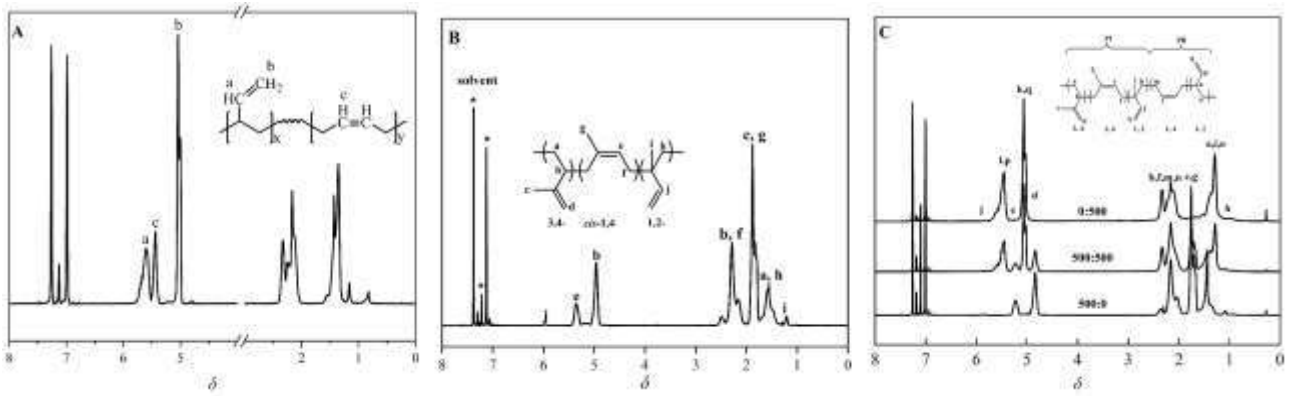


Figure 2. ^{1}H NMR spectra of polybutadiene (A), polyisoprene (B) and butadiene-isoprene block copolymer (C)

The DSC curves in Figure 3 show that polybutadiene displays a low melting point (Tm, 64.0~104.6 ℃), and the molar fraction of 1,2-unit can reach up to 80.2%. The molar fraction of 3,4-unit of polyisoprene is between 48.8%~52.4%, and the Tg is kept from -18.5 ℃ to -15.8 ℃. Furthermore, the unimodal distribution high-temperature gel permeation chromatography curve indicates that the catalytic system has a single active center. Moreover, the quasi-living polymerization characteristics of the catalytic system are verified through kinetics and seeding polymerization experiments of isoprene. Feasible block co-polymerization of 1,3-butadiene and isoprene further supports the living nature of the catalyst bestowed with. However, the high molecular weight of the polymers presents processing challenges. Exploring suitable molecular weight regulators will be crucial for the industrial viability of this system.

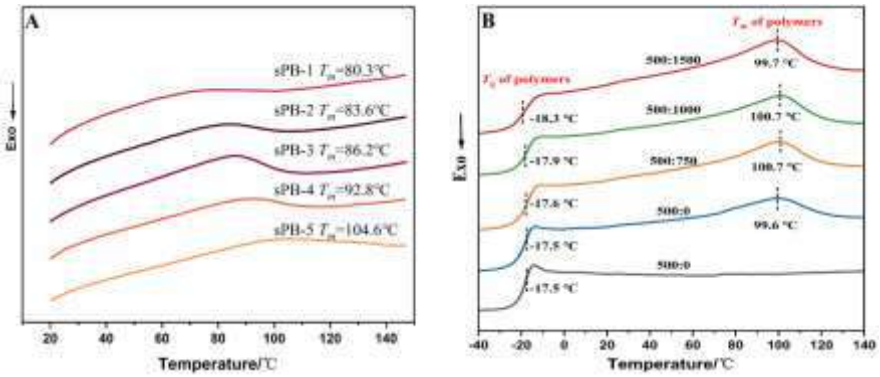


Figure 3. DSC curves of polybutadiene (A) and butadiene-isoprene block copolymer (B)

Acknowledgement

This work was financially supported by the National Key R&D Program of China (No. 2022YFB3704700).

References

1. Ge J, Chen B, Gong D, *Polym. Chem*., 2024, 15: 3751.
2. Gong D, Ying W, Zhao J, Li W, Xu Y, Luo Y, Zhang X, Capacchione C, Grassi A, *J. Catal*., 2019; 377: 367.
3. Liu X, Zheng H, Wang X, Jiang Z, Gu J, Liu H, Zhang C, Yang Q, Zhang X, *Eur. Polym. J*., 2023; 196: 112333.
4. Gong D, Dong W, Hu Y, Bi J, Zhang X, Jiang L, *Polymer*, 2009; 50: 5980.
5. Gong D, Zheng Y, Hu Y, *J. Mol. Catal*., 2024; 555: 113854.
6. Hu W, Xu Y, Ying W, Hu Z, Luo W, Tang F, Huang W, Jia X, Gong D, *J. Mol. Catal*., 2020; 497: 111219.

International Rubber Conference 2025 (IRC2025)
1-3 December 2025 @ BITEC, Bangkok, Thailand

ECIU Rubber Chair - An Inter-University Organisation Focused on Rubber Science and Intersectoral Impact

R. ANYSZKA[1]

[1] *Institute of Polymer and Dye Technology, Faculty of Chemistry, Lodz University of Technology, Lodz, Poland.*

rafal.anyszka@p.lodz.pl

Keywords: ECIU, Rubber, Science, Economy, Society, Environment

The European Consortium of Innovative Universities (ECIU) is an alliance of 13 universities established in 1997. This makes it one of the oldest university alliances. The goals of ECIU stem from solving real-life challenges by fostering collaboration between universities, society, cities, and businesses [1].

ECIU Rubber Chair was established this year with a Seed Grant provided by ECIU to three rubber-oriented groups from ECIU member universities: the Institute of Polymer and Dye Technology (at the Lodz University of Technology, Poland [2]), the Plastics and Elastomer Technology group (at the Tampere University, Finland [3]), and the Elastomer Technology and Engineering chair (at the University of Twente, The Netherlands [4]). The aims of the ECIU Rubber Chair reflect the goals of the ECIU alliance, specifically focused on rubber's impact on technology, economy, society, local communities, and the environment.

Currently, ECIU Rubber Chair is focused on establishing educational program for PhD students within EU-funded Marie Skłodowska-Curie Action grants [5], as well as an educational offer for all ECIU students via developing rubber-oriented challenge and micro-module [6]. In the future, it is planned to assist legal and business fields related to rubber market and involve local communities in actions related to rubber influence on the environment and its recycling.

The goal of this presentation is to introduce the ECIU Rubber Chair to the audience of IRC and foster future collaboration in broadly understood rubber-related activities.

Acknowledgement

This initiative is funded by the ECIU Seed Grant SP1 – ECIU Rubber Chair.

References

1. https://www.eciu.eu/ (accessed on 27.06.2025).
2. https://p.lodz.pl/en (accessed on 27.06.2025).
3. https://www.tuni.fi/en (accessed on 27.06.2025).
4. https://www.utwente.nl/en/ (accessed on 27.06.2025).
5. https://marie-sklodowska-curie-actions.ec.europa.eu/ (accessed on 22.08.2025).
6. https://engage.eciu.eu/browse (accessed on 22.08.2025).

International Rubber Conference 2025 (IRC2025)
1-3 December 2025 @ BITEC, Bangkok, Thailand

Polyrotaxane-Based Hybrid Crosslinking for Tunable Elastic and Thermal Response in Epoxidized Natural Rubber

A. THITITHAMMAWONG, K. AMIN, S. SALAEH, S. SAIWARI, B. THONGNUANCHAN, N. HAYEEMASAE

Research Unit of Advanced Elastomeric Materials and Innovations for BCG Economy (AEMI), Department of Rubber Technology and Polymer Science, Faculty of Science and Technology, Prince of Songkla University, Pattani Campus, Pattani

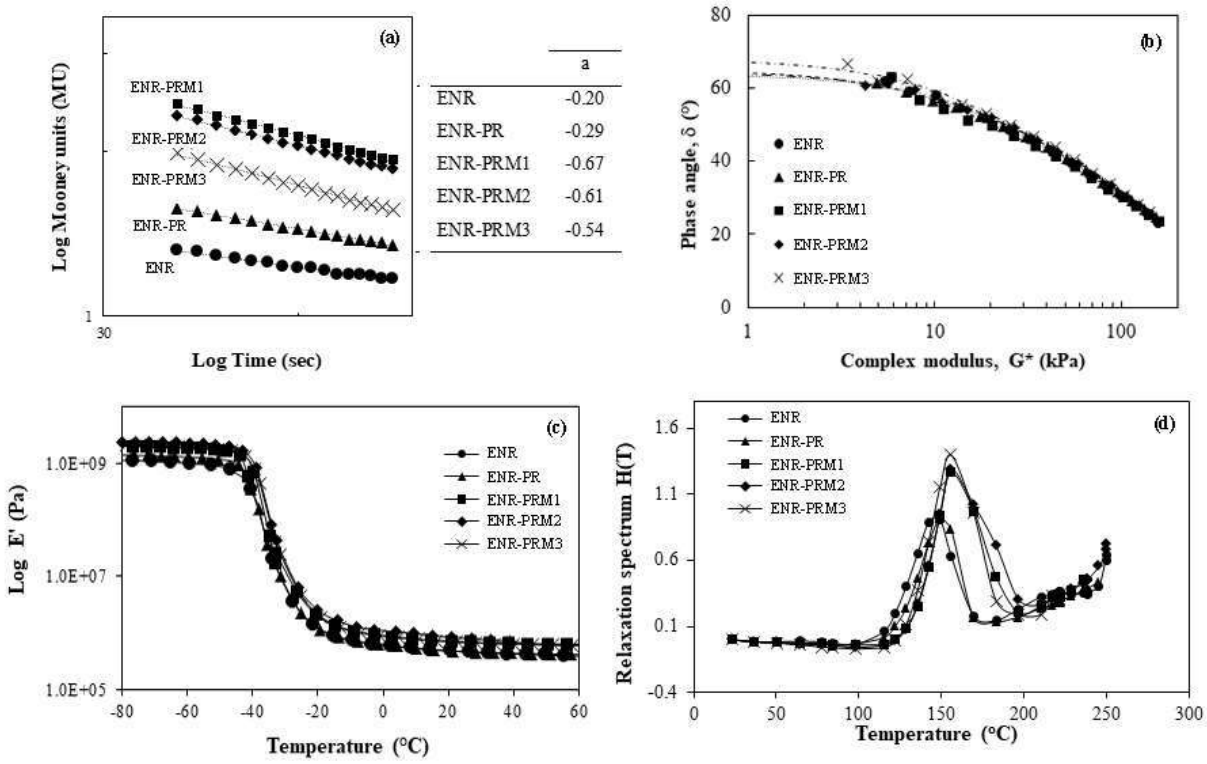
e-mail address of the presenting author (anoma.t@psu.ac.th)

Keywords: Epoxidized natural rubber, Polyrotaxane, Crosslink, Mercaptosilane, Relaxation

Polyrotaxanes (PRs), consisting of cyclic molecules threaded onto a linear polymer and capped with bulky groups, have emerged as dynamic crosslinkers in rubber due to their mechanically interlocked structures and pulley effect, which allows the rings to move along the backbone and distribute stress more evenly[1,2]. This motion contributes to enhanced elastic recovery, energy dissipation, and self-healing properties in elastomers[3]. Recent studies have demonstrated that incorporating PRs into rubber matrices can significantly improve tensile strength, toughness, thermal stability and dynamic durability [4,5]. Their supramolecular nature also allows for stimuli-responsive behavior, making them promising components in next-generation smart rubber materials[6].

This work aims to investigate the effect of PR *in-situ* grafted with mercaptosilane groups as a novel dynamic crosslinker in epoxidized natural rubber (ENR) to improve its stress relaxation and dynamic mechanical response. Rubber compounds were prepared using an internal mixer, where ENR was blended with the PR crosslinker and other compounding ingredients under controlled conditions followed by vulcanization using a hot press.The dynamic behavior and relaxation properties of the uncured and cured materials were evaluated using Mooney stress relaxation testing, dynamic mechanical analysis (DMA), and temperature scanning stress relaxation (TSSR). These tests were used to assess the viscoelastic performance, stress decay behavior, and temperature-dependent relaxation characteristics of the modified ENR compounds compared to conventional crosslinked systems.

Results in Figure 1 show that the incorporation of mercaptosilane-functionalized PR into ENRs significantly enhanced the material's stress relaxation resistance and dynamic performance. The modified rubber compounds exhibited reduced stress relaxation rates and increased thermal stress retention, indicating restricted chain mobility and stronger network interactions. These effects are attributed to a combination of hydrogen bonding, covalent grafting, and hybrid crosslinking between ENR, PR, and mercaptosilane groups. An optimal amount of silane (1–2 phr) further reinforced the network, improving modulus and elastic behavior, while excessive silane (3 phr) led to overplasticization and partial loss of crosslink efficiency. Overall, the hybrid crosslinking system based on movable PR segments and dynamic H-bonds provided a more elastic and thermally stable rubber network, capable of dissipating stress efficiently under dynamic and thermal loading.



	a
ENR	-0.20
ENR-PR	-0.29
ENR-PRM1	-0.67
ENR-PRM2	-0.61
ENR-PRM3	-0.54

Figure 1. Dynamic behavior and relaxation properties of the uncured and cured ENRs

Acknowledgement

The authors gratefully acknowledge the National Science, Research and Innovation Fund (NSRF) and Prince of Songkla University for financial support (Grant No. SAT6601168d).

References

1. Harada A, Takashima Y, Yamaguchi H, *Macromol. Rapid Commun*., 2009; 30 (11): 861.
2. Bruns C J, Stoddart J F, *Acc. Chem. Res.*, 2014; 47 (6): 2186.
3. Watanabe J, Takashima Y, Yamaguchi H, Harada A, *Polym. J.*, 2015; 47: 776.
4. Tanaka Y, Kato, K, Harada A, *Polym. Chem.*, 2019; 10: 1366.
5. Watanabe J, Nomura S, Takashima Y, Harada A, *Polym. J.*, 2015; 47: 776.
6. Liu Y, Zhang S, Wang Y, Li Y, *J. Mater. Chem. A*, 2020; 8: 8022.

Actuation Programming of Liquid Crystal Elastomers

Binjie Jin[1,2], Baochun Guo[1,2], Liqun Zhang[2]

[1] *School of Materials Science and Engineering, South China University of Technology, Guangzhou, China*

[2] *Institute of Emergent Elastomers, South China University of Technology, Guangzhou, China*

binjiejin@scut.edu.cn

Keywords: Functional elastomer, Polymer actuator, Liquid crystal elastomer

Soft robotics leverages programmable polymeric actuators to achieve high deformability and intrinsic biocompatibility [1]. Among these, liquid-crystal elastomers (LCEs)-cross-linked networks combining mesogen anisotropy with rubber elasticity-stand out as leading candidates. However, three key challenges remain: (1) actuation introduction still requires specialized devices or complex molecular design, (2) dynamic shape evolution during actuation is difficult to control, and (3) thermal, optical, and electrical actuation modes operate independently. To address these limitations, we first report several innovative actuation programming strategies for LCEs, as illustrated in Figure 1, which includes a solvent-induced phase separation decoupled from the nematic–isotropic transition, enabling universal actuation introduction/erasing via directional solvent evaporation/swelling [2]. Next, we develop topology-isomerizable LCE networks with spatially programmable actuation temperatures, achieved through light-regulated heterolytic dynamic bond exchange, allowing precise control over actuation sequences [3]. Finally, we introduce LCE dielectric actuators capable of autonomous mode-switching upon heating/cooling, driven by geometry-dependent electromechanical behavior and bending stiffness variations during thermo-triggered shape changes [4]. Together, these advances establish a programmable platform for next-generation soft robotic systems.

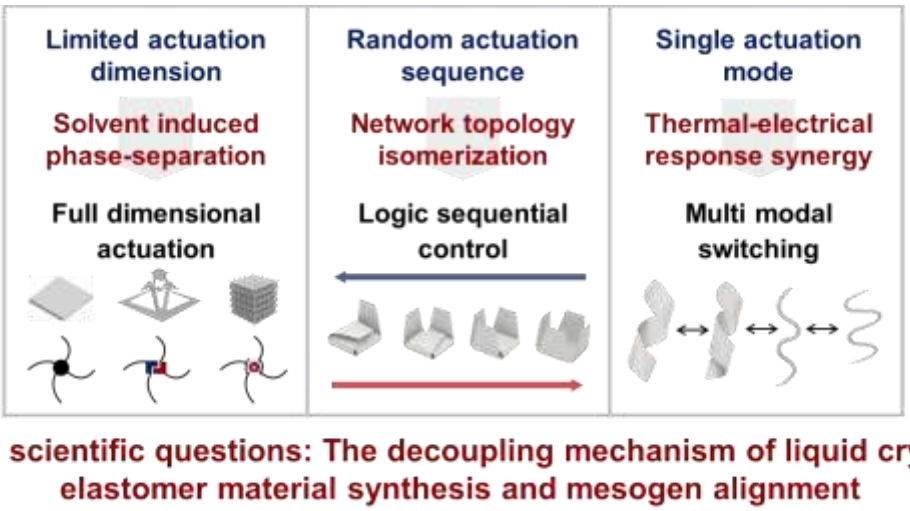


Figure 1. Actuation programming of liquid crystal elastomers

Acknowledgement

The authors would like to express their gratitude to the National Science Foundation of China.

References

1. Herbert K.M, Fowler H.E, McCraken J.M, Schlafmann K.R., Koch J.A, White T.J, *Nat. Rev. Mater.* 2021; 7: 23.
2. Jin B, Liu J, Shi Y, Chen G, Zhao Q, Yang S, *Adv. Mater.* 2022; 34: 2107855.
3. Chen G, Feng H, Zhou X, Gao F, Zhou K, Huang Y, Jin B, Xie T, Zhao Q, *Nat. Commun.* 2023; 14: 6822.
4. Zhang C, Chen G, Zhang K, Jin B, Zhao Q, Xie T, *Adv. Mater.* 2024; 36: 2313078.

Biomimetic Design and Development of Natural Rubber-based Soft Robotics

M. SRIRING[1], T. WATCHARAKAN[1], C. SIRISINHA[1]

[1] *Rubber Technology Research Centre (RTEC), Faculty of Science, Mahidol University, Nakhon Pathom, Thailand*

*e-mail (manus.sri@mahidol.ac.th)

Keywords: Natural rubber, Soft robotics, Pneumatic, Grippers, Actuator

Soft robotics represents an evolution in robot, utilising mechanically soft and flexible materials such as silicone rubber and hydrogels. The system is often inspired by biomimetic mechanisms, including worms, octopus arms [1], and human hands [2] etc. (Figure 1). Compared to traditional rigid robots, soft robots offer several advantages, including safer interaction with humans and fragile objects, adaptability to unstructured environments, and enhanced flexibility for performing complex tasks. Among various actuation approaches, pneumatic actuation has gained significant attention due to its lightweight nature, low cost, ease of fabrication, and ability to produce motion through simple inputs [3]. Pneumatic actuators are typically fabricated from silicone rubber and consist of two primary layers, including an extensible top layer and an inextensible, but flexible bottom layer. These layers are incorporated together with embedded pneumatic networks (PNs) in the structure. The deformation and motion of soft pneumatic robots are achieved by applying air or fluid pressure to these embedded PNs. As a result, materials used in such robotic applications must possess excellent flexibility, elasticity, high tear strength, and favourable dynamic properties. Natural rubber (NR) emerges as an excellent material choice for such applications, owing to its outstanding mechanical properties, biocompatibility, cost-effectiveness, and renewable origin. These attributes make NR an especially attractive option for developing sustainable soft robotic systems.

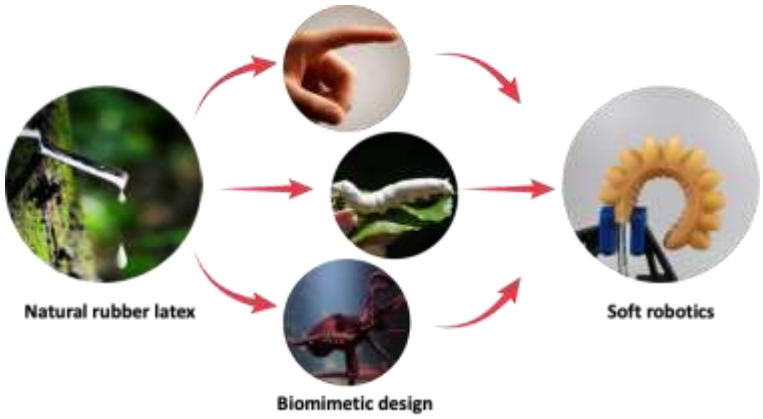


Figure 1. Concept workflow for development of natural rubber-based soft robotics

In this present work, we aim to develop strategies for utilising natural rubber (NR) in advanced and high-value soft robotics applications. A human finger-inspired soft robotic actuator was designed based on the fast-PNs concept [2], incorporating variations in key physical parameters such as chamber height, wall thickness, and the number of PNs. Moulds for each design were fabricated using a stereolithography (SLA) 3D printer. The soft robotic actuators were produced by casting prevulcanised NR latex into the moulds, following a specific fabrication protocol developed by RTEC. The bending performance of the actuators was evaluated as a function of actuation pressure. To further investigate the relationship between material properties and actuation behaviour, additional

actuators were fabricated using NR latices with varying crosslink densities. These were prepared by adjusting the sulphur content in the formulation (0.30, 0.75, and 1.20 phr), while maintaining a fixed accelerator-to-sulphur (A/S) ratio of 0.67.

The results demonstrated that NR-based soft robotics exhibited effective biaxial bending under both positive and negative pressures, as shown in Figure 2. The actuation performance of the actuators was found to be directly influenced by the height and number of pneumatic chambers, with increased height and chamber numbers leading to improved bending capabilities. In contrast, actuation performance was inversely related to the wall thickness of the PNs, as thicker walls reduced the actuation ability. These differences in actuation behaviour are attributed to variations in the inflatable response of the material resulting from each structural design. The findings provide valuable insight for optimising soft robotic architectures tailored to specific applications.

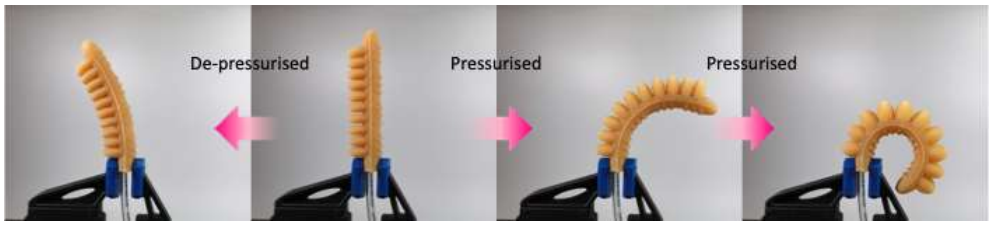


Figure 2. Actuation mechanism of NR soft robotics actuator under negative and positive air pressure

In addition, the actuation efficiency of soft actuators was also found to depend on the material properties. With higher sulphur content, the crosslink density of the NR samples increased from approx. 3.26×10^{-5} mol/g (at 0.30 phr) to approx. 6.94×10^{-5} mol/g (at 1.20 phr), resulting in significant improvements in modulus (60%), tensile strength (70%), tear strength (50%), and dynamic performance of the vulcanisates. As a result, soft actuators fabricated from NR with higher crosslink densities required greater actuation pressure due to reduced deformability. However, their increased stiffness made them more effective for tasks requiring higher interaction forces, such as grasping or lifting heavier objects. These findings highlight the potential of NR latex as a sustainable, high-performance alternative to synthetic materials in advanced soft robotic applications, including space exploration, search and rescue systems, biomimetic devices, surgical tools, and rehabilitation technologies.

Acknowledgement

This project is funded by National Research Council of Thailand (NRCT): N42A670197.

References

[1] Z. Xie, A.G. Domel, N. An, C. Green, Z. Gong, T. Wang, E.M. Knubben, J.C. Weaver, K. Bertoldi, L. Wen, Octopus Arm-Inspired Tapered Soft Actuators with Suckers for Improved Grasping, Soft Robot 7(5) (2020) 639-648.

[2] S. Li, J. Wang, X. Li, Z. Huang, Information Express of Soft Bionic Finger Based on Visual Recognition, 2022 IEEE International Conference on Cyborg and Bionic Systems (CBS), 2023, pp. 240-244.

[3] B. Mosadegh, P. Polygerinos, C. Keplinger, S. Wennstedt, R.F. Shepherd, U. Gupta, J. Shim, K. Bertoldi, C.J. Walsh, G.M. Whitesides, Pneumatic Networks for Soft Robotics that Actuate Rapidly, Advanced Functional Materials 24(15) (2014) 2163-2170.

Epoxidized Natural Rubber and Its Composite-Based Sensors and Energy Harvesters

Titash Mondal

Rubber Technology Centre, Indian Institute of Technology Kharagpur, Kharagpur, India-721302

e-mail address of the presenting author (titash@rtc.iitkgp.ac.in)

Keywords: TENG, Sensors, Energy Materials, Composite

Rubber nanocomposites, which combine elastomers with nanomaterials such as graphene, carbon nanotubes, and nanoparticles, are emerging as transformative materials for this paradigm. These composites offer unique properties, including flexibility, lightweight design, mechanical robustness, and enhanced electrical conductivity, making them pivotal in various applications.

One prominent use of rubber nanocomposites is in sensors, wherein the electrical conductivity of the conductive fillers is leveraged for developing resistive sensors that could show changes in the relative resistance values upon application of external stimuli. In this talk, specific examples of epoxidized natural rubber (ENR)-based multifunctional sensors will be discussed. In the study window, ENR-graphene (ENRG) based sensor demonstrated a gauge factor of −506 and 407 in the bending strain regimes of 0–0.04% and 0.04%–0.09%, respectively, while the temperature sensitivity was noted to be −0.96%/°C. [1] The work was extended to the domain of triboelectric nanogenerators (TENGs). A novel vitrimeric composition was made using ENRG along with textile, with targeted application as textile TENGs. The record high output performance with a power density of 4.69 W m^{-2} accomplished using a single fabric layer with a thickness of 0.56 mm supports the amalgamation of dielectrically optimized elastomeric coatings with textiles for next-generation self-powered wearables. [2,3] Also, the strategic utilization of dynamic covalent chemistry imparted self-healing properties to the coating.

Further, the work was extended by adopting a filler-free composition based on ENR for developing a TENG for a self-powered wearable application. Naturally occurring Tannic acid was used as modifier for ENR. The tannic acid modified ENR demonstrated This modified material was utilized as a tribo-positive pair for TENG construction, which resulted in a very high output voltage of 751 V (at 9 Hz) and 568 V (at 5 Hz). The maximum obtained power density recorded at 9 Hz is 37 W m^{-2} at 1 MΩ external load resistance, and an average power density is 20 W m^{-2} at a load resistance of 10–100 MΩ. [4,5]

Accordingly, this talk highlights the potential of rubber and its nanocomposites as a cornerstone for achieving sensors and TENG developmental goals, offering solutions for automation and greener energy harvesting technologies.

References

1. Sharma S, Selvan T M, Naskar S, Mondal S, Mukhopadhyay T, Mondal T, *ACS Applied Mater. Interfaces.*, 2022; 14: 57265.
2. Sharma S, Mondal T, *Small.*, 2025; 21: 2500481.
3. Sharma S, Mondal T, *Small.*, 2024; 20: 2404771.
4. Guchait A, Haridas CP A, Chattopadhyay S, Mondal T, *Small.*, 2025; 21: 2411410.
5. Guchait A, Saxena A, Chattopadhyay S, Mondal T, *Small.*, 2025; 21: e06264.

International Rubber Conference 2025 (IRC2025)
1-3 December 2025 @ BITEC, Bangkok, Thailand

Elastomeric Ionomer based on Maleated Bromobutyl Rubber

S. SALAEH[1], B. MARSRI[1], S. WIESSNER[2,3], A. DAS[2]

[1] *Department of Rubber Technology and Polymer Science, Faculty of Science and Technology, Prince of Songkla University, Pattani campus, Pattani, 94000, Thailand.*

[2] *Leibniz-Institut für Polymerforschung, Dresden e. V., Hohe Straße 6, D-01069, Dresden, Germany.*

[3] *Institute of Materials Science, TUD Dresden University of Technology, D-01069, Dresden, Germany.*

e-mail address of the presenting author (subhan.s@psu.ac.th)

Keywords: Ionomer, Zinc-carboxylate, Ionic bonds, Maleic anhydride, Bromobutyl rubber

Ionomers are a class of polymers characterized by a hydrocarbon-based backbone and a relatively small proportion (typically less than 15 mol%) of attached ionic or ionizable groups. The backbone is typically composed of polyolefins, while the side groups often include ammonium ions or acidic functionalities, such as carboxylic, sulfonic, or phosphoric acid groups. The ionomeric elastomers are usually prepared from carboxylated acrylonitrile butadiene rubber (XNBR), maleate or sulfonated ethylene propylene diene copolymer (EPDM), and maleate natural rubber (MNR) [1-3]. Currently, the research on a new ionomeric elastomer based on other rubbers is still in progress, and diverse performances need to be further explored.

Polyisobutylene (PIB)-based elastomers have garnered considerable attention due to their broad range of commercial applications due to their high elasticity, excellent resistance to gas and water permeation, and remarkable chemical stability. One of the most important derivatives of PIB is brominated isobutylene-isoprene rubber (BIIR), which is produced by brominating butyl rubber (isobutylene-co-isoprene). This modification not only enhances the vulcanization rate but also improves compatibility with unsaturated rubbers without compromising the material's thermal and chemical resistance, damping behavior, or low permeability. These reactive bromine sites enable the functionalization of BIIR, paving the way for the development of advanced ionomeric materials. Various nucleophilic agents, such as pyridine, imidazole, triphenylphosphine, and tetraethylammonium sulfite, have been employed to introduce functional groups, leading to the synthesis of BIIR-based ionomers with tailored properties [4-6].

In this work, we developed a rubber-based ionomer from ionically cross-linked BIIR-*graft*-maleic anhydride (MBIIR), as summarized in **Figure 1**. First, BIIR was chemically modified with various amounts of maleic anhydride (MA) in the melt state (160°C). Grafting degree and efficiency increased with temperature and MA content. The FTIR spectra revealed that carboxylic acid was successfully grafted onto the MBIIR backbone, which was further used for the preparation of ionic elastomer. The MBIIRs containing different MA loadings (i.e., 2.5, 5, 7.5, and 10 phr) were mixed with zinc oxide (ZnO) (5 phr) and stearic acid (StA) (5 phr). During vulcanization, ionic bonds were formed in MBIIRs through zinc-carboxylate networks and multi-ion-pair clusters, which enhanced the mechanical properties and elasticity of ionomer based on MBIIR. The tensile strength was significantly improved from ~0.5 MPa for neat BIIR and MBIIRs to > 15 MPa for MBIIR ionomers. At the same time, ionically cross-linked MBIIR exhibited higher tensile strength and elongation at break than that of sulfur-cured BIIR. The results also showed that mechanical performance, cross-link density, dynamic mechanical behavior, and morphology were strongly dependent on ZnO and StA contents. Consequently, this study demonstrates that zinc-carboxylate interactions are feasible

for improving the physical and dynamic properties of MBIIR ionomers, which can offer new applications in aerospace, construction, automotive, and medical devices.

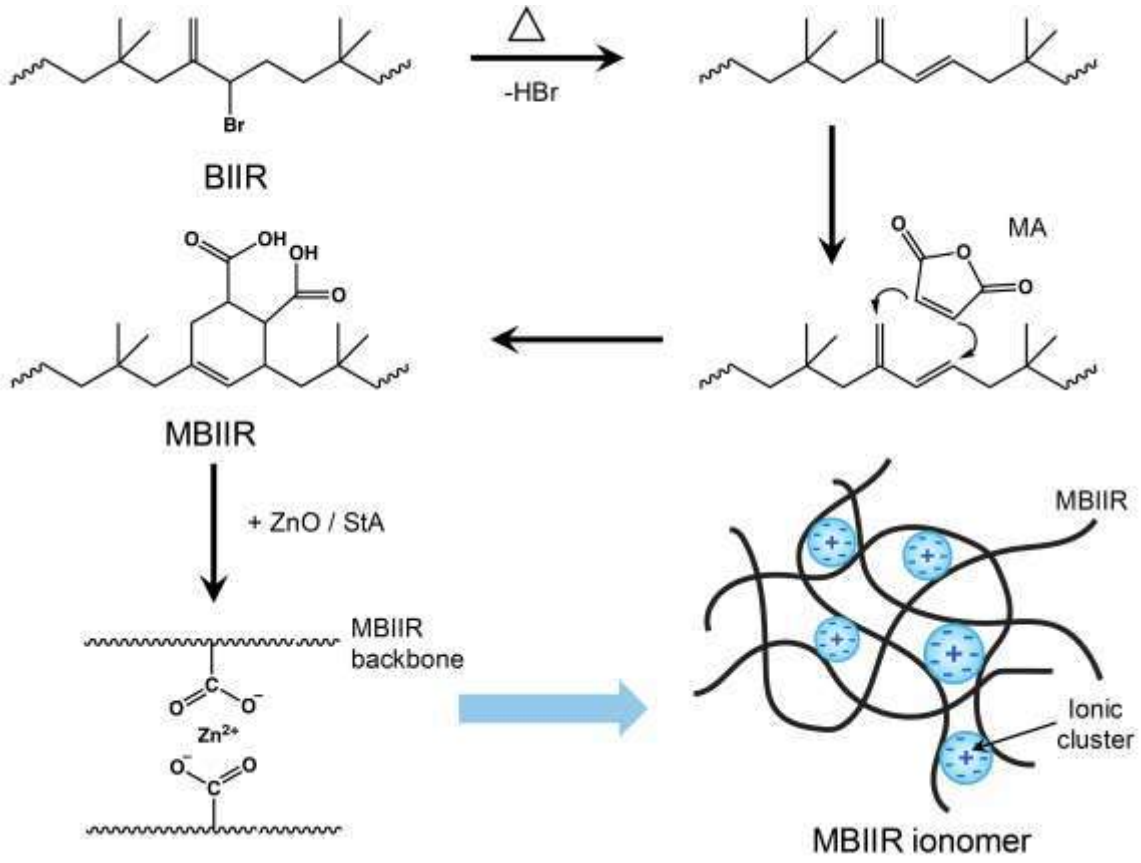


Figure 1. Chemical modification of BIIR with MA and synthesis of MBIIR ionomer

Acknowledgement

This research was supported by Prince of Songkla University (SAT6703035S).

References

1. Jia T, Wang R, Zhang M, Ren C, YangY, Wang J, Yang Y, *Chem Bio Eng*., 2024; 2: 156.
2. Malmierca M A, González-Jiménez A, Mora-Barrantes I, Posadas P, Rodríguez A, Ibarra L, Nogales A, Saalwächter K, Valentín J L, *Macromolecules*, 2014; 47: 5655.
3. Basu D, Das A, Stöckelhuber K W, Jehnichen D, Formanek P, Sarlin E, Vuorinen J, Heinrich G, *Macromolecules*, 2014; 47: 3436.
4. Behera P K, Kumar A, Mohanty S, Gupta V K, *Ind. Eng. Chem. Res.* 2022; 61: 16910.
5. Das A, Sallat A, Böhme F, Suckow M, Basu D, Wießner S, Stöckelhuber K W, Voit B, Heinrich G, *ACS Appl. Mater. Interfaces*, 2015; 7: 20623.
6. Zhang L, Wang H, Zhu Y, Xiong H, Wu Q, Gu S, Liu X, Huang G, Wu J, *ACS Appl. Mater. Interfaces*, 2020; 12: 53239.

Properties and Crosslinking Mechanisms of 1,2-Polybutadiene Derivative-Based Rubber Formulations

Hiroki HASHIMOTO, Hokuto OHURA, Yasuhisa SHIBATA,

NIPPON SODA CO., LTD., Development dept., Chemical Business div., 2-7-2 Marunouchi, Chiyoda-ku, Tokyo, Japan
e-mail address of the presenting author (hi.hashimoto@nissogr.com)

Keywords: 1,2-Polybutadiene, 1,2-Epoxydized polybutadiene, Crosslinking, GECO (Epichlorohydrin/Ethylene Oxide/Allyl Glycidyl Ether Terpolymer), Acid acceptor

Introduction

1,2-Polybutadiene (1,2-PB) exhibits heat curing properties through 1,2-vinyl crosslinking reactions, clearly distinguishing it from conventional liquid polybutadienes(PB) containing 1,4-olefin units[1]. Despite its use as an additive, between the crosslinking mechanisms of 1,2-vinyl and 1,2-epoxidized PB and the resulting material properties has not been systematically investigated.

1,2-Epoxidized PB containing both 1,2-vinyl units and 1,2-epoxydized units was synthesized using 1,2-PB as the starting material. It exhibits both crosslinking and acid-accepting properties, making it useful for halogenated rubber formulations. Our research showed that 1,2-epoxidized PB contribute to providing an alternative to lead monoxide (PbO) in halogenated rubber formulations, particularly for epichlorohydrin rubber (GECO: Epichlorohydrin/Ethylene Oxide/Allyl Glycidyl Ether Terpolymer) applications. This innovative solution using 1,2-epoxidized PB not only provides superior rubber performance but also supports sustainable rubber formulations that comply with environmental standards by replacing hazardous materials such as PbO.

GECO (Epichlorohydrin Rubber) formulation

In this presentation, we report the effectiveness of 1,2-epoxidized PB as an acid acceptor for GECO rubber. The structural formulas are shown in Figure 1 and Figure 2.

The mixing ratios of GECO and 1,2-epoxidized PB are presented in Table 1, and the rubber properties are shown in Table 2. Comparative studies with the conventional acid acceptor MgO demonstrated superior acid resistance properties, which were confirmed to be attributing to the epoxy units through comparison with non-epoxidized 1,2-PB.

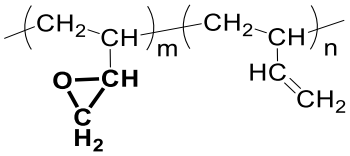


Figure 1. 1,2-Epoxylated Polybutadiene

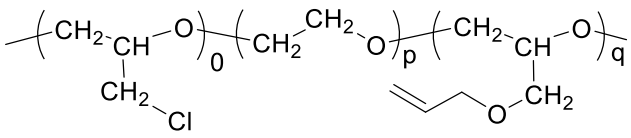


Figure 2. GECO (Epichlorohydrin/Ethylene Oxide/Allyl Glycidyl Ether Terpolymer)

The 1,2-epoxidized PB contains two types of functional units: 1,2-epoxy units and 1,2-vinyl units. These functional units can promote crosslinking reactions through 1,2-vinyl unit polymerization and ring-opening reactions of the epoxy units.

GECO formulations without acid acceptors (Entry 1) exhibit inferior hardness, compression set, and acid resistance compared to PbO-containing formulations (Entry 5). MgO, as an alternative to PbO (Entry 4), shows comparable hardness and compression set but significantly inferior acid resistance compared to PbO (Entry 5). In contrast, 1,2-epoxidized PB shows acid resistance comparable to that of PbO, and increases the hardness and compression set values in relation to the content ratio (Entries 2, 3 vs. 5).

Table1. 1,2-Epoxidized PB / GECO formulation

	Entry						
	1	2	3	4	5	6	7
GECO [1)]	100	100	100	100	100	100	100
1,2-Epoxidized PB [2)]	0	3	10	0	0	0	0
MgO	0	0	0	3	0	0	0
PbO	0	0	0	0	5	0	0
1,2-PB	0	0	0	0	5	3	10
Sorbitan stearate	2	2	2	2	2	2	2
Carbon black	40	40	40	40	40	40	40
α,α'-Di(t-butylperoxy) diisopropylbenzene	1.3	1.3	1.3	1.3	1.3	1.3	1.3

1) EPICHLOMER CG (OSAKA SODA CO., LTD.)
2) NISSO PB JP-100 (NIPPON SODA CO., LTD.)

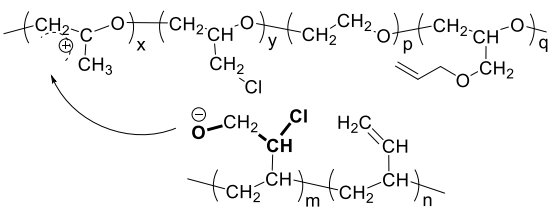


Figure 3. Crosslinking reaction

Table2. The properties of 1,2-Epoxidized PB / GECO formulation

Entry	Mechanical properties			Water/Acid resistance [4)]		
	Shore hardness	Tensile strength at break [MPa]	Compression Set(%) [3)]	Pure water ΔV [%]	600ppm Cl_2 ΔV [%]	20% HCl ΔV [%]
1	A65	8.98	44	+9	+12	+10
2	A76	7.81	32	+5	+6	+8
3	A83	9.86	25	+4	+4	+6
4	A78	10.50	32	+20	+22	+33
5	A81	9.96	25	+4	+4	+7
6	A68	8.60	41	+8	+10	+9
7	A67	7.62	38	+8	+10	+9

3) Temperature 100 ± 1°C, Time 72 hours
4) Temperature 80 ± 2°C, Time 168 hours, volume change

To confirm the specific contribution of epoxy units, comparative studies were conducted with non-epoxidized 1,2-PB (Entries 6, 7). The observed differences in hardness between epoxidized and non-epoxidized PB formulations (Entries 2, 3 vs. 6, 7) indicate that epoxy unit crosslinking is proceeding. The superior acid-accepting properties exhibited by epoxidized PB-containing systems suggest that chlorine is captured by epoxy units, leading to ring opening and subsequent crosslinking (Figure 3).

Conclusion

This study shows that 1,2-epoxidized PB serves as an effective dual-functional additive for GECO rubber, providing both crosslinking and acid acceptance. The material exhibits PbO-equivalent or superior performance with environmental advantages, offering valuable insights for sustainable rubber formulation development.

Acknowledgement

The authors gratefully acknowledge OSAKA SODA CO., LTD. for their generous provision of GECO "EPICHLOMER CG", which made this evaluation study possible.

References

[1] Hiroki HASHIMOTO, Hiroshi SAKAI and Izumi TANDO, *Journal of the Society of Rubber Science and Technology*, 2020; 93: 273.

International Rubber Conference 2025 (IRC2025)
1-3 December 2025 @ BITEC, Bangkok, Thailand

Property and Application of Perfluoropolyether-modified Functional Rubber

Zheming Tong[1], Yuzhi Feng[1], Zhiyang Tong[1,2], Shuai Xu[1], Yulin Yi[1], Guangbi Gong[1]

[1]*PetroChina (Shanghai) New Materials Research Institute Co., Ltd., Shanghai, China..*

[2] *Zhejiang University, Hangzhou, China.*

E-mail address of the presenting author (zhemingtong@126.com)

Keywords: Perfluoropolyether, NBR rubber, Silicone rubber, Functional modification

In recent years, with the rapid development of new energy vehicles and the petroleum industry, the use of rubber sealing materials has been increasing significantly. When components operate under dynamic conditions, friction causes the rubber product surface to heat up significantly and undergo wear, gradually weakening the sealing performance. Therefore, anti-friction agents play a critical role in rubber seals, effectively reducing wear and thereby extending the service life of sealing components. Additionally, these rubber components must also meet requirements for corrosion resistance, anti-fouling, hydrophobicity, oleophobicity, and antibacterial properties, which further elevate the demands on the surface and interface performance of rubber products.

Fluorinated elastomers have better resistance to high temperature, oil, aging and chemical media due to the presence of strong electronegative fluorine atoms and high bonding energy carbon-fluorine bonds[1]. Among them, perfluoropolyether (PFPE) based elastomers are elastomers synthesized by further crosslinking and vulcanizing prepolymers (such as polysiloxanes or butadiene-acrylonitrile oligomers), which are modified or grafted with perfluoropolyether chains[2]. Since PFPE polymers have only fluorocarbon, carbon oxygen and carbon-carbon bonds, it exhibits excellent molecular chain flexibility, low glass transition temperature (Tg), high temperature thermal stability, corrosion resistance, wear resistance, etc., which makes this type of elastomers have a wide temperature range and long term resistance to chemicals and fuel media[3].

Fluorinated silica modified nitrile butadiene rubber (NBR) was synthesized from NBR and double-ended silohydro-perfluoropolyether-b-polysiloxane (PFPE-b-PSi-H) anti-friction agents (Figure 1), which were prepared from PFPE allyl ether (PFPE-ally) and 3 types of double-ended hydrogen containing silicone oil (PSi-H) with different hydrogen mass fractions (referring to the H in the Si-H bond). The results showed that the addition of PFPE-b-PSi-2, prepared from PSi-H with a hydrogen mass fraction of 0.115wt%, better improved the performance of modified NBR. Moreover, when the amount of PFPE-b-PSi-2 added was 2.0wt% of the mass of NBR, the Akron abrasion volume decreased from 0.250 cm^3 to 0.125 cm^3, the static friction coefficient decreased from 2.589 to 1.402, the dynamic friction coefficient decreased from 2.176 to 1.209. All the data suggested that the friction reducer added decreased the resistance to internal segment movement and surface wear of NBR.

In addition, PFPE was used in the modification of silicone polyurethane rubber. Silicone rubber has excellent flexibility and biocompatibility, but its strength, solvent resistance and antifouling properties are inferior to those of organofluorinated rubbers. Therefore, we introduced functionalized PFPE chains into silicon polyurethane rubbers for cross-linking and curing. The mechanical properties (tensile strength and Young's modulus) of the silicon polyurethane rubber modified by PFPE were not deteriorated. At the same time, its resistance to organic solvents was significantly enhanced, and the surface energy was significantly reduced to 20 mN/m. The modified silicone rubber

was prepared as a coating, and its self-cleaning performance and antifouling performance were significantly improved. The coating exhibited excellent anti-adhesion properties against inorganic pollutants, bacteria, algae and marine organisms.

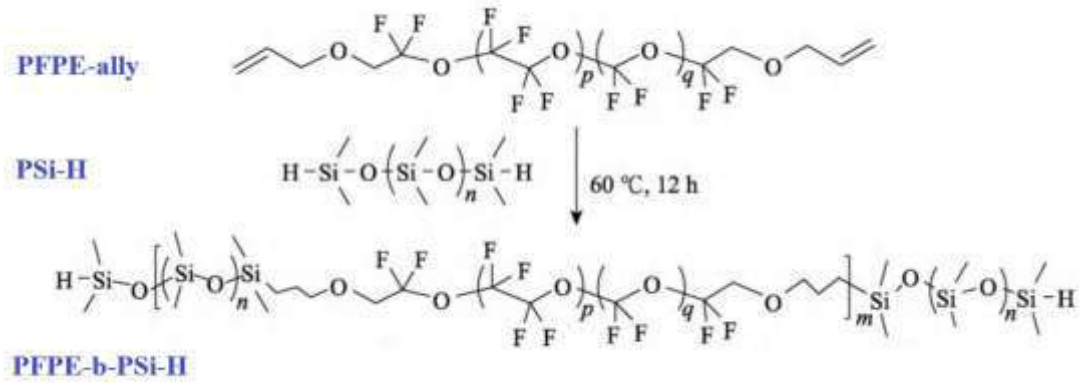


Figure 1. Synthesis process and structure of silicone-modified PFPE polymer chain (PFPE-b-PSi-H)

References

1. Chadron M F , Bruno A, *Prog. in Polym. Sci.*, 2018; 81: 238.
2. Ma Q, Liao S, Ma Y, *Adv. Mater.*, 2021; 33: 2102096.
3. Ameduri B, Boutevin B, *J. Fluorine Chem.*, 2005; 126: 221.

Session IV : Progress in Rubber Characterisation

Oral Presentations

International Rubber Conference 2025 (IRC2025)
1-3 December 2025 @ BITEC, Bangkok, Thailand

Formulations of finite hyperelasticity and viscoelasticity using invariants of stretch tensors

Alexander Lion [1], Michael Johlitz[1]

[1] *University of the Bundeswehr Munich, Werner-Heisenberg-Weg 39, 85579 Neubiberg, Germany.*

Alexander.lion@unibw.de

Keywords: hyperelasticity, viscoelasticity, material modelling, stretch tensors

In order to represent the mechanical behaviour of isotropic, incompressible and elastic materials in continuum mechanics, constitutive models of finite hyperelasticity are commonly used. In most cases, the associated specific Helmholtz free energy depends on the invariants of the left or the right Cauchy-Green tensor. The best known example from this category is the generalized Mooney-Rivlin model. Other approaches, for example statistically or micromechanically-based formulations or the models developed by Ogden, use the eigenvalues of the stretch tensors as arguments. As a consequence of their mathematical structure, the Cauchy-Green tensors are pronounced nonlinear deformation measures. Even the simple Neo-Hookean model of finite hyperelasticity with only one material parameter, whose Cauchy stress tensor depends linearly on the left Cauchy-Green tensor, shows a pronounced nonlinear behaviour.

In the presentation, the right and left stretch tensors are used as intrinsic arguments of the Helmholtz free energy density because these deformation measures depend rather linearly on the deformation. In order to formulate such a model compatible with the 2nd law of thermodynamics and to derive a consistent potential relation, the polar decomposition of the deformation gradient is considered and the stress power is reformulated using associated stress- and deformation rate tensors.

The evaluation of the Clausius-Duhem inequality by the standard method yields the potential relation for the co-rotated Kirchhoff stress tensor. A transformation leads to the Cauchy stress as function of the left stretch tensor. Based on this outcome, some simple and more complicated energy functions are evaluated for uniaxial tension/compression, simple and pure shear as well as for biaxial tension.

In the final step, this approach is transferered to finite multiplicative viscoelasticity, where the specific Helmholtz free energy is assumed to be a function of an elastic stretch strensor. The outcomes of this stretch tensor-based formulation are compared with simulations based on classical Cauchy-Green tensor-based models and discussed.

International Rubber Conference 2025 (IRC2025)
1-3 December 2025 @ BITEC, Bangkok, Thailand

Numerical modeling of the non-isothermal viscoelastic flow behavior of rubber compounds based on the PHAN-THIEN-TANNER (PTT) model

H. Damanik[1], A. Fatima[1], S. Turek[1], J. Petzke[2], D. Kleinschmidt[2], F. Bruening[2]

[1] *Lehrstuhl 3 für Angewandte Mathematik, TU Dortmund University, Vogelpothsweg 87, 44227 Dortmund, Germany*

[2] *Kunststofftechnik Paderborn, Paderborn University, Warburger Straße 100, 33098 Paderborn, Germany*

hdamanik@mathematik.tu-dortmund.de

Keywords: numerical simulation, material modeling, computational fluid dynamics, PHAN-THIEN-TANNER

The numerical simulation of CFD for rubber materials is seeing growing demand in industry, yet most simulations rely on nonlinear viscosity functions rather than true viscoelastic laws. The main bottleneck is the mathematical difficulty in modeling rubber materials by differential viscoelastic constitutive equations such as PTT [2], and in particular, it is challenging to determine the nonlinear material parameter ε that governs rubber behaviour in the PTT model, see [1]. Standard Rubber Process Analyzer (RPA) measurements using oscillatory deformation, as in Table 1, provide only linear material data like G' (Storage modulus) and G" (Loss modulus), failing to characterize nonlinear rheology. In this work, a nonstandard RPA approach is introduced (see Table 2), wherein the cone rotates continuously to induce shear on the sample, and the resulting measurements are used to derive shear and thus nonlinear ε values from the PTT model directly. The measured quantities G' and G", together with the derived nonlinear parameter ε, form the complete set of viscoelastic parameters to be determined, typically expressed as (G_i, λ_i, ε_i), representing both the linear viscoelastic response and the nonlinear material behavior essential for realistic simulation.

For material characterization, a D-RPA 3000 from MonTech Werkstoff-Prüfmaschinen GmbH (Buchen, Germany) was utilized, featuring a cone–cone configuration with a cone angle of 7.167°, which generates a homogeneous shear rate field across the entire sample and functions as a closed cavity rheometer. For experimental investigations, a styrene-butadiene rubber (SBR) compound was used, consisting of 90 phr SBR, 10 phr natural rubber (NR), 41.18 phr plasticizer, 64.71 phr silica, 64.71 phr kaolin, 3.82 phr pigment, and 19.71 phr processing additives. The process parameters applied for material data identification using the RPA are listed in Tables 1 and 2. For the investigations conducted in oscillatory mode, a frequency sweep was carried out for each strain amplitude and each temperature. Under steady shear conditions, a shear rate sweep was performed at each temperature.

Table 1. Process parameters of the RPA investigations under oscillatory shear

Process parameters	**Processing steps**												
Temperature [°C]	60	80	100	120	-	-	-	-	-	-	-	-	-
Frequency [Hz]	0.001	0.01	0.05	0.1	0.5	1	2	5	10	20	50	70	100
Amplitude [%]	0.1	1	10	-	-	-	-	-	-	-	-	-	-

Table 2. Process parameters of the RPA investigations under steady shear

Process parameters	**Processing steps**													
Temperature [°C]	60	80	100	120	-	-	-	-	-	-	-	-	-	-
Shear rate [1/s]	0.05	0.07	0.1	0.2	0.5	0.7	1	2	5	7	10	20	50	70

The unsteady incompressible Stokes equations are formulated using the deformation tensor to describe the fluid flow, and are extended by coupling with multi-mode viscoelastic PTT models to account for the complex material response with additional temperature equation such as:

$$\begin{cases} \frac{\partial u}{\partial t} - 2\eta_s \nabla \cdot D(u) - \nabla \cdot \sigma + \nabla p = (1 - \gamma\theta) \cdot g, \ \nabla \cdot u = 0, \sigma = \sum_i {}^{\eta_i}/_{\lambda_i} (\tau_i - I) \\ \exp\left(\frac{\varepsilon_i \lambda_i}{\eta_i} tr(\tau_i)\right) \tau_i + \lambda_i \tau_i' = 2\eta_i D, \ \tau' = \frac{\partial \tau}{\partial t} + (u \cdot \nabla)\tau - (\nabla u)^T \cdot \tau - \tau \cdot (\nabla u). \\ \frac{\partial \theta}{\partial t} + (u \cdot \nabla)\theta = \eta_T \Delta\theta + Q_\Theta \end{cases}$$

The set of viscoelastic parameters to be determined is (G_i, λ_i, ε_i). The (G_i and λ_i) represent the linear parameters Modulus and relaxation time, while (ε_i) corresponds to the nonlinear parameters. Using a quadratic error measure, we identified a set of 4-mode data, visualized in Figure 1.

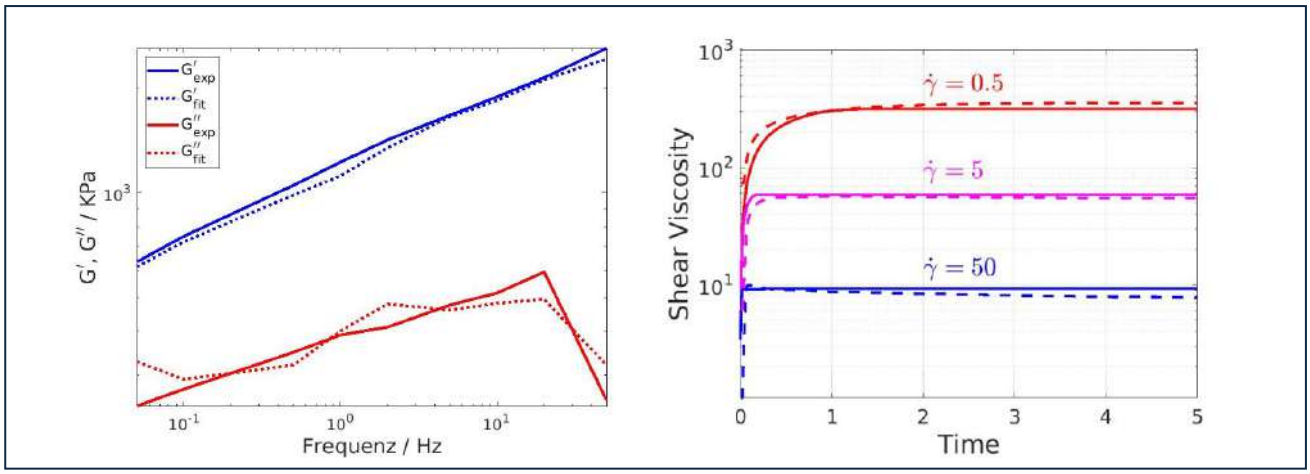


Figure 1: SBR material at T=80° : (Left) G' (R^2=0.995) and G''(R^2=0.821) fitting with the experimental data. (Right) Shear viscosity with three different values of shear rate (R^2=0.0.689, 0.841, 0.051).

Qualitatively, these data sets are optimal for use in CFD simulation. This implies that the error and the number of modes are kept low while the model still captures the full behavioral spectrum without significantly increasing memory demand due to the basic employed numerical strategy as in [3].

Acknowledgement

The authors gratefully acknowledge the financial support provided by the German Aerospace Center (DLR) (IGF No. 01IF22861N). This research was funded by the Federal Ministry for Economic Affairs and Climate Action (BMWK), based on a resolution of the German Bundestag. Furthermore, we would like to thank the companies represented in the project advisory committee for their constructive collaboration.

References

1. Obendrauf, W. Neue Methoden zur Temperatur- und Dehnviskositätsmessung für die Simulation von Kunststoffverarbeitungsprozessen. Dissertation, 1996.
2. Thien, P.; Tanner, R. A new constitutive equation derived from network theory. Journal of Non-Newtonian Fluid Mechanics, 2:353-365, 1977.
3. Damanik, H.; Hron, J.; Ouazzi, A.; Turek, S. A monolithic fem approach for the log-conformation reformuation (LCR) of viscoelastic flow problems. Journal of Non-Newtonian Fluid Mechanics, 165 (19-20): 1105-1113, 2010.

Method for Analyzing Mechanical Property Degradation of Polymer Materials Using Artificial Intelligence

Sangin Park[1]

[1] *Chassis Polymer Materials Development Team, Hyundai Motor Company, Hwaseong 18280, Republic of Korea*

e-mail address of the presenting author (6829656@hyundai.com)

Keywords: Polymer Recycling, Mechanical Property Degradation, Stress–Strain Curve Analysis, Convolutional Neural Network (CNN), Intensity Segmentation, Explainable AI

The ever-increasing demand for sustainable plastics solutions has intensified efforts to improve mechanical recycling processes for thermoplastic polymers. A critical challenge in such recycling workflows is the reliable assessment of how repeated thermal and mechanical processing degrades tensile performance, a key indicator of material integrity and suitability for reuse. In this study, we develop a domain-focused artificial intelligence (AI) framework that automates the analysis of stress–strain behavior and accurately classifies recycled polymer specimens according to their degradation state.

Initially, raw tensile test outputs—recorded as time-series force versus strain data—are transformed into high-resolution, two-dimensional stress–strain curve images. Tensile tests were conducted in accordance with ISO 37 standards using Type 2 dumbbell-shaped specimens. To optimize computational efficiency and highlight physically meaningful features, we apply an intensity segmentation algorithm to eliminate background noise and redundant pixels, retaining only the curve's active regions. This preprocessing reduces data dimensionality by approximately 60% while preserving critical morphological information.

Subsequently, a convolutional neural network (CNN) classifier is trained on the segmented images to differentiate between virgin and mechanically degraded polymers. The network learns to recognize subtle shifts in peak stress, yield point transitions, and strain-hardening slopes induced by molecular-weight reduction. Model training leverages a stratified dataset of over 2,000 labeled specimens and employs early stopping and learning-rate scheduling to prevent overfitting.

To ensure transparency and foster trust in AI-driven decisions, we integrate explainable AI techniques—namely Grad-CAM and activation mapping—to visualize the curve segments that most strongly influence classification outputs. These visualizations consistently highlight known strain intervals associated with initiation of microvoiding and strain localization, corroborating domain expertise.

Comprehensive evaluation on a held-out test set demonstrates that our approach achieves a classification accuracy exceeding 95% and an F1-score of 0.92. Comparative ablation studies confirm that intensity segmentation contributes a 7% boost in convergence speed and a 4% improvement in final accuracy. By automating repetitive analysis tasks and offering clear interpretability, this domain-centric AI workflow has the potential to accelerate material screening cycles, reduce reliance on manual inspection, and enhance decision-making confidence in polymer recycling operations. Future

work will extend this methodology to multimodal data inputs, including thermal degradation profiles and dynamic mechanical analysis curves.

Importantly, the proposed AI workflow is readily adaptable for integration into pilot-scale recycling facilities, enabling near real-time quality assurance during processing. By optimizing the CNN inference pipeline for low-latency execution on edge computing hardware, in situ feedback can be provided to adjust extrusion and temperature parameters dynamically, thereby minimizing material waste and maximizing throughput. Such online monitoring not only accelerates process control but also supports continuous improvement cycles by flagging suboptimal batches for targeted reprocessing or material segregation.

In conclusion, this work delivers a scalable, AI-driven platform that unites advanced machine learning methodologies with polymer domain expertise, establishing a new paradigm for sustainable materials lifecycle management. The high predictive performance, combined with transparent Grad-CAM visualizations, offers a practical blueprint for extending this framework to diverse polymer chemistries and other recycling streams, ultimately contributing to circular economy goals and reduced environmental impact.

Acknowledgement

This research was supported by funding from Hyundai Motor Group.

References

1. Selvaraju RR, Cogswell M, Das A, Vedantam R, Parikh D, Batra D, arXiv Prepr., 2016; 1610.02391
2. Yang C, Kim Y, Ryu S, Gu GX, Mater. Des., 2020; 189:108509
3. Nasir NHM, Usman F, Woen EL, Ansari MNM, Supian ABM, Saloma S, Recycling, 2023; 8:11

Microstructural Modelling of Carbon Black Aggregates for Sustainable Next-Generation Tyre Design

Sarah Pedroni[1], Lewis Tunnicliffe[2], Keizo Akutagawa[1], James J.C. Busfield[1]

[1] *School of Engineering and Materials Science, Queen Mary University of London, London E1 4NS, UK.*

[2]*Birla Carbon, Marietta, GA 30062, USA*

s.pedroni@qmul.ac.uk

Keywords: Carbon Black, Microstructural Modelling, Fıller Design, Void Volume, Energy Dissipation.

The development of sustainable next-generation tyres requires a clear understanding of how microstructural features affect energy dissipation and wear. Rolling resistance contributes about 7–10% of a vehicle's fuel consumption in urban driving. Reducing it by 30% can improve fuel efficiency by roughly 3%. Moreover, 90% of tyre-related CO_2 emissions arise from rolling resistance during use, lowering it offers both economic savings and meaningful environmental benefits [1].

Among the reinforcing fillers used in rubber compounds, carbon black (CB) plays a critical role in determining mechanical, thermal, and frictional characteristics. However, its complex morphology presents a significant challenge in correlating filler microstructure with composite performance.

Numerous mesoscale models have been proposed to simulate filled rubbers and investigate the influence of filler morphology [2, 3]. However, realistic CB aggregate representation remains a critical challenge due to their irregular, fractal-like structures [4]. In existing finite element analysis (FEA) studies, the CB morphology introduced in the representative volume element (RVE) is typically derived from either TEM-based reconstructions or simplified idealised geometries. While both approaches offer valuable insights into the correlation between the microscopic and macroscopic behaviour of the compound, they are either time-consuming or do not account for the complexity of real aggregates, hence limiting the predictive power of the resulting simulations.

In this study, a three-dimensional carbon black (CB) aggregate generation method was developed using a mathematically defined monomer-cluster aggregation algorithm, guided by experimentally derived descriptors such as particle and aggregate size distributions. A void volume validation protocol was introduced to assess the structural accuracy of the aggregates, with comparisons made to COAN (Crushed Oil Absorption Number) measurements, an experimental indicator of aggregate structure and packing. A higher COAN generally corresponds to a greater void volume, indicating more complex and less densely packed structures, which affect energy dissipation and reinforcement in rubber compounds, as described by Kyei-Manu et al. [5].

The generated aggregates are embedded into representative volume elements (RVEs) and prepared for finite element simulations, with a focus on analysing nanoscopic strain distributions under macroscopic tensile strain. Indeed, strain amplification effects caused by the fillers are believed to be closely linked to energy dissipation [1].

Our results show that the synthetic aggregates replicate the void volume characteristics of commercial CB grades and can be packed into RVEs for efficient and scalable microscale

simulations. An initial FEA trial using a voxel-based mesh is presented. Future developments will focus on generating conformal meshes and incorporating bound and occluded rubber phases to improve accuracy.

This approach provides an efficient and meaningful alternative to TEM-based reconstruction and can support the design of lower rolling-resistance compounds. Ultimately, it enables a deeper understanding of filler-matrix interactions and contributes to the improved design of sustainable rubber materials.

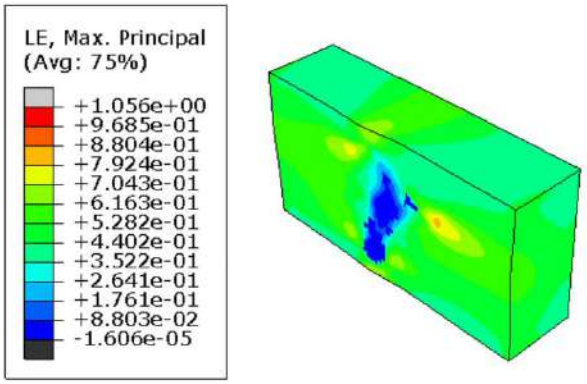


Figure 1. FEM analysis of a Representative Volume Element (RVE) with Periodic Boundary Conditions (PBCs) embedding a reconstructed carbon black (CB) aggregate.

Acknowledgement

One of the authors, Sarah Pedroni would like to thank Birla Carbon for funding her research and for providing the data analysed in this study.

References

1. Akutagawa K. Technology for Reducing Tire Rolling Resistance. Tribol Online. 2017;12(3):99–102.

2. Barghamadi M, Ghoreishy MHR, Karrabi M, Naderi G. Multiscale modeling of hyperviscoelastic behavior of particulate rubber composites based on hybrid silica/carbon black filler system. Polym Compos. 2024 Apr 10;45(5):4359–73.

3. Kulkarni SS, Tabarraei A. A Stochastic Analysis of the Damping Property of Filled Elastomers. Macromol Theory Simul. 2019;28(2):1800062.

4. Herd CR, Tunnicliffe LB. Carbon Black: Manufacturing Processes and Fundamental Properties. In: Harris PJF, editor. Elemental Carbon [Internet]. Royal Society of Chemistry; 2024 [cited 2025 Jun 2]. p. 155–237. Available from: https://books.rsc.org/books/book/2247/chapter/8277418/Carbon-Black-Manufacturing-Processes-and

5. Kyei-Manu WA, Herd CR, Chowdhury M, Busfield JJC, Tunnicliffe LB. The Influence of Colloidal Properties of Carbon Black on Static and Dynamic Mechanical Properties of Natural Rubber. Polymers. 2022 Jan;14(6):1194.

International Rubber Conference 2025 (IRC2025)
1-3 December 2025 @ BITEC, Bangkok, Thailand

Study on the dispersion of silica in SBR using time-resolved ultra small angle X-ray scattering

Shotaro Nishitsuji[1], Takayuki Yoshida[1], Daisuke Iwahara[1],
Naoya Amino[2], Yuki Watanabe[2], Mikihito Takenaka[3]

[1] *Graduate School of Organic Material Science, Yamagata University,*
4-3-16 Jonan, Yonezawa, Yamagata 992-8510, Japan.

[2] *The Yokohama Rubber Co., Ltd., Japan.*

3 *Institute for Chemical Research, Kyoto University, Japan.*

e-mail: nishitsuji@yz.yamagata-u.ac.jp

Keywords: Dispersion, SBR, USAXS

Introduction

Recently, due to environmental concerns and the depletion of fossil fuel resources, high-performance tires have been increasingly required. To achieve improved performance, it is important to investigate the relationship between filler dispersion in rubber/filler systems and the resulting enhancement of mechanical properties.

Koga et al. reported that SBR/CB blends exhibit a hierarchical structure composed of primary particles, aggregates formed by the aggregation of primary particles, and agglomerates formed by the aggregation of aggregates into a network, as shown in Figure 1 [(1)]. Similarly, Schaefer et al. reported that SBR/silica systems possess a comparable hierarchical structure [(2)]. Furthermore, by using synchrotron radiation X-rays as the incident beam, in situ measurements under deformation can be performed. Due to the high intensity of synchrotron X-rays, scattering images can be collected at short intervals.

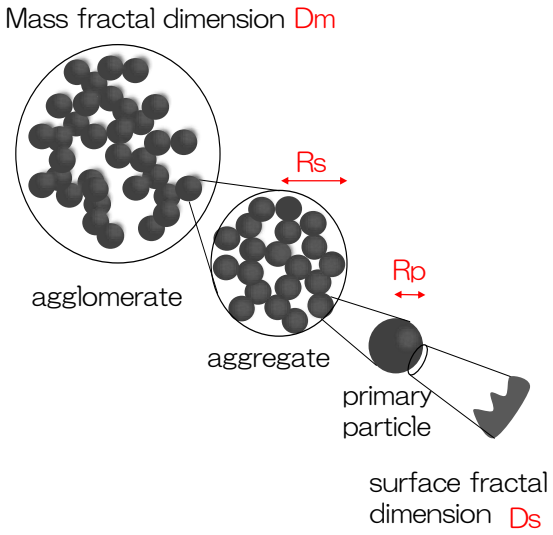


Figure 1 Schematic view of hierarchical structure

In this study, time-resolved ultra-small-angle X-ray scattering (USAXS) was used to investigate the dispersion of silica in SBR. In particular, we focused on changes in the inter-aggregate distance under uniaxial elongation, employing the Polydisperse Born-Green Approximation (PBG) analysis [(3)].

Experimental

In this study, styrene-butadiene rubber (SBR, weight-average molecular weight M_w= 500,000) was mixed with silica and a silane coupling agent as fillers. Silica was added at volume fraction of 5, 10, 15, and 20, 25 vol%. Time-resolved USAXS measurements were conducted on these samples under uniaxial elongational deformation, during which both stress and strain were recorded. The measurements were carried out at beamline BL03XU at SPring-8.

Result and Discussion

Figure 2 show the 2D scattering images at applied strains of 0 %, 30 %, 60 % and 100 %. At 0% strain, the scattering image is isotropic. In contrast, after elongation, the scattering images become anisotropic in the direction of elongation. This anisotropy in the scattering patterns arises from the inhomogeneous distribution of silica aggregates. In the SBR/silica system, SBR is soft while silica is hard. As a result, spatial inhomogeneity in the stress field develops during deformation. This means that the SBR-rich regions deform more easily than the silica-rich regions. Under elongation, the SBR matrix deforms significantly, whereas the silica aggregates exhibit little deformation. Consequently, the contrast between the soft and hard region increases with strain. These results indicate that interparticle correlations are enhanced during deformation, which leads to the appearance of anisotropic scattering patterns under elongation.

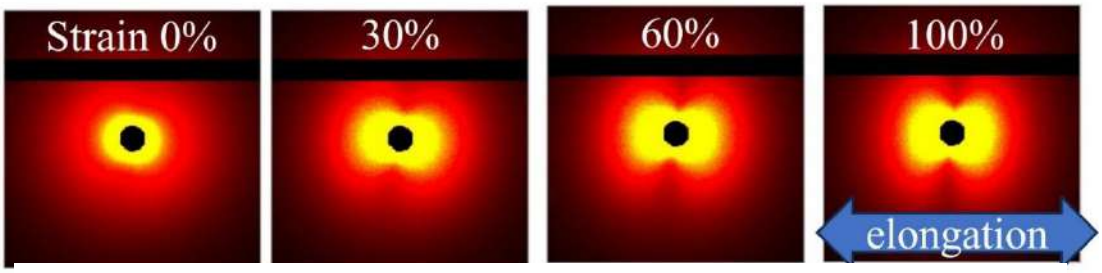


Figure 2 Scattering patterns of SBR/Silica at strain 0 %, 30 %, 60 % and 100%

From the scattering patterns, one-dimensional (1D) profiles in the directions parallel and perpendicular to the elongation were obtained, and the correlation distances between aggregates were estimated using the Unified Guinier power/law approach and PBG analysis. Figure 3 shows the correlation distance of aggregates as a function of strain in both the parallel and perpendicular directions to the elongation. The results indicate that the correlation distance in the parallel direction increases with increasing strain, while that in the perpendicular direction decreases. PBG analysis is shown to be effective in quantitatively estimating the evolution of inter-aggregate correlation distances during elongation.

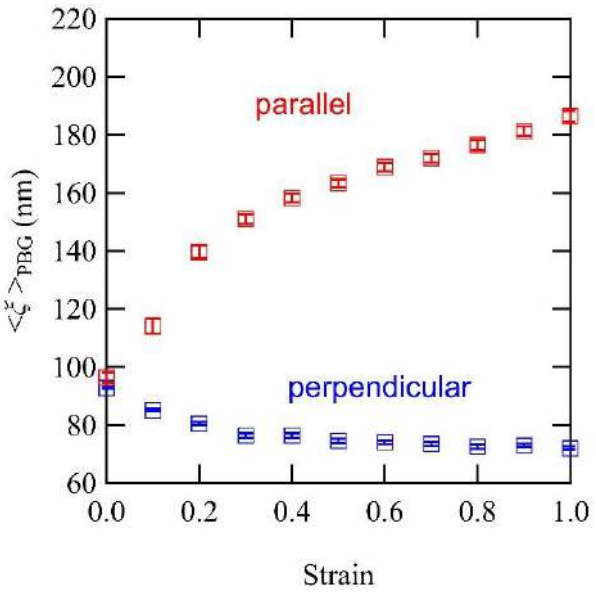


Figure 3 The correlation distance of aggregate in the parallel and perpendicular direction to the elongation as a function of strain

References

1. Koga T, Hashimoto T, Takenaka M, Aizawa K, Amino N, Nakamura M, Yamaguchi D, Koizumi S, *Macromolecules*, 2008; 41: 453.

2. Schaefer D W, Rieker T, Agamalian M, Lin J S, Fischer D, Sukumaran S, Chen C, Beaucage G, Herde C, Ivie J, *J. Appl. Cryst*, 2000; 33: 587.

3. McGlasson A, Rishi K, Beaucage G, *Chauby M, Kuppa V, Ilavsky J, Rackaitis M, *Macromolecules*, 2020; 53: 2235.

International Rubber Conference 2025 (IRC2025)
1-3 December 2025 @ BITEC, Bangkok, Thailand

Correlative analysis of morphological and functional properties in high-performance elastomer blends

Dean VIDAKOVIC[1], Fatma SARAÇ[1], Nina EGGERS[3], Bettina TASCHNER[3], Harald PLANK[1,2]

[1] *Graz Centre for Electron Microscopy, Steyrergasse 17, 8010 Graz, Austria*

[2] *Institute of Electron Microscopy and Nanoanalysis, Graz University of Technology, Steyrergasse 17, 8010 Graz, Austria*

[3] *Voith Austria GmbH, Maretgasse 45, 2632 Wimpassing, Austria*

(dean.vidakovic@felmi-zfe.at)

Keywords: polymer blend, NBR/(H)NBR, NBR/EPDM, correlative microscopy, characterization

Rubber-based paper roll coatings consist of complex multi-component systems, which, during the past decades, have experienced significant challenges due to constantly shifting needs of the paper industry. The material requirements are therefore demanding high thermal resistance, elasticity, wear resistance and the ability to withstand exposure to various media (e.g. oils, moisture, polar substances). As a consequence, blends of nitrile butadiene rubber (NBR) with varying acetonitrile (ACN) contents, with hydrogenated nitrile butadiene rubber (HNBR) or with ethylene propylene diene monomer rubber (EPDM) are particularly suited for paper roll covers, because of their combined thermal and mechanical properties.

Although microscopic studies have been conducted [1-3] comprehensive correlative microscopic investigations of the aforementioned blends and their individual mutual implications remain largely underrepresented in the literature. Consequently, a systematic correlative microscopy and spectroscopy approach is indispensably needed as used in this study. Depending on the targeted information, we apply (scanning) transmission electron microscopy ((S)TEM), electron energy loss spectroscopy (EELS), scanning electron microscopy (SEM), X-Ray diffraction (XRD), atomic force microscopy (AFM) and quantitative nanomechanical mapping (QNM). The relevance of these methods and related preparation procedures (e.g. cryo microtomy) are being discussed.

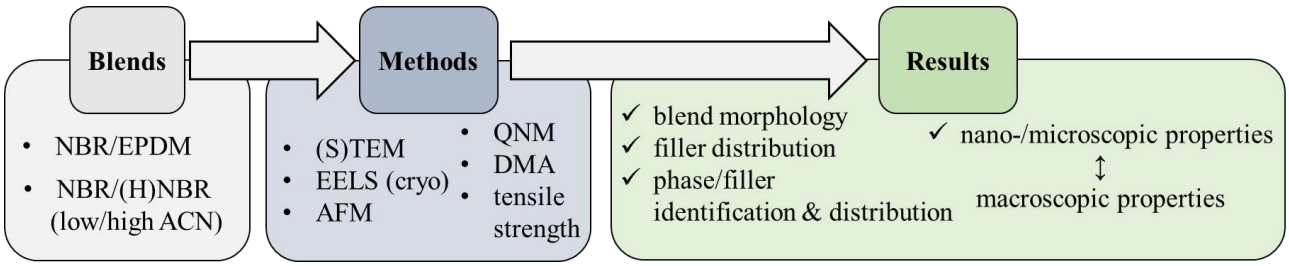


Figure 1. The figure shows the investigated blends & the used methods revealing the key results.

The data correlation from all these methods together with mechanical properties (i.e. DMA, tensile strength) makes it then possible to bridge the gap from nano-/microscopic peculiarities to the macroscopic world and explain phenomena occurring in the macroscopic scale (see Figure 1). Using this correlative approach enables the differentiation between NBR and (H)NBR with sufficiently distinct ACN contents, as well as the analysis of phase and filler distributions in the blends mentioned

above. Additionally, identification is essentially supported through spectroscopic or nanomechanical methods to gain comprehensive micro- and nanoscopic insights.

The long-term scope of these activities is the exploration of new functionalities and synergy effects between the individual blend components. Macroscopic measurements help link micro- and nanoscale features with large-scale mechanical properties. This supports a better understanding and paves the way to specifically add new functions for future materials. By that, the goal is to move towards a more deductive design process, which reduces trial-and-error, limits the number of components, and contributes to long-term sustainability.

Acknowledgement

The authors would like to express their gratitude to the grant sponsors Austrian Research Promotion Agency (FFG) and those who contributed to the study.

References

1. Mostafa N, *J. of Applied Polymer Sci.*, 2008; 108: 3001.
2. Botros S H, Tawfic M L, *Journal of Elastomers & Plastics*, 2005; 37: 299.
3. Hoikkanen M, Poikelispää M, Das A, Honkanen M, Dierkes W, Vuorinen J, *Polymer-Plastics Technology and Engineering*, 2015; 54: 402.

Chemical fingerprinting for environmental detection of tyre rubber emissions

Nick Molden, James Hobday, Ime Usen

Emissions Analytics, UK

jameshobday@emissionsanalytics.com

Keywords: Tyres, Sustainability, 6PPD, emissions, non-exhaust-emissions

Abstract

Over 2.3 billion tires are produced globally per year, with an ever-increasing complexity of chemical additives to optimise safety and performance. Greater understanding of the chemicals and polymer degradation products allows the environmental impact of tyres – in air, soil and water – to be better understood. This presentation shows an untargeted, multi-dimensional pyrolysis GC-MS method to analyse tyre rubber for environmentally important chemicals to develop a comprehensive tyre chemical source profile – from over 500 tires from light, medium and heavy-duty sectors in Europe and the USA.

Concern has been growing in recent years about the environmental effect of tyre emissions since a preservative in tyres was linked to the mass die-off of coho salmon in the USA. Experiments by multiple organisations, including Emissions Analytics, has shown that increased weight due to a vehicle battery can lead to an increase of 20% or more in tyre mass emissions. However, this is not the whole story, as greater wear in terms of mass emissions, does not necessarily correlate with greater toxicity, tyre companies are innovating with new tyre formulations to carry the extra weight, and mitigations such as torque control can be implemented by the vehicle manufacturers.

Emissions Analytics has sourced over 500 tyres to independently analyse tyre chemical composition. The method involved pyrolysis and two-dimensional gas chromatography which enables us to discover, identify and quantify over 400 compounds per tyre. Summarised results will be shared.

The headline findings are that the switch the electric vehicle creates a material risk of higher wear and greater toxicity, but this does not have to be the outcome if industry and regulators establish an effective framework for evaluating tyre emissions. These findings will be used to interpret the likely effects of the proposed Euro 7 regulations as well as the California 6PPD rule.

References

Not applicable as all research was independently conducted immediately by Emissions Analytics

Advancing sustainability in rubber industries involves optimizing testing through the utilization of Rubber Process Analyzer

Wan Li[1], Peih-Shyun Wu[1], Unal C. Yilmazoglu[2]

[1] *Long Pan Rd. Malu, Shanghai, China.*

[2] *Hudson, OH U.S.A.*

li.wan@alpha-technologies.com

Keywords: Rubber Process Analyzer, RPA, Sub-Zero, quality consistency, sustainable testing

The rubber industry's shift towards sustainable development involves enhancing energy efficiency while minimizing waste in the form of rework or scrap. This objective, combined with ensuring consistency in the performance of rubber products, contributes to the realization of an environmentally friendly approach.

Rubber product manufacturing involves a batch process that necessitates managing material variations. The variability in raw rubber leads to inconsistencies in the quality of the mixed rubber compound. Due to discrepancies in the dimensions, rework becomes unavoidable during the processing of variable rubber compounds. Consequently, there is a decrease in energy efficiency and an increase in scrap rather than a viable end product. To achieve sustainability in the industry, Rubber Process Analyzer, the Premier RPA, with the Sub-Zero technology (Figure 1) offers a viable solution. By establishing control from the mixing operation to the final product performance (Figure 2), seamless processing and designed quality are ensured at every production phase.

The Premier RPA is equipped with the capability to provide valuable insights derived from data to effectively address any challenges encountered during the batch processing [1]. By employing a simple frequency sweep in both linear and nonlinear regions, industries can make informed decisions when selecting raw rubber, leveraging insights into molecular architecture and processing performance prediction [2]. A comprehensive assessment of mixed batch consistency can be achieved through strain sweep testing, extending beyond the Payne effect for dispersion quality to optimize batch mixing, silanization reaction extent, prediction of bound rubber content and processing performance [3]. Furthermore, Sub-Zero technology addresses the temperature gap in RPA testing. An evaluation conducted on tread compounds under dynamic strain-controlled conditions demonstrated the RPA data on modulus and hysteresis showed correlation with indicators of rolling resistance, wet traction and heat buildup [4]. This confirmed the relevance of laboratory measurements to end-use performance.

The exceptional ability of the Premier RPA to handle multiple tasks simultaneously, along with its high precision, is truly remarkable. This capability allows QC to distinguish between different lots or batches, and to identify issues even before mixing stage, factory processing, product curing, and compliance testing. The use of RPA screening improved batch uniformity and reduced the amount of reprocessing that required additional energy.



Figure 1. Schematic diagram of Premier RPA with Sub-Zero Technology™

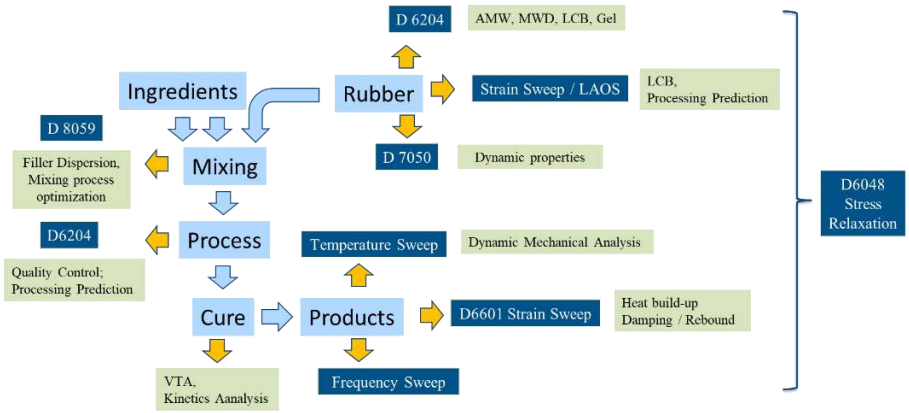


Figure 2. Establishing control on every step of the rubber manufacturing process

References

1. J. S. Dick, Evolution of "RPA test methods for industry" Rubber and Plastics News, August 2015.
2. Michele Scacchi, Techniques to detect long chain branching in polymers Rubber and Plastics News, October 2020.
3. Rubber Chemistry and Technology, Vol. 91, No. 3, pp. 521–536 (2018).
4. Berrin Degirmenci and Michele Scacchi, Striving for Excellence beyond just a Rubber Process Analyzer, presented at IRC 2024.

Rubber Blend Compatibility Analysis Using Large-Amplitude Oscillatory Shear (LAOS) on RPA

Zühra ÇINAR ESİN[1], Murat ŞEN[1,2]

[1] *Hacettepe University, Department of Chemistry, Polymer Chemistry Division, 06800, Beytepe, Ankara, TURKEY*

[2] *Hacettepe University, Institute of Science, Polymer Science and Technology Division, Beytepe, 06800, Ankara, Turkey.*

zuhracinar@gmail.com

Keywords: Silicone, Hydrin, Polymer Compatibility, RPA

Vinyl methyl silicone (VMQ) rubbers exhibit excellent thermal stability, hydrophobicity, chemical resistance, and electrical insulation. However, their oil resistance and mechanical strength are inferior compared to epichlorohydrin (ECH)-based rubbers. ECH rubbers—available as homopolymers, copolymers, and terpolymers—offer superior oil resistance and damping properties, though they possess lower thermal stability and hydrophobicity than VMQ.

This study investigates the compatibility between VMQ and three types of epichlorohydrin-based rubbers: poly(epichlorohydrin) (CO), poly(epichlorohydrin-co-ethylene oxide) (ECO), and poly(epichlorohydrin-co-ethylene oxide-co-allyl glycidyl ether) (GECO), aiming to develop blends that integrate the advantageous properties of both components.

Traditional techniques such as the log-additive rule, quadratic mixing rule, and differential scanning calorimetry (DSC) are frequently employed for compatibility studies. Initially, CO, ECO, and GECO polymers were blended with VMQ at various ratios and evaluated according to the log-additive and quadratic mixing rules. The results obtained from quadratic mixing rule are presented in **Fig. 1**. Based on the obtained results, it was observed that while the CO polymer was incompatible, the ECO polymer exhibited compatibility.

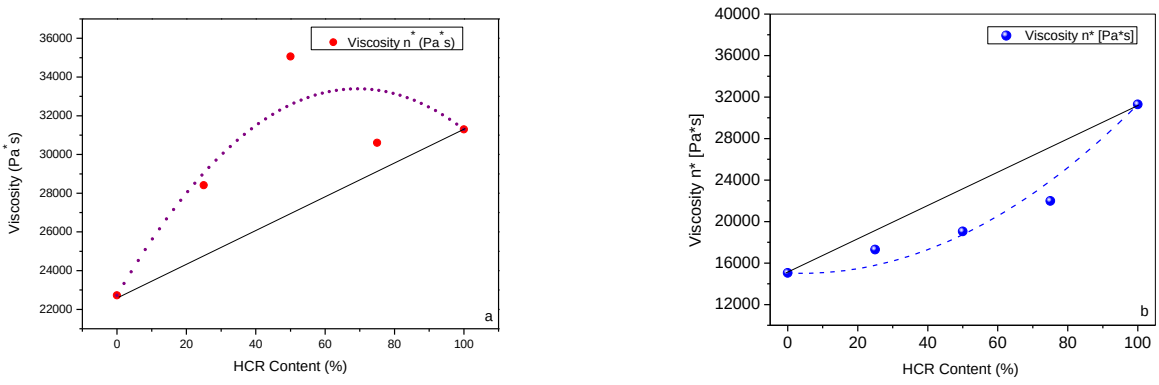


Figure 1. Variation of viscosity of a) ECO/HCR and b) CO/HCR blends with HCR content

The rheological behavior of these blends was analyzed using a Rubber Process Analyzer (RPA) under Large-Amplitude Oscillatory Shear (LAOS) conditions, enabling a detailed assessment of nonlinear viscoelastic responses under large deformations. The long-chain branching (LCB) index is a parameter that provides insight into whether a polymer exhibits a linear or branched architecture.

In this study, the LCB index was quantitatively determined using a rotational rheometer equipped with an RPA module, based on an empirical equation that utilizes harmonic moduli (G_1', G_3' and G_5') obtained from large amplitude oscillatory shear (LAOS) measurements.

$$LCB = \frac{G'_1}{G'_5} - \left[\frac{5}{4} + \frac{1}{4}\left(\frac{G'_3}{G'_5}\right)^2 - \frac{1}{2}\left(\frac{G'_3}{G'_5}\right)\right]$$

LAOS remains underutilized in this context. This study proposes LAOS as a complementary approach, enabling a more detailed evaluation of phase interactions through nonlinear rheological metrics. Subsequently, LAOS experiments were conducted, and the quadratic mixing rule equation was adapted to the LCB index values. The initial evaluation was carried out for the CO polymer, and as shown in **Fig. 2**, results consistent with the quadratic mixing rule were obtained.

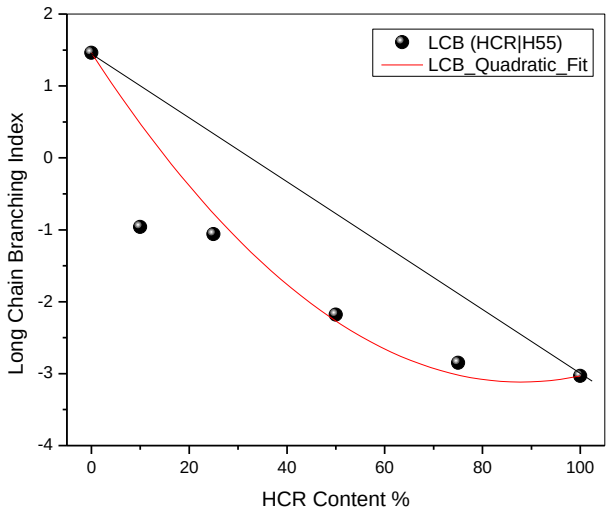


Figure 2. Variation of LCB index value of CO/HCR blends with HCR content

The findings demonstrate that LAOS can serve as a powerful tool for characterizing the behavior of elastomer blends, potentially facilitating the design of rubber materials with balanced mechanical, thermal, and damping properties.

Acknowledgments

The authors gratefully acknowledge financial support from The Scientific and Technological Research Council of Türkiye, under the 2224-A Grant Program for Participation in Scientific Meetings Abroad.

References

1. Šebenik, U., Zupančič-Valant, A., & Krajnc, M. (2006). Investigation of rubber–rubber blends miscibility. Polymer Engineering and Science, 46(11), 1649–1659. https://doi.org/10.1002/pen.20645
2. Tainstruments. (n.d.). https://www.tainstruments.com/pdf/literature/RT006.pdf

Performance Evaluation of Silicone-Based Isolators Under Varying Temperatures and Excitation Levels Using a Thermal Chamber Shaker

E.R. SENOZ[1], U. CALIK[2]

[1&2] *Balıkhisar, Koca Seyit Onbaşı Sk. No:1, 06750 ASELSAN Akyurt/Ankara TURKEY*

ersenoz@aselsan.com

Keywords: Vibration Isolator, Silicone, Frequency, Transfer Function, Temperature

In this study, the variation of the performance of isolators from 3 different manufacturers under the same test load was investigated. The isolators were selected to understand how temperature change affect the test results for different manufacturers. Three variable parameters were used in the tests. These parameters are temperature change, different input vibrations and different input drive directions.



Figure 1. Tested Three Different Isolators

All of the isolators shown in Figure 1 are silicon-based isolators with high damping characteristics. These isolators are tested by placing them together with the test device on the vibration shaker with thermal cabinet the positions of the isolators and the test setup shown in Figure 2. The tests are carried out under three different temperatures. These temperatures are +23°C, +75°C, and -40°C. The temperature at which the isolators reach the specified temperature is measured with the help of thermocouples placed on the material and kept at certain temperatures for at least 3-4 hours before the tests.

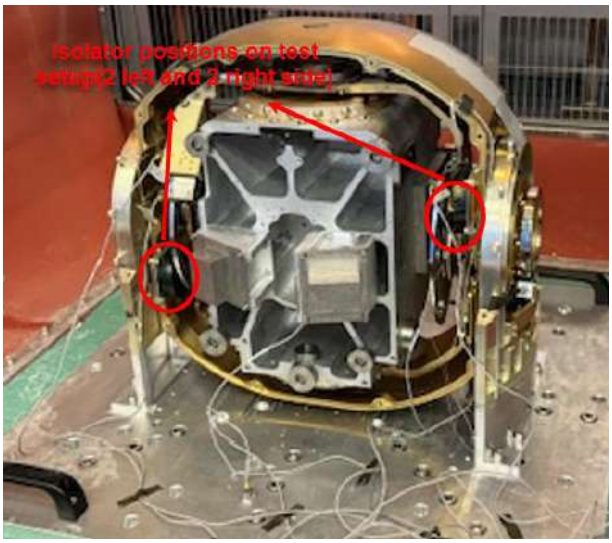


Figure 2. Assembly of the Test Setup on Shaker with Temperature Cabinet

Sine sweep, white noise and shock vibration profiles were applied to the test device at each specified temperature to determine the performance of the isolators. The isolators were also tested in two directions, radial and axial. The test results obtained for each isolator are presented in Table 1, Table 2 and Table 3 for the radial axis.

Table 1. Isolator 1 Test Results

Test Input	Temperature	Natural Frequency
Sine Sweep		15.0
White Noise	+23°C	17.5
Shock		14.0
Sine Sweep		14.0
White Noise	+75°C	15.0
Shock		13.0
Sine Sweep		22.0
White Noise	-40°C	24.0
Shock		15.0

Table 2. Isolator 2 Test Results

Test Input	Temperature	Natural Frequency
Sine Sweep		12.8
White Noise	+23°C	14.0
Shock		12.0
Sine Sweep		11.0
White Noise	+75°C	12.0
Shock		11.0
Sine Sweep		16.5
White Noise	-40°C	19.5
Shock		13.0

Table 3. Isolator 3 Test Results

Test Input	Temperature	Natural Frequency
Sine Sweep		20.5
White Noise	+23°C	23.5
Shock		16.5
Sine Sweep		16.5
White Noise	+75°C	19.0
Shock		16.0
Sine Sweep		22.5
White Noise	-40°C	29.5
Shock		18.5

According to the test results, isolator number 3 shows a stiffer behavior, although similar products were obtained from the manufacturer. The temperature dependent frequency change occurred at least in isolator number 2 according to the inputs given.

Acknowledgement

I would like to thank ASELSAN for providing test equipment support in the studies.

Tribological behavior of soft polymers against model substrates

Sophie BISTAC[1],

[1] *UHA-LPIM 3b rue Alfred Werner 68093 Mulhouse, France.*

sophie.bistac@uha.fr

Keywords: Friction, surface energy, silicone rubber, amphiphilic copolymer

Tires, wiper blades, or transmission belts or shoe sole are just a few of the many industrial and practical uses in which friction of rubber materials plays a major role. Because of their low stiffness and glass transition temperatures, the tribological behavior of soft polymers can be complex, with a significant effect of adhesion and interfacial interactions. In order to better understand the influence of surface energy on the friction of soft polymers (in the rubbery state), model substrates with high stiffness, very low roughness and controlled surface chemistry were used. These model substrates are glass or silicon plates, whose surface chemistry can be modified by chemical grafting of silane molecules in order to obtain different surface energies.

Two kinds of soft polymers have been studied: silicone rubbers (polydimethylsiloxane, PDMS with two different crosslinking densities) and amphiphilic diblocks copolymers (polyethylene-b-polyethylene glycol, PE-b-PEG). Three different PE-b-PEG copolymers, with various PE/PEG ratios are used. PE-b-PEG are amphiphilic copolymers composed of a polar (hydrophilic) block (polyethylene glycol, PEG) and a non-polar (hydrophobic) block (polyethylene). Furthermore, both blocks can crystallize, with the degree of crystallinity varying according to the copolymer composition (PE/PEG ratio).

Friction of soft polymers against hydrophilic and hydrophobic substrates is studied by using a pin on disk tribometer, at 25°C under controlled normal forces and speeds. The friction force divided by the applied normal force is equal to the friction coefficient μ.

The friction results obtained for silicone rubbers show that both rubbers have equal friction coefficients, no matter the friction speed or normal force, the suggesting that the crosslinking density has very slight effect. However, the friction coefficient is larger against hydrophilic substrates than hydrophobic ones, indicating a considerable influence of the substrate surface energy, although only for low normal forces. At greater normal forces, however, the substrate surface energy has less effect. The impact of friction speed has also been investigated, and the results indicate that at low friction speeds, silicone rubbers have different friction coefficient values against hydrophilic and hydrophobic substrates. At greater speeds, however, the surface energy effect becomes insignificant and the friction coefficients measured against both substrates are comparable.

The friction results obtained for the PE-b-PEG copolymers demonstrate a significant influence of the copolymer composition, with a low friction coefficient measured for the copolymer with the highest PEG content against the hydrophilic substrate. This unexpected result is explained by the PEG block crystallinity degree (lower amount of mobile amorphous phase). The influence of substrate surface energy is also investigated. Interfacial interactions between hydrophilic and hydrophobic blocks seem to play an important role. However, because both PE and PEG blocks can crystallize, the crystallinity of each block has a major impact on the friction behavior of copolymers via the chain mobility of the corresponding amorphous phase.

The influence of the nature of the substrate is then discussed. Results obtained for the silicone rubbers have shown that the effect of surface energy of the substrate can become negligible for high friction speeds. Concerning the friction of PE-b-PEG copolymers, the effect of the surface energy of the substrate will strongly depends on the competition between interfacial interactions and PE/PE or PEG/PEG interactions. Moreover, both blocks being able to crystallize, their respective crystallinity has also a major influence effect on the tribological behavior of these copolymers. To conclude, the role of surface energy in tribology is not so evident.

References

1. Bistac S, Brogly M, Bindel D, *Polymers*, 2022; 14:3639.
2. Brogly M, Bistac S, Bindel D, *Polymers*, 2024;16:1244.

NR Film Visualization via AFM Imaging

K S TAN[1], EVELYN LIM H M, NURUL HAYATI YUSOF

[1] *RRIM Sungai Buloh, Malaysia.*

kstan@lgm.gov.my

Keywords: Atomic Force Microscopy, Phase Imaging, Topography, Natural Rubber Blends

Atomic Force Microscopy (AFM) is a popular advanced imaging technique to study surface morphology of substrates in high resolution. Through phase imaging, AFM can be employed to probe the distribution of materials on a surface based on certain material properties. Natural rubber (NR) often mixed with other materials, including other polymers, to achieve new or composite materials for specific applications. The objective of this study was to provide supporting data for mechanical testing results. Synthetic rubber (SR) is one of the common materials for blending with NR. NR-SR blends were prepared by mixing the two materials in latex stage mechanically for 24 hours prior to dipping. The dried dipped films were not peeled off the glass formers but directly subjected to AFM imaging using a Park System NX10 AFM. Both the topography and phase imaging images were recorded simultaneously. The process of capturing AFM images as well as the image analysis is presented in this report. With significant variations in mechanical properties, the phase imaging can differentiate NR from SR and hence distribution of each rubber can be visualized. The distribution pattern of these two types of rubbers appeared differently if a compatibilizer was added, as shown in Figure 1, where the NR, appears in blue, seemed distributed more evenly.

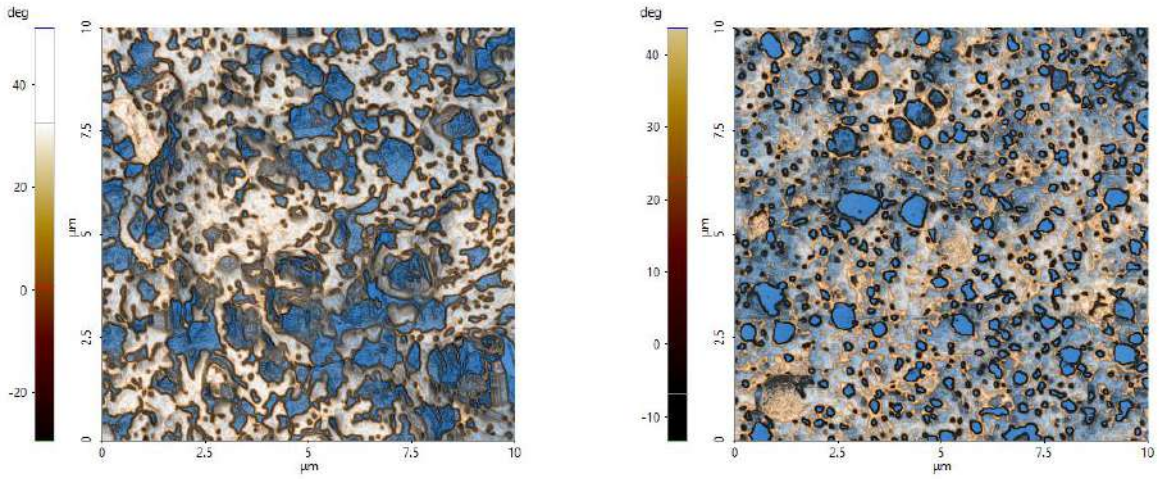


Figure 1. AFM phase images of NR-SR blends with and without (left) compatibilizer. The areas with blue and whitish colors represent NR and SR respectively.

AFM-Based Investigation of Polyisoprene-Inorganic Interface Adhesion at Multiple Scales

Hexuan Mao[1], Xiaobin Liang[1], Ken Nakajima[1]

[1] *Department of Chemical Science and Engineering, Institute of Science Tokyo, Tokyo, Japan.*

mao.h.b3fe@m.isct.ac.jp

Keywords: Interfacial interaction, Interface adhesion, Single-molecule force spectroscopy, Nano-palpation

[Introduction]

Polymer–inorganic interface (PII) is pivotal in determining the macroscopic performance of hybrid materials due to its distinct interfacial structures and interactions. In carbon-black (CB) filled rubber systems, the interfacial polymer region (IPR), formed via spontaneous adsorption of polyisoprene (PI) chains onto CB surfaces, critically contributes to mechanical reinforcement.[1] However, conventional bulk characterization techniques lack the molecular-level resolution required to probe such interfaces. In this study, single-molecule force spectroscopy (SMFS) based on AFM was employed to directly investigate the physical adsorption behavior of single PI chains at CB surfaces and was further compared with the interactions on other inorganic surfaces. Force–extension curves were analyzed to reveal adsorption conformations and the corresponding interfacial interactions. Furthermore, chemical vapor deposition (CVD) was utilized to fabricate nanoscale inorganic coatings on AFM probes, enabling precise nano-palpation and adhesion quantification by fitting the force-deformation curves to the Johnson–Kendall–Roberts (JKR) model.[2] Through the integration of these two AFM based techniques, SMFS and nano-palpation, this work bridges interfacial adsorption at the single molecule level with adhesive behavior at the polymer aggregate scale, offering a comprehensive multiscale understanding of PII interactions in filler reinforced rubber systems.

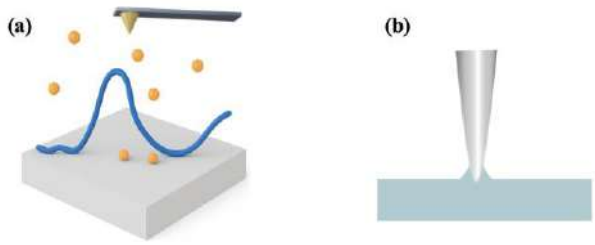


Figure 1. (a) Schematic of SMFS, showing the AFM probe approaching a polymer single chain adsorbed on inorganic surface. (b) Schematic of nano-palpation, depicting the adhesion response during probe retraction from the cross-linked rubber surface.

[Experiment]

For SMFS, ultra-dilute cis-1,4-polyisoprene solutions (1 μmol·L^{-1}) were deposited onto various inorganic surfaces including CVD-coated carbon and aluminum, HOPG, and mica. After rinsing to remove weakly adsorbed chains, measurements were conducted in liquid environments using non-functionalized Si_3N_4 probes and solvents with increasing solubility parameters (Table 1). During tip retraction from the surface, the AFM recorded force responses corresponding to the segment-by-segment detachment of single polymer chains. Each desorption event generated a characteristic signature in the force–extension curves. These curves enabled direct analysis of adsorption conformations and quantification of interfacial interactions under varied solvent

conditions at the single-molecule scale. For nano-palpation, cross-linked PI rubber was prepared using sulfur and ZnO as vulcanization components (Table 2 for formulation). During the process in which the CVD-coated AFM probe was pressed into and retracted from the rubber surface, adhesive deformation responses were captured, reflecting the interfacial adhesion strength at the microscale.

Table 1. Information on the organic solvents selected for this study.

Product code	Reagent name	Solubility Parameter ($MPa^{1/2}$)
034-05006	Cyclohexane	16.8
204-01861	Toluene	18.2
137-01823	Methanol	29.7
	Water	47.3

Table 2. Formulation of the cross-linked PI rubber.

Component	Composition (phr)
Isoprene rubber, IR	100
Sulfur	2
Stearic acid	5

[Conclusion]

This study employed AFM-based SMFS to investigate the physical adsorption of PI chains on various inorganic surfaces. Solvent-dependent changes in adsorption conformations revealed the role of solubility parameters and confirmed the involvement of vdW interactions. Notably, desorption forces were significantly higher on aluminum surfaces, attributed to differences in surface energy. To extend the analysis to bulk states, nano-palpation experiments were conducted on cross-linked PI rubber using CVD-coated AFM probes. Adhesion energies were quantified using the JKR model, with SEM imaging confirming uniform probe coatings. Contact radii were determined by controlling the Young's modulus of the rubber to ensure fitting accuracy. Both single-chain and bulk-scale results consistently demonstrated stronger physical interactions with aluminum. These findings provide new insights into weak interfacial forces and material-dependent polymer adhesion. Future work will focus on AFM imaging of adsorption morphologies, refined solvent selection for identifying conformational thresholds, and temperature-controlled measurements to further explore interfacial energetics.

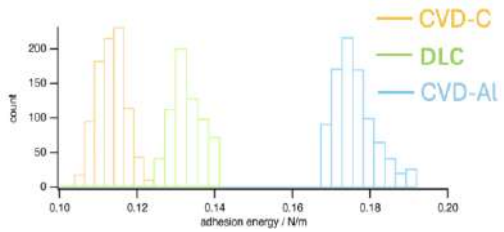


Figure 2. Adhesion energy distribution measured with three types of probes.

Acknowledgement

We sincerely thank Mr. Kōki and Mr. Kukichi, Institute of Science Tokyo, for the preparation of the CVD substrates and SEM imaging.

References

1. Liang X, Nakajima K. *Macromolecules*, 2022; 55(14): 6023-6030.
2. Nakajima K, Ito M, Nguyen HK. *Rubber Chem Technol*, 2017; 90: 272–284.

Improving Seal Life Prediction: Faster Crack Growth Testing in HNBR

O. Ramekaj[1], J. Busfield[1], K. Akutagawa[1]

[1] *Queen Mary University, London, United Kingdom.*

(o.ramekaj@qmul.ac.uk)

Keywords: Testing, Fracture, Tearing Energy, Seals, Service Life Prediction, Crack Growth Rate

The objective of this research is to improve the prediction of seal service life under static loading by characterising slow and intermediate crack growth rates in elastomeric compounds. A rubber formulation based on carbon black–filled HNBR with a peroxide cure system was selected due to its widespread use in oil, gas, and geothermal sealing applications [1–2]. A new quasi-static pure shear crack growth test method is introduced to obtain crack growth rate versus strain energy release rate data more efficiently, requiring fewer samples while yielding more comprehensive information.

Crack growth behaviour in elastomers is a critical factor in long-term performance, especially under the static conditions found in downhole environments. Conventional pure shear crack growth tests apply a constant strain to a notched specimen and measure average crack growth speed, producing a single data point on a T vs dc/dt plot [3-4]. While effective, this approach is time-consuming and material-intensive. In contrast, the method presented here enables continuous crack growth measurements across a range of tearing energies using a single specimen, significantly improving efficiency and data resolution.

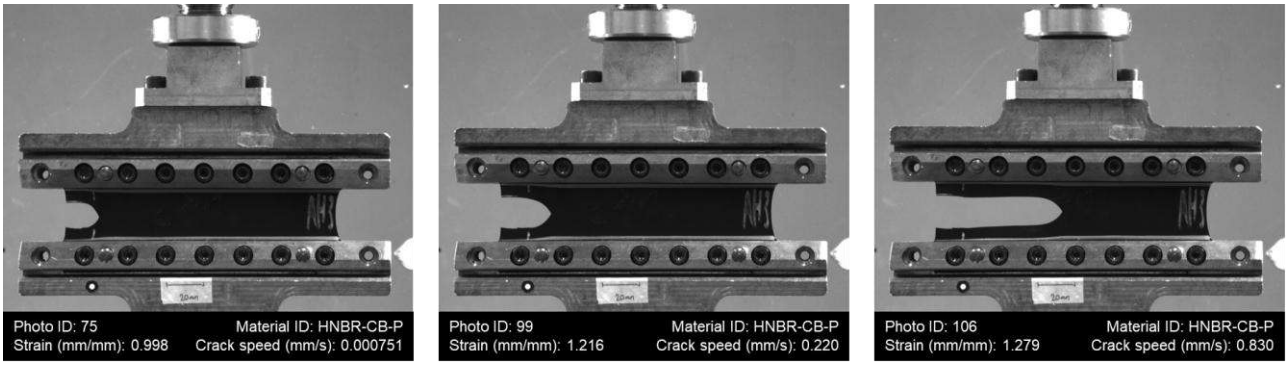


Figure 1: Examples of photographs taken during pure shear testing at various instances. The instantaneous strain and calculated crack speed are shown in each image.

The experimental approach involves gradually loading a pure shear crack growth test piece under a linearly increasing strain. This continuously varies the tearing energy applied, inducing a corresponding increase in crack speed. Images taken during testing (**Figure 1**) are used to extract crack lengths over time data, which are then curve fitted (**Figure 2**) by two exponential functions that are differentiated to calculate the instantaneous values of the crack growth rate at any given time. These values are then plotted against the stored energy release rate to generate a semi-continuous T vs dc/dt graph (**Figure 3**). Compared to traditional methods, this technique yields significantly more information from a single test, offering a faster and more efficient way to characterise crack growth in elastomers. As expected, the carbon black–filled HNBR exhibits significantly greater toughness

than the unfilled NBR sample. A transition from slow to intermediate crack growth rates is clearly identifiable.

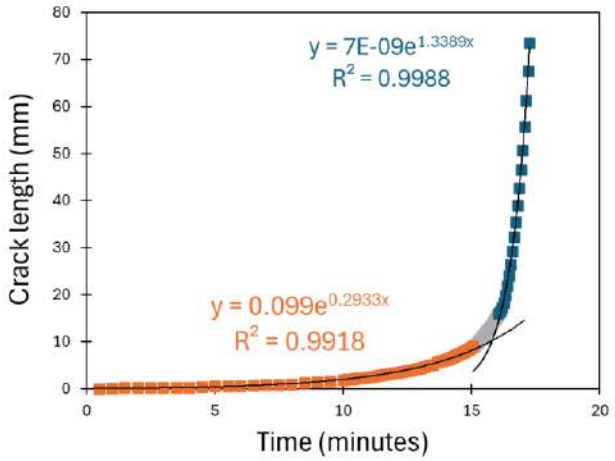


Figure 2: Crack length versus time for a sample subjected to continuously increasing strain. Curves are fitted to the slow crack growth and transition crack speed regions.

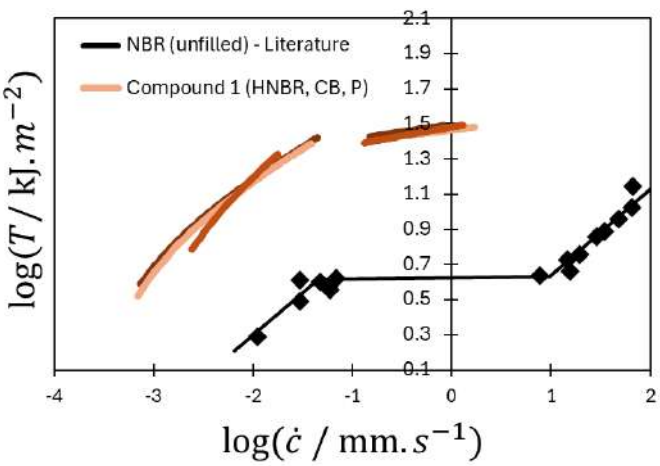


Figure 3: Tearing energy versus crack speed. Results for unfilled NBR [4] and Compound 1 tested using the continuously increasing strain method are shown, including repeat measurements.

While the experimental method applies a gradually increasing strain, the crack growth data obtained span a broad range of tearing energies, including the low-energy regime typical of static sealing conditions. This enables the identification of critical transitions in crack growth behaviour and the estimation of slow crack growth rates, which are directly relevant to predicting seal life under constant stress in real-world applications.

This work introduces a more efficient method for characterising quasi-static crack growth behaviour in elastomeric materials, using a single pure shear crack growth specimen to generate a semi-continuous dataset across a wide range of tearing energies. This approach significantly reduces the number of samples and time required compared to traditional methods, while offering enhanced insight into crack growth dynamics. The method is demonstrated using a carbon black–filled HNBR formulation, enabling detailed evaluation of its fracture performance. By linking crack growth behaviour with material properties, this approach provides a faster and more comprehensive means of assessing and predicting seal performance in demanding applications.

Acknowledgement

The authors would like to express their gratitude to SLB, the sponsor of this research.

References

1. Ciesielski A, *An Introduction to Rubber Technology*, Rapra Technology Limited, 1999; 11.
2. Ilseng A, Skallerud BH, Clausen AH, *Polym. Test.*, 2016; 49: 128.
3. Rivlin RS, Thomas AG, *J. Polym. Sci.*, 1953; 10(3): 291.
4. Kadir A, Thomas AG, *Rubber Chem. Technol*., 1981; 54: 15.

International Rubber Conference 2025 (IRC2025)
1-3 December 2025 @ BITEC, Bangkok, Thailand

Study on the Effect of Silane Coupling Agents on Mechanical Behavior of Silica-Filled Styrene-Butadiene Rubber under Elongation using In Situ Nano-Palpation Atomic Force Microscopy

M. MALINEERAT[1], M. ITO[1], X. LIANG[1], K. NAKAJIMA[1]

[1] *Department of Chemical Science and Engineering, Institute of Science Tokyo,*
2-12-1, Ookayama, Meguro-ku, Tokyo 152-8550, Japan.
malineerat.m.3ab5@m.isct.ac.jp

Keywords: Microscopic mechanical properties; Silica-filled SBR; Silane coupling agents; Interface; Uniaxial elongation

Silica-filled styrene-butadiene rubber (SBR) is a key material for fuel-efficient tires due to its low rolling resistance and good braking performance, which result from the addition of silica filler. However, the dispersibility of silica in rubber is poor, leading to the formation of silica aggregates. To address this, silane coupling agents (SCAs) are commonly used to improve silica dispersion, as they chemically bond silica and rubber. The macroscopic properties of silica-filled SBR vary depending on the type of SCAs. However, the causes of these differences in physical properties have not yet been clarified. This study aimed to investigate the influence of different silane coupling agents on the microscopic deformation behavior and microstress distribution of silica-filled SBR under elongation using in situ nano-palpation atomic force microscopy (AFM), and to gain insight into the microscopic reinforcement mechanism of silane coupling agents in filled rubber.

The samples used in the experiments were silica-filled SBR (40 phr) vulcanizates. *n*-Octyl-triethoxysilane (TEOS) and bis-(3-(triethoxysilyl)propyl) tetrasulfide (TESPT) were employed as silane coupling agents. The amount of SCAs was adjusted based on the molar number of ethoxy groups. A sample without SCA was also prepared as a control. Each sample was cut at -120°C with a cryo-microtome to obtain an observation surface. In situ stretching AFM measurements were performed using a unique, self-developed stretcher [1]. This technique enables the tracing of local structural changes due to elongation at the exact sample location.

The results of in situ AFM measurements under elongation revealed that the elastic modulus increased with strain in all samples, however, the stress distribution was inhomogeneous. Notably, stress primarily concentrated at the interface and progressively spread into the surrounding rubber matrix with increasing strain, as shown in Figure 1. This stress distribution mechanism induced the intermediate-modulus region, comprising the interface and adjacent high-stress response matrix.

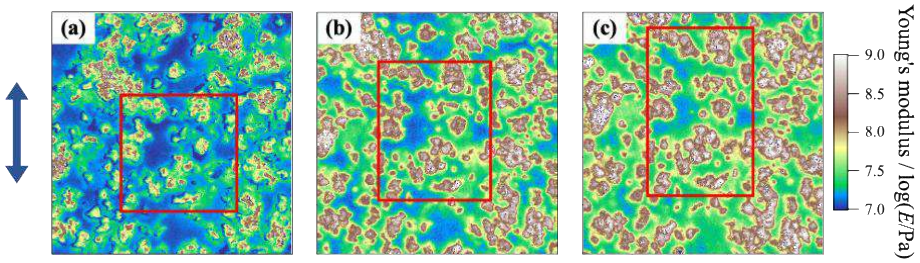


Figure 1. In situ AFM elastic modulus mappings for silica/SBR with TESPT in 1.0×1.0 μm areas under elongation of (a) 0%, (b) 16%, and (c) 45%. Areas in the red frames refer to identical locations.

To better understand the stress distribution mechanisms, quantitative analyses were performed to evaluate the content and modulus of each region during deformation. When modulus mappings were divided into rubber and intermediate-modulus regions, the ratio of the rubber region gradually decreased with elongation in all samples, while that of the intermediate-modulus region increased. Furthermore, the elastic modulus of the rubber matrix increased only slightly, while the intermediate-modulus regions exhibited a more pronounced rise, as shown in Figure 2. Notably, the extent of modulus increase in the intermediate-modulus regions varied with the type of SCAs. In the untreated and TEOS-treated samples, these regions showed a similar increasing trend, with the TEOS-treated sample exhibiting a slightly greater modulus increase (1.7 times) compared to the untreated one (1.6 times). However, the TESPT-treated sample showed a significantly larger increase of 3.5 times. These differences are attributed to variations in the interfacial strength, influenced by the structural and functional characteristics of the SCAs. A stronger interface, particularly enabled by reactive sulfur groups in TESPT, leads to greater stress concentration and a greater increase in local modulus.

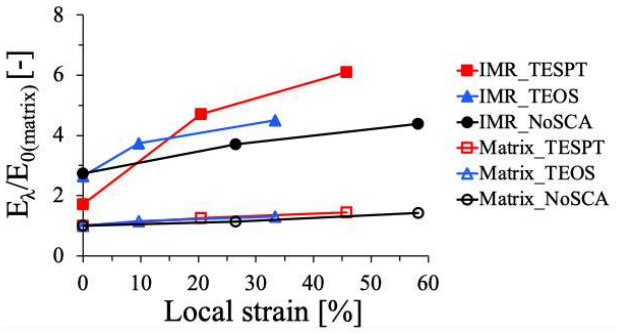


Figure 2. Ratios of elastic modulus of matrix and intermediate-modulus region (IMR) at each local strain to elastic modulus of matrix in the unstretched state.

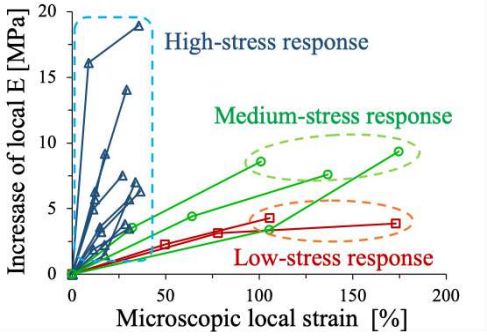


Figure 3. The local strain-local stress relationship in the specific regions for silica/SBR with TESPT.

To further investigate the relationship between local strain and local stress distribution, the digital image correlation (DIC) method was employed for data analysis. The results revealed an inhomogeneous local strain. Combined with AFM results, the local stress response behaviors were clarified. For example, Figure 3 shows the relationship between local strain and microscopic elastic modulus increase in the TESPT-treated sample. Near the silica aggregates, local strain increased only slightly, while the modulus increased significantly, suggesting that these regions served as high-stress zones where stress was concentrated. However, variations in interfacial strength introduced by SCAs led to differing stress concentration levels and modulus increases among samples. In contrast, the rubber matrix generally functioned as a low-stress response region, showing a substantial increase in strain but only a modest increase in modulus. Notably, in the TESPT-treated sample, a medium-stress region was also observed, attributed to enhanced filler-rubber interaction facilitated by TESPT.

Acknowledgement

The measured samples were provided by Yokohama Rubber Co., Ltd.

Reference

1. Liang X, Miyafuji K, Hara K, Mogi K, Nishida R, Liu H, Nakajima K, *Polymer*, 2022; 259: 125343.

International Rubber Conference 2025 (IRC2025)
1-3 December 2025 @ BITEC, Bangkok, Thailand

Friction Behaviour in Relation to Wear Morphology

T.H. PHAM, K. AKUTAGAWA, J.J.C. BUSFIELD

School of Engineering and Material Science, Queen Mary University of London, London E1 4NS, United Kingdom.

e-mail address of the presenting author (h.t.pham@qmul.ac.uk)

Keywords: Tyre friction, abrasion, wear, wear pattern

Tyres are the only part of a vehicle that come into contact with the road. They must simultaneously fulfil these three key performance characteristics, known as the ‘magic triangle’ of tyre functionality: high wet grip, low rolling resistance and good wear resistance. Balancing these three aspects influences the safety, fuel consumption, performance, control of the vehicle and longevity of the tyre. As different environments demand different performance levels, tyres must adapt to various conditions. For example, tyre developers for normal passenger cars aim to reduce fuel consumption by reducing rolling resistance. However, in motorsport, performance is favoured by increasing grip to give the driver more control over the car when cornering. Understanding the underlying friction process between a tyre and the road is critical for predicting tyre friction and developing tyres that deliver the desired performance.

It is known that the coefficient of friction depends on external factors such as the applied forces, temperature and roughness of the road. Additionally, the friction coefficient can change due to the development of abrasion patterns on the tyre surface with repeated frictional sliding, even when the influencing factors remain constant. This study aims to understand how tyre friction behaviour changes depending on the wear and abrasion patterns produced by variation of external influences. The objective is to understand how these processes interact and are initiated, allowing for the prediction and control of the friction between a tyre and the road to optimise performance.

Blade abrasion experiments were conducted to evaluate the friction behaviour, using a setup similar to that previously described [1]. This method involves moving a blade down onto an underlying rubber sample until a given normal load is reached. The blade is then rotated. After rotation, the blade is moved out of contact and rotated back to the initial position where the abrasion process is then repeated. This periodic, unidirectional motion of the blade was chosen because it resembles the process of a contact patch of a rolling tyre repeatedly contacting the road. The external influences on friction that will be experimented with are variations in blade angle, temperature and contact load as well as different rubber formulations. The experimental setup allows for the simultaneous measurement of the normal forces and the torque. These values can be used to calculate an average coefficient of friction over each sliding cycle. Repeated sliding shows how the coefficient of friction changes over successive cycles. Additionally, photographs were taken of the rubber surface to document the changes in the surface induced by the development of wear patterns.

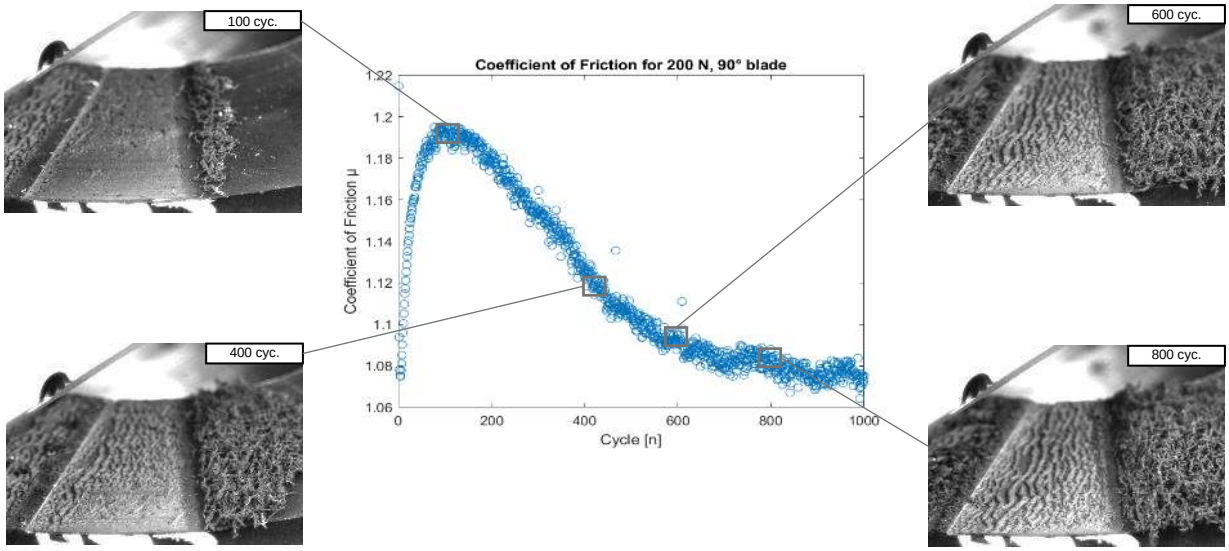


Figure 1. The coefficient of friction evolved over 1000 cycles with a blade with a 90° angle and a 200N normal load.

Shown in Figure 1 is the change in the coefficient of friction over 1000 cycles for a blade with an angle of 90°, using a rotation angle of 20° at high normal load of 200 N with pictures of the rubber surface at selected cycles. The detailed evolution of the friction and wear pattern is evaluated for a wide range of different elastomers and input conditions. Optical analysis of the rubber sample during rotation shows that the surface topography depends not only on the load, but also on the number of abrasion cycles undergone. This is due to changes in the surface, which also affect the friction behaviour. For the example shown in Figure 1, the change in the coefficient of friction over 1000 cycles face is apparent. Initially, the friction increases, which is believed to be due to the formation of a thin smear film layer. This sticky layer attaches to the blade, increasing the contact area and the adhesion component of friction, thereby resulting in a higher friction coefficient. With successive frictional sliding, a very fine abrasion pattern forms, which then increases in size until a coarser pattern emerges, with larger ridges and greater spacing. As the ridge spacing increases, the blade comes into contact with the rubber less frequently, resulting in a smaller contact area during sliding and therefore a smaller friction coefficient. This continues until the geometric features of the rubber become constant, at which point the friction coefficient also reaches a plateau.

The friction behaviour changes depending on whether the abrasion mechanism is chemical or mechanical, leading to smear wear or abrasive wear. Experiments have shown that the abrasion mechanism can change over time, particularly at the beginning when the rubber has not yet developed a pattern. The understanding of this is important for example in new fitted tyres where the formation of the abrasion pattern from the beginning determines the abrasion rate of the tyre in the future.

Acknowledgement

The authors would like to express their gratitude to those who contributed to the study.

References

1. Plaschka E.H., Akutagawa K., Di Federico E., Busfield J.J.C. , *Polymer Testing*, 2025; 143:108688.

S4T7-O-17

International Rubber Conference 2025 (IRC2025)
1-3 December 2025 @ BITEC, Bangkok, Thailand

In situ methods to characterize deformation-induced mechanisms in NR

Eric Euchler[1], Lutz Zybell[2], Sven Wießner[1,2], Konrad Schneider[2]

[1] *Leibniz Institute of Polymer Research Dresden e.V., Hohe Straße 6, 01069 Dresden, Germany.*

[2] *TUD Dresden University of Technology, Hohe Straße 6, 01069 Dresden, Germany.*

(euchler-eric@ipfdd.de)

Keywords: Natural Rubber, Multiaxial Deformation, Strain-Induced Crystallization, Advanced Testing

Elastomeric materials, such as natural rubber (NR), exhibit complex mechanical behavior that depends on their intrinsic material structure and deformation-induced changes of their structure. For NR, the strain-induced crystallization (SIC) phenomenon is of high importance because it immensely affects its outstanding mechanical performance [1]. Via *in situ* measurements, supplementary methods, such as digital image correlation (DIC), infrared (IR) thermography or X-ray scattering, are coupled with standard testing techniques, e.g. tensile experiments, providing unique databases. Such information enhances the understanding of structure-property relationships.

In this contribution, novel approaches for systematic investigations on deformation-induced structural changes in NR-based elastomers are introduced. *In situ* testing was performed in the lab using universal testing machines (ZWICK/Roell, Germany), equipped with advanced camera systems for DIC and IR analysis to estimate strain and temperature fields. In cooperation with the German synchrotron facility, *Deutsches Elektronen-Synchrotron* (DESY), *in situ* X-ray measurements were realized to study SIC behavior at various loading conditions. All measurements were conducted under quasi-static deformation at standard temperature and humidity. The NR-based elastomers were mixed with additives of common sulfur-cured systems without containing reinforcing fillers. Specimens were cured in a hot press at 140°C with vulcanization times according to the results of RPA measurements. Specific specimen geometries were produced for different purposes of multiaxial tensile loading.

Figure 1 shows a snapshot of the monotonic loading of a pre-notched NR-based elastomer specimen (left) and the corresponding strain field by a zoom-in of the crack tip zone (right). Locally, strains that are larger than 400 % occur at the very crack tip [2]. This observation contributes to explanations of the high resistance of NR against crack propagation, since it is known that at strains higher than 400 %, SIC improves the local stiffness of the NR network [3].

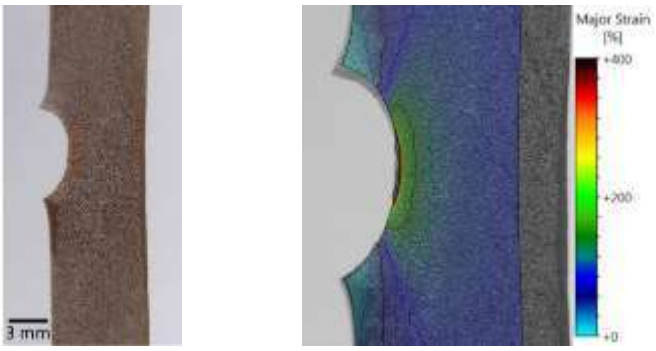


Figure 1. Strain field analysis at the crack tip of a pre-notched NR specimen (from [2]).

In-depth studies on the SIC behavior of NR-based elastomers have been realized using *in situ* synchrotron X-ray and IR measurements [4]. In Figure 2, representatively, a wide-angle X-ray scattering (WAXS) pattern indicates the formation of crystallites by the presence of Bragg peaks (top left), while IR imaging captured the heat generation due to the crystallization process (bottom left). SIC is most dominant at uniaxial tension which occurs in the homogeneous deformation of strip-like specimens as well as at the very front of a crack tip (Fig. 1). The correlation of crystalline fraction, which is equal to the SIC index, and the heat generation under cyclic loading is shown in Figure 2 (right). For both, the SIC index and temperature change, the hysteresis loops represent the reversibility of the SIC mechanism. Notably, the deformation-induced mechanism is related to the mechanical stress, instead of frequently used strain values.

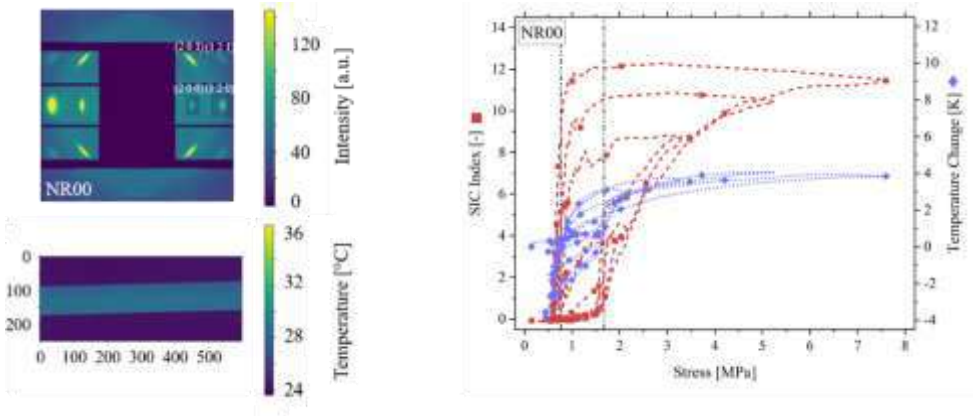


Figure 2. WAXS and IR data representing the SIC behavior of NR under cyclic loading (from [4]).

Acknowledgement

The authors would like to express their gratitude to the support of the P03 beamline staff at DESY, Hamburg, Germany. This study was partly supported by the German Research Foundation under the grant number 492017525.

References

1. Mars W V, Fatemi A, *Rubber Chem. Technol.*, 2004; 77(3): 391.
2. Zybell L, Euchler E, et al. (in preparation)
3. Xiang F, Schneider K, Heinrich G, *Int. J. Fatigue*, 2020; 135: 105508.
4. Euchler E, Schneider K, Sambale A K, Schwartzkopf M, Wießner S, in Heinrich G, Kipscholl R, Le Cam J B, Stoček R (eds.) *Adv. Polym. Sci.*, 2024; 294: 168.

International Rubber Conference 2025 (IRC2025)
1-3 December 2025 @ BITEC, Bangkok, Thailand

The Role of Deformation Mode on Rubber Hysteresis and Its Denpendency on Viscoelasticity

Shouliang NIE*, Wei HUANG, Xiaorong WANG

Zhongce Rubber Group Co. Ltd, Hangzhou, Zhejiang Province, China.

e-mail address of the presenting author (slnie@chaoyang.com)

Keywords: Viscoelasticity, Hysteresis, Deformation Mode, Heat Build-Up, Rolling Resistance

Rubber and its composites filled with nanoparticles are extensively utilized in critical industrial applications such as tires and air springs due to their excellent mechanical properties. As a typical viscoelastic material, their hysteresis loss is of great interest for both industry and academia.[1] Furthermore, it is important to noticed that the rubber components in the products could be loaded at quite different deformation modes, depending on the location and operating conditions.[2] In the stress-strain curve, the hysteresis loss is defined as the integral of the loop formed by stress-strain curve.[1] This can be expressed by the viscoelastic parameters in various formats for the *three types of deformation modes: I) energy-, II)stress- or III) strain-controlled*, allowing for the identification of the decisive viscoelastic parameters accordingly. [3]

The impact of deformation mode on the relationship between hysteresis and viscoelasticity has yet to be validated through practical experiments. In this presentation, we aim to verify it in two common perspectives within tire industry: 1) Heat Build-Up (HBU) of rubber with varying levels of moduli and crosslinking type; 2) Rolling-Resistance of tire utilizing different tread compounds.

1) Rubber Heat Build-Up:

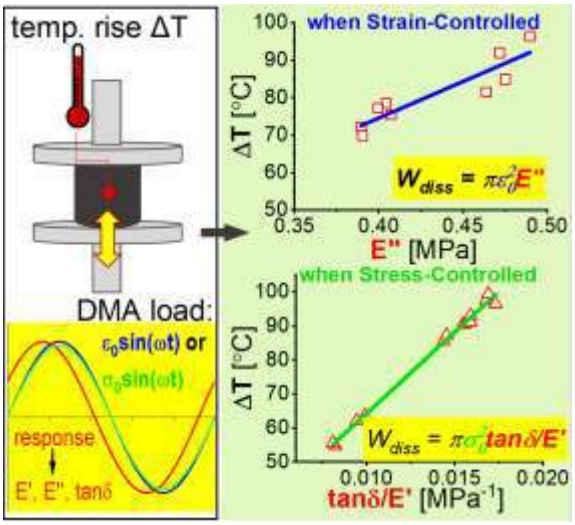


Figure 1. The rubber heat build-up amplitude ΔT due to hysteresis exhibits a distinctive dependency on viscoelasticity: (upper plot) at strain-controlled deformation, ΔT is determined by E″; (lower plot) while at stress-controlled mode, ΔT correlates to tanδ/E′.[3]

The HBU test of rubber is typically conducted as separate experiment from its characterization of viscoelastic properties. [4] Such correlation study often fails due to differing control modes and deformation conditions in the respective setups. In present work, coupled experiments were performed on an advanced dynamic mechanical analyzer (DMA), incorporating a HBU test fixture. During the test, DMA precisely controlled the cyclic deformation either at strain-controlled (constant strain amplitude) or stress-controlled (constant stress amplitude). The temperature rise ΔT was monitored via an inserted thermocouple in the sample core, as depicted in Figure 1 (left).

As demonstrated by the correlation plots in Figure 1 (right) from our experiments, ΔT from HBU exhibits distinct dependencies on viscoelastic parameters.[3] Under strain-controlled compression, ΔT shows a linear correlation with the loss modulus, E''. While in the stress-controlled situation, ΔT is determined by the combined parameter defined as $\tan\delta/E'$. These findings experimentally validate those decisive viscoelastic parameters for each corresponding deformation mode.

2) Tire Rolling Resistance:

The rolling resistance (RR) of tire is another key characteristic, governed by the hysteresis. For the first time, we employ practical experiments to investigate the correlation between tread viscoelasticity and tire RR performance with five types of tread compounds fabricated onto small size two-wheel tires. The tire body structure and tread pattern were kept the same across all samples, ensuring the only difference between the five groups of tires was tread compound.

Our results reveals that the RR value of five tires does not directly correlate to the $\tan\delta$ at 60°C. A deformation index *m* must be incorporated into a combined parameter $\tan\delta/E''^{m}$ to satisfy the correlation. This suggests that the deformation mode of tire tread under rolling conditions is predominantly stress-controlled, which is consistent with the trend observed in previous FEA simulated results reported in the literature.[2]

Conclusion:

The current experimental correlation study demonstrates how does the deformation mode affacet hysteresis-origenated phenomena in terms of rubber heat build-up (HBU) and tire rolling resistance (RR). Under strain-contrlled deformation, the temperature rise of rubber ΔT is governed by the loss modulus, E''. However, ΔT is determined instead by $\tan\delta/E'$ in the stress-controlled case. The RR of tire from tread rubber is, not fully by in a predominate manner, a stress-controlled scenario. A deformation index *m* can be applied on $\tan\delta/E''^{m}$ as the characterization parameter.

Acknowledgements

The authors expressed gratitude to Dr. Christopher G. Robertson for the helpful discussion.

References

1. Ferry JD, *Viscoelastic Properties of Polymers, 3rd Ed.,* John Wiley & Sons, Inc, New York, 1980.
2. Futamura S, Goldstein AA, Prediction and simulation of tire performance characteristics based on deformation index concept, *Rubber Chem. Tech., 2016; 89:1.*
3. Nie S, Huang W, Ren P, Wang X, *Macromol. Rapid Commun. 2025;* 2400847.
4. ASTM D623-07, ASTM International, West Conshohocken, USA 2019.

On the Decoupling of Chemical and Mechanical Surface Contributions in Soft Polymer Network Adhesion

M. BROGLY[1]

[1] *UHA-LPIM – 3b rue Alfred Werner, Mulhouse, France.*

maurice.brogly@uha.fr

Keywords: Soft polymer networks, Adhesion, Surface chemistry, Surface modulus, AFM

The relationship which connects the different factors that influence polymer adhesion, at the macroscale, is widely developed in the literature. Nevertheless the precise determination of the interplay between chemical and mechanical contribution to adhesion is much less developed, mainly due to experimental difficulties related to surface phenomena such as non-isotropic properties or gradients from the top surface to the core of the material. Indeed, adhesive properties of soft polymer networks or rubbery polymer surfaces result from the complex contribution of surface chemistry and activation of sliding [1] and dissipative mechanisms within the polymer surface layer.

This study represents an attempt to develop new relationships of the adhesion at the nanoscale using the atomic force microscopy (AFM) [2]. The use of the AFM allows deducing quantitative values at the nanoscale such as thermodynamic work of adhesion, surface energy, Young modulus, energy dissipative function as well as temperature and speed dependence of the nano-adhesion energy. Measurements of local adhesion forces [3] between a silicon nitride AFM tip and model substrates are performed by using the AFM contact mode, at ambient temperature, in the air. Considering that the main technical uncertainties have been listed and minimized, surface force measurements are, in a first step, done on chemically modified silicon substrates grafted with dedicated functional groups (hydroxyl, amine, methyl and ester). In order to investigate the effects of mechanical or viscoelastic contributions, force measurements on model rubbery polymer networks, whose surfaces are chemically grafted with the same functional groups as for silicon substrates, were achieved. As rubbery networks, crosslinked polydimethylsiloxane (PDMS) networks were synthetized. Mc values, that represent the average macromolecular weights between crosslinks, are ranging between 800 g/mol and 34 000 g/mol. Mc values were determined by swelling experiments. Flory's law of rubber elasticity [4], which represents the reciprocal tensile modulus versus Mc, is satisfied for the synthetized networks. This proves that a good control of the network synthesis and of macroscopic mechanical properties is achieved.

In a first step, AFM force–distance curves on rigid silicon substrates of controlled surface chemistry were recorded. The tip-sample pull-off force was then measured and the DMT theory [5] was used to access the thermodynamic work of adhesion (W_0) of the grafted substrates. Results show that the thermodynamic work of adhesion is proportional to the surface energy deduced from classical wettability measurements. We also demonstrate that measurements are sensitive to relative humidity and that capillary forces contribute to adhesion force.

In a second step, AFM force–distance curves on crosslinked rubbery PDMS surfaces of controlled surface chemistry were recorded. A comparison between the force–distance curves obtained on a silicon substrate and on a PDMS surfaces clearly shows the significant contribution of the mechanical properties of the polymer. First, compared to silicon substrates, during the tip-polymer separation process, the jump-off contact occurs over a large piezo displacement scale and could

correspond to a progressive dewetting of the tip by polymer chains during retracting. Second, the jump-off amplitude is higher than for silicon substrates and finally, the loading and unloading slopes in the deflection-distance representation are much lower than unity in the case of rubbery polymer networks. Considering all these specificities, we succeed in determining Young moduli from force-indentation curves deduced from deflection-distance curves.

Last, the ratio F^{adh}_{PDMSX} / $F^{adh}_{SiX,}$ where F^{adh}_{PDMS} and F^{adh}_{Si} represent the adhesion force measured on respectively PDMS networks and silicon substrates and X represents the functionality of the grafting, were calculated for all the grafting and PDMS networks and compared. It appears that for a given network, the ratios are independent of the surface chemistry, whereas for a given grafting, the ratios depend on the mechanical properties of the network, with the same values for all the grafting funxtionalities. Thus, for a given network, $F^{adh}_{PDMSX} = F^{adh}_{SiX} . k$ (k is a constant). However, for an rigid substrate, the DMT theory gives: $F^{adh}_{SiX} = 2.R.W_0$ (where R is the tip radius and W_0 is the thermodynamic work of adhesion). Then, $F^{adh}_{PDMSX} = 2.R.W_0.k$ and if introducing a dimensional constant ($k'=(2.R)^{-1}$) the relationship becomes: $G^{adh}_{PDMSX} = W_0.k.2.R.k'$ or :

$$G^{adh}_{PDMSX} = W_0. \phi(v,T)$$

where G is the separation energy and $\phi(v,T)$ is a viscoelastic dissipation function that depends on temperature T and separation rate v. This relationship clearly expresses the mechanical contribution from the chemical one in a force curve measurement with AFM. $\phi(v,T)$ is determined for each rubbery network for a given rate and a given temperature and is independent of the surface chemistry.

Last, we have studied the influence of surface chemistry by modifying the chemical properties of the AFM silicon tip with hydrophobic and hydrophilic self-assembly monolayer. We point out the advantage of AFM in the quantitative determination of the thermodynamic properties of the soft polymer networks, such as surface energy and thermodynamic work of adhesion, by comparison with the values obtained by wettability or JKR experiments. Nano indentation experiments give us the opportunity access surface mechanical properties and to probe the influence of the temperature and of the speed on the adhesion energy at the nanoscale. It is shown that WLF time-temperature formalism is still applicable at the nano-scale for soft rubbery polymers.

References

1. Brogly M, Bistac S, Fahs A, *Surfaces*, 2024; 7, 666.
2. Brogly M, Awada H, Noel O, in *Nanosciences and Technology, Applied Scanning Probe Methods XI*, B. Bhushan & H. Fuchs Eds., Springer Berlin Heidelberg, 2009; 1, 73.
3. Brogly M, in *Handbook of Adhesion Technology*, 2nd edition, L.F.M. da Silva, A. Öchsner, R.D. Adams Eds., Springer Berlin Heidelberg, 2018; 1, 39
4. Flory P.J, *Chem. Rev*, 1944; 35, 51.
5. Derjaguin B.V, Muller V.M, Toporov Y.P, *J. Colloid Interface Sci*., 1975; 53, 314.

International Rubber Conference 2025 (IRC2025)
1-3 December 2025 @ BITEC, Bangkok, Thailand

Wear particle formation mechanism investigated using LAT100

Shinya NAKANO[1], Takanobu KAWAMURA[1], James J. C. BUSFIELD[2]

[1] *Sumitomo Rubber Industries, Ltd., Kobe, Japan.*

[2] *Queen Mary University of London, London, United Kingdom.*

e-mail address of the presenting author (shinya-nakano.az@srigroup.co.jp)

Keywords: Rubber Wear, Smear Wear Layer, Wear Particle Formation, Tyre and Road Wear Particles

Tyre and road wear particles (TRWP) has recently attracted attention due to their environmental and health concerns. Fine particles, such as PM10 (particles with a diameter of 10 micrometers or less), remain suspended in the air and can travel long distances, making them difficult to capture. To mitigate the impact of TRWP on the environment and health, it is essential to understand the formation mechanism of wear particles and to control their size distribution. TRWP is composed of tyre tread fragments and road surface elements, with the components being highly mixed and often coated with various other substances. Therefore, a smear wear layer, which is a "sticky" degraded rubber layer observed on the rubber surface under specific wear conditions [1-3], is a key factor in elucidating the formation mechanism of TRWP. In this study, we investigated the wear particle formation mechanism with a focus on the smear wear layer.

Figure 1 shows the experimental procedure. Wear particles were generated and collected using LAT100. Powder, which is mixture of aluminum oxide and magnesium oxide, was supplied between a rotating rubber sample wheel and a corundum substrate disc. To investigate the wear particle formation mechanism, the powder feeding rate was regulated, as it has been revealed that the smear wear layer is removed by interacting with powder [3, 4]. Density separation was performed to separate rubber wear particles, which contain powder, from isolated powder. The powder content of the wear particles was evaluated by TGA. The size of the wear particles was calculated using optical microscope images and image analysis. Two different tyre tread formulations were investigated, as presented in Table 1. The effects of the other compound formulation and the powder size were also examined.

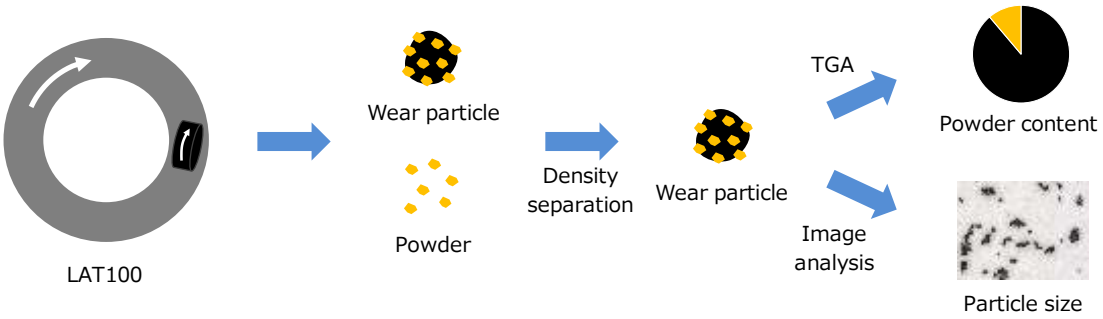


Figure 1. Experimental procedure

Table 1. Sample compositions

Compound	Polymer	Filler
IRN220	IR	N220 (70 phr)
SBRN220	SBR	N220 (70 phr)

Figure 2(a) shows the wear rate as a function of the drying powder feeding rate. When a small amount of powder was supplied, the wear rate increased significantly. Figure 2(b) represents the powder content in the wear particles measured by TGA. The increase in the powder content corresponds to the increase in the wear rate. Even when a large amount of powder (more than 10 times the amount of rubber wear) was supplied, the powder content in the wear particles did not change significantly. There was a large difference in powder content between the two compounds, which may be attributed to the characteristics of the smear wear layer. Figure 2(c) illustrates the volume-weighted average diameter of wear particles. As the powder content in the wear particles increased, their size decreased. Comparing the two compounds, these results suggested that a smear wear layer capable of incorporating a larger amount of powder leads to larger particle sizes and a lower wear rate.

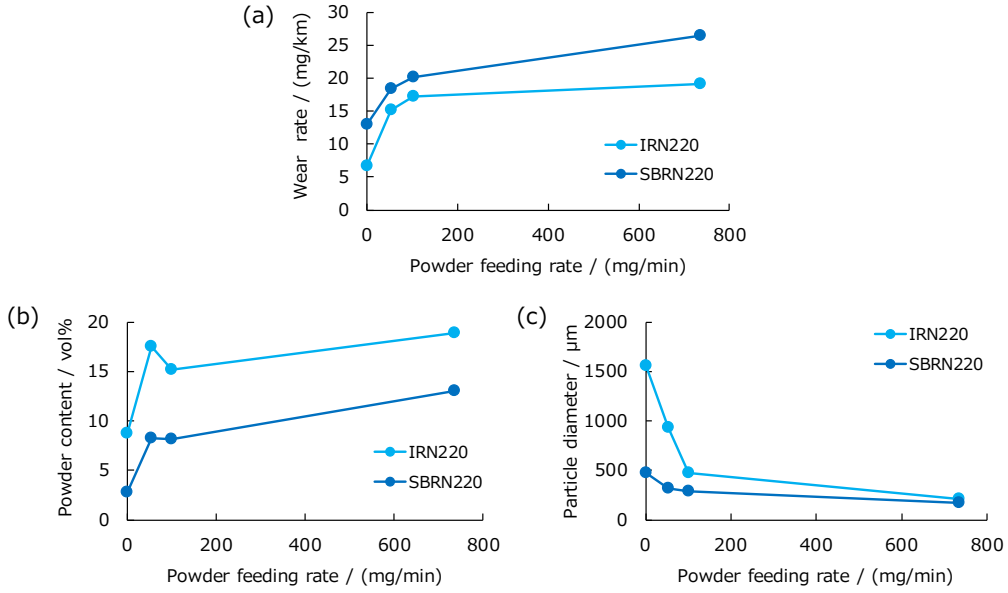


Figure 2. The effect of powder feeding rate on wear rate (a), powder content (b), and particle diameter (c).

Based on the obtained results, the wear particle formation mechanism was estimated. Firstly, a smear wear layer is formed on the rubber surface due to the friction with the road surface. Secondly, powders attach to the adhesive smear wear layer surface. Thirdly, powders are incorporated into the smear wear layer by the shear force applied from the road surface. Finally, the smear wear layer detaches from the rubber surface as wear particles. We have attempted to verify this mechanism using other methods such as adhesion measurement and contact angle measurement.

References

1. Wu, G., Sotta, P., Huang, M., Tunnicliffe, L., Busfield, J., *Rubber Chem. Technol.*, 2023; 96: 588.
2. Koliolios, E., Nakano, S., Kawamura, T., Busfield, J., *Polymer*, 2024; 300: 126982.
3. Koliolios, E., Ph.D. Thesis, Queen Mary University of London, 2025.
4. Nakano, S., Koliolios, E., Kawamura, T., Busfield, J., IRC 2024, 2024.

International Rubber Conference 2025 (IRC2025)
1-3 December 2025 @ BITEC, Bangkok, Thailand

Why Lab Studies Matter for Understanding Tyre Wear Emissions

M. Stěnička[1], R. Stoček[1,2], M. Pöschl[1], S. Datta[1]

[1] *Centre of Polymer Systems, tř. Tomáše Bati 5678, 76001, Zlín, Czech Republic.*

[2] *Coesfeld GmbH & Co. KG, Tronjestraße 8, 44319 Dortmund, Germany.*

e-mail address of the presenting author (stenicka@utb.cz)

Keywords: Rubber, Tyre, Wear, Particle, Emission, Laboratory analysis

Tyres represent the sole component of a vehicle that comes into contact with the road surface, thus fulfilling a pivotal function in the provision of traction, stability and safety. However, it is estimated that approximately 6 million metric tonnes of tyre wear particles (TWPs) are released into the environment on an annual basis as a consequence of vehicle operation. Following detachment, these particles interact with non-exhaust emissions (NEEs), including brake dust and road minerals, to form tyre and road wear particles (TRWPs). TRWPs have been identified as a significant source of microplastics in the environment and a major contributor to NEEs [1–3].

The endeavours to diminish TRWPs emissions are confronted with a fundamental challenge, namely the technical complexity of collecting and analysing these particles directly behind a moving tyre [4, 5]. It is evident that environmental factors, including but not limited to turbulence, adhesion and dispersion, render the consistent capture and validation of these particles on the road a challenging task, given the current technological capabilities.

The present study adopts a divergent approach by shifting the focus to controlled laboratory testing. Instead of endeavouring to replicate authentic wear and tear, the DIN abrasion test (ISO 4649) is utilised as a simplified, widely accessible method for the generation of wear particles under repeatable conditions. It is important to note that the intention of this method is not to simulate actual tyre-road interactions, but rather to offer a standardised platform for investigating how material properties influence particle formation and recovery potential. Furthermore, the intrinsic strength required to initiate crack and thus wear was determined by means of an Intrinsic Strength Analyser™ (Coesfeld, Germany).

A total of four rubber compounds, differing in their ratio of natural rubber (NR) to butadiene rubber (BR), were produced (Table 1). The purpose of the model compounds under consideration here was to demonstrate a correlation between DIN abrasion and intrinsic strength of the cured rubber materials under laboratory conditions (Figure 1, left).

Table 1. Specimen composition

Components [phr]	**Specimen notations**			
	100/0	**80/20**	**60/40**	**0/100**
NR	100	80	60	0
BR	0	20	40	100
Carbon black (N 234)	50	50	50	50
IPPD	3	3	3	3
TMQ	2	2	2	2
Wax 2124	2	2	2	2
TBBS	1.75	1.75	1.75	1.75

Sulphur	2.5	2.5	2.5	2.5
ZnO	5	5	5	5
Stearic acid	3	3	3	3

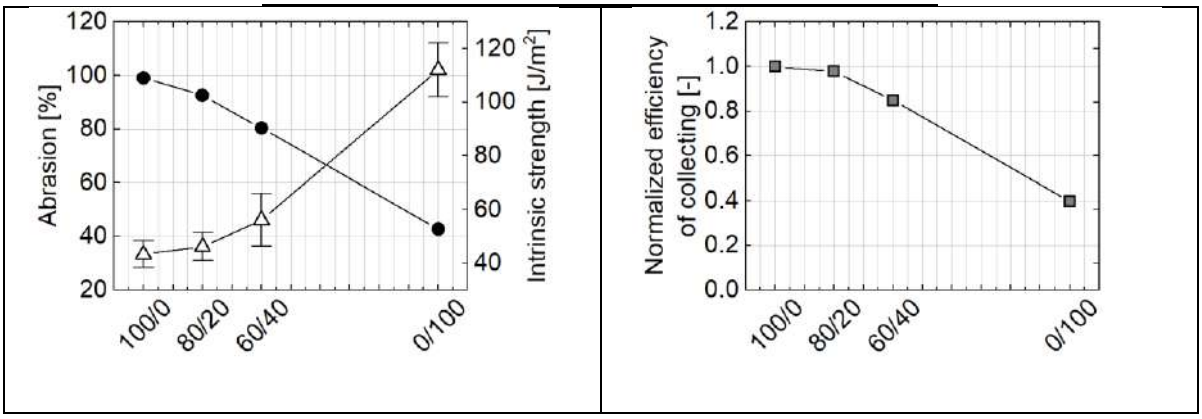


Figure 1. The graphs on the left illustrate the abrasion resistance (circles) and the intrinsic strength (triangles) of rubber compounds with various NR/BR ratio, while the graph on the right shows the efficiency of collecting abraded particles (squares)

The preliminary findings of this study demonstrate that, even within optimised laboratory settings, complete recovery of rubber wear particles (rWPs) is not always attainable. It is evident that the inherent complexity of the problem is underscored by the persistence of losses attributable to adhesion, surface effects and secondary dispersion. Should reliable capture prove elusive in such a fundamental configuration, this would give rise to valid questions regarding the readiness of real-world collection technologies. The collection efficiency has been observed to approach close to 100 % for pure NR. However, as the BR content increases, the collection efficiency decreases significantly (Figure 1, right). This property is probably related to the fact that as the BR content increases, the particle size of rWPs decreases.

The central theme of this study is not to discard the possibility of collecting TRWPs behind a tyre, but rather to underscore the necessity for a stepwise approach, commencing with laboratory-based studies that facilitate the elucidation of the mechanisms underlying particle generation. In order to achieve substantial progress in reducing emissions, it is imperative to comprehend the wear mechanism and the role of diverse rubber type in this process.

Laboratory investigations, even when based on simplified tests, offer crucial insights. The employment of these methodologies facilitates the isolation of variables, the comparison of materials, and the development of a predictive understanding that can ultimately inform both tyre design and future strategies for emission control in real driving environments.

Acknowledgement

This work is financed by the Ministry of Education, Youth and Sports of the Czech Republic DKRVO (RP_CPS_2024_28_006).

References

1. Gieré R, Dietze V, *Adv. Polym. Sci.* 2022; 289:71.

2. Zhang M, Yin H, Tan J, Wang X, Yang Z, Hao L, Du T, Niu Z, Ge Y, *Atmos. Environ.*, 2023; 297: 119597

3. Mattonai M, Nacci T, Modugno F, *TrAC, Trends Anal. Chem.* 2022; 154: 116650

4. Mun S, Chong H, Lim Y, Kwon S, *Sustainability*, 2024; 16: 10395

5. Khardi S, *Atmos.*, 2024; 15: 665

Study of standard laboratory for testing medical rubber gloves according to ISO/IEC 17025

Hassarutai Yangthong[1], Supitta Suethao[1,2], Wirasak Smitthipong[1,2]

[1] *Specialized center of Rubber and Polymer Materials in agriculture and industry (RPM),*

Department of Materials Science, Faculty of Science, Kasetsart University, Bangkok 10900, Thailand

[2] *Hub of Talents in Natural Rubber, National Research Council of Thailand (NRCT), Bangkok, 10900, Thailand*

e-mail address of the presenting author (fscihty@ku.ac.th)

Keywords: Natural rubber, Rubber glove, Standard, Laboratory, ISO/IEC 17025

Thailand is the world's second largest producer and exporter of rubber gloves, after Malaysia. The demand for rubber gloves is expected to continue to increase at a rate of 10 percent per year due to the aging society, the epidemic situation, and the government's policy to promote rubber gloves as a product champion and a hub for natural rubber glove production in Thailand. This has led to a continuous increase in demand for rubber gloves. Currently, most of the rubber glove production bases are in Malaysia, which is a process for producing gloves from synthetic rubber such as nitrile rubber. However, the mechanical properties of nitrile rubber are still inferior to natural rubber. Therefore, this issue is an advantage for Thailand, a producer and exporter of natural rubber, as well as Thailand's strength as a source of concentrated latex, which is an important raw material for rubber glove production. In addition, the government's investment promotion by specifying that rubber glove production is in the group of natural rubber product manufacturing businesses that are entitled to an 8-year corporate income tax exemption, which has attracted new entrepreneurs, both Thai and foreign, such as the United States, Germany, and China, to invest in Thailand more. Therefore, it is possible to produce quality and standard rubber gloves, as well as at a reasonable price. However, one way to promote and push the use of natural rubber gloves to replace synthetic rubber gloves is to create standards and credibility for rubber glove products that are internationally accepted. Currently, there are less than 10 rubber glove testing laboratories in Thailand, both public and private. There are only three government agencies have been certified for their laboratory competence according to the ISO/IEC 17025 standard for rubber glove testing, which is not enough to meet the needs of the industry. Therefore, this research aims to study the expansion of standard laboratory for testing rubber gloves used in medical application according to the ISO/IEC 17025 system to support testing of disposable medical diagnostic gloves following to method of TIS 1056-2556 Part I [1] include: dimensions (i.e., width, length, thickness), watertightness, tensile properties before and after aging (i.e., force, elongation at break).

The research results showing the calibration values of related instruments are shown in Table 1. It can be seen that the instruments used in all testing have calibration or verification that results passed the ISO/IEC 17025 criteria.

Table 1. Results of calibration or verification of instruments

Testing	Instruments	Calibration or verification			Status[a]
		Unit	Criteria	Result	
Dimensions (i.e., width, length, thickness)	Steel ruler	mm	± 1	0.027 – 0.223	/
	Thickness gauge	mm	± 0.03	0.00063 – 0.01175	/
Watertightness	Mandrel Pipe	mm	≤ 60	60	/
		mL	± 50	2	/
	Cylinder	mL	± 10	4.535	/

Testing	Instruments	Calibration or verification			Status[a]
		Unit	Criteria	Result	
Tensile properties (i.e., before and after aging)	Universal Testing Machine	N	± 0.5	0.007 – 0.011	/
		mm	± 1.0	0.0010 – 0.3402	/
	Geer oven	°C	± 1.0	0.47 – 0.60	/

[a] Status / represents available instrument and x represents unavailable instrument

In addition, the results of intralaboratory comparison and interlaboratory comparison according to ISO/IEC 17025 are shown in Table 2. It can be seen that the results between individuals are not significantly different. That is, the t_{Stat} less than the $t_{Critical}$. Similarly, the results between laboratories that were conducted for comparison with the Rubber Authority of Thailand (RAOT). It was found that the test results between laboratories of both agencies did not differ significantly, therefore they passed the test criteria.

Table 2. Results of intralaboratory and interlaboratory comparison

Testing	Unit	Number of gloves (Piece)		Criteria	Intralaboratory comparison		Interlaboratory comparison	
		RPM	RAOT		Result	Status[b]	Result	Status[b]
Dimensions - width	mm	13	13	$t_{Stat} < t_{Critical}$	$t_{Stat} = 1.4$, $t_{Critical} = 2.1$	/	$t_{Stat} = 1.4$, $t_{Critical} = 2.1$	/
- length	mm	13	13	$t_{Stat} < t_{Critical}$	$t_{Stat} = 1.7$ $t_{Critical} = 2.1$	/	$t_{Stat} = 0.1$ $t_{Critical} = 2.1$	/
- thickness	mm	13	13	$t_{Stat} < t_{Critical}$	$t_{Stat} = 0.4$ $t_{Critical} = 2.1$	/	$t_{Stat} = 1.5$ $t_{Critical} = 2.1$	/
Watertightness	unit	200	200	< 10	HY[c] = 7, HK[d] = 6	/	RPM = 5, RAOT = 6	/
Tensile properties - force before aging	N	13	13	$t_{Stat} < t_{Critical}$	$t_{Stat} = 0.3$ $t_{Critical} = 2.1$	/	$t_{Stat} = 1.9$ $t_{Critical} = 2.1$	/
- EB[a] before aging	%	13	13	$t_{Stat} < t_{Critical}$	$t_{Stat} = 1.3$ $t_{Critical} = 2.1$	/	$t_{Stat} = 1.6$ $t_{Critical} = 2.1$	/
- force after aging	N	13	13	$t_{Stat} < t_{Critical}$	$t_{Stat} = 0.4$ $t_{Critical} = 2.1$	/	$t_{Stat} = 1.9$ $t_{Critical} = 2.1$	/
- EB[a] before aging	%	13	13	$t_{Stat} < t_{Critical}$	$t_{Stat} = 0.5$ $t_{Critical} = 2.1$	/	$t_{Stat} = 1.5$ $t_{Critical} = 2.1$	/

[a] Elongation at break, [b] Status / represents passed and x represents failed results, [c]HY and [d]HK are the first and second scientist's watertightness results.

Therefore, this research has been applied for the certification of laboratory competence in testing gloves for single-use medical examination according to TIS 1056-2556 Part I for eight tests include: dimensions (i.e., width, length, and thickness), water leakage, tensile properties before and after aging (i.e., force, elongation at break), which has positive effects to increase the number of government laboratories that are impartiality in testing rubber gloves products.

Acknowledgement

The authors gratefully acknowledge the support from National Research Council of Thailand (NRCT), Fund Project no. N21A670609. We also express our gratitude for the valuable assistance provided by the specialized center of Rubber and Polymer Materials in agriculture and industry (RPM), Department of Materials Science, Faculty of Science, Kasetsart University.

References

1. TIS 1056-2556 Part I Single-use medical examination gloves

International Rubber Conference 2025 (IRC2025)
1-3 December 2025 @ BITEC, Bangkok, Thailand

Visualizing Nanoscale Interface in Direct Adhesive Rubbers Containing Reversible Coordination Linkages

Hung K. NGUYEN[1], Kyohei KOTANI[2], Katsuhiko TSUNODA[2], Ken NAKAJIMA[1]

[1] *Department of Chemical Science and Engineering, Institute of Science Tokyo, Tokyo, Japan.*

[2] *Sustainable Materials and Compounds, Bridgestone Corporation, Tokyo, Japan.*

e-mail address of the presenting author (nguyen.k.af@m.titech.ac.jp)

Keywords: Adhesion, Coordination cross-linked rubbers, Nanoscale interface, Atomic force microscopy

Enhancing adhesion between cross-linked rubbers is crucial in rubber product manufacturing, as it can lead to extending product lifespan and performance. Incorporating reversible linkages, such as dynamic covalent bonds, host-guest interactions, and metal-ligand coordination bonds into rubbers has attracted significant attention as a strategy to improve direct adhesion between cross-linked rubbers.[1] Among these, metal-ligand coordination bonds are particularly promising due to their tunable bonding energy, which can be adjusted by modifying the type and concentration of metal salts as well as newly designing ligands on polymer chains. For example, Kotani et al. have recently developed functionalized rubbers incorporating zinc dimethacrylate (ZDMA) coordination linkages, which exhibited significantly enhanced adhesion strength compared to traditional cross-linked rubbers.[2,3] They also demonstrated that increasing the density of coordination linkages can dramatically increase the adhesion strength.[2] Despite these promising results and their potential applications in the rubber industry, physical mechanisms underlying adhesion at the interface between two crosslinked rubbers remain poorly understood.

In this study, we employ advanced atomic force microscopy (AFM)-based techniques to directly visualize the mechanical behavior at the nanoscale interfacial region between two cross-linked rubbers containing metal-ligand coordination bonds. For materials, functionalized styrene-butadiene rubbers (SBR) were synthesized via tetrazine click reactions with 3,6-di(2-pyridyl)-1,2,4,5-tetrazine (DPT) during the rubber-kneading process, followed by mixing with ZDMA during thermal curing. Figure 1a illustrates the reaction steps for preparing DPT-SBR/ZDMA composites. Further details on sample preparation are available elsewhere.[2] For AFM characterization, we conducted both quantitative nanomechanical mapping (QNM) and nanoscale dynamic mechanical analysis (nDMA) using a Bruker Dimension Icon AFM equipped with a Nanoscope 6 controller (Bruker, USA). The QNM method has been well established for high-resolution modulus mapping of rubber materials,[4] while nDMA has recently demonstrated the ability to simultaneously quantify several dynamic mechanical properties of polymers at the nanoscale, such as storage modulus, loss modulus, and loss tangent, analogous to those obtained from conventional dynamic mechanical analysis.[5]

Figure 1b presents a schematic of the adhesive sample preparation for AFM measurements. Both sheets A and B consist of DPT-SBR/ZDMA composites but can differ in the concentrations of ZDMA and/or DPT, thus they are expected to exhibit different mechanical responses.[2] In addition, a small fraction of carbon black (CB) filler (~5 phr) was added into sheet A as a marker, allowing easy identification of the right interface between two sheets during microtome sectioning and AFM imaging. Figure 1c shows representative height and elastic modulus (in log scale) maps obtained via QNM method across the interfacial region between two cross-linked rubbers with different DPT/ZDMA linkage densities. The right interface is identifiable in the height image due to the

presence of CB exclusively in sheet A. The modulus map reveals a gradual variation in elastic magnitude across several micrometers near the interface, which can be explained due to the interdiffusion of coordination linkages through the interface between the two sheets. We also found that both the density of linkages and the preparation temperature significantly influence the extent of this mechanically modified interfacial region, nicely consistent with changes in adhesive strength measured via peel tests.

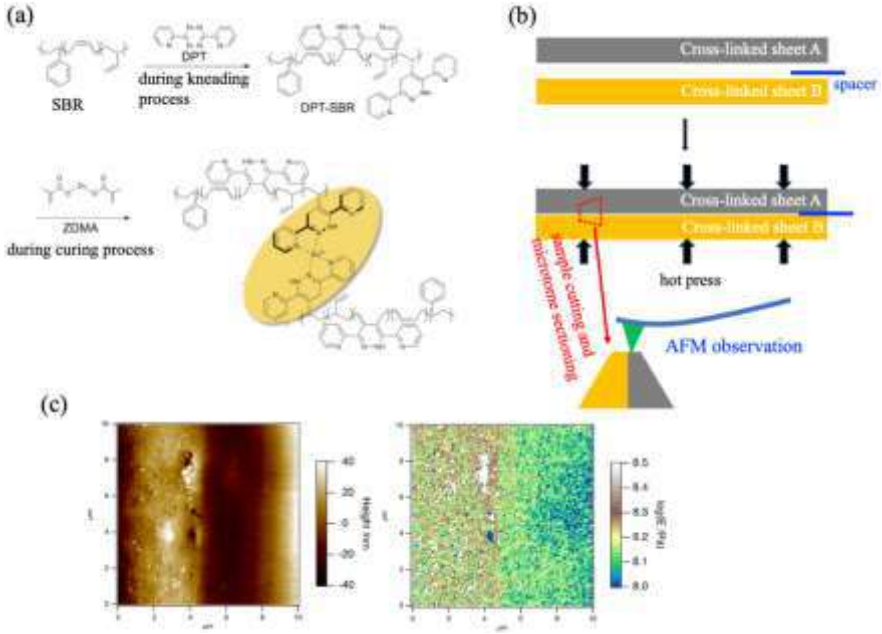


Figure 1. (a) Schematic illustration of the reaction process used to prepare DPT-SBR/ZDMA composites.[2] (b) Schematic of the adhesive sample preparation for AFM experiments. (c) Height and elastic modulus (in log scale) maps measured using QNM method across the interface between two rubber sheets.

Acknowledgement

This work was supported by the JST-Mirai Program Grant Number JPMJMI18A2, Japan.

References

1. Tsuruoka A, Takahashi A, Aoki D, Otsuka H, *Angew. Chem., Int. Ed.*, 2020; 59: 4294.
2. Kotani K, Tsunoda K, Otsuka H, *RSC Appl. Polym.*, 2023; 1: 229.
3. Kotani K, Kitamura Y, Tsunoda K, Takahashi A, Otsuka H, *RSC Appl. Polym.*, 2025; 3: 347.
4. Nakajima K, Ito M, Nguyen HK, Liang X, *Rubber Chem. Tech.*, 2017; 90: 272.
5. Nguyen HK, Shundo A, Ito M, Pittenger B, Yamamoto S, Tanaka K, Nakajima K, *ACS Appl. Mater. Interfaces*, 2023; 15: 38029.

Study on Delamination Mechanism of Rubber-Adhesive Interface in Sealing Materials

Hiromu KAWASAKI[1], Takahiro ANZAI[1], Yuichi AOYAGI[1], Xiaobin LIANG[2], Ken NAKAJIMA[2]

[1] *NOK CORPORATION, 4-3-1 Tsujido-Shinmachi, Fujisawa-shi, Kanagawa-ken 251-0042 Japan.*

[2] *Institute of Science Tokyo, 2-12-1 Ookayama, Meguro-ku, Tokyo 152-8550 Japan.*

Kawasaki.20.Hiromu@jp.nokgrp.com

Keywords: Adhesive Peeling, Interface, Atomic Force Microscopy

Oil seals are one of the most common sealing devices mainly used on rotating shafts. Their main role is to prevent various fluids such as lubricating oil, water, chemicals, and gases used in machine products from leaking from the inside of the machine, and to prevent foreign substances from entering the machine from the outside at the same time. Sealing performance is achieved when a part called the lip contacts the rotating shaft. Because the lip must be able to follow the moving mating surface reliably and resist fluids, a typical oil seal consists of synthetic rubber, a metal ring, a spring, and an adhesive that connects the rubber and metal (Fig. 1). Therefore, if peeling occurs at the rubber metal ring interface, a sealing function cannot be fulfilled, which is fatal.

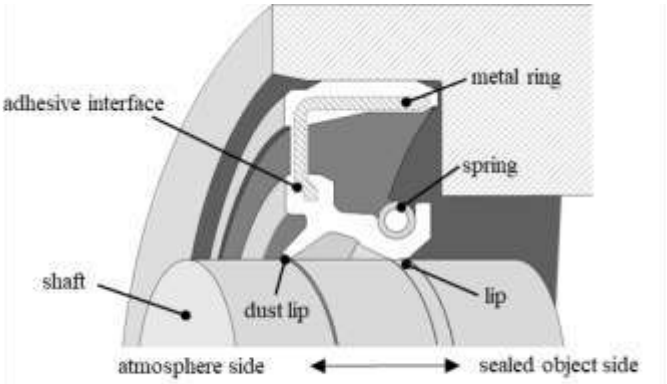


Fig. 1 Structure of oil seal.

Oil seals need to withstand long-term use, but it is estimated that degradation of the interface gradually proceeds by various factors such as heat, oxygen, oil, and fatigue due to repeated deformation. Thus, it is very important to understand the structural change due to degradation of the adhesive interface for improving the durability. In order to do so, it is necessary to visualize the microstructure and confirm its changes. Therefore, in this study, we attempted to clarify the mechanism of rubber adhesive interface peeling by observing the microstructure of the adhesive interface using AFM and obtaining the mechanical properties of the adhesive interface with a thickness of about several μm.

Specimens consisting of rubber, adhesive, and resin were used as model samples to verify the mechanism (Fig. 2). ACM for rubber, phenolic resin for adhesive, and nylon for resin were prepared. After the adhesive was applied to the resin, the specimens were prepared by vulcanizing and bonding the rubber fabric. The prepared specimens were placed in an oven at a predetermined temperature and subjected to heat treatment that simulates an actual product. The cross sections of the collected specimens were polished by using Leica's ultramicrotome and AFM measurements were performed

near the rubber adhesive interface by Bruker's Icon. Elastic modulus was calculated by two-point JKR method (ISO 21222:2020).

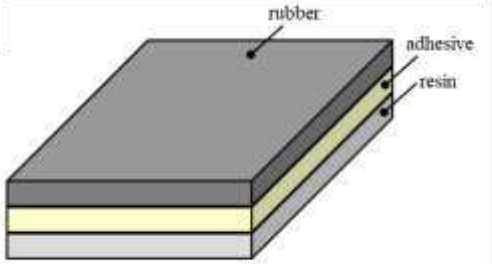


Fig. 2 Image of test specimen.

The acquired elastic modulus mapping and the profile of the adhesive layer are shown in Fig. 3. The elastic modulus profile of the adhesive layer confirms that the elastic modulus of the adhesive decreases near the interface with the rubber. This phenomenon was not observed under conditions where no heat treatment was applied, and we consider that heat and the diffusion of oxygen from the rubber side promoted the degradation of the adhesive [1]. In addition, the rubber layer shows an increase in elastic modulus due to oxidative degradation.

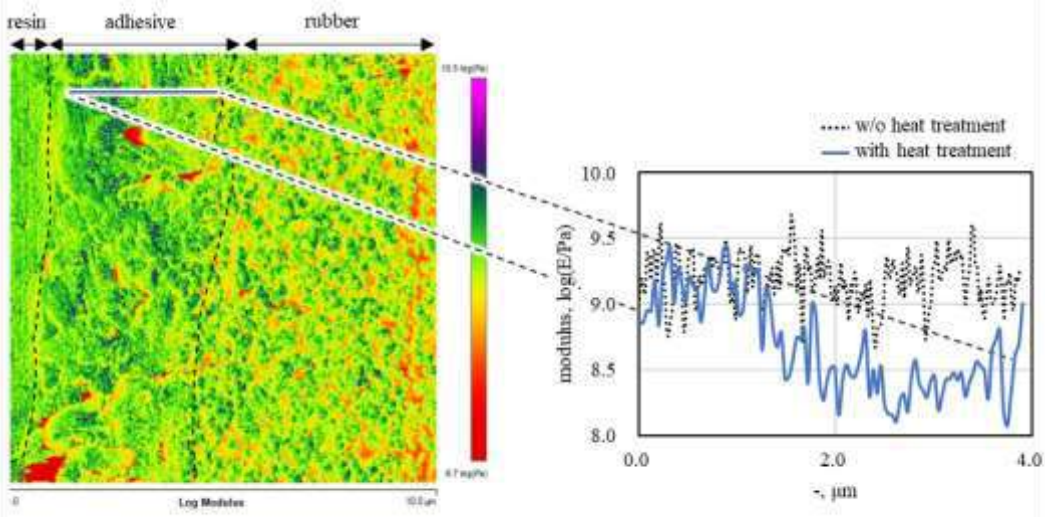


Fig. 3 AFM measurement results.

Therefore, as the mechanism of rubber adhesive interface peeling, heat and oxygen first reduce the elastic modulus of the adhesive near the interface, while the elastic modulus of the rubber increases. It is estimated that this change in elastic modulus reduced the rigidity of the adhesive near the interface, resulting in excessive deformation due to increased shear strain, leading to cohesive failure.

Reference

1. Conley R, Bieron J, *Applied Polymer*., 1963; 7: 103.

Analysis of Allergenic Proteins in Natural Rubber after Radiolysis by Mass Spectrometry Technique

A. NIMPAIBOON[1]

[1]*Rubber Technology Research Centre, Faculty of Science, Mahidol University, Nakhon Pathom 73170, Thailand.*

adun.nim@mahidol.ac.th

Keywords: Natural rubber, Allergenic proteins, Mass spectrometry

Natural rubber (NR) latex from *Hevea brasiliensis* is one of the most important bio-sustainable material and widely used in various applications. However, its utilization is limited by the presence of allergenic proteins, which can provoke a variety of allergic reactions, particularly the life-threatening Type I (immediate) allergy with symptoms such as anaphylaxis. The World Health Organization (WHO)/International Union of Immunological Societies (IUIS) Allergen Nomenclature Sub-Committee has identified allergenic proteins in NR latex, designated Hev b 1 to Hev b 15 and their isoallergens [1]. Presently, ionizing radiation has gained significant interest for use in vulcanization of NR latex. It has been reported the potential of γ-ray irradiation from a Cobalt-60 source for removing proteins from NR latex [2].

The aim of this work is to analyze allergenic proteins present in NR latex before and after radiolysis as a result of electron beam (EB) irraiation by mass spectrometry. The results in Table 1 show that non-targeted label-free nanoscale liquid chromatography coupled to tandem mass spectrometry (Nano-LC-MS/MS) could both qaulitatively and quantitatively analyze allergenic proteins in NR. Downregulated expression could predict the multiple effects of EB on the allergenic proteins, including chain scission, crosslinking and side chain modification.

Table 1 List of NR allergens and their isoallergens identified as differential expression (abundances)

Allergen/Isoallergen	**Differential expression (abundances) (Log_2 fold change)**
	(300 kGy-irradiated /Non-irradiated)
Hev b 1	(-)
Hev b 2	(-)(-)
Hev b 3	(-)(-)
Hev b 4	(-)(-)
Hev b 5	(-)(-)
Hev b 6 Hev b 6.01 Hev b 6.02 Hev b 6.03	(-)(-)

Hev b 7 Hev b 7.02	(-)
Hev b 8 Hev b 8.0102 Hev b 8.0201 Hev b 8.0202 Hev b 8.0203 Hev b 8.0204 (majority)	(-)(-)
Hev b 9	(-)
Hev b 10 Hev b 10.0101 Hev b 10.0102 (majority) Hev b 10.0103	(-)(-)
Hev b 13	(-)
Hev b 14	(-)(-)

(−) = Downregulated >|0.5| (-)(-) = Downregulated >|1|

Acknowledgement

The author would like to thank the Rubber Technology Research Centre (RTEC) for providing the equipment and facilities used in this study.

References

1. Palosuo, T.; Reinikka-Railo, H.; Kautiainen, H.; Alenius, H.; Kalkkinen, N.; Kulomaa, M.; Reunala, T.; Turjanmaa, K., Latex allergy: the sum quantity of four major allergens shows the allergenic potential of medical gloves. *Allergy* **2007,** *62* (7), 781-6.
2. Varghese, S.; Katsumura, Y.; Makuuchi, K.; Yoshii, F., Production of Soluble Protein Free Latex by Radiation Process. *Rubber Chem. Technol.***2000,** *73* (1), 80-88.

NR Symposium

IRC 2025
BANGKOK, THAILAND

International Rubber Conference 2025 (IRC 2025)

Sustainability Risks are Business Continuity Risks: A Systemic Response through GPSNR's Assurance and Shared Investment Framework

S. SAVI[1]

[1] *Global Platform for Sustainable Natural Rubber*

The natural rubber (NR) industry, foundational to tire manufacturing and global mobility, faces sustainability risks that are often indistinguishable from business continuity risks. With 85% of global NR production supplied by six million smallholders, the sector faces declining replanting rates (1.2 – 1.7% versus a 4% stability threshold as per latest IRSG data), aging tree stock, and market volatility. This is furthered by climate variability and rising compliance costs.

In response, the **Global Platform for Sustainable Natural Rubber (GPSNR)**, whose members account for over 50% of global NR demand, has developed an integrated response through a **Risk-Based Assurance System** and a **Shared Investment Mechanism (SIM)**.

The Assurance System standardizes policy commitments across environmental, social, and governance dimensions, supported by self-assessments and made credible by independent verification and third party assessments. Meanwhile, the SIM mobilizes collective industry finance from GPSNR Manufacturers, exceeding **USD 3 million in 2025**, to implement smallholder-centered projects in major rubber producing countries, focused on replanting, agroforestry, land legality, and conservation. Together, these mechanisms form a systemic approach to managing sustainability as a core determinant of long-term supply security and business resilience.

In the last two years, GPSNR has also played a role in bringing the industry under one umbrella to understand and form guidance for evolving **regulatory frameworks** such as the **European Union's Regulation on Deforestation-free Products (EUDR)**. Through the Assurance System, GPSNR enables members to align with some regulatory baselines, and often go beyond them. The platform's due diligence guidance, legality studies, and crosswalks to emerging regulations not only support compliance but drive proactive transformation, positioning sustainability as a competitive and operational advantage rather than a compliance burden.

Looking ahead, as both the Assurance System and SIM move into full implementation, GPSNR's focus is on ensuring **efficient scaling, governance integrity, and measurable impact**. The organization is enhancing its capacity to monitor performance, refine risk methodologies, and maintain transparent reporting while ensuring the system remains adaptable to national contexts and supply chain complexities. This transition from design to implementation marks a critical phase in operationalizing sustainability across the global NR value chain.

International Rubber Conference 2025 (IRC2025)
1-3 December 2025 @ BITEC, Bangkok, Thailand

The Role of Thailand Contributing to Sustainability of Natural Rubber Supplies

N. LEKAWIPAT[1]

[1] *Rubber Research Institute of Thailand, Rubber Authority of Thailand.*

Thailand prioritizes the social and environmental sustainability of its agricultural sector, particularly concerning natural rubber (NR), a key global commodity. The Rubber Authority of Thailand (RAOT), a state enterprise under the Ministry of Agriculture and Cooperatives (MOAC), is the primary agency responsible for the administration, research, and development of the entire domestic rubber system. RAOT is mandated to ensure price stability, promote replanting, and, crucially, lead the sustainable transformation of the industry by strengthening both smallholders and entrepreneurs. RAOT's strategy for achieving sustainable NR supply is multifaceted: it emphasizes sustainable rubber plantation management, efficient natural resource utilization, minimized environmental impact, and the establishment of a fundamental mechanism to upgrade the entire industry.

The strategy focuses on integrating stakeholder needs and developing specific market channels for sustainably sourced rubber products to enhance farmer income and institutional strength. Key initiatives include promoting agroforestry (Integrated Rubber Plantation), targeting 50,000 *rai* (8,000 ha) annually and over 1.8 million *rai* (288,000 ha) cumulatively in immature plots; pursuing international certification (such as FSC or PEFC) for a total of 530,000 *rai* (84,800 ha); and expanding the rubber carbon credit project to cover 1 million *rai* (160,000 ha) of farmers' plantations by 2026. Furthermore, to meet stringent international standards, notably the European Union Deforestation Regulation (EUDR), RAOT is implementing a robust national traceability system. This system involves registering 90% of the total rubber plantation area and the smallholders (who account for 95% of production), linking their verified land titles to raw materials traded through the Central Rubber Market. This ensures end-to-end verification of origin, allowing buyers to trace the product back to the specific registered farmer and location. Through these efforts, Thailand is actively establishing a global benchmark for responsible and sustainable natural rubber production.

Novel Green Technologies for Production of User-friendly and Consistent Properties NR

N. MOONPRASITH, C. KONGKAE[1], P. SUWANDITTAKU[1], S. MONTHA, S. LOYKULNANT

[1] *National Metal and Materials Technology Center, 114 Thailand Science Park, Phahonyothin Road, Khlong Nueng, Khlong Luang, Pathum Thani, 12120, Thailand Tel: +66 615636969.*

nantinm@mtec.or.th

Advancing the sustainability and performance of natural rubber (NR) is key to expanding its role in high-value applications. This presentation highlights five green technologies developed to enhance safety, consistency, and environmental compatibility in NR production.

1. Ammonia- and Nitrosamine-Free Concentrated Latex: A novel preservation system enables the production of high-purity latex without ammonia, TMTD, or ZnO. This latex is ideal for sensitive applications such as baby nipples and medical products, offering improved user safety and microbial stability.
2. Ultra-Low Ammonia Latex for Asphalt (LOMAR): Designed for road construction, this latex enhances asphalt flexibility and water resistance while minimizing ammonia emissions and handling risks.
3. Ultra-Low Ammonia Latex for Foam (ParaFIT): Engineered for latex foam production, it delivers consistent foaming behavior, softness, and workplace safety.
4. BeThEPS – Fresh Latex Stabilizer: A solution for smallholder farmers to preserve fresh latex without ammonia, supporting efficient processing into high-quality sheet rubber.
5. OdorClearSTR20 – Odorless Coagulation for Cup-Lump Rubber: A low-odor coagulation system that improves working conditions and sensory quality of STR20 block rubber without compromising mechanical performance.

International Rubber Conference 2025 (IRC2025)
1-3 December 2025 @ BITEC, Bangkok, Thailand

Perspective on Dipped Rubber Product Biodegradability: MRB Research Highlights and Future Pathways

SHABINAH F. M. S.[1], AZIANA A. H.[1], NORHANIFAH M. Y.[1]

[1] *Technology and Engineering Division, Malaysian Rubber Board, 47000, Sungai Buloh, Selangor, Malaysia*

shabinah@lgm.gov.my

Keywords: Biodegradation, Natural rubber latex glove, Synthetic glove, Biodegradability, Waste management

Malaysia as one of the leading producer countries of dipped rubber products such as disposable non-medial gloves, balloons, and condoms faces growing environmental concerns linked to the disposal of rubber waste which ends up in landfills. This review draws on over two decades research by the Malaysian Rubber Board (MRB) to evaluate the biodegradability of these products through soil burial tests and to highlights the key factors that influence the biodegradation process. Through soil burial and controlled composting experiments, the degradation rates and mechanisms are analyzed based on changes in physical integrity, weight loss, surface morphology and microbial activity. Findings from these studies concluded that natural rubber exhibits appreciable biodegradability than synthetic rubber which is facilitated by various interrelated factors including environmental conditions, microbial activity, nutrient availability and sample surface area. Looking ahead, it is essential for all stakeholders in the dipped rubber products industry to align with global sustainability aspiration by advancing research on biodegradable formulations, applying biotechnological methods to improve degradation, promoting the use of natural rubber, and implementing eco-labelling for responsible product disposal. Future efforts may also involve developing standardized testing protocols and biodegradability standards, which could serve as a useful reference for enhancing sustainability practices across the rubber industry.

International Rubber Conference 2025 (IRC2025)
1-3 December 2025 @ BITEC, Bangkok, Thailand

Study of Biodegradation Efficiency of Natural Rubber Products by Various Microorganism

N. BOONYUEN[1], C. SURIYACHADKUN[1], P. KWANTONG[1], S. NUANKAEW[1], P. KANOKRATANA[1], C. CHUASEEHARONNACHAI[1], S. PATTANAWANIDCHAI[2], P. SAEOUI[2], T. LEEJARKPAI[2], V. CHAMPREDA[1], C. BOONMEE[1], S. LOYKULNANT[2]

[1] *National Center for Genetic Engineering and Biotechnology (BIOTEC), National Science and Technology Development Agency (NSTDA), Khlong Nueng, Khlong Luang, Pathum Thani 12120, Thailand.*

[2] *National Metal and Materials Technology Center (MTEC), National Science and Technology Development Agency (NSTDA), Khlong Nueng, Khlong Luang, Pathum Thani 12120, Thailand.*

Keywords: Natural rubber biodegradation, Actinomycetes, Microbial consortium, Latex-clearing protein (*Lcp*), FTIR/SEM/TGA, Composting, Circular economy

Natural rubber (NR) waste—gloves, sheets, and compounded products—poses a growing end-of-life challenge in Thailand and beyond. We investigated culture-dependent microbial solutions and enzyme pathways to accelerate NR biodegradation under ambient and thermophilic conditions. Environmental samples from plantations, compost and landfill sites were screened on MSM–latex media to isolate rubber degraders (bacteria, actinomycetes, fungi). Degradation performance was quantified by 1–2-month mass-loss assays using NR glove coupons (25–55 °C), with surface/chemical changes verified by SEM, FTIR (1,300–1,900 cm^{-1}) and TGA (30–900 °C). Top single strains—*Nocardia* sp. R20160, *Streptomyces* spp. ALD47/ALD38, and *Gordonia* sp. ABSL11-1—consistently outperformed legacy benchmarks, while thermotolerant candidates (*Thermomonospora curvata* CALD04; *Actinomadura* sp. CALD31) retained activity at 50–55 °C relevant to composting. A non-antagonistic 3-member consortium (R20160 + ALD38 + ALD47; "Formula 8") delivered the highest weight-loss at both 1 and 2 months, indicating complementary roles. Mechanistically, emergent FTIR C=O bands (≈1,700–1,740 cm^{-1}), SEM-observed cracking/pitting, and altered TGA profiles support oxidative chain scission. Heterologous expression and activity assays of latex-clearing protein (*Lcp*) corroborate an *Lcp*-initiated oxidation of cis-1,4-polyisoprene as a primary route. Collectively, these results establish (i) robust isolate resources preserved in national biobanks, (ii) a validated consortium strategy that surpasses single-strain performance, and (iii) an enzyme-level mechanism to guide bioaugmentation in compost/landfill settings. This work outlines a practical, low-carbon pathway for NR waste valorization consistent with circular-economy goals and provides a ready platform for pilot-scale demonstrations.

Background

Thailand is the world's leading producer of natural rubber; end-of-life rubber products (e.g., gloves, compounded sheets) are accumulating and difficult to treat using conventional landfill or incineration. We investigated culture-dependent microbial solutions and enzyme pathways to accelerate biodegradation of natural-rubber (NR) products and inform scalable end-of-life management.

Methods

Environmental samples (rubber plantations across 9 provinces, compost, landfill) were screened to isolate rubber-degrading microbes (bacteria, actinomycetes, fungi). Assays included: (i) clear-zone formation on MSM-latex agar; (ii) two-month mass-loss tests on NR glove coupons in liquid media at 25–55 °C; (iii) SEM for surface morphology; (iv) FTIR (1,300–1,900 cm^{-1}) and TGA (30–900 °C) for chemical/thermal changes; (v) antagonism tests to design non-inhibitory consortia; (vi) metagenomics of communities colonizing additive-containing NR; and (vii) cloning/expression and activity assays of latex-clearing protein (lcp) to confirm enzymatic oxidation of cis-1,4-polyisoprene.

Results

Isolates & top performers (25 °C, 2 months): Among 198 actinomycete isolates tested, four single strains consistently exceeded benchmarks (DRNA-75, TBRC 7106): *Nocardia* sp. R20160 (45.61% weight loss), Streptomyces sp. ALD47 (34.36%), *Streptomyces* sp. ALD38 (30.72%), and *Gordonia* sp. ABSL11-1 (30.42%). Thermotolerant candidates (50–55 °C): *Thermomonospora curvata* CALD04 (21.21%) and *Actinomadura* sp. CALD31 (8.18%) retained activity under elevated temperatures relevant to composting. Consortia outperform singles: A 3-member blend (R20160 + ALD38 + ALD47; "Formula 8") produced the highest mass-loss at both 1 and 2 months without mutual antagonism, indicating complementary degradation roles.

Mechanistic evidence: FTIR revealed emergent C=O bands (1,700–1,740 cm^{-1}) consistent with oxidative chain-scission to keto/aldehyde end-groups; SEM showed cracking, pitting, and perforations; TGA profiles indicated altered thermal stability after biodegradation—patterns stronger with consortia containing R20160.

Enzyme validation: Heterologous lcp expression (*E. coli* BL21) was confirmed by Western blot; plate and LC-MS assays detected oligo-isoprenoids characteristic of enzymatic oxidation of NR, supporting an *Lcp*-initiated pathway in our top isolates.

Resource outcomes: High-value strains have been preserved for research at national biobanks (TBRC/NBT), and experimental designs for controlled compost/landfill simulations are established for pilot-scale validation.

Conclusions

We provide bench-scale proof that carefully designed microbial consortia significantly accelerate NR product degradation versus single strains or legacy references. The combined evidence (mass loss, FTIR, SEM, TGA, and enzymology) indicates oxidative cleavage via Lcp-type pathways as a primary mechanism. These results outline a practical route to biologically assisted end-of-life treatment for NR waste under ambient and thermophilic conditions and create an isolate/enzyme foundation for field pilots and future bioaugmentation products.

Significance

This work advances microbial–enzymatic strategies for sustainable NR waste management, aligning with circular-economy goals while leveraging Thailand's bioresource strengths.

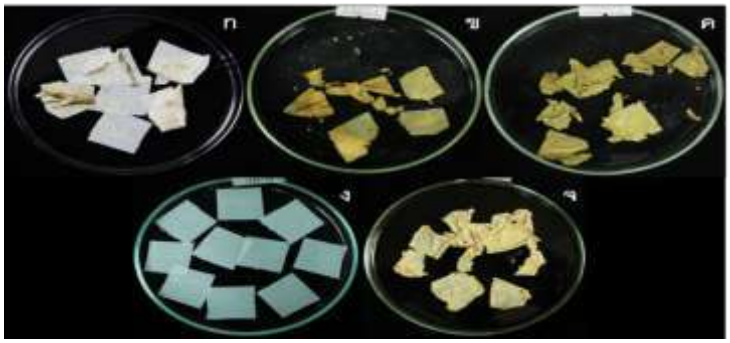


Figure 1. Rubber glove sheets after incubation with actinomycetes at T = 25 °C for 2 months: ก. ALD25 = 35.13%; ข. ALD37 = 34.22%; ค. ALD47 = 33.85%; ง. Control rubber glove sheet; จ. Rubber glove sheet incubated with strain DRNA 75 = 18.14%

International Rubber Conference 2025 (IRC2025)
1-3 December 2025 @ BITEC, Bangkok, Thailand

Reducing Extractable Protein in Latex Gloves to Lower Latex Allergy: Evidence from Thailand and International Studies

N. CHAIEAR[1]

[1] *Faculty of Medicine, Khon Kaen University, Khon Kaen, Thailand.*

Keywords: Latex allergy, Extractable protein, Powder-free gloves, Latex-specific IgE, Healthcare workers, Occupational health, Thailand, LMICs, Type I hypersensitivity.

Background:
Latex gloves produced from natural-rubber latex (NRL) remain indispensable in healthcare infection control yet are recognized as an important cause of Type I hypersensitivity mediated by allergenic Hev b proteins. Early reports in the 1990s documented sensitization rates of up to 10–17% among healthcare workers (HCWs) in hospitals that used powdered, high-protein gloves (Yunginger et al., 1994; Tarlo et al., 1997). Since then, global strategies—particularly the transition to powder-free and low-protein manufacturing—have sharply reduced prevalence. However, latex-free alternatives (e.g., nitrile or neoprene gloves) are substantially more expensive, limiting adoption in low- and middle-income countries (LMICs). A feasible and cost-effective approach in such settings is to reduce extractable protein content in NRL gloves to below 200 µg/g, as defined by EN 455-3 and ASTM D5712 standards. Accumulating Thai and international data now confirm that reducing extractable protein can markedly lower both clinical latex allergy and latex-specific immunoglobulin E (IgE)sensitization.

Objective:
This synthesis aims to summarize national and international evidence—focusing on Thai hospital-based studies—demonstrating that lowering extractable-protein concentrations in NRL gloves reduces the incidence and severity of latex allergy. It consolidates findings from (1) cross-sectional analytical research on Thai hospital personnel and (2) global studies comparing glove protein content with serologic and clinical outcomes.

Methods:
The key Thai investigation, a cross-sectional study among 646 hospital staff, stratified participants by glove exposure: (1) low-extractable-protein (<200 µg/g) gloves and (2) high-extractable-protein (≥200 µg/g) gloves. Latex sensitization was assessed using serum latex-specific IgE measured by ImmunoCAP (cut-off ≥0.35 kUA/L). Clinical allergy symptoms—including urticaria, angioedema, and respiratory irritation—were evaluated by validated self-administered questionnaires. Statistical analyses included comparison of geometric means, medians, and odds ratios (ORs ± 95% CIs). Supporting literature was retrieved from PubMed and WHO/ILO repositories, emphasizing controlled studies evaluating glove protein content and allergic outcomes.

Results (Thailand):
The response rate was 95% (323 per group). Latex-specific IgE positivity did not differ significantly between low- and high-protein groups (2.8% vs 3.1%; OR 0.90, 95% CI 0.35–2.29). Nevertheless, quantitative sensitization intensity was clearly protein-dependent: geometric mean IgE = 1.61 kUA/L (high-protein) vs 0.78 kUA/L (low-protein); p = 0.053. Median IgE = 1.49 kUA/L vs 0.68 kUA/L (p < 0.001). Clinically, current latex-allergy symptoms occurred significantly more often among high-protein-glove users (OR 2.60, 95% CI 1.36–5.22). After multivariable adjustment, high extractable

protein remained an independent predictor of urticaria and angioedema (adjusted OR 2.19, 95% CI 1.04–4.02). Among HCWs without prior inflammatory dermatitis, the association strengthened (adjusted OR 3.48, 95% CI 1.88–9.96). Personal factors—particularly atopic disease (adjusted OR 2.18, 95% CI 1.11–4.75) and hand dermatitis (adjusted OR 2.66, 95% CI 1.27–5.57)—further increased susceptibility.

Complementary Thai Evidence:
Ngamchokwathana et al. (2024) evaluated glove protein levels <50 µg/g and observed that replacing powdered gloves with powder-free, low-protein versions reduced symptomatic latex allergy from 9.8% to 1.2% (adjusted OR 0.18, 95% CI 0.04–0.86). Luengtongkam et al. (2025) reported similar trends across multiple hospitals: high-protein glove exposure (≥200 µg/g) increased odds of probable latex allergy (AOR 2.21; 95% CI 1.08–4.58), and powdered glove use conferred an AOR 2.31 (95% CI 1.61–8.71). Both studies identified atopy and prior hand eczema as consistent cofactors. These results echo the earlier decline in Thai sensitization prevalence—from 8–12% in the 1990s to <3% after national adoption of powder-free, low-protein gloves around 2018.

International Evidence:
Globally, similar reductions have been confirmed. In Finland and Germany, mandatory introduction of gloves <50 µg/g protein content reduced sensitization among nurses from 10% to 1–2% within five years (Holme et al., 2000). In the United States, after NIOSH and FDA issued powder-free-glove advisories in 1997, the prevalence of latex-specific IgE among HCWs fell from 12.1% to 4.3% (Kelly et al., 2019). Singapore's national surveillance similarly documented a 70% reduction in occupational latex allergy cases once high-protein gloves were eliminated. Across all studies, a clear dose–response relationship emerges: every 50–100 µg/g increment in extractable protein corresponds to a proportional rise in symptomatic reactions.

Mechanistic Insights:
Allergenic proteins such as Hev b 1, Hev b 3, Hev b 5, and Hev b 6.02 are water-soluble and can leach from gloves onto the skin or aerosolize via powder. Reducing extractable protein through improved leaching, multiple rinses, and powder elimination minimizes dermal and inhalational exposure. Powder also acts as an airborne carrier; its removal greatly decreases allergen dispersion. While IgE titers may persist in previously sensitized individuals, the reduction in clinical reactions reflects lower antigenic load and decreased exposure frequency.

Discussion:
Evidence from Thailand provides one of the clearest demonstrations that technological modification—rather than complete latex substitution—can yield meaningful risk reduction. The studies' consistent adjusted ORs ≈2–3 for high-protein exposure and ≈0.2 for low-protein use signify strong protective effect sizes. The near-identical findings across Thai, European, and U.S. datasets underscore generalizability. Importantly, clinical improvement often precedes measurable declines in IgE positivity, suggesting that lowering extractable protein suppresses symptom expression even if immunologic sensitization remains detectable. These results support WHO's recommendation to prioritize engineering controls at the manufacturing stage—namely multi-stage leaching and post-washing—before resorting to costly latex-free transitions.

From a health-policy standpoint, low-protein, powder-free gloves (<50–200 µg/g) represent an achievable standard for LMICs, balancing safety and affordability. Thai experience demonstrates successful nationwide procurement reform through the Ministry of Public Health and hospital-level

initiatives such as Srinagarind Hospital's Personnel Safety Goals: SIMPLE Thailand 2018. By 2024, reports to the Workmen's Compensation Fund indicated a >60% drop in compensated latex-allergy claims among HCWs.

Conclusions:

Reducing extractable protein levels in NRL gloves—particularly when combined with powder elimination—substantially lowers both clinical latex allergy and latex-specific IgE sensitization. High-protein gloves (≥200 μg/g) remain a significant independent risk factor for urticaria and angioedema, especially among atopic or dermatitis-prone personnel. Evidence from Thailand and corroborating international studies demonstrates that this simple manufacturing improvement achieves a 70–90% reduction in allergic morbidity without sacrificing barrier performance. In resource-limited healthcare systems, prioritizing low-protein, powder-free latex gloves is therefore an effective, sustainable, and equitable strategy for preventing occupational latex allergy.

References

1. Luengtongkam C, *Assoc. between extractable protein levels in natural rubber latex gloves and latex sensitization among hospital personnel*, Khon Kaen Univ., 2025.
2. Ngamchokwathana C, et al., *J Occup Med Toxicol*., 2024;19:27.
3. Luengtongkam C, et al., *J Med Health Sci*., 2025;32(2):115-127.
4. Yunginger JW, et al., *N Engl J Med*., 1994;331:1601-1605.
5. Tarlo SM, et al., *J Allergy Clin Immunol*., 1997;99(3):495-501.
6. Kelly K, et al., *Ann Allergy Asthma Immunol*., 2019;122(2):123-129.
7. Holme SA, et al., *Occup Environ Med*., 2000;57:301-306.
8. WHO. *Latex Allergy and the Health-Care Sector: Global Review.*, Geneva, 2023.

From Allergen to Assurance: A Comprehensive Review of Natural Rubber Product Safety and MRB's Strategic Role

AZIANA A. H.[1], NURULHUDA A. A.[1]

[1] *Technology and Engineering Division, Malaysian Rubber Board, 47000, Sungai Buloh, Selangor, Malaysia.*

aziana@lgm.gov.my

As the demand for latex-based consumer and medical products rises globally, it is more crucial than ever to ensure the safety of natural rubber (NR) latex products. NR latex products have historically raised safety concerns due to allergenic proteins and chemical residues. A proactive approach to ensuring the safety of NR latex products must start at the manufacturing stage, where early intervention is essential to mitigate potential health and environmental risks posed by the materials and chemicals employed in production. While technological advancements and continuous monitoring have significantly assisted in managing the incidence of Type I (IgE-mediated) latex allergies, the recent shift towards non-NR latex has redirected attention toward addressing the growing concern of Type IV hypersensitivity reactions. Additionally, the inherent properties of certain polymer materials may induce cross-reactive responses in sensitized individuals, further complicating safety considerations. This review presents a comprehensive assessment of NR product safety across its entire lifecycle, encompassing evaluations of cytotoxicity, allergenicity, microbiological safety, barrier integrity, environmental and occupational safety, as well as clinical and regulatory compliance. These aspects are critical for addressing the evolving health and safety challenges associated with both NR and non-NR latex products. It also outlines the crucial role of the Malaysian Rubber Board (MRB) in strategically contributing through technological development and regulatory measures such as the Standard Malaysian Glove (SMG) scheme and *Lesen Mengeksport Sarung Tangan Getah* (LMSTG) license which demonstrates Malaysia's commitment to ensure that NR products are safe for customers and meet international safety standards.

Pioneering a Sustainable Biorefinery of Natural Rubber Serum for New Bioactives in Cosmetics, Food, Nutraceuticals, and Pharmaceuticals

T. PITAKPORNPREECHA[1]

[1] *Center of Excellence in Natural Rubber Latex Biotechnology Research and Development (CERB), division of Health and Applied Science (Biochemistry), Faculty of Science, Prince of Songkla University, Hat-yai, Songkhla, 90110, Thailand.*

Keywords: Natural rubber serum, Bioactive compounds, Novel food, Biorefinery, Novel rubber industrial chain, BCG, SDGs

Natural rubber serum, comprising 60–70% of natural latex, has long been overlooked as industrial waste despite its richness in biomolecules such as proteins, enzymes, and carbohydrates. In Thailand, over one billion liters are discarded annually, posing significant environmental and economic challenges. Because rubber trees are tapped daily, repeated wounding activates defense mechanisms that lead to the synthesis of diverse bioactive phytochemicals essential for the trees' survival. Recognizing this untapped potential, the Center of Excellence in Natural Rubber Latex Biotechnology Research and Development (CERB) has redefined this waste stream through a pioneering Bio-Circular-Green (BCG) biorefinery model. This initiative transforms natural rubber serum into a sustainable source of high-value bioactive compounds, opening new frontiers in biotechnology and promoting circular innovation across the cosmetics, food, nutraceutical, and pharmaceutical industries (fig.1).

Through extensive research, CERB has developed innovative industrial processes that utilize serum-derived components as enzyme sources for producing bioactive oligosaccharides such as β-glucan oligosaccharides (BGOs) or hydrolyzed yeast β-glucan (HBGs) [1]. The team has also achieved industrial-scale extraction of a novel bioactive compound, Hevea latex polysaccharides (HeLP) [2–3]. Both BGOs and HeLP are currently undergoing novel food registration with Thailand's Food and Drug Administration (FDA). Additionally, the production processes yield other valuable by-products, including quebrachitol and proteins. These bioactives—BGOs, HeLP, and quebrachitol—exhibit a wide range of biological activities, including anti-wrinkle, wound-healing, anti-inflammatory, immunomodulatory, anti-cancer, anti-ulcer, anti-diabetic, and prebiotic effects, while latex serum proteins show strong potential as future plant-based protein sources.

To enable commercial-scale production, the first biorefinery factory dedicated to natural rubber serum is being established at the Southern Industrial Estate by Innozus Co., Ltd. This facility will produce all aforementioned compounds for applications across multiple sectors, including cosmetics, future foods, functional foods, dietary supplements, and pharmaceuticals. This initiative delivers substantial environmental, economic, and social benefits by reducing pollution, lowering waste management costs, and increaseing the value of latex and serum. Furthermore, it strengthens Thailand's biorefinery sector by converting agricultural and biological resources into high-value bioproducts. Aligned with the principles of the BCG Economy model, this initiative promotes sustainable economic growth, equitable income distribution, and regenerative resource utilization—ultimately transforming rubber latex by-products into innovative, high-value biomaterials that contribute to achieving the United Nations Sustainable Development Goals (SDGs).

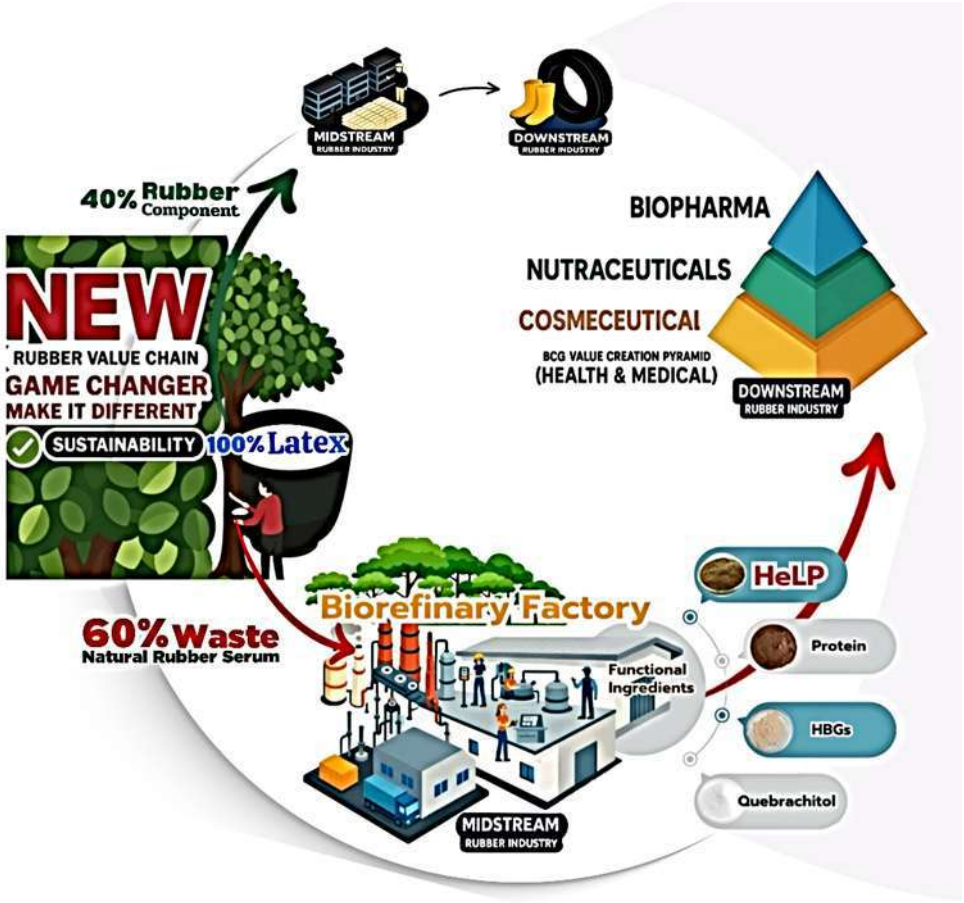


Figure 1. Novel rubber industrial chain

References

1. Pitakpornpreecha T. *Biotechnological process for preparing hydrolyzed yeast beta-glucan by using enzyme cocktail derived from waste liquid in the rubber, manufacturing industry*. Thai Patent Application No. 2501003472A. 2025. Department of Intellectual Property, Bangkok, Thailand.
2. Pitakpornpreecha T. *Process for extracting Hevea latex polysaccharides from effluent of the rubber manufacturing industry, polysaccharide extract, composition and use thereof.* Thai Patent Application No. 2101006111A. 2021. Department of Intellectual Property, Bangkok, Thailand.
3. Pitakpornpreecha T. *Process for extracting Hevea latex polysaccharides from effluent of the rubber manufacturing industry, polysaccharide extract, composition and use thereof.* International Patent Application No. PCT/TH2022/050007. 2023. World Intellectual Property Organization (WIPO).

International Rubber Conference 2025 (IRC2025)
1-3 December 2025 @ BITEC, Bangkok, Thailand

Utilizing Natural Rubber Seeds for Biorefinery

K. KAWATANI[1], J. PHOJAROEN2AUTHORC[2]

[1] *9-10F 3-2-123 Umeda Kita-Ku Osaka-City Osaka 530-0001, Japan.*

[2] *Thailand Institute of Scientific and Technological Research (TISTR) 35 Moo 3 Techno Thani, Khlong 5, Khlong Luang, Pathum Thani 12120, Thailand.*

koryu@innovare.world

Keywords: Natural Rubber Seeds, Rubber Seed Oil, Biochar, Lignin

Innovare Co., Ltd explores the comprehensive utilization of natural rubber seeds (RS). RS is an underutilized byproduct of the rubber plantation through a biorefinery approach to support carbon neutrality and sustainable innovation. The primary goal is to transform RS into valuable products such as biofuels, biochar, activated carbon, and biogas, thereby advancing circular economy models within the ASEAN region.

Previous studies highlight the potential of rubber seed oil (RSO) for second-generation biodiesel production, offering a sustainable alternative to edible oil-based biofuels [2,3]. Research on rubber seed kernel (RSK) residues emphasizes their high protein content and suitability for animal feed [1], while rubber seed shell (RSS) has been identified as a promising feedstock for biochar and lignin-derived materials [4,5]. Collectively, these findings establish RS as a versatile feedstock for biorefinery applications that address environmental and economic sustainability.

RS from Thai plantations was separated into RSK and RSS via a cracking machine. RSO was extracted via mechanical screw pressing (Figure 1), avoiding solvent-based contamination. The oil composition and fatty acid profile were analyzed, revealing high levels of unsaturated fatty acids suitable for biodiesel synthesis via transesterification. RSS was characterized by its high lignin content (44%), enabling conversion through pyrolysis into biochar and bio-oil, as well as pretreatment processes for lignin extraction.

In 2025, Innovare successfully secured the first lot of RS from a Thai rubber plantation, totaling approximately 8–9 tons. We have also set up the pre-pilot testing for the separation of RSS and RSK, RSO extraction, and lignin production. Furthermore, Innovare is actively considering a biochar production project from RSS. Collectively, this integrated process minimizes waste, enhances resource efficiency, and directly aligns with net-zero emission goals.

Innovare demonstrates that natural rubber seeds can serve as a sustainable and versatile feedstock within a biorefinery framework, producing renewable fuels and high-value materials. This approach supports carbon sequestration, waste minimization, and the circular economy in the rubber sector. Limitations include the need for scale-up studies, economic feasibility assessments, and optimization of pretreatment methods. Future research should focus on integrated process modeling, techno-economic analysis, and commercial pilot-scale implementation to validate industrial applicability.



Figure 1. Mechanical screw pressing machine

Acknowledgement

In advancing this initiative, Innovare. has been supported and assisted by its shareholders, the Japan Startup Support Association and the Ritsumeikan Social Impact Fund, as well as the Thailand Institute of Scientific and Technological Research, local government agencies across Thailand, and local partner organizations, including natural rubber plantation farmers. We hereby express our deepest gratitude to all these stakeholders.

References

1. Yang M, Zhu W, Cao H. *Biorefinery of Rubber Seed Kernels for Comprehensive Utilisation*. 2020.
2. Das S, Reshad AS, Bhuyan N, Sut D, Tiwari P, Goud Vv, Kataki R. Utilization of nonedible oilseeds in a biorefinery approach with special emphasis on rubber seeds. In: *Waste Biorefinery: Integrating Biorefineries for Waste Valorisation*. Elsevier; 2020. p. 311-336
3. Martin MA. First generation biofuels compete. *New Biotechnology*. 2010;27(5):596-608
4. Osagiede CA, Aisien FA. Rubber Seed Shell Biochar Sulphonation: A Process Optimization and Conditions' Effect Analysis. *J Energy Technol Environ.* 2022;4(2):2022–2134.
5. Hanis N, Latif A, Brosse N, Ziegler-Devin I, Chrusiel L, Hashim R, Hussin MH. A Comparision of Alkaline and Organosolv Lignin Extraction Methods from Coconut Husks as an Alternative Material for Green Applications. *BioResources*. 2022;17(1):469-491

Modified Natural Rubber: Current Progress and Challenges in Malaysia

K. V. BARATHA NESAN[1], N. H. YUSOF[1], S. IBRAHIM[1]

[1] *Advancement and Innovation of Speciality Material Unit, Technology and Engineering Division,*

RRIM Research Station, Malaysian Rubber Board (MRB), Sungai Buloh, Malaysia

krishnaveni@lgm.gov.my

Natural rubber (NR) from *Hevea brasiliensis* is a renewable polymer known for its excellent elasticity, resilience, and mechanical strength. However, its high unsaturation and non-polar nature limit its performance in applications requiring oil resistance, weathering stability, and flame retardancy. To address these limitations, the Malaysian Rubber Board (MRB) has carried out extensive research on chemical and physical modification of NR to enhance its properties and broaden its applications in the tyre, non-tyre, and latex sectors.

Physical modification focuses on reducing non-rubber constituents; mainly proteins to produce deproteinized natural rubber (DPNR), which offers improved stability and lower allergenicity. Chemical modification introduces functional groups through routes such as epoxidation, depolymerisation, and graft copolymerisation.

Epoxidized natural rubber grades like ENR-25 and ENR-50 deliver superior oil resistance and polarity compatibility. Liquid epoxidized NR (LENR), obtained through controlled degradation, provides reactive functionalities ideal for adhesives, coatings, and polyurethanes. DPNR produced via enzymatic or chemical processes supports high-purity medical and dynamic applications. Methyl methacrylate (MMA)-modified NR latex offers improved tensile strength and solvent resistance, while hydroxyl-telechelic NR (HTNR) enhances processing, adhesion, and crosslinking, making it a valuable precursor for polyurethanes and other functional elastomers.

The innovative use of modified NR spans both tyre and non-tyre applications, yielding notable gains in performance, sustainability, and product versatility. In the tyre sector, green rubber technologies have enabled retreads, passenger car, motorcycle, and solid tyres with up to 40% higher mileage, 25% lower rolling resistance, and fuel savings of about 5%. These improvements contribute to reduced CO2 emissions and better grip, handling, noise control, and safety. Beyond tyres, modified NR supports diverse latex-based products including sound insulators, road bumps, modular floor mats, and high-performance footwear, all offering enhanced durability, recyclability, and comfort. Additional applications such as memory foam, natural adhesives, artwork paints, and non-toxic interior/exterior coatings further highlight NR’s versatility as a safe and eco-friendly material.

Overall, these advancements reflect MRB’s ongoing commitment to transforming natural rubber into sustainable, high-value materials for a wide range of industries. Through targeted chemical modification, NR’s inherent limitations have been effectively addressed, expanding its role in automotive, adhesive, coating, and specialty markets. Modified NR products such as ENR, DPNR, LENR, MMA-modified NR, and HTNR strengthen Malaysia’s competitiveness while supporting the nation’s green and circular economy goals. Future efforts at MRB continue to prioritise formulation optimisation, production scaling, and the exploration of new functional modifications to further elevate NR’s industrial and environmental potential.

International Rubber Conference 2025 (IRC2025)
1-3 December 2025 @ BITEC, Bangkok, Thailand

Challenges for the Future of Natural Rubber Latex and NRL Products, and Its Oppourtunities

AMIR HASHIM M.Y.[1], TAN C.Y., NOR AKILAH SAIDIN, FELIX DARREL

[1] *MARGMA Technical Sub Committee*

The future of natural rubber (NR) latex as a material for examination gloves is characterized by both opportunity and challenge. While NR latex remains valued for its superior tactile sensitivity, comfort, and biodegradability, it faces strong competition from synthetic alternatives—particularly nitrile—that offer enhanced chemical and puncture resistance. Despite declining demand in general medical applications due to latex allergy concerns, NR latex continues to maintain relevance in niche markets that require exceptional dexterity, such as surgical and dental procedures. Ongoing innovations, including hypoallergenic formulations, improved barrier coatings, and sustainability-focused manufacturing, aim to mitigate its weaknesses and reinforce its environmental advantages. Moving forward, the examination glove market is expected to evolve into a dual-material ecosystem, where NR latex and synthetic gloves coexistence serving distinct performance and sustainability priorities.

The presentation shall elaborate on the subject and demonstrated some of the key areas for R&D and challenges to ensure the sustainability of NR Latex as the preferred material for examination gloves.

International Rubber Conference 2025 (IRC2025)
1-3 December 2025 @ BITEC, Bangkok, Thailand

Challenges and Opportunities for Future Applications of Natural Rubber

B. JUNHASAVASDIKUL[1]

[1] *Chairman of Innovation Group, Innovation Group (Thailand) Ltd., Bangkok 10240, Thailand*

Natural rubber (NR) is the first polymer of mankind from Amazon rainforest to become a miracle material that hardly replaced by other materials. Rubber plantation was considered as the cause of deforestation, biodiversity loss and environmental pollution. With the Good Agricultural Practice (GAP) in managing natural rubber plantation, now-a-day, natural rubber plantation becomes a green and environmental friendly green forest that absorbs carbon dioxide and releasing oxygen. Natural rubber is a source of income of million Thai small families. However, natural rubber is a natural polymer producing from photosynthesis, quantity and quality of natural rubber varies from clone of rubber tree, season, and area of plantation and method of tapping, transportation and process. Engineering and process diversification in quality management is applying in this total supply chain of NR starting from rubber plantation, latex tapping, transportation and rubber processing to produce good quality and consistent quality of NR that meet requirements of industry. Good Agricultural Practice (GAP) and Good Manufacturing Practice (GMP) are applied in Thai natural rubber to obtain good quality of natural rubber that meets requirements of users. Meanwhile, there are many trade regulations coming out from European countries, e.g., EUDR, FSC, PEFC, and CBAM in controlling trade and usage of NR supplying to European countries. This requires support and cooperative from government authorization, related to natural rubber, working with total supply of natural rubber to meet these international regulations.

Because of it's excellent in mechanical and physical properties, natural rubber is consumed almost half of the total rubber consumption at 15 million metric tons per year. More- ever, natural rubber is consider as a natural green polymer from natural resource, bio-degradable and carbon footprint or greenhouse gas (GHG) emission, many applications using synthetic rubber will be convert more and more to natural rubber. Besides the latex, many researchers found out that seed of rubber tree contain Omega 3 and oil of the seed has high value as fuel for air crafts.

End of life of natural rubber product which was considered as hazardous wastes. De-linking process has been developing for industrial recycling and post-consumer recycling to produce value products. Pyrolysis is the solution of huge quantity of used tire. Pyrolysis process in used tire produces useful green carbon black and processing oil for further rubber processing.

Concept Product/Market Development

Three key factors to make product and market development success are:

Value-Creation
Product Performance
Cost

In case of natural rubber, it has it value as Green polymer and customer can gain carbon credit in converting from synthetic rubber to use natural rubber. However, end-product using natural rubber must prove to meet end-use product performance. Other important factor which critical in development success is the cost the meet customer or end-user requirement.

Researches & Developments od natural rubber at Innovation Group

As the world is moving toward social sustainability and looking for low carbon dioxide emission products. Innovation Group is promoting as a green polymer that comes from natural source, biodegradable and reduces carbon footprint or greenhouse gas (GHG) emissions. Technical developments and innovations have been developed in total value chain of natural rubber to produce natural rubber that serve industrial requirements, develop natural rubber to replace synthetic rubber either partially or fully replacement synthetic rubber. Many innovative products have been developed using natural rubber.

- Innovation Group is working with Rubber Authority of Thailand in promoting GAP/GMP along the supply chain in producing quality natural rubber. We emphasize no hazardous chemical allow in GAP process. method and time in tapping to gain higher yield. Latex must be filtered to avoid contamination before deliver to factory. We also emphasize using formic acid only in the coagulation process.
- Ammonia is added into the concentrate natural latex as a preserve chemical. In the dipping goods factory, Ammonia has to remove out from the latex before the process. Ultra-low Ammonia natural latex was developed. This is for the benefit for the dipping goods process to improve the processing environment and saving time to remove ammonia from natural latex before the process.
- Ultra-low ammonia natural rubber latex has been developed in producing 'Green ABS' by replacing butadiene with natural rubber. Percentages of natural rubber in ANRS can be varied to give different properties of 'Green ANRS'.
- Ultra-low protein or non-allergic protein natural rubber have been developed by using single centrifuging or double centrifuging process for latex using in producing latex glove and sporting goods to prevent protein allergy of the users.
- Process development at the natural rubber factory to produce to produce very clean natural rubber with low Lovibon. Clean and low Lovibon natural rubber has been developed to replace synthetic rubber in making solvent glue for medical tape and also using as a resin in can coating.
- Clear natural rubber solvent glue is also used in making tennis ball.
- Because of good bouncing properties of natural rubber and as a green polymer, Innovation Group worked with valley ball manufacturer to replace inner tube of valley ball, used butyl rubber to natural rubber.
- Many developments have been carried on using NR to replace, either partially or fully replace synthetic rubber (SR).
    - Innovation Group worked with car part makers, replacing 40% EPDM has been replaced by natural rubber in weathering strip application and automotive parts.
    - Replace TPE in children toys.
    - Replace EPDM in TPV with NR, NR-TPV is eco-friendly thermoplastic recyclable resin.
- Because natural rubber is in bulk form, the mixing process has to be done in the internal mixer. Within the internal mixer, natural rubber had to be well mixed and dispersing with curing agent. Temperature at the mixing chamber had been hold constantly for the reaction of rubber curing been happened. Then thermoplastic (Polypropylene) was discharged into the chamber. Properties of NR-TPV can be varied by ration of natural rubber and thermoplastic.

- Because of the requirement of environmental friendly products, people in sporting goods are looking for natural rubber to replace synthetic polymers. Natural rubber to replace synthetic rubber (chloroprene) in making wet-suit. Besides of gaining carbon credit, the other benefit to change from chloroprene rubber to natural rubber is the cost advantage.
- In tire application, development of "Green Tire" Epoxidized natural rubber has its potential and it is the new field of natural rubber development of Innovation Group. Introducing epoxy group into natural rubber changes chemical and mechanical properties of natural rubber. Low epoxy group natural rubber (8-10%) and high epoxizide natural rubber (20%) is developing at research lab of Innovation Group and being introduced as polar natural rubber.
    - Party replaces Ethylene Vinyl Acetate (EVA) in making out-sole foam in sporting shoe. 8% of epoxidize natural rubber can replace almost half of EVA in high quality out-sole foam without scarified physical and mechanical properties of out-sole foam with the cost benefit.
    - Innovation Group is working with tire manufacturers in 8% epoxizize natural rubber and 20% epoxized natural rubber 8% epoxizide natural rubber is developing as a polar polymer, enhance the dispersion capability of silica dioxide to natural rubber in the mixing process of tire compound. 20% epoxidize natural rubber gives good wet-grip properties in "Green Tire" Development is working toward to replacing or party replace SSBR with 20% epoxidize natural rubber.

Conclusion

"Natural rubber is a natural green polymer that meets the world sustainable requirement. However, Technical development and innovation have to implement along the total value chain of NR in developing its values"

Poster Presentations

IRC 2025
BANGKOK, THAILAND

International Rubber Conference 2025 (IRC 2025)

Session I : Natural Rubber, Bio-based Rubbers and Rubber Chemicals

Poster Presentations

International Rubber Conference 2025 (IRC2025)
1-3 December 2025 @ BITEC, Bangkok, Thailand

Design and molecular dynamics simulation of Biomass Ion-conductive elastomer

Jiajun Qu[1], Liqun Zhang[1,2], Jun Liu[1]

[1]*State Key Laboratory of Organic-Inorganic Composites, Beijing University of Chemical Technology, Beijing 100029, China*
[2]*Xi'an Jiaotong University, Xi'an, China*

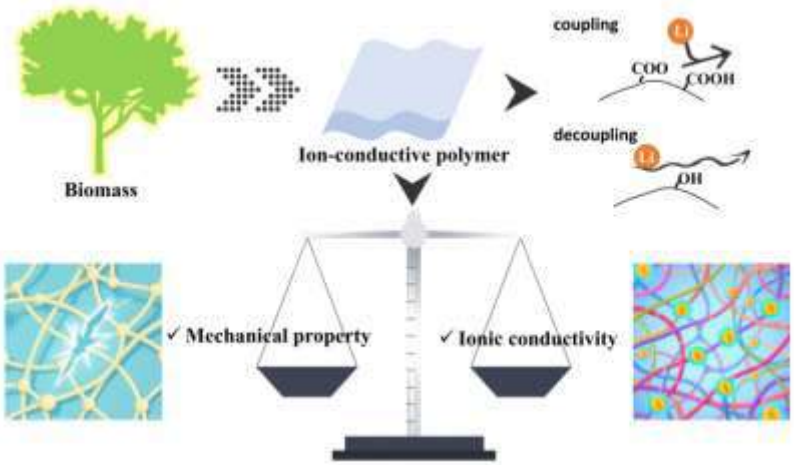
E-mail address of the presenting author: 18903452162@163.com

Abstract

As an eco-friendly alternative to traditional petroleum-based polymers, bio-based ion-conductive elastomers derived from unsaturated biomass acids exhibit tremendous potential. In this work, all-atom molecular dynamics (MD) simulations were employed to investigate the structure-property relationships of ferulate-based ion-conductive elastomers. The systems were constructed from polymer chains randomly copolymerized by ferulic acid, ethylene glycol acrylate, and ethylene units, incorporated with lithium bis(trifluoromethanesulfonyl)imide (LiTFSI) at different mass fractions. Lithium ions (Li^+) coordinates primarily with oxygen atoms from ester, carboxyl, and hydroxyl groups, maintaining stable local coordination despite lithium salt concentration variations. The study uncovers two conduction modes: direct Li^+ hopping via decoupling from -COO-/-COOH groups and coupled conduction with -OH groups in polymer segments. Ionic conductivity exhibits a non-monotonic trend, optimized via the synergy between carrier density and mobility. Mechanical properties of the systems were systematically characterized via diverse approaches, including uniaxial tension, tension-recovery, shear deformation, and fracture-healing tests. After that, the design parameters (lithium salt content and molar fraction of monomers) were extended as input features, and the electrical conductivity and mechanical properties were used as label values. A machine learning study was conducted using a Gaussian Process Regression (GPR) model to summarize the parameter design directions for enhancing the performance. Multi-objective optimization maps the parameter space for peak performance, forecasting an ionic conductivity of 6.13×10^{-4} $S\cdot cm^{-1}$ alongside a Young's modulus of 104.1 MPa, which is superior to many existing bio-based ion conductors. This work establishes a data-driven design framework integrating MD with GPR to balance ionic transport and mechanical stability, paving the way for the development of bio-based ion-conductive elastomers in the field of intelligent flexibility.

Keywords: Biomass, Ion-conductive elastomer, Molecular Dynamics

TOC graphics:



Acknowledgments

We acknowledge the National Science Fund for Excellent Young Scholars (52122311) and the National Natural Science Foundation of China (52373222). The super-calculation center of “Tianhe number two” and the cloud calculation platform of Beijing University of Chemical Technology (BUCT) are both greatly appreciated.

International Rubber Conference 2025 (IRC2025)
1-3 December 2025 @ BITEC, Bangkok, Thailand

Wide-angle X-ray diffraction studies on thermal melting behavior of crystallites formed by planar elongation of vulcanized natural rubber

Shoei Okamoto[1], Hiroto Okumura[1], Maho Nakada[1], Shinichi Yagi[1], Huaizhong Xu[1],

Hiroyasu Masunaga[2], Hideaki Takagi[3], Noriyuki Igarashi[3], Yuji Kitamura[4], Katsuhiko Tsunoda[4],

Kenji Urayama[5], and Shinichi Sakurai[1]

[1]*Department of Biobased Materials Science Kyoto Institute of Technology, Kyoto 606-8585, Japan*

[2]*Japan Synchrotron Radiation Research Institute, Sayo-gun, Hyogo 679-5198, Japan*

[3]*High Energy Accelerator Research Organization, Oho, Tsukuba, Ibaraki, 305-0801, Japan*

[4]*Sustainable and Advanced Materials Division, Bridgestone Corporation, Ogawahigashi-cho 3-1-1, Kodaira Tokyo ,187-8531, Japan*

[5]*Department of Material Chemistry, Graduate School of Engineering, Kyoto University Nishikyo-ku, Kyoto 615-8510, Japan*

Email : shin@kit.ac.jp

Keyword: Natural rubber, Starin-induced crystallization, wide-angle X-ray diffraction, thermal melting

Natural rubber (NR) has the property of not fracturing, even when subjected to large deformation or instantaneous stress. The phenomenon of strain-induced crystallization (SIC), whereby NR toughens and crystallizes when stretched and strained, has been identified as a contributing factor to this ability. Since aircraft tires made of natural rubber are exposed to high temperatures due to friction when landing, it is important to understand the robustness of the crystallites formed by SIC at high temperatures. This study was aimed at investigating the thermal melting behaviors of crystallites formed by planar elongation by conducting wide-angle X-ray diffraction (WAXD) measurements at synchrotron radiation to analyze the lattice constants and crystallite size. Unlike uniaxial elongation, planar elongation is a deformation mode in which the specimen is strained so that it does not shrink from its initial length in the direction perpendicular to the elongation direction.

A cross-shaped vulcanized natural rubber (being vulcanized with 1.40 phr sulfur) was used as the specimen. Specifically, the specimen was planar stretched up to 5.8 times to generate crystallites at room temperature. The temperature of the stretched specimen was then gradually increased to 358 K at a constant heating rate of 1.95 K/min while X-rays were irradiated from the normal direction of the specimen to measure the 2D WAXD pattern. The specimen was kept in a constant state of stretching throughout the heating process. Measurements were performed at BL-10C at the Photon Factory of

the High Energy Accelerator Research Organization (KEK), with an X-ray wavelength of 0.1 nm, a camera length of 0.26 m, irradiation time 1 second, and a Pilatus3 2M detector was used as a detector.

The temperature dependence of *a*-axis length and *c*-axis length of the lattice constants calculated from the positions of the 200 and 201 plane reflection peaks, and those of the crystallite sizes L_{200} and L_{201} calculated from their peak widths are shown in Fig. 1. The *a*-axis length increased with increasing temperature, while the *c*-axis length decreased. This can be explained by the thermal expansion of the *a*-axis length due to the temperature increase and the contraction of the *c*-axis length due to the increase in thermal vibration of the molecular chains inside the crystal lattice. The crystallite size decreased with increasing temperature, but the decrease trend for L_{201} appears to be smaller than that for L_{200}. This suggests that the crystallite size in the *c*-axis direction did not decrease much. This is presumably due to the fact that the crystallites grew in the *c*-axis direction even during the heating process, as the stress increased in the elongation direction with the temperature rise. Such grain growth in the *c*-axis direction has been reported in our previous paper [1]. Another very interesting result of the crystallite size change during melting is that, as shown in Fig. 1 (the vertical dashed line indicates the melting point of 324.8 K, which is the temperature at which the 200 and 201 plane reflection peaks completely disappeared), the crystallites do not decrease to zero during melting, but reach a finite size. This suggests that the crystallites melted at once when they reached a finite size, rather than decreasing to zero during melting. Although this is the opposite to the case of crystal nucleation and growth during crystallization, it also suggests that the crystallites were destabilized when they decreased their size to the critical nucleus size and then melted instantaneously.

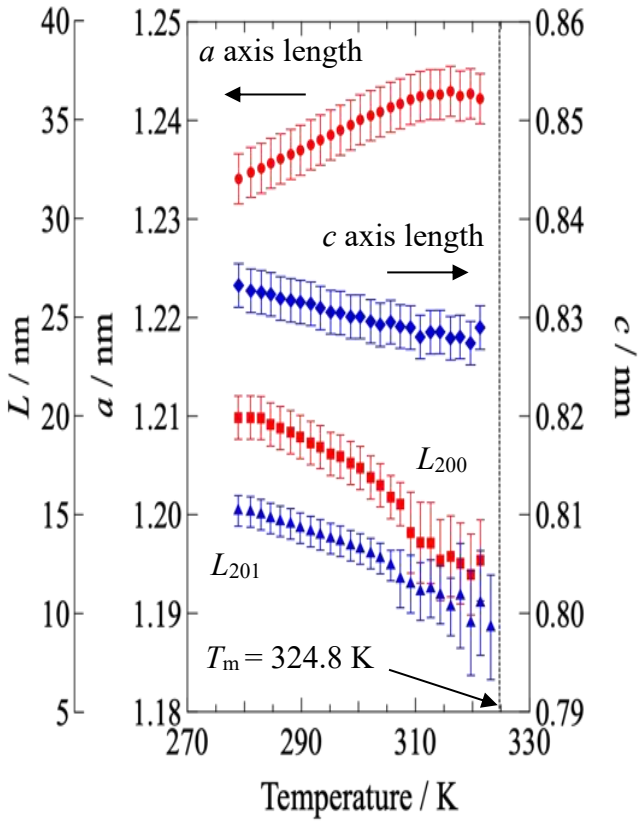


Fig.1 Temperature dependence of lattice constants (*a*, *c*) and crystallite size (L_{200}, L_{201})

Acknowledgement: This work was financially supported by JST CREST (Grant No. JPMJCR2091).

Reference: [1] Tanaka et. al., ACS Appl. Polym. Mater. 6, 5, 2799–2806 (2024)

International Rubber Conference 2025 (IRC2025)
1-3 December 2025 @ BITEC, Bangkok, Thailand

Strain-Induced Crystallization of Carbon Black-Reinforced Vulcanized Natural Rubber by Biaxial Elongation

Hiroto Okumura[1], Shoei Okamoto[1], Maho Nakada[1], Yuki Jotatsu[1], Shinichi Yagi[1], Huaizhong Xu[1], Yuji Kitamura[2], Katsuhiko Tsunoda[2], Hiroyasu Masunaga[3], Kenji Urayama[4] and Shinichi Sakurai[1]

[1]*Department of Biobased Materials Science, Kyoto Institute of Technology, Kyoto 606-8585, Japan.*

[2]*Sustainable and Advanced Materials Division, Bridgestone Corporation, Ogawahigashi-cho 3-1-1, Kodaira Tokyo, 187-8531, Japan.*

[3]*SPring-8, Japan Synchrotron Radiation Research Institute (JASRI), Kouto 1-1-1, Sayo-cho, Sayo-gun, Hyogo 679-5198, Japan.*

[4]*Department of Material Chemistry, Kyoto University, Kyoto 615- 8510, Japan.*

e-mail: shin@kit.ac.jp

Keywords: Natural Rubber, Carbon Black, Wide-Angle X-ray Diffraction, Strain-Induced Crystallization, Biaxial Elongation

Natural rubber (NR) possesses elastomeric properties and the ability to withstand momentary stress during large deformations without fracturing, making it widely utilized in various fields ranging from industrial applications to daily products. It is well known that strain-induced crystallization (SIC), a phenomenon whereby polymer chains align and crystallize when rubber is stretched, plays a critical role in exhibiting these properties. In vulcanized natural rubber, crystals formed through SIC have been reported to significantly increase tensile strength during uniaxial stretching. One common application of NR is in tires, where its strength is enhanced by incorporating fillers such as carbon black (CB). In such usage environments, the deformations experienced by tires are not simple uniaxial stretches but rather complex deformation modes, such as multiaxial stretching. Therefore, clarifying the correlation between SIC and mechanical strength under multiaxial stretching is crucial for improving tire performance. However, studies on the SIC behavior of NR under multiaxial stretching are currently limited. In this study, we investigated the SIC behavior of CB-reinforced NR during biaxial stretching with varying stretching speed ratios. This was achieved through simultaneous measurements using wide-angle X-ray diffraction.

The samples used in this study were vulcanized NR containing 50 phr of CB, prepared at Bridgestone Corporation. The vulcanization temperature and time were set at 160°C and 8 minutes, respectively, with 1.40 phr of sulfur. The raw materials, additives, and formulations used for the vulcanization process are summarized in Table 1, and the geometry of specimen is shown Fig. 1. Wide-angle X-ray diffraction (WAXD) measurements were performed at the BL03XU beamline of SPring-8 using a wavelength of 0.1 nm, a beam size of 0.3 mm in both vertical and horizontal directions, a camera length of 0.276 m, a Pilatus 2M detector, and an exposure time of 1 s with a 5 s

cycle. Additionally, biaxial stretching measurements were conducted by simultaneously varying the stretching speed ratio in the x and y directions.

This experiment involved stretching the specimen simultaneously in the horizontal (x-) and vertical (y-) directions while varying the stretching speed ratio, followed by contracting the specimen at the same speed to return it to its original state. The results revealed differences between the strain where crystallites formed by SIC were first observed during the stretching process and the strain where these crystallites disappeared during the contraction process. During the stretching process, diffraction peaks corresponding to crystallites formed by SIC appeared when the strain in the more stretched direction exceeded approximately 3.0 for the case of NR specimen without carbon black. On the other hand, during the contraction process, these diffraction peaks disappeared when the strain was more decreased to around 2.0–2.5. This hysteresis may indicate the requirement of supercooling even for the case of SIC. We compare the results quantitatively for the carbon black reinforced NR specimen.

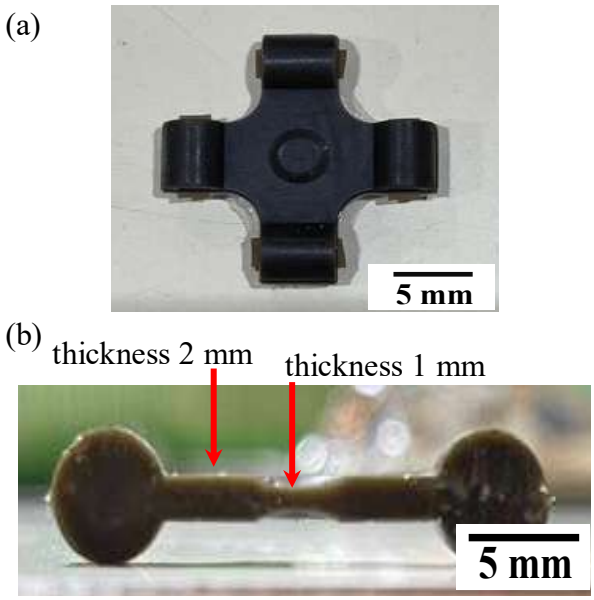


Fig.1. Cross-shaped natural rubber specimen for biaxial elongation.
(a) Top-view photo and(b) side-view photo

Table 1. Formulation of the specimen.
(g per 100 g of rubber)

Materials and additives	phr
Natural rubber	100
Carbon Black	50
Stearic Acid	2.00
Micro Crystalline Wax	2.00
Sulfur	1.40
Zinc oxide	2.22
N-1,3-Dimethylbutyl-*N*-phenyl-*p*-phenylenediamine(6PPD) (Anti Aging Agent)	1.00
Diphenyl guanidine (DPG) (Accelerator)	0.35
N-Cyclohey-2-benzothiazole sulfonamide (CBS) (Accelerator)	1.77

Acknowledgement

This work was financially supported by JST CREST (Grant No. JPMJCR2091).

References

1. X. Chen et al., *ACS Appl. Mater. Interfaces*, 11, 47535-47544 (2019).

International Rubber Conference 2025 (IRC2025)
1-3 December 2025 @ BITEC, Bangkok, Thailand

Study on Melting Behavior of Crystallites in Carbon Black-Filled Vulcanized Natural Rubber Upon High-Speed Shrinkage from Its Highly Elongated State

Maho Nakada[1], Shoei Okamoto[1], Hiroto Okumura[1], Taichi Uemura[1], Shinichi Yagi[1], Huaizhong Xu[1], Hiroyasu Masunaga[2], Yuji Kitamura[3], Katsuhiko Tsunoda[3], Kenji Urayama[4], and Shinichi Sakurai[1]

[1] *Kyoto Institute of Technology, Matsugasaki, Sakyo-ku, Kyoto 606-8585, Japan*

[2] *SPring-8, Japan Synchrotron Radiation Research Institute (JASRI), Kouto 1-1-1, Sayo-cho, Sayo-gun, Hyogo, 679-5198, Japan*

[3] *Sustainable and Advanced Materials Division, Bridgestone Corporation, Ogawahigashi-cho 3-1-1, Kodaira, Tokyo, 187-8531, Japan*

[4]*A Department of Material Chemistry, Kyoto University, Kyoto 615- 8510, Japan s*

Email: shin@gmai.com

Keywords: natural rubber, carbon black, stain-induced crystallization, wide-angle X-ray scattering, high-speed shrinkage

Natural rubber (NR) exhibits strain-induced crystallization (SIC), in which the rubber crystallizes and toughens when stretched and strained. While the mechanism of SIC under high-speed elongation has been extensively studied, there are very few reports on the melting behavior of crystallites formed by SIC during high-speed unloading, especially for NR containing 50 phr of carbon black, which more closely reflects the composition of major rubber products, compared to unfilled natural rubber (NR0). It is generally believed that the instantaneous occurrence of SIC upon contact with the ground prevents tires from bursting and ensures safety. In the case of aircraft tires, which reach speeds of up to 120 km/h at the moment of landing and complete one full rotation in approximately 50 milliseconds, crystallites formed by SIC may accumulate if they do not melt within a single rotation. This accumulation could lead to undesirable effects such as tire hardening. This study investigates the melting behavior of SIC-induced crystallites during rapid unloading using wide-angle X-ray scattering (WAXS) with synchrotron radiation, in combination with a homemade device that enables high-speed shrinkage of NR specimens. It explores how the presence of 50 phr carbon black affects the melting dynamics of SIC crystallites during rapid unloading, given carbon black's known effects on the formation of SIC dissipation crystallites.

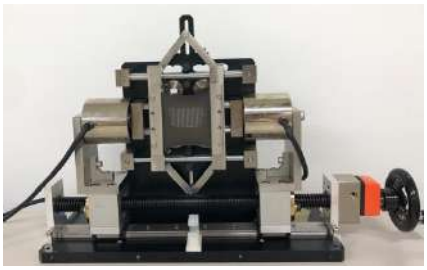


Fig 1. High-speed shrinkage device.

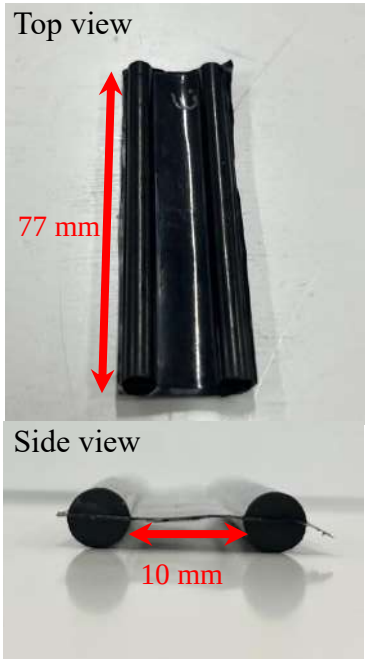


Fig 2. NR50 specimen (thickness 1.0 mm).

To achieve this, we developed a device that utilizes the retractive force of stretched NR50 to perform high-speed shrinkage. The device is equipped with two electromagnets that hold the planar-stretched NR50 sample in place to prevent premature contraction. From outside the experimental hatch, the electromagnets are turned off to release the stretched specimen. In this way, rapid shrinkage is achieved by harnessing the intrinsic retractive force of the rubber (Fig 1).

The device was installed at beamline BL03XU of SPring-8. Time-resolved wide-angle X-ray scattering (WAXS) measurements were performed every 1 millisecond using a specialized two-dimensional detector, synchronized with a high-speed camera that captured the actual shrinkage behavior of the specimen at the same 1-millisecond intervals. The specimen used was a vulcanized natural rubber with cylindrical protrusions at both ends, compounded with 1.40 phr of sulfur (Fig 2). The specimen, initially 10 mm in length, was stretched in-plane up to seven times its original length and subjected to rapid shrinkage (Fig 3). Time-resolved 2D-WAXS measurements were carried out at room temperature during the contraction process.

The results for NR0 showed that the integrated intensity of the (200) reflection peak decreased and nearly vanished after 25 milliseconds, indicating that the crystallites had completely melted almost simultaneously with the strain returning to zero. This suggests that the crystallites persisted for a millisecond even after the strain had fully relaxed, indicating that, unlike in low-speed unloading where crystallites disappeared at the strain of 2.0, they remained present for a longer duration. Since the timing at this strain value for the case of the high-speed shrinking experiment was found to be 20 milliseconds, this implies that the crystallites survived 5 milliseconds. Furthermore, it was found that the crystallinity and the size of the crystallites increased in the initial and intermediate stages of the shrinking (melting) process and then decreased in the final stage of melting. Another significant result is that the crystallites remained a finite size at the moment of the complete melting. This result may suggest the idea of the critical nucleus even for the melting of the crystallites in the shrinking process. We compare the results quantitatively for the carbon black-filled NR specimen.

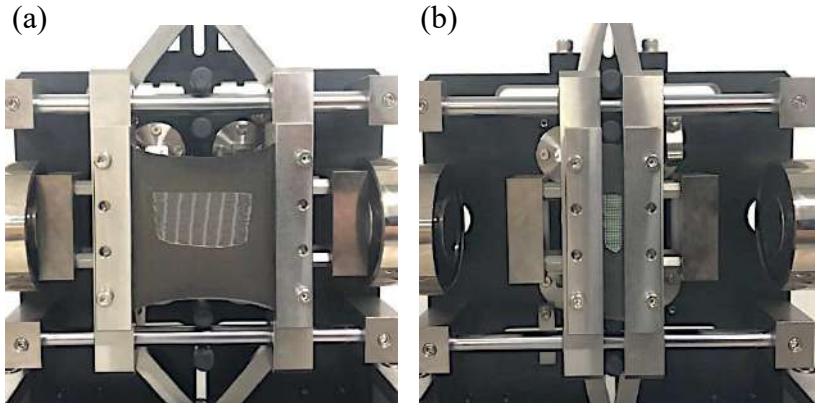


Fig 3. (a) Stretched 7 times and (b) after shrinking.

Acknowledgement

This work was financially supported by JST CREST Japan (grant number JPMJCR2091).

International Rubber Conference 2025 (IRC2025)
1-3 December 2025 @ BITEC, Bangkok, Thailand

Natural-Rubber-Based Adhesives for Housefly (Musca domestica) Control

P. WIROONPOCHIT[1], B. MULSENA[2], K. HATTHAPANIT[1], T. KAEWPRAKOB[1], Y. CHISTI[3], N. HANSUPALAK[2,4]

[1] *National Metal and Materials Technology Center, Pathum Thani 12120, Thailand.*

[2] *Faculty of Engineering, Kasetsart University, Bangkok 10900, Thailand.*

[3] *Institute of Tropical Aquaculture and Fisheries, Universiti Malaysia Terengganu, Terengganu 21030, Malaysia*.

[4] *Faculty of Science, Kasetsart University, Bangkok 10900, Thailand.*

kannikh@mtec.or.th

Keywords: natural adhesives, insect-trapping glue, fly-trapping adhesives, natural rubber, palm olein

Housefly (Musca domestica) is a common pest around outdoor markets and food stalls especially in the warmer regions. Fly control outdoors is difficult [1], but necessary in view of the flyborne transmission of many diseases [2]. Inexpensive and nontoxic methods of control are wanted in preference to insecticides to prevent harm to humans and animals. Trapping flies on adhesive surfaces is an inexpensive and widely used method of control especially in open areas [1,3]. Adhesive traps are effective without pesticides. Commercial adhesives often use petrochemicals-derived polymers such as poly(vinyl alcohol) and acrylate [4,5]. Potentially, the petrochemicals-based materials can be fully replaced with biobased natural products in making adhesive fly traps to reduce environmental impact and dependence on petroleum, a nonrenewable resource.

Adhesives derived from natural biomaterials—specifically natural rubber (NR) and palm olein—were developed for the control of flying insects, particularly houseflies, in premises used for food handling. The insect-trapping performance of the adhesives was influenced by both the formulation composition and the average molar mass of the rubber component. Increasing the palm olein content or reducing the average molar mass of the rubber chains led to a decrease in adhesive viscosity. The former was attributed to the plasticizing effect of palm olein, while the latter resulted from a reduction in chain entanglement. In either case, lower viscosity improved wetting and contact with the insect surface, thereby enhancing adhesion. However, excessive viscosity reduction caused adhesive loss due to gravity-driven dripping, negatively impacting performance.

The optimal formulation consisted of 1 kg of NR with an average molar mass of $6.0\times10^5 \pm 2.1\times10^4$ kg kmol^{-1} dissolved in 2 kg of palm olein. This formulation demonstrated high fly-trapping efficiency in field tests and was more cost-effective than commercial insect-trapping adhesives. In parallel field tests (Figure 1), the optimal adhesive composition of the present work was at least as effective as the commercial insect trapping glue MYFIX® in total insect capture and was substantially more effective than a different commercial product. A schematic representation of the natural adhesive system is shown in Figure 2.

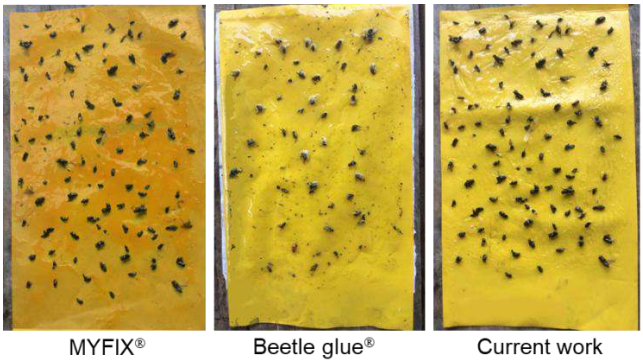


Figure 1. Insects trapped after 6 h use of the traps with different adhesives

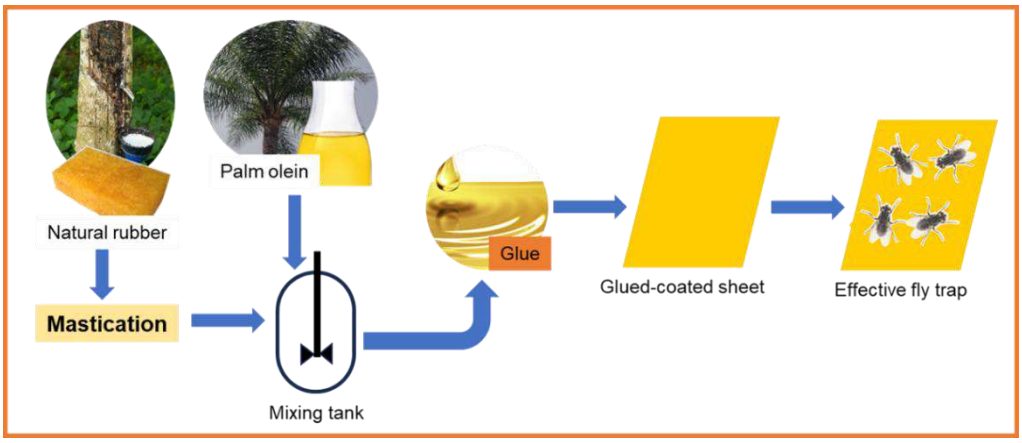


Figure 2. The schematic of natural biomaterial-based adhesives

Acknowledgement

The authors would like to express their sincere gratitude to the Kasetsart University, National Metal and Materials Technology Center (MTEC), Thailand, for the grant support.

References

1. Hinkle, et al. A review of alternative controls for house flies. Insects 2021, 12, 1042.
2. Issa, R. Musca domestica acts as transport vector hosts. Bull. Natl. Res. Cent. (Egypt) 2019, 43, 73.
3. Kim, J. et al. Development of insect-proof starch adhesive containing encapsulated cinnamon oil for paper box adhesion to inhibit Plodia interpunctella larvae infestation. J. Food Sci. 2020, 85, 3363–3371.
4. Yang, K. et al. A novel adhesive trunk trap net for trapping Eucryptorrhynchus brandti (Coleoptera: Curculionidae). Pest Manage. Sci. 2019, 75, 3218–3225.
5. Zhu, J. J. et al. Development and first evaluation of an attractant impregnated adhesive tape against blood-sucking flies. Insect Sci. 2022, 29, 603–612.

International Rubber Conference 2025 (IRC2025)
1-3 December 2025 @ BITEC, Bangkok, Thailand

In Situ Silica Reinforced Natural Rubber: A Novel Approach for Enhanced Performance and Application

S. Montha, P. Suwandittakul, W. Intiya and C. Kongkaew*

[1] *MTEC, National Science and Technology Development Agency, 114 Thailand Science Park, Phahonyothin Road, Khlong Nueng, Khlong Luang, Pathum Thani 12120, Thailand*.

*E-mail: suriyakm@mtec.or.th

Abstract

To overcome multiple problems from silica dust pollution in the rubber industry, a new approach for preparing silica filled natural rubber (NR) by generating the *in situ* silica particles inside the NR matrix *via* the sol-gel reaction in NR latex using sodium silicate as a silica precursor was proposed. Effect of sodium silicate sources, type and concentration of acid, and precipitation pH on the morphology and physical properties of precipitated silica was monitored. X-ray fluorescence (XRF) spectrometry confirmed that precipitated solid obtained from sol-gel reaction of sodium silicate composed of silica as a major component (75-85%). Conversion of sodium silicate to the *in situ* silica particles within NR matrix was in a range of 90-93%. Average sizes of *in situ* silica particles within the NR matrix were quite similar to those of precipitated silica and commercial silica. Interestingly, scorch time and optimum cure time of *in situ* silica filled NR compound were shorter than those of *ex situ* silica filled NR compound. The mechanical properties, *i.e.* modulus at 100%, 300% and 500% stains, tensile strength and elongation at break of *in situ* silica filled NR vulcanizate were comparable with those of *ex situ* silica filled NR vulcanizate.

Keywords: natural rubber, silica, sodium silicate, sol-gel

Keywords: sol-gel, natural rubber, silica, sodium silicate

1. Introduction

Precipitated silica stands as a critical reinforcing filler within the rubber industry, particularly for high-performance tire applications. Its integration confers substantial advantages, including a reduction in rolling resistance and enhancement of wet traction, while concurrently preserving acceptable tread-wear characteristics in contemporary tire designs. Traditionally, the incorporation of precipitated silica powder into a solid rubber matrix is achieved through mechanical blending processes, typically employing two-roll mills or internal mixers. However, this conventional methodology is fraught with considerable challenges. The generation of fine silica dust during processing contributes significantly to air pollution, necessitates high energy consumption, and leads to accelerated machine abrasion. Furthermore, extant human epidemiological evidence indicates the carcinogenicity of inhaled crystalline silica, specifically in its quartz or cristobalite forms, when derived from occupational exposures [1]. In response to these persistent issues, various attempts have been made to overcome these limitations, notably through the development of in situ silica formation techniques directly within the rubber matrix [2-4].

This work systematically investigates a novel methodology for the preparation of silica-filled natural rubber (NR) by facilitating the in situ generation of silica particles. This is achieved via a sol-gel reaction occurring within the NR latex, utilizing sodium silicate as the primary silica precursor. Our investigation encompassed a

detailed examination of the effects of sodium silicate sources, the type and concentration of acid, and the precipitation pH on the morphology and resultant physical properties of the precipitated silica. The study also evaluated the efficiency of incorporating these in situ-formed silica particles within the NR matrix. Crucially, a comparative analysis was performed on the cure characteristics and mechanical properties of the newly developed in situ silica-filled NR vulcanizates against those prepared through conventional (ex situ) methods.

Experimental Section

Materials

Ammonia-preserved fresh natural rubber (NR) latex was procured from a rubber plantation located in Rayong province, Thailand. Characterization of the latex revealed a total solid content (TSC) of 39.5%, a dry rubber content (DRC) of 36.4%, and a non-rubber content (NRC) of 3.10%. Three commercially available grades of sodium silicate solution were employed as precursors for silica generation. Commercial silica (Hisil-233) was supplied by Oriental Silicas Corporation. Hydrochloric acid (HCl), sulfuric acid (H2SO4), formic acid (HCOOH), and acetic acid (CH3COOH), all of analytical reagent grade, were purchased from Ajax Finechem.

Precipitation of Silica from Sodium Silicate Solution

An acidic solution was gradually introduced into the sodium silicate solution under constant mechanical stirring. The addition of acid was terminated upon achieving the predetermined desired precipitation pH. The resulting suspension was then subjected to vacuum filtration using Whatman paper No. 1. The isolated precipitated solid was subsequently dried in a hot air oven at 100°C until a constant mass was recorded. The percentage of solid content was quantitatively determined using the following equation:

$$\text{Solid content (\%)} = [W_1/W_0] \times 100 \quad (1)$$

where W0 denotes the initial mass of the sodium silicate solution and W1 represents the mass of the dried solid.

Particle size distribution measurements of the samples were conducted using laser diffraction (Zetasizer Nano-ZS, Malvern) equipped with a He-Ne laser source operating at a wavelength of 488 nm. Prior to analysis, each sample underwent ultrasonic treatment for 5 minutes. Deionized water served as the dispersion medium. The elemental composition of the samples was ascertained via X-ray fluorescence (XRF) spectrometry (PHILIPS PW2404), utilizing a standardless scan mode.

Preparation of In Situ Silica-Filled NR by the Sol-Gel Method

Sodium silicate solution was added to fresh NR latex under continuous mechanical stirring at ambient temperature. An acid solution was then progressively introduced into the mixture to adjust the pH to 9.0–9.5, thereby promoting the in situ formation of silica particles within the latex. A distinct increase in the viscosity of the mixture was observed during this stage. Further acid addition reduced the pH to 4–5, leading to the coagulation of the NR latex. The resultant coagulum was thoroughly washed with deionized water and subsequently dried in a hot air oven at 70°C until a constant mass was achieved.

A portion of the dried sample was calcined in a crucible at 950°C until a constant mass was obtained. The residual solid from calcination was then subjected to XRF analysis to determine its composition. The concentration of in situ silica within the NR matrix, expressed in parts per hundred rubber (phr), was calculated as follows:

$$\text{Silica content (phr)} = [W_1/W_0] \times 100 \quad (2)$$

where W0 represents the mass of the organic fraction lost upon calcination and W1 corresponds to the mass of silica in the residual solid.

Compounding and Testing

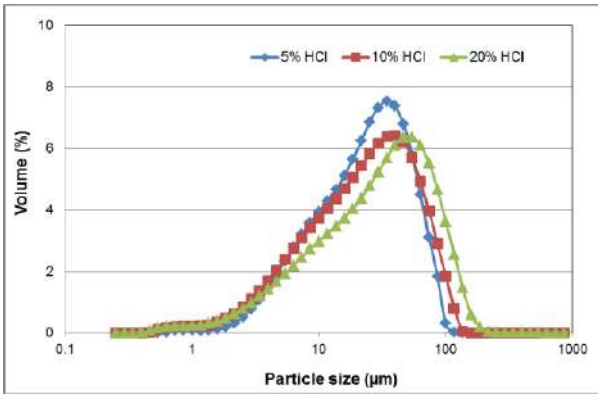
Compounding procedures were executed using a laboratory-scale internal mixer (Brabender Plasticorder 350E) for two distinct batches. The first batch consisted of ex situ silica, NR, and a predetermined suite of compounding chemicals. The second batch utilized the in situ silica-filled NR and an identical set of compounding chemicals. The formulation for both batches comprised 35.0 phr of silica, 3.0 phr of ZnO, 2.0 phr of stearic acid, 1.0 phr of 6PPD, 1.0 phr of TMQ, 2.5 phr of Si-69, 3.0 phr of aromatic oil, 1.2 phr of TBBS, 0.3 phr of TMTD, and 2.0 phr of sulfur.

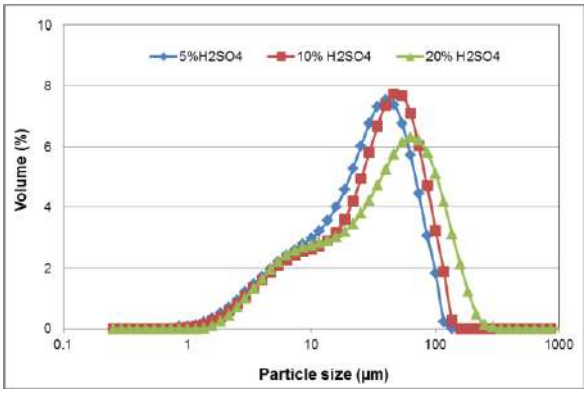
The mixing process was segmented into two sequential steps. In the initial step, NR, silica, ZnO, stearic acid, 6PPD, TMQ, Si-69, and aromatic oil were incorporated. The mixing parameters for this stage were: a fill factor of 0.75, an initial chamber temperature of 80°C, a rotor speed of 40 rpm, and a mixing duration of 10 minutes. In the subsequent step, the compounded material from the first stage was further mixed with TBBS, TMTD, and sulfur. The mixing conditions for this second stage were: a fill factor of 0.75, an initial chamber temperature of 60°C, a rotor speed of 40 rpm, and a mixing duration of 2 minutes. Post-mixing, the compounds were sheeted on a two-roll mill.

Cure characteristics, including minimum torque (ML), maximum torque (MH), scorch time (ts1), and optimum cure time (tc90), were assessed using a moving die rheometer (MDR, TechPro MD+) at 150°C, in accordance with ISO 6502. Vulcanization of the compounded materials was performed in a compression mold at 150°C, with the curing time determined by the optimum cure time obtained from the MDR analysis. Tensile properties were measured using a universal testing machine (Instron 3366 series), following ISO 37 (die type 1).

Results and Discussion

This section would typically present the findings of the experimental work. Three commercial grades of sodium silicate solutions yielded precipitated solid contents ranging from 28-35%. The particle size distribution of these solids was unimodal, ranging from 1.20 µm to 200 µm, with average sizes of 39.49 µm, 39.80 µm, and 34.29 µm for sodium silicate solutions (type A), (type B), and (type C), respectively. XRF analysis confirmed that silica (SiO2) constituted the major component of the precipitated solid, with concentrations of 82.84%, 77.10%, and 83.36% for types A, B, and C, respectively.





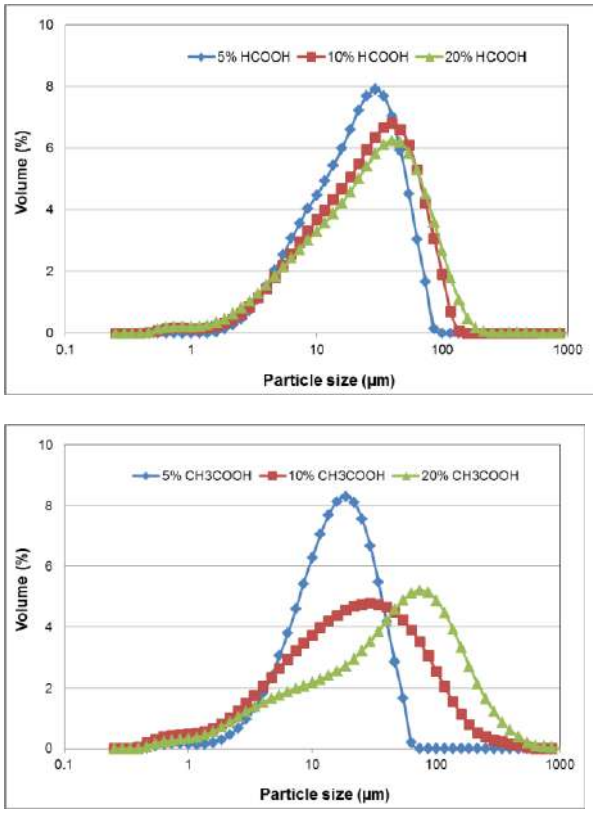


Figure 1: Particle size distribution of precipitated silica obtained from treating sodium silicate solution with various types and concentrations of acid.

Figure 1 illustrates the observed changes in the particle size distribution of precipitated silica as a function of acid type and concentration. Higher acid concentrations (e.g., 20% acid) consistently yielded larger precipitated silica particles compared to lower concentrations (10% and 5% acids), a trend consistent across all acid types investigated. This suggests that the characteristics of the precipitated silica are significantly influenced by the specific acid type and its concentration.

Acidification of sodium silicate solution with 5% hydrochloric acid, 5% sulfuric acid, 5% formic acid, and 5% acetic acid at varying pH values revealed an inverse relationship between precipitated silica content and precipitation pH. A sharp increase in precipitated silica content was observed when the precipitation pH reached 9.0-9.5, with a more gradual increase from pH 9.0-9.5 to pH 4.0-5.0. This trend was consistent across different acid types. The pH range of 4.0-5.0 is particularly interesting as it not only maximizes the precipitated silica content but also corresponds to the pH range at which NR latex coagulation occurs.

Analysis of the in situ silica particles within the NR matrix indicated that the experimental yield was slightly lower than theoretical calculations. A small fraction (1.4-10.3%) of in situ silica particles was lost from the NR matrix during the sol-gel reaction, with higher losses observed at higher concentrations of sodium silicate solution. Consequently, the retained in situ silica particles within the NR matrix ranged from 90-93%.

A crucial aspect of this study involved comparing the cure characteristics and mechanical properties of in situ silica-filled NR compounds with those of ex situ silica-filled NR compounds. As presented in Table 1, both in situ and ex situ compounds exhibited comparable torque difference (MH−ML) values, suggesting similar cross-link densities. Importantly, the scorch time (ts2) and optimum cure time (tc90) of the in situ silica-filled NR compound were notably shorter than those of the ex situ silica-filled NR compound. This reduction in curing times could be attributed to increased protein content in the in situ silica-filled NR, as reported in literature regarding interactions between silica surfaces and protein molecules [5, 6]. This observation further supports the significant role of protein content in NR vulcanization [7, 8]. Furthermore, Table 1 also demonstrates that the mechanical properties specifically, modulus at 100%, 300%, and 500% strains, tensile strength at break, and elongation at break of the in situ silica-filled NR compounds were comparable to those of the ex situ silica-filled NR compounds.

Table 1: Cure characteristics and Mechanical properties of in situ silica-filled NR compound and ex situ silica-filled NR compound.

Properties	In situ silica filled NR compound	*Ex situ* silica filled NR compound
Minimum torque, dN.m	2.38	1.87
Maximum torque, dN.m	12.54	12.05
Scorch time (ts2), min	2.59	4.25
Optimum cure time (ts90), min	4.3	6.37
Modulus 100%, MPa	1.53	1.54
Modulus 300%, MPa	7.35	6.63
Modulus 500%, MPa	18.62	17.87
Tensile stress at break, MPa	29.3	30.22
Tensile strain at break, %	647	659

Conclusion

This study successfully demonstrated the preparation of in situ silica-filled natural rubber through the sol-gel reaction of sodium silicate within NR latex. The amount of precipitated solid varied depending on the sodium silicate source. Silica was identified as the primary component in the precipitated solid. Changes in particle size distribution were observed to be dependent on the type and concentration of acid used, with lower acid concentrations generally yielding smaller precipitated silica particles. The highest amount of precipitated silica was obtained at a precipitation pH of 9.0-9.5. The concentration of in situ silica particles remaining within the NR matrix after the sol-gel reaction ranged from 90-93%. Significantly, the in situ silica-filled NR compound exhibited shorter scorch time (ts2) and optimum cure time (tc90) compared to the ex situ silica-filled NR compound. Furthermore, the mechanical properties of the in situ silica-filled NR compound were comparable to those of its ex situ counterpart. This new approach offers a promising pathway for more sustainable and efficient production of reinforced natural rubber composites.

References

1. Rice, F. L.; Park, R.; Stayner, L.; Smith, R.; Gilbert, S.; Checkoway, H. *Occup. Environ. Med.* **2001**, *58*, 38.
2. Mark, J. E.; Pan, S. J. *Macromol. Chem. Rapid Commun.* **1982**, *3*, 681.
3. Tangpasuthadol, V.; Intasiri, A.; Nuntivanich, D.; Niyompanich, N.; Kiatkamjornwong, S. *J. Appl. Polym. Sci.* **2008**, *109*, 424.
4. Poompradub, S.; Thirakulrati, M.; Prasassarakich, P. *Mater. Chem. Phys.* **2014**, *144*, 122.
5. Holing, G. J.; York, R. L.; Onorato, R. M.; Thompson, C. M.; Webb, N. E.; Yoon, A. P.; Somorjai, G. A. *J. Am. Chem. Soc.* **2011**, *133*, 6243.
6. Mathe, C.; Devineau, S.; Aude, J. C.; Lagniel, G. L.; Chedin, S.; Legros, V.; Mathon, M. H.; Renault, J. P.; Pin, S.; Boulard, Y.; et al. *PLOS ONE* **2013**, *8*, 1.
7. Kongkaew, C.; Dokkhan, C.; Pattanawanidchai, S.; Chaikumpollert, O.; Loykulnant, S. *Biomass Bioenerg.* **2012**, *46*, 233.
8. Mekkreingkrai, D.; Sakdapipanich, J. T.; Tanaka, Y. *Rubber Chem. Technol.* **2006**, *79*, 366.

International Rubber Conference 2025 (IRC2025)
1-3 December 2025 @ BITEC, Bangkok, Thailand

Application of Ozone Treatment to Reduce Foul Odor in Cup Lump Rubber Production

C. KONGKAEW[1], P. SUWANDITTAKUL[1], S. MONTHA[1], P. RAKDEE[1],
N. MOONPRASITH[1], S. LOYKULNANT[1]

[1] *National Metal and Materials Technology Center, Pathum Thani, Thailand.*

chaveer@mtec.or.th

Keywords: Ozone treatment, Odor reduction, Cup lump rubber, Oxidation-reduction potential

Foul odor emitted from cup lump rubber—primarily resulting from microbial decomposition during latex coagulation and storage—poses a persistent challenge for rubber producers. Not only does it affect the working environment and community well-being, but it also undermines product competitiveness in international markets [1,2]. Traditional deodorization methods often involve chemical residues or impractical processes at the plantation level [3,4]. This study explores ozone (O_3), a strong oxidant known for its high reactivity and zero residual contamination, as a promising and environmentally responsible alternative for odor reduction in cup lump rubber processing [5,6].

This study investigates the behavior and stability of ozone when applied to three liquid media: deionized water (DI), 5% sulfuric acid, and 5% formic acid. Ozone gas was introduced into each solution under controlled conditions, and oxidation-reduction potential (ORP) was monitored in real time. All systems exhibited an initial increase in ORP, reflecting ozone dissolution. Notably, the 5% sulfuric acid solution demonstrated the greatest ORP values, while the formic acid system showed fluctuating ORP values likely due to secondary redox reactions.

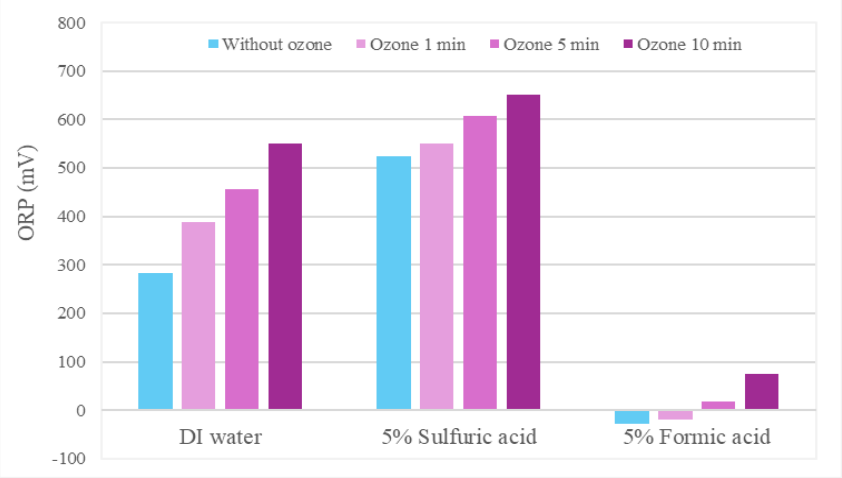


Figure 1. Comparison of oxidation-reduction potential (ORP) in deionized water, 5% sulfuric acid, and 5% formic acid after ozone treatment for 1, 5, and 10 minutes

To assess practical applicability, 5% sulfuric acid solutions were pre-treated with ozone for 1, 5, and 10 minutes before being used as coagulants in the preparation of cup lump rubber from fresh field latex. The rubber lumps were then left to age under ambient conditions for one week. After aging, each sample was cut open to observe internal bubble formation and assessed for odor intensity

using sensory evaluation. Results showed that increasing the ozone treatment time reduced both the number and size of internal gas bubbles—visual indicators of suppressed anaerobic decomposition. In parallel, the odor level decreased from 4 to 3 on a 5-point scale, suggesting that ozone pre-treatment of the acid coagulant can effectively reduce foul odor during rubber coagulation.

Table 1. Effect of ozone treatment time in 5% sulfuric acid solution on bubble formation, internal appearance, and odor level of cup lump rubber

Ozone treatment time in 5% sulfuric acid solution (minutes)	Degree of bubble formation	Internal appearance of cup lump rubber	Odor level of rubber
0	High		4
1	High		4
5	Medium		3-4
10	Low		3

These findings demonstrate that ozone treatment in mildly acidic media, especially in sulfuric acid systems, can effectively reduce foul odor in cup lump rubber without introducing chemical residues. The technique is clean, scalable, and potentially integrable with existing STR20 processing lines. Future work will focus on pilot-scale field trials, long-term odor stability, and impact on rubber properties.

Acknowledgement

The authors would like to express their sincere appreciation to the Bangbut Rubber Farmers Group in Rayong province for providing fresh field latex and experimental facilities essential to the success of this study.

References

1. Hoven VP, Rattanakaran K, Tanaka Y. *Rubber Chem Technol*. 2004;92(4):2253.
2. Botondi R, Barone M, Grasso C. *Foods*. 2021;10(4):748.
3. Idris NF, Le-Minh N, Hayes JE, Stuetz RM. *J Environ Manage*. 2022;305:114426.
4. Sakdapipanich J, Insom K. *Kautschuk Gummi Kunststoffe*. 2006;59(7–8):382–387.
5. Lim S, Shi JL, von Gunten U, McCurry DL. *Water Res*. 2022;213:118053.
6. Waste Advantage Magazine. Using ozone for composting odor control. *Waste Advantage Magazine*. 2018 Jun.

Changes in nanostructural changes during tearing of elastomeric poly(butylene succinate)/poly(butylene succinate adipate) blend films

Kazuki IMAI[1], Keito SHIMAKAWA[1], Ryu MIYAJIMA[1], Nana TSUJI[1], Khuat Thi Khanh VAN[2], Hiroyasu MASUNAGA[3], An Yingjun[4], Atsushi TAKAHARA[4], Sono SASAKI*[1,2,5]

[1]606-8585, Grad. Sch. of Sci. and Tech., Kyoto Inst. of Tech., Matsugasaki Hashikami-cho, 1, Sakyo-ku Kyoto, *Japan*, [2]606-8585 Sch. of Sci. and Tech., Kyoto Inst. of Tech, Matsugasaki Hashikami-cho, 1, Sakyo-ku Kyoto, *Japan*, [3] 679-5198, Japan Syn. Rad. Res. Inst., 1-1-1, Sayo-cho, Sayo, Hyogo, *Japan*, [4] 819-0395, K-NETs, Kyushu Univ., Motooka 744, Nishi-ku, Fukuoka, *Japan*, [5] 679-5148,Riken SPring-8 center, Koto 1-1, Sayo-cho, Sayo, Hyogo, *Japan*

e-mail: m4661002@edu.kit.ac.jp

Keywords: Poly(butylene succinate), Poly(butylene succinate adipate), Blend film, Tearing, Higher-order crystalline structures, Crystallinity, Crystallite size, Monoclinic crystal

Polybutylene succinate (PBS) and polybutylene succinate adipate (PBSA) have attracted attention in recent years as biodegradable plastics[1]. These materials do not contain aromatic structures and have elastomeric elasticity. In particular, PBSA becomes almost amorphous when the adipate content exceeds 30%, making it a more elastomeric material. Although there have been many studies on nanostructural changes of PBS and PBSA in tension, there have been no studies on nanostructural changes in tearing. The nanostructural changes of PBS and PBSA in tension have been studied extensively. The aim of this study was to investigate the nanostructural changes during tearing in elastomeric PBS, PBSA, and their blended films by in-situ X-ray scattering and diffraction measurements using synchrotron radiation.

Press films of PBS, PBSA (BioPBSTM, PTT MCC Biochem Co., Ltd.) and their blends having PBS:PBSA ratios of 20:80, 50:50, and 20:80 (Mitsubishi Chemical Co.) were used as samples. Wide-Angle X-ray Scattering (WAXD) and Small-Angle X-ray Scattering (SAXS) measurements were carried out for the films at the BL38B1 beamline of SPring-8 (RIKEN) using an X-ray beam having a wavelength of 0.1 nm and a PILATUS detector (Dectris Ltd.) and Flat Panel. A uniaxial stretching device and a laser displacement meter were set up in a measurement system. A film was irradiated with the X-ray beam at a position 2 mm away from the onset portion of the notch. The tip of tearing passed through the X-ray irradiation position by stretching the lower part of the film in the direction of the blue arrow as shown in Fig. 1. Note that the other side

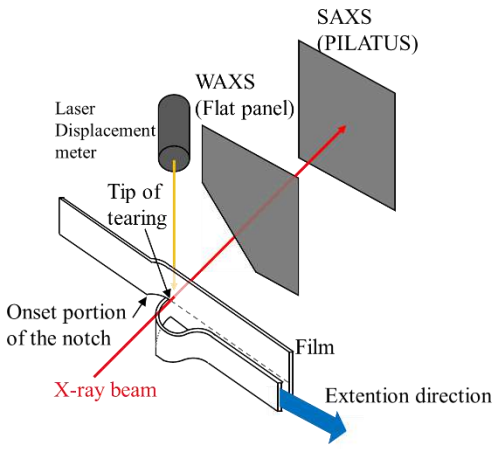


Fig.1 Schematic illustration of SAXS/WAXS simultaneous measurements along with tearing of the notched film.

of the higher part of the film was fixed throughout the experiment. The uniaxial stretching device was operated at a speed of 1,3 and 5 mm/min, the tip of tearing progressed to the irradiation position of the incident X-ray beam and passed through it. In this experiment, changes in higher-order crystalline structures of the film were traced by time-resolved WAXD/SAXS measurements. X-ray irradiation time was 2 s per pattern. 200 diffraction patterns were collected at an interval time of 3 s during film tearing.

PBS film. The crystallite size in the monoclinic [110] direction increased slightly for the PBSA film, while it decreased for the PBS film during tearing. As for the crystal orientation, the monoclinic *c* axis (the chain axis) of the PBSA crystal changed from random to oriented with a tilt angle of ca. 20 deg. to the tearing direction, whereas that of the PBS crystal became almost parallel to the direction of tearing. The lamellar thickness and long period decreased for the PBSA film, indicating the formation of thin lamellae between the existing lamellar stacks. Those of the PBS films slightly increased. These results suggested that the formation of thin lamellae with a low orientation distribution during the tearing process was related to the high tearing strength of the film. The changes in the hierarchical structures for the blend films will be presented in our poster.

Acknowledgement

This work was supported by JST (Moonshot R&D Program, Grant Number JPNP18016)

References

1. N Jacquel, et al., *J. Polym. Sci. A Polym. Chem*., **2011**, 49, 5301–5312.

Effect of chitosan bio-based filler on the mechanical reinforcement of ENR composites

Ploypailin Juntosree[1], Nantinee Choosang[1,2], Wirasak Smitthipong[1,3]

[1] *Specialized center of Rubber and Polymer Materials in Agriculture and Industry (RPM), Department of Materials Science, Faculty of Science, Kasetsart University, Bangkok 10900, Thailand.*

[2] *Bangkok Metropolis Motor Co., Ltd., Samut Sakhon 74110, Thailand.*

[3] *Hub of Talents in Natural Rubber, National Research Council of Thailand (NRCT), Bangkok 10900, Thailand*.

E-mail address of the presenting author: ploypailin.ju@ku.th

Keywords: ENR composite, chitosan, uncrosslinked, mechanical property

Natural rubber (NR) can be modified by the epoxidation process to obtain epoxidized natural rubber (ENR) (Figure 1) [1]. The ENR is produced through the action of hydrogen peroxide and formic acid [2]. Chitosan is known as a linear polymer and is biodegradable. It is the most important requirement for a filler to have good interaction with the rubber matrix [3]. So, this research is conducted to investigate ENR compounds incorporating chitosan as a bio-based filler in ENR composite to improve mechanical properties and minimize environmental impact.

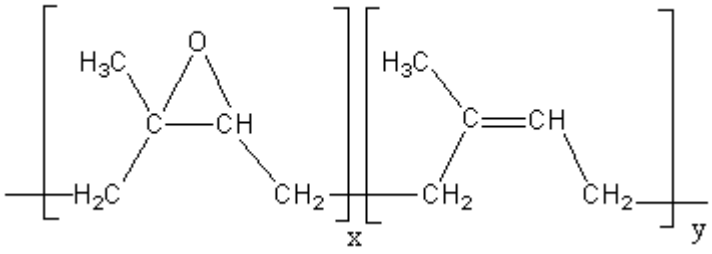


Figure 1. Chemical structure of epoxidized natural rubber (ENR)

Uncrosslinked ENR samples was prepared by mixing ENR with chitosan at different proportions of 10 and 20 phr. The compound was masticated by a two-roll mill. The ENR ≈ 25% of epoxidation was verified by nuclear magnetic resonance spectroscopy (NMR). The chemical functional groups of ENR were also characterized by Fourier transform infrared spectroscopy (FTIR).

From the mechanical property point of view, tensile strength increased with the increase of chitosan (Table 1). However, a reduction in the elongation at break was observed, possibly due to restricted rubber chain mobility caused by chitosan addition.

Table 1. Mechanical properties of ENR samples

Sample name	Results	
	Tensile strength (MPa)	Elongation at break (%)
ENR	2.0 ± 0.05	462 ± 4.5
ENR/Chitosan 10	2.9 ± 0.05	460 ± 5.5
ENR/Chitosan 20	3.7 ± 0.40	386 ± 5.5

Thermogravimetric analysis (TGA) was used to study the thermal stability of ENR samples. Moreover, the hyphenation system of TGA-FTIR, combined with GC-MS, is being applied to qualify and quantify the ENR samples at the same time. Atomic force microscopy (AFM) is also being used to characterize the morphology of the ENR samples. Future studies should focus on the effect of different epoxidation levels on ENR-chitosan composites. SEM can be used to investigate filler dispersion, while spectroscopic techniques will help analyze chemical bonding. Evaluation of long-term durability and environmental performance are also recommended.

Acknowledgement

This research was supported by specialized center of Rubber and Polymer Materials in agriculture and industry (RPM), Department of Materials Science, Faculty of science, Kasetsart University (Thailand).

References

1. Buaksuntear K, Kohl P, LI Y, Smitthipong W, *ACS Appl. Polym. Mater.*, 2025*; 7*: 3576.
2. Huang S, Luo Z, Yang Y, LI S, Zhang J, Kong N, TAN S, Li J, TAO J, *Int. J. Biol. Macromol.*, 2025; 308: 142431.
3. Ismail H, Shaari S, Othman N, *Polym. Test.*, 2011; 30 :784.

Identification and Reduction of residual allergenic rubber proteins in Natural Rubber latex gloves via Alkaline and Surfactant Treatments

P. PORNCHARUKIT[1] and J. SAKDAPIPANICH[1,2*]

[1] *Rubber Research Group, Department of Chemistry, Faculty of Science, Mahidol University, Nakhon Pathom 73170, Thailand*

[2] *The Rubber and Rubber Glove Academician Association, Bangkok, 10900, Thailand*

Presenting author: pimnaraporn.pon@student.mahidol.edu

*Corresponding author: jitladda.sak@mahidol.ac.th

Keywords: Deproteinized natural rubber, Latex gloves, Allergenic proteins, Sodium hydroxide, SDS-PAGE

Allergic reactions caused by residual proteins in natural rubber latex (NRL) are a major concern in the medical industry, especially for products such as gloves that come into direct contact with the skin. This study aims to address this issue by optimizing the manufacturing process for gloves made from deproteinized natural rubber (DPNR), with the objective of reducing allergenic protein content in high-ammonia (HA) latex (Figure 1). Building upon previous studies that identified water-soluble proteins in natural rubber as the primary contributors to Type I latex allergy, this work explored targeted deproteinization strategies to mitigate allergenicity.

To achieve this objective, the study evaluated the effectiveness of protein removal using combinations of surfactants and alkalis, with particular focus on sodium lauryl sulfate (SDS) and sodium hydroxide (NaOH) as processing additives. Residual protein content was quantified via the Lowry method, while allergenic protein profiles were characterized by sodium dodecyl sulfate-polyacrylamide gel electrophoresis (SDS-PAGE) (Figure 2).

The results demonstrated that NaOH markedly enhanced protein removal by disrupting ester linkages within the latex matrix, thereby substantially reducing the levels of allergenic proteins remaining in the final product. In contrast, SDS alone was less effective in breaking down protein-latex associations. The combined approach utilizing NaOH represents a promising strategy for improving the hypoallergenic properties of natural rubber gloves intended for medical use.

This work provides a feasible pathway toward the development of safer latex-based medical products while underscoring the need for further investigation into the long-term stability and mechanical integrity of DPNR processed under alkaline conditions. Future research should also assess the scalability and economic feasibility of this method for large-scale industrial glove production.

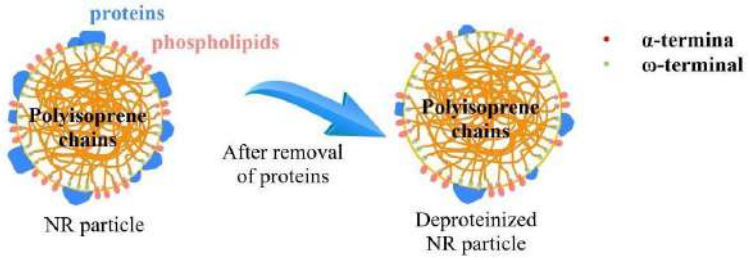


Figure 1. Deproteinization of natural rubber latex using NaOH and surfactants.

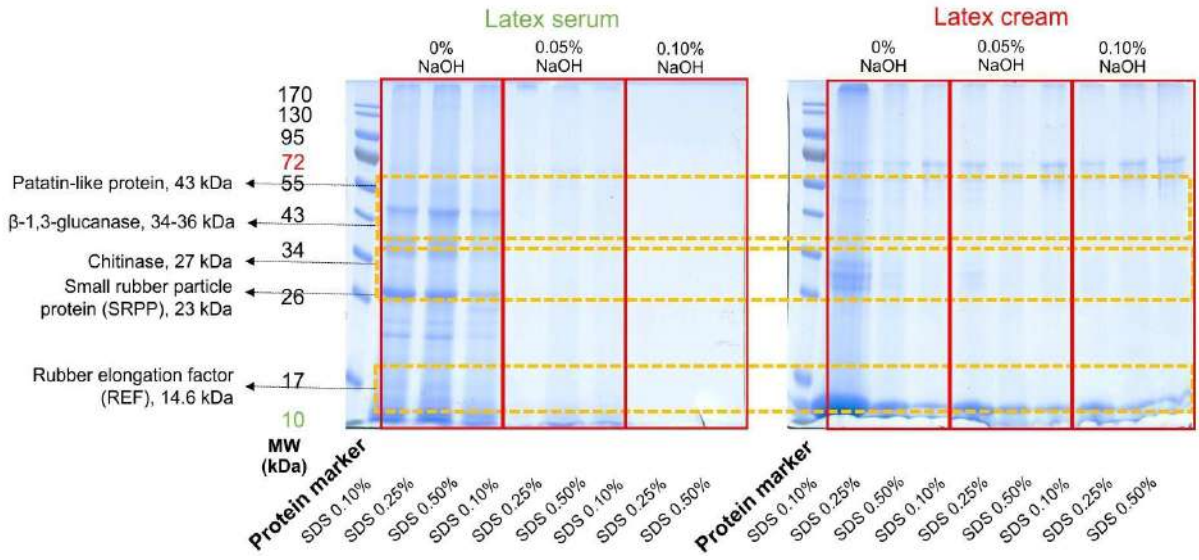


Figure 2. SDS-PAGE profiles of residual proteins in latex serum and cream fractions after treatment.

References

1. P. Rojruthai, J. Sakdapipanich, J. Wiriyanantawong, C.-C. Ho, and N. Chaiear, *Polymers* 14, 4679 (2022).

International Rubber Conference 2025 (IRC2025)
1-3 December 2025 @ BITEC, Bangkok, Thailand

Influence of Bio-Based Epoxidized Natural Rubber as a Compatibilizer on Thermoplastic Polyurethane/Natural Rubber Blends for 3D Printing Applications

T. SRISUWANNO[1], P. LUANGCHUANG[2], C. Bascucci[3], F. Clemens[3], Y. NAKARAMONTRI[1]

[1] *Sustainable Polymer & Innovative Composite Materials Research Group, Department of Chemistry, Faculty of Science, King Mongkut's University of Technology Thonburi, Bangkok 10140, Thailand.*

[2] *Department of Advanced Materials and Surfaces, Empa-Swiss Federal Laboratories for Material Science and Technology, Ueberlandstrasse 129, Dübendorf 8600, Switzerland.*

e-mail address of the presenting author (Torfan.sris@mail.kmutt.ac.th)

Keywords: Thermoplastic polyurethane, Natural rubber, Epoxidized natural rubber, Compatibilizer, 3D printing

In this study, thermoplastic vulcanizates (TPVs) composed of thermoplastic polyurethane (TPU) and bio-based natural rubber (NR) were successfully developed *via* the material extrusion additive manufacturing (MEx-AM) process for 3D printing applications. TPU was selected as the primary matrix polymer due to its distinctive crystalline multi-block copolymer structure, which consists of alternating hard and soft segments. However, TPU also presents certain limitations, including relatively poor elasticity, damping properties, water resistance, and dimensional stability following processing [1,2]. To address these issues, combination of TPU and NR was addressed through the incorporation of ENR as a compatibilizer. Dynamically vulcanized TPU/NR blends with varying ENR contents were prepared using an internal mixer before evaluating their effects on blend's properties. It was found that the addition of ENR significantly enhanced the mechanical properties of the TPU/NR blends, including tensile strength, elongation at break, and toughness. Notably, the formulation containing 3 phr ENR exhibited the highest impact strength and energy absorption, attributed to enhanced shear viscosity and improved interfacial interactions between the polar functional groups of TPU and ENR [3,4]. Furthermore, ENR promoted efficient dispersion of rubber domains within the TPU matrix. However, excessive ENR content (>3 phr) led to rubber particle agglomeration, resulting in diminished mechanical performance. The optimal formulation containing 3 phr ENR was selected for 3D printing trials. Successful printing was achieved at a nozzle temperature of 210 °C, bed temperature of 60 °C, and print speed of 7 mm/s, yielding smooth surfaces and structurally robust components. Preliminary trials demonstrated the ability to fabricate complex honeycomb structures with high flexibility and good structural integrity. However, higher rubber content resulted in nozzle clogging, indicating the need for further refinement of both material formulation and processing parameters as can be seen that proposed prototype in Figure 1.

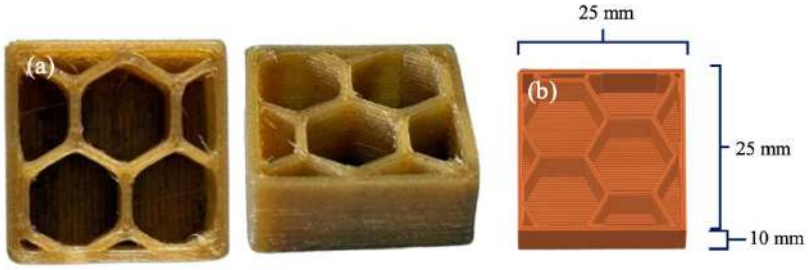


Figure 1. (a) 3D-printed structures fabricated using a TPU/NR-ENR 95/5 blend containing 3 phr of ENR, and (b) 3D model of the honeycomb structure.

Acknowledgement

This work was supported by the Petchra Pra Jom Klao Master's Degree Research Scholarship from King Mongkut's University of Technology Thonburi. Also, this research project is supported by King Mongkut's University of Technology Thonburi (KMUTT), Thailand Science Research and Innovation (TSRI), and National Science, Research and Innovation Fund (NSRF) Fiscal year 2025 Grant number FRB680074/0164.

References

1. Pichaiyut S, Nakason C, Vennemann N, *Iran Polym. J.*, 2012; 21: 65.
2. Kalkornsurapranee E, Nakason C, Kummerlöwe C, Vennemann N, *J. Appl. Polym. Sci.*, 2013; 128: 2358.
3. Pongdong W, Kummerlöwe C, Vennemann N, Thitithammawong A, Nakason C, *J. Polym. Environ*., 2018; 26: 1145.
4. Nakason C, Pichaiyut S, Vennemann N, Kaesaman A, *Polym. Bull*., 2023; 80: 8627.

International Rubber Conference 2025 (IRC2025)
1-3 December 2025 @ BITEC, Bangkok, Thailand

Development of Natural Rubber Insulating Gloves: Influence of Latex Centrifugation and Leaching on Mechanical and Electrical Properties

Promsak Sa-nguanthammarong[1], Chayapha Nimsuwan[1], Chotiros Dokkhan[1], Bundit Putasaeng[1]

[1] *National Metal and Materials Technology Center, 114 Thailand Science Park, Khlongluang, Pathumthani, Thailand.*

e-mail address of the presenting author (promsaks@mtec.or.th)

Keywords: Natural rubber latex, Insulating glove, Leaching, Mechanical properties, Dielectric strength

This research aims to develop natural rubber insulating gloves for high voltage applications through the systematic optimization of latex grade, compounding formulation, and leaching conditions. This study responds to national initiatives aimed at increasing domestic value creation and supports end-user needs in the Provincial Electricity Authority, by developing insulating gloves that conform to international standards such as ASTM D120-14a and IEC 60903:2014.

Previous studies have highlighted natural rubber's potential as an effective electrical insulator [1-3], and its dielectric performance can be enhanced through material purification and nanoparticle incorporation [4]. Building on this foundation, rubber sheets (Figure 1) were prepared using latex concentrates obtained via single and double centrifugation. These were compounded with customized additives (Table 1) and subjected to leaching treatments in water and sodium dodecyl sulphate (SDS) across varied temperatures and durations.

The results showed that double-centrifuged latex exhibited superior dielectric strength up to 15.4 kV/mm in unvulcanised form, attributed to its lower non-rubber contents. After compounding, leaching significantly enhanced both mechanical and electrical properties, with SDS treatment at ambient temperature for 24 hours providing optimal outcomes. The post-leaching samples met all mechanical performance requirements and showed comparable results to commercial gloves (Table 2). Additionally, extractable protein content was effectively reduced to as low as 25 µg/g, which is well within the range observed in commercial products (13–36 µg/g).

In conclusion, the study demonstrates that controlled latex purification, compounding, and leaching can potentially produce insulating gloves that meet international standards for both mechanical performance and electrical insulation. These findings support the potential for domestic glove production, reducing reliance on imports and aligning with national policies aimed at promoting the utilization and value enhancement of natural rubber.



Figure 1. Rubber sheet sample preparation

Table 1. Compounding formulation

Ingredient	Parts per hundred rubber (phr)
Concentrated natural rubber latex	100
KOH	0.10
ZnO	0.25
ZDBC	0.25
Sulphur	0.75
Antioxidant	0.75
Polyvinyl methyl ether	0.80

Table 2. Mechanical property requirement and comparison of commercial insulating gloves and study samples

Property	Requirement	Commercial 1	Commercial 2	SC-LCS*	DC-LCS**
200% Modulus (MPa)	2.1 (max)	1.06 ± 0.03	0.83 ± 0.01	0.82 ± 0.05	0.84 ± 0.03
Tensile Strength (MPa)					
- Before aging	17.2 (min)	26.8 ± 1.6	28.3 ± 1.3	19.5 ± 0.5	21.8 ± 0.4
- After aging 70°C, 7d	>80% of original	97%	95%	87%	87%
%Elongation at break					
- Before aging	600 (min)	817 ± 14	919 ± 12	769 ± 36	800 ± 26
- After aging 70°C, 7d	>80% of original	99%	98%	108%	105%
%Tension set at 400%	25 (max)	2.1 ± 0.2	2.6 ± 0.1	4.0 ± 0.5	4.0 ± 0.3
Tear Strength (kN/m)	21 (min)	47.9 ± 3.9	44.8 ± 4.3	43.6 ± 5.7	42.0 ± 3.8
Hardness (Shore A)	47 (max)	41.0 ± 1.0	39.0 ± 0.9	37.2 ± 0.8	37.1 ± 0.7

*single centrifuge latex compound sheet, **double centrifuge latex compound sheet

Acknowledgement

The authors gratefully acknowledge the support from the Provincial Electricity Authority (PEA), Thailand, for funding the research under the project “Research and Development of Natural Rubber Gloves for High Voltage Electrical Work” Project No. C-056-62.

References

1. Junian S, Makmud M, and Sahari J, Natural Rubber as Electrical Insulator: A Review. *Journal of Advanced Review on Scientific Research*. 2015; 6: 28-42.
2. Roland CM. Electrical and Dielectric Properties of Rubber. *Rubber Chemistry and Technology*. 2016; 89(1): 32-53.
3. González N, Custal M, Lalaouna S, Riba J-R, Armelin E. Improvement of dielectric properties of natural rubber by adding perovskite nanoparticles. *European Polymer Journal.* 2016; 75: 210-22.
4. Mathew S, Varghese S. Effect of Compounding Characteristics on Heat Sensitization of PVME Blended Natural Rubber Latex Compound. *International Journal of Innovative Research and Development.* 2015; 4(8): 232-9.

International Rubber Conference 2025 (IRC2025)
1-3 December 2025 @ BITEC, Bangkok, Thailand

Evaluation of a Non-Traditional Preservative System for Enhancing Natural Rubber Latex Stability

Maneephan Sukkho[1] and Jitladda Sakdapipanich[1,2*]

[1]*Rubber Research Group, Department of Chemistry, Faculty of Science,*
Mahidol University, Nakhon Pathom 73170, Thailand.

[2]*The Rubber and Rubber Glove Academician Association, Bangkok 10900, Thailand*

Presenting author: maneephan.suk@student.mahidol.edu

*Corresponding author: jitladda.sak@mahidol.ac.th

Keywords: Natural rubber, Non-Carcinoganic, Preservative, Latex stability, Sustainable

Natural Rubber (NR) latex, a colloidal biopolymer consisting of rubber particles dispersed in an aqueous medium, is prone to destabilization under ambient conditions, resulting in coagulation and odor formation that adversely affect its processing and performance. Preservatives are thus commonly added during storage to maintain latex quality. Currently, ammonia serves as the primary preservative, while tetramethyl thiuram disulfide/zinc oxide (TMTD/ZnO) is used as a secondary preservative system. However, oncerns regarding the carcinogenic potential of TMTD/ZnO due to nitrosamine formation have prompted the search for safer alternatives.

This study investigates the performance of a novel preservative system compared to TMTD/ZnO over an 84-day storage period. Both preservative systems yielded NR latex that complied with ISO quality standards. The new preservative-treated latex (CNR-PA) exhibited a higher mechanical stability time (MST) during early storage, although it decreased after 84 days, whereas CNR-TZ displayed an increasing MST trend. Despite these differences, both systems maintained volatile fatty acid (VFA) values below 0.06, indicating effective microbial suppression. Viscosity measurements showed that CNR-TZ samples consistently exceeded 60, while CNR-PA maintained a steady value of 100 throughout the entire storage period.

Significantly, the new system reduced the zinc content to 36.83 ppm compared to 330.28 ppm in the TMTD/ZnO system as shown in Figure 1., offering a more environmentally responsible approach. Gel content increased over time for both formulations. The yellow index (YI) of CNR-PA started lower (8.2) than that of CNR-TZ (13.8) but surpassed it by the end of storage. Atomic force microscopy (AFM) analysis revealed comparable surface topography and nanomechanical characteristics between samples.

Collectively, these results demonstrate that the new preservative system provides a viable alternative to conventional TMTD/ZnO, offering comparable latex stability and mechanical quality, with the added advantages of lower environmental impact and improved sustainability.

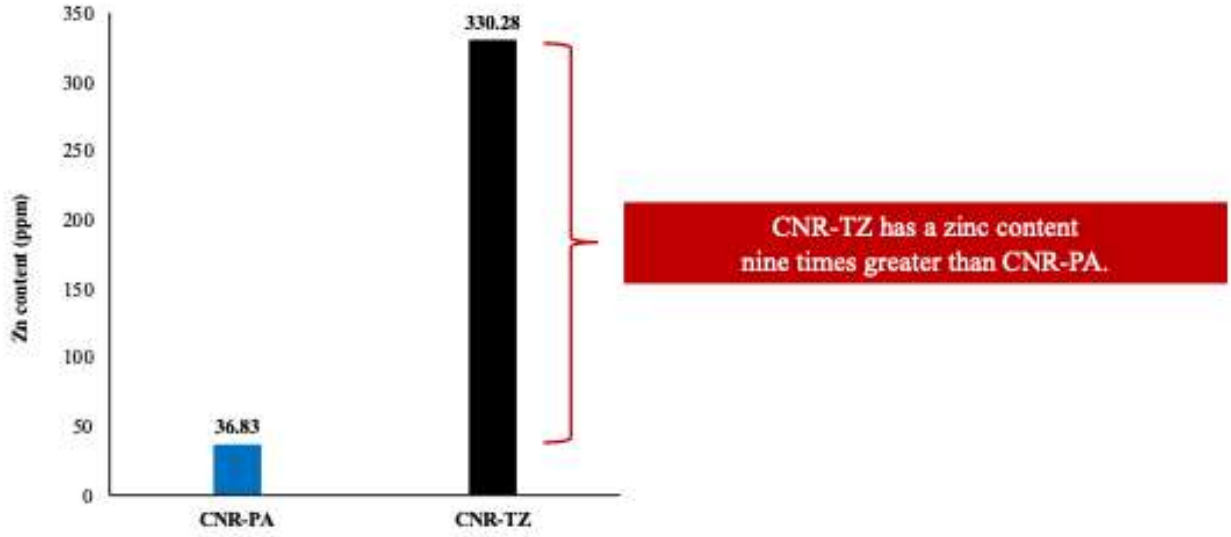


Figure 1. Zinc Content of Natural Rubber Latex Preserved with Conventional TMTD/ZnO and the Novel preservative System

Acknowledgement

The authors express their gratitude to the Thai Rubber Latex Group Public Company Limited for supplying fresh natural rubber latex, and to the KaO Thailand for providing new preservative.

Reference

1. Rojruthai P, Rodgerd P, Ho C.C, Sakdapipanich J, *J Rubber Res*, 2021; 24(5): 783.

Study on the Impact of Purified Natural Rubber Latex and Accelerators on Rubber Allergens in Natural Rubber Gloves

Pitchaya Theedee[1], Jinjutha Wiriyanantawong[1] and Jitladda Sakdapipanich[1,2*]

[1] *Rubber Research Group, Department of Chemistry, Faculty of Science, Mahidol University, Nakhon Pathom 73170, Thailand*

[2] *The Rubber and Rubber Glove Academician Association, Bangkok, 10900, Thailand*

Presenting author: pitchayatheedee@gmail.com

*Corresponding author: jitladda.sak@mahidol.ac.th

Keywords: Natural rubber (NR), NR glove, Rubber allergens, Purified NR, Rubber accelerators

Natural rubber (NR) gloves are widely used as personal protective equipment, especially in medical and industrial fields, to prevent the transmission of infectious diseases. However, the use of NR gloves can lead to latex protein allergies, which is a common problem among users, particularly those who come into direct contact with latex for prolonged periods. This issue has resulted in numerous complaints about protein allergies from medical glove users in recent years, prompting the development of processes to reduce allergens in NR latex, including washing techniques to eliminate proteins and chemical allergens that may be present in the latex. However, the development of technology to eliminate allergens from latex remains crucial for creating safer products for users.

This research aims to study the purification of NR latex and its application in preparing gloves using an allergen-free rubber compound formula, to develop NR gloves that are free from allergens, thus reducing the risk of protein allergies. The purification of NR latex in this study was carried out using deproteinization and saponification methods. Deproteinization helps reduce the amount of protein in NR latex, while saponification reduces potential allergens in the latex. Both methods were analyzed using various techniques, such as chemical testing and protein analysis as shown in Figure 1, the FTIR spectra reveal that the broad band around 3280 cm^{-1}, corresponding to N–H stretching, clearly disappears in the DPNR and SPNR samples. These findings are consistent with the measured nitrogen content. The evaluation any remaining allergens in the latex. The experimental results showed that latex processed by saponification, or saponified NR (SPNR), is a highly purified latex with no allergenic proteins present. This makes it the least likely to cause Type I allergies compared to untreated natural latex.

Subsequently, NR gloves were prepared using rubber compound formulas with different accelerators, such as zinc diethyldithiocarbamate (ZDEC), zinc dibutyldithiocarbamate (ZDBC), and zinc-2-mercaptobenzothiazole (ZMBT). The tests showed that when substances were extracted from the gloves using artificial sweat, ZDBC was not detected, indicating that ZDBC poses the least risk for Type IV allergies compared to the other accelerators. In terms of evaluating the morphological and physical properties of the rubber films, it was found that the films made from SPNR latex mixed with ZDBC were thinner and lighter in color than typical rubber films, with a more uniform internal structure shown on Figure 2. They also exhibited mechanical properties comparable to commercial

NR gloves, demonstrating the potential for developing and using allergen-free products to reduce the risk of protein allergies in users of natural rubber gloves.

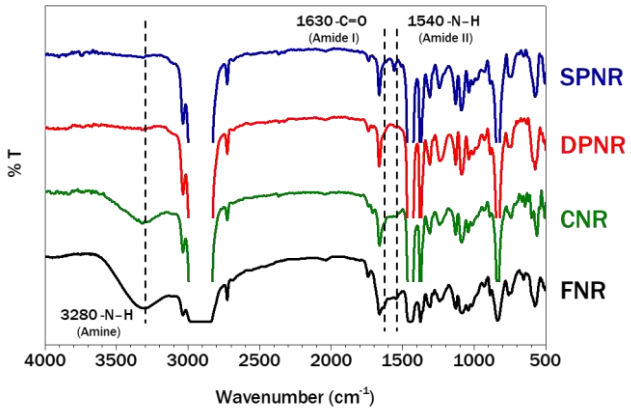


Figure 1. FTIR spectra of FNR, CNR, DPNR, and SPNR.

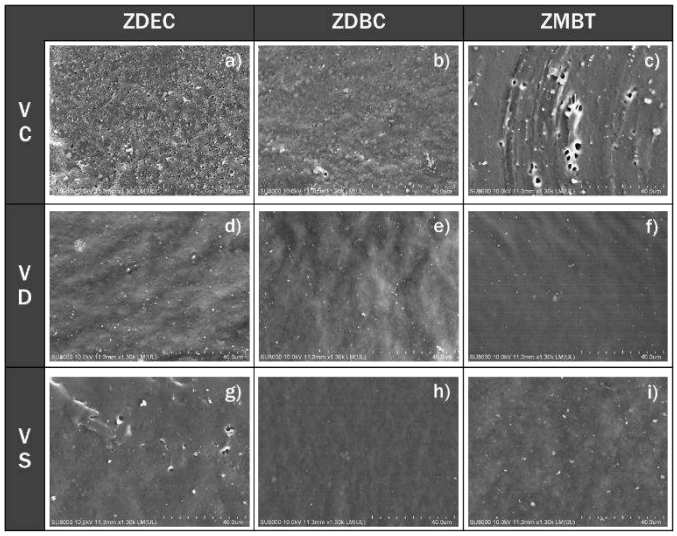


Figure 2. SEM images of a cross-section of finger cots prepared from various latex types and accelerators.

Acknowledgement

The authors gratefully acknowledge the financial support from Thai Rubber Latex Group Public Company Limited.

References

1. Mylon, P.; Lewis, R.; Carré, M. J.; Martin, N.; Brown, S. *Am. J. Infect. Control* **2014**, *42*(1), 48–54.
2. Ownby, D. R. *J. Allergy Clin. Immunol.* **2002**, *110*(2), S27–S32.

International Rubber Conference 2025 (IRC2025)
1-3 December 2025 @ BITEC, Bangkok, Thailand

Optimized UVA-Irradiation Silane-Grafting onto Saponified Skim Rubber for Enhanced Silica-Natural Rubber Compatibility

Areeya Anuwatprakit[1], Apisara Sillapasuwan[1] and Jitladda Sakdapipanich[1,2]

[1]*Rubber Research Group, Department of Chemistry, Faculty of Science,*

Mahidol University, Nakhon Pathom 73170, Thailand.

[2]*The Rubber and Rubber Glove Academician Association, Bangkok 10900, Thailand*

Presenting author: areeya.anw@student.mahidol.edu

*Corresponding author: jitladda.sak@mahidol.ac.th

Keywords: Natural rubber, Silica, Silane coupling agent, Grafting, UVA irradiation, Compatibility

Silica is extensively utilized as a reinforcing filler in the rubber industry due to its capility to enhance mechanical strength and durability. However, the incorporation of silica into natural rubber (NR) often results in poor interfacial compatibility, primarily due to the inherent polarity mismatch between the r non-polar rubber matrix and the polar filler. non-polar rubber matrix and the polar

This study proposes a surface modification strategy as shown in Figure 1. in which a silane coupling agent (KBM-502) is grafted onto saponified skim natural rubber (SSNR) *via* UVA irradiation, employing benzoyl peroxide (BPO) as the photo-initiator. SSNR, a low-cost by-product possessing a linear molecular structure, was selected for its favorable reactivity toward chemical grafting.Optimal grafting conditions were identified as 1 phr of KBM-502 and 5 phr of BPO under 8 minutes of UVA exposure. The resulting grafted rubber (G-SSNR) was subsequently incorporated into silica-filled NR compounds. These modified formulations exhibited markedly enhanced silica dispersion, diminished filler-filler interactions, increased bound rubber content, and accelerated vulcanization behavior. In contrast, the direct incorporation of free KBM-502 yielded only limited improvements.

Furthermore, the use of G-SSNR resulted in increased modulus and tensile strength without compromising elongation at break. This surface grafting strategy offers a promising and energy-efficient route for producing high-performance NR composites with enhanced silica compatibility and processability under mild processing conditions. processing conditions.

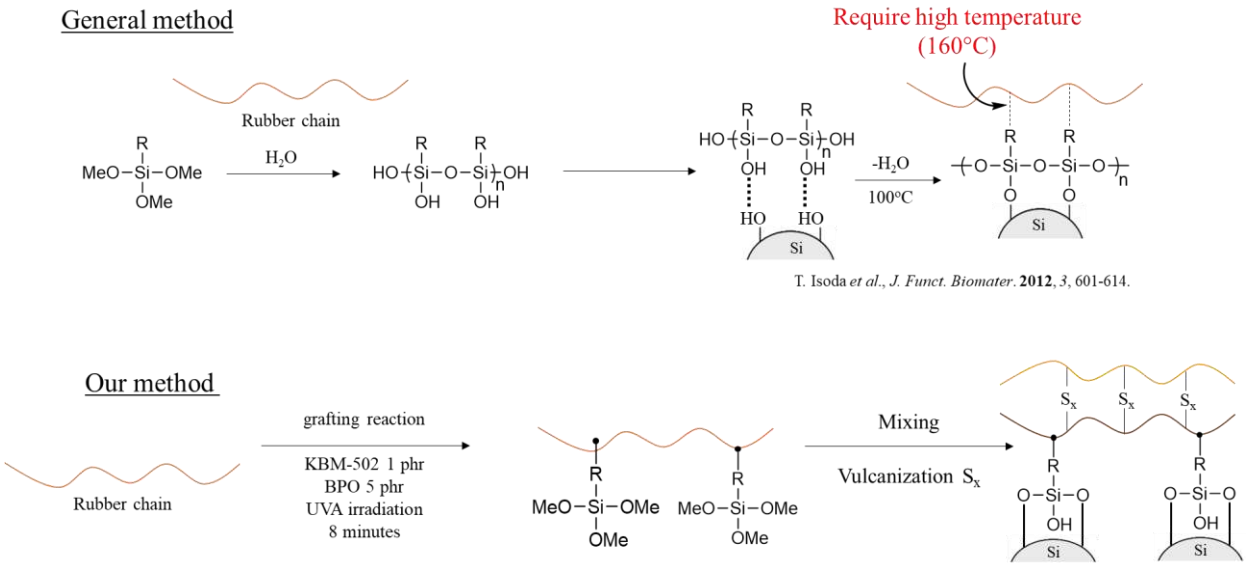


Figure 1. Silane coupling mechanism comparison between conventional blending and UVA-induced grafting onto SSNR

Reference

1. Dechnarong, N.; Nimpaiboon, A.; Kumarn, S.; Phinyocheep, P.; Sakdapipanich, J. Surface modification of natural rubber for silica compatibility. Journal of Polymer Research 2017, 25, 17. https://doi.org/10.1007/s10965-017-1177-3

Strain-induced crystallization behaviors of natural rubber with additional lipids

Tomoaki Nakatsuka[1], Yui Tsuji[1], Masunaga Hiroyasu[2], Keiji Numata[1,3]

[1] *Kyoto university department of material chemistry, Kyoto, Japan.*

[2] *Japan Synchrotron Radiation Research Institute, Harima, Japan.*

[3]*RIKEN Center for sustainable resource science, Wako, Japan*

nakatsuka.tomoaki.42n@st.kyoto-u.ac.jp

Keywords: Natural rubber, Non-rubber component, Lipid, Strain-induced crystallization

Natural rubber (NR) is widely used in various fields of our daily life, particularly in the tire industry, due to its superior properties such as good elasticity, high tensile strength and crack growth resistance. These outstanding properties are believed to arise from a phenomenon called strain-induced crystallization (SIC), which is caused by the alignment of polymer chains during stretching. Generally, SIC in NR is known to occur at lower strains compared to synthetic *cis*-1,4-polyisoprene rubber. However, the promoting factor and the mechanism of SIC have not been clarified yet.

The most plausible hypothesis is non-rubber components such as proteins and lipids in NR act as cross-linking points by interacting with NR chain ends [1]. Recent advanced NMR analysis clarified that NR molecules have an α-terminal, which has been identified as containing ester or hydroxyl groups, at one end, and an ω-terminal, which is connected to *trans*-oligoisoprene units, at the other end [2]. Furthermore, computational study has shown that the α-terminal is likely to interact with the hydroxyl groups of non-rubber components via hydrogen bonding [3]. Given this hypothesis, the current study aims to clarify the role of non-rubber components with hydroxyl groups, particularly lipids, in influencing the SIC performance of NR.

Here, three different lipids in number of possessing hydroxyl group depending on the number of stearic acids bound to glycerol—glycerol monostearate (GMS), glycerol distearate (GDS), and glycerol tristearate (GTS)—were mixed with NR, and their effects on SIC behavior were examined by WAXD measurement under stretching conditions (Fig.1). The result showed that, contrary to the initial hypothesis, an increase in the number of hydroxyl groups of additional lipids did not enhance the SIC property. Instead, GTS microcrystals acted as nucleating agents and promoted the SIC onset. In contrast, GMS and GDS did not act as nucleating agents, and rather delayed the SIC onset by simply reducing the crosslinking density (Fig.2). Therefore, the nucleating effect of GTS is attributed to the combination of the strong affinity with NR ensured by high hydrophobicity and its high crystallization ability due to efficient packing of its alkyl chains. These findings indicate the rate-limiting step in SIC is in the nucleation process, and SIC can be promoted by nucleating agents, maximizing crystallinity at a given strain. In addition, we conclude that hydroxyl groups of additional lipids are unlikely to interact with the α-terminal of NR chains to promote SIC in this solution mixing method. This new insight will help to deepen the understanding of SIC behavior in NR [4].

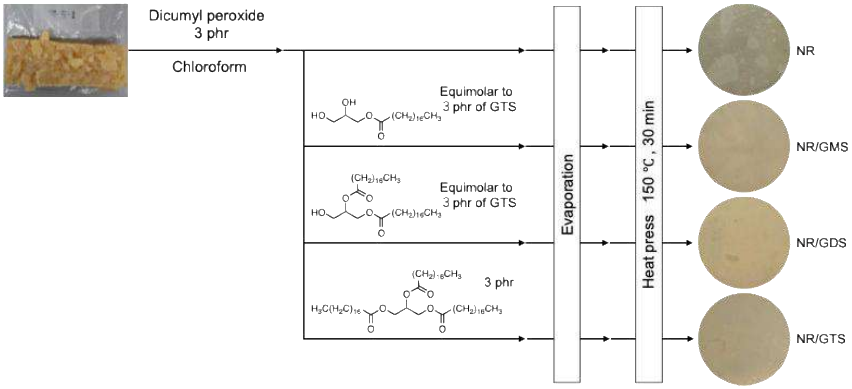


Figure 1. The sample preparation process of NR, NR/GMS, NR/GDS, and NR/GTS.

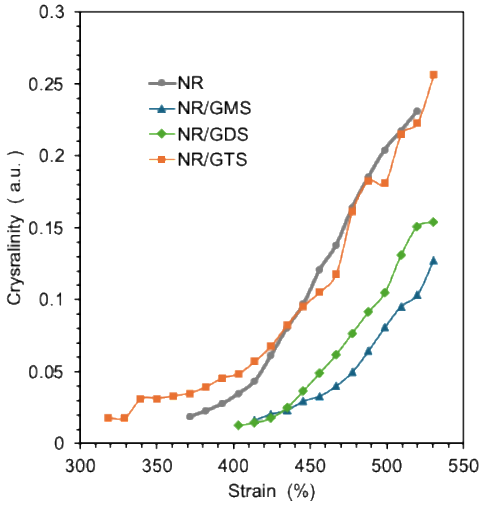


Figure 2. Crystallinity index of NR, NR/GMS, NR/GDS, and NR/GTS as a function of strain.

Acknowledgement

This work was supported by Japan Science and Technology Agency CREST (Grant Number JPMJCR2091), JST COI-Next (Grant Number JPMJPF2114), and the MEXT Program: Data Creation and Utilization-Type Material Research and Development Project (Grant Number JPMXP1122714694), Japan. The X-ray experiments were performed at BL05XU of SPring-8 (Harima, Japan). Sincere appreciation is extended to Bridgestone Corporation for kindly providing the natural rubber samples.

References

1. Y.Tanaka, *Rubber Chem. Technol.*, **2001**, *74*(3), 355-375.
2. M. Oouchi, J. Ukawa, Y. Ishii, H. Maeda, *Biomacromlecules*, **2019**, *20*(3), 1394-1400.
3. J. Gimenez-Dejoz, K. Tsunoda, Y. Fukushima, K. Numata, *Polym. J.* **2021**, *54*(2), 229-233.
4. T. Nakatsuka, H. Masunaga, Y. Tsuji, K. Numata, *Polymer*, **2025**, *332*, 128575.

Light-driven latex engineering: Scalable photopolymerization for semicrystalline polythioether nanoparticles

Cuong-Minh-Quoc Le[1,2], Arnaud Spangenberg[1,2], Karine Mougin[1,2], Abraham Chemtob[1,2*]

[1]*Institut de Science des matériaux de Mulhouse (CNRS)*

[2]*Université de Haute-Alsace*

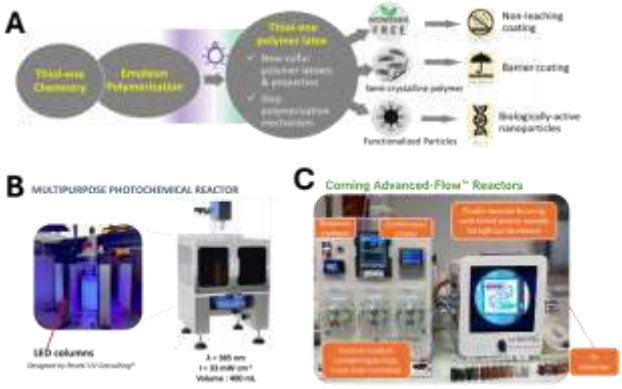
[1] *15 rue Jean Starcky, 68057 Mulhouse, France*

[2] *2 Rue des Frères Lumière, 68093 Mulhouse Cedex, France.*

*E-mail: abraham.chemtob@uha.fr

Abstract

Visible-light emulsion photopolymerization presents a disruptive approach for next-generation synthetic latex production, offering both process scalability and material property innovation. We have developed LED-based batch and flow photoreactor platforms (10–500 mL), enabling ambient temperature polymerization of thiol-ene monomer pairs to yield colloidally stable latexes with >97% monomer conversion in under one hour and solid content up to 40 wt%. By employing photocatalyzed thiol-ene chemistry (lithium acyl phosphinated salt for UV-LED 385 nm, or eosin-Y for green-LED 530 nm), we obtain semicrystalline poly(thioether) latexes with tunable molecular weights (6–13 kg mol^{-1}), narrow particle size distributions (~70–100 nm), and crystallinity up to 45%, confirmed by DSC and XRD. The crystalline is modulated by monomer structure, offering design control over thermal properties and mechanical performance. Mechanistic studies reveal enhanced polymerization kinetics under air, and real-time process control via light intensity. The developed platforms and structure-property relationships open promising questions: Can photopolymerization-based modifications introduce crystallinity or functional coatings to natural rubber latex for advanced applications? How can scalable light-driven processing support zero-carbon and quality consistency targets in industrial latex production? Collaboration opportunities are invited to bridge synthetic photochemistry and natural rubber technologies.



Scheme 1: (A)Thiol-ene emulsion photopolymerization and its potentials for sustainable latex production, (B,C) batch and continuous photoreactors for up-scaled production of latex.

Keywords: *Emulsion photopolymerization, Thiol-ene chemistry, Semicrystalline latex, Poly(thioether) nanoparticles*

References

1. C. M. Q. Le, G. Schrodj, I. Ndao, B. Bessif, B. Heck, T. Pfohl, G. Reiter, J. Elgoyhen, R. Tomovska, A. Chemtob, *Macromol. Rapid Commun.* **2022**, *43*, e2100740.

2. C. M. Q. Le, A. Chemtob, *J. Polym. Sci.* **2022**, *61*, 323.

3. C. M. Q. Le, M. Schmutz, A. Chemtob, *Macromolecules* **2020**, *53*, 2369.

Session II : Advancements in Sustainable Rubber Technology

Poster Presentations

International Rubber Conference 2025 (IRC2025)
1-3 December 2025 @ BITEC, Bangkok, Thailand

Preparation of high performance rubber nanocomposites by complex coupling agent system

Dengfeng Shi[1], Hong Yao[2], Xuan Qin[3], Liqun Zhang[*4]

The Key Laboratory of Beijing City on Preparation and Processing of Novel Polymer Materials, Beijing University of Chemical Technology, Beijing, People's Republic of China[*]

e-mail. 2574913974@qq.com

Keywords: Dispersion, Silica, Silica/SSBR composites

Silica is a key filler in the manufacture of green tires, yet its high surface energy and abundance of surface hydroxyl groups lead to poor compatibility and aggregation within the rubber matrix. To overcome these drawbacks, silane coupling agents are employed to enhance silica dispersion and interfacial bonding. In this study, a novel compound silane coupling system based on the synergistic reactivity of 3-aminopropyltriethoxysilane (KH-550) and 3-(glycidoxypropyl)triethoxysilane (KH-561) was developed to replace the conventional bis-[3-(triethoxysilyl)propyl]-disulfide (Si-75). The coupling system was evaluated using solution-polymerized styrene-butadiene rubber (SSBR)/silica nanocomposites prepared by an internal mixing process. Experimental characterization included Payne effect, tensile and dynamic mechanical analyses, abrasion, and heat build-up tests. The results demonstrate that the KH-550/KH-561 system markedly enhances silica dispersion and interfacial interaction, leading to a 25.4% increase in wet-slip resistance, a 25.5% reduction in abrasion loss, and a significant decrease in rolling resistance compared with Si-75. Moreover, the proposed system uses readily available, lower-cost silanes, offering improved performance without increasing material costs, thus providing a more sustainable and economically feasible coupling strategy for green tire production.

A Synergistic Enhancement of Bio-Based Eucommia Ulmoides Gum Nanocomposites through Epoxidized Natural Rubber and Silane Coupling Agent Integration: Advancements in High-Performance Engineering Tires

ZHİ CHEN[1,2], DEXIAN YIN[1,2], JICHUAN ZHANG[1,2], XIUYING ZHAO[1,2]

[1] *State Key Laboratory of Organic-Inorganic Composites, Beijing University of Chemical Technology, Beijing, China.*

[2] *Beijing Engineering Research Center of Advanced Elastomers, Beijing University of Chemical Technology, Beijing, China.*

chenzhi199911@163.com, zhaoxy@mail.buct.edu.cn

Keywords: Epoxidized natural rubber, Eucommia ulmoides gum, Silica, Nanocomposite, High-performance engineering tires

As the demand for high-performance engineering tires increases, tire materials are required to simultaneously achieve reduced rolling resistance, lower heat generation, and improved wear and cut resistance under increasingly complex service conditions [1]. In this work, a novel nanocomposite based on Eucommia ulmoides gum (EUG), natural rubber (NR), and styrene-butadiene rubber (SBR), reinforced with silica, was developed. To address the issue of silica agglomeration, epoxidized natural rubber (ENR (50% epoxidation degree)) was introduced into the EUG/NR/SBR (20/40/40) matrix (The content of silica and coupling agent bis[3-(triethoxysilyl)propyl]tetrasulfide are 60 phr and 6 phr respectively). Primarily, the interaction between ENR and silica was explored. As shown in **Figure 1,** the results demonstrate that ENR reduces the surface activity of silica via hydrogen bond effect and grafting reaction [2], thus enhancing the silica dispersion.

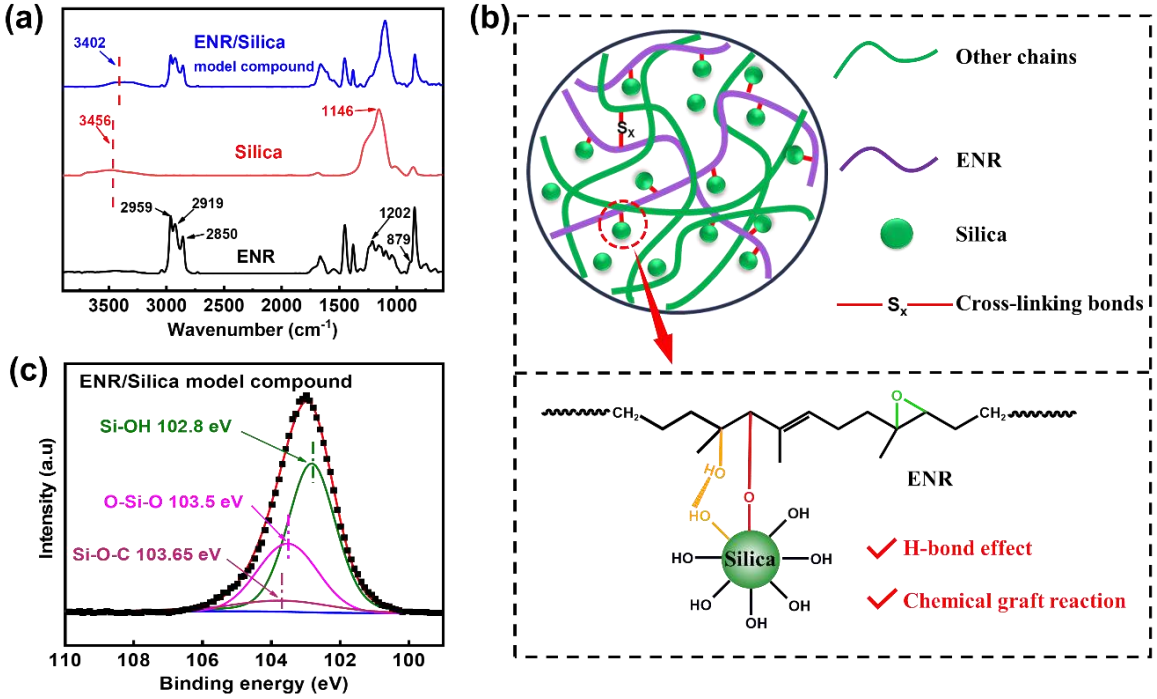


Figure 1. (a) FTIR spectra of ENR, silica and ENR/silica model compound; (b) XPS high-resolution spectra of ENR/silica model compound (c) Schematic diagram of the enhancement mechanism of ENR.

Furthermore, the influence of ENR dosage on the filler network structure of nanocomposite was investigated. As ENR content increases, silica dispersion within the nanocomposites improves, improved the static and dynamic mechanical properties of the nanocomposites, as shown in **Figure 2**. Specifically, the dynamic temperature rise is 25.6°C with a reduction of 12.2%, and the Akron abrasion volume is 0.135 $cm^3 \cdot 1.61\ km^{-1}$ with a reduction of 21.1% at an ENR content of 9 phr, compared to the NR/SBR/EUG nanocomposites without the ENR addition. Furthermore, the dynamic cutting volume and tear strength are 2.35 g and 65 $kN \cdot m^{-1}$, which is qualified for application standards of high-performance engineering tires.

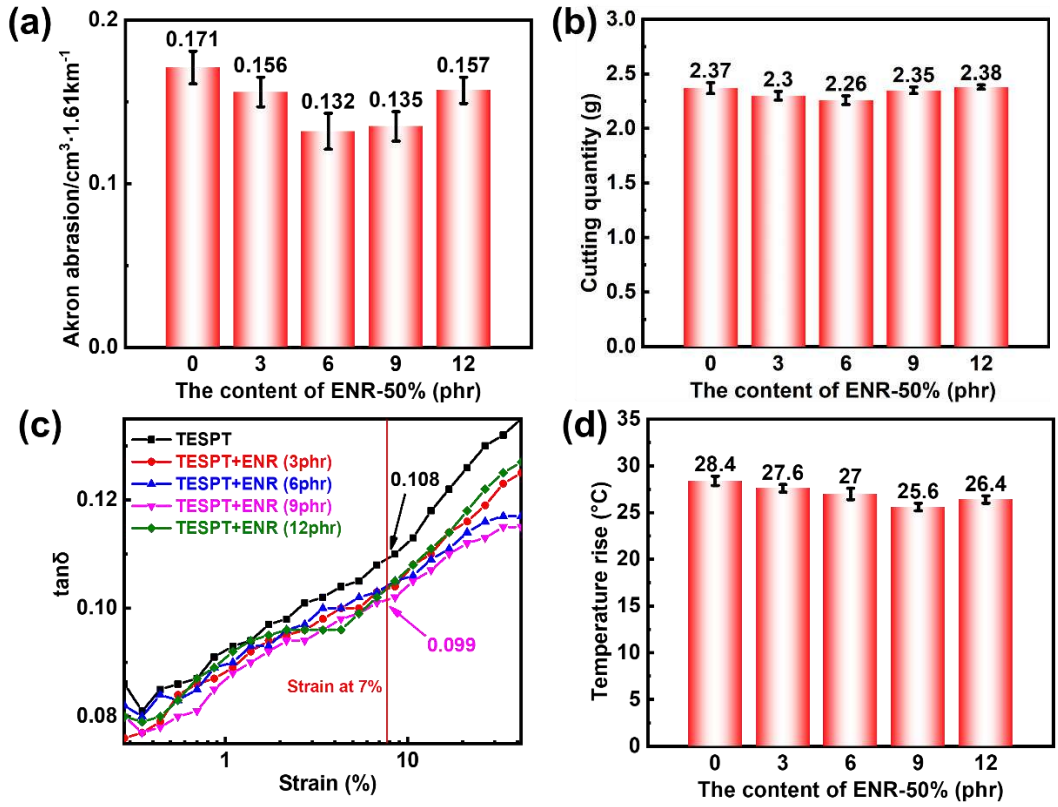


Figure 2. (a) Akron abrasion, (b) cut resistance, (c) curves of tan δ-strain at 60°C and (d) temperature rise of EUG/NR/SBR nanocomposites with different ENR dosages.

Acknowledgement

This work was supported by the National Natural Science Foundation of China [grant numbers 52250357].

This work has been published in [*Journal of Polymer Science*, 2025]

References

1. Z. Chen, Q. Dong, X. Wang, S. Hu, D. Yin, L. Liu, J. Zhang and X. Zhao, *Ind. Crops Prod.*, 2024, 208, 117911.
2. S. Li, X. Zhai, Z. Chen, D. Han, X. Ye and L. *Zhang, Compos. Commun.*, 2024, 46, 101836.

Synthesis and Application of Novel Green Coupling Agents in Silica/Natural Rubber Composites

Shuaiqi Li[1], Xin Ye[1]

[1] *Engineering Research Center of Elastomer Materials on Energy Conservation and Resources, Ministry of Education, Beijing University of Chemical Technology, Beijing 100029, PR China.*

E-mail: lsq5018@163.com; yexin@buct.edu.cn

Keywords: Coupling agents, silica/natural rubber composites, rolling resistance, wet skid resistance.

Nowadays, tires are widely used in automobiles due to their reliability and stability. In the rubber industry, the rolling resistance, abrasion resistance, and wet skid resistance of tires directly influence fuel efficiency, service life, and driving safety, respectively. These three key performance indicators are interrelated and often mutually restrictive, making it difficult to enhance them simultaneously. As such, they are collectively referred to as the "magic triangle" of tire performance [1]. In the context of energy shortages and the pursuit of green development, the advancement of high-performance tires has become an inevitable trend. Natural rubber (NR), as a biomass-based material, possesses excellent processing and mechanical properties. To enhance its overall performance, inorganic fillers such as carbon black and silica are commonly added in the rubber industry. Silica, as an eco-friendly reinforcing filler, effectively reduces rolling resistance and has therefore gained widespread use in tire manufacturing. Nevertheless, the abundant polar silanol groups on the surface of silica result in poor compatibility with NR, easy agglomeration, and weak interfacial interaction. Consequently, silica is typically used in combination with coupling agents.

Currently, the most widely used industrial coupling agent is bis-[γ-(triethoxysilyl) propyl] tetrasulfide (Si69). However, its reaction with silica generates a large amount of ethanol (volatile organic compound, VOC), which poses challenges to environmental protection and sustainable development. Currently, long-chain coupling agents such as γ-mercaptopropyl-ethoxy-bis-(tridecyl-pentaethoxy-siloxane) (Si747) can be utilized to replace conventional silane coupling agents, or epoxidized styrene-butadiene rubber (E-SBR) can be employed to avoid the use of coupling agents, thereby reducing VOC emissions [2-3]. In this work, a novel coupling agent, A3M1, was synthesized by reacting Si69 with aliphatic alcohol polyoxyethylene ether (AEO3) as the monomer. The reaction is illustrated in Fig. 1. The presence of polyether long chains is expected to inhibit VOC emissions during the subsequent reaction of A3M1 with silica.

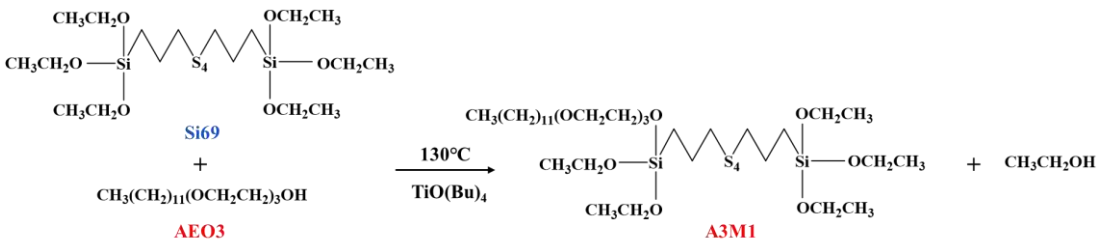


Figure 1. Synthesis reaction of A3M1.

To evaluate the potential application of A3M1 in silica/NR composites, the effects of different coupling agents (Si69, A3M1, and Si747) on the comprehensive performance of the composites were investigated. The experimental formulations are shown in Table 1. The silica/NR composites and

coupling agent as well as other additives are successively mixed in a HAAKE internal mixer and in a two-roller mill. The rubber compound is vulcanized in a plate vulcanizer at 150°C. The results demonstrated that the long polyether alkyl chains in A3M1 could form hydrogen bonds with the silanol groups on silica surface, effectively improving silica dispersion. Compared with Si69, the use of A3M1 reduced the rolling resistance of silica/NR composites by 16.7%, enhanced wet skid resistance by 12.8%, reduced heat build-up and maintained excellent abrasion resistance.

Table 1. Formulation of silica/NR composites with different coupling agents.

Components [phr]	**Sample notations**			
	Pure Silica	**Si69**	**A3M1**	**Si747**
NR[a]	100	100	100	100
Silica	50	50	50	50
ZnO	5	5	5	5
Coupling Agents[b]	0	5	5	5
Stearic acid	2	2	2	2
Accelerator[c]	2.5	2.5	2.5	2.5
Antioxidant[d]	2	2	2	2
Sulfur	2	2	2	2

[a] Natural rubber. [b] Coupling Agents represents Si69, A3M1, and Si747 respectively. [c] 2 phr N-cyclohexyl-2-benzothiazole sulfonamide, 0.5 phr Tetrabenzylthiuram Disulfide. [d] N-1,3-dimethylbutyl-N'-phenyl-p-phenylenediamine.

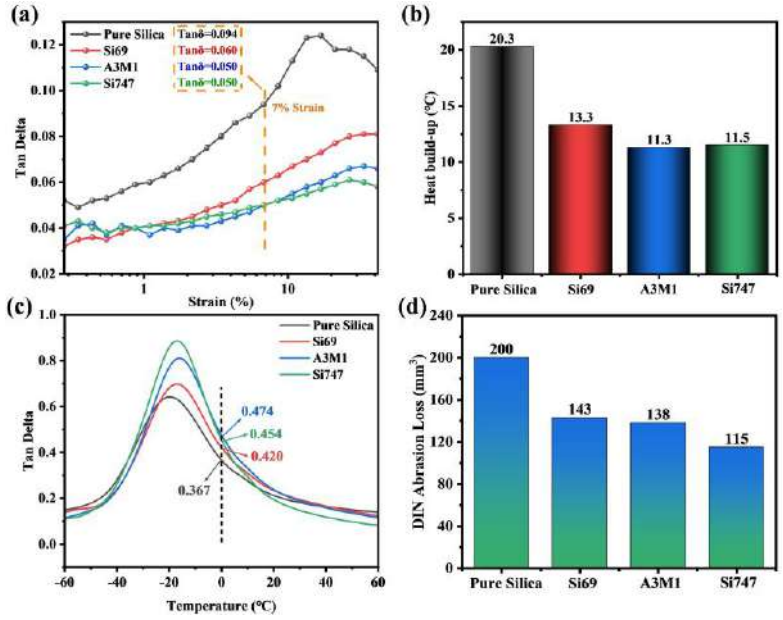


Figure 2. (a) Tan Delta-strain curves at 60°C, (b) Heat build-up, (c) DMA curves and (d) DIN abrasion loss of silica/NR composites.

Acknowledgement

This research did not receive any specific grant from funding agencies in the public, commercial, or not-for-profit sectors.

References

1. Li S Q, Zhai X B, Chen Z, et al. *Compos. Commun.*, 2024; 46: 101836.
2. Pang S, Yang Y, Zhang L Q, et al. *Compos. Sci. Technol.*, 2021; 213: 108903.
3. Liu C H, Guo M M, Zhai X B, et al. *Polymers.*, 2021; 12: 6.

Eco-Tread: The Compounds from Rice Husk Silica and Deproteinized Natural Rubber

Luat Dai TRAN[1], Thang Manh TRAN[2], Hang Thi LE[1], Hoang Van NGUYEN[1], Thanh Binh Thi BUI[1], Hong Nhung Thi LE[1], Seiichi KAWAHARA[3], Nghia Trung PHAN[1*]

[1] *Rubber Science and Technology Center, Hanoi University of Science and Technology, No. 1 Dai Co Viet, Hai Ba Trung, Ha Noi, Viet Nam*

[2] *Hanoi Irradiation Center, Km 12, Street 32, Minh Khai ward, Bac Tu Liem, Ha Noi, Viet Nam*

[3] *Nagaoka University of Technology, 1603-1 Kamitomioka, Nagaoka-shi, Niigata-ken, Japan*

e-mail address of the presenting author: nghia.phantrung@hust.edu.vn, tranluat15@gmail.com

Keywords: hydrophilic silica, rice husk, reinforced deproteinized natural rubber, green car tire tread.

The increasing demand for environmentally friendly materials in the tire industry has drawn attention to natural rubber (NR) and silica derived from biomass. Conventional tire treads rely on synthetic rubber and carbon black, which pose environmental concerns due to poor biodegradability and petroleum origin [1]. In this work, deproteinized natural rubber (DPNR) was selected as a green matrix, while hydrophilic silica extracted from rice husk ash (Hi-Silica) was investigated as a sustainable reinforcing filler [2]. This combination aims to enhance tire tread durability and promote the concept of eco-tread compounds.

Prior studies demonstrate that removing proteins from NR reduces allergenic potential and improves resistance to thermal aging [3]. Meanwhile, rice husk contains up to 22% ash, with silica content exceeding 90%, making it an abundant and renewable filler source. Previous reports have shown that silica improves hardness and abrasion resistance, but may reduce elasticity at high loadings [4]. However, systematic optimization of Hi-Silica content in DPNR for tire tread applications remains limited [5].

DPNR was prepared from field latex using urea and sodium dodecyl sulfate (SDS) treatment, followed by centrifugation [3]. The decreasing of protein content in DPNR was confirmed by Proton Nuclear Magnetic Resonance Spectroscopy ^{1}H NMR (JEOL ECA-400 FT-NMR). Hi-Silica was obtained from rice husk ash and characterized by Fourier Transform Infrared Spectroscopy FT-IR (Jasco 6300 FTIR instrument) to confirm silanol groups. Rubber compounds were prepared with varying silica loadings (0–70 phr). Compounds with 0–70 phr silica were evaluated for curing (Rotorless Rheometer Model RLR-4), Tensile (A Toyoseiki Strograph VG5E), Shore A hardness (Teclock GS-709N), DIN abrasion (GTFO12D), Swelling-based crosslink density, and Thermogravimetric Analysis/Derivative Thermogravimetry TGA/DTG (Labsys TG/DSC1600, TMA instrument).

FT-IR confirmed the presence of Si–O–Si and silanol groups on Hi-Silica, indicating hydrophilicity. Rheometer analysis showed prolonged cure times and reduced cure rates with higher silica content. Tensile strength increased significantly from 0 phr (17.16 MPa) to 40 phr (optimum, >25 MPa), then decreased due to filler agglomeration at higher loadings. Crosslink density generally decreased with silica content, except at 10 phr, where a confinement effect was observed. Hardness

increased steadily, while abrasion resistance was maximized at 40 phr. TGA indicated high thermal stability, with major degradation occurring about 380 °C, leaving ~25% residual mass at 688 °C.

This study demonstrates that Hi-Silica derived from rice husk is a viable sustainable filler for reinforcing DPNR in green tire tread formulations. The optimal filler content was identified at 40 phr, balancing tensile strength, hardness, abrasion resistance, and thermal stability. Limitations include filler agglomeration and reduced elasticity at high silica loadings. Future research should focus on surface modification of Hi-Silica to improve filler–rubber interactions and on scaling up for industrial applications. The findings contribute to advancing sustainable materials for eco-friendly automotive tires.

Reference

1. Wei YC, Xia JH, Zhang L, Zheng TT, Liao S, *Colloid Polym. Sci*., 2020; 298: 1263.
2. Choophun N, Chaiammart N, Sukthavon K, Veranitisagul C, Laobuthee A, Watthanaphanit A, Panomsuwan G, *J. Compos. Sci*., 2022; 6: 369.
3. Chaikumpollert O, Yamamoto Y, Suchiva K, Nghia PT, Kawahara S, *Polym. Adv. Technol*., 2012; 23: 825.
4. Prasertsri S, Rattanasom N, *Polym. Test*., 2011; 30: 515.
5. Lolage M, Parida P, Chaskar M, Gupta A, Rautaray D, *Sustain. Mater. Technol*., 2020; 26: e00232.

Role of Lipase Enzyme in Controlling Storage Hardening and Mechanical Properties of Natural Rubber

K. BOONCHUAY[1], C. SIRISINHA[1], A. NIMPAIBOON[1]

[1]*Rubber Technology Research Centre, Faculty of Science, Mahidol University, Nakhon Pathom 73170, Thailand.*

kattareen.boo@mahidol.ac.th

Keywords: Natural rubber, Lipase, Storage hardening, Mechanical properties

Natural rubber (NR) is composed of *cis*-1,4 polyisoprene and various non-rubber components, such as proteins, lipids, sugars, inorganic substances, and abnormal groups (e.g., aldehyde, epoxide, and lactone) [1]. NR exhibits excellent mechanical properties especially green strength and elasticity compared to its synthetic counterpart [2]. However, one of its drawbacks is the increase in viscosity during long-term storage under ambient conditions, known as the storage hardening phenomenon, which negatively affects its processability. This phenomenon is associated with aldol condensation of aldehyde groups and the presence of lipids [3]. Although chemicals like hydroxylamine can suppress storage hardening, their industrial application is limited due to toxicity concerns [4]. Lipid removal through transesterification is another approach, but it involves the use of hazardous chemicals [5]. Recently, lipase enzymes have shown potential to break down lipids in NR [5], offering a safer and more scalable method to prevent storage hardening and support the production of constant viscosity NR.

This study aims to examine how lipase treatment influences the storage hardening and mechanical properties of NR. Lipase-treated NR was successfully prepared by treating fresh NR (FNR) latex with 0.04%w/v lipases from *Candida lipolytica* (L-NR). The storage hardening behavior of L-NR was characterized by an accelerated storage hardening test (ASHT) under a phosphorus pentoxide atmosphere, and compared with FNR and hydroxylamine-treated NR (H-NR). Additionally, carbon black-filled L-NR vulcanizates were prepared using a sulfur curing system to evaluate curing behavior and mechanical properties.

The results showed that *Candida lipolytica* lipases could partially remove long-chain fatty acid ester groups of phospholipids in NR. Only slight increases in Mooney viscosity and Wallace plasticity values of L-NR were observed during ASHT, suggesting that lipase treatment effectively suppressed the storage hardening of NR. Moreover, the mechanical properties of the carbon black-filled vulcanized samples showed no significant differences. The reduction in network density due to phospholipid removal by lipase treatment did not negatively impact the performance of NR vulcanizates. These results suggest that L-NR can serve as a suitable alternative to H-NR.

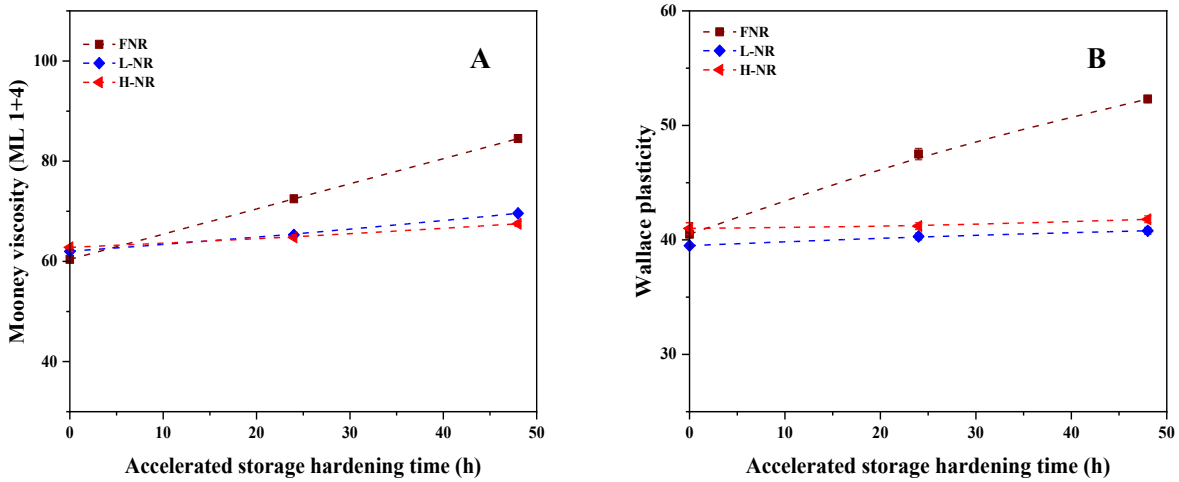


Figure 1. Changes in Mooney viscosity (A) and Wallace plasticity (B) of FNR, L-NR, and H-NR during accelerated storage hardening.

Table 1. Mechanical properties of vulcanized samples

Mechanical properties	Samples		
	FNR	L-NR	H-NR
300% modulus (MPa)	14.9 ± 0.3	14.5 ± 0.3	14.6 ± 0.1
Tensile strength (MPa)	27.5 ± 0.7	27.0 ± 0.1	27.0 ± 0.4
Elongation at break (%)	485 ± 3	509 ± 8	494.7 ± 10
Hardness (Shore A)	66.9 ± 0.3	66.2 ± 0.2	66.6 ± 0.6

Acknowledgement

This research project was supported by the Rubber Authority of Thailand. The authors would like to thank the Rubber Technology Research Centre (RTEC) for providing the equipment and facilities used in this study.

References

1. Hwee EA. Non-rubbers and abnormal groups in natural rubber. In: Thomas S, Chan CH, Pothen LA, Rajisha KR, Maria HJ, editors. *Natural rubber materials: Volume 1 – Blends and IPNs*. Cambridge: Royal Society of Chemistry; 2014. p. 53–72.
2. Malmonge JA, Camillo EC, Moreno RMB, Mattoso LHC, McMahan C M, *J. Appl. Polym. Sci*., 2009;111(6): 2986–2991.
3. Sekhar B, *Rubber Chem. Technol*., 1962;35(4): 889–895.
4. Gross P, Smith RP, *CRC Crit. Rev. Toxicol*., 1985;14(1): 87–99.
5. Yunyongwattanakorn, J, Tanaka Y, Kawahara S, Klinklai W, Sakdapipanich J, *Rubber Chem. Technol*., 2003;76(5): 1228–1240.

Sustainable Vulcanization of Natural Rubber Latex Using Electron Beam

S. Sichumphuang[1], C. Dokkhan[1], P. Kovitcharoenkul[2], C. Charaschimpleekul[3], P. Wiroonpochit[1]

[1] *National Metal and Materials Technology Center, National Science and Technology Development Agency, Phahonyothin Road, Pathum thani, 12120 Thailand*

[2]*Irradiation Center, Thailand Institute of Nuclear Technology (Public Organization), Nakhon Nayok 26120, Thailand*

[3]*Enginearing and Nuclear Instrument Center, Thailand Institute of Nuclear Technology (Public Organization), Nakhon Nayok 26120, Thailand*

E-mail: suthathip.sic@ncr.nstda.or.th

Keywords: Natural rubber latex, irradiation prevulcanization, Electron beam

The development of Electron Beam Vulcanized Natural Rubber Latex (EBVNR) aims to support and expand the Thai natural rubber latex industry by addressing key challenges in both concentrated latex production and product manufacturing. A major goal is to reduce the reliance on chemical vulcanizing agents, which are related to allergic reactions and environmental concerns. This study explores the vulcanization of natural rubber latex using high-energy electron beam irradiation (10 MeV) at doses of 60 - 250 kGy and the addition of 1,6-hexanediol diacrylate (HDDA) 0 1 and 2 phr as a sensitizer. The results indicate that the mechanical properties—such as tensile strength, modulus, and elongation at break—are enhanced with increasing of irradiation doses and the HDDA addition. The addition of HDDA enables the production of strong and tranparent latex even at lower electron beam dose, indicating the potential to reduce both energy consumption and chemical usage during processing.

Acknowledgement

This work was supported by Thailand Institute of Nuclear Technology (Public Organization) and National Research Council of Thailand (NRCT).

References

1. K.Makuuchi, F.Yoshii, J.A.G.S.G. Gunewardena, Radiation vulcanization of NR latex with low energy electron beam, *Radiation Physics Chemistry*, 46(4-6), 979-982, 1995.

International Rubber Conference 2025 (IRC2025)
1-3 December 2025 @ BITEC, Bangkok, Thailand

Comparative Evaluation of Natural Rubber Composites Reinforced with Macadamia Carbon and Carbon Black

Patcharapron Pimput[1] and Jitladda Sakdapipanich[1,2*]

[1] *Rubber Research Group, Department of Chemistry, Faculty of Science, Mahidol University, Nakhon Pathom 73170, Thailand*

[2] *The Rubber and Rubber Glove Academician Association, Bangkok, 10900, Thailand*

Presenting author: patcharapron.pim@student.mahidol.edu

*Corresponding author: jitladda.sak@mahidol.ac.th

Keywords: Natural Rubber, Macadamia Carbon, Carbon Black, Mechanical Properties, Bio-based Fillers

This study investigates the influence of Macadamia carbon as an alternative bio-based filler on the properties of natural rubber (NR) composites, in comparison with conventional carbon black (N330). Macadamia carbon powders were prepared at various particle sizes by sequential ball milling and high-speed milling processes, achieving sizes down to approximately 0.7 µm and incorporated into the rubber matrix at filler loadings of 1, 3, 5, and 10 phr. Macadamia-derived carbon typically contains 70–90 wt.% carbon. These fillers were incorporated into NR compounds at defined loadings, and the resulting composites were characterized in terms of cure characteristics, viscosity, mechanical performance, and thermal behavior.

Results demonstrated that the particle size and the inherent composition of Macadamia carbon, particularly the presence of manganese and copper, significantly affected the curing kinetics, leading to prolonged scorch and cure times relative to N330. Mechanical testing indicated that while fine-particle Macadamia carbon improved tensile strength and modulus over unprocessed carbon, the overall mechanical reinforcement and heat build-up resistance remained inferior to N330-filled composites, mainly due to weaker filler–rubber interactions and lower compatibility.

These findings suggest that Macadamia carbon, although a sustainable and renewable filler source, requires further modification to match the performance of traditional reinforcing fillers. The study contributes valuable insights into the development of bio-filler technologies for eco-friendly rubber composites.

Acknowledgement

The authors gratefully acknowledge the financial support from Thai Rubber Latex Group Public Company Limited.

References

1. Ismail S. N. S., Ibrahim N. N. I. N., Rasli S. N., Majid N. A., Wahab N. M. A., Jamal S. N., Zakaria S, Nazir K, Reinforcement of Charcoal Activated Carbon (CAC) in Natural Rubber (NR) Compound: In Comparison with Carbon Black. *ASEAN Eng. J.* 2022; 12 (2); 161–167.
2. Karunanayake L, Etampawala T, De Silva D. J., Bandara J, Rajapaksha A. U., Vithanage M. Role and Potential of Biochar as a Sustainable Alternative Reinforcing Filler to Carbon Black in Rubber Composites. *Biochar* 2025; 7 (1).

Sustainable Rubber Compounding: Application of Silane-Grafted Palm Oil in Silica-Filled SBR/BR Blends

C. HAYICHELAEH[1], A. MINGSAMOH[1], K. BOONKERD[1,2]

[1] *Department of Materials Science, Faculty of Science, Chulalongkorn University, 254 Phayathai Road, Bangkok 10330, Thailand.*

[2] *Center of Excellence in Green Materials for Industrial Application, Faculty of Science, Chulalongkorn University, 254 Phayathai Road, Bangkok 10330, Thailand.*

(h.chesidi@gmail.com)

Keywords: SBR/BR blend, Palm oil, Processing oil, Silica, Silane coupling agent

In rubber compounding, processing oils play a crucial role in facilitating the incorporation of fillers and additives into the rubber matrix. These oils reduce the viscosity of rubber compounds, enhance the dispersion of reinforcing fillers, and improve the overall workability of the rubber during processing. Petroleum-based oils—such as aromatic, paraffinic, and naphthenic types—are among the most widely utilized processing oils in rubber compounding. For unsaturated rubbers, aromatic oils have been particularly favored due to their excellent compatibility with the rubber molecules. However, despite their technical advantages, petroleum-derived oils present significant environmental and health concerns. They are obtained from non-renewable fossil resources and are not biodegradable, contributing to long-term environmental pollution. In addition, aromatic oils often contain hazardous polycyclic aromatic hydrocarbons (PAHs), which are known carcinogens and pose serious health risks. There has been extensive research on the use of vegetable oils—such as coconut, palm, soybean, and sunflower oils—in rubber compounding, as they offer a renewable and environmentally friendly alternative to petroleum-based oils. One key finding from these studies is that the double bonds present in the molecular structure of vegetable oils can significantly influence the properties of rubber compounds. These unsaturated bonds may participate in side reactions during vulcanization or interact with the rubber matrix, thereby affecting the final performance of the rubber product [1, 2]. To address this issue, this study proposes a chemical modification of palm oil to reduce the undesired reactivity of its double bonds and to enhance its compatibility with the rubber matrix and fillers. Specifically, this study focuses on investigating the effects of modified palm oil on the properties of silica-reinforced SBR/BR blends. The modified palm oil was synthesized by grafting silane, serving as a coupling agent, onto the palm oil molecules.

The modification of palm oil with bis[3-(triethoxysilyl)propyl]tetrasulfide (TESPT) was performed in a laboratory-scale setup. A three-neck round-bottom flask equipped with a mechanical stirrer (operating at 100 rpm), thermometer, and condenser was charged with 500 mL of palm oil. The palm oil was heated to 170 °C and maintained at this temperature. Once the temperature stabilized, 250 mL of TESPT was added dropwise to the flask. The reaction mixture was maintained at 170 °C for two hours to ensure sufficient reaction between palm oil and TESPT.

The effect of modified palm oil on the properties of 70/30 ESBR/BR blends was investigated, with the amount of processing oil fixed at 10 phr. The properties of the blends—specifically the Payne

effect and crosslink density—are summarized in Table 1. The results show that the Payne effect, which reflects the degree of filler–filler interaction, was most pronounced in the blend without any processing oil (WO). This indicates that the absence of processing oils hinders filler dispersion, leading to stronger filler–filler networks. Incorporation of processing oils improved the dispersion and distribution of silica fillers, as evidenced by the reduced Payne effect. Among the oils tested, TDAE oil achieved lower filler–filler interactions compared to unmodified palm oil. Notably, grafting palm oil with TESPT further reduced filler–filler interactions, resulting in a Payne effect even lower than that observed with TDAE oil. Regarding crosslink density, the blend without processing oil exhibited the highest value. The addition of processing oils led to a reduction in crosslink density, with palm oil showing a more pronounced decrease than TDAE oil. This reduction is attributed to the unsaturated segments of palm oil, which can interfere with the vulcanization process. Interestingly, grafting palm oil with TESPT reversed this effect, increasing the crosslink density compared to unmodified palm oil. This improvement is likely due to the reduced reactivity of the unsaturated groups and enhanced interaction between the modified oil and the silica–rubber matrix.

Table 1. Payne effect and crosslink density of silica-reinforced SBR/BR blends.

	Payne effect (kPa)	Crosslink density (mmol/cm^3)
WO	640	0.49
TDAE	350	0.36
Palm oil	390	0.33
Modified palm oil	320	0.36

Based on the experimental results, it can be concluded that silane-grafted palm oil holds significant potential as a sustainable processing oil in silica-reinforced SBR/BR blends. The modified oil demonstrated superior performance by reducing filler–filler interactions more effectively than both unmodified palm oil and commercial TDAE oil. Furthermore, it enhanced the crosslink density of the blends compared to unmodified palm oil, highlighting its dual benefit of improving filler dispersion while lessening the negative impact of unsaturated structures on vulcanization.

Acknowledgement

This research is funded by the Ratchadapisek Somphot Fund for Postdoctoral Fellowship, Chulalongkorn University. Additionally, the authors sincerely thank the Center of Excellence in Green Materials for Industrial Application for supporting our participation by sponsoring the registration for IRC 2025.

References

1. Li J, Isayev AI, Ren X, Soucek MD, *Polymer*, 2015; 60: 144.
2. Hayichelaeh C, Boonkerd K, Nun-Anan P, Purbaya M, *Polym. Adv. Technol.*, 2022; 33: 303.

Cure Characteristics of NR Compounds with Sulfur Sludge from Biogas - Wastewater Treatment in Palm Oil Industry

P. Saramolee[1], P. Srithong[1], K. Sathaporn[1], K. Seneesrisakul[1]

[1] *School of Engineering and Technology, Walailak University, Nakhon Si Thammarat 80160, Thailand.*

(sprachid@mail.wu.ac.th)

Keywords: Natural rubber, Vulcanization, Sulfur sludge, Biogas, Palm oil wastewater

This study investigates the feasibility of utilizing sulfur sludge, a by-product of biogas biodesulfurization from water treatment in palm oil plants, as an alternative crosslinking agent in the vulcanization of rubber materials. A comprehensive characterization of the sulfur sludge was conducted before and after a purification process using a solvent extraction method aimed at removing impurities and enhancing sulfur purity. The treated sulfur (T-sulfur) and commercial-grade sulfur (C-sulfur) samples were analyzed using a range of advanced techniques, including Fourier Transform Infrared Spectroscopy (FT-IR), Thermogravimetric Analysis (TGA), X-ray Fluorescence (XRF), pH, and particle size determination via laser diffraction. The treated sulfur demonstrated high purity of 99.88% sulfur and a yield of approximately 70%. The sulfur particle size distributions suitable for rubber compounding.

Natural rubber (NR) compound was prepared using a laboratory two-roll mill. The formulations of the NR compound samples containing 2 types of sulfur are provided in Table 1. NR was masticated for 3 mins., followed by the addition of other chemicals and curatives at last for 12 mins. The compounds were then sheeted out and left at room temperature for at least 24 h. before testing of cure characteristic at 150°C by Moving die rheometer (MDR).

Table 1. NR Compound Formulations

Components	Amount [parts per 100 parts of rubber, phr]	
	C-Sulfur	T-Sulfur
RSS-3[a]	100	100
ZnO	5	5
Stearic acid	1	1
CBS	1.2	1.2
DPG	1	1
BHT	1	1
Sulfur	2	2

[a] Ribbed Smoked Sheet grade 3, [b]N-Cyclohexyl-2-benzothiazole sulfenamide, [c]Diphenyl guanidine, [d]Butylated HydroxyToluene

The scorch (T_{s2}) and cure times (Tc_{90}), minimum torque (M_L), and maximum torque (M_H) of natural rubber vulcanized with treated sulfur sludge were comparable to those obtained using commercial-grade sulfur, indicating similar crosslinking behavior and vulcanization efficiency. The results confirmed that the sludge-derived sulfur exhibited comparable crosslinking performance, suggesting its technical viability in rubber manufacturing.

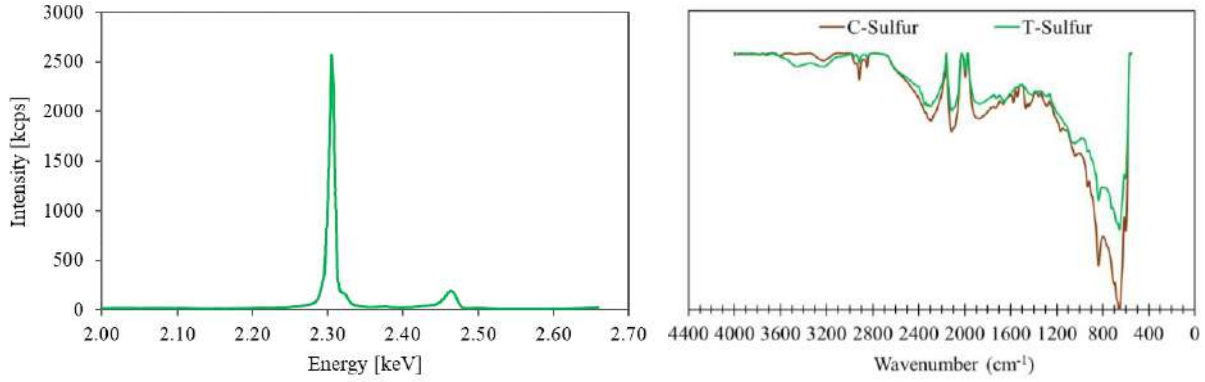


Figure 1. XRF spectrum of treated sulfur sludge (a) and FTIR spectra with various sulfur (b).

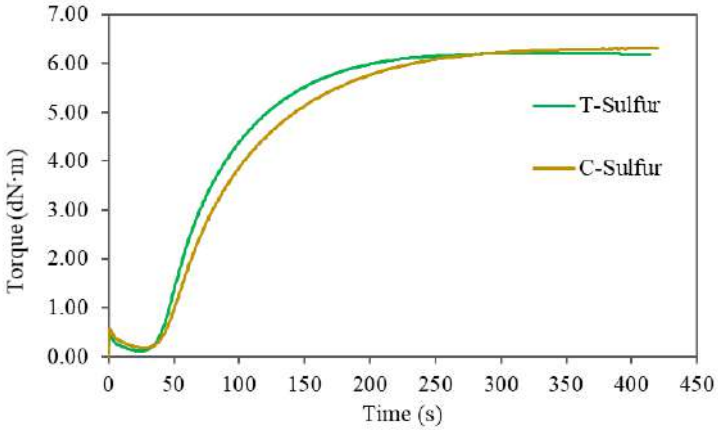


Figure 2. Cure curves of NR compound with various sulfur.

Raw sulfur sludge derived from industrial processes typically exhibits high acidity and is contaminated with metal oxides, rendering it unsuitable for rubber vulcanization. This study investigates a solvent-extraction technique to remove impurities from sulfur sludge. The treated sulfur exhibited characteristics comparable to commercial-grade sulfur, particularly in terms of acidity, composition, particle size and purity. When incorporated into natural rubber compounds, the refined sulfur successfully promoted crosslink formation with cure characteristics similar to that of conventional vulcanizing agents. These findings indicate the potential of recovered sulfur as a sustainable rubber compounding and processing.

Acknowledgement

The authors gratefully acknowledge the financial support from Center of Excellence on Wood and Biomaterials, School of Engineering and Technology Walailak University.

References

1. Suárez-Gómez, S, Bonavera, L, Carballido-Landeira, J, Blanco, P, Blanco, F, Sánchez, ML, de Cos FJ, *J. Mat. Res. Tech.*, 2020; 9(4): 8117-8124.
2. Mol, AR, van der Weijden, RD, Klok, JBM, Buisman, CJN, *Minerals*, 2020; 10, 433.

Feasibility Study of Tamarind Shell Powder as a Bio-Based Secondary Accelerator for Rubber Flooring

W. Intiya, P. Jittham, U. Tepsuwan, and P. Sae-oui

National Metal and Materials Technology Center (MTEC), National Science and Technology Development Agency (NSTDA), Khlong Nueng, Khlong Luang, Pathum Thani 12120, Thailand.

E-mail address : weenusai@mtec.or.th

Keywords: Rubber, Flooring, Tamarind shell, Additives, Mechanical properties

Thailand has recently emerged as one of the largest producers of sweet tamarind, generating approximately 100,000 tons annually and producing large volumes of tamarind shells as agricultural waste. Rich in nitrogen-containing compounds, these shells offer potential as bio-based secondary accelerators in rubber vulcanization [1]. This study examines the feasibility of using tamarind shell powder (TSP) as a sustainable alternative to conventional secondary accelerators in rubber flooring formulations.

Tamarind shells from the "Golden" cultivar were oven-dried, finely ground using a high-speed grinder, and sieved through a 200-mesh screen (Figure 1). The resulting powder was incorporated into rubber compounds at loadings of 2, 4, 6, 8, and 10 parts per hundred rubber (phr) and compared with formulations containing TBzTD at 0.1, 0.2, 0.3, and 0.4 phr to evaluate substitution potential. The rubber compound was based on a commercial flooring formulation provided by a manufacturer; due to confidentiality, full formulation details are not disclosed. The effects of TSP and TBzTD on curing behavior (Figure 2) and mechanical properties (Table 1) were systematically evaluated.

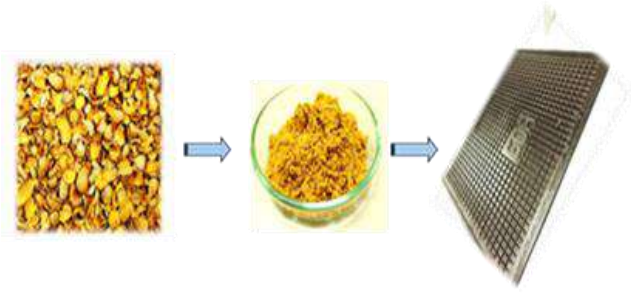


Figure 1. Preparation of tamarind shell as a green additive for rubber flooring

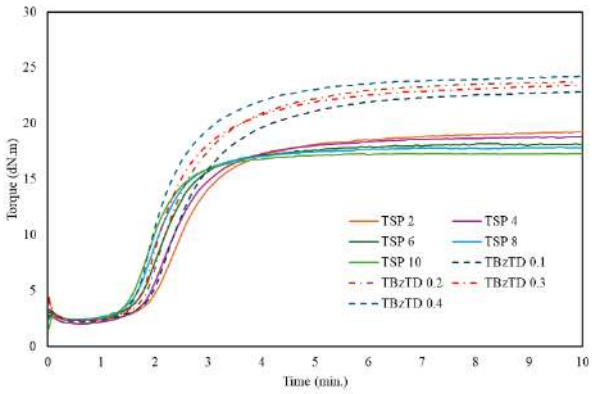


Figure 2. Cure curves of the rubber compounds

Table 1. Mechanical properties of the rubber vulcanizates.

Property	TIS Standard	TBzTD 0.1	TBzTD 0.2	TBzTD 0.3	TBzTD 0.4	TSP 2	TSP 4	TSP 6	TSP 8	TSP 10
Hardness (Shore A)	70 ± 5	69.4±0.3	69.9±0.3	70.6±0.2	71.2±0.2	68.2±0.2	69.9±0.3	68.6±0.3	69.2±0.2	70.8±0.2
Tensile Strength (MPa)	≥ 4.0	8.4±0.6	8.5±0.3	8.4±0.6	8.5±0.4	8.6±0.4	8.4±0.3	8.6±0.1	8.5±0.1	8.0±0.2
Elongation at Break (%)	≥ 150	328±11	319±13	285±15	306±14	349±4	332±4	388±2	388±1	361±13
Δ Hardness (Shore A)	≤5	0.9	1.0	0.6	0.5	3.1	1.0	4.5	4.2	1.3
Δ Tensile Strength (%)	≤25	-1.2	0.2	-3.5	-3.6	1.2	-14.4	-8.1	-4.5	-6.2
Δ Elongation at Break (%)	≤50	-14.6	-10.7	-9.2	-9.7	-5.7	-10.7	-18.6	-18.6	-15.8

Δ = Change after aging at 70 °C for 72 h.

Increasing TSP content resulted in a leftward shift of the cure curves, indicating reduced scorch and cure times. Apart from differences in maximum torque, the cure profile of the compound with 4 phr TSP closely matched that with 0.1 phr TBzTD, while 10 phr TSP produced a profile similar to 0.3 phr TBzTD. Notably, higher TSP contents reduced marching modulus behavior, suggesting more stable vulcanization. Although TSP-based compounds exhibited moderately lower torque differences—implying lower crosslink density and hardness—they maintained comparable tensile strength and demonstrated higher elongation at break. These mechanical properties remained within acceptable limits after accelerated aging.

All TSP-containing formulations complied with the Thai Industrial Standard (TIS 2377-2559, Type 1), confirming their suitability for rubber flooring applications. These results highlight the potential of tamarind shell powder as a renewable, eco-friendly secondary accelerator that supports the value-added utilization of agricultural waste.

Acknowledgement

This research was funded by (1) Thailand Science, Research and Innovation (TSRI), Thailand, through Program Management Unit for Competitiveness (PMU-C), contract number C10F650199, (2) Siam United Rubber Co., Ltd., Nakhon Pathom, Thailand, and (3) National Science and Technology Development Agency (NSTDA).

Reference

1. Purushotham, G.; Yathin, K.L. Study of Mechanical behavior for tamarind shell powder and coconut coir fiber epoxy composite for aerospace application. Int. J. Trend Sci. Res. Dev. 2018, 3, 941–949.

International Rubber Conference 2025 (IRC2025)
1-3 December 2025 @ BITEC, Bangkok, Thailand

Rubber composites reinforced with carbon black and calcium lignosulfonate

I. HUDEC, M. DŽUGANOVÁ, J. KRUŽELÁK

Department of Plastics, Rubber and Fibres, Faculty of Chemical and Food Technology, Slovak University of Technology in Bratislava, Radlinského 9, 812 37 Bratislava, Slovakia

e-mail address of the presenting author (ivan.hudec@stuba.sk)

Keywords: rubber composites, carbon black, lignosulfonate, glycerol

Rubber compounds based on styrene-butadiene rubber (SBR) and acrylonitrile-butadiene rubber (NBR) were filled with constant amount of carbon black – 25 phr and calcium lignosulfonate – 30 phr. Glycerol as cheap and environmentally friendly softener was added into the rubber compounds in concentration scale from 0 to 20 phr to plasticize the rubber matrix and the biopolymer and to improve the adhesion between the components of rubber compounds. For cross-linking of rubber composites, sulfur-based curing system was used. The study was focused on the investigation of glycerol on cross-linking process of rubber compounds, morphology, mechanical and dynamic-mechanical properties of composites.

The rubber formulations were fabricated by using a Brabender laboratory kneading machine in two mixing steps at a temperature of 90 °C and 55 rpm. The curing process was carried out using a Fontijne hydraulic press following the optimum cure time of each rubber compound. The curing temperature was 170 °C and the pressure was 15 MPa. The tensile tests were performed according to valid technical standards using a Zwick Roell/Z 2.5 tearing equipment. The cross-head speed was set up to 500 mm.min^{-1} with a gauge length of 25 mm. The surface morphology was evaluated using scanning electron microscope JEOL JSM-7500F. Dynamical-mechanical performances were obtained by using a dynamical-mechanical analyzer DMTA MkIII, fy Rheometric Scientific.

The results demonstrated that glycerol influenced the course of curing isotherms and decelerated the curing kinetics. This was reflected in the decrease of cross-linking degree, which was more pronounced for composites with higher amount of glycerol. The higher the amount of glycerol in rubber compounds, the lower their viscosities. This points out to plasticizing effect of glycerol on rubber formulations. The dynamic-mechanical analysis revealed that two transition regions occurred on loss factor - temperature dependencies for composites with higher glycerol content, suggesting the formation of two polymer phases (Figure 1). The first peak that represents the glass transition temperature of composites is strongly dependent on the type of rubber matrix. Though, it was not influenced by the amount of glycerol. The second peak relates with glass transition temperature of lignosulfonate, and it was evident that the higher was amount of glycerol, the lower the *Tg* of the biopolymer. This points out to higher plasticizing effect of glycerol on lignosulfonate than on rubber matrices. The softened lignosulfonate was then better dispersed and distributed within the rubber formulations. Glycerol also contributed to better compatibility and adhesion between the biopolymer and rubber matrices on their interface, resulting in the improvement of tensile characteristics of composites. Better distribution of the biopolymer within the rubber matrix based on NBR and higher adhesion on the filler-rubber interface resulted in higher enhancement of tensile strength for the equivalent composites (Figure 2 on the left). As also shown in Figure 2 on the right, the elongation at break for both composite types showed an increasing trend with increasing content of glycerol just up to 15 phr of glycerol. The increase of elongation at break can be attributed to the plasticizing effect of glycerol on rubber compounds, weakening of physical interactions between rubber chain segments

and increase of their mobility and elasticity. This subsequently leads to the increase in elongation at break.

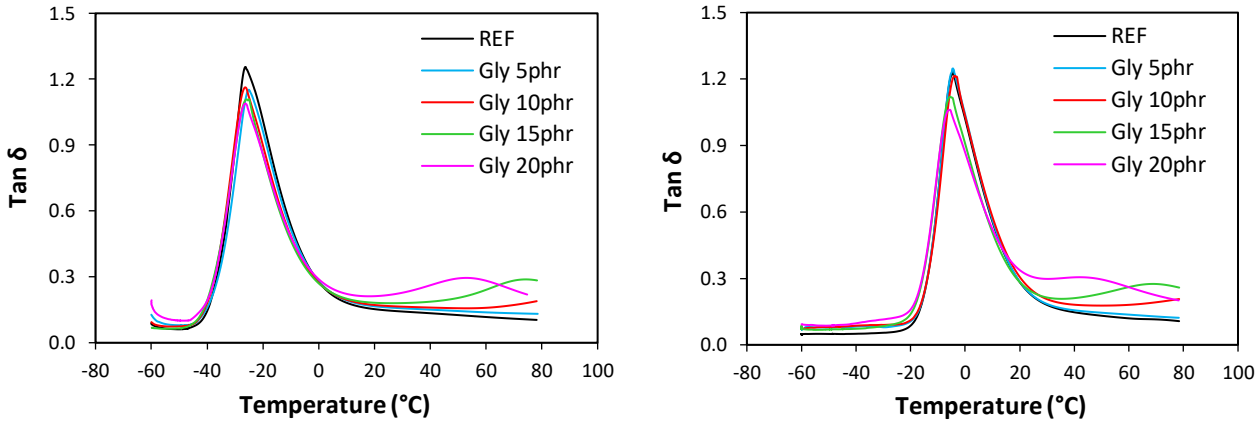


Figure 1. Temperature dependences of loss factor *tan δ* for composites based on SBR (left) and NBR (right)

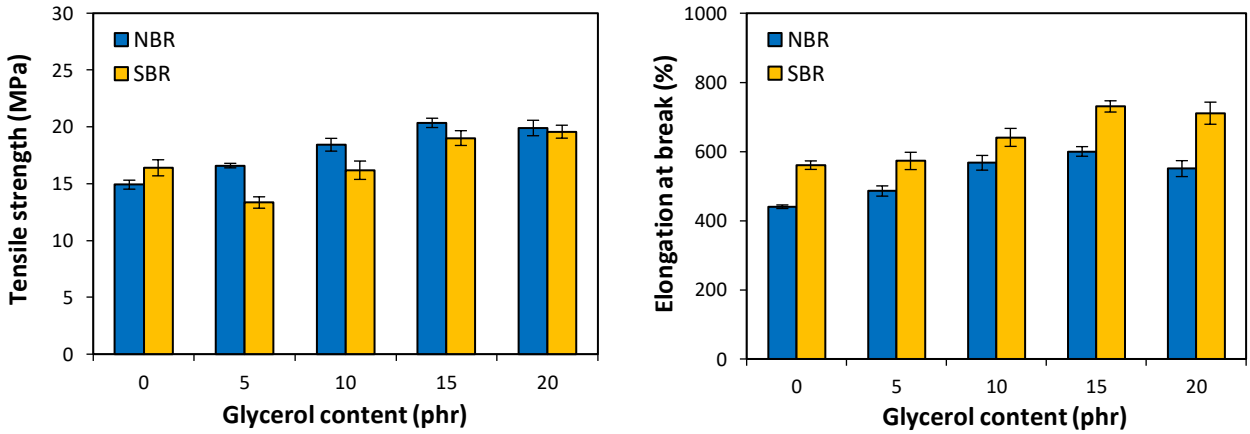


Figure 2. Influence of glycerol content on tensile strength (left) and elongation at break (right) of composites

The main output of the work was the knowledge that the improvement of physical-mechanical properties of biopolymer filled composites can be easily obtained by simple addition of very cheap and environmentally friendly plasticizer into the rubber compounds during their processing without additional treatment or procedures. The enhancement of physical-mechanical properties of rubber compounds filled with biopolymer filler might contribute to the broadening of their potential applications. Moreover, not only can the price of the final rubber products be reduced but more pronounced ecological aspects will be emphasized, too.

Acknowledgement

This work was supported by the Slovak Research and Development Agency under the contract No. APVV-22-0011

International Rubber Conference 2025 (IRC2025)
1-3 December 2025 @ BITEC, Bangkok, Thailand

Rubber composites based on devulcanized tire crumb and lignin as a stabilizer

J. KRUŽELÁK[1], M. DŽUGANOVÁ[1], I. HUDEC[1], J. HRONKOVIČ[2], J. PREŤO[2]

[1] *Department of Plastics, Rubber and Fibres, Faculty of Chemical and Food Technology, Slovak University of Technology in Bratislava, Radlinského 9, 812 37 Bratislava, Slovakia*

[2] *VIPO a.s., Gen. Svobodu 1069/4, 958 01, Partizánske, Slovakia*

e-mail address of the presenting author (jan.kruzelak@stuba.sk)

Keywords: rubber composites, lignin, tire crumb, devulcanization

Devulcanization aims to break C–S and S–S bonds (cross-links) while preserving C–C bonds (the polymer backbone) in the rubber network. Although C–C bonds theoretically require more energy to break than C–S and S–S bonds, in practice, both chain scission and cross-link breakage occur during devulcanization. The most effective devulcanization method maximizes cross-link breakage while minimizing chain scission. Regardless of the devulcanization method, some of the main polymer chains are broken during devulcanization and, thus, the properties of the treated material are different compared to the original rubber. The use of devulcanized rubber can reduce the cost of final products. Depending on the desired application, the devulcanized rubber can be reused as obtained or mixed in different amounts with virgin rubber or other polymers. This paper describes mechanical devulcanization of rubber crumb, the influence of kraft lignin on the devulcanization process and compounding such devulcanized rubber crumb with virgin SBR compound.

Styrene-butadiene rubber was filled with 50 phr of carbon black. Sulfur vulcanization system was used for cross-linking. Virgin SBR-based compound was used as a reference and subsequently mixed with devulcanized rubber crumb and lignin. Devulcanized rubber crumb (RC), obtained as a waste from tread part of truck tires, which is generated during the process of retreading truck tires, was incorporated at 25 wt.%. To further enhance sustainability, an additional 5 wt. % of the virgin compound was substituted with kraft lignin. Glycerol was added as a plasticizer to improve processing and enhance the lignin/rubber interface. Based on previous research, a glycerol content of 20 wt. % relative to the lignin content was used.

Devulcanization of the RC was carried out by mechanical treatment on a two-roll mill, with roller friction 1:2. The processing time was 15 minutes and the temperature of RC during processing was kept at 65°C (RC 65). One sample (RCL) was processed together with 5 wt.% of lignin, under the same conditions as RC 65. To evaluate the devulcanization process, and unprocessed RC was also included in the experiment.

Subsequently rubber compounds were prepared using a two-step mixing process. The first step was carried out in a semi-industrial kneading machine Buzuluk, set at 100°C and 60 rpm. Initially, the rubber was masticated for 1 minute, followed by the addition of RC 65 and lignin (or RCL) and glycerol, and mixed for another minute. Additives and half of the carbon black were then introduced and mixed for 2 minutes. Finally, the remaining carbon black and processing oil were added and mixed for an additional 2 minutes. The resulting compound was shaped into strips and homogenized using a two-roll mill. After cooling, the second mixing step was performed on the two-roll mill, where accelerator and sulphur were blended into the compound at 70°C for 8 minutes.

During the devulcanization process, crosslink scissions generate a significant number of free radicals, which tend to slowly re-crosslink over time. To address this issue, the radical scavenging activity of lignin is proposed as a potential stabilizing strategy. The antioxidant capability of lignin

arises primarily from the homolytic dissociation of its phenolic O–H bonds. This process, characterized by its bond dissociation enthalpy, enables lignin to act as a radical stabilizer by transferring hydrogen atoms to the polymer-based radicals, thereby neutralizing them and inhibiting further crosslinking. The FTIR analysis confirmed the presumption and clearly revealed a lower degree of main elastomer chain scission in the presence of lignin, pointing to its potential stabilizing effect during the devulcanization process.

The mechanical properties of the composites are summarized in Figure 3a. The addition of RC in general reduces tensile strength and moduli compared to reference. Incorporating lignin in the SBR/RC65/L composite further decreases these properties because lignin displaces virgin rubber, reducing the available vulcanizable matrix. In this role, lignin behaves as an inert filler - forming domains that do not participate in cross-linking - consistent with the lower cross-link densities shown in Figure 3b. In contrast, when RC and lignin are pre-processed together on a two-roll mill before incorporation (SBR/RCL), the resulting composite's tensile strength matches that of SBR/RC65, and its 300% modulus is approximately 2 MPa higher than in SBR/RC65. This improvement suggests altered cross-linking behaviour and supports the hypothesis that lignin participates in the devulcanization of RC during processing. The higher cross-link density observed in SBR/RCL indicates an improved ability to undergo revulcanization, possibly due to the preservation of longer polymer chains during the devulcanization treatment.

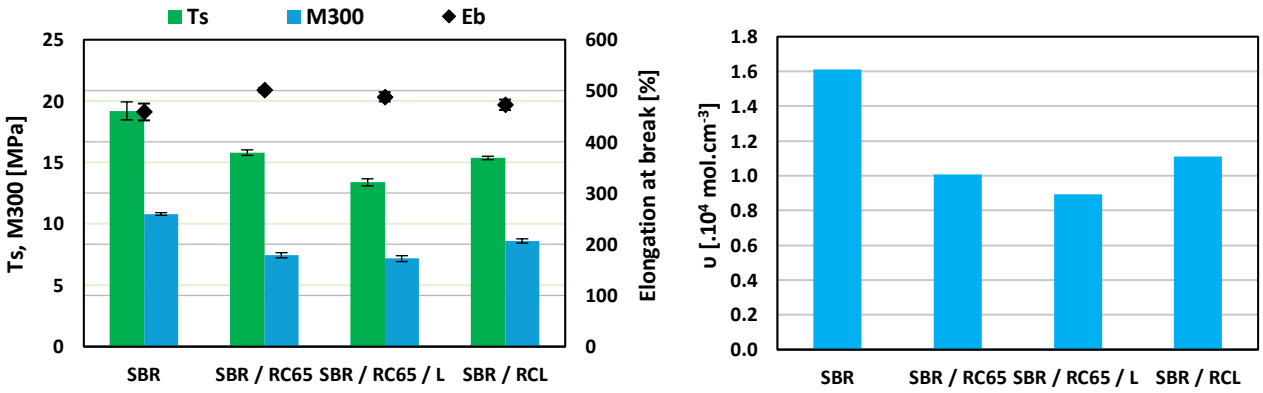


Figure 1. Mechanical properties (a) tensile strength *Ts*, modulus *M300* and elongation at break *Eb* and (b) cross-link density *υ* of composites

This study demonstrated that kraft lignin can play a beneficial role in the devulcanization and reprocessing of rubber crumb obtained as a waste from tread part of truck tires, for use in next-generation rubber composites. Mechanical devulcanization on a two-roll mill, particularly when combined with lignin, resulted in reclaimed rubber with improved properties. FTIR analysis indicated that lignin helps preserve the integrity of the polymer backbone while enhancing selective cross-link scission. When incorporated into a virgin SBR matrix, the pre-treatment of rubber crumb with lignin improved cross-link density and mechanical properties compared to untreated or post-mixed lignin systems. These findings suggest that kraft lignin not only contributes to the sustainability of rubber recycling but also enhances the performance of the resulting composites, making it a promising additive for circular economy applications in the rubber industry.

Acknowledgement

This work was supported by the Slovak Research and Development Agency under the contract No. APVV-22-0011

International Rubber Conference 2025 (IRC2025)
1-3 December 2025 @ BITEC, Bangkok, Thailand

Mediating Carbon Black-Natural Rubber Interface by Thioamide-Functionalized Polysulfide for Energy-Saving Composites

Ruoyan Huang, Dong Wang, Zhenghai Tang,* Baochun Guo*, Liqun Zhang

Institute of Emergent Elastomers, School of Materials Science and Engineering, South China University of Technology, Guangzhou, China.

1360692098@qq.com

Keywords: Rubber composites; Interfacial modifiers; Hysteresis loss; Inverse vulcanization; Energy-saving

Interfacial modification of carbon black (CB)-filled natural rubber (NR) composites is crucial for achieving uniform CB dispersion and robust interfacial interaction, with the goals of improving mechanical properties and reducing hysteresis loss.[1, 2] In this study, we reported a one-step synthesis of thioamide-functionalized polysulfide (SCA) via inverse vulcanization of sulfur with cyclohexylamine and the simultaneous conversion of amine to thioamide groups. SCA could serve as a novel interfacial modifier for NR/CB composites, in which thioamide groups form robust hydrogen bonds with oxygen-containing groups on CB surface, and the polysulfide fragments cleave and covalently couple with NR,[3] enabling the establishment of SCA-mediated bridges between NR and CB. Consequently, the incorporation of SCA remarkably suppresses CB aggregation and enhances interfacial interaction, resulting in substantial decrease in the hysteresis loss of the composites. More importantly, the effects of SCA molecular structure on the composite structure and properties are systematically investigated. The thioamide content is found to be critical for improving CB dispersion within the composites, while the reactivity between NR and polysulfide fragments in SCA is the dominant factor governing interfacial interaction.



Figure 1. (a) Possible reaction pathways between 2-(1-cyclohexenyl) ethylamine (CA) and S_8. (b) Proposed coupling mechanism between CB and rubber by SCA.

Acknowledgement

The work was funded by the National Natural Science Foundation of China (52322303 and 52130305), Guangdong Basic and Applied Basic Research Foundation (2023B1515020085).

References

1. Fang S., Li F., Liu J., et al. *Nano Energy*, 2021, 83.
2. Wang D., Tang Z., Huang R., et al. *Chemistry of Materials*, 2023, 35, 764-772.
3. Wang D., Chen J., Tang Z., et al. *Macromolecules*, 2024, 57, 470-480.

International Rubber Conference 2025 (IRC2025)
1-3 December 2025 @ BITEC, Bangkok, Thailand

Characterization of polyisoprene blended with urethane compounds

Takashi Kakubo[1] , Hirokazu Kageyama[1] , Ryuga Honda[2] , Sakito Sugii[2] , Naoya Amino[1] , Hiromu Saito[2]

[1] *Materials Performance Laboratory, Research and Advanced Development Division,*

The Yokohama Rubber Co., Ltd., Oiwake, Hiratsuka, Kanagawa 254-8601, Japan.

[2] *Department of Organic and Polymer Materials Chemistry,*

Tokyo University of Agriculture and Technology, 2-24-16 Naka-cho, Koganei, Tokyo 184-8588, Japan.

Takashi Kakubo (takashi.kakubo@y-yokohama.com)

Keywords: Urethane, Polyisoprene, Tensile strength, Strain-induced crystallization

Polyurethane is known for its high fracture property, and is used in many industrial products. Cured rubber materials blended with polybutadiene-urethane copolymers have been reported to exhibit high elongation, high tearing energy and self-healing properties [1]. Therefore, we focused on urethane compounds containing isoprene and urethane and investigated the reinforcing effect of polyisoprene blended with urethane compounds containing different amounts of hard urethane using tensile testing. The reinforcing effect was discussed in terms of strain-induced crystallization of polyisoprene, as evaluated by wide-angle X-ray diffraction (WAXD) measurements.

Table 1 shows the composition of the urethane compounds synthesized in this study. Hydroxyl-terminated polyisoprene (HTPI) was used as the polyol, while carbodiimide-modified methylene diphenyl diisocyanate (Millionate MTL), and diphenylmethane diisocyanate (Millionate NM) served as the isocyanate components. Dimethylthiotoluenediamine (DMTDA) and 1,5-pentanediol were employed as chain extenders to prepare the urethane compounds. The raw materials were mixed for 10 min using a planetary centrifugal mixer. The mixtures were then reacted at 60 °C for 24 hours to synthesize the urethane compounds containing isoprene and urethane.

Table 1. Composition of urethane compounds

Urethane Compounds	Polyol (A)	Isocyanate (B)	Chain Extender (C)	Molar Ratio (A : B : C)
PUT2403	HTPI Mn = 2,500	Millionate MTL	HARTCURE30 (DMTDA) Mn = 214	1 : 4 : 3.5
PUT2405	HTPI Mn = 2,500	Millionate NM	1,5-Pentane diol Mn = 104	1 : 2.5 : 1.5

The raw polyisoprene rubber and rubber ingredients (5 phr of stearic acid and 3 phr of zinc oxide) were blended with the 10 phr urethane compound using a small rotary kneader. Specifically, the PUT2403 and PUT2405 urethane compounds were blended at 140°C and 80°C for 10 min, respectively. Then, the vulcanizing agents (1 phr of sulfur, 1.2 phr of accelerator) were incorporated at 80°C, and the polyisoprene rubber blend was vulcanized at 160 °C for 20 min. Tensile test and wide-angle X-ray diffraction (WAXD) analysis were conducted on the cured rubber specimens, which were punched into No. 7 dumbbell-shaped test pieces according to JIS K 6251.

Figure 1 shows the stress-strain curves of neat polyisoprene (PI) and its blends (PI / PUT2403 and PI / PUT2405). Compared to PI, the PI / PUT2403 showed an increased modulus at low strain and higher elongation at break, while the abrupt increase in stress at high strain was small. In contrast, the PI / PUT2405 showed a lower modulus at a low strain than the PI / PUT2403. However, the

increase in stress at high strain was larger. These results suggest that the stress of the polyisoprene blended with urethane compounds inverts with strain. The difference might be attributed to the difference in hardness and the interaction with PI, which depend on the isocyanate composition.

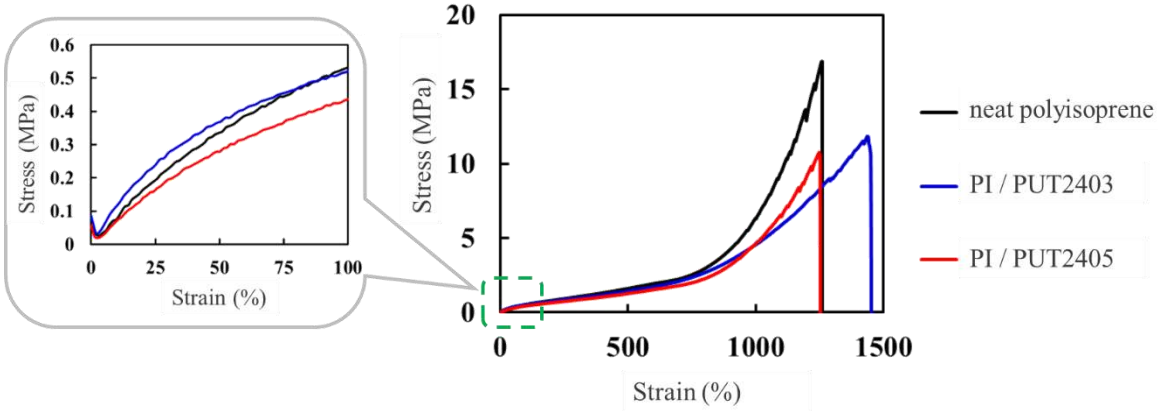


Figure 1. Stress-strain curves of polyisoprene blended with urethane compounds.

Figure 2 shows the WAXD results at 800 % and 1200 % strain, in which an abrupt increase in stress started to occur at around 800 % strain and the slope of stress increase was high at around 1200 % strain, as shown in Figure 1. A crystalline reflection peak was observed at 800% strain in both neat PI and the PI / PUT2403. However, this peak was not observed in the PI / PUT2405. This indicates that strain-induced crystallization occurs at 800% strain in neat PI and the PI / PUT2403, but not in the PI / PUT2405. The crystalline reflection peak of the PI / PUT2405 was larger than that of the PI / PUT2403, indicating a larger enhancement of strain-induced crystallization at high strains in the PI / PUT2405. Therefore, the larger increase in stress at high strain in the PI / PUT2405, as shown in Figure 1, is attributed to the larger enhancement of strain-induced crystallization.

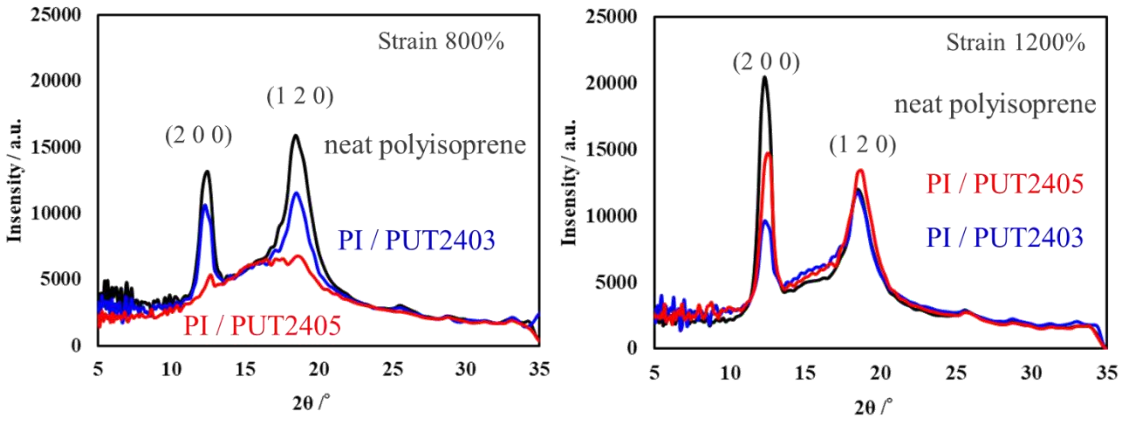


Figure 2. Wide angle X-ray diffraction (WAXD) profiles at 800 % and 1200 % strain.

Depending on the type of urethane compound blended, differences in the modulus and strain-induced crystallization behavior of polyisoprene rubber were observed. The incorporation of urethane compounds was found to suppress strain-induced crystallization while enhancing the elongation at break of the polyisoprene rubber.

References

1. Shoda Y, Aoki D, Tsunoda K, Otsuka H, *Polymer*, 2020; 202: 12200.

Facile and efficient preparation of functionalized diene-elastomers via dynamic covalent polymerization

Xinglong An, Siwu Wu*, Baochun Guo*, Liqun Zhang

Institute of Emergent Elastomers, School of Materials Science and Engineering, South China University of Technology, Guangzhou,China.

1045921550@qq.com

Keywords: Rubber, Sulfur-crosslinked network, Dynamic covalent polymerization, Functionalized rubber

Abstract: The strategic incorporation of functional moieties into rubber matrices has emerged as an effective approach for achieving intrinsic functionalization of diene rubbers. Nevertheless, conventional functionalization methodologies remain constrained by critical limitations, including catalyst system dependency, inevitable side reactions, and restricted substrate adaptability. This study presents an innovative catalyst-free strategy through the rational design of high-sulfur-crosslinked networks in diene rubbers. Under solvothermal conditions, the dynamic covalent polymerization (DCP) between di-/polysulfide linkages and unsaturated monomers[1, 2] or m-Phenylenediamine (MPD)[3, 4] demonstrates dual functionality: it simultaneously induces network disassembly and enables covalent grafting of functional vinyl monomers or MPD onto the rubber backbone. Remarkably, this approach exhibits exceptional versatility, successfully functionalizing various vulcanizates with diverse vinyl monomers or MPD to yield tailored rubber derivatives. The developed DCP-mediated network engineering strategy offers three distinctive advantages[5]: (1) elimination of catalytic requirements, (2) broad substrate compatibility, and (3) precise control over functionalization. This paradigm-shifting methodology not only provides fundamental insights into dynamic covalent chemistry of sulfur-rich networks but also establishes a commercially viable platform for manufacturing advanced functional rubbers, demonstrating both scientific merit and industrial application potential.

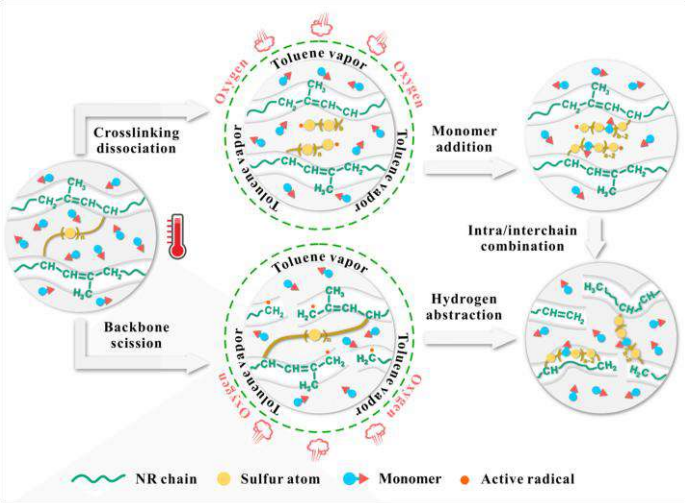


Figure 1. Schematic of the pyrolysis and functionalization of vulcanizates via the dynamic covalent polymerization process.

Acknowledgement

The work was funded by the National Science Fund for Distinguished Young Scholars (51825303) and National Natural Science Foundation of China (52130305 and 51903085).

References

1. Zhang Y, Konopka K, Glass R, Char K, Pyun J, *Polym. Chem.*, 2017; 8: 5167–5173.
2. Westerman C, Jenkins C, *Macromolecules*, 2018; 51: 7233-7238.
3. Karayilan M, Kleine T, Carothers K, Griebel J, Frederick K, Loy D, Glass R, Mackay M, Char K, Pyun J, *J. Polym. Sci.*, 2019; 58: 35-41.
4. Wang D, Tang Z, Huang R, Duan Y, Wu S, Guo B, Zhang L, *Chem. Mater.*, 2022; 35: 764-772.
5. An X, Wu S, Xiong S, Yu S, Tang Z, Guo B, Zhang L, *J. Mater. Chem. A*, 2023; 11: 8647-8655.

Development of Phosphorylated Cellulose Nanofibers/ Natural Rubber Composites

Ryotaro TAKAYAMA[1]

[1] *Oji Holdings Corporation, 1-10-6 Shinonome, Koto-ku, Tokyo, Japan.*

(takayama050618@oji-gr.com)

Keywords: Cellulose Nanofibers, CNF, NR.

【Introduction】

In recent times, the utilisation of woody biomass has been expected for a variety of applications, with the notable attribute of being both carbon-neutral and a renewable resource. In particular, cellulose nanofibres (CNFs) have garnered significant interest as a novel biomass material.

【Our phosphorylated CNFs】

We have established a method for manufacturing phosphorylated CNFs by introducing phosphate groups to the hydroxyl groups of wood pulp, followed by mechanically processing of the resulting phosphorylated pulp (Figure 1). The introduced phosphate groups via phosphorylation pretreatment enable easy nanofibrillation by strong electric repulsion. The obtained CNF aqueous dispersion is highly transparent, viscous, and stable over a wide pH range.

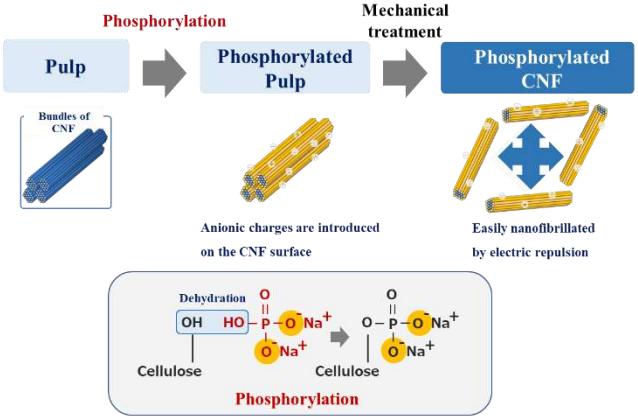


Figure 1. Schematic of the phosphorylated CNF manufacturing process

To promote the practical use of our CNF technology, we are developing natural rubber (NR)/CNF composites. The NR/CNF composites are 100% biomass-derived composites and exhibit unique features compared to NR/carbon black(CB) composites.

In May 2024, we announced the introduction of rubber/CNF composites masterbatch manufacturing equipment with a production capacity of approximately 100 tons per year. A representative sample of the masterbatch produced using this equipment is shown in Figure 2.



Figure 2. NR/CNF masterbatch

【Mechanical properties of NR/CNF composites】

Natural rubber, a material with a wide range of applications in various industries, including tyre and hose manufacturing, is typically reinforced with CB, but CB tends to reduce the elongation of the rubber. The NR/CNF composites we have developed offers comparable reinforcing effect to CB while maintaining the rubber's elongation (Figure 3). Since the amount of CNF added is 1/3 of that of CB, it also contributes to weight reduction of the final product.

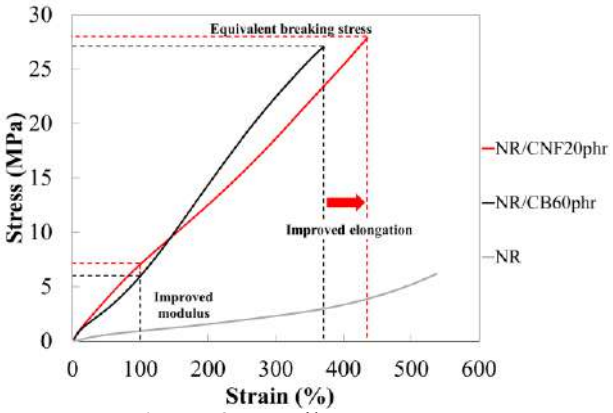


Figure 3. Tensile test

Furthermore, a repeated tensile test was conducted, and the mechanical properties of two cycles were investigated. As shown in Figure 4, the redcution rate of strain energy during loading (cycle1) and re-loading (cycle2) was roughly comparable between CNF and CB.

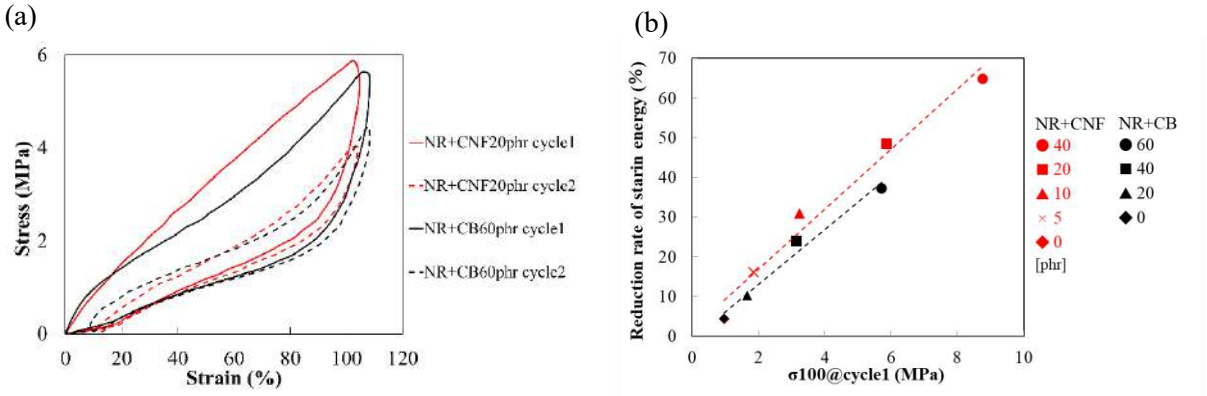


Figure 4. Repeated tensile test (a) strain-stress curve at 100% tensile and (b) 100% modulus in 1st cycle vs. hysteresis loss

In this poster session, we will explain the mechanical properties of NR/CNF composites in detail.

Study on the Effect of Compatibilizer Content on the Mechanical Properties of NR/BR/NBR Blends

S. Kanokporn[1], C. Natchawut [1] and K.Wirunya [1]

[1]*Department of Chemistry, Faculty of Science, Kasetsart University, Bangkok 10900, Thailand*

Corresponding author: fsciwyk@ku.ac.th

Keywords: Ternary rubber blend, NR, BR, NBR, Compatibilizer

At present, the rubber industry continues to play a significant role in global industries. Natural rubber (NR), butadiene rubber (BR), and acrylonitrile-butadiene rubber (NBR) are commonly used in manufacturing processes and product development,each possessing unique properties suitable for a wide range of applications. Blending different rubbers is an effective approach to enhance the properties of rubber materials for broader applications. However, blending rubbers with different polarities remains a significant challenge. NR and BR are non-polar polymers, while NBR is polar. This results in phase mismatches within the blended rubber system. Poor compatibility between rubbers can adversely affect the mechanical and overall properties of the rubber material.

Several studies investigating the combination of different rubbers for improved properties have focused on enhancing compatibility by adding compatibilizers during polymer blending . One such study by Abdelsalam et al.examined NR/SBR/NBR rubber blends with 3 phr of UB4000 compatibilizer and found that using 3 phr of compatibilizer improved the compatibility of the blended rubber [1]. Additionally, most studies commonly use this concentration of 3 phr [2,3].

This research aims to study the effect of adding the compatibilizer (Therpol AST Peletizado) at different loadings of 0, 1, 3, and 5 phr into NR/BR/NBR blends with a fixed ratio of 70/20/10 phr. The properties of the blends were analyzed using FTIR, SEM, DMA, and TGA/DTG techniques to evaluate the effect of the compatibilizer on phase compatibility, mechanical properties, and thermal stability of the blends. The results showed that the addition of compatibilizer, especially at 3 phr, effectively increased phase adhesion, reduced phase separation, and significantly improved the mechanical properties, phase compatibility, and thermal stability of the blended rubber.

Acknowledgement

I would like to express sincere gratitude to all individuals and institutions who contributed to the completion of this study. Special thanks are extended to Wirunya Keawwattana whose guidance, knowledge, and encouragement greatly supported the development of this research. Appreciation is also given to the Department of Chemistry, Faculty of Science, Kasetsart University for providing essential resources and facilities.

References

1. Abdelsalam, M. E.; Shash, S. M.; El-Nashar, D. E. A Comparative Study on Mechanical and Rheological Properties of Ternary Rubber Blends. *J. Thermoplast. Compos. Mater.* **2019**, *33* (6), 839–854.
2. Kunanuruksapong, R.; Somnuk, S.; Sakulkalavek, A. Thermoplastic Vulcanizates Derived from Modified Natural Rubbers and Their Reprocessability. *Polymers* **2023**, *15* (16), 3495.
3. Srinivas, V.; Jagatheeshwaran, M. S.; Vishvanathperumal, S.; Elayaperumal, A. The Effect of Nanosilica on Mechanical and Swelling Resistance Properties of Ternary Rubber (NR/SBR/NBR) Blend Nanocomposites with and without Bis(triethoxysilylpropyl)tetrasulfide. *Silicon* **2024**, *16*, 1669–1688.

Influence of Balanced Ratios between Mica and Carbon Black on Rheological and Mechanical Behaviors of Elastomeric Materials

Won-young Jung [#], Seong-woo Cho [#], Tae-Hee Lee and Keon-Soo Jang *

Department of Materials Science and Engineering, School of Chemical and Materials Engineering, The University of Suwon, Hwaseong, Gyeonggi-do,18323, Republic of Korea

e-mail address of the presenting author (ksjang@suwon.ac.kr)

[#]:They contributed equally; Co-1st authors

Keywords: Ethylene Propylene Diene Monomer (EPDM), Polybutadiene (PB), hybrid filler, surface-modified mica, carbon black

This study explores the development of high-performance and eco-friendly Ethylene Propylene Diene Monomer (EPDM)/Polybutadiene (PB) rubber composites by partially replacing carbon black (CB) with natural mica and ureidopropyltrimethoxysilane (URE)-modified mica (SM) as hybrid fillers. The hybrid filler system was designed to mitigate the environmental impact of CB while maintaining or enhancing the curing behavior, mechanical strength, and elastic performance of the rubber matrix. Curing analysis revealed that high loadings of unmodified mica delayed vulcanization due to poor thermal conductivity and accelerator adsorption, whereas SM-filled systems showed comparable curing kinetics to CB-only composites. Mechanical testing demonstrated that the CB20/SM10 formulation achieved superior tensile strength, elongation, and toughness, surpassing conventional CB systems. Furthermore, dynamic mechanical analysis and rebound resilience tests confirmed reduced hysteresis and enhanced elasticity in SM-containing composites. SEM observations revealed improved filler dispersion and interfacial adhesion in the presence of SM, supporting the enhanced physical properties. These findings highlight the effectiveness of surface-modified mica as a sustainable co-filler, offering a practical strategy to reduce CB usage without compromising performance in elastomeric applications.

Acknowledgement

This work was supported by the Technology Innovation Program (or Industrial Strategic Technology Development Program- Nano fusion innovative product technology development) (No. 20014475, Anti-fog nano-composite-based head lamp with <10% of low moisture adsorption in surface area) funded By the Ministry of Trade, Industry & Energy (MOTIE, Korea). This work was supported by the Materials/Parts Technology Development Program (20024384, Development of a battery housing cover using high orientation

composite material with a fiber content of 40% and using recycled fibers and engineering plastics) funded By the Ministry of Trade, Industry & Energy (MOTIE, Korea). This research was also supported by Advanced Materials Analysis Center, The University of Suwon.

Fatigue Properties of Rubber Composites with Different Glass Transition Temperatures

Jiaye Li[1], Shipeng Wen[1]

[1] *State Key Laboratory of Organic-Inorganic Composites, Beijing University of Chemical Technology, Beijing, China.*

Shipeng Wgen (wensp@mail.buct.edu.cn)

Keywords: Rubber composites, Fatigue; Glass transition temperatures

Rubber, one of the three most essential polymer materials, possesses unique properties such as viscoelasticity, a low modulus of elasticity, and an ability to undergo large reversible deformation. These characteristics make it highly suitable for a range of applications including transportation, sealing and protection, shock absorption, and damping. Due to its significant role in modern industrial construction and national defense, rubber materials are classified as important strategic materials[1].

During practical use, rubber products are frequently exposed to prolonged quasi-static or cyclical dynamic loads. This continuous loading can result in damage to the rubber products, thereby impacting their normal functionality and causing economic losses. To mitigate the significant losses associated with fatigue damage in rubber products, it is crucial to investigate the fatigue life of rubber materials. By conducting such studies, it becomes possible to identify the point at which repair or replacement is necessary to prevent potential fractures or failures. The investigation of the fatigue mechanism in rubber materials holds direct relevance to the durability and safety of rubber products. Consequently, the study of rubber fatigue has consistently captivated professionals working within the rubber field[2].

This paper focuses on the preparation of rubber composites with varying glass transition temperatures (Tg). By varying the proportion of different rubber species, the objective is to examine the impact of different glass transition temperatures on the fatigue properties of these rubber composites.

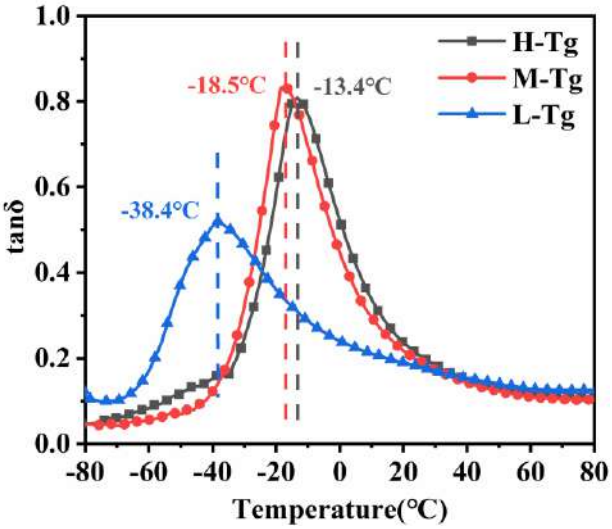


Figure 1. Loss factor versus temperature for different Tg rubber composites

The Tg of the various rubber composites were determined using DMA, as presented in the accompanying figure. Notably, the L-Tg exhibits smaller loss peaks, suggesting reduced internal friction among the molecular chains of the low Tg rubber.

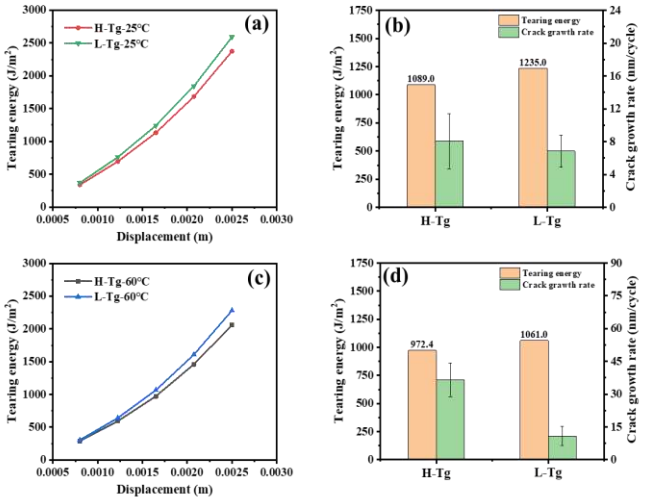


Figure 2. (a) and (c) Tearing energy - displacement curve; (b) and (d) Tearing energy and Crack growth rate at 20% deformation

As depicted in Fig. 2 (a) and (b), the tearing energy of the L-Tg surpasses that of the H-Tg and demonstrates a decrease at elevated temperatures. Moreover, at the same strain, rubber composites with lower tearing energy exhibit a higher rate of crack growth. This phenomenon is particularly pronounced at higher temperatures. Furthermore, the L-Tg exhibits lower rates of crack growth across different temperatures, which indicates superior fatigue resistance properties. In this study, rubber composites with varied glass transition temperatures were formulated by adjusting the ratios of SSBR and BR. The viability of this design approach was confirmed through DMA, which enabled the evaluation of the dynamic properties of the different Tg rubber composites. Additionally, fatigue tests revealed that the L-Tg displayed improved fatigue properties, characterized by larger tearing energy and a reduced rate of crack extension.

References

1. Guo H, Ji P, Halasz I Z, et al. Materials, 2020, 13(24).
2. Xu Z, Jerrams S, Guo H, et al. International Journal of Fatigue, 2020, 131.

International Rubber Conference 2025 (IRC2025)
1-3 December 2025 @ BITEC, Bangkok, Thailand

Development of Tire Tread Formulations for Military Light-Truck Tires

Pairote JITTHAM[1], Puchong THAPTONG[1], Pongdhorn SAE-OUI[1]

[1] *MTEC, National Science and Technology Development Agency (NSTDA), 111 Thailand Science Park, Phahonyothin Road, Khlong Nueng, Khlong Luang, Pathum Thani, Thailand.*

pairotej@mtec.or.th

Keywords: Tire tread compound, Wear resistance, Wet grip performance, Rolling resistance.

The tires used in military vehicles differ significantly in performance from those used in standard civilian vehicles. Military tires require higher strength, durability, and performance under various harsh operational conditions. These requirements make it impossible to simply substitute civilian tires for military use. Therefore, this study aims to develop a tread compound formulation for military light-truck tires. The target tire size is 265/75R16, with performance specifications suitable for 4x4 vehicles, models 50, 51A, and 51B. These vehicles are currently in use across various terrains throughout the country.

The compound was developed using a rubber blend of natural rubber (NR), emulsion styrene-butadiene rubber (ESBR), and butadiene rubber (BR). The research results revealed that the developed compound demonstrated improvements through laboratory testing and evaluations of key tire performance properties. These include heat build-up, wear resistance, wet grip performance (WGP), and rolling resistance. Compared to commercial tire tread currently used by the military, the developed tire tread has slightly higher hardness (approximately 4%), which is within the acceptable range. In addition, it offers improved wear resistance and fuel efficiency (FE) of approximately 12% and 13%, respectively, while maintaining comparable WGP.

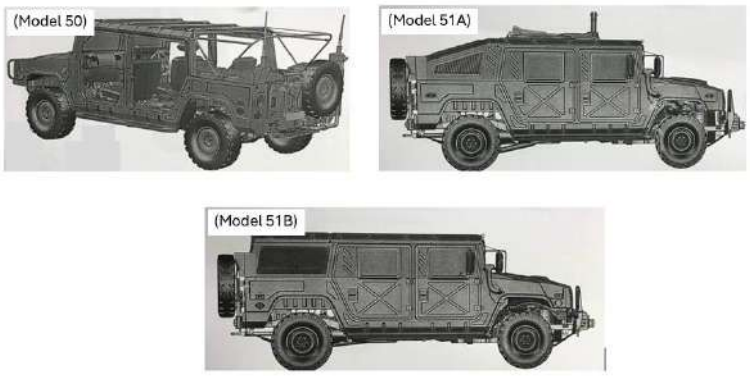


Figure 1. Military light-trucks models 50, 51A, and 51B.

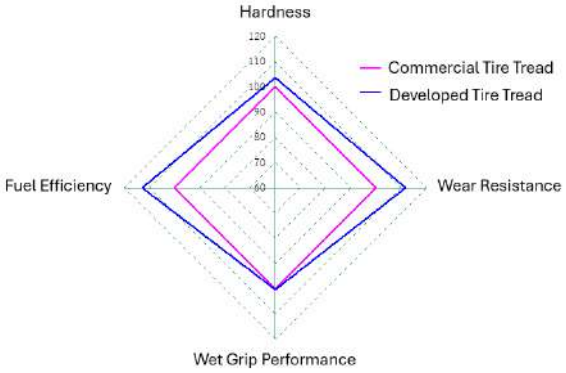


Figure 2. Normalized graph comparing key properties of the developed tread compound with the commercial tire tread used by the Military

Table 1. Properties of the Developed Tread Compound Compared to the Commercial Tire Tread Currently Used by the Military

Properties	Test Conditions	Test Standards	Commercial Tire Tread	Developed Tire Tread
Hardness (Shore A)	Room temperature	ISO 48-4	63.0±5.0	65.8±0.3
Tensile Strength (MPa)	Die type 1, load cell 1 kN, 500 mm/min	ISO 37	-	21.5±0.3
Tear Strength (N/mm)	Method C, 500 mm/min	ISO 34	-	102.7±7.8
Heat Build-up (°C)	100°C, 30 Hz, 245 N, 4.45 mm	ISO 4666-3	-	17.4±0.6
Volume Loss (mm^3)	DIN, Room temperture	ISO 4649 Method B	82.8±2.2	73.1±1.9
tanδ @ 0°C (an indicator for WGP)[1]	Static strain 1%, dynamic strain 0.15%, 10 Hz, -80°C to 80°C, 2°C/min	-	0.202	0.203
tanδ @ 60°C at 5% strain (an indicator for FE)[2]	Static strain 12%, dynamic strain 0.03%-10%, 10 Hz, 60°C	-	0.214	0.186

Acknowledgment:

The authors would like to express their gratitude to the National Research Council of Thailand (NRCT) for supporting the research funding for the fiscal year 2020. Special thanks also go to the Rubber Technology Engineering Center (RTEC), Mahidol University, P.S. Industrial Rubber Co., Ltd., and the Army Ordnance Department for their collaboration in testing the tire performance.

References:

1. Bisschop R, Grunert F, Ilisch S, Stratton T, Blume A, *Polym. Test.*, 2021; 99: 107219.
2. Sirisinha C, Sae-oui P, Suchiva K, Thaptong P, *J. Appl. Polym. Sci.*, 2020; 137(20): 48696.

International Rubber Conference 2025 (IRC2025)
1-3 December 2025 @ BITEC, Bangkok, Thailand

Enhancing Mechanical and Antibacterial Properties of Natural Rubber/Tire Waste Blends through Dual-Phase Processing Techniques

N. KINGKOHYAO[1], T. BOONSIRI[2], Y. NAKARAMONTRI[1]

[1] *Sustainable Polymer & Innovative Composite Materials Research Group, Department of Chemistry, Faculty of Science, King Mongkut's University of Technology Thonburi, Bangkok 10140, Thailand.*

[2] *Department of Microbiology, Phramongkutklao College of Medicine, Bangkok 10400, Thailand.*

e-mail address of the presenting author (napasorn.king@mail.kmutt.ac.th)

Keywords: Latex processing, Melt processing, Nanocomposites, Natural rubber, Tire waste

This research aims to enhance the antibacterial activity and mechanical performance of natural rubber (NR) composites by incorporating recycled tire waste (TW) obtained from the reclamation process and epoxidized natural rubber (ENR), with zinc oxide modified with nanosilica (ZnO-SiO_2) at a ZnO:SiO_2 ratio of 90:10 wt% as a functional filler. NR is a renewable elastomer widely used in industry but is limited by thermal degradation, poor resistance to non-polar solvents, and a lack of antibacterial properties [1]. ENR, derived from NR latex, offers improved polarity and compatibility with polar fillers [2], while recycled rubber can enhance stiffness and abrasion resistance [3]. ZnO nanoparticles provide antibacterial activity against *Staphylococcus aureus (S. aureus)* and *Escherichia coli (E. coli)* [4–5]; however, nanoparticle agglomeration remains a key challenge, often reducing the uniformity and performance of the final composite. To improve dispersion, ZnO was surface-modified with SiO_2 to strengthen filler-rubber interactions. Given that processing methods strongly influence the properties of rubber composites, particularly those containing recycled materials and nanofillers, this study compares the effects of two processing techniques—melt blending and latex blending—on curing behavior, mechanical properties, antibacterial performance, and morphological characteristics. TW/ENR/NR composites containing ZnO-SiO_2 were prepared at a formulation ratio of 50/50/10/10 wt%. Two processing routes were employed: melt blending, and latex blending via a two-step hybrid method. The latex-blended samples, with and without NR latex, exhibited accelerated vulcanization, as evidenced by reduced scorch time (T_{s2}) and optimum cure time (T_{c90}), along with a higher torque difference (M_H–M_L), indicating increased crosslink density. These improvements are attributed to the finer dispersion of ZnO-SiO_2 and stronger filler-rubber interactions facilitated by the two-step blending approach. However, an increase in crosslink density limits the extension of rubber molecular chains, thereby reducing tensile strength and elongation at break, while increasing the modulus, which reflects strength at low strain. In contrast, the melt-blended samples, with lower chain movement, allow greater molecular chain extension which related to the increase of the strain-induced crystallization [6]. Moreover, both methods achieved over 90% antibacterial activity within 8 h against *E. coli* and *S. aureus*, attributed to the synergistic action of Zn^{2+} ion release and reactive oxygen species (ROS) generation at the ZnO-SiO_2 interface [7]. Slightly higher antibacterial activity observed in the latex-blended samples was associated with the residual acidity of ENR latex and more effective dispersion of the hybrid nanofillers, as illustrated in Figure 1. Therefore, this study highlights the trade-offs between processing strategies: latex blending enhances curing efficiency and antibacterial activity, whereas melt blending improves mechanical properties and durability, providing guidance for selecting processing methods to develop high-performance, sustainable NR-based composites for specific applications.

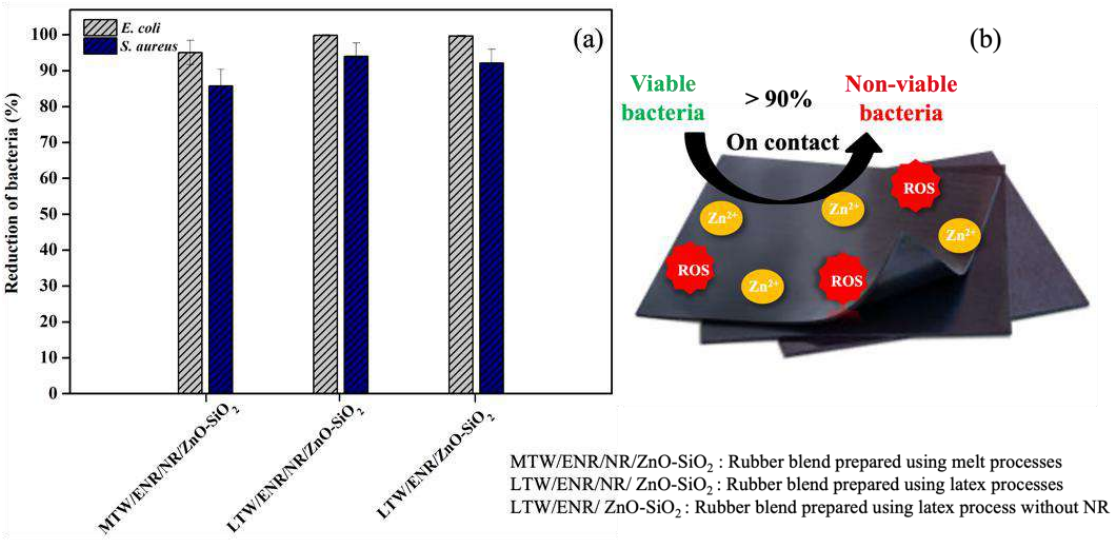


Figure 1. (a) Antibacterial activity of TW/ENR/ZnO-SiO_2 blends with and without NR prepared using melt and latex processes against *E.coli* and *S. aureus*; (b) Proposed mechanism of antibacterial action of the TW/ENR/ZnO-SiO_2 blend with and without NR, illustrating the release of Zn^{2+}ions and generation of reactive oxygen species (ROS), leading to bacterial inactivation upon contact.

Acknowledgement

This work was supported by the Asahi Glass Foundation under KIRIM ID: 27480. The authors also gratefully acknowledge the support from the Petchra Pra Jom Klao Master's Degree Research Scholarship, King Mongkut's University of Technology Thonburi.

References

1. Juntuek P, Ruksakulpiwat C, Chumsamrong P, Ruksakulpiwat Y, *J. Appl. Polym*., 2011; 122: 3152.
2. Poh BT, Chen MF, Ding BS, *J. Appl. Polym. Sci.*, 1996; 60: 1569.
3. Saimi NS, Mamauod SN, Majid NA, Sarkawi SS, Abidin ZZ, *AIP Conf. Proc.,* 2021; 2339: 020116.
4. Gudkov SV, Burmistrov DE, Serov DA, Rebezov MB, Semenova AA, Lisitsyn AB, *Front. Phys.,* 2021; 9: 641481.
5. Rathnayake WG, Ismail H, Baharin A, Bandara IM, Rajapakse S, *J. Appl. Polym. Sci.*, 2014; 131: 39601.
6. Nie Y, Gu Z, Wei Y, Hao T, Zhou Z, *Polym. J.*, 2017; 49: 309.
7. Lallo da Silva B, Abuçafy MP, Berbel Manaia E, Oshiro Junior JA, Chiari-Andréo BG, Pietro RC, Chiavacci LA, *Int. J. Nanomed.*, 2019; 2: 9395.

Durazone D37 as a potential alternative to 6PPD: balancing ozone resistance and dynamic performance

CHUTIMA SAEHENG, PUCHONG THAPTONG

National Metal and Materials Technology Center (MTEC), NSTDA, Pathum Thani, Thailand.

(chutima.sae@mtec.or.th)

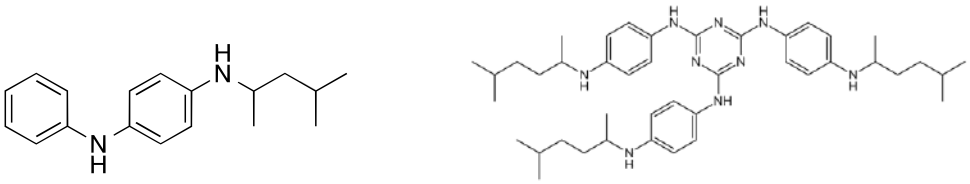
Keywords: 6PPD, Durazone D37, antiozonant, ozone resistance, dynamic performance

Rubber tires require antidegradants to ensure durability against oxidative and ozone-induced degradation, with N-(1,3-dimethylbutyl)-N′-phenyl-p-phenylenediamine (6PPD) (Figure 1(a)) being the most widely used. However, its transformation product, 6PPD-quinone, has been identified as highly toxic to aquatic organisms. Tire wear particles containing 6PPD enter waterways through road dust and runoff, where 6PPD-quinone has been linked to acute mortality in coho salmon and related species [1]. This challenge highlights the urgent need to identify safer alternatives that can maintain tire performance while reducing environmental impact.

This study investigated 2,4,6-tris-(N-1,4-dimethylpentyl-p-phenylenediamino)-1,3,5-triazine (Durazone D37) (Figure 1(b)), a triazine-based antidegradant, as a potential alternative to 6PPD in natural rubber (NR) compounds filled with carbon black (CB). The goal was to evaluate its technical performance relative to 6PPD and to identify an optimal dosage range for practical use. In this work, NR filled with CB (N339) was compounded with individual or blended antidegradants (6PPD and D37). Experimental evaluation covered curing behavior, mechanical properties, abrasion resistance, dynamic viscoelastic behavior, and ozone resistance under both static and dynamic modes.

Results showed that D37 was fully compatible with sulfur vulcanization and maintained tensile strength, hardness, and abrasion resistance comparable to 6PPD. Critically, D37 provided superior ozone resistance, preventing surface cracking even under cyclic dynamic strain. Dynamic mechanical thermal analysis (DMTA) revealed an additional relaxation at 40–60°C in D37-containing compounds as shown in Figure 2, attributed to restricted chain mobility in interfacial bound-rubber regions [2, 3]. This phenomenon increased hysteresis and implied higher rolling resistance. Blended antidegradant systems mitigated this effect while preserving ozone resistance. Based on these results, an optimum D37 dosage was identified in CB-filled NR compounds as a practical balance between ozone durability and dynamic performance.

In conclusion, Durazone D37 offers superior ozone resistance and technical viability as a partial replacement for 6PPD in NR-based tire compounds. However, its impact on hysteresis highlights the need for dosage optimization and further validation. Future research should include pilot-scale compounding, field aging, and environmental fate assessment to confirm industrial applicability.



(a) (b)

Figure 1. Chemical structures of (a) 6PPD and (b) Durazone D37.

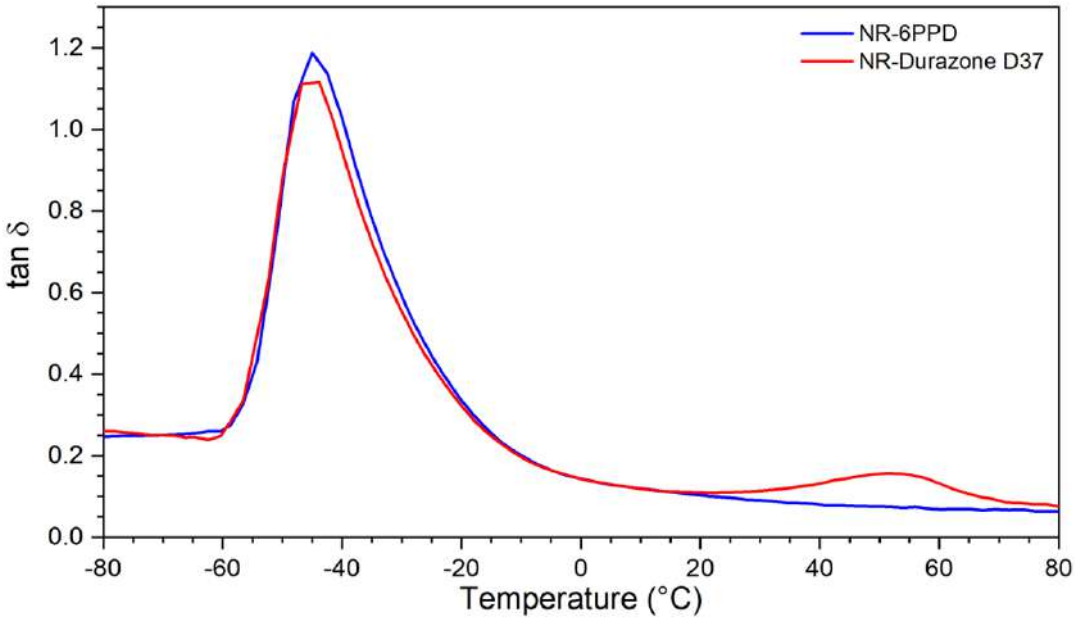


Figure 2. DMTA results of CB-filled NR vulcanizates containing 6PPD and Durazone D37.

Acknowledgement

The authors gratefully acknowledge the financial and technical support provided by SVIZZ-ONE CORPORATION LTD. for this research. This partnership between research and industry played a vital role in shaping the objectives of the study, providing essential resources, and ensuring that the outcomes address both scientific advancement and practical relevance to tire manufacturing.

References

1. Z. Tian, M. Gonzalez, C. A. Rideout, H. N. Zhao, X. Hu, J. Wetzel, E. Mudrock, C. A. James, J. K. McIntyre, E. P. Kolodziej, *Environ. Sci. Technol. Lett.*, 2022; 9: 140.
2. C. G. Robertson, C. M. Roland, Rubber Chemistry and Technology, 2008; 81: 506.
3. V. Arrighia, I. McEwena, H. Qiana, M. Serran, Polymer, 2003; 44: 6259.

International Rubber Conference 2025 (IRC2025)
1-3 December 2025 @ BITEC, Bangkok, Thailand

Effect of Carbon Black and Barium Titanate Hybrid Filler on the Change of Electrical Signal in Epoxidized Natural Rubber Composites

L. BOEURN[1], F. CLEMENS[2], Y. NAKARAMONTRI[1], S. SRISAWADI[3], T. CHANTHASOPEEPHAN[4]

[1]*Sustainable Polymer & Innovative Composite Materials Research Group, Department of Chemistry, Faculty of Science, King Mongkut's University of Technology Thonburi, Bangkok, Thailand.*

[2]*Empa, Swiss Federal Laboratories for Materials Testing and Research, Laboratory for High Performance Ceramics, Ueberlandstrasse 129, 8600 Duebendorf, Switzerland.*

[3]*National Metal and Materials Technology Center, 114 Thailand Science Park, Phahonyothin Road, Khlong Nueng, Khlong Luang, Pathum Thani 12120, Thailand.*

[4]*Department of Mechanical Engineering, King Mongkut's University of Technology Thonburi, 126 Prachautit Road, Bangmod, Tungkru, Bangkok, 10140, Thailand*

e-mail address of the presenting author (lyhav.boeu@kmutt.ac.th)

Keyword: Epoxidized natural rubber, Electrical properties, Hybrid filler

Epoxidized natural rubber (ENR) is a chemically modified form of natural rubber (NR) in which epoxide groups are introduced along the polymer backbone. This structural modification imparts enhanced oil resistance, reduced resilience and air permeability, and increases the glass transition temperature [1, 2]. With 25 mol% epoxidation (ENR-25), the ENR-25 was then compounded with conductive carbon black (CCB), barium titanate ($BaTiO_3$), and a hybrid of the two fillers. The resulting composites were evaluated in terms of their electrical properties to investigate the effect of hybrid filler incorporation. The composites are shown in the proper ratio of the piezoelectric and piezoresistive properties under applied force and strain, respectively. In electrical generation, the ENR-25 composites filled with CCB/$BaTiO_3$ sheet were subject to ball impact before measuring the change in electrical conductivity (σ), dielectric constant (ε'), and also the dielectric loss (ε"). On the other hand, the relative change of the resistance of the composites is measured from the applied strain for a maximum of 300% and elucidates changes in the properties using the electrochemical impedance spectroscopy (EIS) with a Keysight E4990A impedance analyzer (Keysight Technologies, Malaysia). As a result, it was found that the composite containing 10 phr of CCB hybridized with 3 phr of $BaTiO_3$ exhibited optimal values of σ and dielectric ε', along with reduced ε". These improvements are attributed to the synergistic interaction between the conductive network formed by CCB and the high dielectric permittivity of $BaTiO_3$ [3]. Specifically, $BaTiO_3$ enhances filler dispersion and interfacial polarization, while CCB facilitates charge transport via a percolated network. Consequently, these hybrid composites demonstrated superior dielectric performance with minimal energy dissipation [4]. Furthermore, the ball-dropping experiments are expected to showed changes in σ, ε', and ε" with increasing drop height, likely due to disruption of the filler network, an effect indicative of piezoelectric behavior. Therefore, the incorporation of 10 phr CCB and 3 phr $BaTiO_3$ significantly enhances the electrical conductivity and dielectric properties of ENR-25 composites while minimizing energy loss. These findings suggest strong potential for applications in energy harvesting devices, sensors, and capacitors shown in Figure 1.

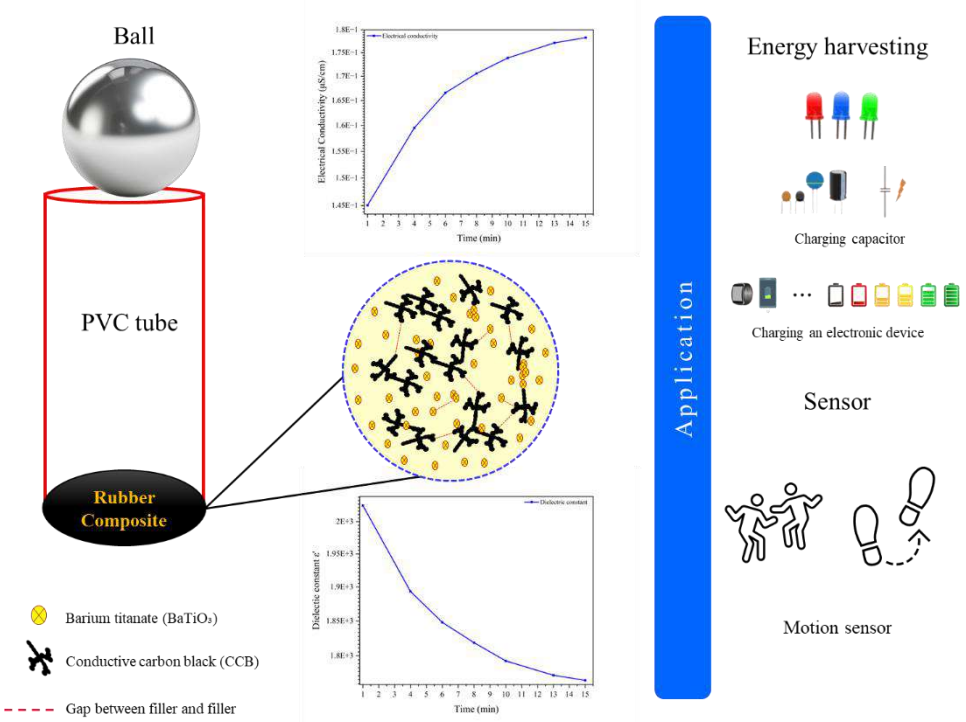


Figure 1. Proposed dropping ball test, mechanism, and application of composites

Acknowledgement

The author would like to express their sincere gratitude to the Swiss National Science Foundation (SNSF) for the scholarship support provided. I am also grateful for the facilities provided by the King Mongkut's University of Technology Thonburi, Department of Chemistry, and this research was conducted under the collaboration between the Swiss Federal Laboratories for Materials Science and Technology (EMPA), specifically the Laboratory for National Metal and Materials Technology Center (MTEC).

References

1. Surya I, Maulina S, Ismail H, IOP Conf. Ser.: Mater. Sci. Eng., 2018; 299: 012061.
2. Chamnanvatchakit P, Prodpran T, Benjakul S, Prasarpran S, Indian J. Sci. Technol., 2015; 8: 1.
3. Zhao H, Xia YJ, Dang ZM, Zha JW, Hu GH, J. Appl. Polym. Sci., 2013; 127: 4445.
4. Dang Z, Shen Y, Nan CW, Appl. Phys. Lett., 2002; 81: 4816.

International Rubber Conference 2025 (IRC2025)
1-3 December 2025 @ BITEC, Bangkok, Thailand

Predicting the glass transition temperature of polymer based on generative adversarial networks and automated machine learning

Zhanjie Liu[1], Jun Liu[1]

[1] *State Key Laboratory of Organic-Inorganic Composites, College of Materials Science and Engineering, Beijing University of Chemical Technology, Beijing 100029, China.*

e-mail address of the presenting author (17865427538@163.com)

Keywords: SSBR, Machine learning, Polymer property prediction, generative adversarial networks, Tree-based Pipeline Optimization Tool

The performance prediction and structural optimization of rubber materials have ushered in a new era, driven by the rapid progress of AI and multi-scale modeling. Solution styrene-butadiene rubber (SSBR) finds wide applications in high performance tire design and various other fields. This study[1] aims to create a quantitative structure-property relationship (QSPR) model linking SSBR's glass transition temperature (T_g) to its structural properties. A dataset of 68 sets of data from published literature was compiled to develop a predictive machine learning model for SSBR's structural design and synthesis using small sample sizes. To tackle small sample sizes, a framework combining generative adversarial networks (GAN) and the Tree-based Pipeline Optimization Tool (TPOT) is proposed. GAN is first used to generate additional samples that mirror the original dataset's distribution, expanding the dataset. The TPOT is then applied to automatically find the best model and parameter combinations, creating an optimal predictive model for the mixed dataset. Experimental results show that using GAN to enlarge the dataset and TPOT regression models significantly enhances model performance, increasing the R^2 value from 0.745 to 0.985 and decreasing the RMSE from 7.676 to 1.569. The proposed GAN-TPOT framework demonstrates the potential of combining generative models with automated machine learning to improve materials science research. This combination accelerates research and development processes, enhances prediction and design accuracy, and introduces new perspectives and possibilities for the field.

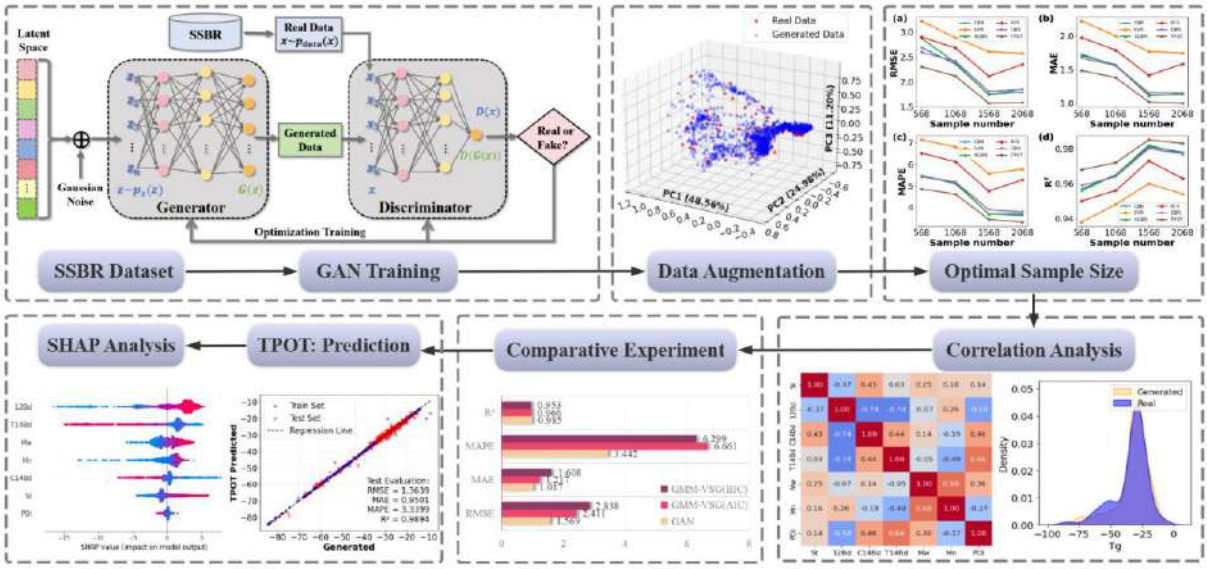


Figure 1. The GAN-TPOT workflow diagram

Acknowledgement

This work is supported by the National Science Fund for Excellent Young Scholars (52122311), the National Natural Science Foundation of China (52373222), and the Open Project of State Key Laboratory of Supramolecular Structure and Materials (Grant number sklssm202512).

References

1. Liu Z, Huo Y, Chen Q, Zhan S, Li Q, Zhao Q, Cui L, Liu J, *MGE Adv.*, 2024, 2 (4), e78.

International Rubber Conference 2025 (IRC2025)
1-3 December 2025 @ BITEC, Bangkok, Thailand

Deproteinization Process of Natural Rubber Latex by Membrane Filtration

Yoko AOYAMA[1], Yuzu TOMEBA[2], Itsuha KUGA[2]

[1] *KOSEN-King Mongkut's Institute of Technology Ladkrabang, 1 Soi Chalongkrung 1, Ladkrabang, Bangkok 10520, Thailand.*

[2] *National Institute of Technology, Numazu College, 3600 Ooka, Numazu, Shizuoka 410-8150, Japan.*

yoko.ao@kmitl.ac.th

Keywords: Deproteinization, Natural rubber latex, Membrane filtration, Microfiltration,

Introduction

Natural rubber latex (NRL) obtained from the sap of Para rubber tree (*Hevea brasiliensis*) contains a few percent of tree-derived proteins which are known to cause Latex allergy. Removal of proteins from NRL has been widely studied [1,2] including either treating with proteolytic enzymes or incubating with urea and surfactants followed by centrifugation. Although these processes are effective to deproteinize NRL, there are some drawbacks of the processes involving centrifugation. Centrifugation/washing for multiple times requires great labor to remove aggregated latex particles generated inside the centrifuge and the serum fluid contains small latex particles which make wastewater treatment difficult.

We have studied deproteinization process of NRL which is denaturation of natural rubber protein by incubation of high ammonia NRL with urea in the presence of surfactant followed by microfiltration as a removal step of denatured and water soluble hevein protein from rubber latex. The objective of this study is to verify the effectiveness of microfiltration membranes for deproteinization. Polyether sulfone membranes with various molecular weight cut-off (MWCO) were examined to separate latex particles and the serum. Ultrasound treatment and addition of basic additives to NRL were also studied to promote deproteinization.

Results and Discussion

High ammonia NRL was diluted to have 30% dry rubber solid content and mixed with urea (0.1w/w%) and sodium dodecyl sulfate (1 wt/wt%). It was incubated for an hour at room temperature and then filtered by using Amicon® Stirred Cell (Merck KGaA) equipped with a polyether sulfone membrane. The nitrogen contents of the dried natural rubber samples were analyzed by Kjeldahl method. The particle size of the latex and the protein size in serum were measured by Zetasizer® (Malvern Panalytical Ltd.).

Among 100, 300, and 1,000 kDa, membrane with higher MWCO showed faster deproteinization (Figure 1). The filtrate with a membrane of 1,000 kDa, however, was turbid and contained small particles of NRL. Filtration with a MWCO 300 kDa was the most suitable in filtering time and deproteinization.

NRL was separated into the top cream layer and the serum by centrifugation. The serum was turbid and contains small latex particles. The cream part has the large latex particles of around 200 nm to 2 μm and the serum contains the small size of latex particles of 100 nm to 400 nm. The small latex particles have large specific surface area and adhere more protein particles on the surface. The latex particles in the serum were filtered to obtain dry rubber samples. The nitrogen content of the serum particles was 1.41 % whereas the nitrogen content of top cream part was 0.107 %. Microfiltration gave the relatively high nitrogen content compared to centrifugation because the small latex particles didn't pass through the pore of the membrane.

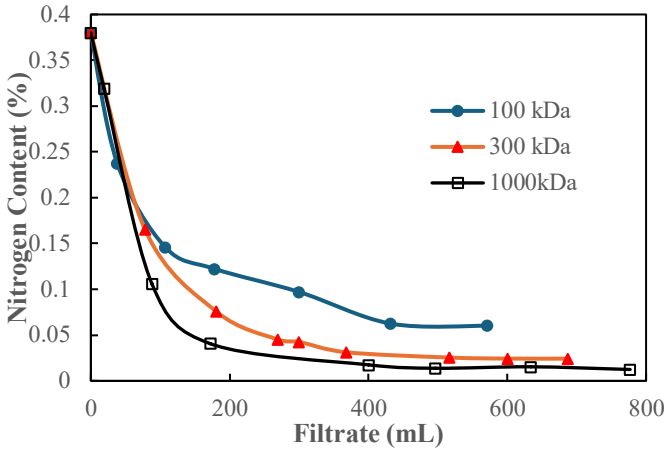


Figure 1. Nitrogen content of DPNR filtered by microfiltration with Amicon® stirred cell unit.

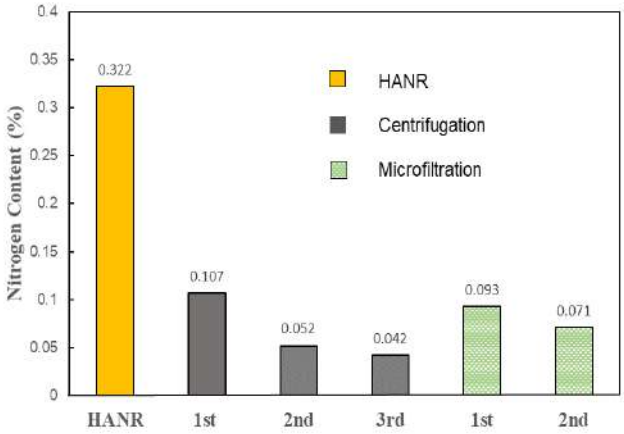


Figure 2. Nitrogen content of DPNR by centrifugation and microfiltration (300 kDa).

Acknowledgement

This study is financially supported by JST/JICA SATREPS, Innovation of Science and Technology on Natural Rubber for Global Carbon Process.

References

1. Perrella, F. W, Gaspari, A. A., *Methods*, 2002; 27: 77.
2. Kawahara, S., Klinklai, W., Kuroda, H., Isono, Y., *Polym. Adv. Technol.*, 2004; 15: 181.

International Rubber Conference 2025 (IRC2025)
1-3 December 2025 @ BITEC, Bangkok, Thailand

Short-term Surface Nanostructure Change of Biodegradable Polyester Thin Films by Seawater Immersion Treatments

Nana Tsuji[1], Hiroto Osakaki[1], Keito Shimakawa[1], Ryu Miyajima [1], Kazuki Imai[1], Khanh-Van Thi Khuat[2], Hiroyasu, Masunaga [3], Yingjun An[4], Atsushi Takahara [4], Sono Sakaki[*1,2,5]

[1]*Grad. Sch. of Sci. and Tech., Kyoto Inst. of Tech., 1 Matsugasaki Hashigami-cho, Sakyo-ku, Kyoto 606-8585, Japan;*

[2]*Fac. of Fiber Sci. and Tech., Kyoto Inst. of Tech., 1 Matsugasaki Hashigami-cho, Sakyo-ku, Kyoto 606-8585, Japan;*

[3]*Japan Syn. Rad. Res. Inst., 1-1-1 Kouto, Sayo-cho, Sayo, Hyogo 679-5198, Japan;*

[4]*K-NETs, Kyushu Univ., Motooka 744, Nishi-ku, Fukuoka 819-0395, Japan;*

[5]*RIKEN SPring-8 Center, 1-1-1 Kouto, Sayo-cho, Sayo, Hyogo 679-5148, Japan.*

E-mail: m4661013@edu.kit.ac.jp

Keywords: biodegradable polyester, marine degradation, grazing-incidence X-ray diffraction (GIXD) measurement, decomposition in seawater, short-term surface nanostructure change.

Introduction

The world production of plastics increased to 380 million tons in 2015 from 2 million tons in 1980 [1] and the runoff of plastics to the environment has become a problem all over the world. In 2010, it was calculated that 4.8 to 12.7 million tons of plastics were discharged into the ocean [2]. Therefore, biodegradable plastics have been attracting attention in recent years, and their global production is anticipated to increase from 2.47 million tons in 2024 to 5.73 million tons in 2029 [3]. Degradability assessment of plastics in the marine environment is typically conducted by immersing samples in the ocean for several months to several years. To shorten this assessment time, the short-term surface degradation of plastics in the ocean can be used to predict long-term bulk degradation, as degradation typically occurs at the surface. However, the surface structure change has not been clarified in detail. The purpose of this study is to investigate the nanostructure changes in marine degradable plastic thin films caused by seawater immersion treatments by grazing-incidence X-ray diffraction (GIXD) measurements using synchrotron radiation. The biodegradation behavior of marine degradable plastics provides valuable methodological insights for investigating the environmental fate of polymeric materials in marine conditions. Previous studies, including those by Aamer Ali Shah, have demonstrated the biodegradability of both natural and synthetic rubber [4]. Building on these findings, the present research may inform future studies on the biodegradation potential of rubber-based materials.

Experiments

A sample used in this study was poly(butylene succinate-*co*-adipate) (PBSA, M_w [the weight-average molecular weight] = 3.10×10^5 g/mol, Mitsubishi Chem. Co. Ltd.). Poly(butylene succinate) (PBS, M_w = 2.57×10^5 g/mol, Mitsubishi Chem. Co. Ltd.) was used for comparison. Thin films were prepared on Si substrates by the spin-coating method with 5 wt% of PBSA and PBS in chloroform. Afterward, the PBSA and PBS thin films were crystallized isothermally for 4 hours at crystallization temperatures, T_cs, of 55 and 85 ℃, respectively, from the melt. The resulting melt-crystallized thin films consisting of spherulite aggregates had a ca. 1.25 μm thickness. Seawater immersion treatments for the films were conducted using the extracted seawater (pH = 7.81) prepared by filtering (5

μmϕ filter) a mixture of natural seawater and sediments collected in Imazu, Fukuoka. The thin films were immersed in the extracted seawater at 25 ℃ under the ambient pressure (0.1 MPa) for up to 10 days. Then, those were rinsed with distilled water and dried under vacuum. GIXD measurements were performed at the BL38B1 beamline in SPring-8 (RIKEN, Hyogo, Japan). The wavelength of the incident X-ray beam was 0.1 nm, and the incident angle to the specimen surface was 0.05 (for near-surface evaluation of the nanostructure) and 0.11 (for whole film evaluation) degrees. The GIXD patterns were measured with a PILATUS3 X 2M detector (Pixcel resolution : 172 × 172 μm^2) (DECTRIS Lid.). Film thickness and surface roughness measurements were performed by using a Surfcorder (Kosaka Laboratory Ltd.). Spherulitic structures in the thin films were observed by a digital microscope VHX-6000 (KEYENCE Co. Ltd.).

Results and Discussion

The observed peaks in the measured GIXD profiles were indexed as the Bragg reflection from the monoclinic crystal structure. The monoclinic lattice constant *a* in the near-surface region of the PBSA thin films was slightly larger than that of the PBS thin films and exhibited an increasing trend after 6 days of seawater immersion treatment. This suggests that surface decomposition in the PBSA thin films occurred due to crystallographic defects or disorder. The crystallite size in the [110] azimuth near the surface of the PBSA thin film also decreased after 6 days of immersion. These results suggest that the PBSA thin film underwent nanoscale degradation in the crystal region after 6 days of immersion in the extracted seawater. On the other hand, there were no changes in the lattice constant *a* and crystallite size in the near-surface region of the PBS thin films, indicating that the PBS thin films maintained their nanostructure just after 10 days of seawater immersion treatment. In our poster presentation, the degradation of both amorphous and crystalline regions will be explained for the PBSA and PBS thin films.

Acknowledgement

This work was supported by JST (Moonshot R & D Program, Grant Number JPNP18016).

References

1. Geyer, R. *et al.*, “Production, use, and fate plastics ever made”, *Science Advances* 3, no.7 (19 Jul. 2017): 1-5. DOI: 10.1126/sciadv.1700782
2. Jambeck, J.R. *et al.*, “Plastic waste inputs from land into the ocean”, *Science* 347, no. 6223 (13 Feb. 2015): 768-771. DOI: 10.1126/science.1260352
3. European Bioplastics, “Bioplastics Market Development Update 2024”, EUBP_Market_Data_Report_2024.pdf
4. Shah, A.A. *et al.*, “Biodegradation of natural and synthetic rubbers: A review”, *Int Biodeterior Biodegrad* 83, (1 Sep. 2013): 145-157. DOI: 10.1016/j.ibiod.2013.05.004

Effect of Seawater Pressure on the Nanostructure Changes in Poly(*l*-lactic acid) Homopolymer and Poly(*d*, *l*-lactic acid) Blend Thin Films

Khanh-Van Thi KHUAT[1], Nana TSUJI[2], Ryu MIYAJIMA[2], Kazuki IMAI[2], Hiroyasu MASUNAGA[3], An YINGJUN[4], Atsushi TAKAHARA[4], Sono SASAKI[*1,2,5]

[1]*Fac. of Fiber Sci. and Eng. Kyoto Inst. of Tech., 1 Hashigami-cho, Matsugasaki, Sakyo-ku, Kyoto 606-8585, Japan.*

[2]*Grad. Sch. of Sci. and Tech., Kyoto Inst. of Tech., 1 Hashigami-cho, Matsugasaki, Sakyo-ku, Kyoto 606-8585, Japan.*

[3]*Japan Syn. Rad. Res. Inst., 1-1-1 Kouto, Sayo-cho, Sayo, Hyogo 679-5198, Japan.*

[4]*K-NETs, Kyushu Univ., 744 Motooka, Nishi-ku, Fukuoka 819-0395, Japan.*

[5]*RIKEN SPring-8 Center, 1-1-1 Kouto, Sayo-cho, Sayo, Hyogo 679-5148, Japan.*

E-mail address: van@kit.ac.jp

Keywords: poly(*l*-lactic acid) thin films, poly(*d*,*l*-lactic acid) blend thin films, seawater-induced surface decomposition, grazing-incidence X-ray diffraction (GIXD) analysis, synchrotron radiation, effect of seawater pressure.

The escalating dependency on petroleum-based polymeric materials has led to widespread plastic pollution, underscoring the urgent need for sustainable alternatives. Biodegradable polymers, such as poly(lactic acid) (PLA), including its stereoisomers poly(*l*-lactic acid) (PLLA) and poly(*d*-lactic acid) (PDLA), have emerged as promising candidates due to their intrinsic biodegradability and derivation from renewable resources. Although PLA has been widely proposed as a viable substitute for conventional petrochemical plastics, its biodegradation performance in seawater remains insufficiently understood. Previous investigations have revealed that PLA degradation in seawater is typically characterized by extended timescales and limited to macroscopic structural changes of the bulk material [1,2]. The long-term bulk degradation behavior of PLA in marine environments may be anticipated from its short-term surface degradation processes. Owing to its higher density relative to seawater, PLA has the potential to sink and accumulate on the seafloor, thereby highlighting the necessity of evaluating its degradation behavior under high-pressure marine conditions. This study investigates the influence of seawater pressure on the surface biodegradation of PLLA and PLLA/PDLA blend thin films with thicknesses under 1 μm. Nanostructure changes in the films were examined following seawater immersion under both ambient pressure conditions, representative of shallow marine environments, and elevated pressure conditions (10.5 MPa), corresponding to seafloor conditions. Grazing-incidence X-ray diffraction (GIXD) measurements utilizing synchrotron radiation were employed to characterize the structural evolution of the films and assess pressure-dependent degradation mechanisms. The biodegradation behavior of PLA in seawater provides critical reference data and methodological frameworks for evaluating the environmental persistence of polymeric systems, including elastomeric materials, in marine environments. Insights into PLA degradation mechanisms and rates can inform the design of standardized assessment protocols and support the development of biodegradable elastomeric composites with enhanced ecological compatibility.

PLLA and PDLA with M_n (the number-averaged molecular weight) of ~10,000 and ~12,000, and M_w (the weight-averaged molecular weight) of ~11,800 and ~14,200 (purchased from Polymer Source Inc.), respectively, were deposited onto silicon substrates via spin-coating. Subsequent isothermal crystallization was performed from the melt at 120 °C for PLLA and 170 °C for the PLLA/PDLA blend. The resulting melt-crystallized thin films exhibited thicknesses in the range of 500–900 nm and featured spherulitic aggregate morphologies. Seawater immersion experiments were conducted using filtered seawater (pH 7.51–7.70), prepared by passing a mixture of natural seawater and sediment collected from Imazu, Fukuoka, through a 5 μmϕ filter. Thin films were immersed at 25 °C under two pressure conditions: ambient (0.1 MPa) and elevated (10.5 MPa), for durations of up to 14 days. Following immersion, the films were rinsed with distilled water and dried under vacuum. GIXD measurements were carried out at the BL38B1 beamline of the SPring-8 synchrotron radiation facility, employing an X-ray beam (wavelength λ = 0.1 nm) and a PILATUS detector to assess nano-structural changes induced by seawater exposure.

A progressive reduction in film thickness was observed with increasing seawater immersion time, with the thinning rate more pronounced in PLLA than in the PLLA/PDLA blend. GIXD intensity profiles for PLLA and PLLA/PDLA blend thin films exhibited diffraction peaks indexed to Bragg reflections corresponding to the orthorhombic and trigonal (hexagonal-type) crystal structures, respectively. Deconvolution of the GIXD profiles into crystalline Bragg reflections and amorphous scattering components enabled the quantitative determination of lattice constant, apparent crystallinity, and crystallite size. The effects of seawater pressure on the nanostructure change of both PLLA and PLLA/PDLA thin films will be discussed in detail in our presentation.

Acknowledgement

This work was supported by JST（Moonshot R&D Program, Grant Number JPNP18016).

References:

1. Tsuji H, Suzuyoshi K, *Polym. Degrad. Stabil.*, 2002; 75: 347–355.

2. Bagheri A R, Laforsch C, Greiner A, Agarwal S, *Glob. Chall.*, 2017, 1: 1700048.

International Rubber Conference 2025 (IRC2025)
1-3 December 2025 @ BITEC, Bangkok, Thailand

Effects of Proteins and Purification in Peroxide-Prevulcanized Natural Rubber Latex for Medical Devices

T. WATCHARAKAN[1,2], M. SRIRING[1], A. NIMPAIBOON[1], P. HAVANAPAN[3], N. PHUNGTHANOM[3], P. TUMWISED[1], C. SIRISINHA[1], K. SUCHIVA[1]

[1] *Rubber Technology Research Centre, Faculty of Science, Mahidol University, NakhonPathom, 73170, Thailand.*

[2] *Polymer Science and Technology Program, Department of Chemistry, Faculty of Science, Mahidol University, Nakhon Pathom, 73170, Thailand.*

[3] *Institute of Molecular Biosciences, Mahidol University, NakhonPathom, 73170, Thailand.*

thitipan.wat@student.mahidol.ac.th

Keywords: Natural rubber latex, Peroxide, Prevulcanization, Enzymatic deproteinization

Natural rubber latex (NRL), obtained from *Hevea brasiliensis*, is widely used in medical and consumer products due to its desirable attributes such as good mechanical properties and elasticity, sustainability, and cost-effectiveness. However, concerns over type I and type IV latex allergies caused by proteins and residual curatives especially for sulfur system present significant challenges for utilizing NR in medical applications [1-3]. Sulfur-based NR vulcanizate often involves accelerators such as thiurams, carbamates, and benzothiazoles, which are associated to allergic reactions and potential carcinogens and zinc oxide (ZnO) as environmental polutantion causing [4-5]. It has been reported that NRL vulcanized by peroxide system using tert-butyl hydroperoxide (t-BHP) and fructose was a more environmentally friendly option compared to sulfur-based systems [6]. However, there is limited research on how purification may affect vulcanization behavior and the resulting properties of the materials.

In the present work, we aim to investigate how peroxide-vulcanization process affects protein alterations in NRL and elucidate the impact of purification on its vulcanization behaviors and properties. NRLs before and after purification using enzymatic deproteinization were vulcanized with t-BHP and fructose at 60ºC. Changes in allergenic protein in latex, vulcanization efficiency, and the mechanical and dynamic properties of the resulting vulcanizate films were systematically analyzed.

The results demonstrated that naturally occurring proteins in NRL significantly enhanced vulcanization, as evidenced by increased crosslinking density and improved mechanical properties in NR samples [7]. Additionally, the vulcanization reaction also modified certain allergenic proteins. In contrast, deproteinized NRL exhibited a significant reduction of vulcanization efficiency, leading to much lower mechanical and dynamic properties compared to the original NRL sample [7]. These findings highlight the important role of proteins in the peroxide-based vulcanization of NRL. Proteins both located at rubber particle (RP) membrane and dispersed in serum phase could act as redox cofactors, promoting the redox reaction between t-BHP and fructose [8]. They may facilitate radical generation, enhance electron transfer across the RP interface, and stabilize reactive radicals, thereby contributing to efficient vulcanization through a bipolar redox mechanism, as proposed in Figure 1.

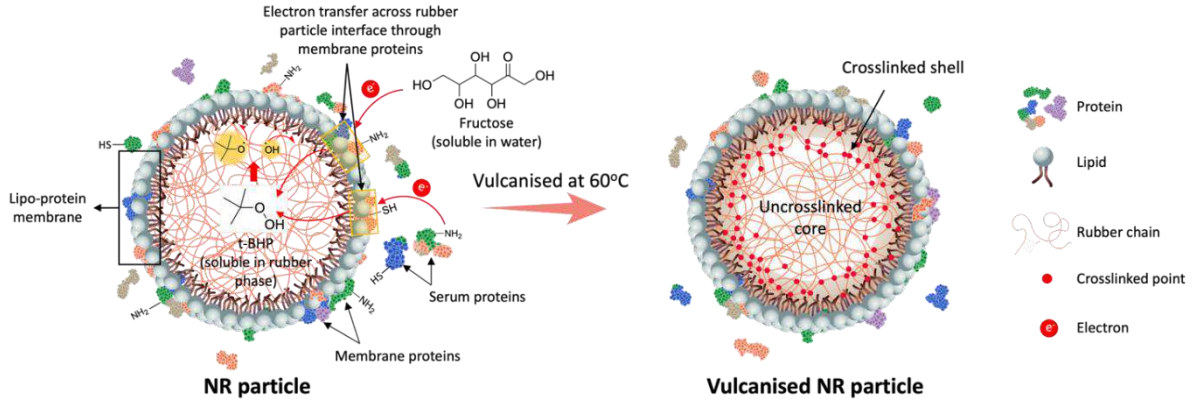


Figure 1. Proposed mechanism of peroxide vulcanization within NR particle facilitated by proteins [9]

To improve latex purity without reducing the material performance, the NRL vulcanized at 60ºC for 3 h was chosen to be purified via a surfactant washing compared to an enzymatic proteolysis approach. The results demonstrated that allergenic and extractable proteins and other extractable contaminants in the vulcanized NR latex were effectively eliminated through multiple washing cycles, with even greater efficiency achieved through enzymatic treatment. Importantly, the purified films retained good mechanical and dynamic properties, indicating the successful preparation of high-purity prevulcanized NR latex suitable for applications in the medical field. These findings highlight the potential for developing an alternative vulcanization system with reduced allergenicity, contamination and lower pollutant emissions.

Acknowledgement

This research project was supported by Mahidol University (MU's Strategic Research Fund) : 2023. Sincere appreciation was extended to Kokoku Innovative Technology Ltd. (KITy) for their financial, instrumental, and technical support.

References

1. Yip E, Cacioli P. The manufacture of gloves from natural rubber latex. *J Allergy Clin Immunol.* 2002;110(2 Suppl):S3-14.
2. Guerra NB, Sant'Ana Pegorin G, Boratto MH, de Barros NR, de Oliveira Graeff CF, Herculano RD. Biomedical applications of natural rubber latex from the rubber tree Hevea brasiliensis. *Mater Sci Eng C Mater Biol Appl.* 2021;126:112126.
3. Davies RT, Gazeley KF. Peroxide prevulcanisation of natural rubber latex with t-butyl hydroperoxide. *J Nat Rubb Res.* 1993;8(3):133–42.
4. Crepy MN. Rubber: new allergens and preventive measures. *Eur J Dermatol.* 2016;26(6):523–530.
5. Sommer S, Wilkinson SM, Beck MH, English JSC, Gawkrodger DJ, Greens C. Type IV hypersensitivity reactions to natural rubber latex: results of a multicentre study. *Br J Dermatol.* 2002;146(1):114–117.

6. Said MZM, Pendle TD, Blackley DC. Peroxide prevulcanisation of natural rubber latex. *J Nat Rubb Res.* 1990;5(1):14–21.
7. Wichaita W, Saengdee P, Sakdapipanich JT. Hollow core-shell structure of grafted rubber particles prepared by redox initiation: Role of proteins and phospholipids in natural rubber latex. *Polymer*. 2016;97:1–10.
8. Longsiri N, Saengdee P, Sakdapipanich JT. Graft copolymerization of PS-co-PAN onto deproteinized natural rubber latex using bipolar redox initiation system. *Bioresour Bioprocess*. 2022;9(1):1–14.
9. Schneider, M, Pith, T, Lambla, M, Preparation and morphological characterization of two- and three-component natural rubber-based latex particles. J. Appl. Polym. Sci. 1996; 62, 273-290.

International Rubber Conference 2025 (IRC2025)
1-3 December 2025 @ BITEC, Bangkok, Thailand

A Sustainable Approach to Viscosity Control and Recycling of Over-matured Prevulcanized Latex in the Elastic Thread Industry

Nuorn Choothong[1], Bawornkit Nekamanurak[1], Teerin Kongpun[1] and Seiichi Kawahara[2]

[1] *Department of materials engineering, Faculty of engineering, Rajamangala university of technology Rattanakosin, Salaya, Nakornprathum 73170, Thailand*

[2] *Department of materials science and technology, Faculty of engineering, Nagaoka University of Technology, Nagaoka, Niigata, Japan, 940-2188*

Nuorn.cho@rmutr.ac.th

Keywords: Over-maturation, prevulcanized natural rubber latex, devulcanization, devulcanizing agent, chemical peptizer

Over-maturation of prevulcanized natural rubber latex (PNRL) is a significant challenge in the elastic thread industry, leading to an irreversible increase in viscosity that renders the material unusable and results in substantial economic and environmental costs. This study presents a sustainable approach to control viscosity and recycle over-matured PNRL through a liquid-phase chemical devulcanization process. The comparative effectiveness and reaction mechanisms of two chemical peptizers, Benzoyl Peroxide (BPO) and Diphenyl Disulfide (DD), were investigated at concentrations of 0.1, 0.3, and 0.5 phr. The devulcanization mechanism was elucidated using swelling tests, Horikx plot analysis, and FTIR spectroscopy. Subsequently, the feasibility of re-blending the reclaimed latex (devulcanized with an optimal 0.3 phr of DD) into virgin PNRL at ratios of 10, 20, and 30% was evaluated, focusing on final product properties critical for industrial application, including permanent set, stress relaxation, and heat aging resistance. The results demonstrated that DD functions as an ideal devulcanizing agent, selectively cleaving sulfidic crosslinks while preserving the polymer main-chain integrity, as confirmed by Horikx plot analysis and FTIR spectroscopy. This selective mechanism allowed the reclaimed latex to retain good mechanical properties. In contrast, BPO was found to act primarily as a degradation agent, causing significant main-chain scission that led to a severe deterioration of all mechanical properties, despite its effectiveness in reducing viscosity. The application study revealed that incorporating up to 20% by dry weight of the DD-reclaimed latex into virgin PNRL maintained the final product's mechanical and application-specific properties within acceptable industrial standards. This research successfully demonstrates that liquid-phase devulcanization using Diphenyl Disulfide is a viable and practical solution for upcycling waste over-matured PNRL.

Acknowledgement

Funding was also received from the Thailand Science Research and Innovation (TSRI) and Fundamental Fund of Rajamangala University of Technology Rattanakosin with funding under contract No. FRB6737/2567 / Research project Reclamation of wasted rubber latex by chemical devulcanization of sulphur (S-S) chains for natural rubber thread industry (2023).

References

[1] J. Shi, K. Jiang, D. Ren, H. Zou, Y. Wang, X. Lv and L. Zhang, J. Appl. Polym. Sci. 2012, 129, 999-1007.
[2] C. Kumnuantip, N. Sombatsompop, Mater. Lett. 2003, 57, 1341-3174.
[3] A.A. Phadke, A.K. Bhattacharya, S.K. Chakraborty and S.K. De, Rubber Chem. Technol. 1983, 56, 1983.

International Rubber Conference 2025 (IRC2025)
1-3 December 2025 @ BITEC, Bangkok, Thailand

Effective degradation of waste tyre rubber using a specific treatment process: A Chemi-biological Method

Pritish R. SHUKLA[1], Utpal ROY[1], Sunil BHAND[2]

[1] *Department of Biological Sciences, Birla Institute of Technology and Science Pilani, K.K. Birla Goa Campus, India.*

[2] *Department of Chemistry, Birla Institute of Technology and Science Pilani, K.K. Birla Goa Campus, India.*

p20210051@goa.bits-pilani.ac.in

Keywords: Biodegradation, Devulcanization, Green Solvent, Rubber-degrading bacteria, Waste tyre rubber

Rubber constitutes a primary component of tyres. Typically, a tyre rubber is composed of 40-50% rubber (including styrene-butadiene rubber, natural rubber, and butyl rubber), 25–40% carbon black, and 10–15% low-molecular-weight additives. Despite their significant economic value, billions of discarded tyres are accumulating globally, with their numbers increasing annually. These stockpiles pose serious environmental and health hazards [1]. With tyre rubber requiring up to 2000 years to fully degrade, millions of tyres are disposed of in landfills, where their combustion results in environmental pollution due to the release of toxic gases, including carbon monoxide, carbon dioxide, and sulfur dioxide [2].

Biodegradation provides an eco-friendly solution for rubber waste problems. It involves the secretion of enzymes by rubber-degrading microorganisms that cleave rubber polymeric chains into smaller molecules, which are subsequently assimilated by microbial cells as carbon and energy sources. However, the microbial breakdown of polyisoprene rubber is inherently slow, often requiring weeks or even months [3]. Similarly, biodesulfurization of rubber is a microbial process aimed at reducing or eliminating sulfur from rubber using microorganisms belonging to the *Thiobacillus* genus, thermoacidophiles of the *Sulfolobales* order, *Gordonia desulfuricans*, and *Rhodococcus* species. This step is crucial for modifying the cross-linked structure of vulcanized rubber, facilitating subsequent biodegradation or biotransformation. However, challenges persist, including low desulfurization efficiency relative to the rubber mass and prolonged treatment durations [4].

A sustainable, environmentally friendly approach, combining a non-toxic chemical and biological treatment, has been proposed to achieve efficient rubber degradation. Effective degradation of vulcanized rubber requires a combination of detoxification, devulcanization, and depolymerization processes. This study presents a novel two-step solution comprising pretreating rubber by a green solvent, involving 24 h of swelling, sonication, and heating at 180°C, followed by filtration and incubation at 30°C for 28 days in a mineral-rich pure culture of a rubber-degrading bacterial isolate at constant shaking under sterile conditions.

Several characterization techniques were employed to confirm the cumulative effect of the approach, including monitoring cell biomass and viability, weight reduction measurement, Schiff's staining, Attenuated Total Reflectance-Fourier Transform IR (ATR-FTIR) analysis, Scanning Electron Microscopy (SEM) imaging, Energy Dispersive X-ray Spectroscopy (EDS), change in sulfur crosslink density, and cytotoxicity of green solvent against rubber-degrading bacterium.

Results demonstrated that pretreated rubber, used as the sole carbon and energy source, supported enhanced bacterial growth, reaching a maximum viable biomass of 1.91×10^{12} CFU/mL by

the 14th day of incubation, a 43.85% increase over unpretreated rubber. The green solvent showed no cytotoxicity, as confirmed by the absence of an inhibition zone when tested against the bacterium in the disc diffusion assay. This synergy contributed to a 17.6% increase in mass reduction and a 33% decrease in sulfur crosslink density, as determined by swelling test using the Flory-Rehner equation. FTIR analysis showed partial cleavage of -C-S-, -S-S-, and C=C bonds, while Schiff's staining confirmed the presence of oligoisoprenoids as an indication of rubber degradation. SEM images revealed increased surface cracks, dents, and roughness. EDS analysis was performed to estimate the changes in the elemental composition of treated rubber, to evaluate the amount of carbon that is potentially available as a nutrient. The EDS analysis showed reductions in weight% of carbon (12.67%), sulfur (46.17%), and zinc (68.45%) contents.

Pretreatment increased carbon availability and utilization up to 5-fold by exposing more C=C bonds in polyisoprene chains, facilitating bacterial enzymatic action and overall biodegradation, underscoring the efficiency of the combinational approach. These findings represent the synergistic potential of green solvent pretreatment and bacterial activity as a two-step sustainable solution for rubber waste management.

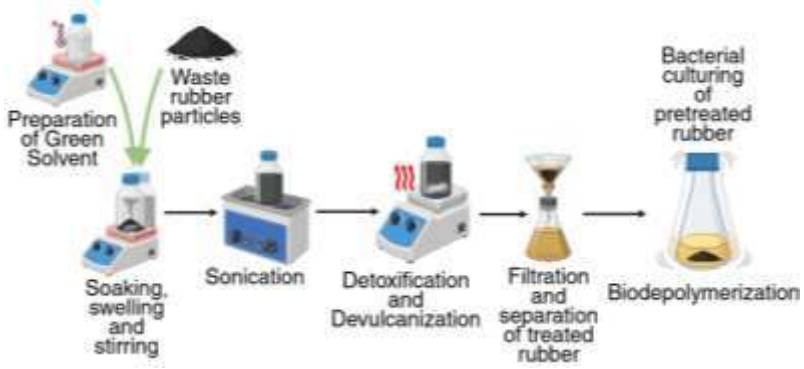


Figure 1. Two-step process for effective rubber degradation

Acknowledgements

The authors gratefully acknowledge the funding and fellowship support from the Corporate Social Responsibility (CSR) of the partner industry, Birla Carbon India Pvt. Ltd., and government agencies, Department of Science and Technology (DST), Government of India and Confederation of Indian Industry (CII).

References

1. Chittella H, Yoon LW, Ramarad S, Lai ZW, *Polym. Degrad. Stab.*, 2021; 194:109761.
2. Cheng Y, Wei Y, Wu H, Zhang T, Li S, Zhu N, Zhang Q, Li W, *Chem. Eng. J.*, 2024; 481:148685.
3. Watcharakul S, Röther W, Birke J, Umsakul K, Hodgson B, Jendrossek D, *BMC microbiol.*, 2016; 16:1-3.
4. Andler R, Cancino C, González-Arancibia F, Rojas J, Castro R, Kasai D, Sanhueza V, *J. Environ. Chem. Eng.*, 2025; 13(2):115598.

Flame-Retardant Performance of Epichlorohydrin-Modified Reclaimed Tire Rubber

Selly M. MAILANDA[1], Rathanawan MAGARAPHAN* [1,2]

[1]*Polymer Processing and Polymer Nanomaterials Research Unit, Petroleum and Petrochemical College, Chulalongkorn University, Bangkok, Thailand.*

[2]*Center of Excellence in Green Materials for Industrial Application, Faculty of Science, Chulalongkorn University, Bangkok, Thailand.*

e-mail address of the presenting author (6578702663@student.chula.ac.th)

*e-mail address: rathanawan.k@chula.ac.th

Keywords: Ground tire rubber, Devulcanization, Functionalization, Revulcanization, Flame-retardant

Natural rubber is known for its excellent thermal insulation due to its low thermal conductivity, which effectively minimizes heat transfer. However, challenges arise with its low fire resistance [1]. Unlike natural rubber, tires are made from vulcanized rubber using sulfur, which improves mechanical properties such as durability, weather resistance, and flexibility. However, the rapid growth of the automotive industry has led to increased tire and waste tire production, creating disposal challenges. Devulcanization agents are crucial for cleaving crosslink bonds and preventing reattachment, thereby enhancing both the devulcanization degree and efficiency. In this study, ground tire rubber (GTR) has been devulcanized using caprolactam as a devulcanizing agent and modified with *p*-coumaric acid (FD-GTR) via thiol-ene click chemistry.

The action of flame-retardants (FRs) in the combustion process involves a gas-phase reaction between fuel and oxygen that proceeds through preheating, volatilization/decomposition, ignition, combustion, and flame propagation. A common mechanism is gas-phase radical quenching, halogenated FRs scavenge reactive radicals that sustain the flame, thereby suppressing flame propagation. Organohalogen compounds can store and deliver halogens within polymers, but not all are effective flame retardants [2]. This study uses epichlorohydrin (ECH), a chlorine-containing epoxy compound, as a flame-retardant agent. The epoxy group reacts with the acid groups of the *p*-coumaric acid, with caprolactam acting as a reaction promoter for the opening of the epoxy rings while retaining the chlorine functionality (FD-GTRECH), as shown in Figure 1 [3].

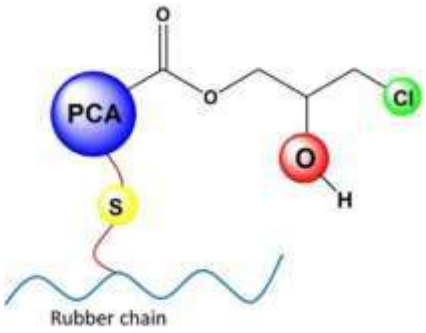


Figure 1. Illustration of the proposed epichlorohydrin-modified reclaimed rubber product (FD-GTRECH).

Differential scanning calorimetry (DSC) was used to assess the thermal behavior of FD-GTR with varying ECH concentrations (4 and 9 phr), as shown in Figure 2. The results suggested

that the optimal temperature for the epoxide ring-opening reaction (ECH) with the carboxylic acid (on the GTR chain) is 70–90 °C, yielding FD-GTRECH.

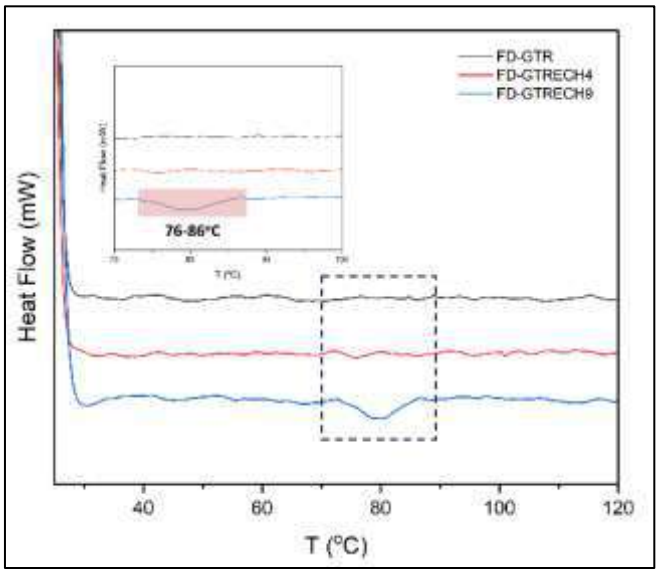


Figure 2. DSC thermograms of FD-GTR and FD-GTRECHs

In Table 1, EDX confirmed ECH uptake with a stepwise increase in chlorine from 0.56 to 1.28 wt%, while O remained relatively constant. Moreover, the LOI test showed that the flame-retardant performance of the reclaimed rubbers improved with increasing ECH content.

Table 1. The EDX results of modifying FD-GTR with ECH

Sample Code	wt%				
	C	O	S	N	Cl
FD-GTR	63.29	26.45	1.98	8.30	0.00
FD-GTRECH4	61.86	27.95	1.76	7.88	0.56
FD-GTRECH9	63.24	26.28	1.49	7.72	1.28

Acknowledgements

The authors would like to thank the National Research Council of Thailand (NRCT) for the financial support for this research. The scholarship program for ASEAN and non-ASEAN countries at Chulalongkorn University also supported this research. We thank Union Commercial Development Co., Ltd, for their support of waste tire rubber and AGC Vinuthai Public Company Limited (AVT) for their support of epichlorohydrin bio-based chemicals.

References

[1] Kodal M,Yazici N, Yildirim R, Karakaya N, Ozkoc G, *Polymers.*, 2023; 15: 23.

[2] Georlette P, *Fire retardant materials.*, 2001; 264-292.

[3] Yan Z, Ma Z, Deng J, Luo G, *Chem. Eng. Sci.*, 2021; 242: 116746.

Session III : Advanced Rubber Materials and Novel Applications

Poster Presentations

International Rubber Conference 2025 (IRC2025)
1-3 December 2025 @ BITEC, Bangkok, Thailand

Preparation and Properties of In-situ Hydrogenated Nitrile Butadiene Rubber Latex

Yang Zhiwei, Yue Dongmei*

(Beijing University of Chemical Technology, Beijing, China)

*e-mail: yuedm@mail.buct.edu.cn

Keywords: Hydrogenated nitrile butadiene rubber latex, Hydrogenation, Hydrogen storage material

Hydrogen storage materials are a type of materials that can reversibly absorb and release hydrogen under certain conditions. In recent years, the use of hydrogen storage materials instead of hydrogen in industrial production has become a research hotspot for scientists. In 2011, Tracy D. Nixon [1] used dimethylamine borane as a hydrogen donor and [Ru (p-cymene) Cl_2] $_2$ as a catalyst to catalyze the hydrogenation of various olefins. Grzegorz K.'s research group [2] developed a transfer hydrogenation reaction of series of olefin compounds, using ruthenium based metal complexes as hydrogenation catalysts and formic acid as a hydrogen donor in 2018.

Hydrogenated nitrile butadiene rubber (HNBR) is the product of selective hydrogenation of unsaturated double bonds in nitrile butadiene rubber (NBR) [3]. The preparation of HNBR latex still requires the addition of H_2 for catalytic hydrogenation [4]. This work has achieved the goal of catalytic hydrogenation of NBR latex without additional H_2. Hydrogen storage materials are used as hydrogen donors instead of using H_2 as hydrogen donors in traditional latex hydrogenation, which greatly reduces the cost of NBR latex's hydrogenation.

The structure of NBR latex's selective hydrogenation product which used ammonia borane and dimethylaminoborane as hydrogen donors was characterized by nuclear magnetic resonance hydrogen spectroscopy and infrared spectroscopy, as shown in Figure 1. The selectivity of this system for NBR catalytic hydrogenation is high, but the hydrogenation effect using ammonia borane as a hydrogen donor is not as good as that of dimethylaminoborane, with a hydrogenation degree of only 52.5%, while the hydrogenation degree of dimethylaminoborane can reach 98.5%. The optimal reaction conditions (hydrogen donor concentration, reaction time, and reaction temperature) for hydrogenation of NBR latex were explored, as shown in Figure 2. The heat resistance of the original rubber and HNBR latex with hydrogenation degrees of 65% and 98% were characterized by thermogravimetric analysis and DTG curves, as shown in Figure 3. The initial thermal decomposition temperature of the original gel before hydrogenation is about 350 ℃[5]. As the hydrogenation degree increases, the initial thermal decomposition temperature of HNBR also increases, while the maximum thermal decomposition temperature remains basically unchanged, about 465℃. When the hydrogenation degree of the product reaches 98%, the initial thermal decomposition temperature of the product is about 450 ℃.

The results showed that ammonia borane compounds as hydrogen donors had a good effect on the hydrogenation of NBR latex. The effects of reaction time, hydrogen donor concentration, and reaction temperature on the hydrogenation products in the system were studied. Hydrogenated nitrile latex with a hydrogenation degree greater than 98% was prepared, and the heat resistance of HNBR latex prepared by this system was comparable to that of HNBR prepared by direct hydrogenation with H_2. This method provides a new idea for saving hydrogen energy, and has important application value in the field of preparing HNBR latex.

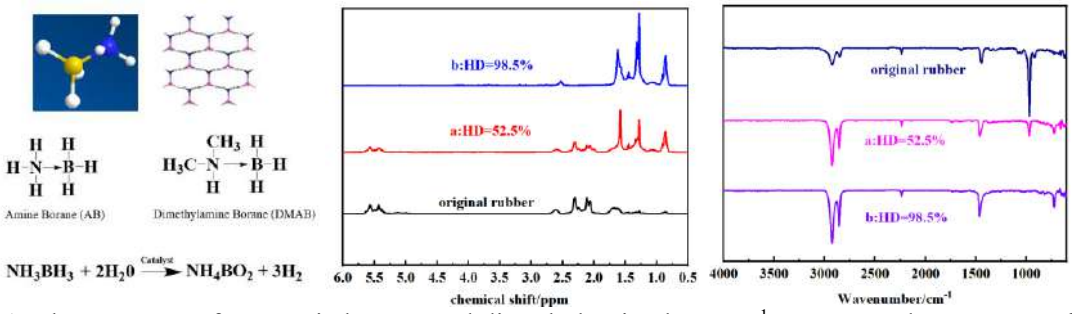


Figure 1. The structure of ammonia borane and dimethylamine borane; ^{1}H NMR and IR spectra of NBR latex hydrogenation using (a) AB and (b) DMAB as hydrogen donors

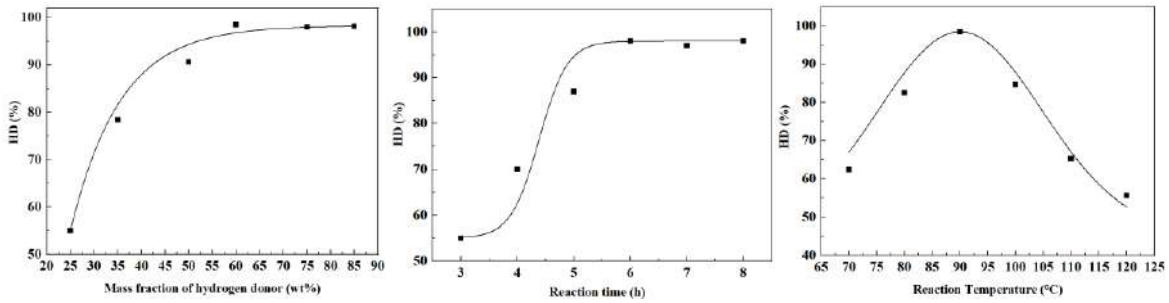


Figure 2. The influence of hydrogen donor concentration, reaction time, and reaction temperature on the hydrogenation of NBR latex

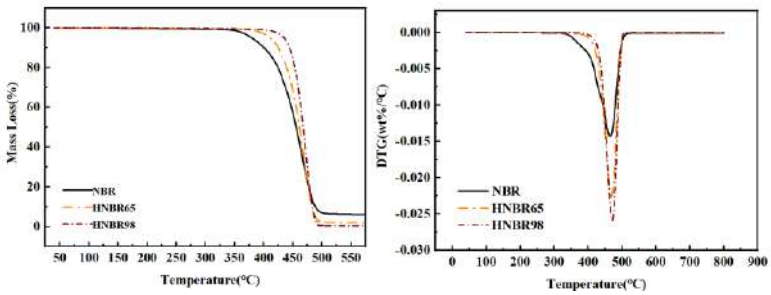


Figure 3. TG and DTG curves of the original rubber and HNBR latex with hydrogenation degrees of 65% and 98%

References

1. Nixon D, Whittlesey K, Williams J, *Tetrahedron Lett.*, 2011; 52: 6652-6654.
2. Zielinski K, Majtczak J, Gutowski M, *J. Org. Chem.*, 2018; 83: 2542-2553.
3. Riehlp S, Nasrallahd J, Schindlerc S, *Chem. Sci.*, 2019; 10: 10267-10274.
4. Chen Z, Kirlikovali O, Idreesk B, *Chem.*, 2022; 8: 693-716.
5. Ozturk Z, Martin P, Parry R, Qilu Z, *Int. J. Hydrogen Energ.*, 2021; 46: 11804-11814.

International Rubber Conference 2025 (IRC2025)
1-3 December 2025 @ BITEC, Bangkok, Thailand

Surface modification of UHMWPE fibers to enhance their interfacial adhesion with rubber

Wencai Wang*[1], Lijie Yin[1], Yichen Lu[1], Wei Li[1], Xiaotong Liu[1], Yanfeng Niu[2]

[1] *State Key Laboratory of Organic-Inorganic Composites, Beijing University of Chemical Technology, Beijing, China.*

[2] *Xingi Technology Co., Ltd., Nantong, China.*

e-mail address of the presenting author (wangw@buct.edu.cn)

Keywords: UHMWPE fiber, Surface modification, Interface adhesion, Fiber-reinforced composites

With the demand for high performance fields, such as lightweight, high strength, and long life, the prospect of the application of ultra-high molecular weight polyethylene (UHMWPE) fibers in fiber-reinforced composites has received widespread attention, and holds broad application prospects in high-strength, lightweight rubber fields such as automotive, defense, and aerospace industries. The interfacial bonding between the fiber and matrix is a key factor in determining the performance of composites, and the chemical inertness of UHMWPE fibers leads to weak interfacial bonding, which affects the comprehensive performance and service life of composites. Traditional resorcinol-formaldehyde-latex (RFL) system's formaldehyde poses health risks, while current eco-friendly alternatives require curing temperatures above 200 °C. Therefore, the study of efficient surface modification methods to improve the chemical activity of UHMWPE fibers and to solve the interfacial bonding between the fibers and the matrix and the molding and processing is the key to the current research.

In this work, to enhance the interfacial adhesion strength between UHMWPE fiber and rubber, we developed a low-temperature dipping strategy tailored for UHMWPE fiber, as shown in Figure 1. This approach employs continuous, low-temperature oxygen plasma treatment (25 ℃/200W/10s) to activate the fiber, replacing the conventional high-temperature activation bath used in traditional dipping systems. This method effectively addresses the issue of poor adhesion of the activation solution while offering high efficiency, lower processing temperatures, and enhanced environmental friendliness. Furthermore, to overcome the limitations of the traditional RFL system, a novel, low-temperature, and eco-friendly dipping system, named benign polyol-isocyanate-latex (PIL) dipping solution, was investigated.

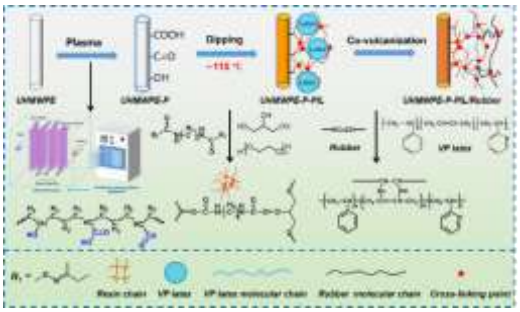


Figure 1. Schematic diagram of the surface modification mechanism of UHMWPE fiber

The PIL dipping solution was prepared by blending specified ratios of Butanone oxime capped hexamethylene diisocyanate (BHDI), polyethylene glycol (PEG300), and glycerol (GI) mixture with

vinylpyridine (VP) latex. The PIL system achieves curing at approximately 120 ℃, forming a crosslinked polyurethane network that replaces the toxic RF resin network. Within this structure, latex particles are embedded, creating an interpenetrating network. During the rubber vulcanization process, latex can co-crosslink with the natural rubber matrix to form vulcanization bonds.

As shown in Figure 2(a), plasma treatment significantly enhanced the hydrophilicity of the UHMWPE fiber, as determined by water contact angle measurements, which facilitates the effective wetting and adhesion of the PIL dipping solution. As shown in Figure 2 (b), the tensile strength loss of UHMWPE-P-PIL remained within 5%. Benefiting from the wetting and bundling effects of the dipping solution between the individual filaments, the breaking force of the impregnated fiber increased, partially compensating for the damage induced by the plasma treatment. As shown in Figure 2 (c-d), following modification, the static interfacial adhesion (H pull-out force) between the UHMWPE fiber and rubber increased by 114%, while the dynamic interfacial adhesion (dynamic fatigue life) showed a remarkable improvement of 525%. Benefiting from the modification, fiber-rubber interface exhibits increased crosslinking density, enhanced adhesion, improved mechanical properties, and superior fatigue resistance.

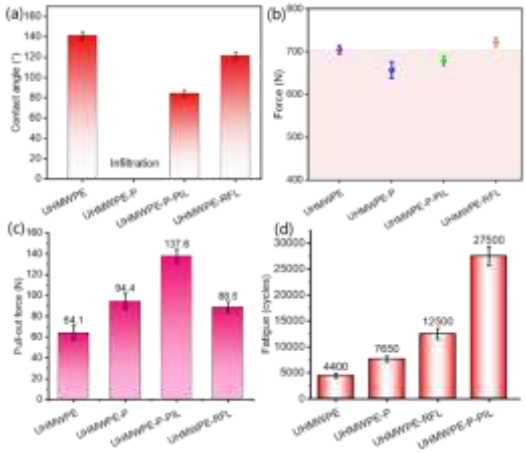


Figure 2. (a) Water contact angle, (b) breaking force, (c) static interfacial adhesion, and (d) dynamic interfacial adhesion of modified fibers.

Acknowledgement

The authors gratefully acknowledge the financial support from the National Natural Science Foundation of China (Grant No. 51833002) and Xingi Technology Co., Ltd.

References

1. Zhang B, Shao X, Tian M, Ning N, Zhang L, Wang W. *Polymer*, 2022; 238: 124414.
2. Wennekes W, Datta R, and J. W. M. Noordermeer, *Rubber Chem. Technol.*, 2007; 804: 565-579.
3. Lin J, Sun C, Min J, Wan H, Wang S, *Composites, Part B*, 2020; 199: 108237.

International Rubber Conference 2025 (IRC2025)
1-3 December 2025 @ BITEC, Bangkok, Thailand

Controllable Modification of Rubber Achieved Through Bio-based Inverse Vulcanized Compounds

Long Li[1], Jiayu Shi[1], Hailan Kang[1], Xiaodong Zhang[2]

[1] *Liaoning Provincial Key Laboratory of Rubber & Elastomer, Shenyang University of Chemical Technology, Shenyang, China.*

[2] *College of Science, Shenyang University of Chemical Technology, Shenyang, China.*

e-mail address of the presenting author (lilong@syuct.edu.cn)

Keywords: inverse vulcanization, vulcanization accelerator, reprocessability, aging resistance, biobased monomer

The bio-based inverse vulcanized compound named poly(sulfur-itaconic acid) (SIA) was synthesized by a reaction between itaconic acid containing double bonds and sulfur to control rubber modification precisely. When applied as vulcanization additives in rubber, SIA not only serves as a vulcanizing agent but also forms complexes between the activator and accelerator, thereby promoting the vulcanization process, as shown in **Figure 1** Utilization of sulfur and SIA could regulate the crosslink density of the vulcanized rubber and improve its mechanical properties, with a 10% increase in tensile strength (up to 28.17 MPa) and a 14% rise in elongation at break (up to 646%), while also promote the filler dispersion. The polysulfides in SIA exhibited the ability to undergo thermal decomposition and reorganization at 150 °C, thereby enabling desirable recyclability for rubber materials. After over three recycling cycles, sample tensile strength remained consistently stable at 8 MPa, while elongation at break maintained a steady value of 400%. As illustrated in **Figure 2**, higher-rank sulfur bonds break, -Sx- undergoes exchange recombination reducing the content of polysulfur chains, and crosslink bonds transform into more stable -S- and -S2-, reinforcing the network during recycling. Further, introducing SIA as a processing aid into the carbon black-filled natural rubber composite system can achieve better aging resistance than the original system. SIA endows rubber composites with excellent mechanical properties, improved interfacial interactions, recyclability and aging resistance. It has the potential to become a bio-based multifunctional additive.

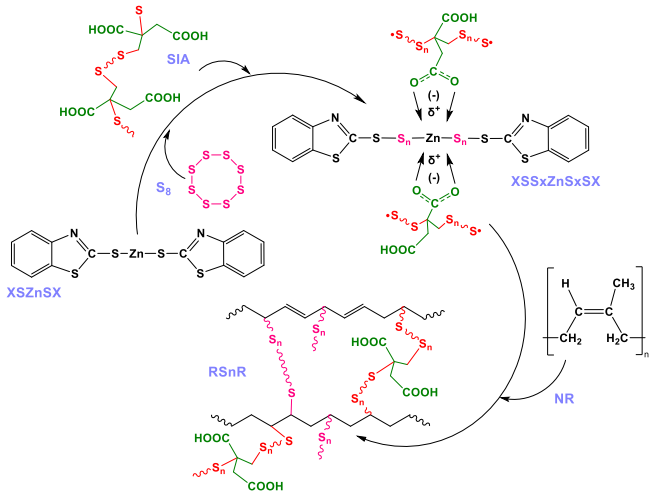


Figure 1. The mechanism of co-vulcanization

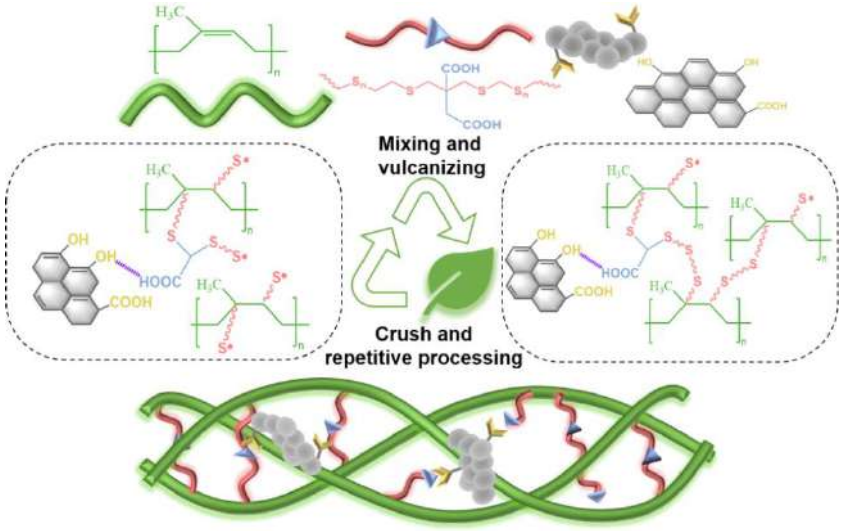


Figure 2. Mechanism of recycling processing

Acknowledgement

This research was supported by the National Natural Science Foundation of China (grant number 52073178); Shenyang Natural Science Foundation special, China (grant number 23-503-6-06); Liaoning Provincial Department of Education Basic Research Project (grant number LJKZZ20220055); the Basic Scientific Research Project of Liaoning Provincial Department of Education, China (grant number JYTMS20231498).

References

1. Jiang L, Kong R, Yi Y, Yang S, Mei Y, Feng X, Yao Z *Polymer*, 2019; 180: 121715.
2. Wreczycki J, Bielinski M., Kozanecki M, Maczugowska P, Mloston G, *Materials,* 2020; 13: 2597.
3. Zhang Y, Griebel J, Dirlam T, Nguyen A, Glass S, Mackay E, Char K, Pyun J, *J. Polym. Sci. Pol. Chem.*, 2017; 55: 107-116

International Rubber Conference 2025 (IRC2025)
1-3 December 2025 @ BITEC, Bangkok, Thailand

UiO-66-NH_2 for the Recovery of Catalyst in Hydrogenation Nitrile Butadiene Rubber and Its Repeated Hydrogenation

Hui Jiao, Dongmei Yue*

Beijing University of Chemical Technology, Beijing, China.

*E-mail: yuedm@mail.buct.edu.cn

Keywords: Hydrogenation nitrile butadiene rubber, Catalyst recovery, Repeated hydrogenation

Hydrogenation nitrile butadiene rubber (HNBR) is a modification method where the C=C unsaturated bonds in the main chain of nitrile butadiene rubber (NBR) undergo selective hydrogenation while the -CN remains unchanged.[1] Due to its excellent oil resistance, mechanical properties, and anti-aging performance, it has been widely used in various aerospace, petroleum, and automotive fields. However, precious metal catalysts with high activity and selectivity are used to increase the production cost during preparing HNBR. Moreover, the catalyst remaining in HNBR also affects its performance, such as the thermal stability, aging resistance, and oil resistance. Therefore, how to recover the residual catalyst from HNBR urgently needs to be addressed.

Currently, the reported methods for catalyst recovery mainly include extraction, precipitation, and adsorption. Ai *et al.* modified large-pore silica microspheres with urea groups and recovered Wilkinson catalyst in HNBR, achieving a rhodium recovery rate of 92.2%.[2] Yang *et al.* used 5-methyl-2,3-diallylamine as a coupling agent to recover rhodium catalyst from HNBR, the rhodium residual was finally reduced from 700 to 59 ppm.[3] Ning *et al.* recovered the catalyst by extracting it from NBR with polyethylene glycol in n-heptane and the recovery efficiency reached 89%.[4] However, the above catalyst recovery methods merely focus on separating the catalyst from HNBR, and the separated catalyst is actually not reused.

In this work, the as-prepared UiO-66-NH_2 with a specific surface area of 2129 m^2/g was used to recover the Palladium (Pd) remaining in HNBR. Finally, the recovered Pd and UiO-66-NH_2 as heterogeneous catalysts were used again as to hydrogenate NBR. This method enables the repeated utilization of the recovered catalyst. As a result, the recovery rate with the addition of formic acid, acetic acid and hydrochloric acid as additives is higher than that with ethanol and methanol due to the stronger acidity of the additives and stronger binding force between Pd and UiO-66-NH_2 (see Figure 1(a)-(c)). The kinetic model of the recovery process was characterized by investigating the relationship between time and recovery rate. The R^2 (coefficient of determination) obtained from the pseudo-first-order kinetic fitting was closer to 1 than pseudo-second-order kinetic, indicating that the adsorption process more closely follows the pseudo-first-order kinetic model and suggested that the rate of the adsorption process is mainly determined by the diffusion rate of UiO-66-NH_2, as the molecular chains of NBR are longer and intertwined (see Figure 1(d)-(f)), resulting in a slower diffusion speed of UiO-66-NH_2 in the HNBR solution. The thermodynamic model of the recovery process was characterized by investigating the relationship between temperature and recovery rate(see Figure 1(g)-(h)). By calculating the slope and intercept, the ΔS (Entropy Change) of the adsorption process is 124.438 $J \cdot mol^{-1} \cdot K^{-1}$ and ΔG (Gibbs Free Energy) is less than 0 $kJ \cdot mol^{-1}$, indicating that the recovery process is a spontaneous endothermic process. Comparing the recovery rates of the catalysts using UiO-66-NH_2 and UiO-66 as adsorbents (see Figure 1(i)). The recovery

rate of UiO-66-NH_2 (95.8%) is higher than the UiO-66 (12.9%). This is because UiO-66-NH_2 contains –NH_2, which have a stronger binding force with Pd than UiO-66. The recovered Pd-catalyst from the HNBR and UiO-66-NH_2 (denoted as Pd/UiO-66-NH_2) for again catalyzing NBR hydrogenation, the hydrogenation degree of HNBR can reach 89.1% (see Figure 1(h)), achieving the recycling of the recovered catalyst.

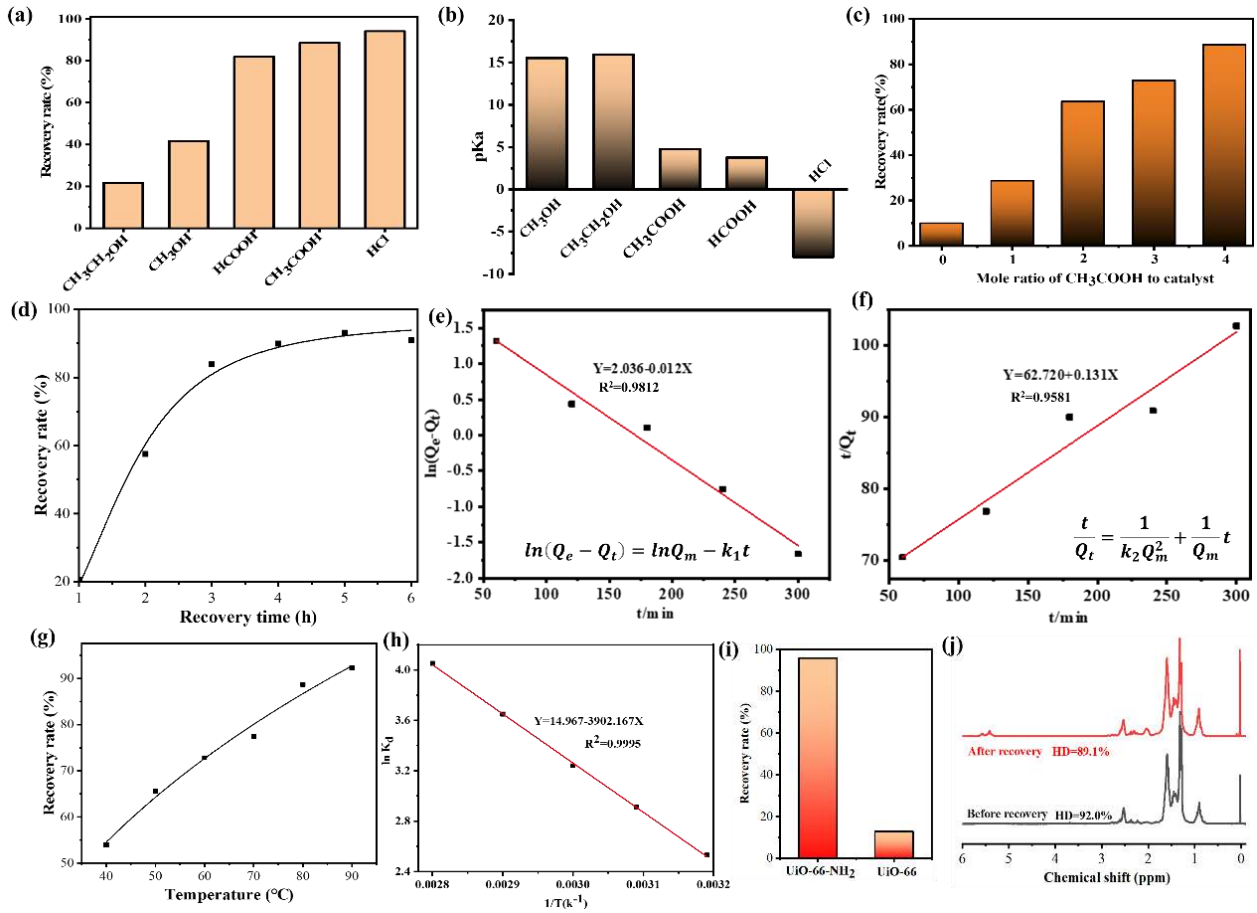


Figure 1. (a) Relationship between additives and recovery rate; (b) pKa values of different additives; (c) Graph showing the relationship between additive dosage and recovery rate; (d) Relationship between recovery rate and time; (e) First-order (f) Second-order kinetic model; (g) Relationship between recovery rate and temperature; (h) Adsorption thermodynamic model; (i) Recovery rates of different types of adsorbents; (j) HNBR nuclear magnetic spectra before and after catalyst recovery

References

1. Cao P, Wu M, Zou R, Zhang L Q, Yue D M, *New J. Chem.,* 2015; 39: 1583-1586.
2. Ai C J, Gong G B, Zhao X T, Liu P, *Powder Technol.,* 2017; 318: 501-506.
3. Yang L J, Pan Q M, Rempel G L, *Catalysis Today.,* 2013; 207: 153-161.
4. Ning S M, Yang S F, Wei X P, Wang W M, Zhang L Q, Yue D M, *J. Appl. Polym. Sci.,* 2012; 123: 1040-1046.

International Rubber Conference 2025 (IRC2025)
1-3 December 2025 @ BITEC, Bangkok, Thailand

Effects of Carbon Nanotube Size on Properties of Eucommia Ulmoides Gum Composite Materials: a Molecular Dynamics Study

Wenchi Han[1,2], Yue Pan[1,2], Qinghong Fang[1,2]

[1] *Liaoning Provincial Key Laboratory of Rubber & Elastomer, Shenyang, China.*

[2] *Shenyang University of Chemical Technology, Shenyang, China.*

e-mail address of the presenting author (hanwenchi@syuct.edu.cn)

Keywords: Carbon nanotubes, Eucommia ulmoides gum, Molecular dynamics, Mechanical properties

Eucommia ulmoides gum (EUG) is an environmentally friendly bio-based material with unique rubber-plastic duality, and shows considerable potentials for multi-industry applications. However, the properties and functional applications of EUG still need to be further developed. Carbon nanotubes (CNTs) have been widely used as efficient fillers to enhance the performances of plastic composites due to their excellent properties. In this study, the molecular dynamics simulation (MD) is adopted to evaluate the effect of the size of carbon nanotubes (CNTs) on the properties of Eucommia ulmoides gum (EUG) composite materials. A series of CNTs/EUG composite system models are constructed by systematically altering the axial dimensions (from 68Å to 128Å) and radial dimensions (from 2.71Å to 16.27Å) of CNTs to investigate the mechanical, electrical and thermal properties at room temperatures.

The results show that the mechanical properties of the CNTs/EUG composites initially increase and then decrease with the increase of the diameter of CNTs, and increase by increasing the length of CNTs. The CNTs with a diameter of 8.14 Å in the axial dimension and a length of 128 Å in the radial dimension have better enhancement effects on the mechanical properties of the CNTs/EUG composites, the modulus of elongation of the CNTs/EUG composite increase by 59.70% and 54.85% compared to CNTs with a diameter of 2.71 Å or a length of 68 Å, respectively. Compared with changing the length of CNTs, changing the diameter has a more significant effect on thermal conductivity of CNTs/EUG composites. The variation range of thermal conductivity of composites is from 0.2361 to 0.3502 W/(m/K), the composites exhibit relatively lower thermal conductivity. Furthermore, the addition of CNTs can reduce the temperature near the friction interface and improve the tribological properties of CNTs/EUG composites. The breakdown field strength of the composites also initially increase and then decrease with the increase of CNTs diameter, and increases with the increase of CNTs length. The variation range of breakdown field strength of composites is from 855 to 1037 KV/mm. The CNTs with a diameter of 8.14 Å in the axial dimension and a length of 128 Å in the radial dimension exhibit higher breakdown field strength and superior tribological properties during the shearing process of composites. The conclusion of this study can provide necessary theoretical support and engineering guidance for improving the performance and functional application of EUG materials in practical applications.

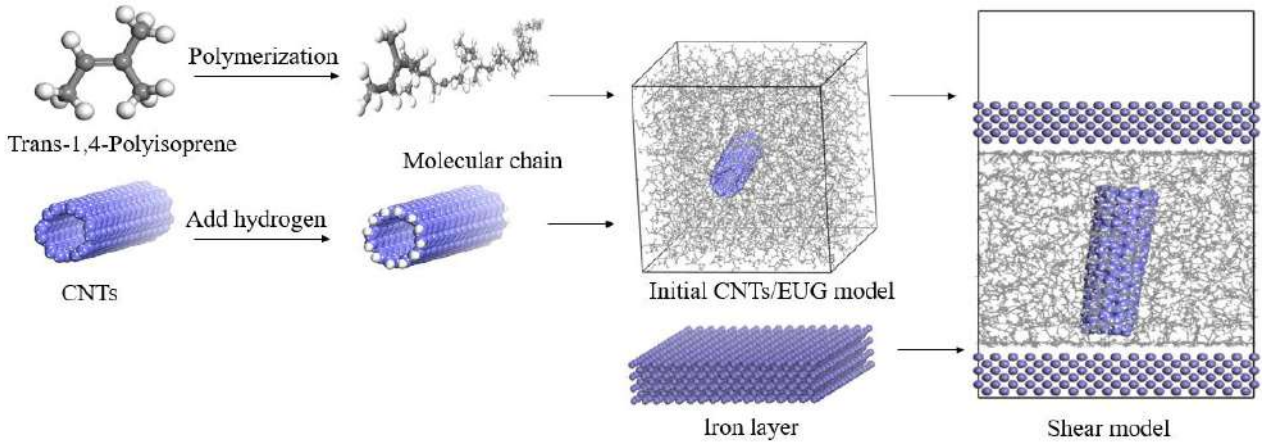


Figure 1. Construction process of molecular models of CNTs/EUG composites

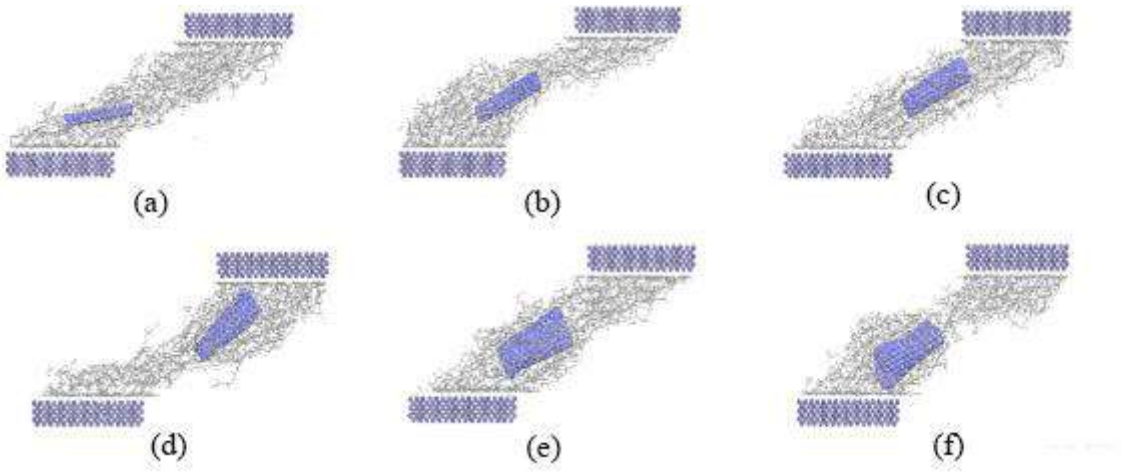


Figure 2. Shear models of CNTs/EUG composites with different CNTs diameters. (a) D2.71-CNTs；(b) D5.42-CNTs；(c) D8.14-CNTs；(d) D10.85-CNTs；(e) D13.56-CNTs；(f) D16.27-CNTs

Acknowledgement

This research is supported by the National Natural Science Foundation of China (grant number 52073178).

References

1. Guo F C, Zhang J P, Pei J Z, *Journal of Molecular Modeling*, 2019; 25: 365.
2. Teng F,Wu J, Su B L, Wang Y S, *Nanomaterials* , 2021; 11: 2464.

International Rubber Conference 2025 (IRC2025)
1-3 December 2025 @ BITEC, Bangkok, Thailand

Analysis of Internal Damage for CNT-Based Soft Nanocomposites

Keni Ma[1], Thanh-Tam Mai[1], Kenji Urayama[1]

[1] *Department of Material Chemistry, Kyoto University, Kyoto 615-8246, Japan.*

ma.keni.46v@st.kyoto-u.ac.jp

Keywords: Soft Nanocomposites, Filler-Reinforced Hydrogels, Chemical and Physical Cross-links

Carbon nanotube (CNT)-reinforced hydrogels stand out for their superior mechanical properties among materials used in hydrogel-based strain sensors. Due to their high elastic modulus, strength and large aspect ratio, CNTs have long been recognized as promising fillers for polymer composites[1]. Their inherent large aspect ratio is also expected to yield unique physical properties distinct from conventional spherical fillers like conductive carbon black. This study aims to analyze internal damage mechanisms in CNT-based hydrogels by distinguishing reversible and irreversible network changes under tensile deformation.

A characteristic feature of filler-reinforced soft materials is the stress-softening effect, in which the stress observed during reloading is significantly reduced compared to the initial loading. This behavior, which is indicative of internal damage without visible macroscopic fracture, is widely observed in various multiphase materials including metal alloys[2]. The underlying mechanisms, however, differ depending on the material system. In this study, we investigate the stress-softening behavior in CNT-based nanocomposite hydrogels that incorporate both physical and chemical cross-links. We decouple the total internal damage into reversible (healable) and irreversible components, and identify the threshold strain at which chemical cross-links begin to rupture.

CNT-reinforced polyacrylamide hydrogel specimens (PAAm-fCNT) were prepared by free-radical polymerization following the method in the literature[3]. Functionalized CNTs (CNTs-COOH, Aldrich, 9.5 nm × 1.5 μm) were chosen as the filler. The crosslinker ((N, N'-methylenebisacrylamide) concentration was 0.03 or 0.1 mol% (represented by X=3 or 10, respectively) relative to the AAm monomer. The AAm monomer concentration at 4 mol·L^{-1}. Gelatin (5 wt.%) was added to CNT/AAm aqueous dispersions as a compatibilizer to enhance CNT dispersion. Among the formulations tested, a CNT concentration of 2 mol% yielded the homogeneous gel with the highest modulus (hydrogel with 2% CNT exhibited the highest work of fracture), designated as PAAm-fCNT-2.

Figure 1(a) shows the tensile loading-unloading curves for PAAm-fCNT-2 with different crosslinker concentrations (X=3 and 10), subjected to a maximum stretch ratio ($\lambda_{x.max}$) equals to 6. The hydrogel with higher X exhibits larger stress at equivalent strain, reflecting its higher chemical cross-link density. Both hydrogels show a pronounced stress-softening effect. The energy dissipation (D) was calculated from the area enclosed by the loading and reloading curves. As shown in **Figure 1(b)**, D increases with $\lambda_{x,max}$ in both samples, and at equivalent $\lambda_{x,max}$, the X = 10 sample consistently exhibits larger D than the X = 3 counterpart.

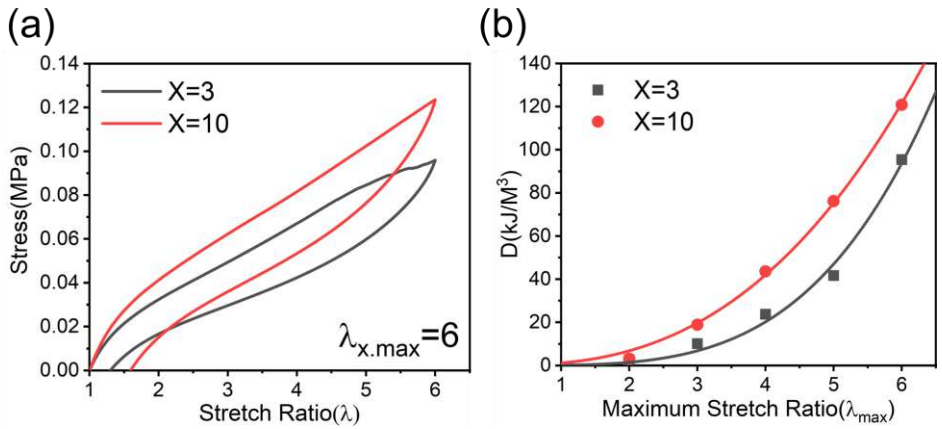


Figure 1. (a) Tensile loading-unloading cycles of PAAm-fCNT-2 (X=3 and 10) at $\lambda_{x.max}$=6 and (b) the corresponding dissipated energies at different $\lambda_{x.max}$.

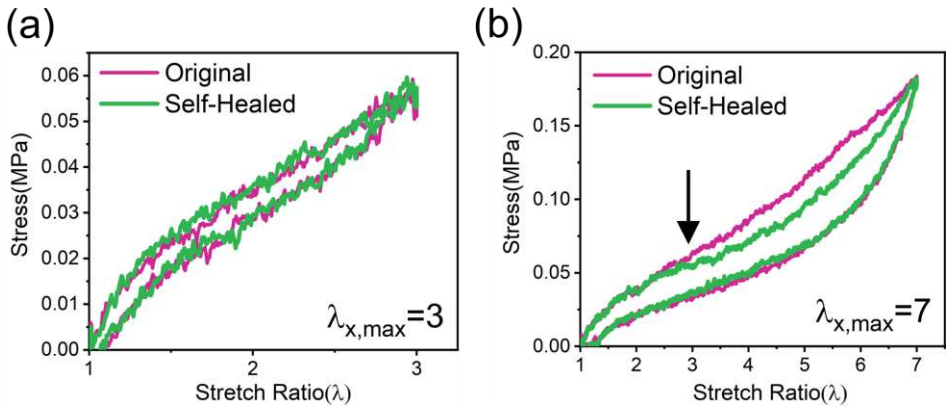


Figure 2. Tensile loading-unloading cycles of the original PAAm-fCNT-2 (X=3) and that after self-healing at (a) $\lambda_{x.max}$=3 and (b) $\lambda_{x.max}$=7.

After tensile loading-unloading cycles with various $\lambda_{x.max}$, the relaxed samples were sealed to prevent water vaporization, and stored for 24 hours to allow self-healing. Subsequent cyclic tensile tests were then performed on these self-healed hydrogels. **Figure 2** compares the tensile responses of the original and self-healed hydrogels. At $\lambda_{x.max}$=3, the loading-unloading curves before and after healing overlap almost perfectly, indicating that the observed internal damage is fully recoverable and arises from the rupture of reversible (healable) physical cross-links between gelation and CNTs. In contrast, at $\lambda_{x.max}$=7, the two loading curves deviate significantly, manifesting the occurrence of irreversible bond breakage under high stretching. Notably, the two loading curves coincide in the regime of λ<3, suggesting that $\lambda \approx 3$ represents the threshold for the onset of irreversible network fracture. This study provides the first clear identification of a strain threshold distinguishing reversible from irreversible damage in CNT-filled hydrogels.

References

1. N. Nurazzi et al., Nanomaterials, vol. 11, no. 9, p. 2186, 2021.
2. K. M. Schmoller and A. R. Bausch, Nature materials, vol. 12, no. 4, pp. 278-281, 2013.
3. X. Sun et al., Chemical Engineering Journal, vol. 382, p. 122832, 2020.

International Rubber Conference 2025 (IRC2025)
1-3 December 2025 @ BITEC, Bangkok, Thailand

Study on the structural control of natural rubber with nanomatrix structure and its vulcanization

Yuanbing ZHOU[1], Sujitra ONUTAI[1], Shuangquan LIAO[1], Seiichi KAWAHARA[2]

[1] *School of Materials Science and Engineering, Hainan University, Haikou, Hainan, China.*

[2] *Department of Materials Science and Technology, Nagaoka University of Technology, Nagaoka, Niigata, Japan.*

E-mail: zhouyb@hainanu.edu.cn

Keywords: Natural rubber, Nanomatrix structure, Hierarchical structure, Structural control

Nanostructure plays an important role in mechanical properties of rubbery materials. For instance, the nanomatrix structure of non-rubber components such as proteins and phospholipids contribute to improvements of mechanical properties for uncured natural rubber (NR) [1]. It is, thus, important to investigate the relationship between nanomatrix structure and mechanical properties[2,3]. However, effects of the nanomatrix structure on the mechanical properties have not been elucidated, yet, due to difficulty to characterize the nanomatrix structure, which is a complicated hierarchical structure composed of NR, proteins and phospholipids. Therefore, it is necessary to prepare a model NR with an artificial nanomatrix structure to investigate the relationship between the nanomatrix structure and the properties, precisely.

In the present study, an attempt to prepare the model NR with the artificial nanomatrix structure was performed by graft copolymerization of vinyltriethoxysilane (VTES) at different concentrations onto the surface of *cis*-1,4-polyisoprene particles of deproteinized NR (DPNR) in latex stage, followed by coagulating and drying the graft-copolymer latex. The graft-copolymer (DPNR-*graft*-SiO_2) was further vulcanized at latex stage, and the mechanical properties are discussed in relation to the morphology of nanostructure.

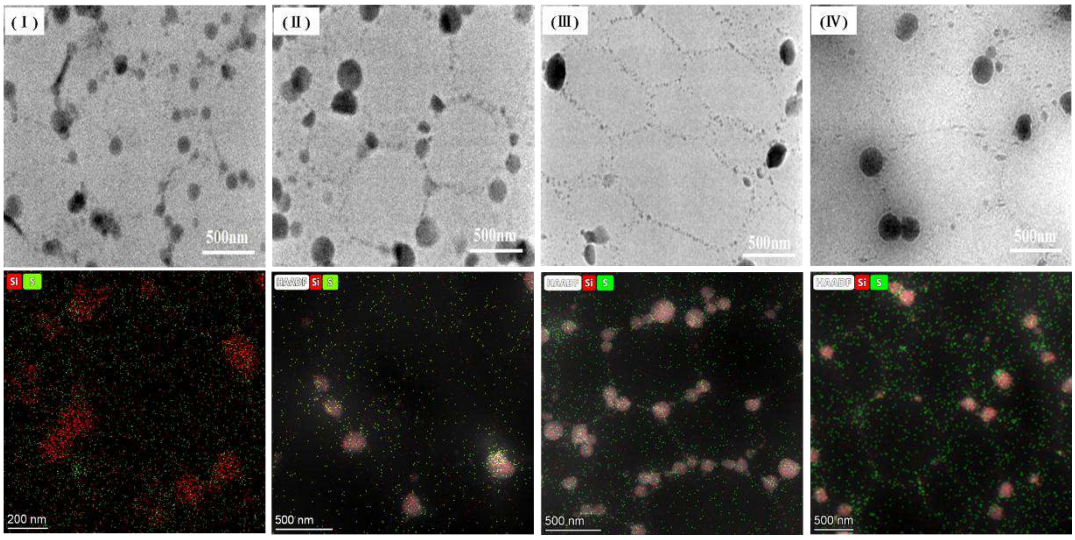


Figure 1. TEM and EDS images for vulcanized DPNR-*graft*-SiO_2

As the results, in the TEM and EDS images, the *cis*-1,4-polyisoprene particles were well dispersed in the nanomatrix consisting of silica nanoparticles, the original silica nanomatrix structure was well retained after vulcanization, sulfur tends to agglomerate with silica particles. The suitable

initiator and VTES concentrations to form the nanomatrix structure were found to be 0.066 and 1.05 mol/kg-rubber, respectively.

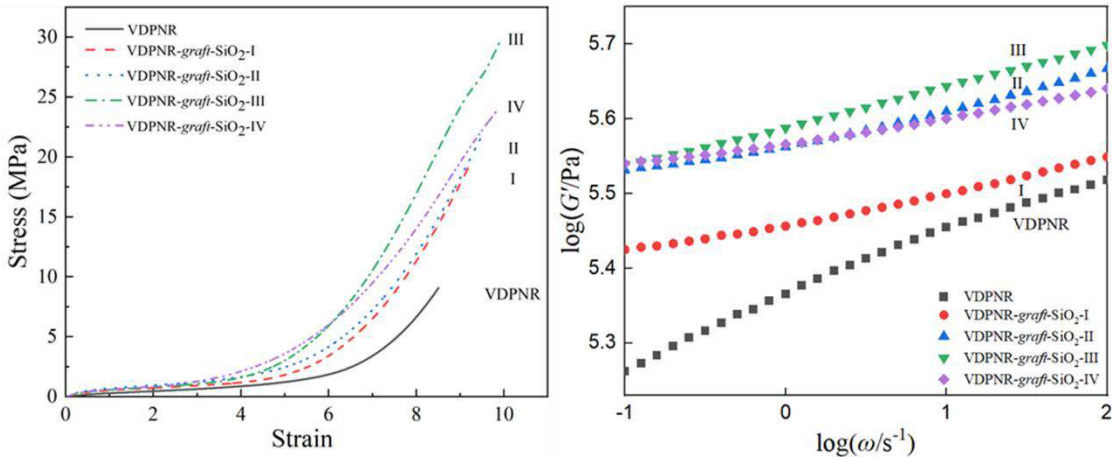


Figure 2. Stress-strain curves and storage modulus versus the frequency for vulcanized DPNR-*graft*-SiO_2

The tensile strength is significantly improved by the formation of a continuous silica nanomatrix structure and high degree of vulcanization. VDPNR-*graft*-SiO_2-III shows the highest tensile strength at 29.79 MPa and the largest break elongation of 992.9%, which is 3 times higher than that of VDPNR. Furthermore, NR with a silica nanomatrix structure showed a remarkable viscoelastic behavior.

Acknowledgement

This work was supported by Hainan Provincial Natural Science Foundation of China (No. 223RC400). The International Science & Technology Cooperation Program of Hainan Province (No. GHYF2025018).

References

1. P. Suksawad, Y. Yamamoto, et.al., *Eur. Polym. J.*, 2011;47: 330.
2. N. T. Thuong, T. A. Dung, N. H. Yusof, et al., *Polymer*, 2020; 195: 122444.
3. Y. Yamamoto, K. Endo, Q. Tévenot, et al., *Langmuir*, 2020; 36 (38): 11341-11348.

International Rubber Conference 2025 (IRC2025)
1-3 December 2025 @ BITEC, Bangkok, Thailand

Enhancing the Mechanical Properties of uncrosslinked Epoxidized Natural Rubber through Non-Covalent Interactions

Muthita Phetpradab[1], Phakamat Limarun[1,2], Wirasak Smitthipong[1,2,3]

[1] *Department of Materials Science, Faculty of Science, Kasetsart University, Chatuchak, Bangkok, Thailand*

[2] *Specialized center of Rubber and Polymer Materials in agriculture and industry (RPM), Department of Materials Science, Faculty of Science, Kasetsart University, Chatuchak, Bangkok, Thailand*

[3] *Hub of talents in natural rubber under the National Research Council of Thailand, National Research Council of Thailand (NRCT), Bangkok, Thailand*

e-mail address of the presenting author (muthita.phe@ku.th)

Keywords: ENR, DOPA, Thermodynamic, Computer modelling

Natural rubber (NR) has a molecular structure containing carbon-carbon double bonds[1]. The important properties of NR are elasticity, high reversible deformation and good tensile strength [1-2]. Due to NR having a double bond structure, it triggers to oxidation reaction [1]. Thus, NR can be degraded. Therefore, NR has been modified through an epoxidation reaction by formic acid and hydrogen peroxide [1-2], it can be transformed to epoxidized natural rubber (ENR). The ENR is better in mechanical properties and more polarity compared to the NR [2].

This work aims to modify ENR, and to improve the mechanical properties of uncrossliked ENR's modification. In this experiment, 6 g ENR was mixed by 1.2 g 2,4,5-Trihydroxy-DL-phenylalanine (DOPA) for 24 h and then 0.3 g $FeCl_3 \cdot 6H_2O$ (Fe) for 15 min. For ENR structure, the difference points between NR and ENR are the change from double bond to epoxide ring [2]. So, if we add DOPA and Fe to ENR, we can enhance the mechanical properties of ENR. The reason for incorporating DOPA and Fe into ENR is to improve its toughness compared to control ENR [3-4] (Figure 1). The DOPA can be covalently linked to the ENR through the epoxide group (Figure 1a), and then Fe can be interacted to oxygen or nitrogen atom of DOPA by metal-ligand coordination (Figure 1b).

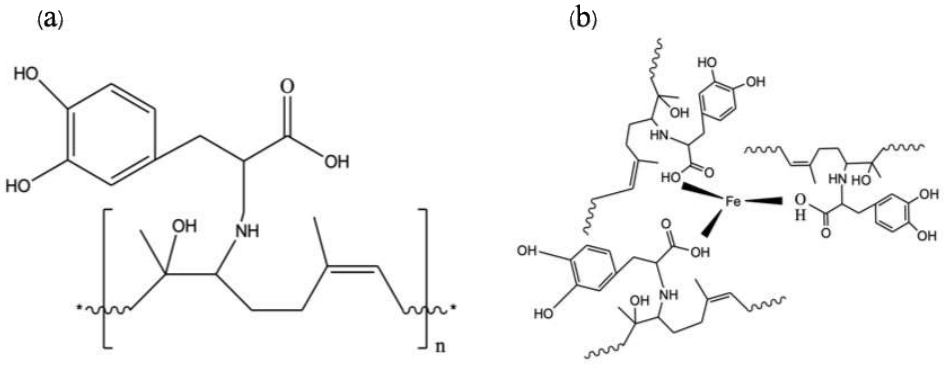


Figure 1. Chemical structure of ENR with DOPA (a), and ENR with DOPA and Fe (b)

This study focuses on preparation and characterization of three different samples: uncrossliked ENR, uncrossliked ENR/DOPA and uncrossliked ENR/DOPA/Fe. They were tested by several techniques, such as FTIR, mechanical properties, computer modelling, and thermodynamics.

Tensile strength increased by 213.46% with the addition of DOPA and Fe, certainly due to the network formation form metal-ligand interaction between Fe and oxygen or nitrogen atom of DOPA. This result is in good agreement with the sample structure from FTIR spectra. The Marc program is being used to study the computer modelling of mechanical properties of modified ENR samples. For the thermodynamics point of view, force decreased with the increase of temperature for all the samples [5]. Moreover, higher %strain possesses higher force. The non-covalent interaction, especially the metal-ligand interaction, can be used to enhance the mechanical and thermal properties of modified ENR. This could be applied to develop a new type of functional rubber.

Acknowledgement

I would like to express my sincere gratitude to specialized center of Rubber and Polymer Materials in agriculture and industry (RPM), Department of Materials Science, Faculty of Science, Kasertsart University for providing the facilities necessary in my project.

References

1. Ngudsuntear K, Limtrakul S, Vatanatham T, Arayapranee W, *ACS Omega*, 2022; 7: 36448-36456.
2. Buaksuntear K, Panmanee K, Wongphul K, Lim-arun P, Jansinak S, Shah D.U., Smitthipong W, *Polymer*, 2024: 291, 126626.
3. Yadav R.K., Yadav R.A., Kostova I., *Appl. Sci.,* 2023: 13, 13336.
4. Hwang D.S., Zeng H, Masic A, Harrington M.J., Israelachvili J.N., Waite J.H., *J. Biol. Chem.*, 2010; 285: 25850-25858.
5. Suethao S, Ponloa W, Phongphanphanee S, Wong-Ekkabut J, Smitthipong W, *Sci. Rep.*, 2021; 11: 6097.

International Rubber Conference 2025 (IRC2025)
1-3 December 2025 @ BITEC, Bangkok, Thailand

A Mechanical property and thermal stability of natural rubber composite filled with multi-walled carbon nanotubes/carbon black or biochar

P. JANTACHUM[1], T. KHOCHAI[1], A. ANLAKHON[1], B. KHUMPAITOOL[1]

[1] *Division of Chemistry, Faculty of Science, Udon Thani Rajabhat University, Udon Thani, Thailand.*

e-mail address of the presenting author (punyarat.ja@udru.ac.th)

Keywords: Natural rubber, Multi-walled carbon nanotubes, Carbon black, Bio-char, Composite

Multi-walled carbon nanotubes (MWCNTs) are widely recognized as high-performance reinforcing fillers for rubber due to their high aspect ratio, superior mechanical strength, and excellent electrical and thermal conductivities. Previous studies have demonstrated that only a small amount of MWCNTs is required to achieve enhanced properties, provided that good dispersion is obtained [1]. In recent years, biofillers have been explored as sustainable alternatives to petroleum-based fillers due to their abundance, renewability, and ecological advantages. Spent coffee grounds, one of the most consumed waste products worldwide, can be converted into biochar (BiO) via pyrolysis and utilized as an alternative filler in rubber composites [2–3].

This study aimed to investigate the effects of MWCNT loading, in combination with carbon black (CB) or biochar (BiO), on the swelling, crosslink density, cure characteristics, tensile properties, and thermal stability of natural rubber (NR) composites.

Biochar was produced from spent coffee grounds through pyrolysis at 800 °C for 2 h, yielding 29.62% moisture content, 51.40% ash, and 18.98% fixed carbon. NR/MWCNT masterbatches containing 0–3 phr of MWCNTs and 20 phr of CB or BiO were prepared using latex compounding and subsequently processed by internal mixing and compression molding at 150 °C. CNT–CB composites exhibited the lowest swelling and the highest crosslink density, attributed to the homogeneous dispersion of MWCNTs in the NR/CB matrix. The maximum torque during vulcanization was highest for CNT–CB composites at 3 phr MWCNTs, reflecting enhanced crosslink density. Increasing MWCNT content leads to a stronger filler network and restricted rubber chain mobility, which increases the material's resistance to deformation and results in higher 100% and 300% modulus, while the elongation at break decreases due to reduced elasticity. Tensile strength of CNT–CB composites improved at 2 and 3 phr MWCNTs, with increases of ~1.0% compared to unfilled NR/CB composites. Thermal analysis further revealed enhanced stability, as Tmax increased from 392 °C (neat NR) to 394–395 °C for CNT–CB composites. In contrast, CNT composites showed moderate improvements, while CNT–BiO composites consistently displayed the lowest performance, suggesting limited reinforcement due to weaker interfacial interactions.

In summary, incorporating 2–3 phr MWCNTs into NR/CB composites significantly enhanced tensile strength, modulus, and thermal stability, confirming a synergistic effect between MWCNTs and carbon black. While CNT composites offered only moderate reinforcement and CNT–BiO composites exhibited limited improvements, the hybrid MWCNT–CB system proved most effective, demonstrating its potential for the development of advanced rubber composites.

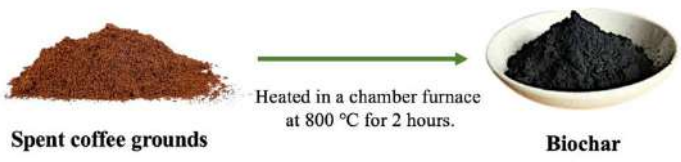


Figure 1. Preparation of biochar from spent coffee ground

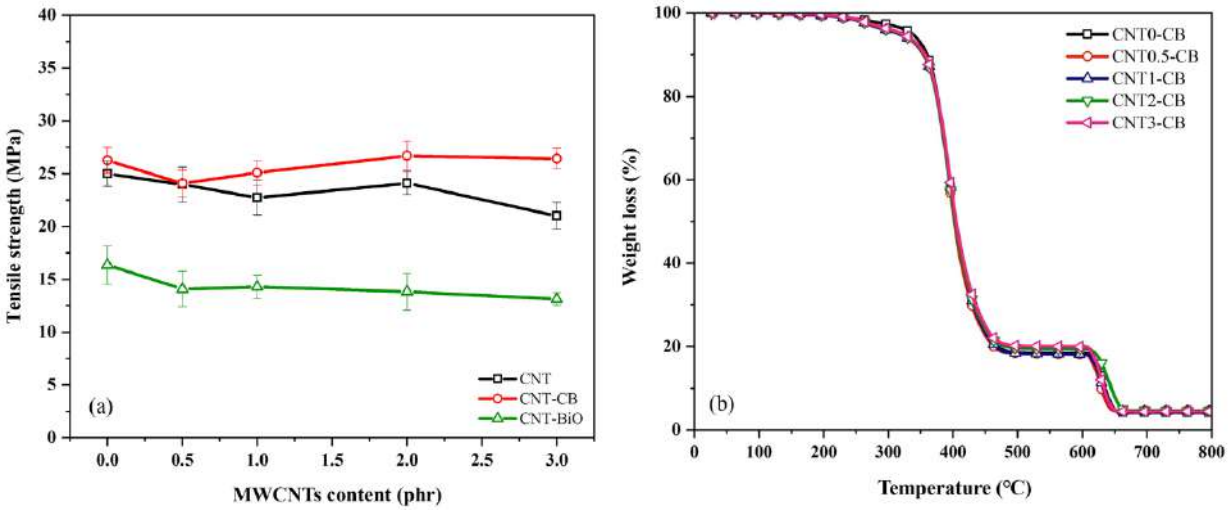


Figure 2. (a) Tensile strength and (b) TGA thermogram of rubber composites

Table 1. Compound formulation of the composites.

Ingredients	Amount (phr)		
	CNT	CNT-CB	CNT-BiO
NR[a]	100	100	100
MWCNT[b]	0, 0.5, 1, 2, 3	0, 0.5, 1, 2, 3	0, 0.5, 1, 2, 3
Carbon black	-	20	-
Biochar	-	-	20
ZnO	5	5	5
Stearic acid	2	2	2
6PPD	1	1	1
CBS	1	1	1
Sulfur	2	2	2

[a] Natural rubber
[b] Multi-walled carbon nanotubes

Acknowledgement

The authors express their sincere appreciation for the financial assistance provided by the Division of Chemistry at the Faculty of Science, Udon Thani Rajabhat University. Additionally, I would like to extend my gratitude to Miss Piyada Bunchai and Miss Wanwisa Namwandee for their assistance in the preparation of the biochar for this project.

References

1. Kodal M, Yazıcı Çakır N, Yıldırım R, Karakaya N, Özkoç G, *Polymers*, 2023; 15: 4503.
2. Siriwong C, Boopasiri S, Jantarapibun V, Kongsook B, Pattanawanidchai S, Sae-Oui P, *J. Appl. Polym. Sci.*, 2018; 46060.
3. Chen Z, Tu Q, Shen X, Fang Z, Bi S, Yin Q, Zhang X, *Polym. Test*., 2023; 126.
4. Suresh Babu KKB, Nataraj M, Tayappa M, Vyas Y, Kumar Mishra R, Acharya B, *Mater. Sci. Energy Technol.*, 2024; 7: 318.
5. Singh M, Salaudeen SA, Norouzi O, Al-Salem S, Gilroyed BH, Dutta A, *Chem. Eng.*, 2023; 109356.

International Rubber Conference 2025 (IRC2025)
1-3 December 2025 @ BITEC, Bangkok, Thailand

Optimizing NR/EPDM/EVA Rubber Foam Formulations for Sustainable Ceiling Board Application

K. BUNSREYNEANG[1], N. JANTAWONG [2,3], K. BOONKERD[1,3], K. HANCHAROEN[4], S. POOMPRADUB[3,5]

[1] *Department of Materials Science, Faculty of Science, Chulalongkorn University, Bangkok, Thailand.*
[2] *Program of Petrochemistry and Polymer Science, Faculty of Science, Chulalongkorn University, Bangkok, Thailand.*
[3] *Center of Excellence in Green Materials for Industrial Application, Chulalongkorn University, Bangkok, Thailand.*
[4] *Center of Building Innovation Technology, Department of Building Innovation, Faculty of Architecture, Kasetsart University, Bangkok, Thailand.*
[5] *Department of Chemical Technology, Faculty of Science, Chulalongkorn University, Bangkok, Thailand*
E-mail: nattayadaploy@gmail.com

Keywords: Natural Rubber Foam, Thermal Insulation, Foam Density and Shrinkage Properties

Due to the escalating impacts of global warming and climate change, rubber researchers around the world have increasingly focused on finding sustainable solutions for developing rubber products. One effective approach is the use of natural rubber (NR), a renewable and biodegradable resource. Many studies have reported the development of various natural rubber–based products as environmentally friendly alternatives to synthetic materials.

In this study, we aimed to develop ceiling boards for construction applications using natural rubber. However, the presence of double bonds in each repeating unit of NR makes it sensitive to weather. To mitigate this, NR was blended with Ethylene-Propylene-Diene-Monomer (EPDM; ASTM designation) at 20, 30, 40, and 50 phr to improve its resistance to environmental degradation. The rubber compounds were prepared by the melt mixing method and processed at 160 °C. Dinitrosopentamethylenetetramine (Supercell DP) was used as the blowing agent, since compared to other foaming agents such as RC720 and EW5, Supercell DP provides the lowest foam density and lowest thermal conductivity, making it the most suitable for thermal insulation ceiling board applications. Preliminary results indicated that using solely NR led to extensive shrinkage after foaming, resulting in a dense rubber foam ceiling board. The NR/EPDM ratio was found to influence the cell structure of the rubber foam. Specifically, the pore size of the foam increased with higher EPDM content, likely because EPDM has a lower viscosity than NR, thereby reducing the viscosity of the matrix. This reduction in viscosity allowed the gas released from the decomposition of the blowing agent to expand more effectively. Moreover, the lower viscosity facilitated better dispersion of the rubber ingredients and blowing agent, which also improved the pore distribution in the foam. The released gas was produced by the decomposition of the blowing agent; the higher the blowing agent loading, the greater the amount of gas released, which accordingly resulted in a larger cell size. Differences in pore structure resulted in variations in the density of the rubber foam: the foam at an NR/EPDM ratio of 80/20 exhibited the highest density of 0.4856 g/cm³, while the foam at an NR/EPDM ratio of 50/50 showed the lowest density of 0.3731 g/cm³.

Although the NR/EPDM ratio of 50/50 resulted in the lowest density, the rubber foam from this formulation continued to shrink even after 10 days. This shrinkage caused dimensional instability and led to imprecision in the shape of the product. To address this issue, ethylene–vinyl acetate (EVA) was incorporated into the rubber foam. Owing to the absence of unsaturated bonds, EVA is also expected to enhance the aging resistance of the rubber foam. Based on the results above, the NR/EPDM rubber foam at the 50/50 ratio demonstrated the best overall performance compared to the other ratios and was therefore selected as the reference compound for further study. In the subsequent experiments, the NR content was fixed at 50 phr, while the EPDM/EVA ratio was varied from 50/0 to 40/10, 30/20, and 20/30.

The results showed that the presence of EVA in the rubber matrix led to a continuous decrease in the density of the rubber foam as the EVA ratio increased. SEM images revealed that increasing the EVA ratio resulted in rubber foam with larger cell sizes, with the formulation at an NR/EPDM/EVA ratio of 50/10/40 exhibiting the largest cell size. This effect can be attributed to the lower viscosity of EVA compared to EPDM, which facilitates easier gas expansion during foaming. In addition, the pore distribution became more uniform as the EVA ratio increased.

Another important property of rubber foam for use as an insulating ceiling board is its thermal conductivity, which indicates how much heat can be transmitted through the ceiling board from the outside to the inside, and vice versa. For a high-performance ceiling board, the heat transmission should be as low as possible. The results showed that the rubber foam with an NR/EPDM/EVA ratio of 50/30/20 exhibited the lowest thermal conductivity, measured at 0.137 W/m·K. This is because rubber has a higher thermal conductivity than air. Once the porous structure was introduced into the rubber matrix, the thermal conductivity was significantly reduced. Moreover, it was found that the thermal conductivity continuously decreased with increasing DP loading. As mentioned above, the increase in blowing agent loading gave the rubber foam a larger cell size, meaning that more air was present in the rubber matrix. Therefore, the reason why the rubber foam with a high DP content had the lowest thermal conductivity was due to the highest amount of air trapped inside the cells. This indicates that such rubber foam possesses the best thermal insulation performance.

Acknowledgement

This work was supported by the National Research Council of Thailand (NRCT). Additionally, we sincerely thank the Center of Excellence in Green Materials for Industrial Application for supporting our participation by sponsoring the registration for IRC 2025.

References

1. Kim B, Nun-anan P, Hancharoen K, Seiichi K, Boonkerd K, J. Phys., 2022; 2175(1): 012018.
2. Jantawong N, Boonkerd K, and Hancharoen K, Solid State Phenom. 2024; 356: 55.

International Rubber Conference 2025 (IRC2025)
1-3 December 2025 @ BITEC, Bangkok, Thailand

A Novel Approach to Using Waste Rubber as a Subsoil Amendment for Improving Soil Quality and Mitigating Hardpan Formation

S. PATTANAWANIDCHAI[1], P. SAE-OUI[1], S. LOYKULNANT[1], T. KUANKHAMNUAN[2]

[1] *National Metal and Materials Technology Center (MTEC), National Science and Technology Development Agency (NSTDA), Khlong 1, Khlong Laung, Pathum Thani 12120, Thailand.*

[2] *Department of Agricultural Engineering, Rajamangala University of Technology Thanyaburi, Khlong 6, Khlong Laung, Pathum Thani 12110, Thailand.*

e-mail address of the presenting author (sirichp@mtec.or.th)

Keywords: Sandy loam soil, Soil compaction, Waste rubber, Bulk density, Water permeability

Soil is a fundamental component of agricultural production, yet intensive tillage and heavy machinery often lead to compaction and hardpan formation, severely limiting crop productivity [1-2]. This study evaluated the potential of incorporating crumb rubber into sandy loam subsoil (50 cm under the top soil) to mitigate compaction and improve soil physical properties. The effects of particle size (S-crumb <1 mm, M-crumb = 1–5 mm, L-crumb >50 mm) and loading (0–35 wt%) on soil bulk density and water permeability were investigated. Bulk density decreased progressively with increasing crumb rubber loading across all particle sizes, with the greatest reduction observed at ~25 wt% S-crumb (Figure 1). Beyond this optimum, further addition of S-crumb produced no significant change. Crumb rubber incorporation also markedly enhanced water permeability of compacted soil, which increased continuously with higher loadings regardless of particle size (Figure 2). At any given loading, S-crumb yielded the greatest improvement, likely due to its poor compatibility with soil and its higher specific surface area, which generated more interfacial voids and facilitated greater water permeability. Overall, the results demonstrate a strong dependence of both bulk density and water permeability on crumb rubber size and loading. Importantly, chemical analyses of crumb water extracts showed that concentrations of most heavy metals were below detection limits; only zinc was detected (35 mg/L), which remained within the U.S. Environmental Protection Agency (EPA) safety threshold (<47 mg/L in freshwater) [3]. These findings indicate that crumb rubber can effectively alleviate soil compaction while maintaining environmental safety, supporting its potential as a sustainable soil amendment. Long-term studies are recommended to verify the persistence of these benefits and assess potential ecological impacts. Future work should also address field-scale applicability and provide recommendations for safe agricultural use, for example, assessing potential implications for root crops compared with non-root crops.

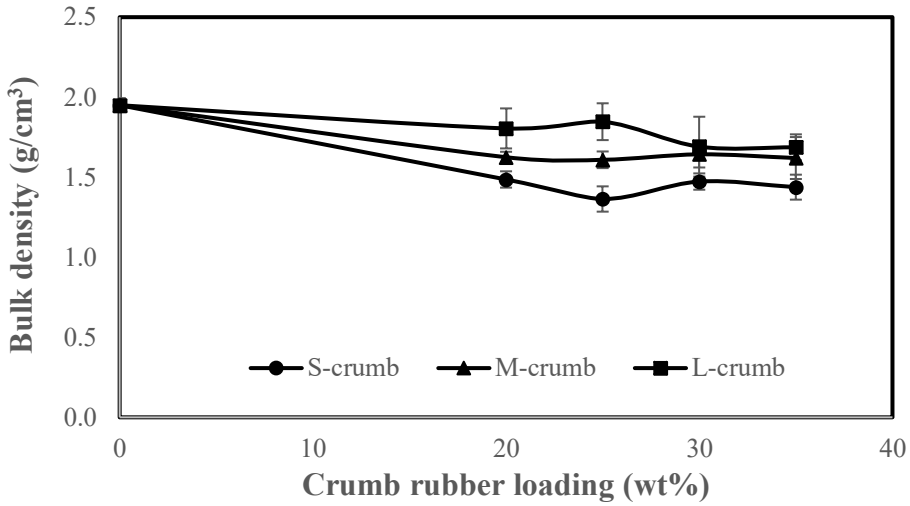


Figure 1. Bulk density of soil amended with different crumb sizes and loadings

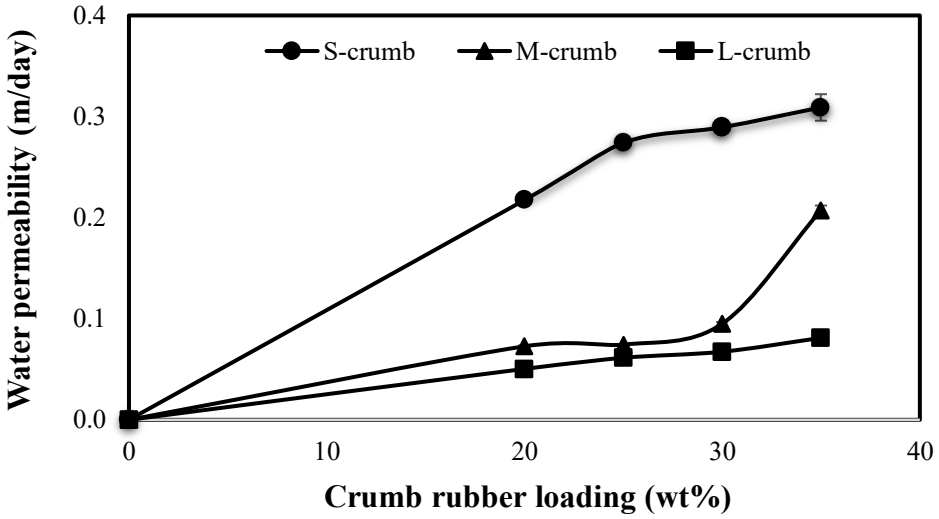


Figure 2. Water permeability of soil amended with different crumb sizes and loadings

Acknowledgement

We gratefully acknowledge the Land Development Regional Office, Nakhon Ratchasima, Thailand, for supporting the field-testing site and related facilities.

References

1. Hamada K, Inoue H, Mochizuki H, Miyamoto T, Asakura M, Shimizu Y, *Soil Tillage Res.,* 2021; 214: 105161.
2. Tekeste M Z, Raper R L, Schwab E B, *Agric. Eng. Inter.*, 2008; 10: 1.
3. United States Environmental Protection Agency, Ambient Water Quality Criteria for Zinc, EPA 440/5-80-079, Washington, DC, USA, Oct. 1980.

Development of natural rubber and polycaprolactone blends as access hole-filling materials for dental implant applications

P. WONGWITTHAYAKOOL[1], K. HATTHAPANIT[2], P. WIROONPOCHIT[2],
C. PONGCHUMYEN[1], S. PANYAKRUA[1], P. GULGOVIT[1]

[1] *Faculty of Dentistry, Thammasat University, Pathumthani, 12120, Thailand.*

[2] *National Metal and Materials Technology Center, Pathumthani, 12120, Thailand.*

panja_w@tu.ac.th

Keywords: Natural rubber/Polycaprolactone blend, Filling materials, Dental implant applications

Microleakage in dental implant systems poses a significant clinical concern, particularly at the abutment-implant interface and the screw access hole [1,2]. An effective sealing material with high efficiency is essential to address this issue. This study explores the development of a thermoplastic elastomer based on a natural rubber (NR) and polycaprolactone (PCL) blend as a novel filling material for implant screw access holes.

NR dough was prepared as the formulation in Table 1, and was blended with PCL at 0%, 10%, and 20% w/w concentrations. Sorption and solubility tests were conducted in artificial saliva to assess material stability. Sealing efficacy was evaluated by measuring methylene blue microleakage through absorbance readings at a wavelength of 595 nm, and results were compared with polytetrafluoroethylene (PTFE) and gutta-percha over 1- and 10-day periods. The handling properties of NR/PCL blends were studied using a plugger and a dental probe (Figure 2) while recording the packing and removal times, respectively. Rheological properties were analyzed to determine the viscoelastic behavior of the NR/PCL blends. Statistical analysis was performed using one-way ANOVA via SPSS.

Table 1. Natural rubber dough compositions

Materials	Contents (phr)
Natural rubber	100
Natural oil	240
Calcium carbonate	850



Figure 2. Removing the NR/PCL blend from the access hole with a dental probe.

Sorption increased with PCL content, whereas solubility remained statistically unchanged across all formulations. Microleakage testing revealed that NR/PCL blends exhibited sealing efficiency comparable to PTFE and gutta-percha, i.e., the NR/PCL blend showed the lowest absorption, as shown in Figure 1. The results from Table 2 illustrate that the NR/PCL blend containing 20% w/w PCL showed the shortest packing and removal times ($p < 0.05$). Rheological analysis indicated that increased PCL concentration enhanced the elastic characteristics of the blend.

The NR/PCL blend with 20% w/w PCL demonstrates promising potential as a novel sealing material for dental implant screw access holes. It offers effective sealing, ease of use, and favorable

rheological behavior. Biocompatibility assessment was not undertaken in the present study. Although the safety of NR and PCL has been supported in the literature, direct evaluation of the developed material remains necessary. It is identified as an important direction for future research.

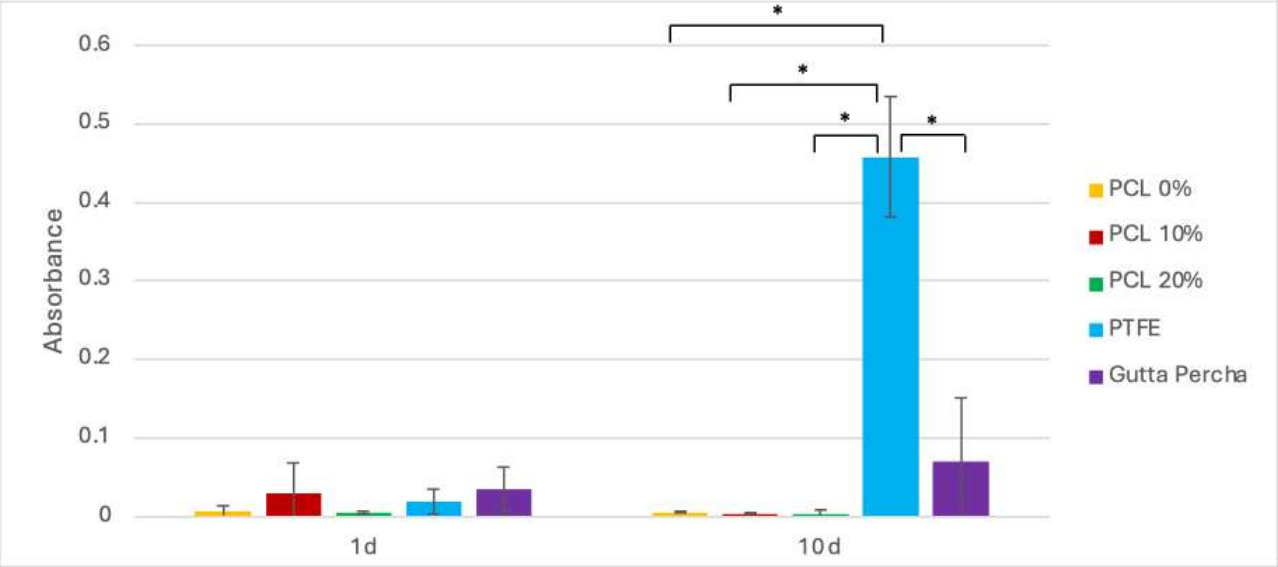


Figure 1. The absorbance average of methylene blue is determined using different sealing materials. Statistical significance was determined using one-way ANOVA followed by Dunnett's multiple comparisons test. $p < 0.05$ was considered significant.

Table 2. The packing and removal times of NR with different PCL contents.

PCL content (% w/w)	Packing time (sec)	Removal time (sec)
0	1.34±0.22[a]	2.20±0.10[a]
10	1.20±0.10[b]	1.66±0.50
20	0.43±0.12[a,b]	0.34±0.08[a]

[a-b]: Different letters in each column indicate statistically significant differences among groups (one-way ANOVA followed by Dunnett's multiple comparisons test, $p < 0.05$).

Acknowledgement

The authors would like to express their sincere gratitude to the Faculty of Dentistry, Thammasat University, Thailand, for the grant support. The authors also gratefully acknowledge the National Science and Technology Development Agency (NSTDA), Thailand, for providing the natural rubber dough preparation and materials used in this study.

References

1. Moráguez OD, Belser UC, *J. Prosthet. Dent.*, 2010; 103: 189–191.
2. Park SD, Lee Y, Kim YL, Yu SH, Bae JM, Cho HW, *J. Prosthet. Dent.*, 2012; 108: 173–180.

International Rubber Conference 2025 (IRC2025)
1-3 December 2025 @ BITEC, Bangkok, Thailand

Effectiveness of Macca Coal Supporter for Osteoarthritis Knee Patients

Varatnane Yaoprukse[1] and Jitladda Sakdapipanich[1,2*]

[1]*Rubber Research Group, Department of Chemistry, Faculty of Science,*

Mahidol University, Nakhon Pathom 73170, Thailand.

[2]*The Rubber and Rubber Glove Academician Association, Bangkok 10900, Thailand*

Presenting author: Varatnane.yao@student.mahidol.edu

*Corresponding author: jitladda.sak@mahidol.ac.th

Keywords: Macca Supporter, Osteoarthritis knee patients, Far-infrared

According to the collaboration with Doi tung development project under royal initiative of Royal Highness princess Srinagrindara, the princess mother, under the topic of "A development of macadamia nut wastes as an economically valuable material". These wastes were altered to be a Macca coal by a high-temperature carbonization process. It has been confirmed previously that this Macca coal has the ability to emit far-infrared (FIR) ranging in wavelengths of 4-20 mm, as a deep-penetrating heat. Thus, the aim of this work was to apply the Macca coal, as its FIR heat generating ability, to prepare supporter and apply to some symptoms that can be healed by heat, like osteoarthritis. In this study, the effectiveness of the Macca knee supporter was elucidated for treating Osteoarthritis Knee Patient (OA).

The carbonized Macca coal was ground and sieved, only the Macca coal with average particle size of 3-5 mm was blended with polyurethane (PU) to make a foam sheet with thickness of 25 mm. The prepared composite was used to prepare knee supporter. OA knee clients (n=114) were randomly divided into control (n=37), placebo or non-Macca (n= 36), and Macca (n=41) groups. The non-Macca (wearing regular knee supports) and the Macca groups (wearing MKS) were suggested to wear the supports at least 4 h a day for 2 months. Modified WOMAC (MWOMAC) scores, visual analog pain scale (VAS) and Quality of life scores (by SF36) were determined at pre, 1st and 2nd month. There were no differences of MWOMAC scores among the three groups at the pre period, whereas at the 2nd month, these scores of both Non-Macca and Macca groups were significantly lower when compared to the control group.

Even though, there were no differences of MWOMAC scores among the groups, it was found that within the Macca group, MWOMAC scores were significantly differences among pre, 1st and 2nd month period. These scores of the non-Macca group were only significantly differences at pre *vs.* 1st and pre *vs.* 2nd month. No significant differences among the 3 groups of all domains of SF36 were found. Energy/fatigue and social functioning domains of the Macca group were significantly increased from pre to the 2nd month, whereas no differences were found within the Control and Non-Macca groups. For the VAS, no differences among the groups were found; however, VAS was significantly decreased within the Macca group. No differences of VAS were found within both the control and non-Macca groups. This indicates that FIR radiated from Macca materials may be a factor responsible for these exceeded therapeutic effects. Therefore, it can be concluded that Macca knee supporter can applied for relief the OA symptom effectively, based on the significant change in the pain and got better in the daily self-assist ability, by the FIR effect from Macca coal incorporating in the supporter.

Reference

1. Rodgerd P., Yakkul S., Sakdapipanich J., *Adv. Mater. Res.*, 2013; 844: 149.

International Rubber Conference 2025 (IRC2025)
1-3 December 2025 @ BITEC, Bangkok, Thailand

Manipulating the Properties of Polymer Vitrimer Nanocomposites by Designing Dual Dynamic Covalent Bonds

Zhenyuan Li[1], Hengheng Zhao[1], Liqun Zhang[1,2], Jun Liu[1]

[1] *Beijing University of Chemical Technology, Beijing, China.*

[2] *Xi'an Jiaotong University, Xi'an, China.*

e-mail address of the presenting author (2024400153@buct.edu.cn)

Keywords: Polymer vitrimer nanocomposites, Molecular dynamics simulation, Functional elastomer material

The development of materials that combines the mechanical strength of thermoset polymers with the reprocessing ability of thermoplastic polymers has been the subject of extensive research. In the pursuit of material that experiences both these exceptional performances, a feasible idea is to introduce dynamic bond exchange reactions (BERs) into the material, which are also known as covalent adaptive networks. In 2011, Montarnal *et al*. [1] first named a new material "vitrimers", which exhibited silica-like viscosity properties across a broad temperature range, while also possessed desirable characteristics such as selfhealing, recyclability, and weldability. Due to its distinctive properties, vitrimer is now frequently classified as a third category of polymer materials, alongside thermoplastics and thermosetting polymers.

To enhance the mechanical and thermal properties of polymers, the approach of incorporating nanoparticles (NPs) has been investigated. This not only reduces the cost of materials but also provides an opportunity to tailor the properties of the nanocomposites. Huang *et al.* [2] constructed polymer vitrimer nanocomposites (PVNs) based on disulfide using epoxy and sulfhydryl-activated silica NPs as fillers, exhibiting excellent mechanical strengthening properties and higher self-healing efficiency. Wu *et al.* [3] reported a strategy to achieve mechanically robust, ductile, and recyclable elastomer vitrimers by implementing dynamic covalent networks in elastomer/silica composites. They also prepared covalently cross-linked but recyclable PVNs by binding exchangeable β-hydroxyl ester bonds to the vitrimer−NP interface. However, a comprehensive understanding of matrix and interfacial bond exchange reactions to tailor the properties of PVNs is still lacking. In this regard, computer simulations play a crucial role in understanding the structure, dynamics, and properties of vitrimers and provide insights into the design and synthesis of new materials.

Herein, we utilized coarse-grained molecular dynamics simulations to investigate model PVNs in which there were two different kinds of DCBs in the vitrimer matrix and at the interface as shown in Figure 1. By varying the bond swap energy barrier (ΔE_{sw}) in the matrix ΔE_{sw}^{mat} or in the interface ΔE_{sw}^{int}, or in both ΔE_{sw}^{all}, a maximum mechanical property is observed at the moderate value of ΔE_{sw}^{mat}, ΔE_{sw}^{int}, or ΔE_{sw}^{all}. Meanwhile, the effect of ΔE_{sw} on the stress relaxation and the bond orientation as a function of the time under a fixed strain is well probed, which both decays more slowly at greater ΔE_{sw}. We simulated the tension−recovery curve to examine the effect of ΔE_{sw} on the hysteresis loss and permanent deformation of PVNs, finding an optimal value to achieve its minimum energy dissipation and maximum recovery ratio. Lastly, we investigated the efficiency of self-healing by building and removing walls from the system. Interestingly, a maximum self-healing efficiency of the stress−strain behavior is observed at moderate ΔE_{sw}. Overall, this study provides

valuable insights into the relationship between the structure and properties of PVNs, offering implications for the manipulation of their mechanical properties and enhancement of their self-healing capabilities.

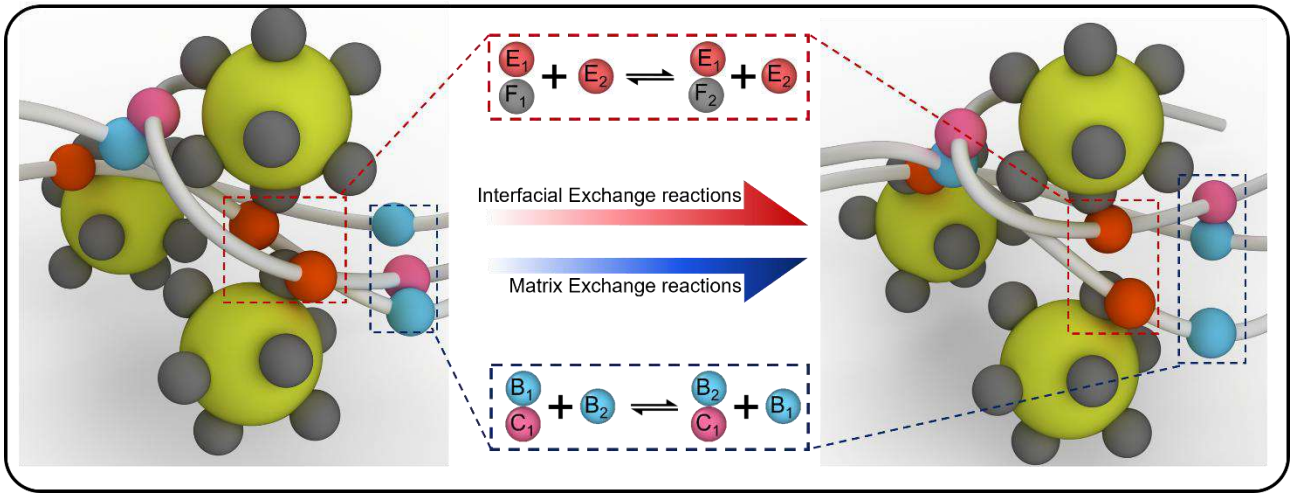


Figure 1. Bond swap mechanism of PVNs. There are two types of dynamic bond swaps: interfacial bond swaps (occur between the reactive beads on the vitrimer and on the NPs, highlighted by the red dashed box) and matrix bond swaps (occur between the active beads of vitrimer itself, highlighted by the blue dashed box). Other unreactive beads on the polymer chain are indicated by white lines.

Acknowledgement

This work was financially supported by the National Science Fund for Excellent Young Scholars (52122311), the National Natural Science Foundation of China (52373222), the Beijing Municipal Natural Science Foundation (2182053), and the Fok YingTong Education Foundation of China (Grant No. 171040). The supercalculation center of “Tianhe numWber two” and the cloud calculation platform of Beijing University of Chemical Technology (BUCT) are both greatly appreciated.

References

1. Montarnal D, Capelot M, Tournilhac F, Leibler L, *Science,* 2011; 334: 965.
2. Huang Z, Wang Y, Zhu J, Yu J, Hu Z, *Compos. Sci. Technol.,* 2018; 154: 18.
3. Wu S, Yang Z, Fang S, Tang Z, Liu F, Guo B, *J. Mater. Chem. A Mater.,* 2019; 7: 1459.

International Rubber Conference 2025 (IRC2025)
1-3 December 2025 @ BITEC, Bangkok, Thailand

Accelerated Prediction of Glass Transition Temperature in SSBR via Integrated Molecular Dynamics Simulation and Machine Learning Framework

Siqi Zhan [1], Jun Liu [1], Liqun Zhang [2]

[1] *15 North Third Ring Road East, Beijing, China*

2022200573@buct.edu.cn

Keywords: SSBR, Glass Transition Temperature, Molecular Dynamics Simulation, Ordinary Kriging, XGBoost, Machine Learning

The development of smart and functional rubber materials increasingly relies on data-driven approaches to accelerate performance optimization. This work proposes a hybrid methodology that integrates all-atom molecular dynamics (AAMD) simulations with machine learning (ML) to efficiently predict the glass transition temperature (T_g) of solution-polymerized styrene-butadiene rubber (SSBR), a key determinant of its mechanical and dynamic behavior. A high-fidelity dataset was constructed using AAMD simulations across a range of copolymer compositions. To address the challenge of limited data availability, an enhanced interpolation scheme was developed by improving Nearest Neighbor Interpolation (NNI) via Ordinary Kriging (OK), which preserves the computational efficiency of NNI while significantly improving prediction accuracy. Four regression models—XGBoost, Ridge, LASSO, and SVR—were systematically evaluated, with XGBoost exhibiting superior performance based on R^2 and RMSE metrics. The resulting NNI-OK-XGBoost model showed strong robustness, maintaining an average R^2 of approximately 0.97 across 900 repeated trials. Validation against new SSBR compositions revealed excellent agreement between ML predictions and AAMD simulation results, with the ML model achieving significantly higher computational efficiency. This approach provides a robust and practical framework for intelligent property prediction in the rational design of functional rubber materials, supporting accelerated screening and optimization for next-generation high-performance elastomers.

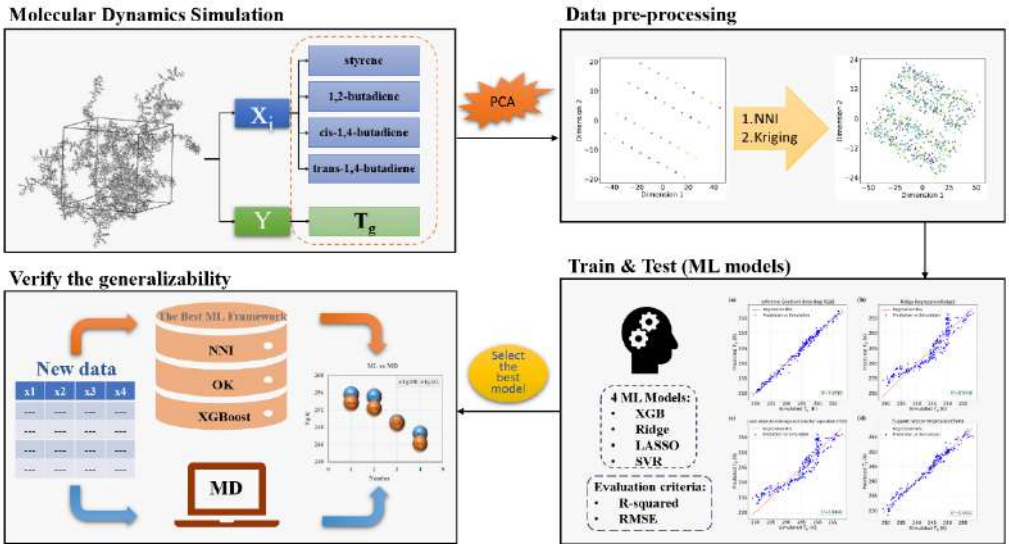


Figure 1. Schematic illustration of the integrated MD-ML workflow for predicting the glass transition temperature of SSBR.

Acknowledgement

J.L. acknowledges the National Science Fund for Excellent Young Scholars (52122311) and the National Natural Science Foundation of China (52373222). This work is supported by Open Project of State Key Laboratory of Supramolecular Structure and Materials (Grant number sklssm202512).

References

1. Ge W, De Silva R, Fan Y, Sisson SA, Stenzel MH, *Adv. Mater.*, 2025; 2413695.
2. Xu P, Ji X, Li M, Lu W, *npj Comput. Mater*., 2023, 9 (1), 1–15.
3. Song C, Gu H, Zhu L, Jiang W, Weng Z, Zong L, Liu C, Hu F, Pan Y, Jian X, *J. Mater. Chem. A*, 2023, 11 (32), 16985–16994.

International Rubber Conference 2025 (IRC2025)
1-3 December 2025 @ BITEC, Bangkok, Thailand

Preparation of DES-containing Polyurethane Elastomer and Its Moisture-dependent Electrical Conductivity

Shogo TAKETA[2], Shintaro YAMAGUCHI[2], Hironobu TAHARA[1], Hiroto MURAKAMI[1]

[1] *Institute of Integrated Science and Technology, 1-14 Bunkyo Nagasaki, Japan.*

[2] *Graduated School of Integrated Science and Technology, 1-14 Bunkyo Nagasaki, Japan.*

e-mail address of the presenting author (hiroto@nagasaki-u.ac.jp)

Keywords: Polyurethane, Deep Eutectic Solvent, Ion Conductivity, Moisture Response

Polyurethanes (PUs) are macromolecules which consist of polyol, diisocyanate, and curing agent. A certain PU forms a microphase separation structure consisting of hard and soft segments that affect their thermal and physical properties. By the way, deep eutectic solvents (DES) are mixtures consisting of two or more hydrogen-bonded donors and hydrogen-bonded acceptors and are liquids at room temperature in which the melting point of the mixture is significantly lower than the melting point of each component. DESs are expected to be a cheap designer solvent in which the physical properties can be controlled and are used in green chemistry due to low-toxicity and low-environmental impact. A DES consisting of quaternary salt and hydrogen-bonded donor possesses ion conductivity that is influenced by moisture. Therefore, we think that the mixing of PU and DES results in the fabrication of moisture-responding rubber materials (Figure 1). In this presentation, we describe the fabrication of DES-containing PU and its moisture-dependent electrical conductivity.

PU was synthesized with poly(tetramethlene glycol) 2000 (PTMG2000), diphenylmethane diisocyanate (MDI), and butanediol by a prepolymer method (Figure 2).[1] A mixture of choline chloride and ethylene glycol (1 : 4.5 mol/mol) was used as a DES. The DES was added into the DMF solution of PU at 50 wt% relative to the weight of PU. The mixture was poured into a Teflon Petri Dish and dried at 80 °C for 2 days to obtain a DES-containing PU film. The thermal and physical properties were evaluated by DSC measurement and tensile test, respectively. The structure of the DES-containing PU film was estimated by FT-IR measurement. The electroconductivity of the film was measured by AC impedance method: E_{ac} = 200 mV; f = 0.01～10000 Hz; film area, 4.0 cm^2; and film thickness, 0.3 mm.

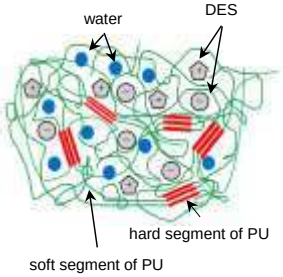


Figure 1. Cartoon of DES-containing PU.

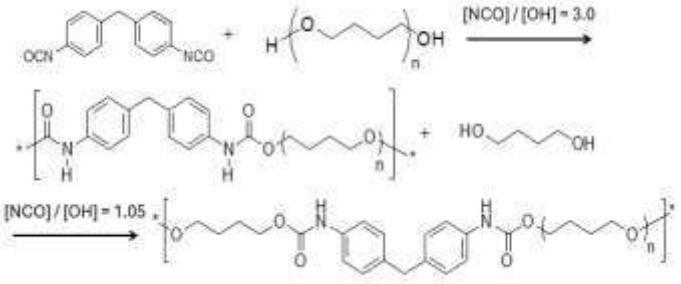


Figure 2. Synthesis scheme for PU by prepolymer method.

The glass transition temperatures of the PU film without DES and DES-containing PU film were observed at 63 and 64 °C, respectively. Both the films also showed exothermic peak around -30 °C and endothermic peak around 5 °C, originating from reorganized crystallization and its melting of the soft segment. This result indicates that the coexistence of DES did not affect the thermal motion of the soft segment of PU.

Stress-strain curves were obtained from tensile tests of the PU film without DES and DES-containing PU film. Young's moduli, elongation strengths, and strain at break were 8.9 MPa, 19.7 MPa, and 2060% for the PU film without DES, and 5.7 MPa, 8.3 MPa, and 1600% for the DES containing PU film. This result suggests that the rubber property is maintained even when the DES is contained in the PU film, but the coexistence of DES causes the decrease in the values for the physical properties.

The formation of hydrogen bond between the urethane bonds in the hard segment of PU was estimated by the ATR-FT-IR measurement. No shift of the peak wavenumbers for the C=O stretching vibration was observed regardless of the addition of DES. This means that the DES is not capable of cleaving hydrogen bonds between the urethane bonds in the hard segment of PU.

The Nyquist diagrams of AC impedance for the DES-containing PU film are shown in Figure 3. The AC impedance of PU without DES could not be measured due to its high resistance. The ionic conductivity at each temperature was evaluated to be 2.2×10^{-10} S cm^{-1} at 25 °C, 8.2×10^{-10} S cm^{-1} at 40 °C, and 4.1×10^{-9} S cm^{-1} at 60 °C. From the result, it was found that the ionic conductivity increases with increasing temperature.

Figure 4a and 4b show a measurement cell for the moisture-dependent electrical conductivity measurement and the time course of electric current value before and after dropping water droplets, respectively. The exposing moisture resulted in the increasing of electric current value; the drying by air resulted in the decreasing of electric current value. Therefore, we have succeeded in developing a prototype PU rubber whose electrical conductivity responds to moisture.

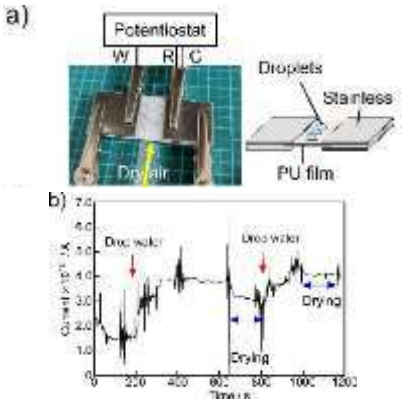


Figure 4. a) Photo and cartoon of a measurement cell for the moisture-dependent electrical conductivity measurement. b) Time course of electric current value: bias voltage, 2.0 V.

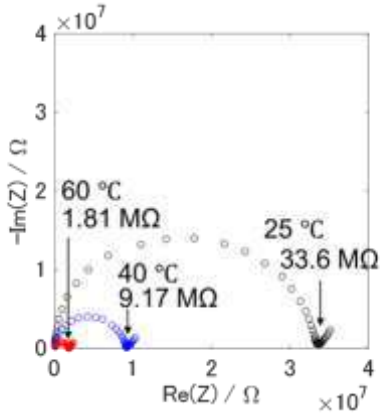


Figure 3. Nyquist diagrams of AC impedance of DES-containing PU. The resistance values in the figure are originated from ionic conduction.

Acknowledgement

This study is supported by the International Polyurethane Technology Foundation, and JSPS KAKENHI Grant Number JP22K05258 and JP23K26630.

References

1. Kojio K, Kugumiya S, Uchiba Y, Nishino Y, Furukawa M, *Polymr. J.*, 2009; 41: 118.

International Rubber Conference 2025 (IRC2025)
1-3 December 2025 @ BITEC, Bangkok, Thailand

A Facile Method in Fabricating Flexible Composite Elastomers with Large-Size Segregated Structures for Electromagnetic Interference Shielding

Liang He[1], Yang Chen[1], Lijie Yin[1], Wencai Wang[1*]

[1]*Center of Advanced Elastomer Materials, College of Material Science & Engineering, Beijing University of Chemical Technology, Beijing 100029, China.*

Presenting author (hl13176189630@163.com), *Corresponding author (wangw@buct.edu.cn)

Keywords: Segregated structures, Electromagnetic Interference Shielding, Conductive composite elastomer

To mitigate the destruction to the conductive network caused by the plastic deformation of polymer particles during hot-press molding, plastic particles with high molecular weights and moduli are typically required for preparing composites with segregated structures; thus, the prepared composites exhibit poor flexibility. Moreover, segregated composites still face preparation complexities, which hinders the advancement from the laboratory to the factory.

In view of this, a facile method for developing flexible composites with segregated structures is proposed. The preparation process for composite elastomers is shown in Figure 1. First, silver-coated polydopamine-modified reduced graphene oxide (Ag@PrGO), as conductive fillers, are prepared by electroless plating. Next, polydimethylsiloxane (PDMS)-coated polyolefin elastomer (POE) beads are put into a self-sealing bag containing the Ag@PrGO. After a simple shaking, the fillers are adhered to the POE surface as the cohesive property of cured PDMS. Finally, flexible composites with large-size segregated structures are obtained via hot pressing. As shown in Figure 2, the prepared composite elastomers exhibit good flexibility and possess remarkable segregated structures. Notably, benefiting from the 2D structure of the Ag@PrGO and the ability to slip during hot-press molding, the conductive networks maintain structural integrity due to the adaptable deformability. With increasing Ag content, the electromagnetic interference shielding effectiveness (EMI SE) of the composite elastomers improves from 9 dB to 70 dB in the X-band at a thickness of 1.9 mm, attributed to the continuous optimization of the conductive network.

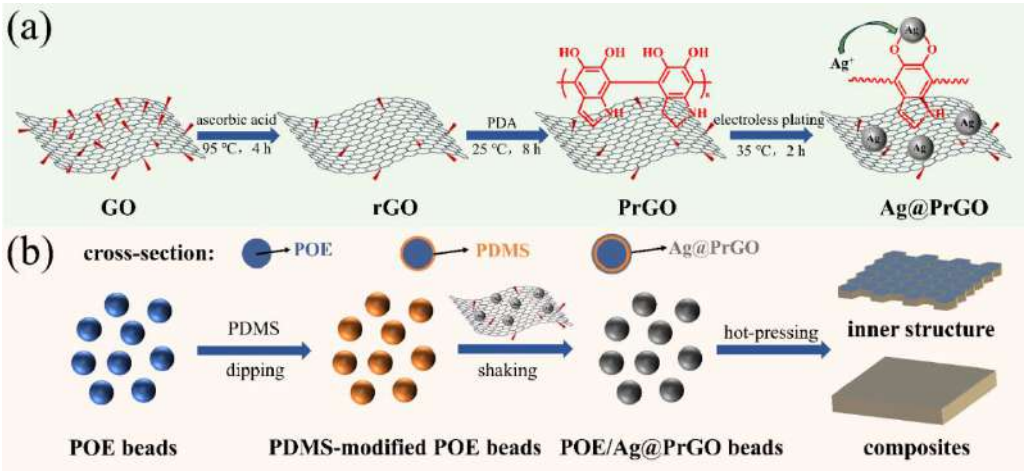


Figure 1. Fabrication process for the (a) Ag@PrGO fillers and (b) POE/Ag@PrGO composites.

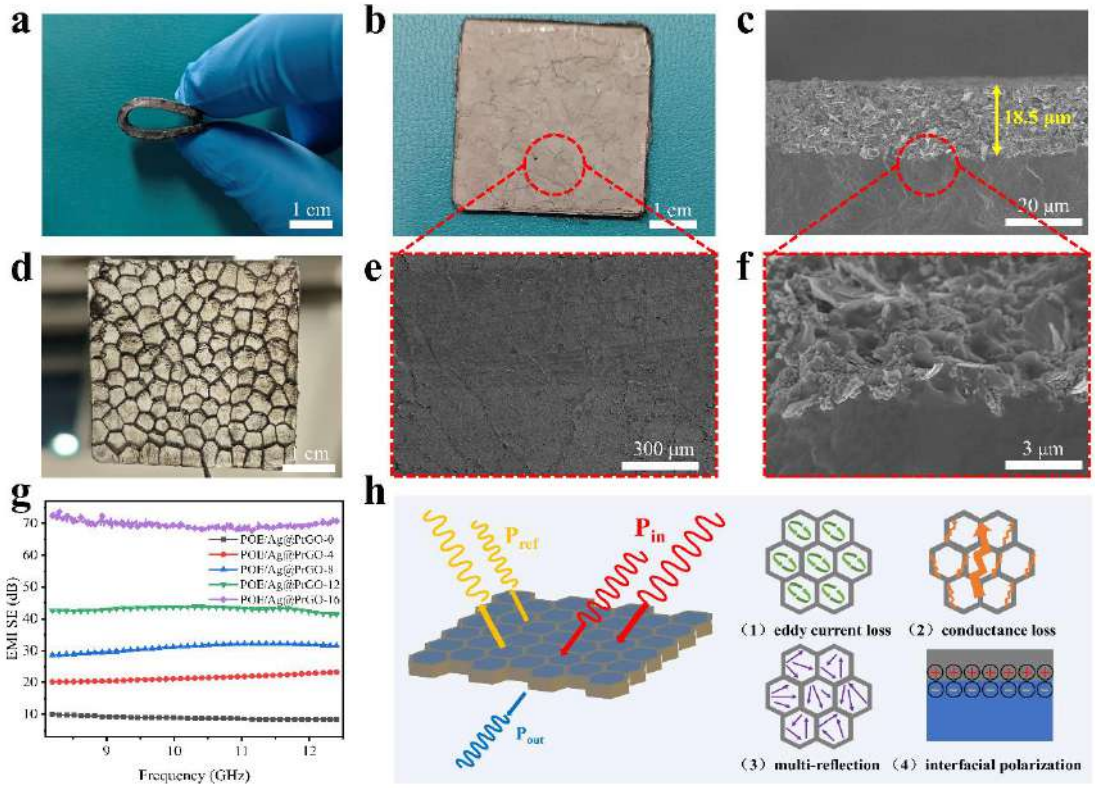


Figure 2. (a) The digital image exhibiting the bending performance of POE/Ag@PrGO composites; (b and e) The digital and SEM images of POE/Ag@PrGO composites; (c and f) SEM images of the cross-section of POE/Ag@PrGO composites; (d) The digital image of POE/Ag@PrGO composites after the conductive layers on the surface have been polished; (g) The EMI SE of POE/Ag@PrGO composites in the X band; (h) The EMI shielding mechanism of POE/Ag@PrGO composites.

Acknowledgement

The authors thank the Center of Advanced Elastomer Materials of BUCT for financial support.

References

1. Dingxiang Yan, Huan Pang, Bo Li, Robert Vajtai, Ling Xu, Penggang Ren, Jianhua Wang, Zhongming Li, *Adv. Funct. Mater.*, 2015; 25: 559-566.
2. Ali Akbar Isari, Ahmadreza Ghaffarkhah, Seyyed Alireza Hashemi, Stefan Wuttke, Mohammad Arjmand, *Adv. Mater.*, 2024; 36: 2310683.
3. Liang He, Yang Chen, Xiaoming Shao, Qiyuan Yao, Ding Feng, Lijie Yin, Wencai Wang, *Macromol. Rapid Commun.*, 2024; 2400585.

International Rubber Conference 2025 (IRC2025)
1-3 December 2025 @ BITEC, Bangkok, Thailand

Highly conductive Ag/pCF/MVQ composite rubber for efficient electromagnetic interference shielding

Yang Chen[1], Liang He[1], Wencai Wang[1*]

[1] *Center of Advanced Elastomer Materials, College of Material Science & Engineering, Beijing University of Chemical Technology, Beijing 100029, China.*

Presenting author (1049729480@qq.com), *Corresponding author (wangw@buct.edu.cn)

Keywords: Electromagnetic interference shielding rubber, Carbon fiber, Polydopamine, Electroless silver plating

The increasing complexity of the space electromagnetic environment is causing substantial electromagnetic interference (EMI) due to the widespread use of electronic equipment and the quick development of wireless communication technologies[1]. As a result, it is imperative to prepare high-efficiency EMI shielding materials. Compared with traditional metal materials, conductive rubber is starting to attract a lot of attention due to its many benefits, including changeable electrical conductivity, superior flexibility, and light weight, which has a lot of potential applications in the realm of EMI[2]. However it is usually necessary to add a large number of conductive fillers to achieve high conductivity. At this time, obtaining high conductivity at low packing fractions is still an important field of research.

In this study, flexible and highly conductive composite rubber at low filler content was successfully prepared through polydopamine (PDA) assisted electroless silver plating plus mechanical mixing. The preparation process for composite rubber is shown in Figure 1. Firstly, carbon fibers (CF) with a length of 100−300 μm and a diameter of 7 μm was activated by PDA to improve the surface activity by self-polymerization reaction. Next, take advantage the metal chelating ability of PDA, silver layer was firmly deposited on the surface of CF through a facile electroless silver plating method. Finally, silver-plated carbon fibers (Ag/pCF) and methyl-vinyl silicone (MVQ) were prepared into composite rubber by mechanical mixing. As shown in Figure 2, the composite rubber filled with only 45 phr Ag/pCF had a high electromagnetic interference shielding effectiveness (100 dB) due to the low density and high aspect ratio of Ag/pCF. The composite rubber has excellent potential for application in the field of electromagnetic interference shielding.

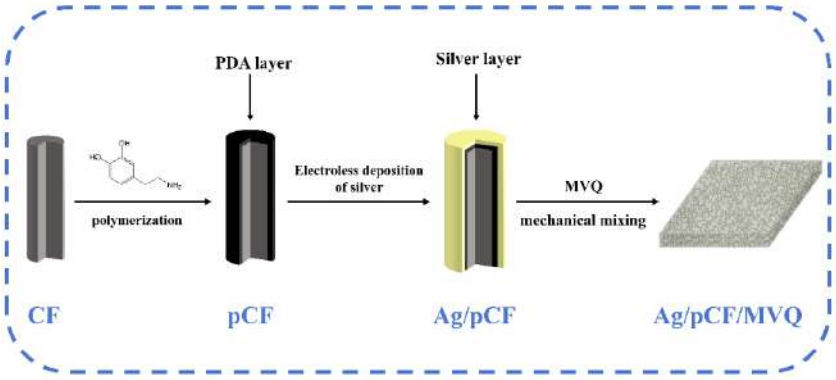


Figure 1. Process for the preparation of Ag/pCF/MVQ composites

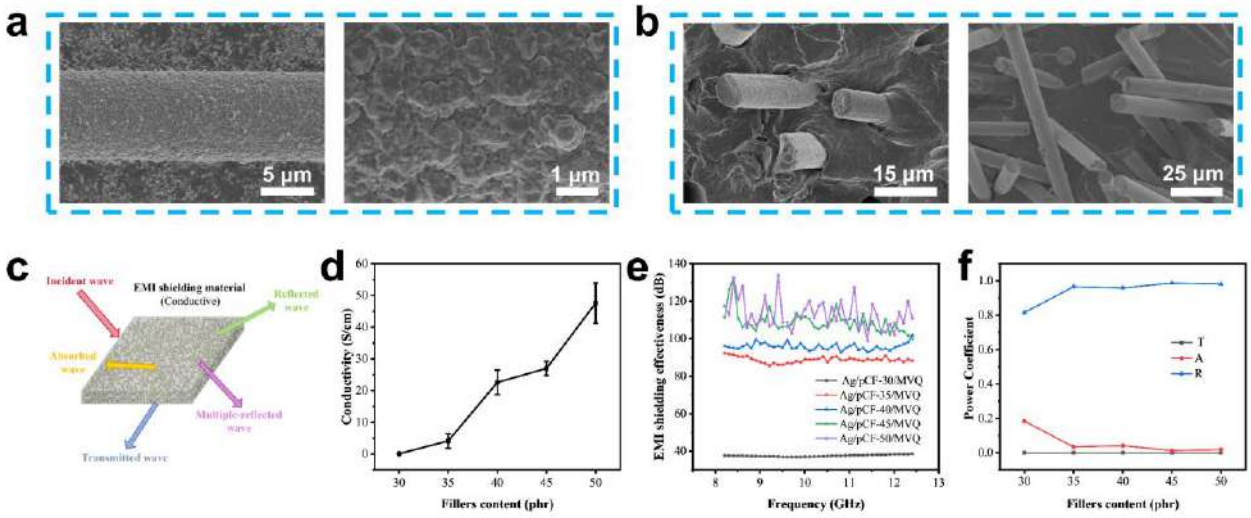


Figure 2. (a) SEM images of Ag/pCF; (b) SEM images of Ag/pCF/MVQ composites; (c) The EMI shielding mechanism of Ag/pCF/MVQ composites; (d) The conductivity of Ag/pCF/MVQ composites; (e) The EMI shielding effectiveness of Ag/pCF/MVQ composites; (f) The power coefficients of of Ag/pCF/MVQ composites

Acknowledgement

This work was financially supported by the National Natural Science Foundation of China (No. 51833002).

References

1. Liu J, Yu MY, Yu ZZ, Nicolosi V, Mater. Today Phys., 2023; 66: 245.
2. Nan Z, Wei W, Lin ZH, Chang JJ, Hao Y, Nano-Micro Lett, 2023; 15: 172.

International Rubber Conference 2025 (IRC2025)
1-3 December 2025 @ BITEC, Bangkok, Thailand

Texture Evolution and Mechanical Response of Cholesteric Liquid Crystal Elastomers with a Lying Helix Structure

Koudai Tanino[1], Tsutomu Furuya[2], Tsuyoshi Koga[2], Kenji Urayama[1]

[1] *Department of Material Chemistry, Graduate School of Engineering, Kyoto University*

[2] *Department of Polymer Chemistry, Graduate School of Engineering, Kyoto University*

urayama.kenji.2s@kyoto-u.ac.jp

Keywords: Liquid Crystal Elastomers, Lying Helix Structure, Cholesteric Elastomers, Soft Elasticity

Cholesteric liquid crystal (CLC) with a lying helix configuration (**Fig.1**), in which the helical axis lies parallel to the substrate, exhibits a fingerprint (FP) texture reflecting its regular structure. Due to its periodicity, this FP texture has the property of diffracting light. By crosslinking this CLC into an elastomer (CE), the diffraction properties become dynamically tunable by mechanical stretching. This positions CE films with FP texture (FP-CE) as promising materials for advanced optical devices, such as dynamic diffraction gratings. Surface undulation of FP-CE in response to temperature variation [1] and electric field [2] has been investigated by several researchers. This study investigates the variations in FP texture and tensile stress of FP-CE films during stretching.

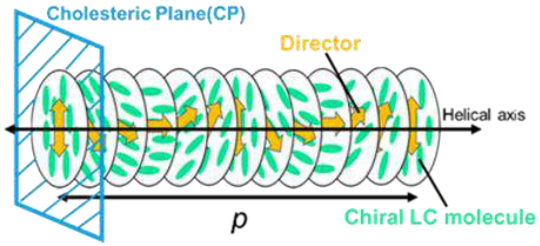


Fig.1 Schematic of CLC

The samples were prepared using a mesogenic diacrylate (RM82), a chiral diacrylate (LC756), a chain extender (BDMT), and a photoinitiator (Irgacure784) (**Fig.2**). This mixture was injected at 110°C into a glass cell (gap: 30 µm) that had been treated for homeotropic (vertical) alignment. Upon cooling to 65°C in the liquid crystal phase, a fingerprint (FP) texture, characteristic of the Lying Helix (LH) structure, was observed. At 65°C, photopolymerization was performed by irradiating with 525 nm light to obtain an FP cholesteric elastomer (FP-CE) film. Change in the FP texture and mechanical response of the FP-CE film to stretching were investigated.

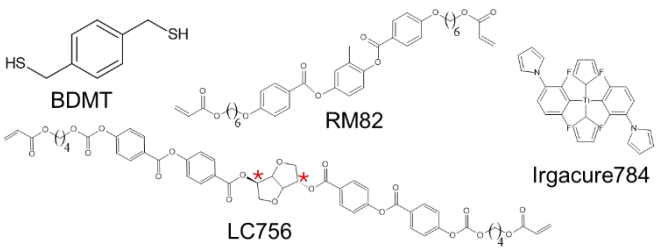


Fig.2 Chemical structures of the compounds

A polarizing optical microscope image verifies a FP texture in the FP-CE film with a helical pitch of 14.6 µm (corresponding to twice the stripe width), where helical axes orient randomly in the film plane (**Fig.3(a)**).Upon uniaxial stretching, regions where the stripes are initially oblique to the stretching axis undergo reorientation along the stretching axis, while maintaining the stripe width (helical pitch) (dipicted by the red dotted lines in **Fig.3(b)**. This behavior indicates that the local directors realign along the stretching axis, resulting in the helical axis becming perpendicular to it. In contrast, domains with stripes initially oriented perpendicular to the stretching axis (closed by the

yellow dotted lines) show a different response: the stripes do not rotate, but the stripe width (helical pitch) increases in the stretching direction. This pinning of stripe direction results from no bias

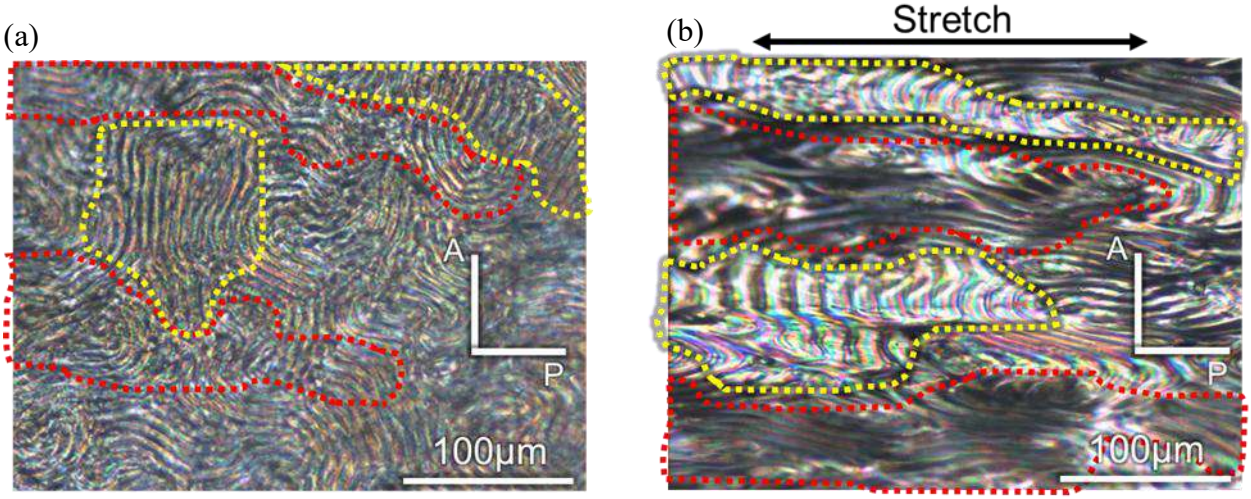


Fig.3 FP textures and of FP-CE in the (a) undeformed and (b) stretched (ε_x=0.9) states. The yellow dotted area depicts a domain with the initial stripes almost perpendicular to the stretching axis.

between the clockwise and counterclockwise rotations of the local directors under stretching, with mechanical work contributing to the widening of the helical pitch.

Figure 4 plots the nominal stress and 2D orientational factor (*f*s) for stripes as a function of true strain. This behavior is characterized by three distinct regions. In Region II, a wide stress plateau is observed. This mechanical response is directly correlated with a significant change in the fingerprint (FP) texture and a sharp increase in *f*s . This suggests an easy alignment of the cholesteric planes (CPs) toward the stretching direction, analogous to the "soft elasticity" in nematic elastomers [3], which significantly reduces the required mechanical work. Subsequently, in Region III, the stress rises steeply, exhibiting typical rubber-like elasticity. In this region, the FP texture remains unchanged, and *f*s reaches saturation, quantitatively confirming the completion of the CP uuuureorientation. Thus, the stress increase in Region III is attributed purely to the elastic deformation of the polymer network itself.

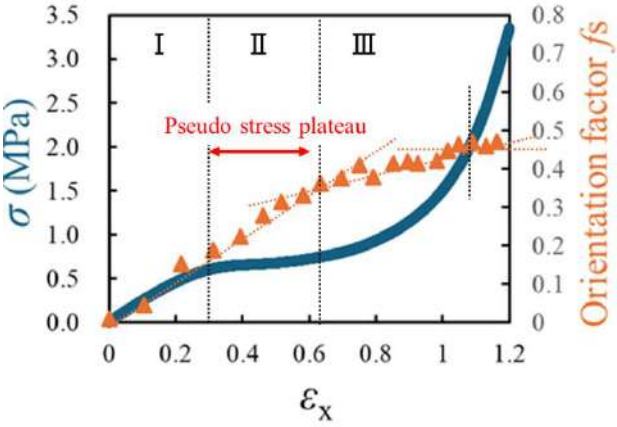


Fig.4 Nominal stress and orientation factor as a function of true stress for FP-CE

References

1. H. Nagai, X. Liang, Y. Nishikawa, K. Nakajima, and K. Urayama, *Macromolecules*, **49**, 9561−9567 (2016)
2. W. Feng, D. J. Broer, L. Grebikova, C. Padberg, J. G. Vancso, and D. Liu, *ACS Appl. Mater. Interfaces*, **12**(5), 5265-5273 (2020)
3. See, for example, H. Tokumoto, Z. Hao, A. Takebe, K. Kamitani, K. Kojio, A. Takahara, K. Bhattacharya, K. Urayama, *Sci. Adv.*, **7**, eabe9495 (2021)

International Rubber Conference 2025 (IRC2025)
1-3 December 2025 @ BITEC, Bangkok, Thailand

Simulation of Rubber Acoustic Coatings under Deep-Sea Pressure Based on Strain-Dependent Viscoelastic Properties

Yue Liu[1], Xiuying Zhao[1]

[1] *Center of Advanced Elastomer Materials, College of Materials Science and Engineering, Beijing University of Chemical Technology, Beijing, China.*

2023430046@buct.edu.cn

Keywords: Acoustic coating, Hydrostatic pressure, Strain-dependent viscoelasticity, Dynamic mechanical analysis (DMA) **,** Underwater acoustics.

The acoustic coating is essential for underwater vehicles to achieve stealth, typically comprising rubber-based materials with embedded cavities that absorb sound through damping and structural effects[1]. In deep-sea environments, hydrostatic pressure causes significant deformation, compressing cavities and altering the rubber's mechanical behavior, which reduces sound absorption[2]. However, most simulation models still treat viscoelastic properties as uniform constants, ignoring strain-induced spatial heterogeneity, thus limiting the accuracy and applicability of acoustic performance predictions.

To overcome this, we propose a strain-driven mapping method for viscoelastic properties that captures their evolution under different strain states and enables localized parameter assignment. Standard styrene-butadiene rubber (SBR) specimens were tested using dynamic mechanical analysis (DMA) across –50% to 100% strain, 1–100 Hz frequency, and –50 °C to 30 °C. Using the Williams-Landel-Ferry(WLF) equation, frequency spectra of storage and loss moduli were obtained at multiple pre-strain levels, as shown in Figure 1. The strain field under hydrostatic pressure was then simulated, and fitted functions were used to map and assign viscoelastic parameters across the deformed model.

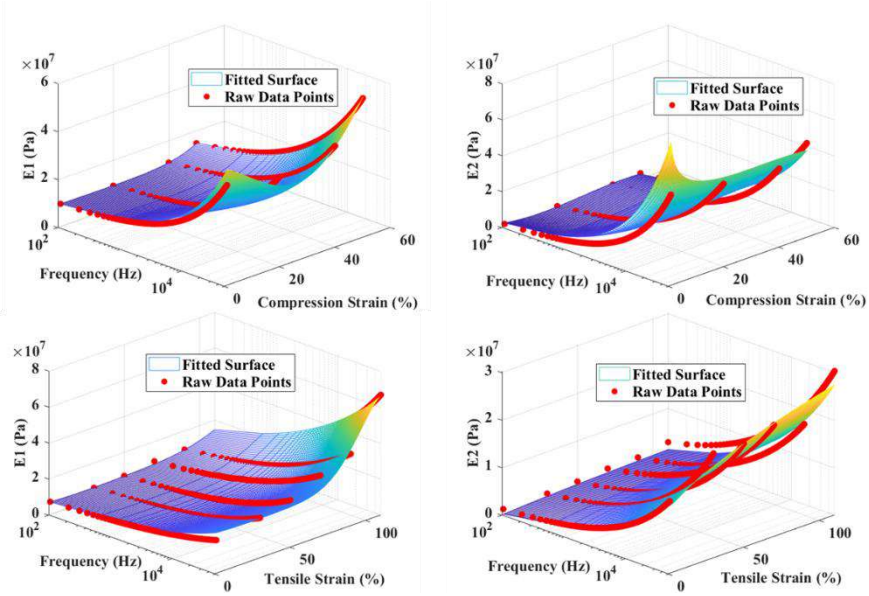


Figure 1. Storage modulus and loss modulus of SBR under different pre-strain

To validate the proposed method, a horn-shaped acoustic coating was simulated under hydrostatic pressure. Prior to performance evaluation, the viscoelastic behavior under 1 MPa pressure was characterized. Figure 2 shows the storage modulus across frequencies, confirming the necessity of strain- and frequency-dependent parameter mapping. The predicted sound absorption, shown in Figure 3, matched experimental results closely. The strain-driven mapping significantly improved the accuracy in capturing the absorption peak's frequency and amplitude compared to conventional uniform-property models, demonstrating its effectiveness in acoustic performance prediction.

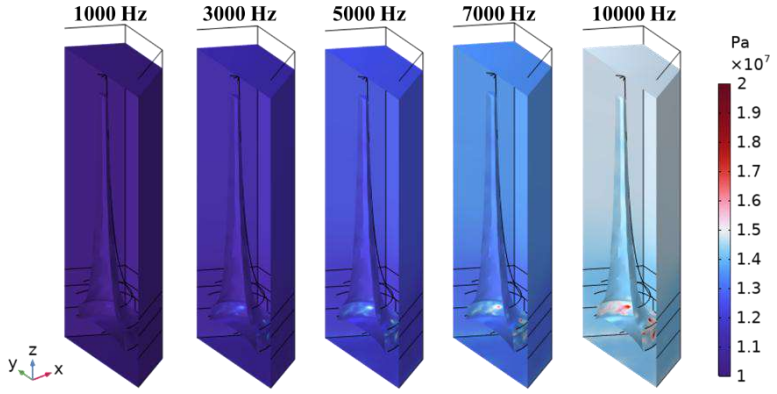


Figure 2. Storage modulus of acoustic coating at different frequencies under 1MPa pressure

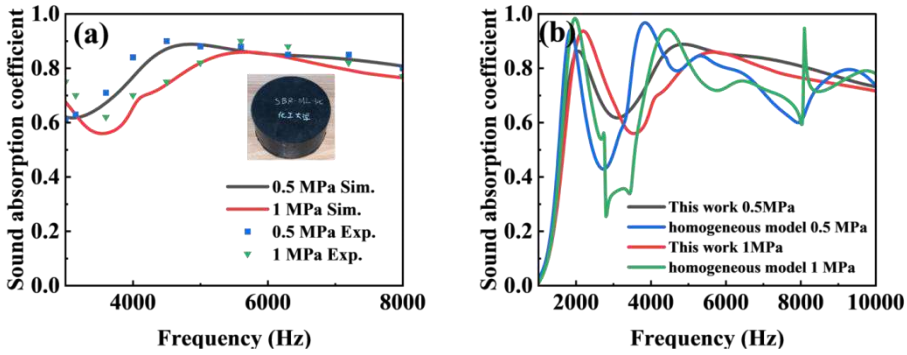


Figure 3. (a) Simulated vs. experimental sound absorption coefficients;
(b) This work vs. homogeneous material model

In summary, the modeling strategy proposed in this study addresses the limitations of conventional methods that neglect the spatial heterogeneity of material properties. It provides a more accurate and physically realistic tool for the design and performance prediction of rubber-based acoustic structures under complex loading conditions, demonstrating strong potential for engineering application and further development.

Acknowledgement

This work was supported by an original explora-tion project funded by National Science Foundation of China (52250357).

References

1. Gu Y, Zhong H, Bao B, Wang Q, Wu J. *Applied Acoustics, J.*, 2021; 172: 107605.
2. Zou H, Su L, Zhang Y, Zhang M, Yu W, Wang X, Xia X, Chen H, Zhang X, Zhao A. *Int. J. Mech. Sci.*, J., 2024; 271: 109137.

International Rubber Conference 2025 (IRC2025)
1-3 December 2025 @ BITEC, Bangkok, Thailand

Influence of vacancy defect on stretching behavior of liquid crystal elastomer membrane

T. KATO [1], Y. OKUMURA[2], H. KIKUCHI[2], K. URAYAMA[1]

[1] *Department of Material Chemistry, Graduate School of Engineering, Kyoto University, Kyoto, Japan.*

[2] *Institute of Material Chemistry and Engineering, Kyushu University, Fukuoka, Japan.*

urayama.kenji.2s@kyoto-u.ac.jp

Keywords: Liquid Crystal, Elastomer, Soft elasticity, Fracture, Digital Image Correlation.

Liquid crystal elastomers (LCEs) (**Figure 1)**, which combines the properties of liquid crystal and rubber, exhibit a unique mechanical property known as "soft elasticity". This arises from the coupling between liquid crystal alignment and rubber elasticity. For a notable example, polydomain LCEs (P-LCEs) with randomly oriented local directors undergo large deformations under nearly constant and extremely low tensile force, until a monodomain state aligned along the stretching direction is attained. The liquid-like mechanical response in P-LCEs is further evidenced by the equalization of true stresses in orthogonal directions under unequal biaxial stretching [1]. The effect of soft elasticity in LCEs under inhomogeneous deformation is intriguing, but it remains largely unexplored while our recent work on the stretching behavior of a P-LCE membrane with initial notch has found an unusual development of strain distribution [2]. This study focuses on inhomogeneous deformation behavior accompanied by the polydomain-to-monodomain transition (PMT) in a P-LCE membrane with a circular flaw.

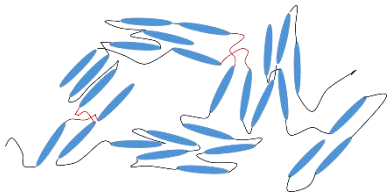


Figure 1 Schematic of LCEs

A main-chain type P-LCE membrane was prepared by mixing liquid crystal diacrylate RM-257, cross linker PETMP, chain extender EDDET, catalyst Dipropyl Amine and solvent Toluene to crosslink by Michael-addition at 25°C. Then, removal of Toluene lead to Polydomain Liquid Crystal Elastomer (P-LCE) as method in the literature [3]. A wide membrane (20 × 75 × 1 mm) with a central circular hole (diameter: 5.0 mm) shown as **Figure 2** was elongated along the x-axis at a constant rate of 3.3 × 10^{-2} % / s which satisfies the quasi-equilibrium condition. The deformation behavior around the hole was analyzed using digital image correlation (DIC) to track the evolution of the hole's shape and the strain distribution across the sample.

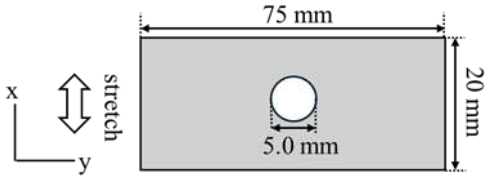


Figure 2 Geometry of the specimens

Figure 3 shows the x- and y-axis lengths λ_x and λ_y, and perimeter length λ_L of the central hole, all normalized by their initial values, as a function of applied true strain E_x. For comparison, the corresponding results for a conventional elastomer (nitrile butadiene rubber; NBR) are also shown. In NBR, all lengths λ_x, λ_y, and λ_L increase monotonically with E_x with $\lambda_x \gg \lambda_y$, indicating the elliptical deformation accompanying a perimeter increase due to strain concentration around the lateral sides of the hole. In contrast, the hole in P-LCE exhibits a non-monotonic shape evolution, which can be divided into three distinct stages. In Region I ($E_x < 0.25$), λ_L increases while maintaining a nearly circular shape ($\lambda_x \approx \lambda_y$), indicating nearly uniform expansion. In Region II ($0.25 < E_x < 0.45$),

λ_x increases while λ_y decreases, with λ_L remaining nearly constant, indicating the elliptical deformation without perimeter growth. In Region III ($0.45 < E_x$), each parameter behaves similarly to NBR. We correlate these observations with the heterogeneous PM transition: the transition initiates locally around the hole in Region I and progresses outward in Region II.

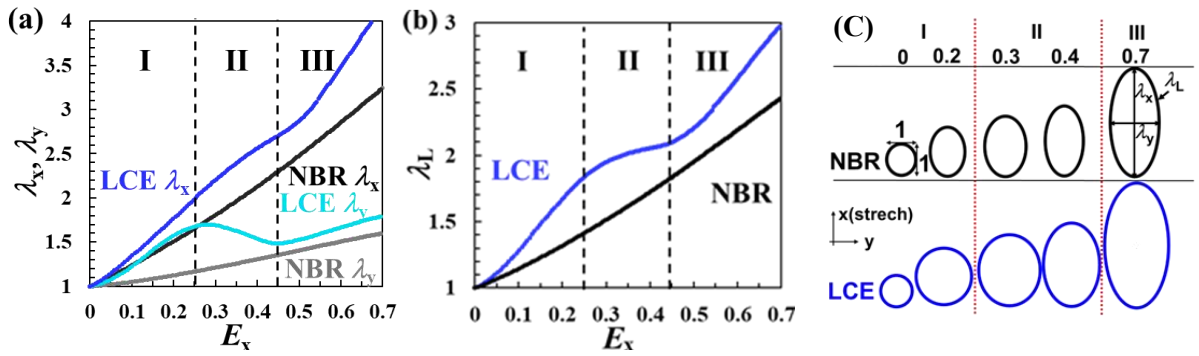


Figure 3 (a) λ_x or λ_y, **(b)** λ_L as a function of E_x for LCE and NBR and **(c)** change of the vacancy

Figure 4 shows 2D distribution of major principal strain ε_1 on LCE and NBR specimens at E_x = 0.25, 0.45 (boundaries between Region I /II and Region II/III) and 0.70. In Region I, due to the effect of soft elasticity, strain is concentrated not only at the side of the circular hole but also along its entire perimeter. As a result, deformation into an elliptical shape is suppressed. At the end of Region I, ε_1 around the entire hole reaches the threshold strain E_x* for PMT, indicating that the material has become monodomain. In Region II, ε_1 increases in areas apart from the hole, suggesting a delayed spatial progression with PMT. Consequently, in this region, the hole is elongated into an elliptical shape along the stretching direction while maintaining a constant perimeter. In Region III, where nearly the entire sample has become monodomain, the material behaves similarly to a conventional rubber.

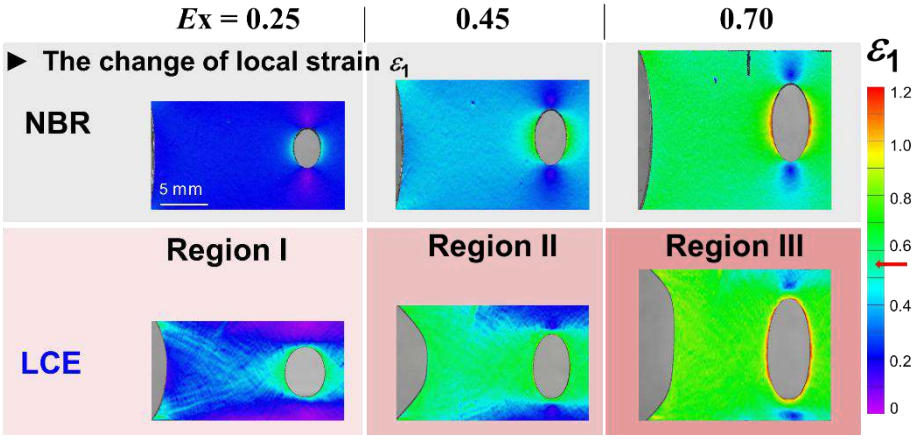


Figure 4 Distribution of major principal strain ε_1.

References

1. Tokumoto H., Hao Z., Takebe A., Kamitani K., Kojio K., Bhattacharya K., Urayama K., Sci. Adv. 7, 25(2021)
2. Imai S., Tokudome Y., Mai T.-T., Urayama K., *ACS Mater. Lett.* **7**, 2805(2025).
3. Yakacki C. M., Saed M., Nair D., Gong T., Reed S., Bowman C. N., *RSC Adv.* **5**, 18997-19001 (2015)

International Rubber Conference 2025 (IRC2025)
1-3 December 2025 @ BITEC, Bangkok, Thailand

Bio-Based Polyurethane/Tannic Acid Composites with Adjustable Damping Property Enabled by Constructing Multiple Sacrificial Networks

DEXIAN YIN[1,2], ZHI CHEN[1,2], XIN WANG[1,2], XIUYING ZHAO[1,2], LIQUN ZHANG[1]

[1] *State Key Laboratory of Organic-Inorganic Composites, Beijing University of Chemical Technology, Beijing, China.*

[2] *Beijing Engineering Research Center of Advanced Elastomers, Beijing University of Chemical Technology, Beijing, China.*

yindx96@163.com; zhaoxy@mail.buct.edu.cn

Keywords: Bio-based polyurethane, Tannic acid, Sacrificial networks, Damping property

Damping materials play a significant role in reducing vibrations and noise. Presently, polyurethane (PU) elastomers fabricated from renewable resources have attracted considerable attention in damping fields owing to their significant benefits towards sustainable development and green production [1-2].

Bio-based millable polyurethane (bio-PU) elastomer is successfully synthesized from bio-based poly (trimethylene ether) glycol (bio-PO3G), bio-based 1,5-pentamethylene diisocyanate (bio-PDI), and 3-allyloxy-1,2-propanediol (APD) (Figure 1). Tannic acid (TA) is then incorporated into the bio-PU elastomer to enhance the damping, mechanical, and thermal properties by constructing multiple sacrificial networks. The composites with PU/TA weight ratios of 100/0, 100/6, 100/12, 100/18, and 100/24 were denoted as the pure PU, PU/TA1, PU/TA2, PU/TA3, and PU/TA4, respectively. Depending on the energy dissipation of sacrificial networks, the fabricated bio-based PU/TA (bio-PU/TA) composites exhibit a mechanical strength of 16.0 MPa (4.9 times higher than that of the bio-PU elastomer), with a glass-transition temperature raised from -63.7 to -26.8 °C and $\tan\delta_{max}$ enhanced from 0.50 to 0.91. In addition, the abundant polyphenolic structures of TA endowed bio-PU/TA composites with excellent ultraviolet absorption capability and high transparency.

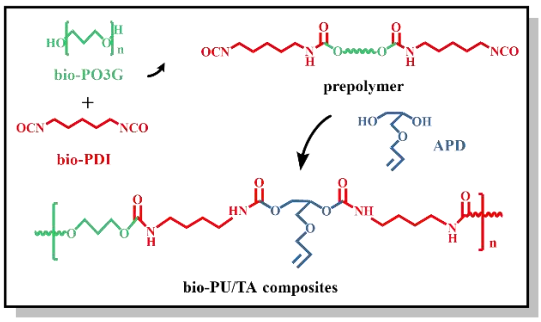


Figure 1. Fabrication routes of bio-PU/TA composites

Figure 2 shows that the storage modulus curves of bio-PU/TA composites increase and exhibit a single transition with increasing TA content. Furthermore, it illustrates that as TA content increased, the $\tan\delta_{max}$ value of bio-PU/TA composites significantly increases, accompanied by a shift in the loss peak towards higher temperatures. The molecular chain movement of bio-PU/TA composites is constrained by strong sacrificial bonds, resulting in an augmented frictional force within the molecular chains. Consequently, more energy is required for the disruption and formation of dynamic bond network, leading to a notable shift of T_g towards higher temperatures and a substantial increase

in $tan\delta_{max}$. Notably, the frequency range of vibrations and noise varies across different engineering fields. For example, the vibration frequency ranges for noise and vehicles are 10^0–10^4 Hz and 10^{-1}–10^6 Hz, respectively. Figure 2 illustrates the variations in storage modulus and tanδ of bio-PU/TA composites at different frequencies. Owing to the strong sacrificial-bond interactions, the introduction of TA not only improves the storage modulus of bio-PU/TA composites but also increases the $tan\delta_{max}$ value and shifts it toward lower frequencies, contributing to the enhancement of the damping performance of bio-PU/TA composites at low frequencies.

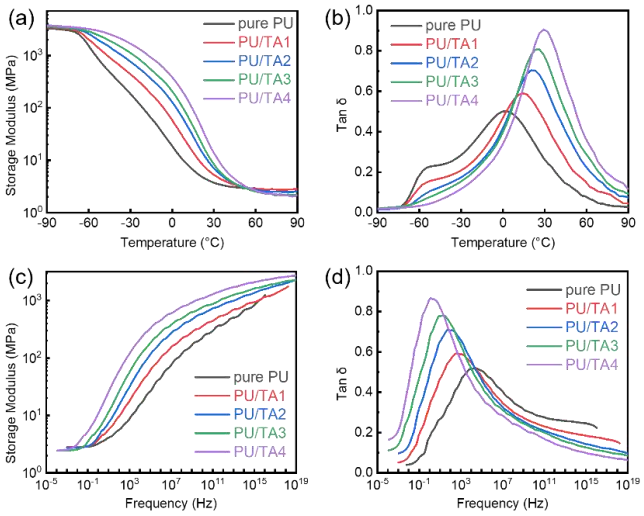


Figure 2. (a) Storage modulus-Temperature curves of bio-PU/TA composites. (b) Tanδ-Temperature curves of bio-PU/TA composites. (c) Storage modulus-*f* curves of bio-PU/TA composites. (d) Tanδ-*f* of bio-PU/TA composites.

In this work, a novel bio-PU elastomer is successfully synthesized from bio-PO3G and bio-PDI, and bio-PU/TA composites are fabricated by incorporating TA to construct multiple sacrificial networks. The chemical structures, thermal properties, mechanical properties and damping properties of the composites are systematically characterized. The results shows that the multiple sacrificial networks provide a large energy dissipation, which improved the T_g value of bio-PU/TA composites from -63.7 to -26.8 °C, $tan\delta_{max}$ from 0.50 to 0.91, and $\Delta S_{tan\delta}$ from 39.4 to 55.2. Bio-PU/TA composites exhibit a tensile strength of 16.0 MPa, which is 4.9 times higher than that of the pure PU. In addition, the abundant polyphenolic structures of TA endowed bio-PU/TA composites with an excellent UV absorption capacity and high transparency. To sum up, this work not only provides a promising strategy for developing bio-based elastomers for damping applications but advances the sustainable growth of PU industry.

Acknowledgement

This work was supported by the National Natural Science Foundation of China [grant numbers 52250357, 52203003].

References

1. Yin D, Wang Y, Shou T, Liu L, Hu S, Zhao X, Zhang L, *Ind. Crop. Prod.*, 2024; 220: 119240.
2. Yin D, Wang X, Wang Y, Zhao X, Zhang L, *ACS Appl. Polym. Mater.*, 2024; 6: 8409-8418.

Changes in Nano Structure upon Uniaxial Stretching of Polyurethane Liquid-Crystalline Elastomers as Analyzed by Small-Angle X-ray Scattering

Yume SUGINO[1], Tomoka NODA[2], Tatsuya ENDO[2], Hideaki TAKAGI[3], Shinichi SAKURAI[1]

[1] *Department of Biobased Materials Science, Kyoto Institute of Technology,*
1 Matsugasaki Hashigami-cho, Sakyo-ku, Kyoto, 606-8585, JAPAN

[2] *Toyo Tire Corporation, 3-10-1 Yato, Kawanishi City, Hyogo, 666-0131, JAPAN*

[3]*Photon Factory, Institute of Materials Structure Science, High Energy Accelerator Research Organization (KEK),*
1-1 Oho, Tsukuba, Ibaraki, 305-0801, JAPAN

E-mail: shin@kit.ac.jp

Keywords: Liquid-Crystalline Elastomers, Thermoplastic Polyurethane, Nano Structure, Small-Angle X-ray Scattering, Uniaxial Stretching

Liquid-crystalline elastomers (LCEs) are materials bearing both liquid-crystalline and elastomeric properties. The length of LCEs changes reversibly along with the change in the mesogenic orientation around the liquid crystal/isotropic transition temperature. Recently, Hasegawa and co-workers reported that by precisely controlling the molecular alignment of mesogenic groups in sheet specimens of LCEs developed by their group, the LCEs can undergo reversible elongation and contraction up to 47,000 cycles near the liquid crystal/isotropic phase transition temperature.[1] This study was aimed at clarifying the nano structural changes upon uniaxial stretching of LCEs by small-angle X-ray scattering (SAXS).

Thermoplastic polyurethane containing the biphenyl mesogenic group (Fig. 1), which is the precursor of the above-mentioned LCEs specimen, was used for measurement: (1) a just-pressed TPU specimen, (2) a UV irradiated specimen from (1), (3) a UV irradiated specimen which was uniaxially stretched from (1) in prior to the UV irradiation (aforementioned LCEs), (4) a specimen obtained by thermally annealing the specimen (3). The above four types of specimens were subjected to two-dimensional small-angle X-ray scattering (2d-SAXS) measurements, which were conducted at BL-6A of Photon Factory (KEK). The wavelength was 0.15 nm and the camera length was 1.0 m. All measurements were conducted in the through view mode, whereby the incident X-ray beam was introduced to the specimen from the direction parallel to the normal of the specimen.

Specimens (1) and (2) initially exhibited random orientation, as indicated by the isotropic ring-shaped peaks observed in Fig. 2(a). Upon uniaxial stretching, the 2d-SAXS pattern transformed into an X-shaped feature (Fig. 2(b)). The first- to third-order peaks observed in these patterns arise from the periodic structure of smectic layers formed by the aggregation of mesogenic groups.[2] The change in pattern upon uniaxial stretching is attributed to the alignment of both the mesogenic units and the urethane segments along the stretching direction, resulting in a tilted orientation of the smectic layers. However, the SAXS profiles shown in Fig. 3 plotted as the logarithm of scattering intensity $I(q)$ versus q, where q is the magnitude of the scattering vector defined as $q = (4\pi / \lambda_X)\sin(\theta/2)$, with θ being the scattering angle and λ_X the X-ray wavelength, demonstrated that the peak positions (q) remained almost unchanged regardless of the stretching ratio λ. This indicates that the periodicity of the smectic layers remained constant even when the specimen was stretched tenfold. This invariance in the smectic layer periodicity was not only observed in specimens (1) and (2), but also

in specimens (3) and (4). We interpret this characteristic behavior as follows by considering a nano structure model as shown in Fig 4: This model comprises ellipsoidal-shaped grains of a periodically alternating structure of the layer formed by aggregated mesogenic groups and the layer formed by aggregated urethane segments. Additionally, surrounding each grain are relatively long polymer chains where mesogenic and urethane units alternate continuously, which exhibit a random coil state in the unstretched specimen. The smectic layer periodic structure forms individual grains that are randomly oriented, each surrounded by an amorphous phase. Thus, these numerous grains are interconnected by relatively long amorphous chains in a random coil state. The polymer chains are subjected to be oriented parallel to the stretching direction so that the grains become obliquely oriented. This structural model allows the specimen to sustain macroscopic deformation without fracture on stretching. Since most grains only reorient without undergoing significant deformation (although some traces of grain damage are evidenced in the 2d-SAXS patterns), the smectic layer periodicity remains unchanged during stretching.

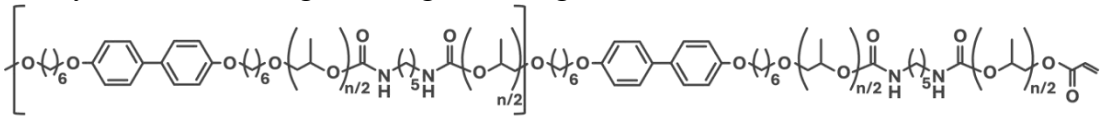


Figure 1. Chemical structure of thermoplastic polyurethane containing the biphenyl mesogenic group.

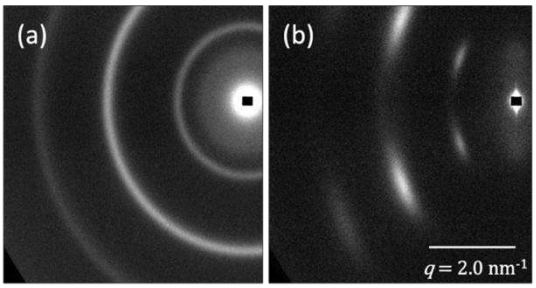


Figure 2. Two-dimensional SAXS patterns of the pressed specimen (a) before stretching and (b) at 10.0-fold uniaxially stretched state.

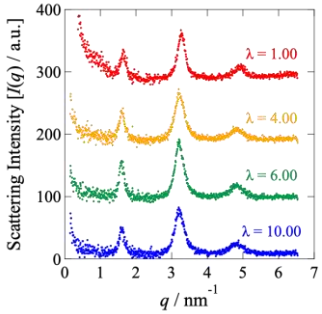


Figure 3. Changes in the one-dimensional SAXS profiles with stretching ratio (λ) for the pressed specimen.

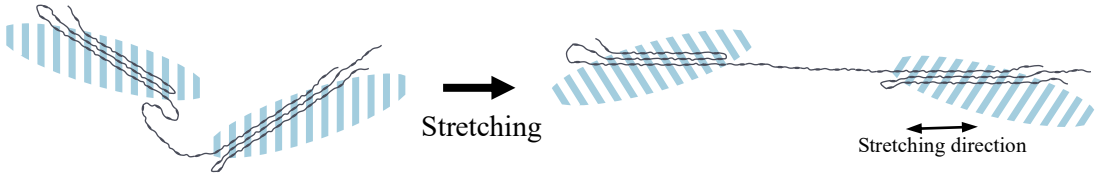


Figure 4. Model of the grains that contain the alternating stacks of the liquid crystalline layers.

Acknowledgement

SAXS measurements were carried out at KEK Photon Factory (BL-6A) under the experimental program (2024G524), and I am grateful to the KEK staff for their technical support.

References

1. Y. Hasegawa, S. Sakurai, Proceedings of the Polymer Materials Forum, 2017, p. 80.
2. Christian Haege, Dr. Stefan Jagiella, Prof. Dr. Frank Giesselmann 2019. "Molecular Electron Density Distribution and X-Ray Diffraction Patterns of Smectic A Liquid Crystals – A Simulation Study." ChemPhysChem 20 (19), 2017, 2466–2472.

International Rubber Conference 2025 (IRC2025)
1-3 December 2025 @ BITEC, Bangkok, Thailand

Novel Properties of Rubber Formulated with 1,2-Polybutadiene Derivatives

H. Ohura, H. Hashimoto, Y. Shibata,

NIPPON SODA CO., LTD., Development dept., Chemical Business div., 2-7-2 Marunouchi, Chiyoda-ku, Tokyo, Japan

e-mail address of the presenting author (h.ohura@nissogr.com)

Keywords: 1,2-Polybutadiene, Crosslinking, EPDM, GECO, Acid acceptor

Introduction or Abstract

1,2-Polybutadiene (1,2-PB, Figure 1) exhibits thermosetting properties due to 1,2-vinyl crosslinking reactions, clearly distinguishing it from conventional liquid polybutadienes containing 1,4-olefin units[1]. Despite its widespread use as an additive, the relationship between 1,2-vinyl content and the resulting material properties has not been systematically investigated. This study clarifies the correlation between 1,2-vinyl content and key characteristics: mechanical properties, oil resistance, and electrical performance in EPDM formulations. Our findings demonstrate that these properties are directly influenced by the 1,2-vinyl content, providing valuable insights for optimizing rubber formulations.

1,2-Epoxidized PB (Figure 2) derived from 1,2-PB possesses both 1,2-vinyl units and 1,2-epoxy units. It exhibits both crosslinking capability and acid acceptance effects, making it a promising additive for halogenated rubber formulations. Our research demonstrated that 1,2-epoxidized PB serves as an effective and environmentally friendly alternative to lead monoxide (PbO) in halogenated rubber formulations, particularly for epichlorohydrin rubber (GECO) applications. This innovative solution provides excellent rubber performance while enabling sustainable formulations that comply with environmental standards, replacing toxic materials such as PbO.

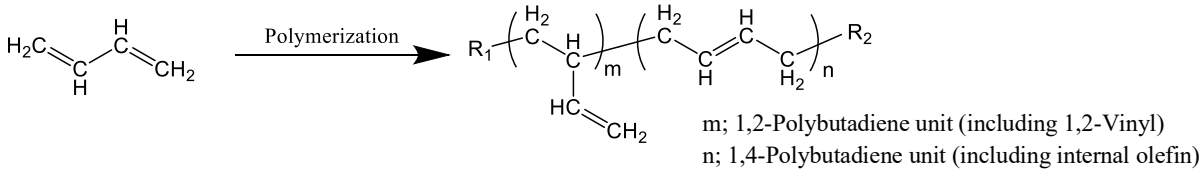


Figure 1. Structure of Polybutadiene [Poly(1-butene-*co*-2-butene)]

EPDM (Ethylene Propylene Diene Terpolymer) formulation

Table 1 presents an example EPDM rubber formulation incorporating 1,2-PB. The results show a distinct correlation between 1,2-vinyl unit content and crosslinking degree. As the 1,2-vinyl content increases, both mechanical strength and oil resistance exhibit significant improvement (Table 2). This enhancement is attributed to the increased crosslinking density within the polymer matrix. Therefore, polybutadiene with high 1,2-vinyl content is essential for the optimal EPDM formulations.

Table 1. Example of EPDM formulated with 1,2-PB

Material name	phr
EPDM [1)]	100
1,2-PB	0, 10
Zinc oxide	5
Stearic acid	1
Calcined clay	120
Carbon black	5
Paraffinic oil	6
Paraffin wax	5
Dicumyl peroxide	7
Dibenzoylquinone dioxime	1.5

1) Ethylene content: 42%, ENB content: 0.7%, ML1+4 (125℃): 27

Table 2. Properties of EPDM with Polybutadiene

Polybutadiene [2)]	phr	Mechanical properties		Oil resistance [3)]		Compression set [4)]
		Shore hardness	Tensile strength at break [MPa]	Standard oil IRM901		23ºC [%]
				Δm [%]	ΔV [%]	
Not added	0	A69	6.69	46	72	17
m/n = 22/78: M_n=2,500	10	A67	7.08	46	70	17
m/n = 92/8: M_n=3,200	10	A71	7.42	38	58	12

2) m: 1,2-vinyl, n: 1,4-vinyl, 3) Temperature: 70°C±2°C, 72hours, 4) Compression ratio: 25%, 72hours

GECO (Epichlorohydrin Rubber) formulation

1,2-Epoxidized PB (Figure 2) contains epoxy and 1,2-vinyl functional groups that enable crosslinking and ring-opening reactions. Its reactivity differs from 1,4-Epoxidized PB due to different epoxy stereochemistry. Table 4 presents properties of GECO formulations shown in Table 3. Incorporating 1,2-Epoxidized PB into GECO rubber improves mechanical properties including hardness and tensile strength through crosslinking reactions. Additionally, it provides equivalent or superior acid resistance compared to conventional acid acceptors.

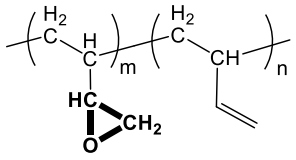


Figure 2. Chemical structure of 1,2-Epoxidized PB

Table 3. Example of GECO formulated with 1,2-Epoxidized PB

	Entry			
	1	**2**	**3**	**4**
GECO [5)]	100	100	100	100
1,2-Epoxidized PB [6)]	0	3	0	0
MgO	0	0	3	0
PbO	0	0	0	5
Sorbitan stearate	2	2	2	2
Carbon black	40	40	40	40
α,α'-Di(t-butylperoxy) diisopropylbenzene	1.3	1.3	1.3	1.3

Table 4. Properties of GECO with 1,2-Epoxidized PB / Exisrting acid acceptors

Entry	Mechanical properties		Water/Acid resistance	
	Shore hardness	Tensile strength at break [MPa]	Pure water	20% HCl
			ΔV [%]	ΔV [%]
1	A65	8.98	+9	+10
2	A76	7.81	+5	+8
3	A78	10.50	+20	+33
4	A81	9.96	+4	+7

5) EPICHLOMER CG (OSAKA SODA CO., LTD.), 6) NISSO PB JP-100 (NIPPON SODA CO., LTD.)

Conclusion

In the EPDM formulation, 1,2-PB increases crosslink density, which significantly improves mechanical strength and oil resistance. In the GECO formulation, 1,2-Epoxidized PB improves the mechanical properties and provides excellent acid resistance. These findings are expected to be useful for eco-friendly and high performance rubber formulations.

Acknowledgement

The authors gratefully acknowledge OSAKA SODA CO., LTD. for their generous provision of GECO "EPICHLOMER CG", which made this evaluation study possible.

References

1. H. HASHIMOTO, H. SAKAI, I. TANDO, *Journal of the Society of Rubber Science and Technology*, 2020; 93: 273.

International Rubber Conference 2025 (IRC2025)
1-3 December 2025 @ BITEC, Bangkok, Thailand

Mechanically Robust and Moisture-Resistant Poly(thioether-thiourea) Elastomers with Glassy-State Self-Healing Capability

Haitao WU, Zhaoyang YUAN, Jing ZHENG, Hao WANG, Mengjin JIANG, Jinrong WU

National Key Laboratory of Advanced Polymer Materials, College of Polymer Science and Engineering, Sichuan University, Chengdu, China.

e-mail address of the presenting author (wht2281007108@163.com)

Keywords: Glassy-state healing, Thiourea-based hydrogen bonds, Moisture resistance, Mechanical robustness

Elastomers play an essential and irreplaceable role in military, aerospace, healthcare, and other cutting-edge fields. Nevertheless, when the service temperatures are below the glass transition temperature (T_g), elastomers transition from rubbery to glassy states, becoming rigid and brittle. This limitation can lead to catastrophic failures. For instance, during the launch of the US space shuttle Challenger, the O-ring elastomer seal on its fuel tank failed due to glass transition at low temperatures, causing fuel leakage and ultimate explosion. Such incidents underscore the urgent need for elastomers that can repair themselves autonomously in the glassy state.[1] Nonetheless, existing elastomers can only self-heal in the rubbery state and are unable to self-heal in the glassy state due to the immobilization of chain segments below T_g, which strongly restricts the reconfiguration of dynamic bonds.[2-3] Therefore, developing glassy-state self-healing elastomers is a significant yet extremely challenging open question.

In this work, we develop a new class of glassy-state self-healing poly(thioether-thiourea) elastomers (PTUEs), featuring a large number of asymmetric, loosely packed thiourea-based hydrogen bonds (Figure 1a). Despite the immobilization of chain segments below T_g, these hydrogen bonds retain high mobility, enabling the rearrangement of hydrogen bond networks and imparting exceptional self-healing capabilities in the glassy state (Figures 1b-c). Remarkably, the damaged material manifests a self-healing efficiency of 97.2% after 36 h at -10 ℃ without external intervention, even though its T_g is 7 ℃. Under mild compression, 100% healing efficiency is achieved within 90 min at -35 ℃. Moreover, by adjusting the number of methylene units between thioether groups, the cohesive energy density of network can be tailored, thereby regulating the physical and mechanical properties of PTUEs. Additionally, PTUEs exhibit outstanding moisture resistance due to the hydrophobicity of thiourea and thioether units, retaining over 95% of both mechanical strength and Young's modulus at 80% relative humidity for 120 h at 25 ℃. This highlights PTUEs potential for advanced insulating and sealing applications in low-temperature, high-humidity environments.

This work represents a significant breakthrough in the field of elastomers by achieving glassy-state self-healing, a challenge that has long been considered insurmountable. Importantly, the novel yet straightforward network design offers a viable pathway to mitigate service failures in low-temperature, high-humidity environments through the development of self-healing and recyclable elastomers.

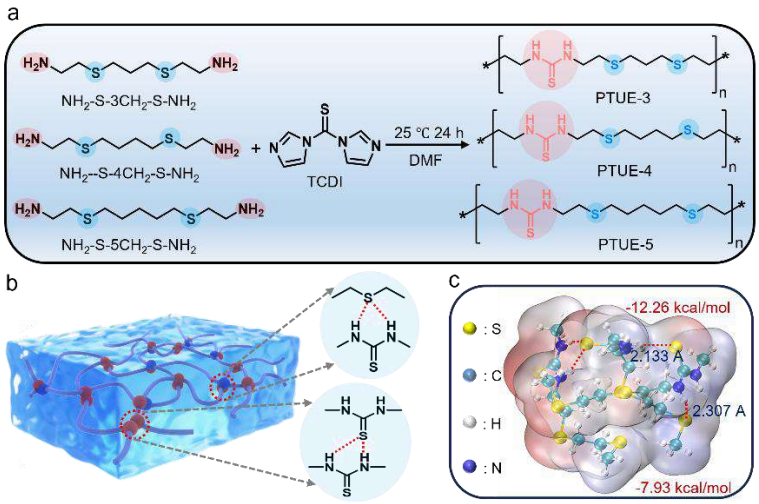


Figure 1. Preparation route and network structure of poly(thioether-thiourea) elastomers (PTUEs).

Acknowledgement

We acknowledge the supports from National Natural Science Foundation of China (Grant Nos. 52525301, 52373061 and 52403076).

References

1. Yanagisawa Y, Nan Y, Okuro K, Aida T. *Science*., 2018; 359: 72.
2. Wang H, Liu H, Cao Z, Li W, Huang X, Zhu Y, Ling F, Xu, H, Wu Q, Peng Y, Yang B, Zhang R, Kessler O, Huang G, Wu J. *Proc. Natl. Acad. Sci. U. S. A.,* 2020; 117: 11299.
3. Xu J, Chen J, Zhang Y, Liu T, Fu J. *Angew. Chem., Int. Ed.*, 2021; 60: 7947.

International Rubber Conference 2025 (IRC2025)
1-3 December 2025 @ BITEC, Bangkok, Thailand

Self-Healing and Impact-Resistant Elastomer Based on a Novel Tetraoxadiborolane Dynamic Bonds

Shiyu GU, Nan LI, Qi WU, Jinrong WU

College of Polymer Science and Engineering, National Key Laboratory of Advanced Polymer Materials, Sichuan University, Chengdu 610065, China

e-mail address of the presenting author (2022323090025@stu.scu.edu.cn)

Keywords: Polymers, Elastomers, Self-healing, Impact resistance, Boron chemistry

Elastomers are widely used for impact resistance due to their distinctive dynamic viscoelastic properties [1]. However, conventional elastomers typically exhibit low loss factors (tanδ < 0.1), limiting their energy dissipation efficacy in practical applications [2]. Incorporating dynamic crosslinking networks into elastomers has emerged as a promising strategy for enhancing impact resistance [3]. This approach enables anti-impact elastomers with self-healing abilities, advancing sustainable multifunctional elastomers via extended service life and recyclability [4]. Recently, B-O bonds have been used to create self-healing elastomers [5]. However, most of these elastomers require external stimuli for efficient healing, which limits their applicability. Compared to the traditional bis-dioxaborolane bond, tetraoxadiborolane bonds (with a B-B framework) exhibit pronounced electron deficiency, weakening adjacent B-O bonds through reduced conjugation stabilization [6].

Herein, we introduced a new chemistry that combines dynamic tetraoxadiborolane bonds (TODB) to achieve ambient-temperature self-healing with excellent impact resistance in elastomers (Figure 1). Time-dependent ^{1}H-NMR and MS spectra demonstrate the rapid ambient exchange of TODB, and the binding energy of TODB is much lower than the traditional dioxaborolane bond (BDOB) due to higher electron deficiency in the B-B framework (Figure 2). Specifically, we demonstrated our concept using a simple model elastomer that was embedded with TODB and BDOB, which are referred to as TODBE and BDOBE, respectively (Figure 3a). Interestingly, TODBE exhibited a reduced activation energy (~2/3 of BDOBE) and an enhanced self-healing efficiency (~2.5 times of BDOBE) (Figure 3b). Besides, TODBE enables exceptional energy dissipation and high loss factor (tanδ = G''/G') via reversible B-O breakage and network rearrangement under impact, demonstrating ~1.7 times greater impact force attenuation than covalently crosslinked elastomers (CCE) as shown in Figure 3c. Furthermore, TODBE shows better thermostability, which is due to its boron-based molecular structure (Figure 3d). With such advantages as rapid room-temperature self-healing properties and outstanding impact resistance, the as-prepared elastomers might be the ideal materials for flexible devices and wearable sensors.

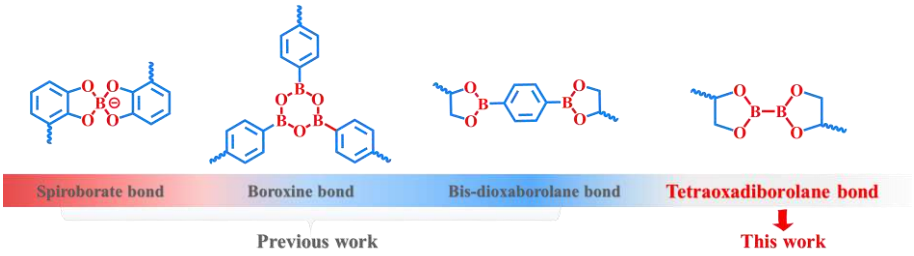


Figure 1. Structural evolution of boronic ester linkages

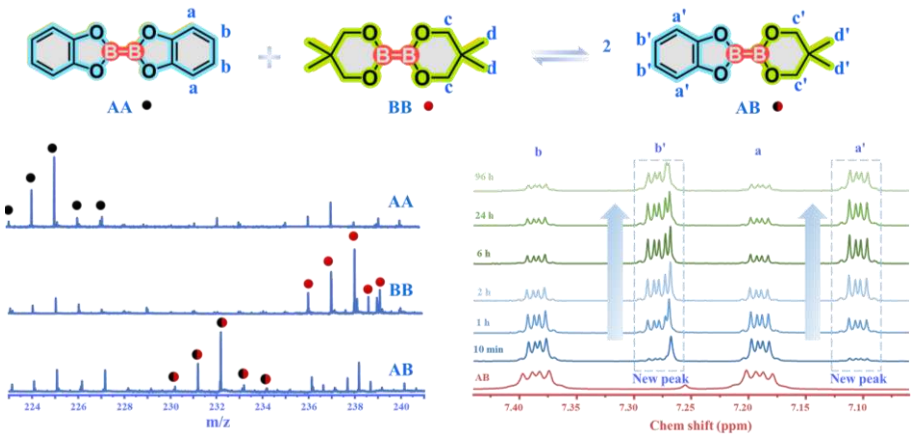


Figure 2. Dynamics validation of the TODB via a small molecule model

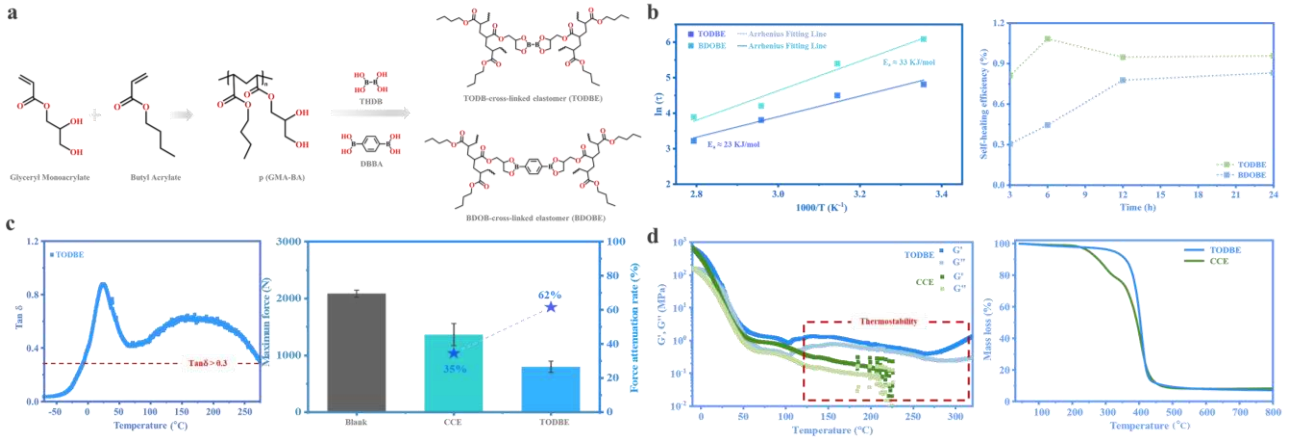


Figure 3. Synthesis and functional performance of the TODBE. (a) Synthesis procedure of TODBE. (b) Activation energy and self-healing efficiency of TODBE relative to BDOBE. (c) Loss factor and anti-impact properties of TODBE. (d) Thermostability of TODBE compared with the covalently cross-linked sample.

Acknowledgement

This work was supported by the National Natural Science Foundation of China (Grant Nos 52203064 and 52373061); China Postdoctoral Science Foundation (2023M732415).

References

1. J. Huang, Y. Xu, S. Qi, J. Zhou, W. Shi, T. Zhao, M. Liu, *Nat. Commun*., 2021; 12: 3610.
2. G. Chen, J. Wu, Z. Wang, H. Zhu, S. Zhu, Q. Zhang, *Sci. Adv*., 2025; 11: eadv5292.
3. Y. Kim, S. Cho, W. Choi, H. Cho, K. Jeong, J.-H. Kim, S. Jo, D. Y. Ryu, S. Lee, Y. Jin, J. Hong, *Adv. Funct. Mater*., 2025; n/a: 2509804.
4. N. Li, S. Gu, Q. Wu, J. Wu, *RSC Appl. Polym*., 2025; 3: 299-316
5. Y. Peng, S. Gu, Q. Wu, Z. Xie, J. Wu, *Acc. Mater. Res*., 2023; 4: 323-333.
6. X. Lou, J. Lin, C. Y. Kwok, H. Lyu, *Angew. Chem. Int. Ed*., 2023; 62: e202312633.

International Rubber Conference 2025 (IRC2025)
1-3 December 2025 @ BITEC, Bangkok, Thailand

UV-A Functionalization of Low Molecular-Weight Natural Rubber Latex Using TiO_2-Coated Hollow-Glass Beads as Photocatalyst

Kanokporn WONGNUKOON[1], Jitladda SAKDAPİPANİCH[1,2*]

[1]*Rubber Research Group, Department of Chemistry, Faculty of Science, Mahidol University, Nakhon Pathom 73170, Thailand.*

[2]*The Rubber and Rubber Glove Academician Association, Bangkok 10900, Thailand*

Presenting author: kanokporn.wou@student.mahidol.edu

*Corresponding author: jitladda.sak@mahidol.ac.th

Keywords: Natural rubber, Functionalized Low Molecular-Weight Natural Rubber, Titanium Oxide (TiO_2), hollow-glass bead (HGB), Photochemical reaction

Natural rubber (NR), a long-chain hydrocarbon polymer composed primarily of *cis*-1,4-polyisoprene and non-rubber constituents, has attracted significant interest due to its high molecular weight (MW) and viscosity. However, the absence of reactive terminal groupsrenders it chemically inert and difficult to modify through conventional functionalization techniques. To enhance the functional properties of NR, low molecular-weight natural rubber bearing reactive groups (FLNR) can be synthesized by introducing functional moieties along the polymer chain. Among various techniques, photochemical degradation process presents an energy-efficient and environmentally benign method for preparing FLNR.

In this study, FLNR was synthesized through photochemical degradation of latex under ultraviolet-A (UVA) irradiation in the presence of hydrogen peroxide (H_2O_2), using TiO_2-coated hollow glass beads (TiO_2- HBG) as photocatalysts [1]. The successful coating of TiO_2 onto HGB was confirmed by the photosensitivity of TiO_2- HBG, evaluated by monitoring the photodegradation of methylene blue (MB) *via* UV/Vis spectrophotometry. The TiO_2-HBG effectively catalyzed the degradation of MB in the presence of H_2O_2 under UVA-irradiation [2]. functional groups were introduced into the NR backbone through UV-A irradiation in the presence of TiO_2-HGB and hydrogen peroxide.

Optimal conditions for FLNR synthesis involved deproteinized natural rubber (DPNR) latex at 10% dry rubber content (DRC) , treated with 30 wt%H_2O_2 and 20 TiO_2 - HBG particles under 1 kW of UVA irradiation for 30 minutes. The resulting FLNR were characterized using Fourier-transform infrared spectroscopy (FTIR), which exhibited characteristic absorption bands at 3450, 1760 and 873 cm^{-1}, corresponding to hydroxyl, carbonyl and epoxide group respectively. Additional analyses included nuclear magnetic resonance (NMR) for microstructural elucidation and gel permeation chromatography (GPC) for molecular weight determination. The molecular weight of natural rubber significantly decreased after TiO_2- HGB- assisted UV-A treatment, as shown in Figure 1.

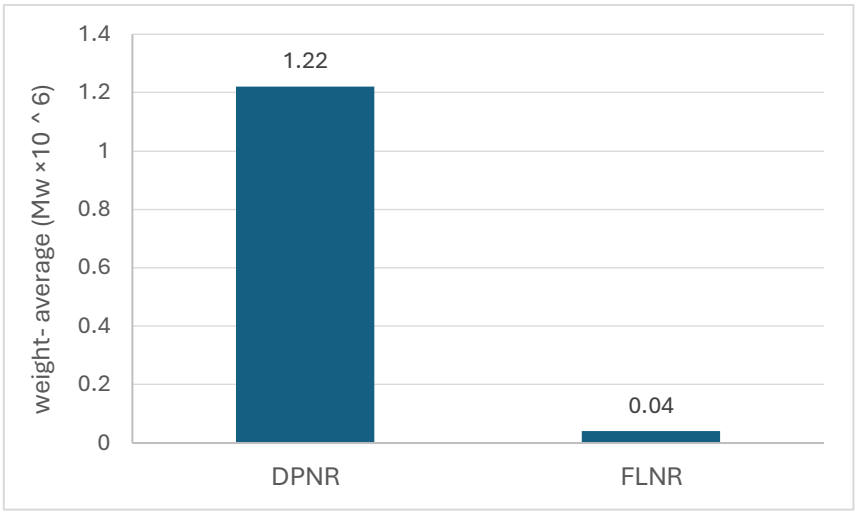


Figure 1. Molecular weight reduction of NR after TiO_2-HGB-assisted UV-A irradiation.

References

1. Kueseng P, Poompradub, S, Thitithanakul N, *Polym. Degrad. Stab.,* 2010; 95(11), 2059.
2. Daneshvar N, Salari D, Khataee A, *J. Photochem. Photobiol. A: Chem*., 2004; 162(2–3), 317.

Preparation and Characterization of Hydroxylated Natural Rubber via Epoxidation and Alkaline Ring-Opening

Thanita SUAKAMRAM[1], Jitladda SAKDAPIPANICH[1,2*]

[1]*Rubber Research Group, Department of Chemistry, Faculty of Science,*
Mahidol University, Nakhon Pathom 73170, Thailand.

[2] *The Rubber and Rubber Glove Academician Association, Bangkok 10900, Thailand*

Presenting author: thanita.sum@student.mahidol.edu

*Corresponding author: jitladda.sak@mahidol.ac.th

Keywords: Natural rubber latex, Epoxidation, Hydroxylation, Surface modification

Natural rubber (NR) is widely used due to its excellent mechanical performance. However, its non-polar nature limits compatibility with polar fillers and synthetic polymers. Epoxidation of NR represents an effective approach for chemical modification that introduces epoxide groups along NR molecular backbone, thereby enhancing polarity and altering key physical properties. Subsequent ring-opening of these epoxide groups generates hydroxyl-functionalized NR (HENR), which incorporates reactive hydroxyl sites suitable for crosslinking, grafting, and adhesion enhancement [1,2].

This work aimed to investigate the optimum conditions for preparing epoxidized NR (ENR) and HENR, with the additional goal of modifying NR through these chemical reactions. ENR latex was synthesized by reacting high-ammonia NR (HANR) latex with performic acid at 20 °C. Hydroxylation was then carrier out using mild alkaline treatment applied to both ENR latexes. Structural characterization was performed using FTIR and ^{1}H-NMR spectroscopy to confirm the conversion of epoxide to hydroxyl groups and further validated by glass transition temperature (T_g) measurements using differential scanning calorimetry (DSC). In addition, gel content and contact angle measurements were employed to validate and further analyze the experimental results.

The results showed that epoxide content increased with both performic acid concentration and reaction time, reaching a maximum of 12.4% for 25% acid after 1 hour. The T_g of ENR and HENR increased progressively, indicating reduced chain mobility due to enhanced polarity. Hydroxylation conducted at pH lower than <1 for 3 hours resulted in a gel content of 66%, which was significantly higher than that of unmodified NR (31%), suggesting the formation of a more entangled network structure. Mechanical testing revealed that ENR exhibited reduced tensile strength and modulus, attributed to diminished strain-induced crystallization. In Figure 1, the surface contact angle decreased from 75° (NR) to 59° (ENR), and further to 35° (HENR), demonstrating enhanced hydrophilicity from hydroxyl group incorporation. Consequently, hydroxylation of ENR via epoxide ring-opening represents an effective strategy for modifying both the structural and surface properties of NR.

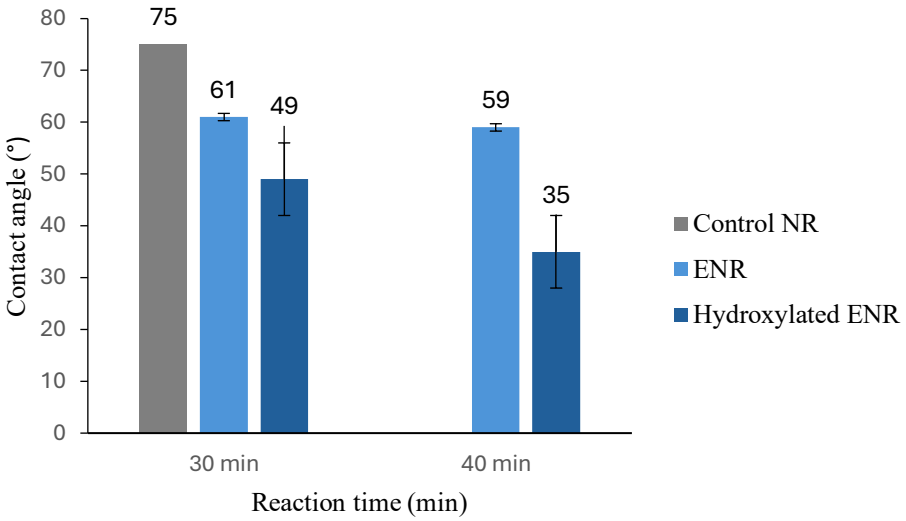


Figure 1. Contact angle measurements of ENR and Hydroxylated ENR obtained at reaction times of 30 and 40 minute.

References

1. Gan S, Hamid ZA, *J. Polym.* 1997, 38, 1953.
2. Baker C, Gelling I, Azemi S, *J. Nat. Rubb. Res.* 1986, 135.

Session IV : Progress in Rubber Characterisation

Poster Presentations

International Rubber Conference 2025 (IRC2025)
1-3 December 2025 @ BITEC, Bangkok, Thailand

Development of an Integrated Design, Analysis and Evaluation System for Rubber Components

Changsu Woo[1], Sangee Choi[2], Sangkyun Kim[3]

[1] *Korea Institute of Machinery & Materials, 156 Gajeongbuk-Ro, Yuseong-Gu, Daejeon, Korea.*

[2] *TSR Co., Ltd, 157 Gongdan-Dong, Gumi, Gyeongsangbuk-Do, Korea.*

[3] *DRB Co., Ltd, 7 Geumsa-Dong, Geumjeong-Gu, Busan, Korea.*

cswoo@kimm.re.kr

Keywords: Rubber components, Material properties, Finite element analysis, Fatigue test, Database

For products aiming to be first class, the application of rubber components for most machines including vehicles have gradually increased to achieve high quality and reliability through low vibration and noise, and enhanced operation. Therefore, requires an analysis and design technology for rubber components is required[1].

As much attention has been paid to the assurance of the quality and durability of vehicles, the development of technology is required to enhance the durability and reliability of anti-vibration rubber components that are the most important components of vehicles[2]. Until now, however, rubber components have been developed by trial and error as well as experiences due to the special properties of rubber. All respects of performance tests including the design and analysis technology, therefore, are now very vulnerable. In particular, the mechanical data of rubber material can be obtained only by experiment as there are many rubber compounds. Therefore, it is very difficult to develop a database of mechanical properties of rubber component and there are many obstacles to overcome in the fatigue lifetime estimation and evaluation technology due to insufficient manpower and technology[3].

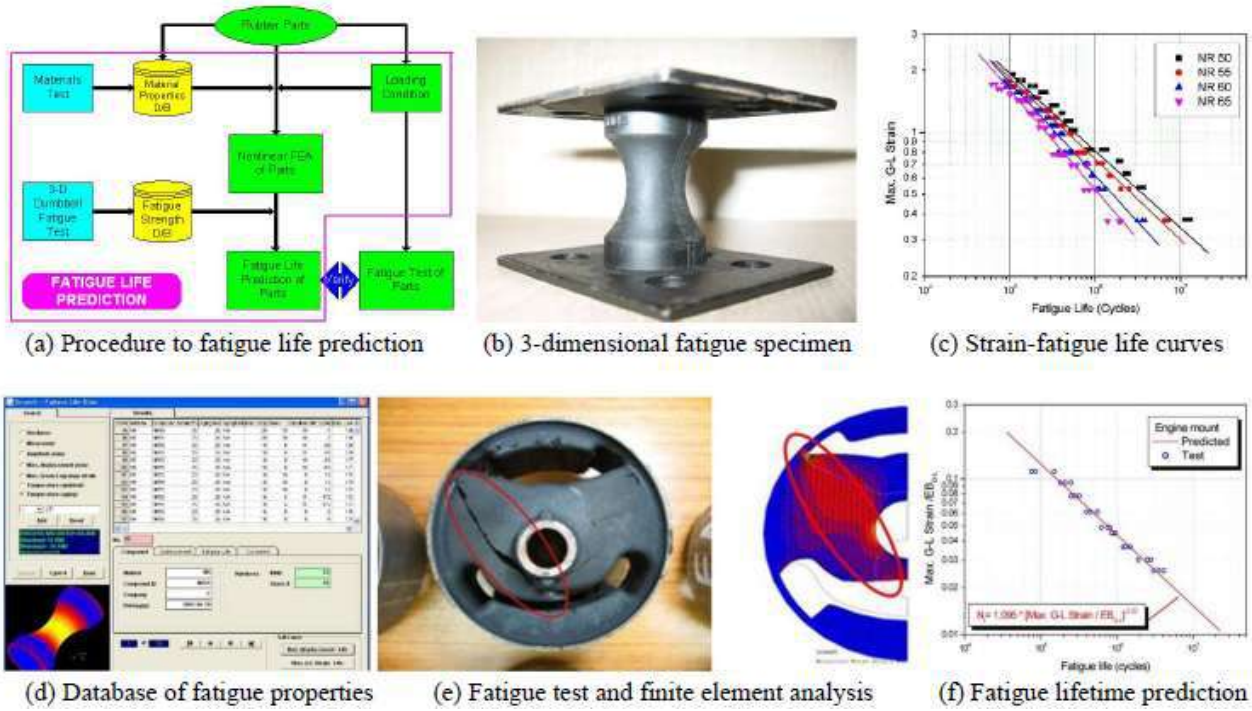
The objectives of this study are to establish test methods of rubber material and to develop a database of rubber material properties and to evaluate the performance of rubber components and to construct the prediction system of fatigue lifetime[4]. The fatigue lifetime prediction methodology of the rubber component was proposed by incorporating finite element analysis and fatigue damage parameters from the fatigue test[5,6]. Database of mechanical properties of anti-vibration rubber material, such as compound conditions, mechanical properties, degradation, and fatigue lifetime were developed.

Fatigue lifetime of engine rubber mount for automobiles was nearly exactly predicted by the developed method and the validity of the fatigue lifetime estimation method was verified. Using the developed integrated design system of rubber components, the time and expense required to develop rubber components were saved and the reliability of products is expected to be enhanced.



(a) Integrated of design system (b) Rubber compound program (c) Database of rubber properties

Figure 1. Integrated Design, Analysis and evaluation system for rubber components



(a) Procedure to fatigue life prediction (b) 3-dimensional fatigue specimen (c) Strain-fatigue life curves

(d) Database of fatigue properties (e) Fatigue test and finite element analysis (f) Fatigue lifetime prediction

Figure 2. Fatigue lifetime prediction of rubber components

Acknowledgement

This work was supported by the materials and components technology development program (20022506) and Elastic material re-launch project in response to key strategic industries (RS-2024-00439120) funded by the Ministry of Trade, Industry and Energy of Korea.

References

1. Charlton. D. J., Yang. J., *Rubber Chemistry & Technology*, *1993*, 67, 481-503.
2. Lake. G.J., *Rubber Chemistry & Technology*, 1997, 68, 435-460.
3. Gent. A. N., Oxford University Press, NY, 1992.
4. Mullin. L., *Rubber Chemistry & Technology*, 1969, 42, 339-362.
5. Takeuchi. K. & Nagakawa. M., *Int'l Polymer Sci*. 1993, 20, 64-69.
6. Fatemi. & Yang., Damage and Life Prediction Theories, *International J. of fatigue*, 1998, 20, 9-34.

International Rubber Conference 2025 (IRC2025)
1-3 December 2025 @ BITEC, Bangkok, Thailand

Spatiotemporal Internal-Damage Distribution During Nonuniform Deformations in Filled Elastomers

Yuki TOKUDOME, Mai THANH-TAM, Kenji URAYAMA

Department of Material Chemistry, Graduate School of Engineering, Kyoto University, Kyoto, Japan

(urayama.kenji.2s@kyoto-u.ac.jp)

Keywords: Stress-softening, Filled elastomers, Digital image correlation, Biaxial deformation

Introducing nano-fillers into soft materials significantly enhances their mechanical properties. These nanocomposite soft materials, such as filled elastomers, often exhibit a stress-softening effect—marked by a notable reduction in stress upon reloading after initial loading. This phenomenon is observed in a broad range of material, not only in nanocomposite soft materials but also in metal alloys.[1] Stress-softening indicates internal damage caused during initial loading, and it has been extensively studied under cyclic uniaxial loading/unloading conditions. Since uniaxial deformation represents only a specific deformation type, the results offer a limited understanding of the phenomena. We investigated stress-softening in several types of filled elastomer under various biaxial stretching conditions, and elucidated a governing strain parameter to describe internal damage in various deformations.[2] In this study, we extended this approach to heterogeneous deformations composed of a range of local deformation modes. The findings in this study are particularly significant because nanocomposite soft materials often experience complicated deformations during practical applications.

Styrene-butadiene rubber filled with carbon black (0.21 vol%) was used as a sample. Load/unload cyclic tests were conducted for the sheet samples using seven different elongation modes (uniaxial elongation, planar elongation, un-equi biaxial elongation with four different strain ratios, and equi-biaxial elongation) with successive increases in maximum strain to quantify the stress-softening effect (**Fig.1**). A wide-width specimen with an initial crack along the width direction was elongated stepwise, and a change in the two-dimensional strain distribution during crack opening was quantified using micro-scale DIC (**Fig.2**).

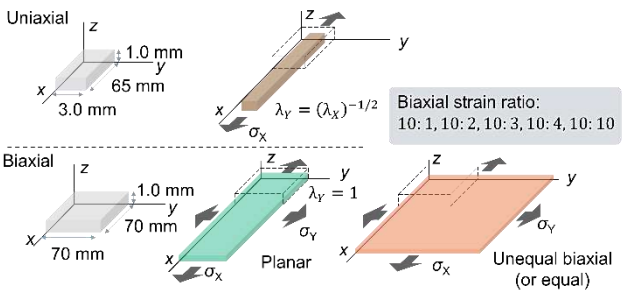


Fig. 1 Schematics of several types of deformation: uniaxial, planar, unequal biaxial (nominal strain ratio $\varepsilon_y/\varepsilon_x$ = 0.1, 0.2, 0.3, 0.4), equi-biaxial.

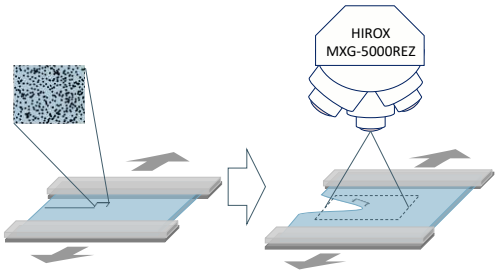


Fig. 2 Schematics of quantification of two-dimensional strain distributions during elongation of a specimen with a hole.

Fig. 3 shows the engineering stress (σ) - elongation ratio (λ) curves in the load/unload cyclic test of un-equi biaxial elongation (10:4). Stress-softening occurs in the two directions in the high(X) and low elongation(Y) axes. The dissipated energy *D* resulting from the stress-softening effect in each cycle was evaluated from the area bounded by the loading and

unloading curves. From the corresponding results in seven types of deformation, the D values were obtained as functions of stretch λ_X and λ_Y. The data of D in various deformations were well approximated by a single equation using the invariants (I_1, I_2) of strain tensor as variables:

$$D(I_1, I_2) = a(I_1 - 3) + b(I_2 - 3) + c(I_1 - 3)(I_2 - 3) \quad (1)$$

where a, b and c are the numerical coefficients.

Fig. 4 shows the development of strain fields around a crack-tip during crack opening. This study focused on steady cracks that occur only at the opening without propagating, with a small elongation strain of the entire sample ($\varepsilon_{y,macro} < 0.47$). ε_1 is the engineering strain in the direction of maximum elongation (principal major strain) at each point, ε_2 is the engineering strain in the direction perpendicular to ε_1, and $\varepsilon_2/\varepsilon_1$ is the strain ratio. The strain distribution is non-uniform around the crack, and the strain is concentrated near the crack-tip.

The obtained strain distributions around the crack (**Fig. 4**) were transformed into the distribution of I_1 and I_2, and subsequently, the distribution of D at each position was obtained using equation (1) (**Fig. 5**). The internal damage due to the stress-softening effect develops as the crack opens, with a pronouncedly non-uniform distribution, and it increases closer to the crack-tip.

This methodology is applicable to various types of nonuniform deformation. In presentation, we also demonstrate how this approach effectively captures non-uniform stress-softening behavior and damage distributions during heterogeneous deformation in a CB-filled rubber sheet with a vacancy defect.

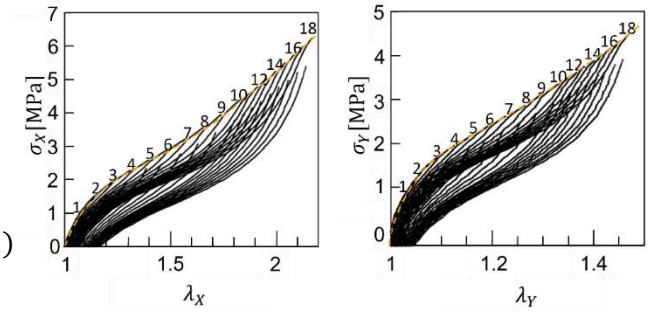


Fig. 3. Nominal stress (σ) - stretch (λ) relations in cyclic loading tests of un-equi biaxial elongation (10:4).

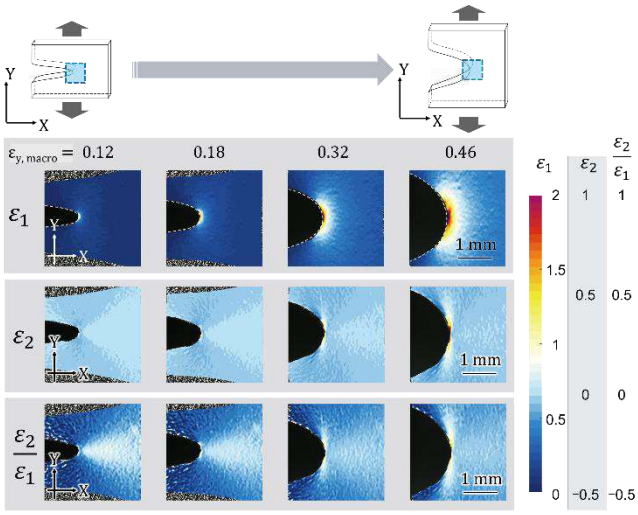


Fig. 4. Development of strain fields around a crack-tip during crack opening.

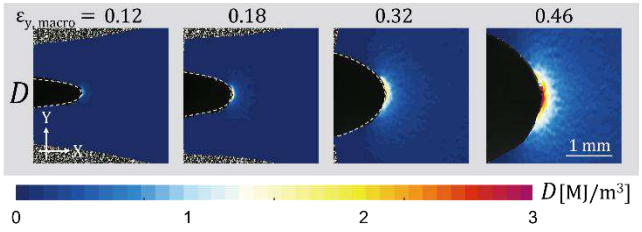


Fig. 5. Development of calculated spatial distributions of D around a crack-tip during crack opening.

References

1. Schmoller, K. M., & Bausch, A. R., *Nat. Mater.*, **12**, 278 (2013).
2. Mai, T. T., Morishita, Y., & Urayama, K., *Soft Matter*, **13**, 1966 (2017).

AFM Nanomechanics of Vulcanized Rubber Containing Silica and Petroleum Resin

Makiko ITO[1], Kouki AZUMA[2], Keisuke CHINO[2], Xiaobin LIANG[1], Ken NAKAJIMA[1]

[1] *Institute of Science Tokyo, 2-12-1 Ookayama, Meguro-ku, Tokyo, Japan.*

[2] *ENEOS Materials Corporation, 8 Chidori-cho, Naka-ku, Yokohama, Japan.*

ito.m.7e5f@m.isct.ac.jp

Keywords: Atomic Force Microscopy, Petroleum Resin, Styrene-Butadiene Rubber, Silica, Nanomechanics

Petroleum resins dissolve and compatibilize with a variety of solvents and polymers, and are used in a variety of applications such as paints, adhesives, and rubber compounding materials. In recent years, the automotive industry has been seeking more fuel-efficient products, and various studies have been conducted on modifying rubber, blending silica and petroleum resins, and so on [1]. Newly developed modified petroleum resins (MPR) have been shown to improve wet grip, fuel efficiency, and abrasion resistance. This study focuses on the compatibility of styrene-butadiene rubber (SBR) and petroleum resins, and aims to clarify the correlation between the nano- and macro-mechanical properties of the developed products.

Table 1 shows the details of the samples. Solution-polymerized SBR is used, and MPR has functional groups that react with rubber. The smooth surface of each sample is prepared with an EM FC6 cryo-ultramicrotome (Leica Mycrosystems, Germany). The atomic force microscope (AFM) used to measure local properties is a MultiMode 8 with NanoScope V (Bruker, USA). Each measurement is conducted in Peak Force QNM mode with the measurement frequency of 1 kHz and in Force Volume mode with that of 5 Hz. The obtained force curves are analyzed using Johnson-Kendall-Roberts (JKR) linearized method [2].

Table 1. Sample compositions

Components [phr]*	**SBR**	**SBR+MPR**	**SBR+Silica**	**SBR+MPR+Silica**
SBR	100	100	100	100
Silica	-	-	30	30
MPR	-	30	-	30

*Parts by weight per 100 parts by weight of rubber

Figure 1 shows Young's modulus images obtained by AFM. The scan size is 2.0 μm. Figure 2 is histograms obtained from the images in Figure 1 after the areas corresponding to silica particles are removed. The Young's modulus is dramatically increased by blending MPR with SBR. The reaction between SBR and MPR is thought to improve compatibility and raise the elastic modulus of the rubber. Usually, adding filler to rubber increases Young's modulus due to the reinforcing effect. In fact, Figure 1 and 2 show that when silica is added to SBR, interfacial regions are formed around the silica particles and overall Young's modulus increases. However, in the case of the SBR+MPR+silica system, the Young's modulus of the matrix is lowered by the addition of silica. Its seems that the addition of silica particles changes the compatibility balance between SBR and MPR.

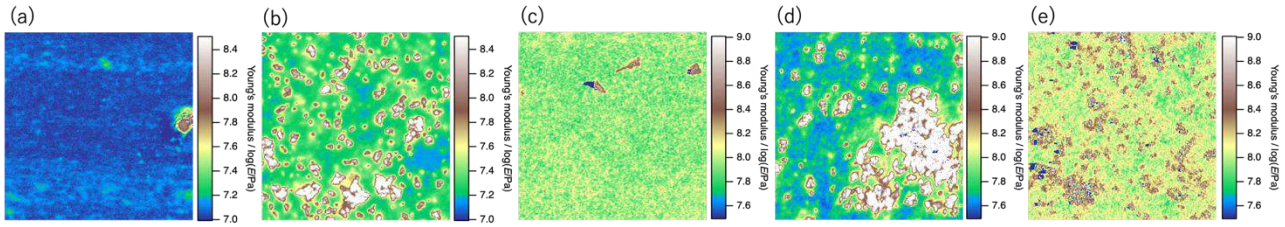


Figure 1. Young's modulus image obtained by AFM. (a) SBR, (b) SBR+Silica, (c) SBR+MPR, (d) SBR+MPR+silica and (e) SBR+MPR+Silica with doubled kneading time. Scan size is 2.0 μm.

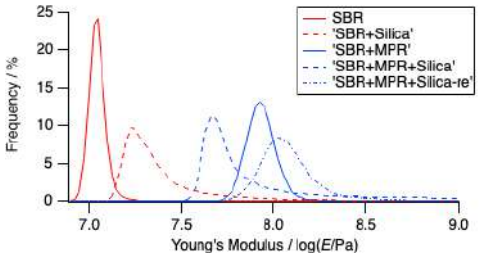


Figure 2. Histogram of Young's modulus for matrix and interface.

Compared to the SBR+silica system, the SBR+MPR+silica systems exhibited twice thicker interface, suggesting that MPR is unevenly distributed at the interface. When the kneading time is doubled (SBR+MPR+silica-re in Figure 2; blue single-dotted line), silica dispersion is improved, interfacial thickness and interfacial modulus decrease, and the matrix modulus increases.

In order to elucidate the correlation between nano- and macro-mechanical properties, AFM modulus values are plotted on the macroscopic master curve for storage modulus as shown in Figure 3. The frequency of each AFM data is calculated using its sample deformation rate. Then, WLF equation is used to shift the frequencies for FV and QNM modes by setting the reference temperature at 10°C. Young's modulus of the SBR+MPR system shows good agreement with the macroscopic storage modulus. For filler-reinforced specimens, the modified Guth-Gold equation, shown in Equation 1, is often used to discuss the effect of reinforcement.

$$G = G_0(1 + 2.5f\phi + 14.1f^2\phi^2) \qquad (1)$$

In the present study, this correction factor f is obtained using two patterns of defining equations: f_1 (equation 2), which considers only the volume fraction, and f_2 (equation 3), which considers the volume fraction and the reinforcement effect of the increased modulus of the interface. In this equation, ϕ_S is the volume fraction of silica, ϕ_I is the volume fraction of the interface, E_M is the modulus of the matrix, and E_I is the modulus of the interface.

$$f_1 = \frac{\phi_S+\phi_I}{\phi_S} \qquad (2) \quad , \quad f_2 = \frac{E_I}{E_M}\left(\frac{\phi_S+\phi_I}{\phi_S}\right) \qquad (3)$$

The modulus calculated with f_2 is closer to the macroscopic storage modulus than the modulus calculated with f_1. The correction factor that also takes into account the high elasticity of the interface is a more accurate evaluation of the contribution of the interface.

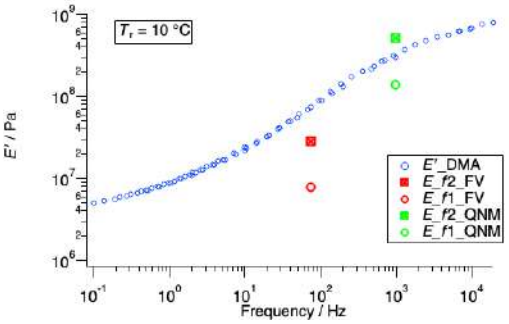


Figure 3. Comparison of macroscopic storage modulus and AFM modulus for SBR+MPR+Silica systems (single kneading).

References

1. Weng P, Tang Z, Guo B, *Polymer*, 2020; 190: 122244.
2. Fujinami S, Ueda E, Nakajima K, Nishi T, *J. Polym. Sci., Part B: Polym. Phys.* 2019, 57, 1279

Mixed-Mode Crack Propagation Criterion in Elastomers

Tomoki MISHIMA[1], Thanh-Tam MAI[1], Katsuhiko TSUNODA[2], Kenji URAYAMA[1]

[1] *Department of Material Chemistry, Graduate School of Engineering, Kyoto University, Kyoto, Japan*

[2] *Sustainable and Advanced Material Division, Bridgestone Corporation, Tokyo, Japan*

mishima.tomoki.48w@st.kyoto-u.ac.jp

Keywords: Crack Propagation, Elastomers, Digital Image Correlation, Mixed-Mode Crack

Crack propagation is a primary mode of material fracture, but its path is highly sensitive to loading conditions around the crack tip. Unlike hard materials such as metals and glass, elastomers undergo large deformations and exhibit strong nonlinear elastic behavior, making their fracture mechanics particularly complex. In this study, we quantify experimentally the strain and strain energy density fields around the crack tip of elastomers under various loading conditions, and elucidate key factors that govern the direction and evolution of crack propagation.

Vulcanized acrylonitrile butadiene rubber (NBR) containing 1.4 phr of sulfur was used as a specimen. NBR films having initial cracks oriented at various angles θ_0 relative to the film's long side were prepared (**Figure 1**: θ_0 =3.1°, 45.9°, 72.8°). The films with random speckle patterns were stretched stepwise along their short axis. The resultant behavior of crack opening and propagation was observed using an optical microscope. The evolution of strain distribution around the crack tip during the stretching was examined by digital image correlation (DIC).

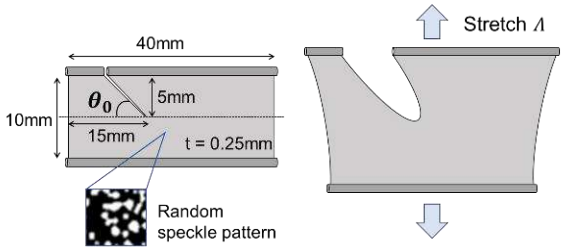


Figure 1. Geometry of crack growth experiment

The crack behavior under sequential stepwise stretching can be classified into three distinct stages before catastrophic failure occurs. In the first stage, where the global stretch Λ is small, the crack simply opens without propagating. When Λ reached a critical threshold Λ_c, the crack begins to propagate slightly but soon arrested: This behavior, characterized by repeated initiation and arrest, is defined as "stable crack growth" and corresponds to the second stage. Stable crack growth continues until Λ reaches a higher threshold Λ_c' ($> \Lambda_c$), and beyond Λ_c', the crack rapidly propagates across the specimen, leading to macroscopic failure. This "catastrophic crack growth" is assigned to the third stage. The path of stable crack growth is curvilinear, while catastrophic crack growth proceeds straight and perpendicular to the stretching direction (**Figure 2**).

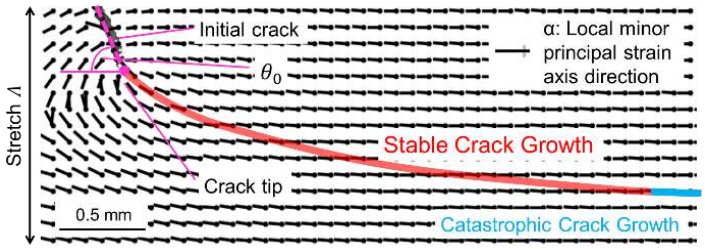


Figure 2. 2D distribution of local minor principal strain axis direction at crack-growth onset for θ_0 = 72.8°. The data are shown in the coordinate system before deformation. The red line represents the path of stable crack growth.

Figure 2 shows the 2D distribution of local minor principal strain axis direction (α) at $\Lambda = \Lambda_c$ for an initial crack angle of θ_0 = 72.8°. The direction α is mapped onto the undeformed coordinate system prior to crack opening. Due to the inclined orientation of the initial crack, the distribution of α is asymmetric. The red line traces the experimentally observed stable crack path, while the blue line indicates catastrophic crack trajectory. Notably, the stable crack follows the curved distribution of α.

Figure 3(a) shows the distribution of strain energy density (U) at the onset of crack growth ($\Lambda = \Lambda_c$). U was calculated from the strain energy density function (W) obtained using the biaxial stress-strain data by a separate measurement. It can be observed that the value of U rapidly increases as the crack tip is approached. **Figure 3(b)** presents a graph plotting U on a semicircle with a radius of 200 μm centered at the crack tip (black solid line in **Figure 3(a)**). In this plot, U is shown as a function of the angle ϕ from the crack tip, where the direction of applied stretching is defined as 0°. This graph exhibits a minimum value at $\phi_c \approx 130°$. The minimum value consistently appeared at $\phi_c \approx 130°$ independent of the semicircle radius. **Figure 3(c)** also shows an enlarged view of the distribution of local minor principal strain axis direction around the crack tip. Unlike **Figure 2**, this figure is presented in the deformed coordinate system. The red line in the figure indicates the direction corresponding to $\phi_c \approx 130°$ as viewed from the crack tip. The red line aligns with the local minor principal strain axis direction, indicating that crack propagation during stable crack growth occurs in the direction with the minimum value of U.

This result suggests that the curved propagation paths during stable crack growth ($\Lambda_c < \Lambda < \Lambda_c'$) under asymmetric loading (i.e., mixed-mode crack) are governed by the local orientation of the principal strain axes at the onset of crack growth at $\Lambda = \Lambda_c$. Furthermore, the crack propagation direction is determined by the direction in which the strain energy density exhibits its minimum value. Similar features were observed for various initial angles θ_0. In presentation, we will compare these criteria with those in natural rubber with strain-induced crystallizability.

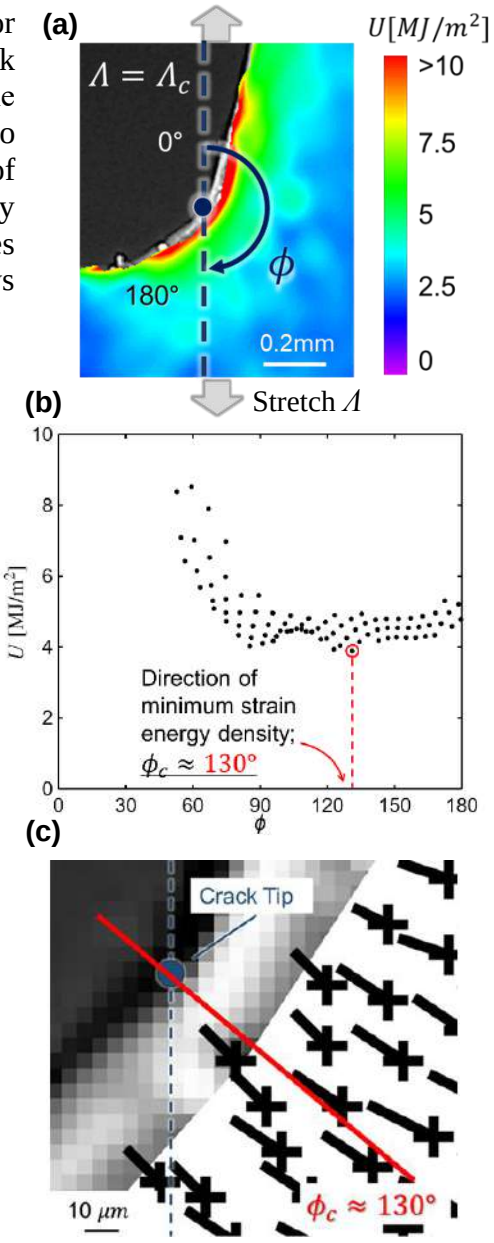


Figure 3(a). Distribution of strain energy density (U) around the crack tip at the crack-growth onset ($\Lambda = \Lambda_c$). **(b).** Polar plot of U. The center is the crack tip, and the radius is 200 μm. **(c).** Distribution of local minor principal strain axis direction at $\Lambda = \Lambda_c$. The red line shows the direction of the minimum value of U.

Thermal Analysis of the Mullins Effect in Filler Reinforced Elastomers

Koshi SHIMAZAKI[1], Kakeru OBAYASHI[1], Katsuhiko TSUNODA[2], Kenji URAYAMA[1]

[1] *Department of Material Chemistry, Kyoto University, Kyoto 615-8246, Japan.*

[2] *Sustainable and Advanced Materials Division, Bridgestone Corporation, Tokyo 187-8531, Japan.*

shimazaki.koshi.43c@st.kyoto-u.ac.jp

Keywords: Mullins effect, stress softening, heat emission

Filler-reinforced elastomers are extensively used in rubber products such as automobile tires due to their superior mechanical performance. A distinct feature of filler-reinforced elastomers is the Mullins effect, which manifests as a notable stress reduction during reloading compared to virgin loading at the same stretch, while peak stress at the maximum stretch remains unchanged. Although this phenomenon has been widely studied, its fundamental mechanism remains unclear.

Loading-unloading cycles in filled elastomers are accompanied by measurable heat emission. However, the correlation between stress reduction and thermal dissipation is still not fully understood. Clarifying this correlation is essential not only for a comprehensive understanding of the Mullins effect, but also for improving the mechanical durability and energy efficiency of rubber components in practical applications. In this study, we investigate the correlations between stress softening and heat emission during cyclic loading, focusing on the influence of filler type and deformation mode.

Vulcanized styrene-butadiene rubber (SBR) filled with either 50 phr of carbon black (CB) or silica particles treated with a silane coupling agent was prepared using 1.4 phr sulfur and as the crosslinking agent. These samples are designated as CB/SBR, Silica/SBR, respectively. Two stretching modes were employed: uniaxial and planar stretching. Planar stretching was achieved by elongating wide sheet specimens along their short axis, restricting lateral contraction and inducing nearly planar deformation in the central region (**Fig. 1-b1**).

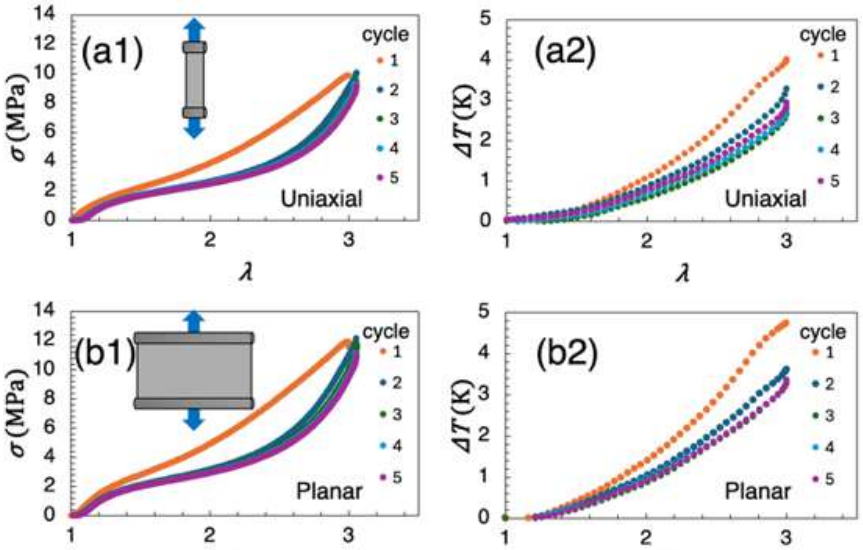


Fig.1 (a1, b1) Engineering stress and (a2, b2) surface temperature increase against elongation for CB-filled SBR in loading processes of multiple loading-unloading cycles by uniaxial stretch(a1, a2) and planar stretch(b1, b2)

Each sample underwent five loading-unloading cycles with a maximum elongation ratio of λ = 3 During these cycles, both the tensile force and surface temperature change (ΔT) were recorded. The ΔT-stretch data were converted into the exothermic energy Q under adiabatic conditions using a thermal diffusion model.

The nominal stress (σ)-λ curves for CB/SBR under uniaxial and planar elongation are shown in **Fig.1(a1) and (b1)**, respectively. Corresponding ΔT-λ curves are presented in **Fig.1(a2) and (b2)**, respectively. For both elongation modes, significant decreases in σ and ΔT were observed during the second loading. However, after the third loading, both values remained nearly constant at the same λ. Similar trend was observed for Silica/SBR, indicating a strong correlation between mechanical stress reduction and thermal response.

Figure 2 compares the reduction in heat generation ($\Delta Q = Q_1 - Q_5$) and mechanical energy loss (D) between the first and fifth loading cycles. The energy loss D was evaluated from the area enclosed by these loading curves. The ratio $\Delta Q/D$ depends primarily on filler type: approximately 0.3 for CB and 0.4 for Silica, with minor dependence on the deformation mode. According to Candau et al.[1], heat emission during uniaxial stretching is mainly attributed to void formation at rubber-filler interfaces. The observed values of ΔQ /D well below 0.5 suggest that the additional mechanisms contribute to the mechanical energy loss D beyond void formation alone. In this presentation, we will further explore the physical origin of the residual energy dissipation ($D - \Delta Q$), with particular emphasis on thermal annealing effects.

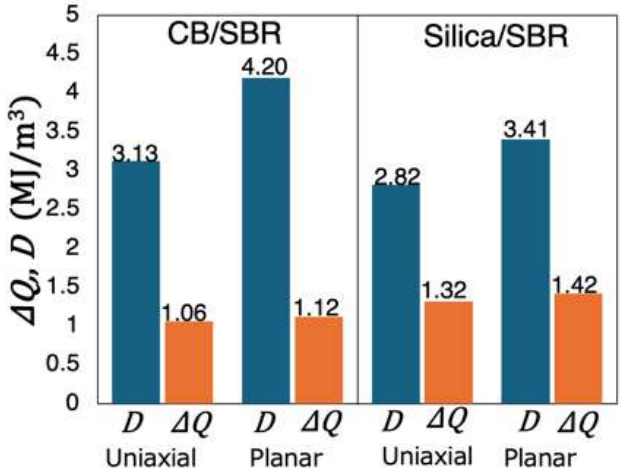


Fig.2 Heat generation difference between the first and fifth loading (ΔQ) and mechanical energy dissipation (D) for each specimen during uniaxial and planar stretch cycles.

1. Candau, N., Fernandes, J. P. C., Vives, E., Mudarra Lopez, M., Neira-Viñas, M., & Maspoch, M. L. ,

A Melt Crystallization and Dewetting Kinetics of Marine-Degradable Polyesters in Thin Films

Ryu Miyajima[1], Nana Tsuji[1], Kazuki Imai[1], Hiroto Osakaki[1], Keito Shimakawa[1], Khanh-Van Thi Khuat[2], Hiroyasu Masunaga[3], and Sono Sasaki[*1,3,4]

[1]*Dept. of Biobased Mater. Sci., Grad. Sch. of Sci. Eng., Kyoto Inst. of Tech.,1, Matsugasaki, Hashikami-cho, Sakyo-ku, Kyoto 606-8585, Japan.*

[2]*Fac. of Fiber. Sci. and Eng., Kyoto Inst. of Tech., 1, Matsugasaki, Hashikami-cho, Sakyo-ku, Kyoto 606-8585, Japan.*

[3]*Japan Syn. Rad. Res. Inst., 1-1-1, Kouto, Sayo-cho, Sayo, Hyogo 679-5198, Japan.*

[4]*RIKEN SPring-8 Cent., 1-1-1, Kouto, Sayo-cho, Sayo, Hyogo 679-5148, Japan.*

E-mail address: m4661018@edu.kit.ac.jp

Keywords: marine-degradable polyester, thin film, isothermal crystallization, crystallization rate, dewetting rate, grazing-incidence wide-angle X-ray diffraction (GIWAXD), synchrotron radiation

The higher-order structure of crystalline polymers can be controlled by crystallization conditions such as temperature, pressure and so on. For the case of linear crystalline polymers in thin films with thicknesses of less than 1 μm, crystallization behavior changes depending on film thickness. With decreasing film thickness, nucleation and crystal growth rates of polymers in thin films usually decrease. This phenomenon was explained as a decrease in molecular mobility with decreasing film thickness[1,2]. The dewetting of polymers on substrates sometimes occurs due to a mismatch in surface free energy between the substrate and polymer. However, crystallization kinetics of polymers during the dewetting process have not been clarified at the molecular scale. This study aims at investigating the early-stage isothermal crystallization behavior of marine-degradable linear polyesters in thin films by X-ray diffraction measurements using synchrotron radiation. The relationship between dewetting and crystallization kinetics of polymers will be discussed for thin films.

Poly(ε-caprolactone) (PCL) with a M_n (the number-averaged molecular weight) of 5.7×10^4 and a M_w (the weight-averaged molecular weight) of 1.3×10^5 was used as a sample. PCL thin films with different thicknesses from ca. 200 to ca. 900 nm were prepared on Si substrates by the spin-coating method. Isothermal crystallization behavior from the melt was traced for each specimen by time-resolved grazing-incidence wide-angle X-ray diffraction (GIWAXD) measurements at BL38B1 of SPring-8 (RIKEN, Hyogo, Japan). The dewetting behavior and spherulitic structure formation in the thin film specimen were observed by a polarized-reflection optical microscope (PROM) under a crossed-Nicol condition.

Dewetting of PCL on the Si substrate started to occur in the melt. Spherulitic structure was generated and grew in the isothermal crystallization process after the temperature jump from the melt. Time dependence of the apparent crystallinity was evaluated from GIWAXD profiles measured during the isothermal crystallization. The initial maximum slope value in the plots of the apparent crystallinity vs. the isothermal crystallization time was evaluated as the crystallization rate (k), and

the onset time of the increase was defined as the induction time of crystallization (t_0). The nucleation rate (N^a) was estimated as the inverse of t_0 ($N^a \sim 1/t_0$). Both the crystallization and nucleation rates were found to decrease with decreasing film thickness. Notably, a significant drop in the crystallization rate was observed around 400–600 nm. This behavior is consistent with previous findings in poly ethylene oxide (PEO) films, which showed that crystallization kinetics begin to deviate from bulk-like behavior below approximately 500 nm in thickness due to the confinement of polymer chains and the resulting suppression of chain mobility required for crystallization[1,2]. However, some specimens exhibited dewetting during the isothermal crystallization process from the melt and showed exhibited different crystallization behavior. In the dewetting specimens, the crystallization and nucleation rates exhibited fluctuations, suggesting that the fluctuation depends on the extent of dewetting.

In thin polymer films (without dewetting), crystallization behavior changes depending on the film thickness. We found that the thickness denpendence of the crystallization rate can be divided into two main regions. In the first region, where the thickness is below a certain critical value, the mobility of polymer chains becomes heavily restricted, resulting in a strong constraint of the crystallization kinetics. Actually, the value of the crystallization rate is about only 20% of its bulk value. In the second region, where the film is thicker than the critical value, the crystallization rate tends to be almost similar to that of the bulk.

In my poster presentation, I will present results demonstrating both the thickness-dependent and thickness-independent regions of crystallization kinetics. The details of the dewetting and crystallization behavior of PCL will also be explained.

References

1. Nguyen, T. V., Nagata, T., Noso, K., Kaji, K., Masunaga, H., Hoshino, T., Sakurai, S., Sasaki, S., *Macromolecules*, 2022; 55: 6076-6089.
2. M.V. Massa, K. Dalnoki-Veress, J.A. Forrest, *Eur. Phys. J. E*, 2003; 11: 191–198.

A Resazurin Reduction Test for Rapid Evaluation of Natural Rubber Latex Putrefaction

Preeyawis Na Ubol [*], Chayanoot Kositanont, Waluree Thongkam[1]

[1] *National Metal and Materials Technology Center, Pathum Thani, Thailand.*

Preeyawis.nau@mtec.or.th

Keywords: Natural Rubber Latex, Resazurin, Putrefaction

The spoilage of fresh natural rubber latex is primarily attributed to bacterial and enzymatic activity, which induces significant alterations in its physical and chemical properties, ultimately resulting in putrefaction and coagulation. One of the standard analytical methods used to evaluate spoilage is the determination of the volatile fatty acid (VFA) number. This parameter quantifies the concentration of volatile fatty acids such as acetic, formic, and propionic acids generated through the microbial degradation of non-rubber constituents within the latex matrix. The VFA number is typically obtained via a combination of steam distillation and titration, providing a measure of the extent of microbial activity. However, conventional VFA analysis may lack the sensitivity required for early detection of spoilage and is susceptible to interference from additives such as soaps or alkaline agents.

Microbial quantification in rubber latex is commonly performed using total plate count and most probable number (MPN) methodologies. Although these techniques offer adequate sensitivity for detecting low microbial loads, they are inherently labor-intensive and time-consuming.

The resazurin reduction test represents a colorimetric approach for the estimation of microbial activity. This method is based on the ability of metabolically active bacteria to reduce the blue dye resazurin to pink resorufin, thereby enabling indirect assessment of latex quality. The present study aims to develop a more rapid and efficient method for the evaluation of rubber latex putrefaction.

In fresh rubber latex, resazurin solution was added to fresh latex sample tube, and incubate at 37°C for 10 minute. Then, observed sample tube for a color change. Initially blue in its oxidized state, resazurin turns pink or even colorless upon reduction by metabolically active cells.

The colour of fresh natural rubber latex after incubated with resazurin dye are shown in table 1. The rate of reduction of resazurin related with number of bacteria in rubber latex sample. Sample no.1 that contain the most microbes has the most rapid reduction rate. We found that in every fresh latex samples, Blue colour of resazurin dye in samples become purple and finally colourness in a few minutes. However, In case of latex samples that not fresh or stored overtime the rate of dye reduction was taken more time.

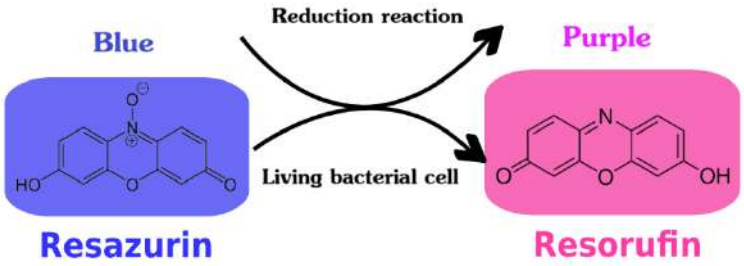


Figure 1. Mechanism of resazurin reduction

Table 1. Colour of fresh natural rubber latex after add resazurin dye for 10 minutes.

Fresh natural rubber latex sample	Colour of resazurin dye reduction test					
	3 hr	6 hr	9 hr	12 hr	24 hr	30 hr
Sample 1	Silver Pink RBG (199, 182, 187)	Silver Pink RBG (197, 184, 194)	Silver Pink RBG (192 ,180, 184)	Silver Pink RBG (201 ,186, 191)	NA	NA
Sample 2	Medium Purple RBG (130,76, 192)	Medium Purple RBG (121,66, 185)	Medium Purple RBG (155,66, 183)	Medium Purple RBG (143,72, 194)	Light purple RBG (215,177, 200)	Silver Pink RBG (197 ,175, 188)
Sample 3	Medium Purple RBG (37,150, 190)	Medium Purple RBG (119,67, 193)	Medium Purple RBG (135, 72, 195)	Medium Orchid RBG (196, 72, 195)	Thistle RBG (204, 182, 192)	Thistle RBG (173 ,157, 193)
Sample 4	Medium Purple RBG (64,148, 185)	Medium Purple RBG (136,65, 190)	Medium Purple RBG (144, 70, 191)	Medium Purple RBG (133, 71, 198)	Medium Purple RBG (120, 76, 191)	Medium Purple RBG (113, 74, 189)
Sample 5	Medium Purple RBG (150,75, 193)	Medium Purple RBG (127, 61, 184)	Medium Purple RBG (131, 70, 190)	Medium Purple RBG (133, 74, 200)	Medium Purple RBG (107, 72, 188)	Medium Purple RBG (113, 80, 195)

References

1. Thanasirikul C, Patumvan A, Lipsky D, Bovonsombut S, Singjai P, Boonchieng E, Chitov T, J Sci AgriTechnol., 2022;4(1):1-7.
2. Elshikh M, Ahmed S, Funston S, Dunlop P, McGaw M, Marchant R, Banat IM. Biotechnol Lett. 2016;38:1015-9.
3. International Organization for Standardization. Documentation bibliographic references. ISO 506. 4th ed. Geneva: ISO; 2020.

Establishment of a library database of some compounding ingredients using a Py-GC/MS technique

P. TUMWISED[1,2*], S. WIRASATE[1], C. SIRISINHA [1]

[1]*Rubber Technology Research Centre, Faculty of Science, Mahidol University, Nakhon Pathom 73170, Thailand.*

[2]*Polymer Science and Technology Program, Department of Chemistry, Faculty of Science, Mahidol University, Nakhon Pathom 73170, Thailand.*

prin.tum@student.mahidol.ac.th

Keywords: Natural rubber, Accelerators, Py-GC/MS, GC-MS library database, Reverse engineering

A rubber compound is a blend of raw rubber and selected additives, including fillers, curing agents, and processing aids. These components are formulated to enhance specific properties, such as strength, flexibility, and durability. The compounding process allows the material to meet the performance demands of various industrial applications. Since 2014, Thailand's rubber compound exports have declined, while exports from other countries have increased. This indicates a decline in Thailand's global market share [1]. One contributing factor may be regulatory restrictions on specific chemical accelerators such as nitrosamines, which are linked to health and environmental concerns. In response, there has been growing interest in developing safer and more environmentally friendly rubber formulations [2-5]. Accelerators significantly influence curing behaviour, mechanical performance, and potential toxicity. Replacing hazardous accelerators with safer options, while maintaining processing efficiency and product quality, remains a major challenge. Evaluating commonly used accelerators in terms of reactivity, decomposition products, and compatibility with various rubber types is crucial for the development of sustainable and regulation-compliant materials [6-8].

This work investigated a powerful method for providing a library database for reverse engineering in the rubber additive industry, utilising the Pyrolysis-GC/MS (Py-GC/MS) technique. This technique offers analyses of raw rubber and additives present in vulcanised rubber, which is crucial for product development in response to trading regulations.

The results showed that pyrolysates at a temperature of 300°C in a cured sample of standard Thai rubber 20 (denoted as C-STR20) detected D-limonene as a characteristic of polyisoprene from NR, and carbon disulfide resulting from sulfur reacting with the NR backbone. In addition, pyrolysates of three accelerators were determined. For the N-Cyclohexyl-2-benzothiazolesulfenamide (CBS), Cyclohexylamine, benzothiazole, 2-(methylmercapto) benzothiazole, and N-cyclohexyl-2-benzothiazolamine were detected. Caprolactam was found as a characteristic of Dithiocaprolactame (DTDC) sulphur-donor accelerator. Dibenzylamine was detected as a characteristic of Tetrabenzylthiuram disulfide (TBzTD). In summary, the Py-GC/MS technique, under proper test conditions, demonstrated the potential to identify curatives in cured rubber products with simple sample preparation and a short test duration.

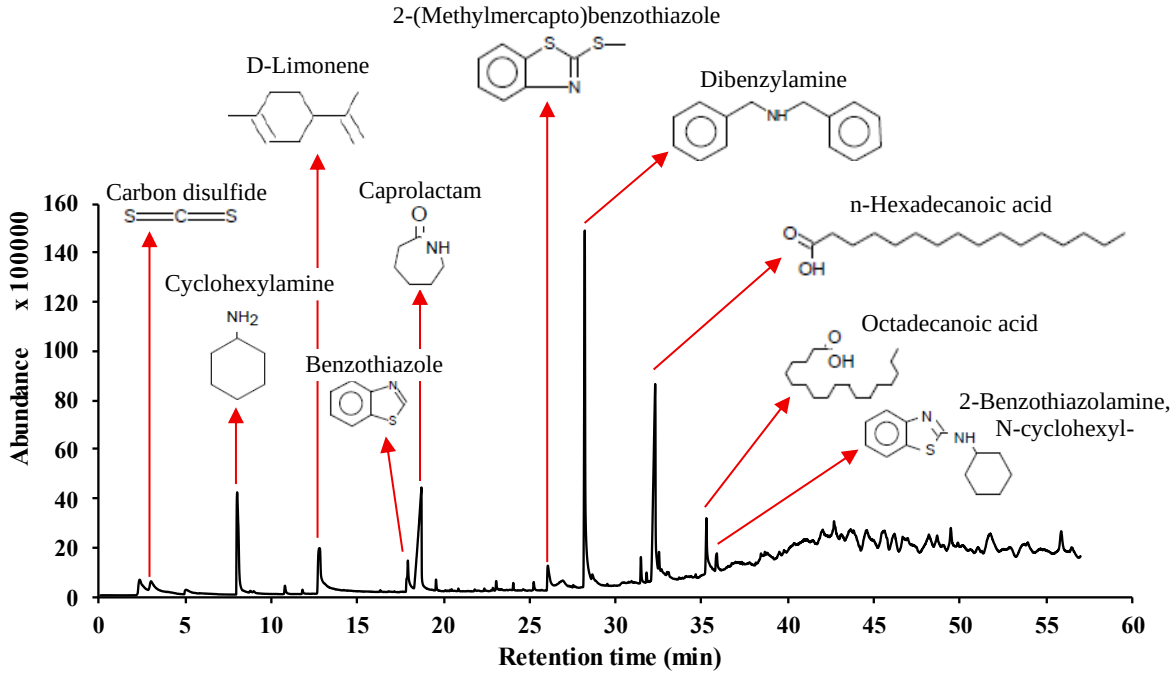


Figure 1. GC-MS chromatogram at 300°C of cured standard thai rubber 20 (C-STR20)

Acknowledgement

The authors would like to thank the Rubber Technology Research Centre (RTEC) for providing the equipment and test facilities used in this study.

References

1. Sowcharoensuk, C. *Thailand Industry Outlook 2025-2027: Rubber Industry*. 2024.
2. Spiegelhalder, B. and R. Preussmann, IARC Sci Publ, 1982; 231-43.
3. Willoughby, B.G. and K.W. Scott, Rubber chemistry and technology, 1998; 71: 310-322.
4. Willoughby, B.G. and K.W. Scott, Rubber chemistry and technology, 1998; 71: 766-777.
5. Manchuri, K.M., et al., Medical Gas Research, 2025; 15: 535-543.
6. Iavicoli, I. and G. Carelli, Journal of Occupational and Environmental Medicine, 2006; 48: 195-198.
7. Sheth, P. and R. Desai, International Journal for Scientific Research & Development, 2013; 1:
8. Alam, M.N., S.C. Debnath, and J. Choi, Journal of Polymer Research, 2021; 28: 317.

Author Index

A

A. Anlakhon 447
A. Blume 93, 181
A. Causa 223
A. Das 259
A. Fatima 266
A. Ichangi 243
A. Matsuura 95, 118
A. Mingsamoh 384
A. Nimpaiboon 314, 379, 423
A. Nintap 207
A. Talma 93
A. Thitithammawong 80, 252
A. Uesugii 95
A. Zych 93
Abraham Chemtob 371
Adisak Khotchomphu 209
Agnieszka Kolodziejczak-Radzimska 27
Airi Sato 128
Akarapong Tuljittraporn 201
Akari Uesugi 209
Alexander Lion 156, 265
Amit Das 20
An Yingjun 353, 421
Andreas Limper 22
Anıl Tatlidilli 49
Anke Blume 59, 157
Annemarie Hillebrecht 137
Anthony Lin 120
Anureet Kaur 10
Anutida Suwan 114
Anuwat Saetung 108, 114
Apinya Chintrakul 211, 213
Apisara Sillapasuwan 367
Apissara Komkay 135
Areeya Anuwatprakit 367
Arnaud Spangenberg 371
Arthittaya Chuaybamrung 205
Atichart Kwanyuang 213
Atsushi Takahara 353, 419, 421
Auke Talma 59
Azizon Kaesaman 35

B

B. Di Credico 223
B. Khumpaitool 447
B. Marsri 259
B. Mulsena 344
B. Sripornsawat 75
B. Thongnuanchan 252
B. Tirthankar 89
Bagdagul Karaagac 81
Baochun Guo 41, 70, 142, 169, 254, 394, 397
Bawornkit Nekamanurak 426
Benjamin Klie 227
Bettina Taschner 276
Binjie Jin 254
Biqiong Chen 10
Boxiao Li 176
Bundit Putasaeng 361

C

C. Ajay 89
C. Bascucci 359
C. Bottier 118
C. Charaschimpleekul 381
C. Dipankar 89
C. Dokkhan 381
C. Hayichelaeh 384
C. Jagannath 221
C. Kongkaew 346
C. Nah 25, 172
C. Natchawut 401
C. Pongchumyen 453
C. Sirisinha 159, 256, 379, 423, 501
Chandresh Dwivedi 178
Changsu Woo 486
Chanon Kongkamol 211, 213
Charoen Nakason 35
Charongpun Musikavong 37
Chayanoot Kositanont 498
Chayapha Nimsuwan 361
Chen Cheng 19
Chen Zhaohui 146
Chenxi Huyan 51
Chomnutcha Boonmee 72
Chomsri Siriwong 207
Chotiros Dokkhan 361
Chris Wu 120
Christopher Bascucci 245

Christopher G. Robertson 19
Chunyu Zhang 183, 249
Chutarat Sathirapanya 211
Chutima Saeheng 411
Cuong-Minh-Quoc Le 371

D

D. Abdulraman 25, 172
D. Kleinschmidt 150, 185, 266
D. Mahuya 89
D. Saikat 89
D. Sudeep 89
D.K. Arti 133
Daisuke Iwahara 274
Danniel C. Liao 120
Dariusz M. Bielinski 27
Darren Yi Sern Low 47
Davut Aksüt 49, 91
Dazylah Darji 141
Dean Vidakovic 276
Dengfeng Shi 372
Dexian Yin 373, 472
Dong Wang 41,163, 394
Donghan Li 165
Dongmei Yue 203, 235, 437

E

E.R. Senoz 283
Ekachai Wimolmala 55
Ekwipoo Kalkornsurapranee 62, 201, 205, 231
Elif Uzun 157
Elmar Moritzer 227
Eric Euchler 297
Evelyn Lim H M 287

F

F. Bruening 150, 185, 266
F. Clemen 75
F. Clemens 243, 359, 413
F. Gay 118
F. Grunert 93
F. Mongioi 243
F. R. Wurm 181
F. Van Elburg 93
Fabian Grunert 59
Fangshuo Li 176
Farshid Zolala 130
Fatma Saraç 276
Fei Chen 51
Feng Wang 176
Feng Yang 97
Florian Löhr 227
Frances van Elburg 59, 157
Frank Clemans 205, 245

G

G. Biswanath 221
G. Prasenjit 221
G.-B. Lee 25
Ganggang Zhang 70
Guangbi Gong 263
Guo-Hua Hu 85

H

H. Damanik 266
H. Hashimoto 476
H. Kikuchi 470
H. Kum-ourm 95, 118
H. Ohura 476
Hailan Kang 97, 435
Haitao Wu 478
Han Song 85
Hang Thi Le 377
Hao Wang 478
Harald Plank 276
Hassarutai Yangthong 308
Heng Liu 183, 247
Hengheng Zhao 456
Hexuan Mao 288
Hideaki Takagi 338, 474
Hiroaki Yoshida 83
Hiroharu Ajiro 83
Hirokazu Kageyama 395
Hiroki Hashimoto 261
Hiromu Kawasaki 312
Hiromu Saito 395
Hironobu Tahara 460
Hiroto Murakami 460
Hiroto Okumura 31, 338, 340, 342
Hiroto Osakaki 419, 496
Hiroyasu 419
Hiroyasu Masunaga 31, 338, 340, 420, 353, 421, 496
Hisayoshi Kobayashi 16

Hoang Van Nguyen 377
Hokuto Ohura 261
Hong Nhung Thi Le 377
Hong Yao 372
Hongze Xu 45
Huaizhong Xu 338, 340, 342
Hubert Gojzewski 157
Hui Jiao 437
Huiqing Fan 233
Hung K. Nguyen 310

I

Ime Usen 278
Itsuha Kuga 417

J

J. Busfield 291
J. Chaiyut 118
J. J. C. Busfield 148
J. Petzke 150, 185, 266
J. Sakdapipanich 357
J.J.C. Busfield 187, 295
Jae Il So 23
Jakrapong Kaewkhao 201
Jakub Wreczycki 27
James Busfield 10
James Hobday 278
James J.C. Busfield 303, 197, 271
Janarthanan Supramaniam 47
Jannik Laages 1
Javier Araujo-Morera 157
Jeong Seok Oh 65
Jhiratchaya Buranawichit 207
Jiajun Qu 336
Jialiang Chen 142
Jian Tang 103
Jianming Zhang 45, 176, 179, 240
Jiashun Yang 19
Jiaye Li 405
Jiayu Shi 435
Jichuan Zhang 373
Jin Sung Seo 23
Jin Yuan 146
Jing Hua 103
Jing Zheng 478
Jinhui Liu 103
Jinjutha Wiriyanantawong 365
Jinrong Wu 42, 139, 237, 478, 480
Jitladda Sakdapipanich 21, 106, 365, 367, 382, 455, 482, 484
Josie Hughes 245
Julia Uth 137
Jun Liu 336, 415, 456, 458
Junqi Zhang 139, 42
Juthamas Jaichuedee 37

K

K S Tan 287
K. Akutagawa 291, 295
K. Amin 252
K. Bandzierz 181
K. Boonchuay 379
K. Boonkerd 384, 449
K. Bunsreyneang 449
K. Filzer 181
K. Hancharoen 449
K. Hatthapanit 344, 453
K. Kanyawararak 95
K. Nakajima 293
K. Sathaporn 386
K. Seneesrisakul 386
K. Suchiva 423
K. Urayama 470
K.Wirunya 401
Kai Liu 103
Kakeru Obayashi 152, 494
Kamolchat Charungchitaree 209
Kannika Sahakaro 39
Kanokporn Wongnukoon 482
Karine Mougin 199, 371
Karnda Sengloyluan 135
Katsuhiko Tsunoda 31, 110, 128, 310, 338, 340, 342, 492, 494
Kazuki Imai 353, 419, 421, 496
Ke Liu 179
Keiji Numata 369
Keisuke Chino 490
Keito Shimakawa 353, 419, 496
Keizo Akutagawa 10, 197, 271
Ken Kojio 152
Ken Nakajima 33, 154, 288, 310, 312, 490
Ken Nakajima 154

Keni Ma 441
Kenji Urayama 3, 31, 110, 152, 338, 340, 342, 441, 466, 488, 492, 494
Keon-Soo Jang 403
Khanh Van 353
Khanh-Van Thi Khuat 419, 421, 496
Khuat Thi 353
Kiadtisak Saenboonruang 55
Kinsuk Naskar 18
Kittipong Insom 106
Konrad Schneider 297
Koshi Shimazaki 494
Koudai Tanino 466
Kouki Azuma 490
Kwanchai Buaksuntear 126
Kyohei Kotani 310

L

L. Boeurn 413
L. Conzatti 223
L. Giannini 223
L. Schmidt 150
L. Tadiello 223
L. Tarachiwin 95, 118
L. Tripaldi 223
L. Vaysse 118
Ladawan Songtipya 231
Lam Ba Nguyen 99
Lewis Tunnicliffe 271
Li Liu 167
Liang He 462, 464
Lijie Yin 433, 462
Lin Wang 203, 235
Lingfeng Cui 217
Lingming Kong 42
Liqun Zhang 5, 29, 41, 51, 70, 85, 142, 169, 254, 336, 372, 394, 397, 456, 458, 472, 240
Long Li 435
Long Zheng 167
Lu Zong 45
Luat Dai Tran 377
Lucksanaporn Tarachiwin 209
Lutz Zybell 297

M

M. Brogly 301
M. D'arienzo 223
M. Di Consiglio 93
M. Ito 293
M. J. J. Dixey 148
M. Malineerat 293
M. Pöschl 305
M. Rabindra 89, 221
M. S. Arkana 229
M. Sriring 256, 423
M. Stěnička 305
M.I. Fathurrohman 133
Maho Nakada 338, 340, 342
Mai Thanh-Tam 488
Maimoon Himmawong 39
Makiko Ito 490
Maneephan Sukkho 363
Manuel Bessler 137
Masami Okamoto 219
Masunaga 419
Masunaga Hiroyasu 369
Mateusz Imiela 27
Matthew Thornton 193
Mengjin Jiang 478
Michael Clayton 193
Michael Johlitz 156, 265
Mikihito Takenaka 274
Milanta Tom 7
Ming Tian 29
Minglong Yao 19
Miroslawa Prochon 27
Mohamad Akmal Abdul Rahim 141
Mujia Yang 57
Mukhopadhyay 13
Murat Şen 49, 281
Muthita Phetpradab 445

N

N. Hansupalak 344
N. Hayeemasae 80, 225, 252
N. Jantawong 449
N. Jehsoh 225
N. Kingkohyao 409
N. Moonprasith 351
N. Onozuka 95, 118
N. Othman 78
N. Phungthanom 423

N. R. Mohamed 78
N. Risangud 229
N. Samerphob 225
N.A. Kinasih 133
Nan Li 480
Nana Tsuji 353, 419, 421, 496
Nanthiya Hansupalak 215
Nantinee Choosang 87
Nantinee Choosang 355
Nanying Ning 29
Naoya Amino 274, 395
Nathapong Sukhawipat 114
Nattapon Uthaipan 135
Nghia Trung Phan 101, 377
Nguyen Ngoc Mai 83
Nguyen Thu Ha 83
Nick Molden 278
Nina Eggers 276
Nitinart Saetung 108, 114
Noriyuki Igarashi 338
Noriyuki Onozuka 209
Nuorn Choothong 426
Nurul Hayati Yusof 141, 287
Nussana Lehman 201, 231

O

O. Ramekaj 291

P

P. Gulgovit 453
P. Havanapan 423
P. Jantachum 447
P. Jittham 388
P. Junkong 25
P. Kovitcharoenkul 381
P. Luangchuang 359
P. Phinyocheep 25, 172
P. Porncharukit 357
P. Rakdee 351
P. Sae-oui 388, 451
P. Saramolee 386
P. Srithavorn 187
P. Srithong 386
P. Stagnaro 223
P. Sunintaboon 25, 172
P. Suwandittakul 346, 351
P. Tumwised 423, 501
P. Wiroonpochit 344, 381, 453
P. Wongwitthayakool 453
P. Y. Cheng 68
Pairote Jittham 238, 407
Pamela Pasetto 114
Panithi Wiroonpochit 215
Patcharapron Pimput 382
Pattanop Kanokratana 72
Pattra Lertsarawut 55
Peeraphong Pokphat 72
Peih-Shyun Wu 279
Peram Prasada Rao 192
Phachara Suklim 213
Phakamat Limarun 238, 445
Philippe Daniel 77
Phillip Kohl 126
Pilar Bernal-Ortega 157
Pisit Pimrat 39
Pitchaya Theedee 365
Pitchayaporn Suwanakood 74
Piyada Bussadee 72
Ploypailin Juntosree 87, 355
Pongdhorn Saeoui 72, 159, 407
Pranee Nuinu 74
Pranee Phinyocheep 122
Preeyanuch Junkong 112
Preeyawis Na Ubol 498
Pritish R. Shukla 427
Promsak Sa-nguanthammarong 361
Puchong Thaptong 159, 407, 411
Purwonegoro Muljawan 189

Q

Qi Wu 237, 480
Qinghogn Fang 97, 439

R

R. Anyszka 251
R. Lacote 118
R. Lim 116
R. Salazar 116
R. Scotti 223
R. Stoček 305
R. Volpe 187
Ramakrishnan S 178
Ratanon Chotima 215
Rathanawan Magaraphan 44, 429

Rattapong Numard 197
Rawiporn Promsung 205, 231
Rui Zhang 167
Ruoyan Huang 394
Ryohei Ikura 83
Ryotaro Takayama 399
Ryu Miyajima 353, 419, 421, 496
Ryuga Honda 395

S

S, Butenko 243
S. Amit 221
S. Datta 305
S. Jantarasunthorn 118
S. Kanokporn 401
S. Liengprayoon 118
S. Loykulnant 351, 451
S. Montha 346
S. Montha 351
S. Mostoni 223
S. Panyakrua 453
S. Pattanawanidchai 451
S. Poompradub 449
S. Puspitasari 133
S. Saiwari 80, 252
S. Salaeh 80, 252, 259
S. Sichumphuang 381
S. Srisawadi 413
S. Suganob 116
S. Thongkham 229
S. Turek 266
S. Wiessner 259
S. Wirasate 501
S. Zhang 68
Sabu Thomas 7
Sakiko Yashiro 83
Sakito Sugii 395
Sakorn Kaewthai 170
Sampatrao D Manjare 174, 178
Sang Eun Shim 23
Sangee Choi 486
Sangin Park 269
Sangkyun Kim 486
Sarah Pedroni 271
Saree Phongphanphanee 87
Sasitorn Srisawad 215
Sayan Sdoodee 37
Sayant Saengsuwan 74
Seiichi Kawahara 14, 83, 99, 101, 124, 377, 426, 443
Selly M. Mailanda 429
Seong-woo Cho 403
Shaoqi Huang 139
Shiliang Xu 249
Shinichi Sakurai 31, 338, 340, 342, 474
Shinichi Yagi 338, 340, 342
Shintaro Yamaguchi 460
Shinya Nakano 303
Shipeng Wen 167, 405
Shiyu Gu 480
Shoei Okamoto 338
Shoei Okamoto 340, 342
Shogo Taketa 460
Shotaro Nishitsuji 274
Shouliang Nie 299
Shuai Xu 263
Shuaiqi Li 375
Shuangjian Yu 142
Shuangquan Liao 443
Shuxue Wang 240
Siah Ying Tang 47
Siqi Zhan 458
Siriprapa Kaewjaeng 201
Siriwan Jansinak 199
Siriwat Radabutra 74
Siwaporn Srimongkol 215
Siwu Wu 142, 397
Sombat Thanawan 122
Somyot Meetha 209
Sono Sakaki 419, 353, 421, 496
Sophie Bistac 285
Sopinya Nithakor 112
Sorn Duangsuwan 53
Spencer Lee 120
Suchart Kothan 201
Sujitra Onutai 443
Sumate Chaiprapat 37
Sunida Kaewchuen 35
Sunil Bhand 427
Supakit Yonphan 201
Supalerk Moonrungsee 209
Supat Isarangkool Na Ayutthaya 209
Supitta Suethao 87, 308

Surapich Loykulnant 72
Sutthinee Keawmaungkom 215
Sven Wießner 297

T

T. Amornsakchai 25, 172
T. Boonsiri 409
T. Brugo 243
T. Chanthasopeephan 413
T. Kaewprakob 344
T. Kalaivendhan 190
T. Kato 470
T. Khochai 447
T. Kuankhamnuan 451
T. Lerksamran 118
T. Srisuwanno 359
T. Tada 95
T. Watcharakan 256, 423
T.H. Pham 295
T.R. Aswath 190
Tae-Hee Lee 403
Taichi Uemura 342
Takahiro Anzai 154, 312
Takanobu Kawamura 303
Takashi Kakubo 395
Takayuki Yoshida 274
Tapas Ranjan Mohanty 178
Tatsuya Endo 474
Taweechai Amornsakchai 53, 122
Teerin Kongpun 426
Teofil Jesionowski 27
Thanawadee Leejarkpai 72
Thang Manh Tran 377
Thanh Binh Thi Bui 377
Thanh-Tam Mai 441, 492
Thanita Suakamram 484
Tharin Sensan 108
Thitiwan Intha 55
Thomas Griggs 10
Thuong Thi Nghiem 101
Tim Yu-Ting Lin 120
Titash Mondal 258
Tomoaki Nakatsuka 369
Tomoka Noda 474
Tomoki Mishima 492
Torfan Srisuwanno 245
Toshio Tada 60
Tran Thi Thuy 83
Tsutomu Furuya 466
Tsuyoshi Koga 466

U

U. Calik 283
U. Tepsuwan 388
Ulrich Giese 1, 227
Unal C. Yilmazoglu 279
Utpal Roy 427

V

V. Ferrer 118
Varatnane Yaoprukse 455
Viet Anh Ta 101

W

W. Intiya 346, 388
W. K. Dierkes 181
W. Waddell 120
Waluree Thongkam 498
Wan Li 279
Wangtong Li 165
Warakorn Noisang 39
Warut Chanasit 211
Wasan Tessanan 122
Wei Huang 299
Wei Li 433
Weijia Wang 233
Weixiao Song 85
Wencai Wang 433, 462, 464
Wenchi Han 439
Wilawan Lekkla 74
Wirach Taweepreda 170
Wirasak Smitthipong 87, 126, 199, 238, 308, 355, 445
Wisut Kaewsakul 195
Wongsathorn Saitrong 53
Won-young Jung 403

X

X. Liang 293
Xiaobin Liang 154, 288, 312, 490
Xiaodong Zhang 435
Xiaohu Ren 233
Xiaohui Wu 85
Xiaorong Wang 19, 161, 299
Xiaotong Liu 433

Xin Wang 247
Xin Wang 472
Xin Ye 375
Xinglong An 397
Xiuying Zhao 373, 468, 472
Xiuze Che 233
Xuan Qin 372
Xuequan Zhang 183, 247, 249
Xueting Wan 57

Y

Y. C. Wang 68
Y. Chisti 344
Y. Kitaura-Sakaguchi 95, 118
Y. Nakaramontri 75, 359, 409, 413
Y. Okumura 470
Y. Shibata 476
Y. Shoda 93
Y. X. Wu 68
Yanchun Han 176
Yanfeng Niu 433
Yang Chen 462
Yang Chen 464
Yang Zhiwei 431
Yao Zhimin 146
Yasuhiro Shoda 110
Yasuhisa Shibata 261
Yeampon Nakaramontri 205, 245
Yichen Lu 433
Yingfeng Tu 57
Yingjun An 419
Yogesh Jadhav 174, 178
Yoko Aoyama 417
Yongxin Duan 176
Yongxin Duan 179
Yoshimasa Yamamoto 14, 101, 124
Youli Li 126
Yuanbiao Gong 233
Yuanbing Zhou 443
Yudong Liu 103
Yue Dongmei 431
Yue Liu 468
Yue Pan 439
Yui Tsuji 369
Yuichi Aoyagi 154, 312
Yuji Kitamura 31, 110, 128, 338, 340, 342
Yuki Jotatsu 31, 340
Yuki Tokudome 488
Yuki Watanabe 274
Yuko Ikeda 16
Yulin Yi 263
Yume Sugino 474
Yunxiao Liu 45
Yuzhi Feng 263
Yuzhu Xiong 217
Yuzu Tomeba 417
Z. A. Laksanaa 229
Z. Q. Zhang 68

Z

Zejun Zhang 179
Zhan Lu 165
Zhanjie Liu 415
Zhaoyang Yuan 478
Zheming Tong 263
Zhenghai Tang 41, 163, 394
Zhengtian Xie 42, 139
Zhengying Li 19
Zhenyuan Li 456
Zhepeng Wang 19
Zhi Chen 373, 472
Zhiyang Tong 263
Zixuan Wang 85
Zühra Çinar Esin 281